

PHYTOPATHOLOGIA MEDITERRANEA

Plant health and food safety

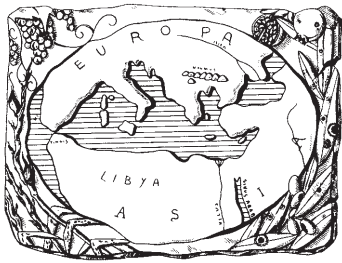
Volume 60 • No. 2 • August 2021

iscritto al Tribunale di Firenze con il n° 4923 del 5-1-2000 - Poste Italiane Spa - Spedizione in Abbonamento Postale - 70% DCB FIRENZE



The international journal of the
Mediterranean Phytopathological Union





PHYTOPATHOLOGIA MEDITERRANEA

Plant health and food safety

The international journal edited by the Mediterranean Phytopathological Union
founded by A. Ciccarone and G. Goidànich

Phytopathologia Mediterranea is an international journal edited by the Mediterranean Phytopathological Union. The journal's mission is the promotion of plant health for Mediterranean crops, climate and regions, safe food production, and the transfer of knowledge on diseases and their sustainable management.

The journal deals with all areas of plant pathology, including epidemiology, disease control, biochemical and physiological aspects, and utilization of molecular technologies. All types of plant pathogens are covered, including fungi, nematodes, protozoa, bacteria, phytoplasmas, viruses, and viroids. Papers on mycotoxins, biological and integrated management of plant diseases, and the use of natural substances in disease and weed control are also strongly encouraged. The journal focuses on pathology of Mediterranean crops grown throughout the world.

The journal includes three issues each year, publishing Reviews, Original research papers, Short notes, New or unusual disease reports, News and opinion, Current topics, Commentaries, and Letters to the Editor.

EDITORS-IN-CHIEF

Laura Mugnai – University of Florence, DAGRI, Plant pathology and Entomology section, Ple delle Cascine 28, 50144 Firenze, Italy
Phone: +39 055 2755861
E-mail: laura.mugnai@unifi.it

Richard Falloon – New Zealand Institute for Plant & Food Research (retired)
Phone: +64 3 337 1193 or +64 27 278 0951
Email: richardefalloon@gmail.com

CONSULTING EDITORS

A. Phillips, Faculdade de Ciências, Universidade de Lisboa, Portugal
G. Surico, DAGRI, University of Florence, Italy

EDITORIAL BOARD

I.M. de O. Abrantes, Universidad de Coimbra, Portugal
J. Armengol, Universidad Politécnica de Valencia, Spain
S. Banniza, University of Saskatchewan, Canada
A. Bertaccini, Alma Mater Studiorum, University of Bologna, Italy
A.G. Blouin, Plant & Food Research, Auckland, New Zealand
R. Buonaurio, University of Perugia, Italy
R. Butler, Plant & Food Research, Christchurch, New Zealand
N. Buzkan, Imam University, Turkey
T. Caffi, Università Cattolica del Sacro Cuore, Piacenza, Italy
J. Davidson, South Australian Research and Development Institute (SARDI), Adelaide, Australia
A.M. D'Onghia, CIHEAM/Mediterranean Agronomic Institute of Bari, Italy
T.A. Evans, University of Delaware, Newark, DE, USA

A. Evidente, University of Naples Federico II, Italy
M. Garbelotto, University of California, Berkeley, CA, USA
L. Ghelardini, University of Florence, Italy
V. Guarnaccia, University of Stellenbosh, South Africa
N. Iacobellis, University of Basilicata, Potenza, Italy
H. Kassemeyer, Staatliches Weinbauinstitut, Freiburg, Germany
P. Kinay Teksür, Ege University, Bornova Izmir, Turkey
A. Moretti, National Research Council (CNR), Bari, Italy
L. Mostert, Faculty of AgriSciences, Stellenbosh, South Africa
J. Murillo, Universidad Publica de Navarra, Spain
J.A. Navas-Cortes, CSIC, Cordoba, Spain
L. Palou, Centre de Tecnologia Postcollita, Valencia, Spain
E. Paplomatas, Agricultural University of Athens, Greece

I. Pertot, University of Trento, Italy
A. Picot, Université de Bretagne Occidentale, LUBEM, Plouzané, France
D. Rubiales, Institute for Sustainable Agriculture, CSIC, Cordoba, Spain
J-M. Savoie, INRA, Villenave d'Ornon, France
A. Siah, Yncréa HdF Lille, France
A. Tekauz, Cereal Research Centre, Winnipeg, MB, Canada
D. Tsitsigiannis, Agricultural University of Athens, Greece
J.R. Úrbez Torres, Agriculture and Agri-Food Canada, Canada
J.N. Vanneste, Plant & Food Research, Sandringham, New Zealand
M. Vurro, National Research Council (CNR), Bari, Italy
A.S. Walker, BIOGER, INRAE, Thiverval-Grignon, France
M.J. Wingfield, University of Pretoria, South Africa

DIRETTORE RESPONSABILE

Giuseppe Surico, DAGRI, University of Florence, Italy
E-mail: giuseppe.surico@unifi.it

EDITORIAL OFFICE STAFF

DAGRI, Plant pathology and Entomology section, University of Florence, Italy
E-mail: phymed@unifi.it, Phone: ++39 055 2755861/862

EDITORIAL ASSISTANT - **Sonia Fantoni**

EDITORIAL OFFICE STAFF - **Angela Gagliar**

Phytopathologia Mediterranea on-line: www.fupress.com/pm/

PHYTOPATHOLOGIA MEDITERRANEA

**The international journal of the
Mediterranean Phytopathological Union**

Volume 60, August, 2021

Firenze University Press

***Phytopathologia Mediterranea*. The international journal of the Mediterranean Phytopathological Union**

Published by

Firenze University Press – University of Florence, Italy

Via Cittadella, 7–50144 Florence–Italy

<http://www.fupress.com/pm>

Direttore Responsabile: **Giuseppe Surico**, University of Florence, Italy

Copyright © 2021 **Authors**. The authors retain all rights to the original work without any restrictions.

Open Access. This issue is distributed under the terms of the [Creative Commons Attribution 4.0 International License \(CC-BY-4.0\)](https://creativecommons.org/licenses/by/4.0/) which permits unrestricted use, distribution, and reproduction in any medium, provided you give appropriate credit to the original author(s) and the source, provide a link to the Creative Commons license, and indicate if changes were made. The Creative Commons Public Domain Dedication (CC0 1.0) waiver applies to the data made available in this issue, unless otherwise stated.



Citation: Y. Du, X. Wang, Y. Guo, F. Xiao, Y. Peng, N. Hong, G. Wang (2021) Biological and molecular characterization of seven *Diaporthe* species associated with kiwifruit shoot blight and leaf spot in China. *Phytopathologia Mediterranea* 60(2): 177-198. doi: 10.36253/phyto-12013

Accepted: February 1, 2021

Published: September 13, 2021

Copyright: © 2021 Y. Du, X. Wang, Y. Guo, F. Xiao, Y. Peng, N. Hong, G. Wang. This is an open access, peer-reviewed article published by Firenze University Press (<http://www.fupress.com/pm>) and distributed under the terms of the Creative Commons Attribution License, which permits unrestricted use, distribution, and reproduction in any medium, provided the original author and source are credited.

Data Availability Statement: All relevant data are within the paper and its Supporting Information files.

Competing Interests: The Author(s) declare(s) no conflict of interest.

Editor: Vladimiro Guarnaccia, DiSAFA - University of Torino, Italy.

Research Papers

Biological and molecular characterization of seven *Diaporthe* species associated with kiwifruit shoot blight and leaf spot in China

YAMIN DU^{1,2,3,4}, XIANHONG WANG⁴, YASHUANG GUO⁴, FENG XIAO⁴, YUHONG PENG⁴, NI HONG^{1,2,3,4}, GUOPING WANG^{1,2,3,4,*}

¹ College of Plant Science and Technology, Huazhong Agricultural University, Wuhan 430070, Hubei, China

² Key Lab of Plant Pathology of Hubei Province, Wuhan 430070, Hubei, China

³ Key Laboratory of Horticultural Crop (Fruit Trees) Biology and Germplasm Creation of the Ministry of Agriculture, Wuhan 430070, Hubei, China

⁴ State Key Laboratory of Agricultural Microbiology, Huazhong Agricultural University, Wuhan 430070, Hubei, China

*Corresponding author. E-mail: gpwang@mail.hzau.edu.cn

Summary. *Diaporthe* species are significant pathogens, saprobes, and endophytes, with comprehensive host association and geographic distribution. These fungi cause severe dieback, cankers, leaf spots, blights, and stem-end rot of fruits on different plant hosts. This study, explored the occurrence, diversity and pathogenicity of *Diaporthe* spp. associated with *Actinidia chinensis* and *A. deliciosa* in the main kiwifruit production areas of China. *Diaporthe* isolates (284) derived from 106 diseased leaf and branch samples were examined. Multi-locus phylogenetic analyses and morphology of 43 representative isolates revealed that seven *Diaporthe* species were obtained, including *D. alangii*, *D. compactum*, *D. eres*, *D. hongkongensis*, *D. sojae*, *D. tectonae*, and *D. unshiuensis*. Pathogenicity tests were performed on kiwifruit fruits, leaves and branches. Koch's postulates confirmed all species were pathogenic. *D. alangii* and *D. tectonae* were the most aggressive species, followed by *D. eres*, *D. sojae*, *D. hongkongensis*, *D. unshiuensis*, and *D. compactum*. Host range evaluation showed that the seven *Diaporthe* species could also infect apricot, apple, peach, pear, and plum. This is the first report of *D. alangii*, *D. compactum*, *D. sojae*, *D. tectonae*, and *D. unshiuensis* infecting kiwifruit in China, increasing understanding of the *Diaporthe* complex causing diseases of kiwifruit plants, to assist effective disease management.

Keywords. *Actinidia*, phylogeny, pathogenicity.

INTRODUCTION

Kiwifruit is known “the king of fruits” due to its rich nutritional content, abundant dietary fibres, balanced nutritional composition of minerals, high vitamin C content, antioxidant properties and other human health-beneficial metabolites, including carotenoids and flavonoids (Huang *et al.*, 2013; Pan *et*

al., 2020; Wu et al., 2020). The centre of origin of kiwifruit is the mountains and ranges of southwestern China (Yue et al., 2020). Kiwifruit has a short history of domestication, starting from the early 20th century (Huang et al. 2013; Li et al. 2017a Wu et al., 2020). Through decades of domestication and substantial efforts for selection from wild plants, several important horticultural species have been commercially cultivated, including *Actinidia chinensis*, *A. deliciosa*, *A. eriantha*, and *A. arguta* (Huang et al., 2013; Song et al., 2020). *Actinidia chinensis* and *A. deliciosa* are the major species cultivated in China (Huang, 2009), which had a kiwifruit cultivation area of 240,000 ha in 2018, producing 2.55 MT of fruit, accounting for nearly 55% of the global kiwifruit (FAO, 2018; Guo et al., 2020a).

During the past decades, with the steadily increasing duration of kiwifruit monoculture and the rapid expansion of production, diseases have become prevalent in orchards and nurseries. Branch blight and leaf spot diseases are widespread and prevalent, and these diseases cause serious economic losses in China, and affect development of the kiwifruit industry. Accurate identification of cause of these diseases is important for development of effective biosecurity and trade policies. The most common disease symptoms observed in kiwifruit plantations consist of branch blight, leaf spot, bacterial blossom blight, and fruit rot. These symptoms are related to several fungi (Hawthorne et al., 1982; Pennycook, 1985; Pan et al., 2018) and bacteria (Zhang et al., 2019).

Vine decline of kiwifruit in Turkey was mainly related to *Phytophthora citrophthora* (Akilli et al. 2011). In Greece, the pathogens which caused distinct cankers on branches of kiwifruit were *Diaporthe neotheicola* and *Botryosphaeria dothidea* (Thomidis et al., 2010, 2013). *Diaporthe ambigua* and *D. australafricana* were reported as causing cordon dieback in Chile (Díaz and Latorre, 2018). In China, the major pathogens causing branch blight were *B. dothidea*, *D. actinidiae*, *D. eres*, and *D. tuliensis* (Li et al., 2013; Bai et al., 2017).

Leaf spot of kiwifruit, caused by *Alternaria alternata*, *Diaporthe* spp., *Glomerella cingulata*, *Pestalotiopsis* spp. and *Phomopsis* spp., has been previously reported in Korea and New Zealand (Jeong et al., 2008; Hawthorne and Otto, 2012). *Didymella bellidis* has been reported as the major cause of leaf spot in China (Zou et al., 2019).

The blossom blight of kiwifruit occurs in many countries. Several pathogens have been reported as the causal agents of this disease, including *Pseudomonas viridiflava*, *P. fluorescens*, *P. syringae*, *P. fluorescens* *P. syringae* pv. *syringae*, *P. syringae* pv. *actinidiae*, and *Botrytis cinerea* (Conn and Gubler, 1993; Koh et al., 2001; Shin et al., 2004; Young et al., 2009; Zhang et al., 2019)

Fruit rot of kiwifruit can be divided into field rot and postharvest fruit rot. Field rot, caused by *Sclerotinia sclerotiorum*, affects immature fruits on vines (Pennycook, 1985). More than seven fungi have been reported to be associated with postharvest fruit rots of kiwifruit (Beraha and O'Brien, 1979; Hawthorne et al., 1982; Pennycook, 1985), *Diaporthe* spp. and *Botryosphaeria* spp. were reported as the major causes of postharvest fruit rot. In New Zealand, *Botrytis cinerea* causes storage rot and *B. dothidea* causes ripening rot. *Botryosphaeria dothidea* also was the major cause of postharvest fruit rot in Iran (Nazerian et al., 2019). *Diaporthe actinidiae* has been reported to cause postharvest fruit rot in China, Iran, Korea, and New Zealand (Sommer and Beraha, 1975; Lee et al., 2001; Koh et al., 2005; Mousakhah et al., 2014; Li et al., 2017b). In addition, *D. ambigua*, *D. australafricana*, *D. novem*, and *D. rudis* have been reported to cause postharvest fruit rot of kiwifruit during cold storage in Chile. *Diaporthe ambigua* was also isolated from postharvest kiwifruit rots in Greece (Thomidis et al., 2013; 2019). *Diaporthe honkongensis* has been reported to cause stem-end rot in Turkey (Erper et al., 2017). *Diaporthe melonis* and *D. pernicioso* have been reported as the major pathogens causing postharvest fruit rots in New Zealand (Beraha and O'Brien, 1979; Hawthorne et al., 1982).

Before the advent of molecular biology technology, identification criteria for *Diaporthe* species were based on the morphological characteristics (e.g., colony appearance in cultures, size and shape of ascomata and conidiomata, sexual state and connections to the asexual state) and host specificity (Rehner and Uecker, 1994; Santos et al., 2011; Gomes et al., 2013; Guarnaccia and Crous, 2017; Yang et al., 2018b). Previous studies demonstrated that these characters were generally not sufficient for species level diagnoses, because some species of *Diaporthe* are not host-restricted and are capable of infecting several taxonomically unrelated host genera (Rehner and Uecker, 1994; Thompson et al., 2011; Elfar et al., 2013; Huang et al., 2013; Thompson et al., 2015). *Diaporthe helianthi*, as the causal agent of stem canker of sunflower, was first reported in the former Yugoslavia. Subsequent studies confirmed *Xanthium italicum*, *X. strumarium*, and *Arctium lappa* as weed hosts of *D. helianthi* (Thompson et al., 2015). Three other *Diaporthe* species, *D. gulyae*, *D. kochmanii*, and *D. kongii*, have been identified as the pathogens of sunflower stem canker (Thompson et al., 2011). In addition, character plasticity and cultural variation of *Diaporthe* hampered species clarification. Application of molecular data has progressed fungal species definition (Hibbett and Taylor, 2013; Yang et al., 2018a). *Diaporthe* species are being redefined, based on the combination of morphological,

cultural and phytopathogenic characteristics, mating types and DNA sequence data (Guarnaccia and Crous, 2017, 2018; Fan *et al.*, 2018). Adoption of multi-locus phylogeny has provided clear resolution of classification and species (Udayanga *et al.*, 2014).

China is an important kiwifruit-growing country and leader in kiwifruit cultivation. However, in recent years, the incidence and systematic identification of the *Diaporthe* species associated with branch blight of kiwifruit were only assessed in two orchards of Hubei and Anhui provinces. Only 36 strains were obtained and identified as *D. tulliensis*, *D. actinidiae* and *D. eres*, and it is unclear which species is responsible for the disease in different host varieties or species in different provinces (Bai *et al.*, 2017). In addition, leaf spot of kiwifruit caused by *Diaporthe* species has been rarely reported in China, which makes effective prevention and control of the disease challenging. Therefore, larger scale surveys are needed to give increased understanding of the relative role of *Diaporthe* spp. in fungal branch blight and leaf spot found on kiwifruit in China.

The present sampled plants with shoot blight and leaf spot symptoms for pathogen isolation. Phylogenetic analyses based on the nuclear ribosomal internal transcribed spacer region (ITS), *translation elongation factor 1-alpha* (*EF1- α*) and *beta-tubulin* (*TUB*) genes, coupled with morphology of representative strains, were carried out to determine the diversity of pathogens. After pathogenicity determination, species associated with kiwifruit shoot and leaf blight were identified. This study has provided valuable information on pathogen ecology, as a basis for improving management strategies for these economically important diseases.

MATERIALS AND METHODS

Sampling and pathogen isolation

Surveys of incidence of shoot blight and leaf spot diseases were conducted in 16 orchards located in nine provinces of China, including Anhui, Chongqing, Henan, Hubei, Fujian, Shandong, Shanxi, Sichuan, and Zhejiang, from October 2017 to May 2019. A total of 106 samples with symptoms of shoot blight and/or leaf spot were collected from *Actinidia chinensis* ('Cuiyu', 'Donghong', 'Hongyang', 'Huangjin', 'Jinyan', and 'Longzanghong'), and *A. deliciosa* ('Cuixiang', 'Hayward', 'Jinkui', and 'Xuxiang'). Six pieces (4–5 mm²) of wood or foliage were cut from each of the diseased tissues neighbouring the asymptomatic regions with a sterile scalpel. After surface sterilization in 1% NaOCl for 45 s, the tissues were treated in 75% ethanol for 45 s, rinsed three

times in sterile distilled water for 1 min each, and then dried on sterilized filter paper (Fu *et al.*, 2018). Each tissue piece was placed on potato dextrose agar (PDA; 20% diced potato, 2% dextrose, 1.5% agar, and distilled water) plates and incubated at 25°C in the dark for 3–5 d until fungal colony formation (Bai *et al.*, 2015). Colonies with typical characteristic of *Diaporthe* spp. were sub-cultured onto fresh PDA plates. The obtained isolates were purified using hyphal tip or single spore methods. Mycelium plugs of purified isolates were transferred to PDA tubes, or stored in 25% glycerol at -80°C for subsequent use (Zhai *et al.*, 2014).

DNA extraction, PCR amplification, and sequencing

Colonies were cultivated on PDA plates where the medium was covered with sterile cellophane which was incubated at 25°C in the dark for 5–7 d. Mycelia was scraped and placed into clean tubes. Total genomic DNA was extracted using a modified CTAB method (Freeman *et al.*, 1996). The quality and quantity of DNA were confirmed visually by staining with Gel Red after electrophoresis in 1% agarose gel and visualization under UV light ($\lambda = 302$ nm) trans illumination (Udayanga *et al.*, 2012; Gao *et al.*, 2017). The internal transcribed spacer (ITS) region of the nuclear ribosomal genes was amplified using the primer sets ITS1/ITS4 (White *et al.*, 1990), the primers EF1-728F/EF1-986R (Carbone and Kohn, 1999) were used to amplify part of *EF1- α* , and the primers Bt-2a/Bt-2b (Glass and Donaldson, 1995) were used to amplify part of *TUB*. For PCR, an aliquot of 50 μ L reaction solution contained 5 μ L of 10 \times *Taq* buffer II (Mg²⁺ Plus) (TaKaRa), 1 μ L of dNTP mixture (2.5 mM each), 1 μ L of each primer, 0.5 μ L of *Taq* (5U μ L⁻¹), 2.0 μ L of DNA template, and 39.5 μ L of ddH₂O (Zhai *et al.*, 2014). PCR parameters were initiated at 95°C for 5 min, followed by 35 cycles, each of denaturation at 95°C for 30 s, annealing at appropriate temperature for 30 s (56°C for ITS, 51°C for *EF1- α* , 61°C for *TUB*), and extension at 72°C for 30 s, and terminated with a final elongation step at 72°C for 10 min (Guo *et al.*, 2020b). The PCR amplicons were purified and sequenced by Sangon Biotech Company, Ltd. The obtained sequences were analyzed on DNAMAN (v. 9.0; Lynnon Biosoft), and deposited in GenBank (Table 1).

Phylogenetic analyses

Novel sequences generated in this study were blasted against the NCBI's GenBank nucleotide database ([www.http://blast.ncbi.nlm.nih.gov/](http://blast.ncbi.nlm.nih.gov/)) to search for closely similar relatives for a taxonomic framework of the studied

Table 1. Sources and GenBank accession numbers of isolates included in this study.

Species	Isolate designation ^a	Host	Country	Genbank accession numbers			
				ITS	<i>EF1-α</i>	<i>TUB</i>	
<i>Diaporthe alangii</i>	CFCC 52556*	<i>Alangium kurzii</i>	China	MH121491	MH121533	MH121573	
	CFCC 52557	<i>Alangium kurzii</i>	China	MH121492	MH121534	MH121574	
	CFCC 52558	<i>Alangium kurzii</i>	China	MH121493	MH121535	MH121575	
	CQ155	<i>Actinidia chinese</i>	China	MT043825	MT109567	MT109603	
	FJHJB57	<i>Actinidia chinese</i>	China	MT043831	MT109562	MT109615	
	HB48	<i>Actinidia deliciosa</i>	China	MT043835	MT109578	MT109619	
	LP-1	<i>Actinidia</i> sp.	China	KX457967	KX457964	/	
	SC74	<i>Actinidia chinese</i>	China	MT043849	MT109592	MT109627	
	SC83	<i>Actinidia chinese</i>	China	MT043850	MT109593	MT109628	
	<i>D. ambigua</i>	CBS 114015*	<i>Pyrus communis</i>	South Africa	KC343010	KC343736	KC343978
<i>D. compactum</i>	LC3078*	<i>Camellia sinensis</i>	China	KP267850	KP267924	/	
	LC3083*	<i>Camellia sinensis</i>	China	KP267854	KP267928	/	
	CQ130	<i>Actinidia deliciosa</i>	China	MT043824	MT109565	MT109601	
	CQ178	<i>Actinidia chinese</i>	China	MT043827	MT109570	MT109606	
	SC42	<i>Actinidia chinese</i>	China	MT043846	MT109589	MT109624	
	SC67	<i>Actinidia chinese</i>	China	MT043848	MT109591	MT109626	
	<i>D. eres</i>	AR5193*	<i>Ulmus</i> sp.	Germany	KJ210529	KJ210550	KJ420799
CBS 267.55		<i>Laburnum × watereri</i> 'Vossii'	Netherlands	KC343082	KC343808	KC344050	
CBS 101742		<i>Fraxinus</i> sp.	Netherlands	KC343073	KC343799	KC344041	
CFCC 52576		<i>Castanea mollissima</i>	China	MH121511	MH121553	MH121593	
CFCC 52578		<i>Sorbus</i> sp.	China	MH121513	MH121555	MH121595	
AH16		<i>Actinidia chinese</i>	China	MT043816	MT109564	MT109600	
HB24		<i>Actinidia chinese</i>	China	MT043833	MT109576	MT109617	
HB25		<i>Actinidia chinensis</i>	China	MT043834	MT109577	MT109618	
HN10		<i>Actinidia deliciosa</i>	China	MT043836	MT109579	MT109620	
WAI-1		<i>Actinidia</i> sp.	China	KX457969	KX 457965	/	
MJL13		<i>Actinidia chinensis</i>	China	MT043839	MT109582	MT109632	
MJL18		<i>Actinidia chinensis</i>	China	MT043841	MT109584	MT109634	
FJ11		<i>Actinidia chinensis</i>	China	MT043828	MT109559	MT109612	
SD16		<i>Actinidia chinensis</i>	China	MT043853	MT109595	MT109638	
SX24		<i>Actinidia deliciosa</i>	China	MT043854	MT109597	MT109630	
<i>D. ganjae</i>		CBS 180.91*	<i>Cannabis sativa</i>	USA	KC343112	KC343838	KC344080
<i>D. goulteri</i>		BRIP 55657a	<i>Helianthus annuus</i>	Australia	KJ197290	KJ197252	KJ197270
<i>D. hongkongensis</i>	LC3484	<i>Camellia sinensis</i>	China	KP267906	KP267980	KP293486	
	CBS 115448*	<i>Dichroa febrifuga</i>	China	KC343119	KC343845	KC344087	
	CQ21	<i>Actinidia chinese</i>	China	MT043821	MT109571	MT109607	
	CQ51	<i>Actinidia chinensis</i>	China	MT043822	MT109572	MT109608	
	FJHJB53	<i>Actinidia chinensis</i>	China	MT043830	MT109561	MT109614	
	MJL19	<i>Actinidia deliciosa</i>	China	MT043842	MT109585	MT109635	
	MJL21	<i>Actinidia deliciosa</i>	China	MT043843	MT109586	MT109636	
	<i>D. manihotia</i>	CBS 505.76*	<i>Manihot utilisissima</i>	Rwanda	KC343138	KC343864	KC344106
	<i>D. neoraonikayaporum</i>	MFLUCC 14-1136*	<i>Tectona grandis</i>	Tailand	KU712449	KU749369	KU743988
	<i>D. raonikayaporum</i>	CBS 133182*	<i>Spondias mombin</i>	Brazil	KC343188	KC343914	KC344156
<i>D. sojae</i>	FAU635*	<i>Glycine max</i>	USA	KJ590719	KJ590762	KJ610875	
	FAU636	<i>Glycine max</i>	USA	KJ590718	KJ590761	KJ610874	
	ZJUD68	<i>Citrus unshiu</i>	China	KJ490603	KJ490482	KJ490424	
	CQ14	<i>Actinidia chinensis</i>	China	MT043819	MT109566	MT109602	
	CQ16	<i>Actinidia chinensis</i>	China	MT043820	MT109568	MT109604	

(Continued)

Table 1. (Continued).

Species	Isolate designation ^a	Host	Country	Genbank accession numbers		
				ITS	<i>EF1-α</i>	<i>TUB</i>
	FJHJB61	<i>Actinidia chinensis</i>	China	MT043832	MT109563	MT109616
	HN59	<i>Actinidia deliciosa</i>	China	MT043838	MT109581	MT109622
	SD8	<i>Actinidia chinensis</i>	China	MT043852	MT109596	MT109639
	SC90	<i>Actinidia chinensis</i>	China	MT043851	MT109594	MT109629
	ZJ5	<i>Actinidia chinensis</i>	China	MT043856	MT109599	MT109631
<i>D. tectonae</i>	MFLUCC 12-0777*	<i>Tectona grandis</i>	Thailand	KU712430	KU749359	KU743977
	MFLUCC 12-0782	<i>Tectona grandis</i>	Thailand	KU712431	KU749360	KU743978
	MFLUCC 13-0476	<i>Tectona grandis</i>	Thailand	KU712433	KU749362	KU743980
	MFLUCC 14-1139	<i>Tectona grandis</i>	Thailand	KU712438	KU749366	KU743985
	CQ58	<i>Actinidia chinensis</i>	China	MT043823	MT109573	MT109609
	CQ166	<i>Actinidia chinensis</i>	China	MT043826	MT109569	MT109605
<i>D. tulliensis</i>	BRIP 62248a*	<i>Theobroma cacao</i>	Australia	KR936130	KR936133	KR936132
<i>D. unshiuensis</i>	CFCC 52594	<i>Carya illinoensis</i>	China	MH121529	MH121571	MH121606
	CFCC 52595	<i>Carya illinoensis</i>	China	MH121530	MH121572	MH121607
	ZJUD51	<i>Citrus japonica</i>	China	KJ490586	KJ490465	KJ490407
	ZJUD52*	<i>Citrus unshiu</i>	China	KJ490587	KJ490466	KJ490408
	CQ7	<i>Actinidia chinensis</i>	China	MT043817	MT109574	MT109610
	CQ9	<i>Actinidia chinensis</i>	China	MT043818	MT109575	MT109611
	FJHJB22	<i>Actinidia chinensis</i>	China	MT043829	MT109560	MT109613
	HN51	<i>Actinidia deliciosa</i>	China	MT043837	MT109580	MT109621
	MJL15	<i>Actinidia deliciosa</i>	China	MT043840	MT109583	MT109633
	MJL35	<i>Actinidia deliciosa</i>	China	MT043844	MT109587	MT109637
	SC41	<i>Actinidia chinensis</i>	China	MT043845	MT109588	MT109623
	SC65	<i>Actinidia chinensis</i>	China	MT043847	MT109590	MT109625
<i>Diaporthe corylina</i>	CBS 121124*	<i>Corylus</i> sp.	China	KC343004	KC343730	KC343972

^a ICMP: International Collection of Micro-organisms from Plants; FAU: Isolates in culture collection of Systematic Mycology and Microbiology Laboratory, USDA-ARS, Beltsville, Maryland, USA; BRIP: Queensland Plant Pathology herbarium/culture collection, Australia; CBS: Westerdijk Fungal Biodiversity Centre, Utrecht, The Netherlands; CFCC: China Forestry Culture Collection Center, China; LC: Corresponding author's personal collection (deposited in laboratory State Key Laboratory of Mycology, Institute of Microbiology, Chinese Academy of Sciences); MFLUCC: Mae Fah Luang University Culture Collection, Chiang Rai, Thailand; ZJUD: Zhejiang University.

* = ex-type culture.

/ = the Genbank accession number is absent.

isolates. Sequence alignments of different gene regions, including sequences obtained from this study and reference sequences based on recent studies of *Diaporthe* species, were initially carried out with the online server (<http://mafft.cbrc.jp/alignment/server/index.html>) (Kato and Standley, 2013), and were then manually adjusted in MEGA v. 7 (Kumar *et al.*, 2016).

An initial maximum likelihood (ML) phylogenetic analysis was conducted based on *EF1-α* sequences of 284 isolates obtained in this study and 31 reference strains including one outgroup taxon (*Diaporthe corylina* CBS121124) deposited in GenBank (Table 1) with a GTR+G substitution model by using IQ-tree v.1.6.8, to give an overview backbone phylogenetic tree for the genus *Diaporthe* (data not shown). A subset of

43 representative isolates was then selected based on the results of the general *EF1-α* analysis, and was processed through different phylogenetic analyses conducted individually for each locus and multiple sequences analyses using concatenated ITS, *EF1-α*, and *TUB*.

Multi-locus phylogenetic analyses were generated using Maximum likelihood (ML) and Bayesian inference (BI). The maximum-likelihood tree was inferred using the edge-linked partition model in IQ-tree (Nguyen *et al.*, 2015; Minh *et al.*, 2020). For the IQ-tree, the best evolutionary model for each partition was determined using ModelFinder (Minh *et al.*, 2020). In the partition model, IQ-TREE can estimate the model parameters separately for every partition. After ModelFinder found the best partition, IQ-TREE immediately starts the

tree reconstruction under the best-fit partition model, Branch supports were assessed with ultrafast bootstrap approximation (UFBoot) of 1000 replicates (Hoang *et al.*, 2017). Additionally, Bayesian inference (BI) was performed on the concatenated loci to construct phylogenies using MrBayes v. 3.2.2 (Ronquist *et al.*, 2003) as described by Crous (2006). MrModeltest v. 2.3 (Nylander, 2004) was used to calculate the best-fit models of nucleotide substitution for each data partition with the corrected Akaike information criterion (AIC). Two analyses of four Markov Chain Monte Carlo (MCMC) chains were conducted from random trees with 8×10^6 generations. The analyses were sampled every 1000 generations, which were stopped once the average standard deviation of split frequencies was below 0.01. The first 25% of the trees were discarded as the burn-in phase, and the remaining trees were summarized to calculate the posterior probabilities (PP) of each clade being monophyletic. Phylogenetic trees were visualized in Figtree v.1.4.2 (Rambaut, 2014).

Morphological and growth rate analyses

Based on the results of the phylogenetic analyses, 17 representative isolates (including *D. alangii*: CQ155, FJHJB57; *D. compactum*: CQ178, SC67; *D. eres*: HN10, HB25, SX24, HB24, CQ3; *D. hongkongensis*: CQ51; *D. sojiae*: CQ14, CQ78, CQ16; *D. tectonae*: CQ58, SC83; *D. unshiuensis*: CQ7, CQ9) were selected for morphological observations and growth rate assessments. Three-day-old mycelium plugs (5 mm diam.) were taken from the margins of actively growing cultures and transferred onto the centres of 9 cm diam. Petri dishes containing potato dextrose agar (PDA) or 2% tap water agar supplemented with sterile fennel stems. Cultures were incubated at 25°C with a 14 h/10 h fluorescent light/dark cycle (Guo *et al.*, 2020b). Colony diameters were measured daily for 3 d to calculate mycelium growth rates (mm d^{-1}). For each representative isolate, these measurements were made in triplicate. Colony shape, density, and pigment production on PDA were noted after seven days. Generation of ascomata and conidiomata on PDA or fennel stems were examined periodically. Shape, colour, and size of asci were observed using light microscopy (Nikon Eclipse 90i or Olympus BX63), and 50 asci, ascospores, conidiophores, and conidia were measured.

Pathogenicity and host range

The 14 representative strains (*D. alangii*: CQ155, SC74; *D. compactum*: CQ178, SC67; *D. eres*: HN10,

HB25; *D. hongkongensis*: CQ21, CQ51; *D. sojiae*: CQ14, CQ16; *D. tectonae*: CQ166, CQ58 *D. unshiuensis*: CQ7, MJL15) were tested for pathogenicity on detached leaves or shoots of kiwifruit, and on branches of five other fruit tree species. One isolate of each species (*D. alangii*: CQ155; *D. compactum*: CQ178; *D. eres*: HN10; *D. hongkongensis*: CQ21; *D. sojiae*: CQ14; *D. tectonae*: CQ58; *D. unshiuensis*: CQ7) was also inoculated onto fruits of kiwifruit to assess pathogenicity.

Leaves of *Actinidia chinensis* ‘Cuiyu’, wounded or unwounded, were inoculated with mycelium plugs of isolates in eight replicates, to assess the pathogenicity of representative isolates selected from the seven *Diaporthe* species. Fresh and healthy leaves were washed under running tap water followed by surface sterilization with 25% ethanol, drying with sterile tissue paper and then air-drying (Hawthorne and Otto, 2012; Mousakhah *et al.*, 2014; Fu *et al.*, 2018). For the wound inoculation method, the mycelium plugs (agar disks) were placed midway on each side of each leaf midrib after wounding three times by pinpricking with a sterilized needle (insect pin, 0.5 mm diam.). For the non-wound inoculation method, mycelium plugs were placed directly on the unwounded leaves. Inoculations with sterile agar plugs were used as negative controls. The experiment was conducted twice. The inoculated leaves were put into a plastic container covered with plastic film and incubated at $25 \pm 1^\circ\text{C}$ with a 12 h/12 h light/dark photoperiod. Symptoms and lesion lengths were recorded at 7 d after inoculation, and re-isolations were made from lesion margins to fulfil Koch’s postulates.

Pathogenicity was also determined on excised segments of 1-year-old woody shoots of *A. chinensis* ‘Cuiyu’, *A. chinensis* ‘Jinyan’, *A. chinensis* ‘Hongyang’, and *A. chinensis* ‘Huangjin’, in five replicates. Green shoots (5–10 mm diam.) were pruned from healthy kiwifruit vines and cut into 10 cm long segments, rinsed with tap water, surface disinfected with 75% ethanol, and then air-dried. Wounding and non-wounding inoculation methods were used. For the wounding treatment, a superficial wound (5 mm diam.) was made on each shoot segment by removing the cortex with a disinfected 5 mm diam. hole punch (Bai *et al.*, 2015; Sessa *et al.*, 2017). Agar plugs (5 mm diam.) from fungus cultures were inserted into the wounds, and the inoculated parts were sealed with Parafilm to maintain humidity (Mostert *et al.*, 2001). For the non-wound inoculation method, the agar plugs were placed on the surface of unwounded shoots directly and the inoculated parts were sealed with Parafilm to maintain humidity. All inoculated shoots were kept in plastic containers covered with plastic film and maintained in the laboratory at 25°C. The experiment was conducted twice. Lesion lengths were measured at

10 d after inoculation, and pieces were excised from the xylem or phloem tissues under canker lesions neighbouring asymptomatic regions and were cultured to fulfil Koch's postulates.

Detached fruits of *A. deliciosa* 'Hayward' were inoculated with seven representative isolates in quadruplicate to determine isolate pathogenicity. The inoculations were conducted using wounded and non-wounded methods as previously described (Diaz *et al.*, 2017; Li *et al.*, 2017a). Healthy fruits were surface-sterilized with 75% ethanol prior to inoculation, washed three times with sterile water, and were air-dried (Zhou *et al.*, 2015; Erper *et al.*, 2017). For the wounded treatment, each mycelium plug was placed on the fruit after wounding once by pinpricking with a sterilized needle (5 mm deep) (Luongo *et al.*, 2011). For the non-wounded method, the mycelium plug was directly placed on the surface of unwounded fruits. Inoculation with sterile agar plugs was used as controls. Inoculation points were individually wrapped with sterilized moist cotton plugs (Zhai *et al.*, 2014; Bai *et al.*, 2015). Fruits were placed in a sealed plastic container at 25°C with a 12 h/12 h light/dark photoperiod. The tests were repeated twice. Seven days post inoculation, symptoms on the fruit were recorded and the lengths of lesions were measured. Recovery isolations were made from the flesh at the margins of developed lesions.

The host range of the seven *Diaporthe* species was determined on detached shoots of five *Rosaceae* fruit tree species, including *Malus pumila* 'Hong Fushi', *Prunus salicina* 'Dahongpao', *Prunus armeniaca* 'Helanxiangxing', *Pyrus pyrifolia* 'Cuiguan' and *Prunus persica* 'Youtao'. Shoots of these plants were wound-inoculated (as described above). Five shoots of each host were used for each inoculation treatment

Statistical analyses

Data from repeated tests and among treatments in each test were analyzed using SPSS Statistics 21.0 (WinWrap® Basic; <http://www.winwrap.com>) by one-way analysis of variance, and means were compared using Tukey's test at a significance level of $P = 0.05$.

RESULTS

Sampling and pathogen isolation

Investigations and analyses of the occurrence and sample collection of kiwifruit branch blight and leaf spot were conducted from October 2017 to May 2019. One hundred and six samples were collected from the surveyed orchards and nurseries for fungus isolations; 80 of the samples were diseased branches and 26 were infected leaves. In total, 284 *Diaporthe* isolates showed typical *Diaporthe* spp. cultural characteristics (Table 2), including fluffy, flattened, white, creamy, sulphur or grayish aerial mycelium, with solitary or aggregated, globose, dark pycnidia and the presence of alpha and/or beta conidia (Sessa *et al.*, 2017; Guo *et al.*, 2020b). Among them, 81 isolates were obtained from diseased leaf samples, and were identified as six species of *Diaporthe* (*D. alangii*, *D. compactum*, *D. eres*, *D. hongkongensis*, *D. sojiae*, and *D. unshiuensis*). In total, 203 isolates were derived from infected shoots, and were identified as seven species of *Diaporthe* (*D. alangii*, *D. compactum*, *D. eres*, *D. hongkongensis*, *D. sojiae*, *D. unshiuensis* and *D. tectonae*). The kiwifruit species and varieties from which these isolates were obtained included *A. chinensis* 'Cuiyu', 'Donghong', 'Hongyang', 'Huangjin', 'Jinyan',

Table 2. Sampling regions and numbers of *Diaporthe* isolates obtained in this study.

Sampling province	Number of isolates	Numbers of isolates from each species						
		<i>Diaporthe unshiuensis</i>	<i>D. eres</i>	<i>D. sojiae</i>	<i>D. hongkongensis</i>	<i>D. compactum</i>	<i>D. alangii</i>	<i>D. tectonae</i>
Chongqing	92	39	19	22	7	2	1	2
Fujian	72	43	8	12	7	1	1	0
Henan	15	3	8	4	0	0	0	0
Hubei	30	4	11	8	4	1	2	0
Shanxi	17	0	17	0	0	0	0	0
Sichuan	30	2	17	7	0	2	1	1
Shandong	8	0	7	1	0	0	0	0
Zhejiang	4	1	0	3	0	0	0	0
Anhui	16	8	7	0	1	0	0	0
Total	284	100	94	57	19	6	5	3

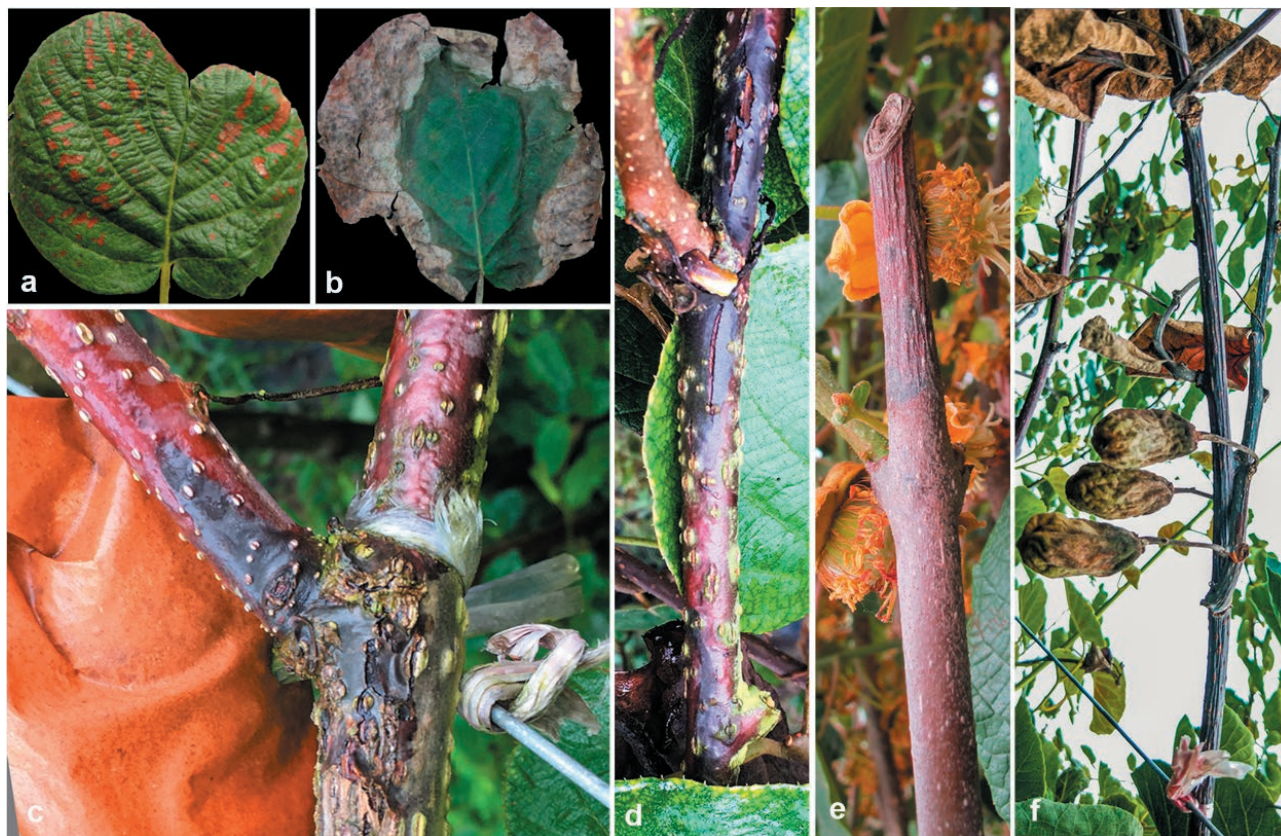


Figure 1. Typical symptoms of kiwifruit leaf spot and shoot blight. a, reddish brown spots on a leaf; b, lesions extend to the margin of a leaf, and small, black pycnidia on the necrotic parts; c, maroon and fusiform lesions on a branch; d, red-black fusiform lesions with internal discoloration formed on a branch; e, necrotic lesions spreading on a branch from the pruning wound; f, whole branch wilted.

‘Longzanghong’, and *A. deliciosa* ‘Cuixiang’, ‘Hayward’, ‘Jinkui’, and ‘Xuxiang’. Branch blight symptoms were commonly observed at the incision or pruned positions, with reddish-black fusiform or irregular necrotic lesions (Figure 1c); the lesions would gradually expand along each incision (Figure 1e). Under dry climate conditions, the infected branches turned brown and cracked, with internal discolorations (Figure 1d). Whole branches were withered (Figure 1f). The diseased leaves developed silvery gray or bronze spots, which were sporadically distributed on the leaves (Figure 1a). In the later stage of disease development, the spots were expanded to the edges of the leaves, and the leaves withered and curled at their margins. Scattered pycnidia were observed on the diseased leaves (Figure 1b).

Phylogenetic analyses of isolated fungi

The 43 representative isolates were subjected to multi-locus phylogenetic analyses with concatenated ITS, *EF1- α* ,

and *TUB* sequences together with 31 reference isolates from previously described species, including the outgroup sequence of *Diaporthe corylina* (culture CBS 121124). A total of 1557 characters (ITS: 1–541, *EF1- α* : 542–935, *TUB*: 936–1557) were included in the phylogenetic analyses. For the Bayesian analyses, the following priors were set in MrBayes for the different data partitions: the SYM+I+G model with invgamma-distributed rates was implemented for ITS; The GTR+G model with gamma-distributed rates was implemented for *EF1- α* ; and the HKY +G model with propinv-distributed rates was implemented for *TUB*. For the IQ-tree inference, the SYM+I+G model was selected for ITS, GTR+I+G for *EF1- α* , and HYK+I+G for *TUB*. Bayesian posterior probability ($PP \geq 0.5$) and Maximum likelihood bootstrap values ($ML \geq 50$) were shown at the dendrogram nodes (Figures 2 and 3).

The multi-locus phylogenetic results showed that 43 representative isolates were assigned to seven species (Figure 2). Five isolates grouped with the type strain and other reference sequences of *D. alangii* (Bayesian posterior probability = 0.52, Maximum likelihood bootstrap

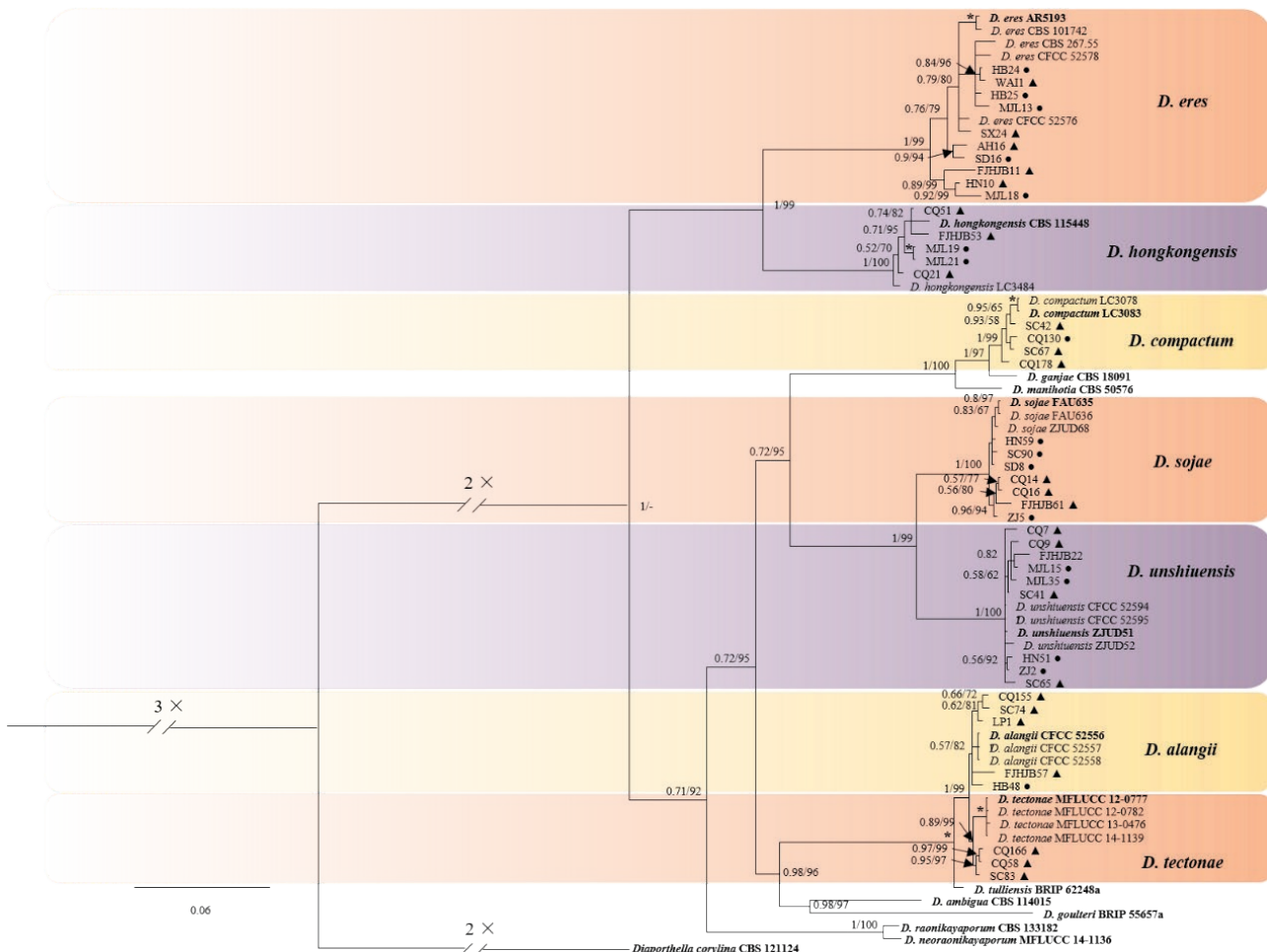


Figure 2. Maximum-likelihood phylogenetic analysis obtained from the combined ITS, *EF1-α* and *TUB2* sequence alignments of 43 *Diaporthe* isolates. The species *Diaporthella corylina* (CBS 121124) was used as the outgroup. Bayesian posterior probability (PP ≥ 0.90), and bootstrap support values > 50% are shown at the nodes. (ML ≥ 50%) were shown at the nodes (PP/ML). Asterisks (*) indicates full support (1/100). Ex-type strains were indicated in bold font. The scale bar indicates 0.06 expected changes per site. Isolate numbers accompanied by circle symbols indicate strains isolated from leaves, and triangle symbols indicate strains isolated from branches.

value 89). Four isolates clustered together with the type strain and other reference strains of *D. compactum* with high support (1.00, 99). Ten isolates clustered together with the ex-type strain and other reference strains of *D. eres* with high support (1.00, 99). Five isolates grouped with the ex-type strain and other reference strains of *D. hongkongensis* with strong support (1.00, 100). Seven isolates clustered together with the type strain and other reference strains of *D. sojae* with strong support (1.00, 100). Three isolates grouped with the reference strains of *D. tectonae* with high support (0.89, 99). Nine isolates were identified as *D. unshiuensis*, forming a highly supported subclade (1.00, 100).

The individual alignments and trees of the three single loci used in the analyses were also compared with respect to their performance in species recognition. Each

gene used differentiated *D. compactum*, *D. eres*, *D. hongkongensis*, *D. sojae*, and *D. unshiuensis*. Moreover, ITS and *EF1-α* gathered *D. tectonae* and *D. alangii* into one clade (data not shown). The phylogenetic analysis of *TUB* sequences showed that similar clades statuses compared with the phylogenetic analyses based on the concatenated ITS, *EF1-α*, and *TUB* sequences (Figure 3). The phylogenetic analysis of *TUB* sequences was conducted with a HKY+I+F substitution model using IQ-tree v.1.6.8, and 436 characters were included in the phylogenetic analysis.

Morphological and growth rate analyses of isolates

Morphological observations coupled with phylogenetic analyses were used to clarify the species delimitation.

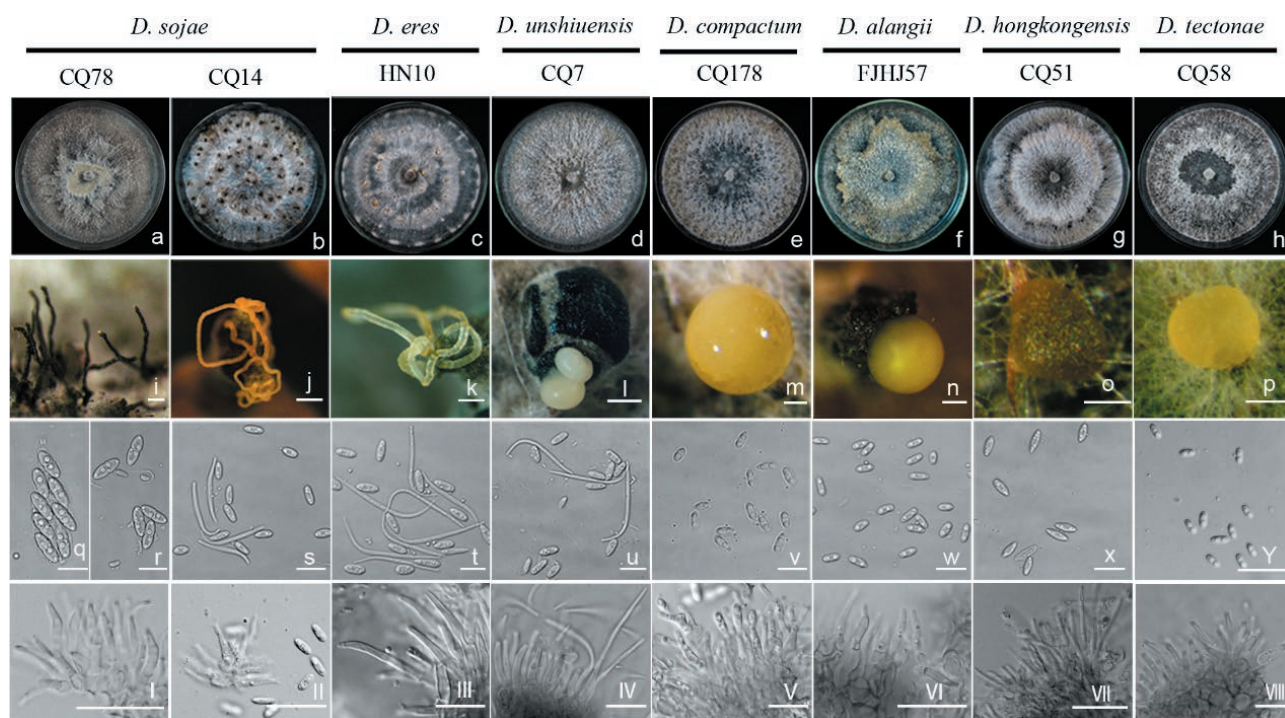


Figure 4. Morphologies of representative isolates selected from seven *Diaporthe* species. a to h, colony characteristics of the representative isolates of belonging to seven species cultured on potato dextrose agar incubated at 25°C in darkness. i, ascomata on fennel stems. j and k, spiral conidial cirri. l to p, conidial droplets. q, asci. r, ascospores. s to u, alpha and beta conidia. v to y, alpha conidia. I–VIII, conidiophores. Scale bars: i, k and n = 200 µm; j and l = 500 µm; m, o and p = 100 µm; q to y = 10 µm. I to III and VI to VII = 20 µm; IV, V, and VIII = 10 µm.

(Figure 4q), ascospores were hyaline, two-celled, often four-guttulate. *Conidiophores* phialidic, hyaline, terminal, ampulliform, 15–23 × 1.5–3.5 µm, tapered towards the apex (Figure 4I). Compared with the description of the ex-type isolate FAU 635, the asci of isolate CQ78 were slightly shorter (32.5–45.5 × 8–12 vs 38.5–46.5 × 7–9 µm; mean ± SD = 38.2 ± 2.9 × 10.0 ± 0.8 µm), and the ascospore were of similar size to the ex-type isolate (10–13 × 4–5 vs 9.5–12 × 3–4 µm), mean ± SD = 11.0 ± 0.7 × 4.3 ± 0.3 µm (Table 3). Of all species obtained from this study, only *D. sojae* produced the sexual state on fennel stems *in vitro*.

Diaporthe eres. Cultures appeared initially as white (surface) and pale yellowish to brownish at the centres with age, colony diam. 25–31 mm in 3 d at 25°C. Aerial mycelia were white, sparse and fluffy. Each colony on PDA contained no less than two wide concentric rings of conidiomata at maturity (Figure 4c). Conidiomata were subglobose to globose, dark brown to black, with spiral conidial cirri extruding from ostioles (Figure 4k). Alpha conidia were hyaline, fusiform or oval (Figure 4t), 7–11 × 3–5 µm, mean ± SD = 8.6 ± 0.9 × 3.7 ± 0.4 µm. Beta conidia were hyaline, filiform, smooth, curved, with truncate bases (Figure 4t), 30–43 × 2–3 µm, mean ± SD

= 34.88 ± 3.56 × 2.35 ± 0.34 µm. Conidiophores were phialidic, hyaline, terminal, cylindrical, 9–13 × 1.5–4 µm, tapered towards the apices (Figure 4III).

Diaporthe unshiuensis. Aerial mycelia were white, sparse, turning to grey with age, and with light gray pigmentation at the colony centres (Figure 4d), with colony diam. 23–28 mm in 3 d at 25°C. Conidiomata were subglobose, black and solitary or aggregated on the medium surface, with opalescent, glossy conidial drops exuding from the ostioles (Figure 4l). Alpha conidia were hyaline, ellipsoidal or clavate, smooth, and aseptate (Figure 4u), 6–8 × 2–4 µm, mean ± SD = 7.0 ± 0.5 × 3.0 ± 0.3 µm. Beta conidia were filiform, hyaline, smooth, curved, with truncate bases (Figure 4u), 22–40 × 2–3 µm, mean ± SD = 28.8 ± 3.5 × 2.2 ± 0.3 µm. Conidiophores were phialidic, hyaline, terminal, and cylindrical, 15–26 × 1.5–2.5 µm, and tapered towards the apices (Figure 4IV).

Diaporthe compactum. Cultures were entirely white from above, and brown, and feathery from below, with neat margins (Figure 4e), and colony diam. 27–30 mm after 3 d at 25°C. Brown or pale gray and spheroidal conidiomata were semi- or fully-embedded in the media, and conidia exuded from ostioles in lustrous, yellowish drops (Figure 4m). Alpha conidia were fusiform, hya-

Table 3. Sizes of alpha and beta conidia, and growth rates in culture, of representative isolates of *Diaporthe* spp. obtained in this study.

Species, isolate	Conidium sizes						Growth rate (mm d ⁻¹)
	Alpha conidia ^a		Beta conidia ^b		Means ± SD of conidia ^c		
	Length (µm)	Width (µm)	Length (µm)	Width (µm)	α-Conidia	β-Conidia	
<i>Diaporthe eres</i>							
HN10	6.56–11.23	3.18–4.88	29.43–43.23	1.69–3.11	8.59 ± 0.86 × 3.69 ± 0.35	34.88 ± 3.56 × 2.35 ± 0.34	10.1
HB25	6.85–10.27	3.18–4.13	26.26–41.96	1.74–3.83	7.91 ± 0.64 × 3.70 ± 0.24	34.42 ± 0.45 × 2.53 ± 0.37	9.2
SX24	6.06–8.52	2.81–4.13	20.91–32.30	1.44–3.09	7.30 ± 0.52 × 3.60 ± 0.28	27.53 ± 2.70 × 2.14 ± 0.30	8.3
HB24	5.86–8.48	2.76–4.70	/	/	7.24 ± 0.58 × 3.67 ± 0.38	/	8.5
CQ3	5.22–7.61	2.75–3.53	/	/	6.44 ± 0.60 × 3.11 ± 0.19	/	11.7
<i>D. hongkongensis</i>							
CQ51	6.97–10.39	3.07–4.65	/	/	8.47 ± 0.76 × 3.78 ± 0.33	/	9.8
<i>D. sojae</i>							
CQ14	5.57–8.27	2.82–4.05	14.43–30.54	1.67–3.29	6.98 ± 0.52 × 3.42 ± 0.29	23.89 ± 3.19 × 2.38 ± 0.16	7.6
CQ78	6.19–9.17	3.10–5.00	/	/	7.81 ± 0.76 × 3.92 ± 0.42	/	12.5
CQ16	6.16–8.11	2.11–3.56	/	/	7.15 ± 0.48 × 2.95 ± 0.27	/	9.8
<i>D. unshiuensis</i>							
CQ7	5.82–8.74	2.40–3.50	21.98–41.15	1.47–2.71	6.96 ± 0.52 × 3.00 ± 0.27	28.77 ± 3.48 × 2.15 ± 0.32	9.3
CQ9	5.81–8.81	2.59–4.05	18.31–30.97	1.85–3.19	7.27 ± 0.67 × 3.28 ± 0.30	25.48 ± 2.18 × 2.88 ± 0.28	7.8
<i>D. tectonae</i>							
CQ58	4.38–7.09	2.11–3.28	/	/	5.60 ± 0.58 × 2.64 ± 0.30	/	12.3
SC83	5.65–6.86	2.56–3.42	/	/	7.91 ± 0.64 × 3.70 ± 0.24	/	10.4
<i>D. compactum</i>							
CQ178	6.19–8.52	2.98–4.24	/	/	7.27 ± 0.52 × 3.73 ± 0.28	/	9.6
SC67	6.19–10.01	2.75–4.40	/	/	7.86 ± 0.54 × 3.53 ± 0.31	/	8.6
<i>D. alangii</i>							
CQ155	5.44–9.28	2.33–4.13	22.33–40.86	1.42–4.00	7.55 ± 0.85 × 3.21 ± 0.45	32.67 ± 4.99 × 2.49 ± 0.49	9.8
FJHJB57	5.72–10.14	2.77–4.45	/	/	7.20 ± 0.76 × 3.64 ± 0.35	/	8.1

^a Minimum and maximum lengths and widths of 50 alpha conidia.

^b Minimum and maximum lengths and widths of 50 beta conidia.

^c Mean conidium sizes of calculated from statistical analyses. Data were analyzed with SPSS Statistics 21.0 (WinWrap Basic; <http://www.winwrap.com>) by one-way analysis of variance, and means were compared using Duncan's test (at $P = 0.05$). SD = standard deviation. / indicates where beta conidia were not produced.

line, usually biguttulate, straight or slightly curved, and both ends of each conidium were blunt, or one end was rounded and the other acute (Figure 4v), $6-9 \times 3-4 \mu\text{m}$, mean \pm SD = $7.3 \pm 0.5 \times 3.7 \pm 0.3 \mu\text{m}$. Beta conidia were not observed. Conidiophores were phialidic, hyaline, terminal, ampulliform, and tapered towards their apices, $9-17 \times 1-3 \mu\text{m}$ (Figure 4V).

Diaporthe alangii. Aerial mycelium was sparse. Colonies were white at first, and becoming light brown due to pigment formation, with neat or petaloid margins (Figure 4f), colony diam. 24–30 mm after 3 d at 25°C. Conidiomata were scattered, black or brown and irregularly distributed over agar surfaces, with yellowish conidial drops exuding from the ostioles (Figure 4n). Alpha conidia were aseptate, hyaline, biguttulate, each usually with one end obtuse and the other acute (Figure 4w), $6-10 \times 3-5 \mu\text{m}$, mean \pm SD = $7.2 \pm 0.8 \times 3.6 \pm 0.4 \mu\text{m}$. Beta conidia were not observed. Conidiophores were phialidic, hyaline, terminal, ampulliform, tapered towards the apices, $9-18 \times 1.5-2.5 \mu\text{m}$ (Figure 4VI).

Diaporthe hongkongensis. Colonies were snow-white, with dense aerial mycelium, which collapsed in the center, and the collapsed parts were moist and sticky (Figure 4g), colony diam. 30 mm after 3 d at 25°C. Conidiomata were spheroidal and enveloped by tangled mycelia. Irregular and yellowish conidial piles were effusing from the ostioles (Figure 4o). Alpha conidia were fusiform, hyaline, septate, and not obtuse at both ends (Figure 4x), $7-10 \times 3-5 \mu\text{m}$, mean \pm SD = $8.5 \pm 0.8 \times 3.8 \pm 0.3 \mu\text{m}$. Beta conidia was not observed. Conidiophores were phialidic, hyaline, terminal, cylindrical, tapered towards their apices, $25-30 \times 1-3 \mu\text{m}$ (Figure 4VII).

Diaporthe tectonae. Colonies were white at first, with gray pigmentation gradually accumulating in the centres until entire colony colonies turned brown (Figure 4h), colony diam. 31–36 mm after 3 d at 25°C. Conidiomata globose, black or brown, scattered, erumpent on PDA, with conidial droplets exuding from the centre ostioles (Figure 4p). Alpha conidia were cylindrical or fusiform, hyaline, usually biguttulate, and septate (Figure 4y), $4-7 \times 2-3 \mu\text{m}$, mean \pm SD = $5.6 \pm 0.6 \times 2.6 \pm 0.3 \mu\text{m}$. Beta conidia were not observed. Conidiophores phialidic, hyaline, terminal, ampulliform, and tapered towards their apices, measuring $11-20 \times 1.5-3 \mu\text{m}$ (Figure 4VIII).

Pathogenicity tests

Two typical symptoms developed on detached leaves of *A. chinensis*, which were observed at the wound sites at 7 d post inoculation. One symptom consisted of reddish-brown, round or suborbicular, small, slowly expan-

sion lesions, while the other consisted of lesions with black necrotic centres surrounded by round or suborbicular brown halos (Figure 5a). The first of these symptoms developed after inoculations with *D. compactum*, *D. eres*, *D. sojae* or *D. unshiuensis*, while the second was induced by inoculations with *D. tectonae*, *D. alangii* or *D. hongkongensis*. Lesion diameters caused by the different fungi differed significantly. *Diaporthe tectonae*, or *D. alangii* caused large lesions (mean diam. = 10–22 mm) on all the inoculated leaves, those caused by *D. hongkongensis* or *D. eres* were smaller (5–8 mm), while those caused by isolates of *D. sojae*, *D. compactum*, or *D. unshiuensis* were smaller still (2–4 mm) (Figure 6a). Unwounded leaves inoculated with *Diaporthe* spp. isolates remained symptomless. In parallel, no lesions were observed on the leaves that were wounded and non-wound inoculated with PDA discs as controls. Koch's postulates were fulfilled by re-isolating each *Diaporthe* sp. isolate only from symptomatic leaves.

In the pathogenicity tests conducted on branches of four kiwifruit varieties, all the *Diaporthe* species were pathogenic to wounded branches. The symptoms induced by representative isolates were similar, as fusiform necrotic lesions and internal discoloration observed at the wound sites (Figure 5b). The lesion lengths caused by the representative isolates tested on different cultivars were diverse. *Diaporthe tectonae* and one isolate of *D. alangii* (SC74) induced large lesions (mean length = 67–83 mm) on *A. chinensis* 'Huangjin', *D. alangii* (CQ155) or *D. eres* caused smaller lesions (20–30 mm), and the other pathogens induced even smaller (2–18 mm) (Figure 6b). *Diaporthe tectonae*, *D. alangii*, and a *D. sojae* isolate (CQ16) caused large lesions (50–106 mm) on *A. chinensis* 'Hongyang', while the remaining isolates caused shorter lesions (4–20 mm) (Figure 6c). *Diaporthe tectonae* or *D. alangii* (SC74) induced large lesions (39–54 mm) on *A. chinensis* 'Jinyan', while *D. eres* (HB25) and *D. alangii* (CQ155) caused smaller lesions on this cultivar (17–22 mm). The remaining isolates caused short lesions on this cultivar (5–12 mm) (Figure 6d). *Diaporthe tectonae* and a *D. alangii* isolate (SC74) caused large lesions (40–68 mm) on *A. chinensis* 'Cuiyu', *D. alangii* (CQ155), *D. compactum* (CQ178), *D. eres* (HB25), or *D. sojae* (CQ16) caused shorter lesions (15–25 mm), and those from the remaining isolates were shorter still (3–10 mm) (Figure 6e). Unwounded shoots of kiwifruit inoculated with *Diaporthe* spp. isolates remained symptomless, and no lesions developed on the shoots that were wounded and non-wound inoculated with PDA discs. Each respective *Diaporthe* species was re-isolated from inoculated symptomatic shoots, fulfilling Koch's postulates for these pathogens.

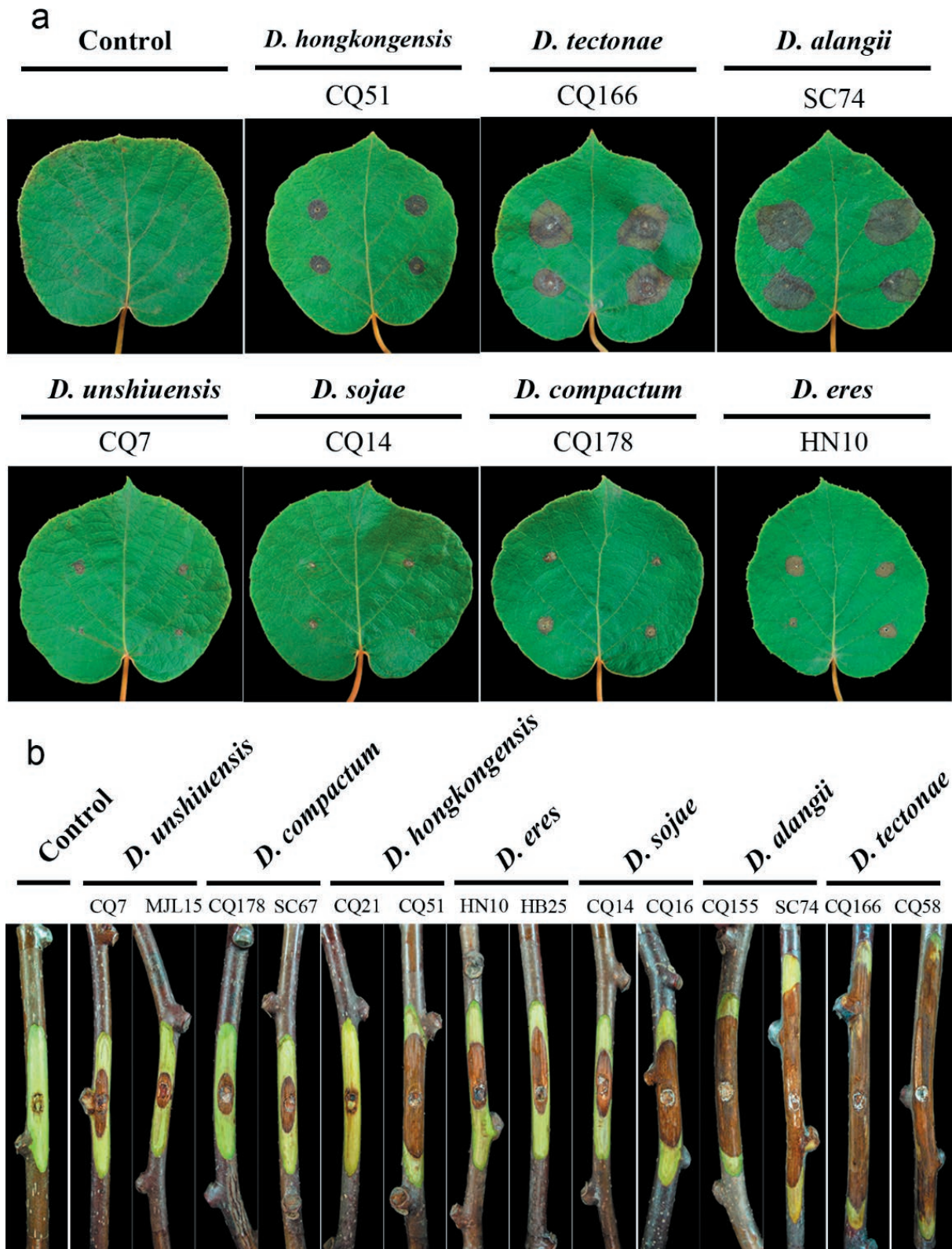


Figure 5. Pathogenesis of seven *Diaporthe* species on kiwifruit leaves and stems. a, symptoms caused after inoculation of wounded kiwi leaves (*Actinidia chinensis* ‘Cuiyu’) with mycelium plugs from cultures of seven *Diaporthe* spp. b, symptoms caused by inoculation of wounded kiwi branches (*Actinidia chinensis* ‘Hongyang’) with mycelium plugs from cultures of seven *Diaporthe* spp.

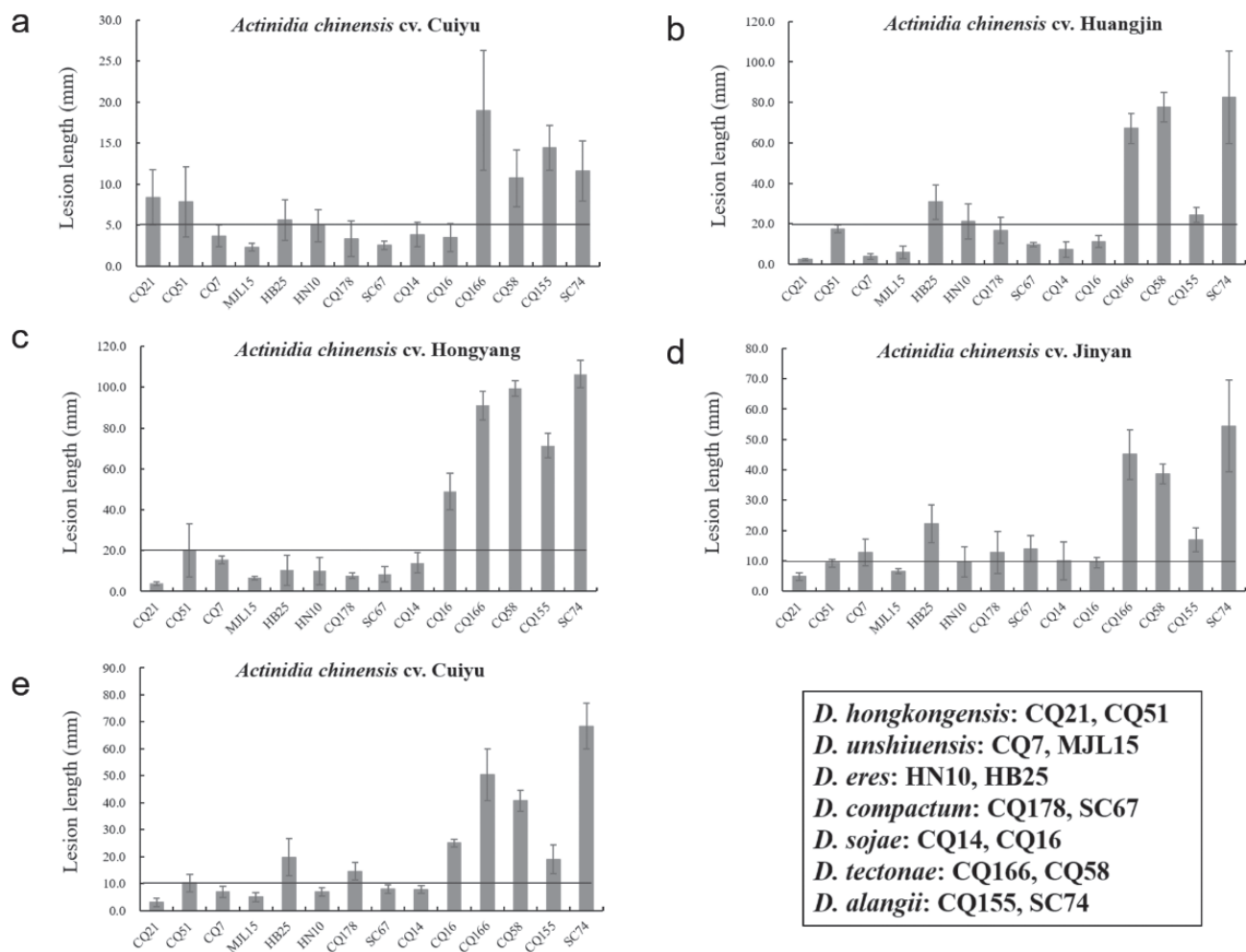


Figure 6. Mean lesion lengths on wounded kiwifruit leaves and shoots at 10 dpi with mycelium plugs of representative isolates of seven *Diaporthe* species. a, lesion length on wounded leaves of *Actinidia chinensis* ‘Cuiyu’. b to e, lesion lengths on the wounded kiwifruit shoots (*Actinidia chinensis* ‘Huangjin’, *Actinidia chinensis* ‘Hongyang’, *Actinidia chinensis* ‘Jinyan’, or *Actinidia chinensis* ‘Cuiyu’).

Fruits were susceptible to the representative isolates selected from each species, and all tested species caused rots on wounded fruits. Typical symptoms were some sarcocarp tissues swollen with internal softening around the inoculation wounds at early stages, transparent drops streaming from the inoculation punctures, epidermis peeling, and brownish, damp and rotted flesh (Figure 7a). Fruits inoculated with *D. alangii* (CQ155), *D. eres* (HN10), *D. sojae* (CQ14), *D. tectonae* (CQ58), or *D. hongkongensis* (CQ21) had larger lesions (mean diam. = 30–42 mm) than those inoculated with *D. unshiuensis* (CQ7) or *D. compactum* (CQ178), (13–17 mm) (Figure 7b). All the non-wounded fruits inoculated with *Diaporthe* spp. isolates remained symptomless. The negative controls of wounded and unwounded fruits did not produce lesions. Each respective *Diaporthe* species was

re-isolated from the symptomatic fruits, fulfilling Koch’s postulates for these pathogens.

In the host range tests, at 10 d post-inoculation, the seven *Diaporthe* species all caused canker symptoms on detached shoots of the five different fruit crop plants. After removing phloem tissues, maroon and fusiform necrotic lesions emerged in the underlying wood below, and these extended along the inoculated branches. In most cases, the affected shoots of pear and apple showed swollen and the bark cracking at the margins, with dark-brown to reddish cankers and abundant gummosis were observed at the inoculation sites on the branch of plum and apricot. The symptoms produced on peach shoots were black depressed cankers. The *Diaporthe* isolates caused different degrees of lesioning on detached branches of the different fruit tree species.

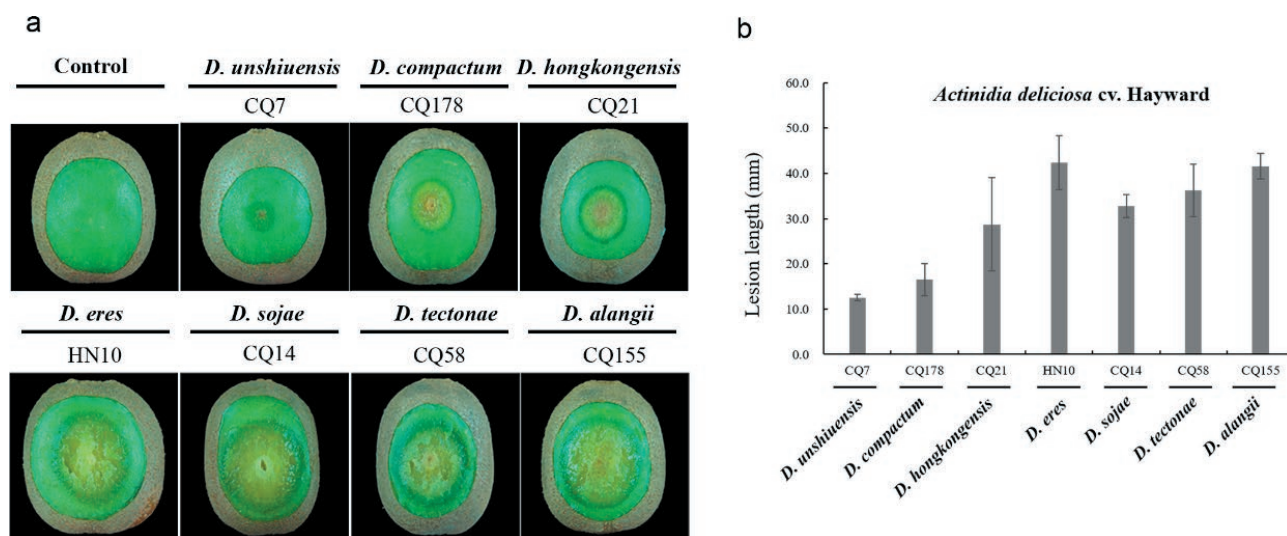


Figure 7. Symptoms and mean lesion lengths caused by inoculation of wounded kiwifruit fruits (*Actinidia deliciosa* ‘Hayward’) with mycelium plugs from cultures of seven *Diaporthe* spp. a, representative symptoms photographed at 10 d post inoculation. b, mean lesion lengths (four replicates) measured at 7 d post-inoculation.

Diaporthe tectonae or *D. alangii* isolates caused large lesions (mean length = 18–39 mm), and *D. compactum*, *D. eres*, *D. hongkongensis*, *D. sojae*, or *D. unshiuensis* caused shorter lesions (5–15 mm) on *Pyrus pyrifolia* ‘Cuiguan’ (Figure 8a). Lesion lengths on *Prunus salicina* ‘Dahongpao’ caused by the seven *Diaporthe* species were of length 5–20 mm, except that two isolates caused larger lesions, with those from *D. sojae* isolate (CQ14) being 30 mm, and those from *D. alangii* isolate (SC74) being 53 mm (Figure 8b). The lesion lengths on *Malus pumila* ‘Hong Fushi’ caused by the seven *Diaporthe* species were mostly 5–15 mm in length, except for those from one isolate of *D. alangii* (SC74) which were longer (70 mm) (Figure 8c). The lesion lengths on *Prunus persica* ‘Youtao’ caused by *D. alangii* isolate CQ155, *D. compactum* isolate CQ178, *D. eres*, *D. hongkongensis*, *D. sojae*, or *D. unshiuensis* were 5–10 mm long, and those from the remaining isolates were larger (15–25 mm) (Figure 8d). *Diaporthe alangii* caused large lesions (60 mm) on *Prunus aremeniaca* ‘Helanxiangxing’, followed by *D. hongkongensis*, *D. eres*, *D. sojae*, *D. tectonae* isolate CQ58, or *D. unshiuensis* isolate CQ7 (15–30 mm), and the remaining isolates caused short lesions (5–10 mm) (Figure 8e). No lesions were induced in the branches inoculated with non-colonized PDA plugs.

DISCUSSION

Diaporthe spp. previously reported on kiwifruit have been associated with fruit stem-end rots (Sommer and

Beraha, 1975; Hawthorne *et al.*, 1982; Lee *et al.*, 2001; Koh *et al.*, 2005; Luongo *et al.*, 2011; Thomidis *et al.*, 2019), and with shoot blight and leaf spots. In the present study, a large-scale investigation of *Diaporthe* species associated with kiwifruit infections was conducted in nine major cultivation provinces of China. Multi-locus phylogenetic analyses and morphological characterization of isolated fungi were employed to evaluate the diversity of *Diaporthe* species associated with shoot blight and leaf spot of kiwifruit, and pathogenicity tests was performed to fulfill Koch’s postulates for representative *Diaporthe* isolates. This study has shown that seven *Diaporthe* species, including *D. unshiuensis*, *D. eres*, *D. sojae*, *D. hongkongensis*, *D. compactum*, *D. alangii*, and *D. tectonae*, were the causal organisms of shoot blight and leaf spot diseases of kiwifruit. As well, *D. unshiuensis*, *D. sojae*, *D. compactum*, *D. alangii*, and *D. tectonae* are here first reported as causes of kiwifruit shoot blight and leaf spot. The study was comprehensive, investigating samples from 16 orchards located in nine major kiwifruit production areas in China, and used phylogenetic analyses and morphology to characterize a large number of fungus isolates.

DNA sequence data are essential for resolving taxonomic questions, redefining species boundaries, and accurate species nomenclature (Guarnaccia and Crous, 2017; Guarnaccia *et al.*, 2017). Phylogenetic analyses individually based on ITS, *EF1- α* , and *TUB* sequence data differentiated *D. compactum*, *D. eres*, *D. hongkongensis*, *D. sojae*, and *D. unshiuensis*. However, ITS and *EF1- α* gathered *D. tectonae* and *D. alangii* into one

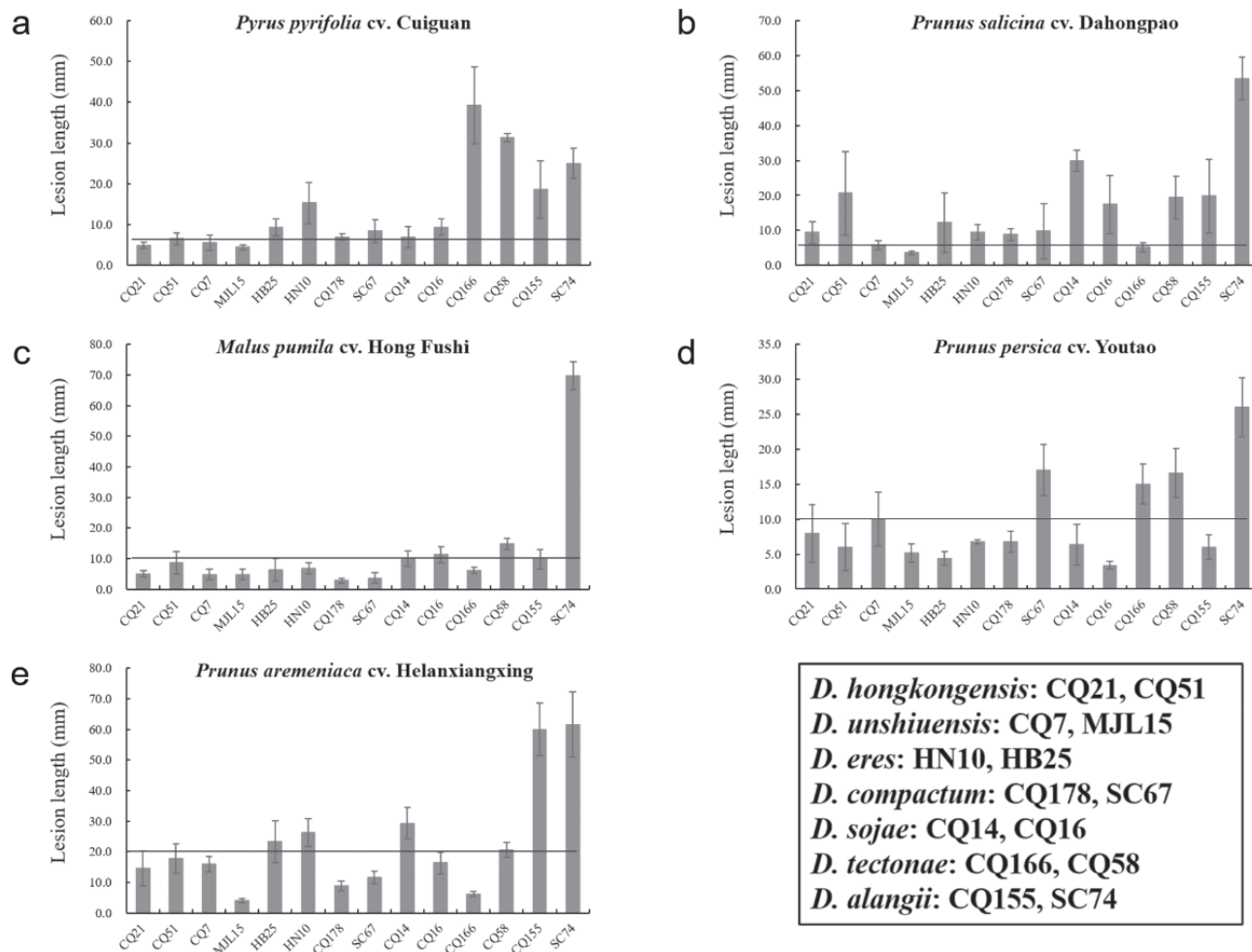


Figure 8. Mean lesion lengths on wounded shoots of pear, plum, apple, peach, and apricot, at 10 d post-inoculation, induced by mycelium plugs from cultures of representative isolates of seven *Diaporthe* species. a, lesion lengths on shoots of *Pyrus pyrifolia* ‘Cuiguan’, b, *Prunus salicina* ‘Dahongpao’, c, *Malus pumila* ‘Hong Fushi’, d, *Prunus persica* ‘Youtao’, or e, *Prunus aremeniaca* ‘Helanxiangxing’.

clade. Several studies have used three to five concatenated genes simultaneously to separate species within *Diaporthe* (Santos *et al.*, 2011; Gomes *et al.*, 2013; Gao *et al.*, 2015; Diaz *et al.*, 2017). As ITS and the *EF1-α* gene have limitations for distinguishing *D. alangii* and *D. tectonae*, the concatenated ITS, *EF1-α*, and *TUB* phylogenetic analysis was successively employed to discriminate these two fungi. The results showed that the two species clustered into two clades with high bootstrap (1.00/99). These two fungi also differed morphologically, with *D. tectonae* having shorter alpha conidia than *D. alangii*.

Prevalence analyses of the seven *Diaporthe* spp. showed that the most dominant species responsible for leaf spot and branch blight of kiwifruit were: *D. unshiuensis* (100 isolates, 35.2%, isolated from Anhui, Chongqing, Fujian, Henan, Hubei, Sichuan, and Zhejiang); *D. eres* (94 isolates, 33.1%, isolated from Anhui, Chongqing,

Fujian, Henan, Hubei, Shandong, Shanxi, Sichuan, and Zhejiang); and *D. sojae* (57 isolates, 20.1%, isolated from Chongqing, Fujian, Henan, Hubei, Shandong, Sichuan, and Zhejiang). The other identified fungi were less common, including: *D. hongkongensis* (19 isolates, 6.7%, isolated from Anhui, Chongqing, Fujian, and Hubei), *D. compactum* (six isolates, 2.1%, isolated from Chongqing, Fujian, Hubei, and Sichuan); *D. alangii* (five isolates, 1.8%, isolated from Chongqing, Fujian, Hubei, and Sichuan), and *D. tectonae* (three isolates, 1.1%, isolated from Chongqing and Sichuan) (Table 2). Analysis of *Diaporthe* species in the sampled areas showed obvious species diversity in Anhui, Chongqing, Fujian, Hubei, Sichuan, and Zhejiang. This may be attributed to the humid and warm climate in these provinces, which is suitable for survival of *Diaporthe* spp. In contrast, only one *Diaporthe* sp. was identified from Shanxi, two from

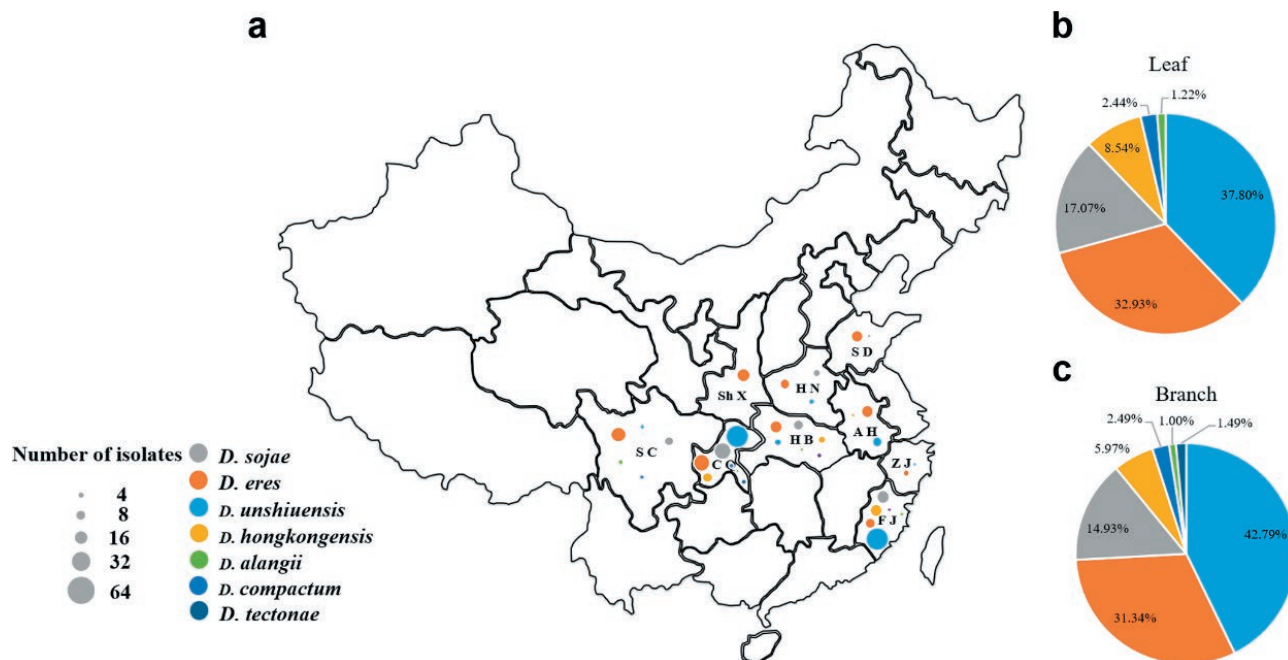


Figure 9. Sample collections of kiwifruit shoot blight and leaf spot diseases, and distribution of *Diaporthe* species in China. a, numbers and species of different *Diaporthe* species from kiwifruit plants. Each coloured circle represents one fungus species, and the size of the circle indicates the number of isolates. Abbreviations indicate provinces or regions of Anhui (AH), Chongqing (CQ), Henan (HN), Hubei (HB), Fujian (FJ), Shandong (SD), Shanxi (ShX), Sichuan (SC) and Zhejiang (ZJ). b, and c, isolation rates (%) of different *Diaporthe* spp. from kiwifruit leaf or branch tissues.

Shandong, and three species were identified from Henan (Figure 9a), which may be related to the dry climate of these three provinces being unsuitable for *Diaporthe*.

Since *Diaporthe* spp. have endophytic, saprobic or pathogenic lifestyles, pathogenicity to kiwifruit was assessed by inoculating leaves, shoots, and fruit of different kiwifruit species, using wound and non-wound inoculation methods. Wound inoculations showed that all the species were pathogenic and caused leaf spot and shoot blight of this host. The different fungi also showed significantly different virulence, with *D. alangii* and *D. tectonae* as the most aggressive species, followed by *D. compactum*, *D. eres*, *D. hongkongensis*, *D. unshiuensis*, and *D. sojae*. It is significant, however, that the inoculations of these seven species on unwounded leaves, branches, and fruits did not cause disease symptoms. These species can be endophytes and opportunist pathogens occurring in a wide range of hosts and later as saprobes on dead host tissues.

Host affiliation has been for species delimitation in *Diaporthe*, but this has proved uninformative because many *Diaporthe* spp. have been recorded on a wide range of hosts (Santos and Phillips, 2009; Udayanga *et al.*, 2012; Gao *et al.*, 2015; Guarnaccia *et al.*, 2020). For example, *D. lithocarpus* was confirmed as the cause of

diseases on five plant hosts belonging to different families, and *Lithocarpus glabra* was shown to host seven different species of *Diaporthe* (Gao *et al.*, 2014). In the present study, the seven *Diaporthe* species isolated from kiwifruit were not host-specific. *Diaporthe tectonae* was first reported to cause branch and twig dieback on *Tectonae grandis* in Northern Thailand (Doilom *et al.*, 2016), and the present study has showed that *D. tectonae* could induce shoot blight of kiwifruit in China. *Diaporthe alangii* was originally isolated from dieback branches of *Alangium* in China (Yang *et al.*, 2018b). The present study confirmed *D. tectonae* as the cause of leaf spot and shoot blight of kiwifruit. *Diaporthe eres*, *D. sojae*, and *D. hongkongensis* are pathogens causing shoot canker of grapevine and pear (Dissanayake *et al.*, 2014; Guo *et al.*, 2020b), as well as kiwifruit shoot blight and leaf spot (present study). *Diaporthe unshiuensis* was reported from the fruit of *Citrus unshiu* with unidentified symptoms and non-symptomatic branches and twigs of *Fortunella margarita* (Huang *et al.*, 2015), and the present study showed weak aggressiveness of this species to kiwifruit. Several *Diaporthe* spp. have been recently recognized as causal agents of diseases of *Rosaceae* fruit crop plants, including peach, pear, and apple (Bai *et al.*, 2015; Sessa *et al.*, 2017; Tian *et al.*, 2018; Guo *et*

al., 2020b). However, kiwifruit is often in mixed plantings with apple, apricot, pear, peach, and plum in many kiwifruit production areas in China. Results of host range and virulence assessments described here have shown the seven *Diaporthe* species were pathogenic, not only to kiwifruit, but also to most other *Rosaceae* fruit crop hosts. This indicates that these pathogens have the potential to infect these alternative hosts, potentially providing pathogen inoculum across these hosts.

In conclusion, identification of these pathogens provides valuable new information to assist understanding of leaf spot and branch blight of kiwifruit. The study has also shown the *Diaporthe* species responsible for these diseases, which will assist the design of potential disease prevention and management strategies for these economically important diseases.

ACKNOWLEDGEMENTS

This study was financially supported by the Key National Project (no. 2018YFD0201406) and the earmarked fund for Pear Modern Agro-Industry Technology Research System (CARS-28-16) of the Chinese Ministry of Agriculture.

LITERATURE CITED

- Akilli, S., Serce, C. U., Katircioglu, Y. Z., Karakaya, A., Maden, S., 2011. Involvement of *Phytophthora citrophthora* in kiwifruit decline in Turkey. *Journal of Phytopathology* 159: 579–581.
- Bai, Q., Zhai, L. F., Chen, X., Hong, N., Xu, W. X., Wang, G. P., 2015. Biological and molecular characterization of five *Phomopsis* species associated with pear shoot canker in China. *Plant Disease* 99: 1704–1712.
- Bai, Q., Wang, G. P., Hong, N., 2017. First report of *Diaporthe tulliensis* and *Diaporthe actinidiae* causing kiwifruit stem canker in Hubei and Anhui provinces, China. *Plant Disease* 101: 508.
- Beraha, L., O'Brien, M. J., 1979. *Diaporthe melonis* sp. nov., a new soft rot of market cantaloupes. *Journal of Phytopathology* 94: 199–207.
- Carbone, L., Kohn, L. M., 1999. A method for designing primer sets for speciation studies in filamentous ascomycetes. *Mycologia* 91: 553–556.
- Conn, K. E., Gubler, W. D., 1993. Bacterial blight of kiwifruit in California. *Plant Disease* 77: 228–230.
- Díaz, G. A., Latorre, B. A., Lolas, M., Ferrada, E., Naranjo, P., Zoffoli, J. P., 2017. Identification and characterization of *Diaporthe ambigua*, *D. australafricana*, *D. novem*, and *D. rudis* causing a postharvest fruit rot in kiwifruit. *Plant Disease* 101: 1402–1410.
- Díaz, G. A., & Latorre, B. A., 2018. First report of cordon dieback of kiwifruits caused by *Diaporthe ambigua* and *D. australafricana* in Chile. *Plant Disease* 102: 446.
- Dissanayake, A. J., Liu, M., Zhang, W., Chen, Z., Udayanga, D., ... Kevin, D. H., 2014. Morphological and molecular characterisation of *Diaporthe* species associated with grapevine trunk disease in China. *Fungal Biology* 119: 283–294.
- Doilom, M., Dissanayake, A. J., Wanasinghe, D. N., Boonmee, S., Liu, J. K., ... Kevin D. H., 2016. Microfungi on *Tectona grandis* (teak) in northern Thailand. *Fungal Diversity* 82: 107–182.
- Elfars, K., Torres, R., Diaz, G. A., Latorre, B. A., 2013. Characterization of *Diaporthe australafricana* and *Diaporthe* spp. associated with stem canker of blueberry in Chile. *Plant Disease* 97: 1042–1050.
- Erper, I., Turkkan, M., Ozcan, M., Luongo, L., Belisario, A., 2017. Characterization of *Diaporthe honkongensis* species causing stem-end rot on kiwifruit in Turkey. *Journal of Plant Pathology* 99: 779–782.
- Fan, X. L., Bezerra, J. D. P., Tian, C. M., Crous, P. W., 2018. Families and genera of diaporthean fungi associated with canker and dieback of tree hosts. *Persoonia* 40: 119–134.
- FAO, 2018. Food and Agriculture Organization of the United Nations. <http://www.fao.org/faostat/en/#data/QC>. Accessed 20 February 2020.
- Freeman, S., Talma, T., Shabi, E., 1996. Characterization of *Colletotrichum gloeosporioides* isolates from avocado and almond fruits with molecular and pathogenicity tests. *Applied and Environmental Microbiology* 62: 1014–1020.
- Fu, M., Crous, P. W., Bai, Q., Zhang, P. F., Xiang, J., ... Wang, G. P., 2018. *Colletotrichum* species associated with anthracnose of *Pyrus* spp. in China. *Persoonia* 42: 1–35.
- Gao, Y. H., Sun, W., Su, Y. Y., Cai, L., 2014. Three new species of *Phomopsis* in Gutianshan Nature Reserve in China. *Mycological Progress* 13: 111–121.
- Gao, Y. H., Su, Y., Sun, W., Cai, L., 2015. *Diaporthe* species occurring on *Lithocarpus glabra* in China, with descriptions of five new species. *Fungal Biology* 119: 295–309.
- Gao, Y. H., Liu, F., Duan, W. J., Crous, P. W., Cai, L., 2017. *Diaporthe* is paraphyletic. *IMA Fungus* 8: 153–187.
- Glass, N. L., Donaldson, G. C., 1995. Development of primer sets designed for use with the PCR to amplify conserved genes from filamentous ascomycetes.

- Applied and Environmental Microbiology* 61: 1323–1330.
- Gomes, R. R., Glienke, C., Videira, S. I. R., Lombard, L., Groenewald, J. Z., Crous, P. W., 2013. *Diaporthe*: a genus of endophytic, saprobic and plant pathogenic fungi. *Persoonia* 31: 1–41.
- Guarnaccia, V., Crous, P. W., 2017. Emerging citrus diseases in Europe caused by species of *Diaporthe*. *IMA Fungus* 8: 317–334.
- Guarnaccia, V., Groenewald, J. Z., Woodhall, J., Armengol, J., Cinelli, T., ... Crous, P. W. 2017. *Diaporthe* diversity and pathogenicity revealed from a broad survey of grapevine diseases in Europe. *Persoonia* 40: 135–153.
- Guarnaccia, V., Crous, P. W., 2018. Species of *Diaporthe* on camellia and citrus in the Azores Islands. *Phytopathologia Mediterranea* 57: 307–319.
- Guarnaccia, V., Martino, I., Tabone, G., Brondino, L., Gullino, M. L. 2020. Fungal pathogens associated with stem blight and dieback of blueberry in northern Italy. *Phytopathologia Mediterranea* 59: 229–245.
- Guo, Y. H., Liu, Q., He, P., 2020a. Current situation, problems and countermeasures of kiwifruit industry in China. *Guizhou Agriculture Science* 48: 69–73.
- Guo, Y. S., Crous, P. W., Bai, Q., Fu, M., Yang, M. M., ... Wang, G. P., 2020b. High diversity of *Diaporthe* species associated with pear shoot canker in China. *Persoonia* 45: 135–162.
- Hawthorne, B. T., Reesgeorge, J., Samuels, G. J., 1982. Fungi associated with leaf spots and post-harvest fruit rots of kiwifruit (*Actinidia chinensis*) in New Zealand. *New Zealand Journal of Botany* 20: 143–150.
- Hawthorne, B. T., Otto, C., 2012. Pathogenicity of fungi associated with leaf spots of kiwifruit. *New Zealand Journal of Agricultural Research* 29: 533–538.
- Hibbett, D. S., Taylor, J. W., 2013. Fungal systematics: is a new age of enlightenment at hand? *Nature Reviews Microbiology* 11: 129–133.
- Hoang, D. T., Chernomor, O., Haeseler, A. V., Minh, B. Q., Vinh, L. S., 2017. UFBboot2: Improving the Ultrafast Bootstrap Approximation. *Molecular Biology and Evolution* 35: 518–522.
- Huang, F., Hou, X., Dewdney, M. M., Fu, Y. S., Chen, G. Q., ... Li, H., 2013. *Diaporthe* species occurring on citrus in China. *Fungal Diversity* 61: 237–250.
- Huang, F., Udayanga, D., Wang, X., Hou, X., Mei, X., ... Li, H., 2015. Endophytic *Diaporthe* associated with citrus: a phylogenetic reassessment with seven new species from China. *Fungal Biology* 119: 331–347.
- Huang, H. W., 2009. History of 100 years of domestication and improvement of kiwifruit and gene discovery from genetic introgressed populations in the wild. *Chinese Bulletin of Botany* 44: 127–142.
- Huang, S., Ding, J., Deng, D., Tang, W., Sun, H., ... Liu, Y. S., 2013. Draft genome of the kiwifruit *Actinidia chinensis*. *Nat Commun* 4: 1–9.
- Jeong, I. H., Lim, M. T., Kim, G. H., Han, T. W., Kim, H. C., Kim, M. J., ... Koh, Y. J., 2008. Incidences of leaf spots and blights on kiwifruit in Korea. *The Plant Pathology Journal* 24: 125–130.
- Katoh, K., Standley, D. M., 2013. MAFFT multiple sequence alignment software version 7: improvements in performance and usability. *Molecular Biology and Evolution* 30: 772–780.
- Koh, Y. J., Lee, D. H., Shin, J. S., Hur, J. S., 2001. Chemical and cultural control of bacterial blossom blight of kiwifruit caused by *Pseudomonas syringae* Korea. *New Zealand Journal of Crop and Horticultural Science* 29: 29–34.
- Koh, Y. J., Hur, J. S., Jung, J. S., 2005. Postharvest fruit rots of kiwifruit (*Actinidia deliciosa*) in Korea. *New Zealand Journal of Crop and Horticultural Science* 33: 303–310.
- Kumar, S., Stecher, G., Tamura, K., 2016. MEGA7: Molecular evolutionary genetics analysis version 7.0 for bigger datasets. *Molecular Biology and Evolution* 33: 1870–1874.
- Lee, J. G., Lee, D. H., Park, S. Y., Hur, J. S., Koh, Y. J., 2001. First report of *Diaporthe actinidiae*, the causal organism of stem-end rot of kiwifruit in Korea. *Plant Pathology Journal* 17: 110–113.
- Li, C., Jiang, J. X., Leng, J. H., Li, B. M., Yu, Q., Tu, G. Q., 2013. Identification of pathogen causing shoot blight of kiwifruit. *Plant Protection* 24: 130–133.
- Li, H., Yu, S., Tang, W., Miao, M., Liu, Y., 2019. First report of *Diaporthe passiflorae* and *Diaporthe nobilis* causing a postharvest kiwifruit rot in Sichuan province, China. *Plant Disease* 103: 771–771.
- Li, L., Pan, H., Chen, M., Zhang, S., Zhong, C., 2017a. Isolation and identification of pathogenic fungi causing postharvest fruit rot of kiwifruit (*Actinidia chinensis*) in China. *Journal of Phytopathology* 165: 782–790.
- Li, L., Pan, H., Liu, W., Chen, M. Y., Zhong, C. H., 2017b. First report of *Diaporthe actinidiae* causing stem-end rot of kiwifruit during post-harvest in China. *Plant Disease* 101: 1054.
- Luongo, L., Santori, A., Riccioni, L., Belisario, A., 2011. *Phomopsis* sp. associated with post-harvest fruit rot of kiwifruit in Italy. *Journal of Plant Pathology* 93: 205–209.
- Minh, B. Q., Schmidt, H. A., Chernomor, O., Schrempf, D., Woodhams, M. D., ... Lanfear, R., 2020. IQ-TREE

- 2: new models and efficient methods for phylogenetic inference in the genomic era. *Molecular Biology and Evolution* 37: 1530–1534.
- Mostert, L., Crous, P. W., Kang, J., Phillips, A. J. L., 2001. Species of *Phomopsis* and a *Libertella* sp. occurring on grapevines with specific reference to South Africa: morphological, cultural, molecular and pathological characterization. *Mycologia* 93: 146–167.
- Mousakhah, M., Jamali, A., Khodaparast, S. A., Ollia, M., 2014. Incidence of leaf spots, blights and fruit rots of kiwifruit (*Actinidia deliciosa*) in Guilan province. *Iranian Journal Plant Pathology* 50: 173–181.
- Nazerian, E., Mirabolghay, M., Ashnaei, S. P., Beiki, F., 2019. Characterization of *Botryosphaeria dothidea* as new pathogen of kiwifruit in Iran. *Journal of Plant Protection Research* 59: 134–137.
- Nguyen, L. T., Schmidt, H. A., Haeseler, A., Minh, B. Q., 2015. IQ-TREE: a fast and effective stochastic algorithm for estimating maximum-likelihood phylogenies. *Molecular Biology and Evolution* 32: 268–274.
- Nylander, J., 2004. MrModelTest v. 2. program distributed by the author. Evolutionary Biology Centre, Uppsala University.
- Pan, H., Hu, Q. L., Zhang, S. J., Zu, D., Li, L., Zhong, C. H., 2018. Kiwifruit disease investigation and pathogen identification in Liupanshui city, Guizhou province. *Plant Protection* 44: 125–131.
- Pan, L., Zhao, X., Chen, M., Fu, Y., Xiang, M., Chen, J., 2020. Effect of exogenous methyl jasmonate treatment on disease resistance of postharvest kiwifruit. *Food Chem* 305: 1–8.
- Pennycook, S. R., 1985. Fungal fruit rots of *Actinidia deliciosa* (kiwifruit). *New Zealand Journal of Experimental Agriculture* 13: 289–299.
- Rambaut A., 2014. FigTree, v. 1.4.2. Institute of evolutionary biology. University of Edinburgh. <http://tree.bio.ed.ac.uk/software/figtree/>.
- Rehner, S. A., Uecker, F. A., 1994. Nuclear ribosomal internal transcribed spacer phylogeny and host diversity in the coelomycete. *Phomopsis*. *Botany* 72: 1666–1674.
- Ronquist, F., Huelsenbeck, J.P., 2003. MrBayes 3: bayesian phylogenetic inference under mixed models. *Bioinformatics* 19: 1572–1574.
- Santos, J. M., Phillips, A. J., 2009. Resolving the complex of *Diaporthe* (*Phomopsis*) species occurring on *Foeniculum vulgare* in Portugal. *Fungal Diversity* 34: 111–125.
- Santos, J. M., Vrandecic, K., Cosic, J., Duvnjak, T., Phillips, A. J., 2011. Resolving the *Diaporthe* species occurring on soybean in Croatia. *Persoonia* 27: 9–19.
- Sessa, L., Abreo, E., Bettucci, L., Lupo, S., 2017. Diversity and virulence of *Diaporthe* species associated with wood. *Phytopathologia Mediterranea* 56: 431–444.
- Shin, J. S., Park, J. K., Kim, G. H., Park, J. Y., Han, H. S., ...Koh, Y. J., 2004. Identification and ecological characteristics of bacterial blossom blight pathogen of kiwifruit. *Research in Plant Disease* 10: 290–296.
- Sommer, N. F., Beraha, L., 1975. *Diaporthe actinidiae*, a new species causing stem-end rot of Chinese gooseberry fruits. *Mycologia* 67: 650–653.
- Song, Y. L., Lin, M. M., Zhong, Y. M., Chen, J. Y., Qi, X. J., ...Fang, J. B., 2020. Evaluation of resistance of kiwifruit varieties (strains) against bacterial canker disease and correlation analysis among evaluation indexes. *Journal of Fruit Science* 41: 1–15.
- Thomidis, T., and Exadaktylou, E., 2010. First report of *Botryosphaeria dothidea* causing shoot blight of kiwifruit (*Actinidia deliciosa*) in Greece. *Plant Disease* 94: 1503.
- Thomidis, T., Exadaktylou, E., Chen, S. F., 2013. *Diaporthe neotheicola*, a new threat for kiwifruit in Greece. *Crop Protection* 47: 35–40.
- Thomidis, T., Prodromou, I., Zambounis, A., 2019. Occurrence of *Diaporthe ambigua* Nitschke causing postharvest fruit rot on kiwifruit in Chrysoupoli Kavala, Greece. *Journal of Plant Pathology* 101: 1295–1296.
- Thompson, S. M., Tan, Y. P., Young, A. J., Neate, S. M., Aitken, E. A. B., Shivas, R. G., 2011. Stem cankers on sunflower (*Helianthus annuus*) in Australia reveal a complex of pathogenic *Diaporthe* (*Phomopsis*) species. *Persoonia* 27: 80–89.
- Thompson, S. M., Tan, Y. P., Shivas, R. G., Neate, S. M., Morin, L., ... Aitken, E. A. B., 2015. Green and brown bridges between weeds and crops reveal novel *Diaporthe* species in Australia. *Persoonia* 35: 39–49.
- Tian, Y., Zhao, Y., Sun, T., Wang, L., Liu, J., Hu, B. S., 2018. Identification and characterization of *Phomopsis amygdali* and *Botryosphaeria dothidea* associated with peach shoot blight in Yangshan, China. *Plant Disease* 102: 2511–2518.
- Udayanga, D., Liu, X. Z., Crous, P. W., McKenzie, E. H. C., Chukeatirote, E., Hyde, K. D., 2012. A multi-locus phylogenetic evaluation of *Diaporthe* (*Phomopsis*). *Fungal Diversity* 56: 157–171.
- Udayanga, D., Castlebury, L. A., Rossman, A. Y., Chukeatirote, E., Hyde, K. D., 2014. Insights into the genus *Diaporthe*: phylogenetic species delimitation in the *D. eres* species complex. *Fungal Diversity* 67: 203–229.
- White, T. J., Bruns, T., Lee, S., Taylor, J., 1990. Amplification and direct sequencing of fungal ribosomal RNA genes for phylogenetics. *Academic Press, San Diego* 18: 315–322.

- Wu, L., Lan, J., Xiang, X., Xiang, H., Jin, Z., Liu, Y. Q., 2020. Transcriptome sequencing and endogenous phytohormone analysis reveal new insights in CPPU controlling fruit development in kiwifruit (*Actinidia chinensis*). *PLoS One* 15 (10): e0240355.
- Yang, Q., Du, Z., Tian, C. M., 2018a. Phylogeny and morphology reveal two new species of *Diaporthe* from traditional Chinese medicine in northeast China. *Phytotaxa* 336: 159–170.
- Yang, Q., Fan, X. L., Guarnaccia, V., Tian, C. M., 2018b. High diversity of *Diaporthe* species associated with dieback diseases in China, with twelve new species described. *MycKeys* 39: 97–149.
- Young, S. L., Hyo, S. H., Gyoung, H. K., Young, J. K., Hur, J. S., Jung, J. S., 2009. Causal agents of blossom blight of kiwifruit in Korea. *The Plant Pathology Journal* 25: 220–224.
- Yue, J., Liu, J., Tang, W., Wu, Y. Q., Tang, ... Zheng, Y., 2020. Kiwifruit genome database (KGD): a comprehensive resource for kiwifruit genomics. *Horticulture Research* 7: 1–8.
- Zhai, L., Zhang, M., Lv, G., Chen, X., Jia, N., ... Wang, G. P., 2014. Biological and molecular characterization of four *Botryosphaeria* species isolated from pear plants showing stem wart and stem canker in China. *Plant Disease* 98: 716–726.
- Zhang, Z. Z., Long, Y., H, Yang, S., Li, L., Yin, X. H., 2019. Occurrence regularity and control measures of kiwifruit blossom blight of kiwifruit. *South China Fruit* 48: 159–164.
- Zhou, Y., Gong, G., Cui, Y., Zhang., D., Chang, X., ... Sun, X., 2015. Identification of *Botryosphaeriaceae* species causing kiwifruit rot in Sichuan province, China. *Plant Disease* 99: 699–708.
- Zou, M. F., Wang, Y. X., Wang, M. F., Zhou, Y. G. Xiong, H., Jiang, J. X., 2019. First report of leaf spot on kiwifruit caused by *Didymella bellidis* in China. *Plant Disease* 104: 1–3.



Citation: A. Moukahel, S.G. Kumari, A.A. Hamed, M. Sharman, S. Ahmed (2021) Distribution and identification of luteovirids affecting chickpea in Sudan. *Phytopathologia Mediterranea* 60(2): 199-214. doi: 10.36253/phyto-12135

Accepted: March 25, 2021

Published: September 13, 2021

Copyright: © 2021 A. Moukahel, S.G. Kumari, A.A. Hamed, M. Sharman, S. Ahmed. This is an open access, peer-reviewed article published by Firenze University Press (<http://www.fupress.com/pm>) and distributed under the terms of the Creative Commons Attribution License, which permits unrestricted use, distribution, and reproduction in any medium, provided the original author and source are credited.

Data Availability Statement: All relevant data are within the paper and its Supporting Information files.

Competing Interests: The Author(s) declare(s) no conflict of interest.

Editor: Nihal Buzkan, Kahramanmaraş Sütçü Imam University, Turkey.

Research Papers

Distribution and identification of luteovirids affecting chickpea in Sudan

ABDULRAHMAN MOUKAHEL¹, SAFAA G. KUMARI^{1*}, ABDELMAGID ADLAN HAMED², MURRAY SHARMAN³, SEID AHMED⁴

¹ International Center for Agricultural Research in the Dry Areas (ICARDA), Terbol Station, Beqaa, Zahle, Lebanon

² Plant Pathology Research Program, Agricultural Research Corporation, Wad Medani, Sudan

³ Department of Agriculture and Fisheries, Brisbane, Queensland, Australia.

⁴ International Center for Agricultural Research in the Dry Areas (ICARDA), Rabat, Morocco

*Corresponding author. E-mail: s.kumari@cgiar.org

Summary. In Sudan yellowing viruses are key production constraints in pulse crops. Field surveys were carried out to identify luteovirids affecting chickpea crops in the major production regions (Gezira Scheme and River Nile State). A total of 415 chickpea plant samples with yellowing and stunting symptoms were collected during the 2013, 2015 and 2018 growing seasons. Serological results (Tissue-blot immunoassays) showed that *Luteoviridae* and Chickpea chlorotic dwarf virus (CpCDV, genus *Mastrevirus*, family *Geminiviridae*) were the most common viruses, with rare infections with Faba bean necrotic yellows virus (FBNYV, genus *Nanovirus*, family *Nanoviridae*). Some samples reacted only with a broad-spectrum luteovirid monoclonal antibody (5G4-MAb), and others showed cross reactions between the specific monoclonal antibodies, suggesting the occurrence of new luteovirid variants. Serological results were confirmed by amplification with reverse transcription-polymerase chain reaction (RT-PCR) and sequencing of the partial coat protein gene. Molecular analyses provided a basic, sufficient and reliable characterization for four viruses affecting chickpea that belong to *Polerovirus* (family *Luteoviridae*). These were Cucurbit aphid-borne yellows virus (CABYV), Pepper vein yellows virus (PeVYV), Pepo aphid-borne yellows virus (PABYV) and Cotton leafroll dwarf virus (CLRDV), that shared high similarity with the type sequences. Phylogenetic analyses also revealed high similarity to luteovirid species. This study has established reliable, rapid and sensitive molecular tools for the detection of luteovirid species.

Keywords. Molecular characterization, sequence alignment, *Polerovirus*, *Luteoviridae*, Sudan.

INTRODUCTION

Chickpea (*Cicer arietinum* L.) is an economically important food crop in West Asia and North Africa (WANA) and in semi-arid areas of the world

(Van der Maesen, 1987). The total world area under chickpea cultivation during the 2018 cropping season was 1.78 million ha with an estimated annual production of 17 million tonnes (FAO, 2018), making chickpea the third most important pulse crop after soybean and common bean. Chickpea is an important source of protein in human diets and plays a significant role in farming systems (Merga and Haji, 2019).

In Sudan, chickpea is the third most economically important food legume crop after faba bean and cowpea, as a cash crop that generates income for farmers and rural communities, and as a significant source of protein for Sudanese people (Mohamed *et al.*, 2015). It is traditionally grown as a winter crop in River Nile State, northern Sudan. However, chickpea production has recently expanded to the central clay plain of central Sudan. The Gezira Scheme is one of the world's largest irrigation systems under one management, centred in the Sudanese state of Gezira, southeast of the confluence of the Blue Nile and White Nile at the city of Khartoum. The major crops in the Gezira Scheme are cotton, vegetable crops, cereals (sorghum and wheat), and currently kabuli type chickpea production is expanding due to its high price and low cost of production. The chickpea area harvested in Sudan during 2018 was 6,716 ha, and yielded 11,698 tonnes (FAO, 2018). The productivity in Sudan is generally low (1.75 t ha⁻¹) (FAO, 2018), partly due to the use of inferior seeds purchased from local markets or imported from neighboring countries. Chickpea fields planted in November each year (early planting) are susceptible to high virus and wilt/root rot infections (Mohamed *et al.*, 2015; 2018). Late planted crops (December/early January) showed low amounts of virus and root rot infections, but are more exposed to heat than early sown crops (Abdelmagid Adlan Hamed, personal communication), and this leads to high amounts of empty pods.

Generally, diseases causing yellowing, stunting and leaf roll symptoms are primarily caused by luteovirids, which are considered the most destructive virus diseases that infect cool season food legumes worldwide (Bos *et al.*, 1988; Makkouk *et al.*, 2003c; 2014; Kumar *et al.*, 2008; Kumari *et al.*, 2009). Virus species in the family *Luteoviridae* are transmitted in a circulative, non-propagative manner by specific aphid vectors. These viruses often cause phloem necroses that spread from inoculated sieve elements and cause symptoms by suppressing translocation, reducing plant growth and prompting chlorophyll loss, which results in characteristic yellowing and dwarfing of infected plants. Several members of the *Luteoviridae* have host ranges largely restricted to one plant family, and other members infect plants

in several or many families. For instance, Bean leafroll virus (BLRV) and Soybean dwarf virus (SbDV) (*Luteovirus*) infect mainly legumes, whereas Beet western yellows virus (BWYV, *Polerovirus*) infects more than 150 species of plants in over 20 families (Domier, 2011).

Serologically, virus species in the *Luteoviridae* (mainly those in *Polerovirus*) cannot be distinguished using polyclonal antisera (Duffus and Russell, 1975; Govier, 1985) and most monoclonal antibodies (MAbs) (Oshima and Shikata, 1990; Smith *et al.*, 1996), due to cross reactions with non-target species. Furthermore, antibodies for many species within this family are not easily available (D'Arcy *et al.*, 1989; Fortass *et al.*, 1996). Molecular assays are generally more sensitive than serological tests, especially with luteovirids, which are present in lower concentrations than many other plant viruses. Reverse transcription-polymerase chain reaction (RT-PCR) technology provides more sensitive assays which have the potential to identify luteovirid-infected plants more reliably, especially in the early stages of infection, and also helps to improve virus classifications (Lemaire *et al.*, 1995; Hauser *et al.*, 2000; Xiang *et al.*, 2008a, 2008b; Mnari-Hattab *et al.*, 2009; Shang *et al.*, 2009; Knierim *et al.*, 2010). For example, virus isolates previously identified as BWYV have been reclassified as four distinct virus species (BWYV, Beet chlorosis virus (BChV), Beet mild yellowing virus (BMV), and Turnip yellows virus (TuYV)) on the basis of differences in host range and molecular characterizations (Hauser *et al.*, 2000; 2002; D'Arcy and Domier, 2005). Using molecular techniques, Chickpea chlorotic stunt virus (CpCSV), identified as a new member of *Polerovirus*, has been shown to naturally infect a range of cool-season food legumes, and cause leaf yellowing and plant stunting in Ethiopia and Syria (Abraham *et al.*, 2006) and in many countries in WANA region (Kumari *et al.*, 2007; Asaad *et al.*, 2009). In addition, many virus isolates that were identified as a luteovirid based on their positive reactions with a broad spectrum MAb "5G4" (Katul, 1992) in the past, did not react serologically with the available specific MAbs (Makkouk *et al.*, 1988; Abraham *et al.*, 2008; Mustafayev *et al.*, 2011; Kumari *et al.*, 2017). These viruses remained unidentified due to the lack of specific antibodies or appropriate molecular tools.

Chickpea can be naturally infected with a number of viruses causing yellowing and stunting symptoms (Nene *et al.*, 1996; Kumar *et al.*, 2008). However, in Sudan, four viruses have been identified to naturally this host and cause significant economic damage. These are, Faba bean necrotic yellows virus (FBNYV, *Nanovirus*, *Nanoviridae*), Chickpea chlorotic dwarf virus (CpCDV, *Mastrevirus*, *Geminiviridae*), CpCSV and BWYV (Abra-

ham *et al.*, 2009; Makkouk *et al.*, 2003b; 1995; Makkouk, 2020). Cucurbit aphid-borne yellows virus (CABYV) has also been reported by Kumari *et al.* (2018) to infect chickpea in Sudan and cause stunting, yellowing and necrosis. However, that study suggested the presence of other luteovirids in survey samples, but the identity of these was not reported.

Previous studies and surveys conducted in many regions of Sudan have indicated the occurrence of unrecognized viruses with wide distributions and sometimes with high incidence. However, the diversity of luteovirid species infecting cool-season food legume crops in Sudan has not been previously and extensively studied, and information on the incidence of specific viruses affecting these crops is limited. To address this knowledge gap, we carried out field surveys in the main chickpea production areas of Sudan to accurately characterize the identity, diversity, variability and geographic distributions of luteovirid species that affect chickpea, using conventional and molecular analyses.

MATERIALS AND METHODS

Field surveys and serological tests

Field surveys were conducted in the major chickpea production areas in Sudan, including areas of the Gezira Scheme (middle, north and south) and River Nile State (Hudeiba Agriculture Research Station, Berber and Shendi). The 204 chickpea samples collected by Kumari *et al.* (2018) in February 2013 and March 2015 were included in the present study, to investigate luteovirid diversity in addition to the CABYV already reported. A further 211 chickpea samples were collected in February 2018 when the crops were at the flowering/pod setting stage. Shoot samples from a total of 415 chickpea plants with yellowing and stunting symptoms were collected from 35 fields (133 plants from ten fields in 2013; 71 plants from four fields in 2015 and 211 plants from 21 fields in 2018). In each field visited, data on field location, crop condition, growth stage, virus disease symptoms, virus disease incidence and aphid populations were recorded. Virus disease incidence in each field was determined on the basis of visual virus symptoms and the number of infected plants per m² at randomly chosen locations in the field, and were grouped into five categories (<1%, 1-5%, 6-20%, 21-50% or >50%). The fresh stem of each sample plant was blotted on nitrocellulose membrane (NCM, 0.45 µm, Bio-Rad, Cat No. 1620115) in ten replicates. The leaves of all collected samples were dried over silica gel or lyophilized for further molecular analyses.

Three replicates of blotted NCMs were tested for the presence of viruses by tissue-blot immunoassay (TBIA; Makkouk and Kumari, 1996), using a broad-spectrum legume luteovirid monoclonal antibody (MAB) (5G4; Katul, 1992), MAB for FBNYV (3-2E9; Franz *et al.*, 1996) and a polyclonal antibody for CpCDV (Kumari *et al.*, 2006).

To identify individual luteovirids, samples that reacted positively with MAB 5G4 in TBIA (23 samples in 2013, 18 samples in 2015, 45 samples in 2018) were retested further, using specific MABs to BWYV (A5977 from Agdia, USA), BLRV (4B10; Katul, 1992), SbDV (ATCC PVAS-650, USA) and a mixture of three MABs (1-1G5, 1-3H4 and 1-4B12) produced against an Ethiopian isolate of CpCSV (CpCSV-Eth) and a mixture of three MABs (5-2B8, 5-3D5 and 5-5B8) produced against a Syrian isolate of CpCSV (CpCSV-Sy) (Abraham *et al.*, 2006, 2009).

Molecular analyses

RNA extraction

Total RNA was extracted from 50 to 100 mg of virus-infected lyophilized tissue following a user-developed protocol using McKenzie lysis buffer (McKenzie *et al.*, 1997) with the RNeasy® Plant Mini Kit (Cat No. 74904, Qiagen). RNAs for all tested samples were stored as solutions in Nuclease free-water at -80°C.

Complementary DNA (cDNA)

Synthesis of cDNA was achieved using the M-MLV Reverse Transcriptase kit (Cat No. 28025013, Invitrogen) as per the manufacturer's instructions, with reverse primer AS3 (Abraham *et al.*, 2008) (Table 1). Three µL of total RNA, 1 µL of 10 µM AS3 primer, 1 µL of Nuclease free water and 1 µL of 10 µM dNTPs (2'-deoxynucleotide 5'-triphosphates) were heated at 65°C for 5 min. The reaction was cooled on ice for 2 min and the following reagents were added: 2 µL 5× First-Strand Buffer, 1 µL 0.1 M DTT and 0.5 µL Nuclease free water. The reaction was incubated at 37°C for 2 min then 0.5 µL of M-MLV RT enzyme was added (final volume 10 µL) followed by a further 50 min at 37°C before deactivating at 70°C for 15 min.

Reverse transcription-polymerase chain reaction (RT-PCR)

The success of reverse transcription was checked by performing a PCR using the generic primer pairs (AS3/Pol3870F) (Sharman *et al.*, 2015) to amplify 370 bp of

Table 1. Luteovirid primer sets used in this study.

Primer pairs	Primer Sequence (5' to 3')	Product Size (bp)	Target virus species ^a	Reference
Generic primers				
AS3	CACGCGTCIACCTATTTIGGRTTITG	370	CLR DV, CpCSV, CABYV, PLRV, BWYV, TuYV, BLRV, CBTV, SbDV	Abraham <i>et al.</i> , 2008
Pol3870F	ATCACBTTCCGGGCCGWSTYTWT CAGA			Sharman <i>et al.</i> , 2015
Specific Multiplex primers				
<i>Master Mix-I</i>				
AS3				
BLRV3589F	CAAGGAGACGTTTACCAGTCGT	551	BLRV	Sharman, unpublished data
BWYV3969F	GTCTCCGARGCCTCTCCCAA	276	BWYV/TuYV	Sharman, unpublished data
SbDV3731F	CGWGTTTTTCRAAGGACGGCA	418	SbDV	Sharman, unpublished data
PBMYV3396F	GGTTGGTTCTTCCAGTCCAAT	838	PBMYV	Sharman <i>et al.</i> , 2021
<i>Master Mix-II</i>				
AS3				
CABYV3635F	GAAACCGCCGACGCCCTAAT	474	CABYV	Sharman, unpublished data
CpCSV3705F	AAYARGCGYMCTGTT CAGCGGGC	566	CpCSV	Sharman, unpublished data
<i>Specific Uniplex primer pairs</i>				
Pol3982R	CGAGGCCTCGGAGATGAACT	310	CLR DV	Sharman <i>et al.</i> , 2015
CLR DV3675F	CCACGTAGRCGCAACAGGCGT			
PeR	TCGCTTGCCCGCCTTTGGTG	1249	PeVYV	Zhang <i>et al.</i> , 2015
PeF	GGAGCGTTGCGGAATGGATGC			

^a Virus acronyms are CLR DV = Cotton leafroll dwarf virus; CpCSV = Chickpea chlorotic stunt virus; CABYV = Cucurbit aphid-borne yellows virus; PLRV = Potato leafroll virus; BWYV = Beet western yellows virus; TuYV = Turnip yellows virus; BLRV = Bean leafroll virus; CBTV = Cotton bunchy top virus; SbDV = Soybean dwarf virus; PhBMYV = Phasey bean mild yellows virus; PeVYV = Pepper vein yellows virus.

the partial coat protein (*CP*) gene (Table 1), using the My Taq polymerase kit (Cat No. BIO-21108, Bioline). The positive samples with sharp band were processed by Multiplex RT-PCR (MP-PCR) (Murray Sharman, unpublished data), using the generic reverse primer AS3 with species-specific primers for Phasey bean mild yellows virus (PBMYV), CpCSV, BWYV, SbDV, BLRV and CABYV (Table 1), and by following the manufacturer's instructions for the My Taq polymerase kit (final volume 10 µL). Due to the proximity in product sizes for some primers, the MP-PCR amplification mixture was divided in two multiplex master mixes; master mix-I included AS3 with primers BLRV3589F, BWYV3969F, SbDV3731F and PhBMYV3396F and master mix-II consisted of AS3 with CABYV3635F and CpCSV3705F (Table 1). These primers amplify partial *CP* gene. Positive controls for all tested viruses were used in both master mixes as checks to accurately identify PCR products of the different viruses. The PCR for both sets consisted of an initial denaturation of 95°C for 1 min, then 35 cycles (95°C for 30 sec, 62°C for 20 sec, 56°C for 10 sec, 72°C for 30 sec) followed by a final extension of 72°C for 3 min. All PCR products were analyzed on 1.5% agarose gel stained with

RedSafe™ Nucleic Acid Staining Solution (20,000×) (Cat No. 21141, iNtRON) with final concentration of 5% in 0.5% TBE (Tris-borate-EDTA) buffer.

In addition to the above primers, two specific uniplex primer pairs targeted Pepper vein yellows virus (PeVYV) (PeF/PeR; Zhang *et al.*, 2015) and Cotton leafroll dwarf virus (CLR DV) (CLR DV3675F/Pol3982R; Sharman *et al.*, 2015) (Table 1) to confirm the sequencing outputs of the DNA fragments generated by AS3/Pol3870F.

DNA sequencing and molecular analysis

PCR amplicons of interest were amplified with total volumes of 50 µL. From each of these, 5 µL was analyzed on agarose gel, and the high-quality products were directly sequenced by the Sanger method following the instructions of a commercial sequencing company (Macrogen). The sequences were compared with available sequences in the GenBank database using the basic local alignment search tool (BLAST; Altschul *et al.*, 1997; 2005). In this study, BLAST search and sequence

analyses were carried out based on the greatest similarity of the submitted sequences with the following four GenBank accessions: GenBank accession Nos. KC685313 for PeVYV, KJ789902 for Pepo aphid-borne yellows virus (PABYV), EU871539 for CLRDV and EX398665 for CABYV. Sequences of 24 Sudanese isolates were submitted to the GenBank (see Table 4 for accession numbers).

Sequence assembly and pairwise comparisons were carried out using MEGA-X (Kumar *et al.*, 2018) for the partial CP sequence of 18 *Polerovirus* isolates (from 13 countries) from the GenBank database and four Sudanese chickpea isolates representing four polerovirus species identified further in the present study (SuCp122-13: CABYV, SuCp31-15: CLRDV, SuCp29-15: PABYV and SuCp42-13: PeVYV). Sequence alignments were generated under the Hasegawa–Kishino–Yano (HKY) (Hasegawa *et al.*, 1985) model with a bootstrap value of 1000 by MEGA-X. Nucleotide pairwise similarities were calculated using SDTv 1.2 (Muhire *et al.*, 2014).

Phylogenetic analyses of nucleotide and amino acid sequences were carried out using a Clustal_X program after multiple alignment of sequences by neighbour joining algorithms with 500 bootstrap replications (Thompson *et al.*, 1997).

RESULTS

Field distribution and serological tests

The most commonly observed symptoms suggestive of virus infection in chickpea fields were yellowing, stunting, chlorosis and reddening of the leaves and tip wilting (Figure 1). Based on the symptoms observed in the fields, 17% of chickpea fields (one field in 2013 and five fields in 2018) had virus incidence of 5% or less, 31% of fields had incidence of 6–20% (two fields in 2013 and nine in 2018), 29% of fields had incidence of 21–50% (four fields in 2013, two in 2015 and four in 2018), and 8

fields (23%) had virus incidence greater than 50% (three fields in 2013, two in 2015 and three in 2018).

TBIA results from 415 symptomatic plant samples collected during the 2013, 2015 and 2018 growing seasons indicated that CpCDV was the most common virus, with average relative infection rates of 59% of the tested samples in 2013, 89% in 2015, and 17% in 2018. In addition, 21% of tested samples reacted positively with a broad-spectrum legume luteovirid MAb (5G4) (23 samples in 2013, 18 in 2015 and 45 in 2018), whereas FBNYV infection was detected in only one sample during 2013 (Table 2). When 86 samples that reacted positively with 5G4 MAb were further tested using specific luteovirid MAbs, 11 samples reacted with BWYV MAb, 22 samples reacted with CpCSV MAbs, 23 samples reacted with both BWYV and CpCSV MAbs, and the 30 remaining samples reacted only with 5G4 MAb (Table 3).

Molecular analyses

According to TBIA reactions with different MAbs, 36 samples were selected for further molecular characterization (eight samples that reacted only with MAb 5G4, seven that reacted positively with 5G4, BWYV and CpCSV MAbs, and 21 samples that reacted positively with 5G4 samples and CpCSV MAbs). The generic primer pair AS3/Pol3870F amplified the expected product size of 370 bp from 33 chickpea samples out of 36 samples tested (Figure 2-A). The MP-PCRs (set 1 and set 2) results showed presence of CABYV in 12 samples with amplicon size of approx. 474 bp (Figure 2-B). However, there were 21 samples that were positive in generic RT-PCR AS3/Pol3870F but were negative in all MP-PCRs. Thus, all unrecognized samples along with five samples that were amplified with CABYV-specific primer pairs were sequenced by Sanger sequencing.

The sequence analyses confirmed presence of CABYV (five samples) with 96% nt similarity with the



Figure 1. Plants showing yellowing and stunting symptoms in chickpea fields in the Gezira Scheme, Sudan during the 2015 cropping season.

Table 2. Results of serological tests (Tissue blot immunoassay, TBIA) for chickpea samples collected from different regions of Sudan during the 2013, 2015 or 2018 growing seasons.

Year/Region	Number of fields visited	Number of samples tested	Number of samples reacted positively with ^a		
			5G4 (MAB)	FBNYV (MAB)	CpCDV (PAb)
2013					
<u>Gezira Scheme</u>					
North	5	68	6	0	63
Middle	3	32	3	1	14
<u>River Nile State</u>					
Hudeiba Agr. Res. station	1	25	14	0	1
Berber	1	8	0	0	1
2015					
<u>Gezira Scheme</u>					
South	4	71	18	0	63
2018					
<u>Gezira Scheme</u>					
North Gezira	7	58	11	0	2
Middle Gezira	8	81	27	0	21
<u>River Nile State</u>					
Shendi	2	19	7	0	10
Hudeiba Agr. Res. station	1	21	0	0	0
Berber	2	32	4	0	4
Total	34	415	86	1	179

^a 5G4 (MAB): broad-spectrum legume luteovirid monoclonal antibody (Katul, 1992); FBNYV (MAB): Faba bean necrotic yellows virus (monoclonal antibody) (3-2E9; Franz *et al.*, 1996); CpCDV (PAb): Chickpea chlorotic dwarf virus (Polyclonal antibody) (Kumari *et al.*, 2006).

type reference sequence for CABYV (GenBank accession no. NC_003688), and three luteovirid species were

detected for the first time from chickpea in Sudan (all belonging to *Polerovirus*), PeVYV (six samples), PABYV (14 samples) and CLRDV (one sample). Sequences were submitted to the GenBank, and the GenBank accession numbers are shown in Table 4.

When six PeVYV samples and one CLRDV sample were subjected to RT-PCR using specific primer pairs for PeVYV (PeF/PeR; Zhang *et al.*, 2015) and CLRDV (CLR DV3675F/Pol3982R; Sharman *et al.*, 2015) (Table 1), amplicons of the expected sizes (1249 bp for PeVYV and 310 bp for CLR DV) were generated (Figure 2-C and 2-D).

The comparison of detection methods between TBIA and MP-PCR clearly showed that there was greater variation in species detected than indicated by TBIA alone, i.e., the common character between the analyzed samples is that all these samples reacted positively with 5G4 MAB, which means there is no false positive reaction or cross reaction with another family of plant viruses. On the other hand, there was no compatibility between the serological results and molecular characterization. It is obvious that CpCSV and/or BWYV were not detected in any of the samples, despite that most samples reacted with CpCSV MAB mixtures and BWYV MAB due to the serological cross reaction which is common for luteovirids (Oshima and Shikata, 1990; Smith *et al.*, 1996) (Table 4)

Pairwise comparisons of CP amino acid sequences of representative isolate for each virus indicated that the virus isolates from Sudan were probably members of recognized *Luteoviridae* species. The nucleotide sequence of the isolate SuCp42-13 showed that it was indistinguishable from PeVYV-Sudan isolate, despite that PeVYV-Sudan was isolated from hot pepper (Table 5). The phylogenetic analysis tree also showed that this isolate was close to PeVYV-Sudan (GenBank acces-

Table 3. Serological results of Tissue blot immunoassay (TBIA) with specific luteovirid monoclonal antibodies (MABs) for chickpea samples collected from different regions of Sudan during the 2013, 2015 or 2018 growing seasons.

Year	Number of samples reacted with 5G4 MAB ^a	Number of samples reacted positively with MABs ^b					Unidentified luteovirids
		BWYV	CpCSV	BLRV	SbDV	CpCSV& BWYV	
2013	23	4	6	0	0	9	4
2015	18	0	1	0	0	7	10
2018	45	7	15	0	0	7	16
Total	86	11	22	0	0	23	30

^a 5G4: broad-spectrum legume luteovirid monoclonal antibody (Katul, 1992).

^b Monoclonal antibodies used are BWYV: Beet western yellows virus (A5977 from Agdia, USA); BLRV: Bean leafroll virus (4B10; Katul, 1992); SbDV: Soybean dwarf virus (ATCC PVAS-650, USA); CpCSV: a mixture of three MABs (1-1G5, 1-3H4 and 1-4B12) produced against an Ethiopian isolate of Chickpea chlorotic stunt virus (CpCSV-Eth), and a mixture of three MABs (5-2B8, 5-3D5 and 5-5B8) produced against a Syrian isolate of CpCSV (CpCSV-Sy) (Abraham *et al.*, 2006, 2009)

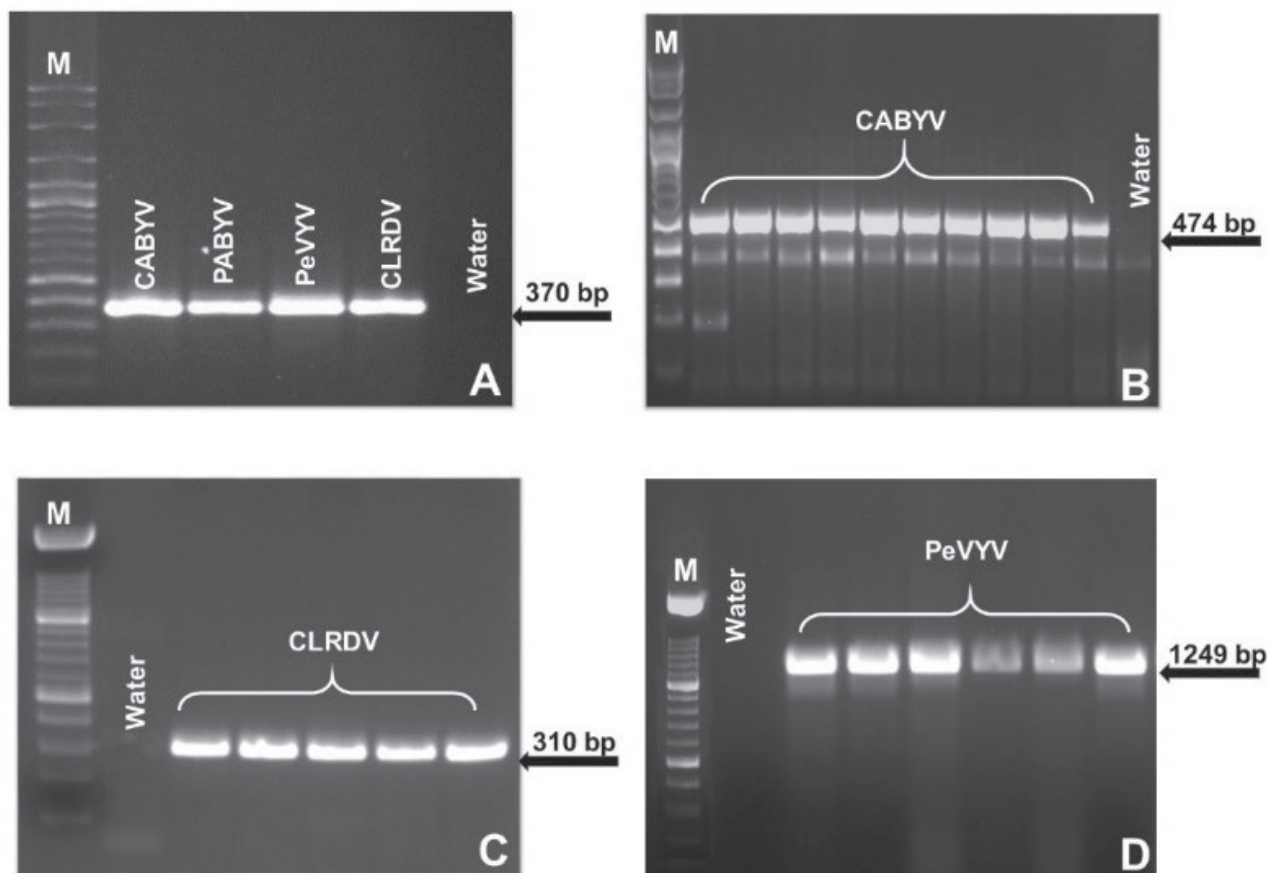


Figure 2. (A) Detection of Cucurbit aphid-borne yellows virus (CABYV), Pepo aphid-borne yellows virus (PABYV), Pepper vein yellows virus (PeVYV) and Cotton leafroll dwarf virus (CLRDV) by RT-PCR using AS3/Pol3870F generic primers; (B) Detection of CABYV by MP-PCR using AS3/CABYV3635F specific primers; (C) Detection of CLRDV by RT-PCR using Pol3982R/CLRDV3675F specific primers (one sample from Sudan and four samples from Uzbekistan were used as positive controls); (D) Detection of PeVYV by RT-PCR using PeF/PeR specific primers. M = DNA Ladder VC 100 bp Plus (Cat No. NL1405, vivantis, Malaysia).

sion no. KC685313) (Figure 3). BLAST analysis of the PCR product generated by AS3/Pol3870F revealed high nucleotide sequence similarity with *Polerovirus* viruses: 95-96% similarity was found with PeVYV (accession no. KC685313) and 93-94% for PABYV (accession no. KJ789902). Similarities of 90% were found for CLRDV (accession no. EU871539) and 90-92% for CABYV (accession no. KX398665) (Table 4). A nucleotide sequence obtained from the isolate SuCp29-15 was also distinct from all other luteovirid sequences. Pairwise comparisons of the predicted CP amino acid sequences showed that isolate SuCp29-15 was close to the PABYV-Cote d'Ivoire isolate (GenBank accession no. KR476816) with 97% similarity (Table 5; Figure 3).

The CP sequence of SuCp31-15 was 96% similar to that of the CLRDV-Brazil isolate, which was the closest phylogenetically. Similarly, isolate SuCp122-13 shared distinct similarity with both CABYV isolates from Tun-

sia (GenBank accession no. EF187345) and Italy (GenBank accession no. EF029113) (Table 5; Figure 3).

The phylogenetic comparison of the nucleotide sequence of the virus isolates grouped the isolates in distinct clusters depending on identical and different sequences which revealed that the grouping model is typically correlated to the geographical origin of the isolates (Figure 3). This result also was supported by a two-dimensional color-coded matrix of pairwise identity scores (Figure 4) generated by species demarcation tool (SDT) (Muhire *et al.*, 2014), which revealed that the representative isolates have overlapping identity range with CP gene from GenBank isolates (59-99%). Despite the fact that some virus isolates were identified from different hosts, the SDT showed similar identity as for isolate SuCp42-13 and reference isolate (PeVYV, GeneBank accession no. KC685313).

Table 4. Designations, geographic origins, comparison and identity with reference GenBank accessions of chickpea luteovirids characterized in this study.

Isolate name ^a	GenBank accession number	Region in Sudan	TBIA reaction with MAb ^b	Virus sequence Blastn_ Reference GenBank accessions ^d	Blastn similarity %
SuCp10-13	MK461113	North of Gezira Scheme	5G4, CpCSV	PeVYV_KC685313	96
SuCp14-13	MK461114	North of Gezira Scheme	5G4	PeVYV_KC685313	96
SuCp42-13	MK461115	Middle of Gezira Scheme	5G4, CpCSV	PeVYV_KC685313	95
SuCp108-13	MK461116	Hudeiba Agr. Res. Station, River Nile	5G4, CpCSV	PeVYV_KC685313	96
SuCp111-13	MK461120	Hudeiba Agr. Res. Station, River Nile	5G4	PABYV_KJ789902	93
SuCp21-15	MK461121	South of Gezira Scheme	5G4, CpCSV, BWYV	PABYV_KJ789902	94
SuCp22-15	MK461122	South of Gezira Scheme	5G4, CpCSV	PABYV_KJ789902	94
SuCp26-15	MK461123	South of Gezira Scheme	5G4	PABYV_KJ789902	94
SuCp28-15	MK461124	South of Gezira Scheme	5G4, CpCSV	PABYV_KJ789902	94
SuCp29-15	MK461125	South of Gezira Scheme	5G4, CpCSV, BWYV	PABYV_KJ789902	94
SuCp30-15	MK461126	South of Gezira Scheme	5G4, CpCSV	PABYV_KJ789902	94
SuCp32-15	MK461127	South of Gezira Scheme	5G4, CpCSV	PABYV_KJ789902	94
SuCp33-15	MK461128	South of Gezira Scheme	5G4, CpCSV	PABYV_KJ789902	94
SuCp34-15	MK461129	South of Gezira Scheme	5G4, CpCSV, BWYV	PABYV_KJ789902	94
SuCp35-15	MK461130	South of Gezira Scheme	5G4, CpCSV	PABYV_KJ789902	94
SuCp36-15	MK461131	South of Gezira Scheme	5G4, CpCSV, BWYV	PABYV_KJ789902	94
SuCp37-15	MK461132	South of Gezira Scheme	5G4, CpCSV	PABYV_KJ789902	94
SuCp38-15	MK461133	South of Gezira Scheme	5G4, CpCSV	PABYV_KJ789902	94
SuCp31-15	MK411565	South of Gezira Scheme	5G4, CpCSV	CLR DV_EU871539	90
SuCp106-13 ^c	MG933685	Hudeiba Agr. Res. Station, River Nile	5G4, CpCSV	CABYV_KX398665	91
SuCp110-13	MK461117	Hudeiba Agr. Res. Station, River Nile	5G4, CpCSV	CABYV_KX398665	91
SuCp117-13	MK461118	Hudeiba Agr. Res. Station, River Nile	5G4	CABYV_KX398665	90
SuCp122-13 ^c	MG933686	Hudeiba Agr. Res. Station, River Nile	5G4, CpCSV	CABYV_KX398665	90
SuCp23-15	MK461119	South of Gezira Scheme	5G4, CpCSV, BWYV	CABYV_KX398665	92

^a The last two numbers refer to year of collection.

^b Information of MAb^s are given in Table 3. Virus acronym used is CpCSV: Chickpea chlorotic stunt virus; BWYV: Beet western yellows virus.

^c All samples were amplified only with generic primer pairs (AS3/Pol3870F) except last 5 samples were amplified with AS3/CABYV3635F in addition to generic primer pairs.

^d Virus acronym used is CLR DV: Cotton leafroll dwarf virus; CABYV: Cucurbit aphid-borne yellows virus; PeVYV: Pepper vein yellows virus; PABYV: Pepo aphid-borne yellows virus.

^e CABYV isolates reported in Kumari *et al.* (2018).

DISCUSSION

The present study has shown that CpCDV and luteovirids were the most common viruses affecting chickpea crops in Sudan, whereas FBNYV was rare. These viruses have been reported on faba bean and chickpea in many countries in the WANA region (Kumar *et al.*, 2008; Kumari and Makkouk, 2007; Makkouk and Kumari, 2009). CpCDV has been reported on faba bean and chickpea (Makkouk *et al.*, 1995), and FBNYV (Makkouk *et al.*, 2003b) and BLRV (Makkouk *et al.*, 1988) were reported on faba bean in Sudan, based on serological assays using polyclonal antibodies.

Based on serological results, 11 samples reacted positively with BWYV MAb, 22 with CpCSV MABs, and 23

samples reacted with both BWYV and CpCSV MABs. However, sequence analyses showed that no samples were infected with either BWYV or CpCSV. This demonstrates that virus identification based solely on serology can be inaccurate due to cross reactions between specific MABs and a range of viruses in *Polerovirus*. Our approach of initially screening large numbers of symptomatic field samples by serology, followed by molecular confirmation of species from serologically-positive samples, has proved to be useful to accurately identify virus species involved in disease outbreaks.

Although results of serological tests confirmed the growing importance and challenge caused by luteovirids in legume crops in the WANA region, there have been many indications that the use of serological techniques

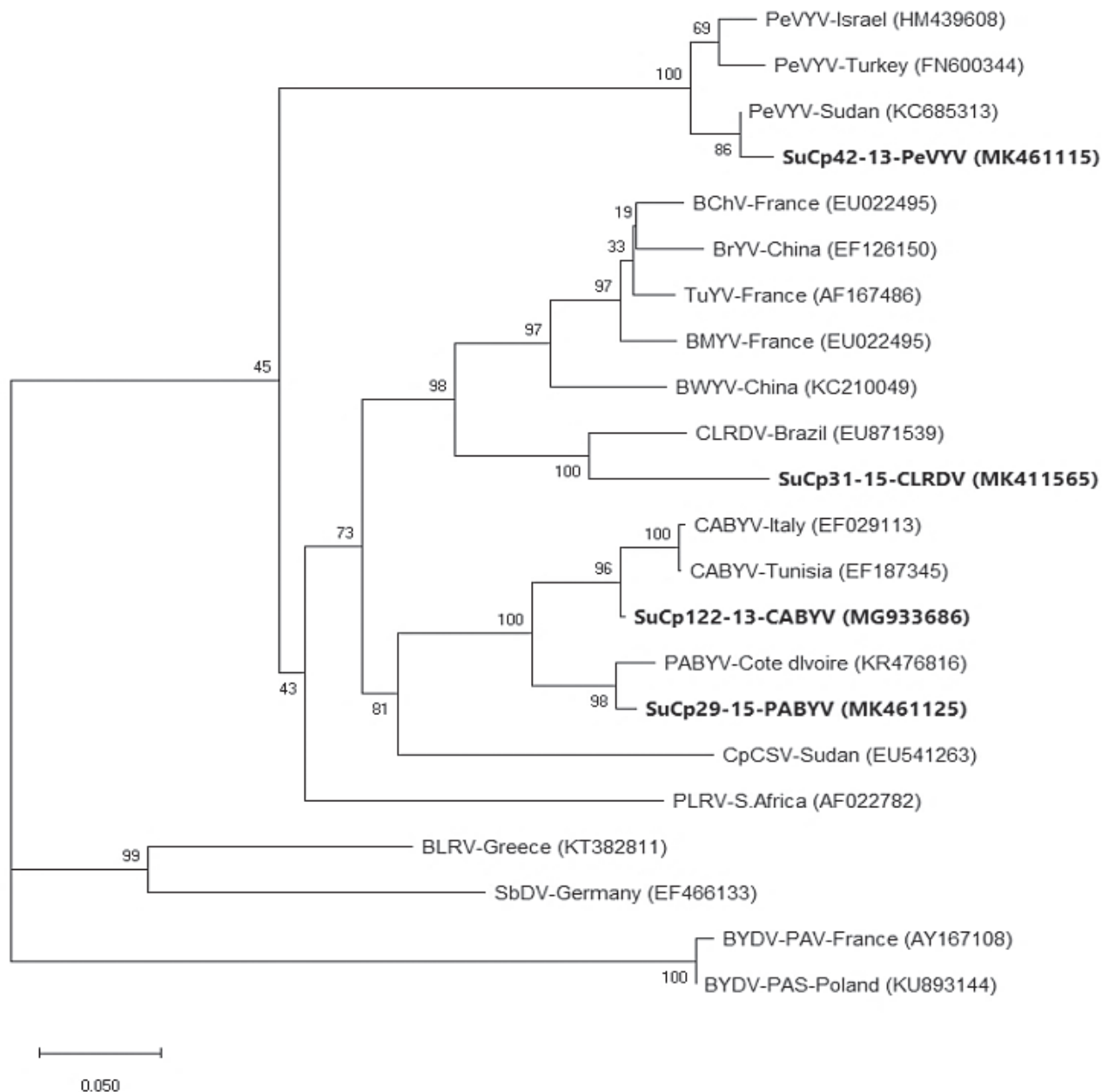


Figure 3. Dendrogram showing the phylogenetic relationships of the predicted partial coat protein amino acid sequences from AS3/Pol3870F fragment of new detected distinct luteovirid isolates with those of other luteovirids from the database. The scale bar represents 0.050 divergence of the Hasegawa-Kishino-Yano dissimilarity index. Bootstrap analysis was carried out with 1000 replicates of the starting tree. Bootstrap values are shown in each branch. Database accession numbers of the luteovirid sequences and the virus acronyms used are presented in Table 5.

are not sufficiently reliable for the identification of luteovirid species, because different luteovirids share a number of epitopes (Martin and D’Arcy, 1990; Fortass *et al.*, 1997; Abraham *et al.*, 2006). However, as Makkouk and Kumari (1996) confirmed, TBIA is a helpful method for easy, rapid and cheap detection of plant viruses,

especially in the developing countries, and TBIA can be an important tool for virus detection in large scale surveys. The molecular detection method for CABYV, PABYV, PeVYV and CLRDV diagnoses used in this study showed the RT-PCR analysis is very reliable for detection of these four viruses in symptomatic samples.

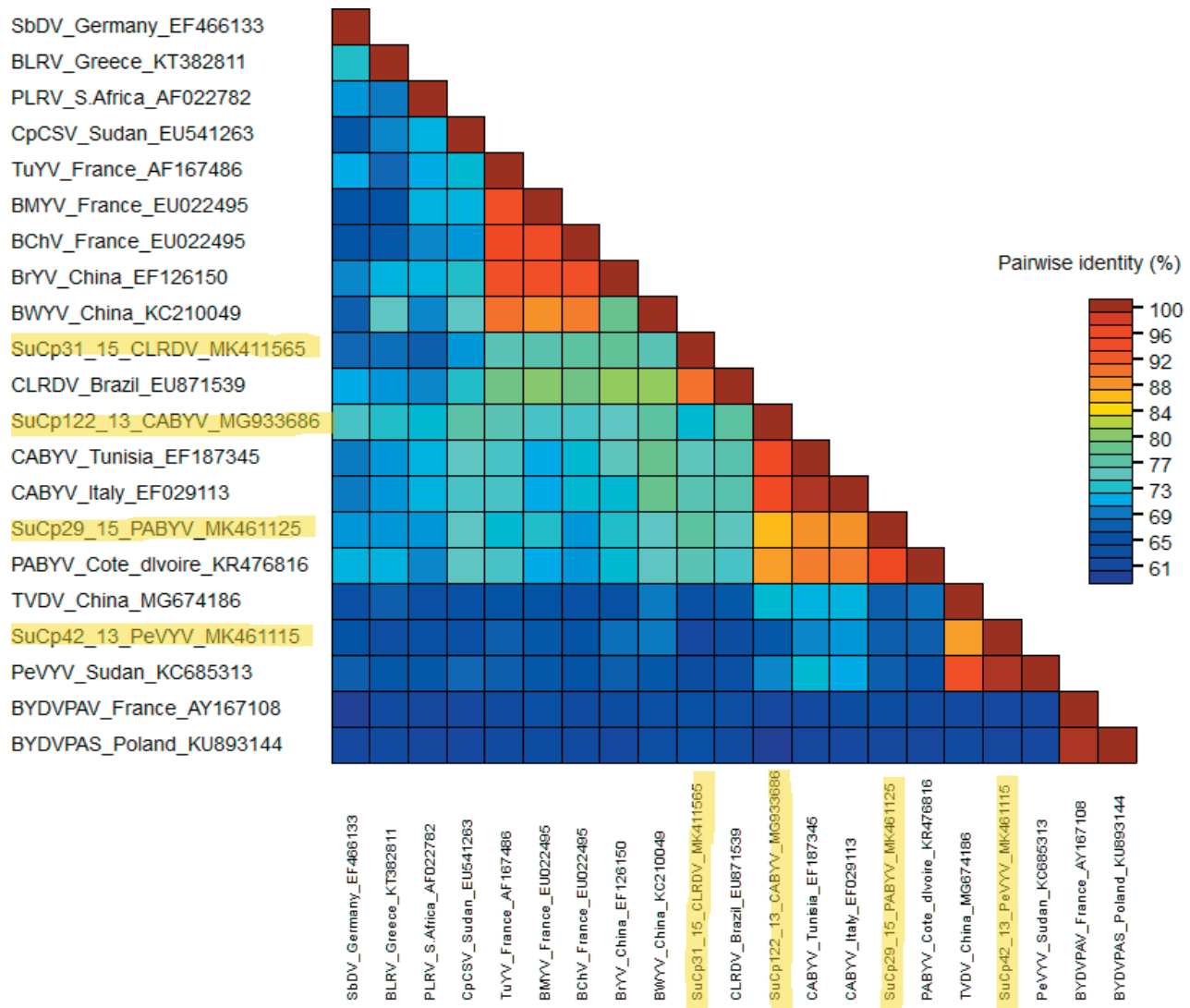


Figure 4. Two dimensional percentage pair wise similarity plot matrix of different selected strains of *Luteoviridae* generated using the Species Demarcation Tool (<http://web.cbio.uct.ac.za/SDT>). Each coloured cell represents a percentage similarity between two sequences (one indicated horizontally to the left and the other vertically at the bottom) displayed in the colour key. The luteovirid isolates from Sudan are highlighted, and all accessions details used for this study are listed in Table 5.

Therefore, the MP-PCR method, which can rapidly identify luteovirids, is an important tool for identifying and determining the distribution of luteoviruses that affect cool season legumes. Generally, MP-PCR technology, in addition to sensitivity and specificity, has the added benefits of saving time and costs compared with Uniplex RT-PCR (Deb and Anderson, 2008; Murray Sharman, unpublished data).

The field surveys carried out in the present study indicated that *Aphis craccivora* is present in most chickpea fields. *Aphis craccivora* is polyphagous and preferences *Fabaceae* hosts, but other host plant families

include *Brassicaceae*, *Cucurbitaceae*, *Malvaceae*, and *Solanaceae*. Crops attacked by this aphid include brassicas, cucurbits, beetroot, peanut, cotton, cowpeas and chickpea. In addition, this aphid is the vector of a number of plant viruses including *Luteoviridae* species. The major crops in Gezira Scheme are cotton, vegetable and chickpeas, and the viruses reported on chickpea in this study also affect cotton and vegetable crops. Further study is therefore needed on behaviour of aphid species in agriculture systems in the Gezira Scheme to use the information for effective management of these viruses. Furthermore, occurrence of these new viruses suggests

Table 5. Pairwise comparisons of the percentage amino acid sequence similarities for partial CP gene (AS3/Pol3870F fragment) of four distinct luteovirid sequences amplified from four representative samples with that of other luteovirids from the database and to each other.

Virus species (source)	Accession Number	Sequenced representative Isolates			
		SuCp42-13 (PeVYV)	SuCp29-15 (PABYV)	SuCp31-15 (CLR DV)	SuCp122-13 (CABYV)
Barley yellow dwarf virus-PAS (Poland)	KU893144	43.43	45.83	42.55	50.00
Barley yellow dwarf virus-PAV (France)	AY167108	43.43	45.83	42.55	49.36
Bean leafroll virus (Greece)	KT382811	52.53	58.95	58.06	64.83
Soybean dwarf virus (Germany)	EF466133	57.58	66.32	60.22	65.73
Beet chlorosis virus (France)	EU022495	65.06	75.31	75.00	76.98
Beet mild yellowing virus (France)	EU022496	62.65	74.07	75.00	77.42
Beet western yellows virus (China)	KC210049	64.65	80.00	78.72	75.00
Brassica yellows virus (China)	EF126150	61.46	76.67	79.78	80.45
Carrot red leaf virus (Mauritius)	FJ969849	57.69	59.18	51.11	61.11
Chickpea chlorotic stunt virus (Syria)	EU541270	60.42	79.12	70.00	80.58
Cotton leafroll dwarf virus (Brazil)	EU871539	61.62	78.95	96.17	76.97
Cucurbit aphid-borne yellows virus (Italy)	EF029113	61.62	89.36	75.79	97.93
Cucurbit aphid-borne yellows virus (Tunisia)	EF187345	60.42	89.01	75.00	97.24
Pepo aphid-borne yellows virus (Cote d'Ivoire)	KR476816	62.11	96.70	73.33	88.97
Pepper vein yellows virus (Sudan)	KC685313	100.00	62.50	60.00	63.16
Potato leafroll virus (South Africa)	AF022782	60.61	65.62	61.70	68.21
Tobacco vein distorting virus (China)	MG674186	74.95	65.62	58.95	65.97
Turnip yellows virus (France)	AF167486	67.47	75.31	75.00	79.84
SuCp42-13-PeVYV (Sudan, this study)	MK461115	-	61.70	59.57	58.89
SuCp29-15-PABYV (Sudan, this study)	MK461125		-	NS*	60.00
SuCp31-15-CLR DV (Sudan, this study)	MK411565			-	75.56
SuCp122-13-CABYV (Sudan, this study)	MG933686				-

* NS: No significant similarity found.

the need for further screening of legume crops, including chickpea, for resistance to luteovirids, and for development of new management strategies to incorporate host resistance as an important component for virus disease control.

Despite the limited number of samples analyzed for sequencing, PABYV sequences were amplified from the majority of the luteovirid-positive samples analyzed (14 samples of 24 sequenced samples), followed by PeVYV and CABYV. This suggests that these viruses are widespread in cool-season food legumes grown in the WANA countries, and are more prevalent than the other luteovirids detected so far from the region, such as BLRV and SbDV (Fortass and Bos, 1991; Tadesse *et al.*, 1999; Abraham *et al.*, 2000; Makkouk *et al.*, 2003a). The observed variability within the sequences together with detection in samples from different locations and different luteovirids, suggest that these viruses have been infecting legumes for many years in Sudan but have remained undetected and/or incorrectly identified as one of the

other legume luteovirids, possibly due to the lack of appropriate diagnostic methods. In addition, PeVYV has been previously reported infecting hot pepper (*Capsicum annum*) in Sudan (Alfaro-Fernández *et al.*, 2014). The molecular analysis found that PeVYV chickpea isolate (SuCp42-13, GenBank accession no. MK461115) was almost identical to the Sudanese PeVYV isolated from pepper (GenBank accession no. -KC685313), indicating that both chickpea and pepper isolates are same, or are very similar, but this virus has not been previously recognized in grain legumes due to antibody cross reactions.

Most previous studies have been based on serological tests that are not reliable for the identification of luteovirids to species level. The present study has confirmed the occurrence of CABYV, PABYV, PeVYV and CLR DV in Sudan, using robust molecular techniques. These samples reacted serologically with one or more of antibodies specific to BWYV and CpCSV, suggesting they share a common epitope with these two viruses.

CABYV was first described in 1992 in France (Lecoq *et al.*, 1992), but was later detected infecting cucurbits in many other countries (Kassem *et al.*, 2013). In addition to cucurbits, CABYV can infect other crop species, including lettuce (*Lactuca sativa*) and fodder beet (*Beta vulgaris*), as well as some common weeds (Kassem *et al.*, 2013), which are thought to be virus reservoirs. Recently, CABYV was reported to infect faba bean (*Vicia faba* L.) in Turkey (Buzkan *et al.*, 2017), and the present study is the first report of CABYV affecting chickpeas. CABYV is transmitted by *Aphis gossypii* and *Myzus persicae* (Lecoq *et al.*, 1992), and both these vectors have very broad host ranges. Further disease surveillance is required to determine if CABYV is also present in other grain legume production regions of the world.

Cotton blue disease (CBD) was first described in the Central African Republic in 1949 (Cauquil and Vaissayre, 1971), although no causal agent was characterized at the time. CLRDV has now been shown to cause Cotton blue disease from Brazil (Corrêa *et al.*, 2005). Our detection of CLRDV from Sudan is the first confirmation of this virus from Africa, and this suggests that this virus may have been unnoticed on chickpea in Sudan, where cotton cultivation is widespread. Hence, further research is required to outline the life cycle of this virus on cool season and warm season crops. More recently, CLRDV has been reported on chickpea in Uzbekistan (Kumari *et al.*, 2020).

Sharman *et al.* (2015) and Mukherjee *et al.* (2016) indicated that the host range of CLRDV is not well understood, but mainly includes plants in *Malvaceae*, especially *Gossypium* spp. While the main vector of CLRDV in cotton is *Aphis gossypii* (Michelotto and Busoli 2007), this virus is also transmitted by *M. persicae* and *A. craccivora* in chickpea (Mukherjee *et al.*, 2016). In Sudan, cotton and chickpea crops are grown in rotation, and they probably share these viruses and their aphid vectors. This may play a role in the epidemiology of these viruses, allowing them to survive between seasons on alternating crops. The study by Reddy and Kumar (2004) on the host range of the chickpea stunt disease associated virus (CpSDaV), most likely synonymous to CLRDV (Naidu *et al.*, 1997; Corrêa *et al.*, 2005), indicated that CLRDV can infect several grain legume species, many of which are commonly cultivated in Sudan, suggesting that CLRDV may have suitable hosts all year around. Mukherjee *et al.* (2016) studied the genetic similarity between CLRDV and CpSDaV in India, and found that these two viruses are possibly two different strains of the same virus. This information would be helpful for managing these serious diseases, possibly by altering the cropping patterns used by producers.

The present study is the first to report CLRDV and PABYV from crops in Sudan, and is the first report of PeVYV isolated from chickpea in this country. Kumari *et al.* (2018) made the first report of CABYV in Sudan, and the present report has greatly extended the understanding of the diversity, geographical range and incidence of CABYV in Sudan. In addition, this study is the first reliable molecular characterization for these four *Polerovirus* species identified from chickpea samples collected in Sudan. Further field investigations and surveys are required to determine more accurately the ongoing impacts and geographical distribution of these newly detected viruses on chickpea and other grain legume crops in the WANA region. Accurate local knowledge of identity of viruses affecting these crops is essential for breeding for disease resistance and effective crop management.

ACKNOWLEDGEMENTS

This research was supported by the Grains Research and Development Corporation, Australia (Project DAN00202), the Arab Fund for Social and Economic Development (AFSED), Kuwait, and the Department of Agriculture and Fisheries, Queensland, Australia.

LITERATURE CITED

- Abraham A.D., Makkouk K.M., Gorfu D., Lencho A.G., Ali K., ... Lencho A., 2000. Survey of faba bean (*Vicia faba* L.) virus diseases in Ethiopia. *Phytopathologia Mediterranea* 39: 277–282.
- Abraham A.D., Menzel W., Lesemann D.E., Varrelmann M., Vetten H.J., 2006. Chickpea chlorotic stunt virus: A new Polerovirus infecting cool-season food legumes in Ethiopia. *Phytopathology* 96: 437–446. <https://doi.org/10.1094/phyto-96-0437>
- Abraham A.D., Varrelmann, M., Vetten H.J., 2008. Molecular evidence for the occurrence of two new luteoviruses in cool season food legumes in North-east Africa. *African Journal of Biotechnology* 7: 414–420. <https://doi.org/10.1007/s00705-009-0374-0>
- Abraham A.D., Menzel W., Varrelmann M., Vetten H.J., 2009. Molecular, serological and biological variation among Chickpea chlorotic stunt virus isolates from five countries of North Africa and West Asia. *Archives of Virology* 154: 791–799. <https://doi.org/10.1007/s00705-009-0374-0>
- Alfaro-Fernández A., ElShafie E.E., Ali M.A., El Bashir O.O.A., Córdoba-Sellés M.C., Ambrosio M. F.S.,

2014. First report of Pepper vein yellows virus infecting hot pepper in Sudan. *Plant Disease* 98: 1446–1446. <https://doi.org/10.1094/PDIS-03-14-0251-PDN>
- Altschul S.F., Madden T.L., Schäffer A.A., Zhang J., Zhang Z., ... Lipman D.J., 1997. Gapped BLAST and PSI-BLAST: a new generation of protein database search programs. *Nucleic Acids Research* 25: 3389–3402. <https://doi.org/10.1093/nar/25.17.3389>
- Altschul S.F., Wootton J.C., Gertz E.M., Agarwala R., Morgulis A., ... Yu Y.K., 2005. Protein database searches using compositionally adjusted substitution matrices. *FEBS Journal* 272: 5101–5109. <https://doi.org/10.1111/j.1742-4658.2005.04945.x>
- Asaad N.Y., Kumari S.G., Haj-Kassem A.A., Shalaby A.A., Al-Shaabi S., Malhotra R.S., 2009. Detection and characterization of Chickpea chlorotic stunt virus in Syria. *Journal of Phytopathology* 157: 756–761. <https://doi.org/10.1111/j.1439-0434.2009.01574.x>
- Bos L., Hampton R.O., Makkouk K.M., 1988. Viruses and virus diseases of pea, lentil, faba bean and chickpea. In: *World crops: cool season food legumes* (R.J. Summerfield, ed.), Kluwer Academic Publishers, London, United Kingdom, 591–615.
- Buzkan N., Arpacı B.B., Apalak A., 2017. First report of Cucurbit aphid-borne yellows virus in *Vicia faba*. *New Disease Reports* 35: 13. <https://doi.org/10.5197/j.2044-0588.2017.035.013>
- Cauquil J., Vaissayre, M., 1971. La “maladie bleue” du cotonnier en Afrique: transmission de cotonnier à cotonnier par *Aphis gossypii* Glover (The “blue disease” of cotton in Africa: transmission cotton to cotton by *Aphis gossypii* Glover). *Coton et Fibres Tropicales* 26: 463–466.
- Corrêa R.L., Silva T.F., Simões-Araújo J.L., Barroso P.A.V., ... Vaslin M.F.S., 2005. Molecular characterization of a virus from the family *Luteoviridae* associated with cotton blue disease. *Archives of Virology* 150: 1357–1367. <https://doi.org/10.1007/s00705-004-0475-8>
- D’Arcy C.J., Torrance L., Martin R.R., 1989. Discrimination among luteoviruses and their strains by monoclonal antibodies and identification of common epitopes. *Phytopathology* 79: 869–873.
- D’Arcy C.J., Domier L.L., 2005. Family *Luteoviridae*. In: *Virus Taxonomy: Classification and Nomenclature of Viruses, Eighth Report of the International Committee on the Taxonomy of Viruses* (C.M. Fauquet, M.A. Mayo, J. Maniloff, U. Desselberger, L.A. Ball, ed.), Elsevier Academic Press, San Diego, CA, USA, 891–900.
- Deb M., Anderson J.M., 2008. Development of a multiplexed PCR detection method for Barley and Cereal yellow dwarf viruses, Wheat spindle streak virus, Wheat streak mosaic virus and Soil-borne wheat mosaic virus. *Journal of Virology Methods* 148: 17–24. <https://doi.org/10.1016/j.jviromet.2007.10.015>
- Domier L.L., 2011. Family *Luteoviridae*. In: *Virus Taxonomy: Classification and Nomenclature of Viruses, Ninth Report of the International Committee on Taxonomy of Viruses* (A.M.Q. King, M.J. Adams, E.B. Carstens, E.J. Lefkowitz, ed.), Elsevier, Oxford, 1045–1053.
- Duffus J.E., Russell G.E., 1975. Serological relationship between Beet western yellows and Beet mild yellowing viruses. *Phytopathology* 65: 811–815. <https://doi.org/10.1094/Phyto-65-811>
- FAO, 2018. Pulse Quantity Production. Food and Agriculture Organization of the United Nations. Statistical Databases, FAO, Italy. Available online at: <http://www.fao.org/faostat/en/>
- Fortass M.F., Bos L., 1991. Survey of faba bean (*Vicia faba* L.) for viruses in Morocco. *Netherlands Journal of Plant Pathology* 97: 369–380.
- Fortass M.F., van der Wilk F., Goldbach R.W., Bos L., van den Heuvel J.F.J.M., 1996. Diversity of viruses infecting faba bean in Morocco and their detection by the polymerase chain reaction. *Agronomie* 16: 61–68. <https://doi.org/10.1051/agro:19960104>
- Fortass M.F., Wilk F., Heuvel J.F.J.M., Goldbach R.W., 1997. Molecular evidence for the occurrence of Beet western yellows virus on chickpea in Morocco. *European Journal of Plant Pathology* 103: 481–484. <https://doi.org/10.1023/A:1008687629522>
- Franz A., Makkouk K.M., Katul L., Vetten H.J., 1996. Monoclonal antibodies for the detection and differentiation of Faba bean necrotic yellows virus isolates. *Annals of Applied Biology* 128: 255–268. <https://doi.org/10.1111/j.1744-7348.1996.tb07321.x>
- Govier D.A., 1985. Purification and partial characterisation of Beet mild yellowing virus and its serological detection in plants and aphids. *Annals of Applied Biology* 107: 439–447. <https://doi.org/10.1111/j.1744-7348.1985.tb03160.x>
- Hasegawa M., Kishino H., Yano T.A., 1985. Dating of the human-ape splitting by a molecular clock of mitochondrial DNA. *Journal of Molecular Evolution* 22: 160–174. <https://doi.org/10.1007/bf02101694>
- Hauser S., Stevens M., Mougel C., Smith H.G. Fritsch C., ... Lemaire O., 2000. Biological, serological, and molecular variability suggest three distinct polerovirus species infecting beet or rape. *Phytopathology* 90: 460–466. <https://doi.org/10.1094/PHYTO.2000.90.5.460>
- Hauser S., Stevens M., Beuve M., Lemaire O., 2002. Biological properties and molecular characterization of Beet chlorosis virus (BChV). *Archives of Virology* 147: 745–762. <https://doi.org/10.1007/s007050200023>

- Kassem M. A., Juarez M., Gómez P., Mengual C. M., Sempere R. N., ... Aranda M.A., 2013. Genetic diversity and potential vectors and reservoirs of Cucurbit aphid-borne yellows virus in southeastern Spain. *Phytopathology* 103: 1188- 1197. <https://doi.org/10.1094/PHYTO-11-12-0280-R>
- Katul L., 1992. *Characterization by serology and molecular biology of Bean leaf roll virus and Faba bean necrotic yellows virus*. PhD Thesis. University of Göttingen, Göttingen, Germany. 115 pp.
- Knierim D., Deng T., Tsai W.S., Green S.K., Kenyon L., 2010. Molecular identification of three distinct Polerovirus species and a recombinant Cucurbit aphid-borne yellows virus strain infecting cucurbit crops in Taiwan. *Plant Pathology* 59: 991–1002. <https://doi.org/10.1111/j.1365-3059.2010.02327.x>
- Kumar P.L., Kumari S.G., Waliyar F., 2008. Virus diseases of chickpea. In *Characterization, Diagnosis and Management of Plant Viruses: Vegetable and Pulse Crops*. Vol 3 (G.P. Rao, P.L. Kumar, R.J. Holguin-Pena, ed.), Studium Press LLC, Texas, USA, 213–234.
- Kumar S., Stecher G., Li M., Knyaz C., Tamura K., 2018. MEGA X: Molecular evolutionary genetics analysis across computing platforms. *Molecular Biology and Evolution* 35: 1547–1549. <https://doi.org/10.1093/molbev/msy096>
- Kumari S.G., Makkouk K.M., Attar N., 2006. An improved antiserum for sensitive serologic detection of Chickpea chlorotic dwarf virus. *Journal of Phytopathology* 154: 129–133. <https://doi.org/10.1111/j.1439-0434.2006.01068.x>
- Kumari S.G., Makkouk K.M., 2007. Virus diseases of faba bean (*Vicia faba* L.) in Asia and Africa. *Plant Viruses* 1: 93–105.
- Kumari S.G., Makkouk K., Asaad N., Attar N., Loh M.H., 2007. Chickpea chlorotic stunt virus affecting cool-season food legumes in west Asia and north Africa. Page 157. In: *Abstract book of 10th International Plant Virus Epidemiology Symposium, on the theme "Controlling Epidemics of Emerging and Established Plant Virus Diseases - The Way Forward"*. 15–19 October 2007, Hyderabad, India. 209 pp.
- Kumari S.G., Larsen R., Makkouk K.M., Bashir M., 2009. Virus diseases of lentil and their control. In: *The Lentil: Botany, Production and Uses* (W. Erskine, F.J. Muehlbauer, A. Sarker, B. Sharma, eds). CABI, UK, 306–325. <https://doi.org/10.1079/9781845934873.0000>
- Kumari S.G., Ziyaev Z., Kemal S., 2017. Viral diseases affecting chickpea crop in Uzbekistan. *Phytopathologia Mediterranea* 562: 356. https://doi.org/10.14601/Phytopathol_Mediterr-20879
- Kumari S. G., Moukahel A.R., Hamed A.A., Sharman M., 2018. First Report of Cucurbit aphid-borne yellows virus Affecting Chickpea (*Cicer arietinum* L.) in Sudan. *Plant Disease* 102: 2048. <https://doi.org/10.1094/PDIS-02-18-0347-PDN>
- Kumari S.G., Sharman M., Moukahel A., Ziyaev Z., Ahmed S., 2020. First report of Cotton leafroll dwarf virus affecting chickpea (*Cicer arietinum* L.) in Uzbekistan. *Plant Disease* 104: 2532. <https://doi.org/10.1094/PDIS-01-20-0085-PDN>
- Lecoq H., Bourdin D., Wipf-Scheibel C., Bon M., Lot H., ... Herbach. E., 1992. A new yellowing disease of cucurbits caused by a luteovirus, Cucurbit aphid-borne yellows virus. *Plant Pathology* 41: 749–761. <https://doi.org/10.1111/j.1365-3059.1992.tb02559.x>
- Lemaire O., Herrbach E., Stevens M., Bouchery Y., Smith H.G., 1995. Detection of sugar beet-infecting Beet mild yellowing luteovirus isolates with a specific RNA probe. *Phytopathology* 85: 1513–1518. <https://doi.org/10.1094/Phyto-85-1513>
- Makkouk K.M., 2020. Plant pathogens which threaten food security: viruses of chickpea and other cool season legumes in West Asia and North Africa. *Food Security* 12: 495–502. <https://doi.org/10.1007/s12571-020-01017-y>
- Makkouk K.M., Bos L., Azzam O.I., Kumari S., Rizkallah A., 1988. Survey of viruses affecting faba bean in six Arab countries. *Arab Journal of Plant Protection*: 6: 53–61.
- Makkouk K.M., Dafalla G., Hussein M., Kumari S.G., 1995. The natural occurrence of Chickpea chlorotic dwarf geminivirus in chickpea and faba bean in the Sudan. *Journal of Phytopathology* 143: 465–466. <https://doi.org/10.1111/j.1439-0434.1995.tb04555.x>
- Makkouk K.M., Kumari S.G., 1996. Detection of ten viruses by tissue blot immunoassay (TBIA). *Arab Journal of Plant Protection* 14: 3-9.
- Makkouk K.M., Kumari S.G., Shahraeen N., Fazlali Y., Farzadfar S., ... Mansouri R.A., 2003a. Identification and seasonal variation of viral diseases of chickpea and lentil in Iran. *Journal of Plant Diseases and Protection* 110: 157–169.
- Makkouk K.M., Hamed A.A., Hussein M., Kumari S.G., 2003b. First report of Faba bean necrotic yellows virus (FBNYV) infecting chickpea (*Cicer arietinum*) and faba bean (*Vicia faba*) crops in Sudan. *Plant Pathology* 52: 412. <https://doi.org/10.1046/j.1365-3059.2003.00833.x>
- Makkouk K.M., Kumari S.G., Hughes J.d'A., Muniyappa V., Kulkarni N.K., 2003c. Other legumes: Faba bean, chickpea, lentil, pigeonpea, mungbean, blackgram, lima bean, horegram, bambara groundnut

- and winged bean. In: *Virus and Virus-like Diseases of Major Crops in Developing Countries* (G. Loebeinstein, G. Thottappilly, ed.), Kluwer Academic Publishers, Dordrecht, The Netherlands, 447–476.
- Makkouk K.M., Kumari S.G., 2009. Epidemiology and integrated management of persistently transmitted aphid-borne viruses of legume and cereal crops in West Asia and North Africa. *Virus Research* 141: 209–218. <https://doi.org/10.1016/j.virusres.2008.12.007>
- Makkouk K.M., Kumari S.G., van Leur J.A.G., Jones, R.A.C., 2014. Control of plant virus diseases in cool-season grain legume crops. *Advances in Virus Research* 90: 207–253. <https://doi.org/10.1016/B978-0-12-801246-8.00004-4>
- Martin R.R., D'Arcy C.J., 1990. Relationship among luteoviruses based on nucleic acid hybridization and serological studies. *Intervirology* 31:23–30. <https://doi.org/10.1159/000150130>
- McKenzie D.J., McLean M.A., Mukerji S., Green M., 1997. Improved RNA extraction from woody plants for the detection of viral pathogens by reverse transcription–polymerase chain reaction. *Plant Disease* 81: 222–226. <https://doi.org/10.1094/PDIS.1997.81.2.222>
- Merga B., Haji J., 2019. Economic importance of chickpea: Production, value, and world trade. *Cogent Food & Agriculture* 5: 1615718. <https://doi.org/10.1080/23311932.2019.1615718>
- Michelotto M.D., Busoli A.C., 2007. Caracterização da transmissão do vírus do mosaico-das-nervuras do algodoeiro pelo pulgão *Aphis gossypii* com relação a persistência e ao tempo necessário para inoculação. *Bragantia* 66: 441–447. <https://doi.org/10.1590/S0006-87052007000300010>
- Mnari-Hattab M., Gauthier N., Zouba A., 2009. Biological and molecular characterization of the Cucurbit aphid-borne yellows virus affecting cucurbits in Tunisia. *Plant Disease* 93: 1065–1072. <https://doi.org/10.1094/pdis-93-10-1065>
- Mohamed A.A., Tahir I.S., Elhashimi A.M., 2015. Assessment of genetic variability and yield stability in chickpea (*Cicer arietinum* L.) cultivars in River Nile State, Sudan. *Journal of Plant Breeding and Crop Science* 7: 219–225. <https://doi.org/10.5897/JPBCS2015.0523>
- Mohamed O.E., Ahmed S., Singh M., Ahmed N.E., 2018. Association of crop production practices on the incidence of wilt and root rot diseases of chickpea in the Sudan. *Arab Journal of Plant Protection* 36: 21–26.
- Muhire B.M., Varsani A., Martin D.P., 2014. SDT: A virus classification tool based on pairwise sequence alignment and identity calculation. *PLoS ONE* 9: e108277. <https://doi.org/10.1371/journal.pone.0108277>
- Mukherjee A.K., Mukherjee P.K., Kranthi S., 2016. Genetic similarity between Cotton leafroll dwarf virus and Chickpea stunt disease associated virus in India. *The Plant Pathology Journal* 32: 580–583. <https://doi.org/10.5423/ppj.nt.09.2015.0197>
- Mustafayev E., Kumari S.G., Attar N., Zeynal A., 2011. Viruses infecting chickpea and lentil crops in Azerbaijan. *Australasian Plant Pathology* 40: 612–620. <https://doi.org/10.1007/s13313-011-0094-2>
- Naidu R.A., Mayo M.A., Reddy S.V., Jolly C.A., Torrance L., 1997. Diversity among the coat proteins of luteoviruses associated with chickpea stunt disease in India. *Annals of Applied Biology* 130: 37–47. <https://doi.org/10.1111/j.1744-7348.1997.tb05781.x>
- Nene Y.L., Sheila V.K., Sharma S.B., 1996. *A world list of chickpea and pigeonpea pathogens*. 5th edition. Patancheru 502324, Andhra Pradesh, India: International Crops Research Institute for the Semi-Arid Tropics (ICRISAT) (Semi-formal publication), 27 pp.
- Oshima K., Shikata E., 1990. On the screening procedures of ELISA for monoclonal antibodies against three luteoviruses. *Annals of the Phytopathological Society of Japan* 56: 219–228. <https://doi.org/10.3186/jjphytopath.56.219>
- Reddy S.V., Kumar P.L., 2004. Transmission and properties of a new luteovirus associated with chickpea stunt disease in India. *Current Science* 86: 1157–1161.
- Shang Q., Xiang H., Han C., Li D., Yu J., 2009. Distribution and molecular diversity of three cucurbit-infecting poleroviruses in China. *Virus Research* 145: 341–346. <https://doi.org/10.1016/j.virusres.2009.07.017>
- Sharman M., Lapbanjob S., Seunruang P., Belot J.-L., Galbieri R., ... Suassuna N., 2015. First report of Cotton leafroll dwarf virus in Thailand using a species-specific PCR validated with isolates from Brazil. *Australasian Plant Disease Notes* 10: 1–4. <https://doi.org/10.1007/s13314-015-0174-1>
- Sharman M., Appiah A., Filardo F., Nancarrow N., Congdon B., ... Wilson C., 2021. Biology and genetic diversity of Phasey bean mild yellows virus, a common virus in legumes in Australia. *Archives of Virology* 166: 1575–1589. <https://doi.org/10.1007/s00705-021-05022-0>
- Smith H.G., Barker I., Brewer G., Stevens M., Hallsworth P.B., 1996. Production and evaluation of monoclonal antibodies for the detection of Beet mild yellowing luteovirus and related strains. *European Journal of Plant Pathology* 102: 163–169. <https://doi.org/10.1007/bf01877103>

- Tadesse N., Ali K., Gorfu D., Yusuf A., Abraham A., ... Kumari S.G., 1999. Survey for chickpea and lentil virus diseases in Ethiopia. *Phytopathologia Mediterranea* 38: 149–158.
- Thompson J.D., Gibson T.B., Plewniak F., Jeanmougin F., Higgins D.G., 1997. The CLUSTAL_X windows interface: flexible strategies for multiple sequence alignment aided by quality analysis tool. *Nucleic Acids Research* 25: 4876–4882. <https://doi.org/10.1093/nar/25.24.4876>
- Van der Maesen L.J.G., 1987. *Cicer* L.: Origin, history and taxonomy of Chickpea. In: *Chickpea* (M.C. Saxena, K.B. Singh, ed.), CAB International, Wallingford, UK., 11–34.
- Xiang H., Shang Q., Han C., Li D., Yu J., 2008a. Complete sequence analysis reveals two distinct poleroviruses infecting cucurbits in China. *Archives of Virology* 153: 1155–1160. <https://doi.org/10.1007/s00705-008-0083-0>
- Xiang H., Shang Q., Han C., Li D., Yu J., 2008b. First report on the occurrence of Cucurbit aphid-borne yellows virus on nine cucurbitaceous species in China. *Plant Pathology* 57: 390. <https://doi.org/10.1111/j.1365-3059.2007.01664.x>
- Zhang S.B., Zhao Z.B., Zhang D.Y., Liu Y., Zhang S.B., ... Peng J., 2015. First report of Pepper vein yellows virus infecting red pepper in Mainland China. *Plant Disease* 99: 1190. <https://doi.org/10.1094/pdis-01-15-0025-pdn>



Research Papers

Bacillus-based products for management of kiwifruit bacterial canker

Citation: E. Biondi, L. Gallipoli, A. Mazzaglia, S.P. Fuentealba, N. Kuzmanovic, A. Bertaccini, G.M. Balestra (2021) *Bacillus*-based products for management of kiwifruit bacterial canker. *Phytopathologia Mediterranea* 60(2): 215-228. doi: 10.36253/phyto-12184

Accepted: March 11, 2021

Published: September 13, 2021

Copyright: © 2021 E. Biondi, L. Gallipoli, A. Mazzaglia, S.P. Fuentealba, N. Kuzmanovic, A. Bertaccini, G.M. Balestra. This is an open access, peer-reviewed article published by Firenze University Press (<http://www.fupress.com/pm>) and distributed under the terms of the Creative Commons Attribution License, which permits unrestricted use, distribution, and reproduction in any medium, provided the original author and source are credited.

Data Availability Statement: All relevant data are within the paper and its Supporting Information files.

Competing Interests: The Author(s) declare(s) no conflict of interest.

Editor: Joel L. Vanneste, Plant and Food Research, Sandringham, New Zealand.

ENRICO BIONDI¹, LORENZO GALLIPOLI², ANGELO MAZZAGLIA², SET PEREZ FUENTEALBA^{1,3}, NEMANJA KUZMANOVIĆ^{1,4,5}, ASSUNTA BERTACCINI¹, GIORGIO M. BALESTRA^{2,*}

¹ *Dipartimento di Scienze e Tecnologie Agro-Alimentari (DISTAL), Alma Mater Studiorum - University of Bologna, Viale Fanin 44, 40127 Bologna, Italy*

² *Dipartimento di Scienze Agrarie e Forestali (DAFNE), University of Tuscia, via S. Camillo de Lellis, 01100 Viterbo, Italy*

³ *Instituto de Ciencias Agroalimentarias, Animales y Ambientales (ICA3), Universidad de O'Higgins, Ruta 90 km. 3, 3070000 San Fernando, Chile*

⁴ *Julius Kühn-Institut (JKI), Federal Research Centre for Cultivated Plants, Institute for Epidemiology and Pathogen Diagnostics, Messeweg 11/12, 38104, Braunschweig, Germany*

⁵ *Julius Kühn-Institut (JKI), Federal Research Centre for Cultivated Plants, Institute for Plant Protection in Horticulture and Forests, Messeweg 11/12, 38104, Braunschweig, Germany (current address)*

*Corresponding author. E-mail: balestra@unitus.it

Summary. *Pseudomonas syringae* pv. *actinidiae* is an important pathogen of kiwifruit (*Actinidia deliciosa*), and bacterial canker of this host is managed by monitoring and chemical control strategies. The efficacy of the bio-pesticides Amylo-X[®] (based on *Bacillus amyloliquefaciens* subsp. *plantarum* strain D747) and Serenade Max[®] (strain QST713 of *B. subtilis*) was evaluated by *in vitro* and *in vivo* experiments. Both antagonists inhibited different biovars of the pathogen in *in vitro* assays; QST713 was more efficient than D747. The two *Bacillus* strains also colonized *A. deliciosa* flowers (c. 10⁵⁻⁷ cfu per flower) up to 96 h after inoculation. D747 persisted on leaves (c. 10⁴⁻⁶ cfu cm⁻²) up to 4 weeks after inoculation, during 2 years in Emilia Romagna and Latium regions of Italy. On flowers, the antagonists reduced pathogen populations, compared to untreated (control) flowers. On *A. deliciosa* and *A. chinensis* plants under controlled conditions, Amylo-X[®] reduced severity of bacterial canker, providing ca. 50% relative protection on *A. deliciosa* and 70% on *A. chinensis*. Serenade Max[®] was less effective, giving 0% relative protection on *A. deliciosa* and 40% on *A. chinensis*. In a field trial, on *A. deliciosa* plants, Amylo-X[®] reduced the severity of bacterial canker on leaves, providing ca. 40% relative protection. The sensitivity of both antagonistic strains to streptomycin sulphate was confirmed by testing the most used concentration where antibiotics are approved for management of bacterial pathogens.

Keywords. Biocontrol agents, *Pseudomonas syringae* pv. *actinidiae*, *in vitro* assays, antagonist survival, population challenge.

INTRODUCTION

In the last decade, bacterial canker of kiwifruit, caused by *Pseudomonas syringae* pv. *actinidiae* (Psa), led to extensive economic losses for kiwifruit producers. The pandemic of this bacterial pathogen started in 2008, mainly in the *Actinidia* spp., and the pathogen was especially aggressive on *A. chinensis* cultivars (Abelaira *et al.*, 2011; Mazzaglia *et al.*, 2012; EPPO, 2016). At present, five biovars of Psa are recognized (Cunty *et al.*, 2015), grouped by biochemical, genetic and pathogenicity characteristics (Renzi *et al.*, 2012; Butler *et al.*, 2013; Vanneste *et al.*, 2013; Vanneste, 2017; Fujikawa and Sawada, 2019). Biovar 3 is the most virulent, and was responsible for the bacterial canker pandemic. Disease control strategies rely on strict orchard hygiene practices, breeding and deployment of resistant host genotypes, and scheduled use of antibacterial compounds or elicitors activating host immune systems (Cotrut *et al.*, 2013; Cellini *et al.*, 2014; Michelotti *et al.*, 2018). As well, the use of biological control agents (BCAs) has also been shown to be effective (Cortesi *et al.*, 2017; Rossetti *et al.*, 2017; Hoyte *et al.*, 2018). New and promising strategies have shown the possibility to reduce the use of chemicals by nanotechnological tools (Fortunati *et al.*, 2016; Mazzaglia *et al.*, 2017; Fortunati and Balestra 2018). Nevertheless, prophylaxis utilizing early diagnostic analyses of asymptomatic plant material remains the most effective method for reducing the primary infection sources (Rees-George *et al.*, 2010; Balestra *et al.*, 2013; Biondi *et al.*, 2013; Gallelli *et al.*, 2013).

Chemical control applications against Psa are preventive and/or applied at early stages of the disease development. In open fields, the amount of effective control is dependent on compounds such as streptomycin and/or copper formulations to prevent bacterial blight occurrence (Koh *et al.*, 1996; Nakajima *et al.*, 2002; Lee *et al.*, 2005; Vanneste *et al.*, 2011a). Antibiotics are allowed on most of the continents to control bacterial plant pathogens, but not in Europe, where copper compounds are mostly employed (Balestra and Bovo, 2003; Balestra, 2007; Lee *et al.*, 2005; Vanneste *et al.*, 2011a). Both compounds have different negative properties, including phytotoxicity, pathogen resistance, fruit residues, and accumulation of metal ions in soils (Goto *et al.*, 2004; Marcelletti *et al.*, 2011; Cameron and Sarojini, 2013). Integrated management of kiwifruit bacterial canker is therefore required using multiple strategies for the effective control of the disease. This could include application of resistance inducers, stimulation of host defence responses, and the use of biocontrol agents (Dong *et al.*, 1999; Cellini *et al.*, 2014).

Several bacterial strains are used as fungicides or bactericides to control different plant diseases; most of these are species of *Bacillus* or *Pseudomonas* (McSpadden Gardener and Driks, 2004; Borriss, 2011), and are used against several plant pathogenic bacteria, including *Erwinia amylovora* (Bazzi *et al.*, 2006; Chen *et al.*, 2009), *Xanthomonas arboricola* pv. *pruni* (Biondi *et al.*, 2009a), and *Pseudomonas syringae* pv. *tomato* (Fousia *et al.*, 2016). Some studies have been carried out on control of Psa using biological methods. These have shown the effectiveness of *Pantoea agglomerans* or *Lactobacillus plantarum*, and some bacteriophages and organic substances (Stewart *et al.*, 2011; Frampton *et al.*, 2014; Daranas *et al.*, 2018; de Jong *et al.*, 2019).

In the present study, bacterial strains D747 of *Bacillus amyloliquefaciens* subsp. *plantarum* and QST713 of *B. subtilis*, the principal components, respectively, of the bio-fungicides Amylo-X[®] and Serenade Max[®], were tested *in vitro* for their ability to inhibit the Psa growth, and for their sensitivity to the antibiotic streptomycin sulphate. *In planta*, under controlled conditions and in field trials, the two BCAs were assessed for their capacity to survive on and colonize kiwifruit plants (leaves and flowers), for their efficacy to inhibit Psa epiphytic populations on flowers, and for their effectiveness in reducing the severity of bacterial canker.

MATERIALS AND METHODS

Bacterial strains

The Psa strains NCPPB 3739 (biovar 1), CRA-FRU 3.1 (biovar 3), CFBP 7286 (biovar 3) and DISTAL (*ex*-IPV-BO) 9312 (biovar 3; Biondi *et al.*, 2018) were routinely grown at 27°C for 48–72 h, on NSA (Crosse, 1959) or KB (King *et al.*, 1954) media. The mutant strain CRA-FRU 3.1rif^r, resistant to rifampicin, was grown at 27°C for 72–96 h on KB medium supplemented with 20 ppm rifampicin.

Bacillus amyloliquefaciens strain D747, the active ingredient of Serenade Max[®], and *B. subtilis* strain QST713, in Amylo-X[®], were routinely grown on LPGA (Ridè *et al.*, 1983) at 27° or 36°C for 24 h.

Release of antibacterial compounds by *Bacillus* strains against different *Psa* strains

The production of antimicrobial compounds by strains D747 and QST713 was assessed *in vitro* using the method of Vanneste *et al.* (1992). Axenic 24-h-old colonies of each strain were transferred with a loop to

the centres of (c. 1 cm spot diameter.) Petri dishes containing minimal medium (MM: K_2HPO_4 , 7.02 g L⁻¹; KH_2PO_4 , 3.02 g L⁻¹; L-asparagine 3.0 g L⁻¹, $(NH_4)_2SO_4$, 2.0 g L⁻¹; nicotinic acid 0.5 g L⁻¹, D-glucose 4.0 g L⁻¹, $C_6H_5Na_3O_7 \cdot 2H_2O$ 0.5 g L⁻¹, $MgSO_4 \cdot 7H_2O$ 0.01 g L⁻¹; Bacto agar, 18.0 g L⁻¹). The dishes were then incubated at 27°C for 48 h. Two diameters of each resulting bacterial macro-colony were then measured, and the colony was then scraped off the plate with a lancet. The plates were then exposed to chloroform vapours for 45 min. Each Petri dish was then homogeneously covered with 5 mL of MM soft-agar (MM medium containing 0.7% agar) inoculated with Psa strains NCPPB 3739, DISTAL 9312 or CRA-FRU 3.1 (ca. 10^6 cfu mL⁻¹). After 48–96 h at 27°C, inhibition haloes were each assessed by subtracting the mean of the diameters of the antagonist macro-colony from the mean of the inhibition halo diameter. Psa strains were used as negative controls, and the assay was repeated three times.

Activity of streptomycin sulphate against Bacillus strains

In vitro experiments using the diffusion plate method were carried out on NA medium (nutrient broth, 8 g L⁻¹; agar 18 g L⁻¹). A water suspension of 24-h-old culture of D747 (approx. 10^6 cfu mL⁻¹) was used for the Petri dish inoculations (100 µL per dish). Three paper disks (6 mm diam.) were placed on the inoculated agar medium in each test dish, and 30 µL of streptomycin at 25 or 50 µg mL⁻¹ were pipetted on two of the discs; 30 µL of sterile distilled water (SDW) were applied to the third disc as the experimental control. After incubation at 27°C for 48 h, the inhibition halo diameters in the test plates were determined by subtracting the antibiogram disk diameters (6 mm) from the halo diameters. This test was repeated five times with three replicates each, and the standard deviations were calculated.

The *in vitro* experiments using macro-dilution were carried out in 50 mL Falcon tubes each containing 15 mL of LB broth (Bacto Peptone 10.0 g L⁻¹, Yeast Extract 5.0 g L⁻¹, NaCl 10.0 g L⁻¹, pH 7.0). The tubes were each inoculated with 150 µL aqueous suspensions containing approx. 10^7 cfu mL⁻¹ of spores of Amylo-X* (2.0 g L⁻¹) or Serenade Max* (3.0 g L⁻¹). The inoculated tubes were then amended with streptomycin sulphate (100 ppm) or SDW as negative controls. The tubes were then incubated at 27°C at 80 rpm for 24 h. The bacterial population in each tube was evaluated after 1 and 24 h by collecting 1 mL of inoculated broth. Each sample was tenfold diluted and, 10 µL from each dilution were added to LPGA, and the inoculated plates were incubated at 27°C for 24 h. The bacterial populations were then quantified

by counting the colonies. The assay was repeated three times, and the standard deviations were calculated.

In planta experiments

Amylo-X* and Serenade Max* against Psa

The efficacy of Amylo-X* and Serenade Max* against Psa were assayed under greenhouse conditions on kiwifruit plants of *A. deliciosa* (cv. Hayward) and *A. chinensis* (cv. Hort16A). The plants were grown in 7.0 L capacity pots in randomized replicates (three plants in four replicates per treatment). Amylo-X* (2.0 g L⁻¹; c. 10^7 cfu mL⁻¹) and Serenade Max* (3.0 g L⁻¹; c. 10^7 cfu mL⁻¹) were applied to the leaves (c. 100 mL per plant) using a sprayer 48 h before inoculation with the pathogen (BPI). After treatment application, the plants were inoculated by spraying a water suspension ($OD_{600} = 0.01$; c. 10^7 cfu mL⁻¹) of the virulent Psa strain DISTAL 9312. The plants were then sealed in polyethylene (PE) bags for 2 d to favour pathogen penetration in the leaves. The greenhouse conditions were set at 16 h light, 23°C and 8 h dark, 17°C, and maintaining the RH% at greater values than 70% (Biondi *et al.*, 2018; Perez *et al.*, 2019) until disease assessments. Streptomycin sulphate (100 ppm) and SDW were used as, respectively, positive and negative experimental controls. Disease severity was evaluated 21 d after Psa inoculations, by counting the number of leaf spots on ten leaves per plant (c. 120 leaves per treatment). The data collected were analysed using ANOVA and Duncan's test at $P \leq 0.05$ with SPSS software Windows v15.0 (SPSS Inc.), and the proportions (%) of protection provided by each treatment relative to the negative controls (SDW-treated plants) were calculated.

Selected symptomatic leaf samples were used for Psa isolation and identification. The leaves were surface sterilized by washing with 2% sodium hypochlorite. Necrotic lesions were aseptically collected and crushed with pestel and mortar with 2 mL of SDW. The resulting plant extract and three ten-fold SDW dilutions were plated (30 mL) on NSA. The plates were incubated for up to 72 h. Psa-like colonies were subcultured on KB plates and identified with PCR assays (Biondi *et al.*, 2013).

Bacillus strain colonization of kiwifruit flowers and their effects on Psa populations

Experiments were carried out on detached flowers of kiwifruit plants of cv. Hort 16A (very susceptible to Psa).

The flowers were kept in Eppendorf tubes containing sterile distilled water. Freshly opened flowers were sprayed with an aqueous spore suspension of Serenade Max[®] (3.0 g L⁻¹, *c.* 10⁷ cfu mL⁻¹) or Amylo-X[®] (2.0 g L⁻¹, *c.* 10⁷ cfu mL⁻¹). The mutant strain CRA-FRU 3.1 Rif^r (*c.* 10⁶ cfu mL⁻¹) was sprayed on the flowers 24 h after application of the bio-control treatments. After incubation at 25°C in humid chamber, five flowers per time point (1, 24, 48, 72 or 96 h from antagonist and pathogen application) were individually washed in 3 mL 10 mM MgSO₄. Antagonist and Psa populations present on each flower were assessed by plating tenfold dilutions in 10 mM MgSO₄ on LPGA or KB plates (amended with 20 ppm of rifampicin) (Biondi *et al.*, 2006), and incubating these at 36°C for 20 h (for LPGA) or 27°C for 72–96 h (for KB). Numbers of bacterial colonies recovered from treated flowers were counted, and the populations of both the antagonists and the pathogen were calculated for each flower. SDW and untreated, non-inoculated flowers were used as experimental controls.

Survival of *Bacillus* D747 on kiwifruit leaves

The ability of *Bacillus* strain D747 to survive on leaf surfaces of *A. deliciosa* cv. Hayward trees was evaluated during 2017 and 2018, in the Emilia Romagna and Latium regions of Italy. Kiwifruit plants (two trees per replicate and four replicates), located in open fields in Faenza (Emilia Romagna) and Viterbo (Latium) provinces, were sprayed with Amylo-X[®] (2.0 g L⁻¹; *c.* 10⁷ cfu mL⁻¹) or SDW (negative controls). The treatments were carried out after blooming: in Emilia Romagna on 15/05/2017 and 08/05/2018, and in Latium on 14/06/2017 and 04/06/2018. The bacterium population survival was monitored up to four weeks: at each time point six leaves were randomly collected from each tree, washed in 250 mL of 100 mM MgSO₄ in a rotating incubator at 120 rpm for 45 min at 25°C. The resulting washing fluids were each filtered through sterile gauze and then centrifuged at 10,000 *g* for 20 min at 4°C, and the resulting pellet was resuspended in 1.0 mL SDW. Bacterial antagonist populations present in the resuspended pellets were determined by plating tenfold dilutions in 10 mM MgSO₄ on LPGA plates, and then incubating these at 36°C for 24 h. The bacterial colonies recovered from treated leaves were counted, and the populations of the antagonist per cm² of leaf was calculated ((bacterial concentration per mL × 250 mL/six leaves) × 1 / mean leaf area). SDW was used as the negative control. DNA was extracted from selected axenic colonies recovered from the field assessments, using the Plant DNeasy Minikit (Qiagen). A BOX-PCR was carried out on DNA templates diluted at 50 ng µL⁻¹.

PCR assays were performed in 50 µL reaction mixture containing 1× PCR Go Taq Flexi buffer, 3.0 mM MgCl₂, 0.2 mM dNTPs, 4 U Go-Taq Flexi DNA polymerase (Promega), 2.0 µM BOXAIR primer (5'-CTACG-GCAAGGCGACGCTGACG-3'), and 4 µL template DNA. The BOX-PCR thermal profile consisted of an initial denaturation step (95°C for 7 min), followed by 30 cycles each at 94°C for 1 min, 53°C for 1 min, and 65°C for 8 min, and a final extension step of 16 min at 65°C (Versalovic *et al.*, 1994). All the amplification products were analyzed on 2.0% agarose gel in TAE buffer (0.04 M Tris, 0.001 M NaEDTA and 0.02 M glacial acetic acid), after staining in 0.03% ethidium bromide and visualization under UV light (312 nm). SDW and the D747 strain were used as, respectively, negative and positive controls.

Field activity of Amylo-X[®] against Psa

In Viterbo (Latium region) during 2018, a kiwifruit orchard (*Actinidia deliciosa*, cv. Hayward) with 7-year-old plants severely affected by Psa (*c.* 30% of plants symptomatic), was used to evaluate activity of Amylo-X[®] against Psa. The trial included two groups of plants divided into four plots (ten plants each) per treatment. One group was treated three times with 1.5 kg ha⁻¹ of Amylo-X[®], before bud opening (on 10/05/2018), then 1 week later at the blooming initiation (on 17/05/2018), and then at 04/06/2018. The second group of plants did not receive any phytosanitary treatment, as experimental controls. A disease severity scale was used to evaluate the treatment results. The scale took account of the number of spots (necrotic areas surrounded by yellow haloes) on leaves of 1- and 2-year-old branches (ten leaves from four branches per plant), for four plants in two replicates. Disease assessments were carried out in the second week of May, June or September, 2018.

Four leaf spot severity classes were defined as: class 1 = 0 (no symptoms), class 2 = 25% leaf surface area affected, class 3 = 50% and class 4 = 75% leaf surface area affected. Disease severity was then calculated using the following formula: N° leaves in class 1 × 0 + N° leaves in class 2 × 0.25 + N° leaves in class 3 × 0.50 + N° leaves in class 4 × 0.75 / total N° leaves assessed. As well, the percentage of branches per plant with healthy (asymptomatic) leaves was also determined. The data obtained were statistically analysed using GraphPad Prism v5.0 software for (ANOVA), and differences among mean values for treatments were determined using Tukey's HSD test ($P \leq 0.05$).

RESULTS

In vitro experiments

Results from the *in vitro* experiments indicated that both antagonist strains, D747 and QST713, produced compounds that inhibited the growth of the three *Psa* strains of different biovars (Figure 1). *Bacillus* strain QST713 was significantly more effective for *Psa* inhibition than D747. Strain QST713 gave mean inhibition haloes ranging from 29 to 31 mm, which were larger than those induced by D747 (22 to 24 mm) (Figure 1). The inhibition haloes produced by antibacterial compounds of each *Bacillus* strain were similar ($P > 0.05$) for the three *Psa* strains tested, belonging to the biovars 1 and 3 of the pathogen.

In the *in vitro* experiments using the diffusion method, streptomycin sulphate reduced the growth of D747 24-h-old living cells. At 25 and 50 ppm, mean inhibition haloes were, respectively, 7.2 and 8.5 mm, while in the control (SDW), the bacterial growth was not reduced, and no inhibition haloes were observed (Table 1).

In the macro-dilution experiments, streptomycin sulphate treatments of spore suspensions of both bio-products did not affect the bacterial populations, which were $c. 10^4$ cfu mL⁻¹, statistically similar to the populations in the control tubes ($c. 10^5$ cfu mL⁻¹). In contrast, at 24 h, streptomycin sulphate reduced the concentrations of D747 ($c. 10^4$ cfu mL⁻¹) and QST713 ($c. 10^4$ cfu mL⁻¹) strains, in comparison with the control ($c. 10^7$ cfu mL⁻¹). After 24 h the sensitivity to streptomycin sulphate

(100 ppm) was statistically similar for D747 and QST713 strains (Table 1).

In planta experiments

Controlled conditions

Strain D747, inoculated at high concentration, colonized the kiwifruit flowers up to 96 h after inoculation. After 1 h the concentration of bacteria was $c. 10^6$ cfu per flower, but from 24 to 72 h, the population rapidly increased, to $c. 10^8$ cfu per flower. At 96 h the population decreased to $c. 10^7$ cfu per flower. The strain QST713 was not able to colonize the flowers, but it could survive on them. The mean bacterial concentration was $c. 10^6$ cfu per flower from 1 to 48 h after application, while at 72 and 96 h, the population decreased to $c. 10^5$ cfu per flower. The concentrations of both antagonist strains were similar after 1 h. From 24 to 96 h, the populations of D747 were larger than those of QST713 (Figure 2). Flowers treated with SDW were free of *Bacillus* sp. No phytotoxicity was observed on flowers treated with Amylo-X[®] or Serenade Max[®].

On the same batch of flowers, the mutant *Psa* strain CRA-FRU 3.1rif^r colonized the flowers treated with SDW (controls) up to 72 h from inoculation. At 1 h, the recorded *Psa* population was $c. 10^6$ cfu per flower, and this increased to $c. 10^7$ and 10^8 cfu per flower at, respectively, 24 and 48 h. At 72 h, the population had decreased but remained high ($c. 10^7$ cfu per flower). On flowers treated with the antagonist strains, the *Psa* populations were significantly less than those on control flowers at most of the time points. After 1 h, the *Psa* populations on QST713-treated flowers was similar to that on those treated with SDW, but up to 96 h, the *Psa* populations were up to two orders of magnitude less than in the control. Similarly, the *Psa* populations on D747-treated flowers were less by more than one order of magnitude than those for the controls, at each time point. In general, QST713 more effectively reduced the *Psa* populations than D747, although QST713 had less ability to colonize flower surfaces than D747. After 1 h, the D747 treated flowers had less *Psa* ($c. 10^4$ cfu per flower) compared to flowers treated with QST713 or SDW ($c. 10^6$ cfu per flower). At 24 h, the *Psa* populations on D747- or QST713-treated flowers were less and with similar concentration ($c. 10^6$ cfu per flower) of those of the controls ($c. 10^7$ cfu per flower). From 48 to 72 h, the populations of *Psa* on flowers treated with both antagonists were reduced ($c. 10^{5-6}$ cfu per flower) compared to those on control flowers ($c. 10^{7-8}$ cfu per flower); in particular, in QST713-treated flowers, the *Psa* populations were less than those detected on flowers treated with D747 (Figure 2).

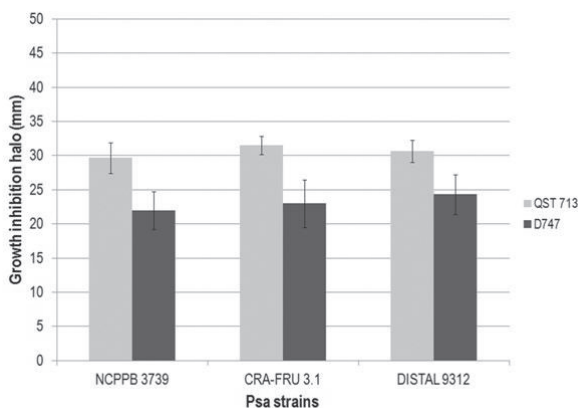


Figure 1. Mean diffusion plate proportions (%) of growth inhibition of three *Psa* strains (biovar 1, strain NCPPB 3739, biovar 3, strains CRA-FRU 3.1 and DISTAL 9312), caused by two strains of antagonistic *Bacillus* strains (QST 713, light histograms; D747, dark histograms). Bars indicate standard deviations ($P \leq 0.05$).

Table 1. Streptomycin sulphate concentrations (ppm) used against strains D747 and QST713 of *Bacillus* sp. for *in vitro* experiments using diffusion and macro-dilution methods.

Diffusion Method		
Strains (inoculated at time 0 h as living cells)	Streptomycin concentration	Growth inhibition halo (standard deviations)
Sterile Distilled Water (negative control)	/	0.00 mm (\pm 0.00)
D747 living cells	25 ppm (0.75 μg^*)	7.2 mm (\pm 0.3)
D747 living cells	50 ppm (1.50 μg^*)	8.5 mm (\pm 0.4)

Macro-dilution Method			
Strains (inoculated at time 0 h as spores)	Streptomycin concentration	Bacterial concentrations (standard deviations)	
		After 1 h	After 24 h
Sterile Distilled Water (negative control)	/	$3.7 \cdot 10^5$ cfu mL ⁻¹ ($\pm 1.3 \cdot 10^5$ cfu/mL)	$1.9 \cdot 10^7$ cfu/mL ($\pm 2.2 \cdot 10^6$ cfu/mL)
D747 spores (Amylo-X [*])	100 ppm	$7.2 \cdot 10^4$ cfu/mL ($\pm 6.9 \cdot 10^4$ cfu/mL)	$8.2 \cdot 10^3$ cfu/mL ($\pm 9.7 \cdot 10^3$ cfu/mL)
QST713 spores (Serenade Max [*])	100 ppm	$8.8 \cdot 10^4$ cfu/mL ($\pm 4.6 \cdot 10^4$ cfu/mL)	$4.2 \cdot 10^3$ cfu/mL ($\pm 4.0 \cdot 10^3$ cfu/mL)

*Streptomycin sulphate quantity in the antibiogram disk (μg).

The experiment performed on *A. deliciosa* plants under greenhouse conditions demonstrated the ability of Amylo-X^{*} to reduce the disease severity (bacterial leaf spots) caused by the inoculated Psa DISTAL 9312 strain. The disease severity was low in all treatments. In particular, the severity on plants treated with Amylo-X^{*} (mean = *c.* 2 spots per leaf) was statistically similar to that recorded on plants treated with streptomycin sulphate (positive control, *c.* 0.3 spots per leaf), and significantly lower than that on the negative controls (*c.* 4 spots per leaf). The disease severity on plants treated with Serenade Max^{*}, in contrast, was similar to the one of the negative control plants (*c.* 4 spots per leaf) (Figure 3).

In the experiment carried out on *A. chinensis* plants, the disease severity was higher than observed on *A. deliciosa* plants. These results confirmed the ability of Amylo-X^{*} to reduce bacterial leaf spot severity caused by the virulent Psa. The disease severity on the plants treated with Amylo-X^{*} (mean = *c.* 14 spots per leaf), was significantly lower than that on control plants (*c.* 62 spots per leaf). The severity was also reduced in the plants treated with Serenade Max^{*} (*c.* 32 spots per leaf), but this was higher than that in Amylo-X^{*} treated plants (Figure 3).

Field trials

On *A. deliciosa* plants in Emilia Romagna, the D747 strain survived on leaf surfaces for up to almost 4 weeks after Amylo-X^{*} application in both field experiments

(2017 and 2018). The D747 strain, employed in both trials at the same concentration, produced larger antagonist populations at 1 h after application in 2017 (*c.* 8×10^6 cfu cm⁻²), in comparison with 2018 (*c.* 2×10^6 cfu cm⁻²). This difference in population remained stable until 6 d, while from 9 to 27 d from application, the populations of D747 were similar in both experiments (10^5 cfu cm⁻²) (Figure 4).

In Latium region, the strain D747 survived on leaf surfaces with high populations for 28 d (from *c.* 10^4 to *c.* 10^5 cfu cm⁻²). In both experiments, the population dynamics of D747 were similar for the first assessments, up to 14 d from Amylo-X^{*} application (*c.* 10^{4-5} cfu cm⁻²). During 2017, populations of the antagonist at 21 and 28 days were larger (*c.* 10^5 cfu cm⁻²) than those evaluated in the second year (approx. 10^4 cfu cm⁻²) (Figure 4).

Although the antagonist populations on the kiwi-fruit trees in Latium were smaller than those recorded in Emilia Romagna from the first to the last assessments, the populations remained high for the whole assayed period.

The plants in the negative control treatments (untreated or SDW) were, in most cases, free of *Bacillus* species. In the other cases, some *Bacillus*-like colonies were found in the re-isolations (*c.* $10-10^2$ cfu mL⁻¹). At each assessment time point, selected re-isolated colonies were identified as strain D747, using BOX-PCR (Figure 1S).

In the assayed kiwifruit orchards, the use of Amylo-X^{*} led to a general reduction of bacterial wilt on diseased branches. In May, the mean disease severity index (DI) of 1-year-old branches in the D747-treated plot was *c.*

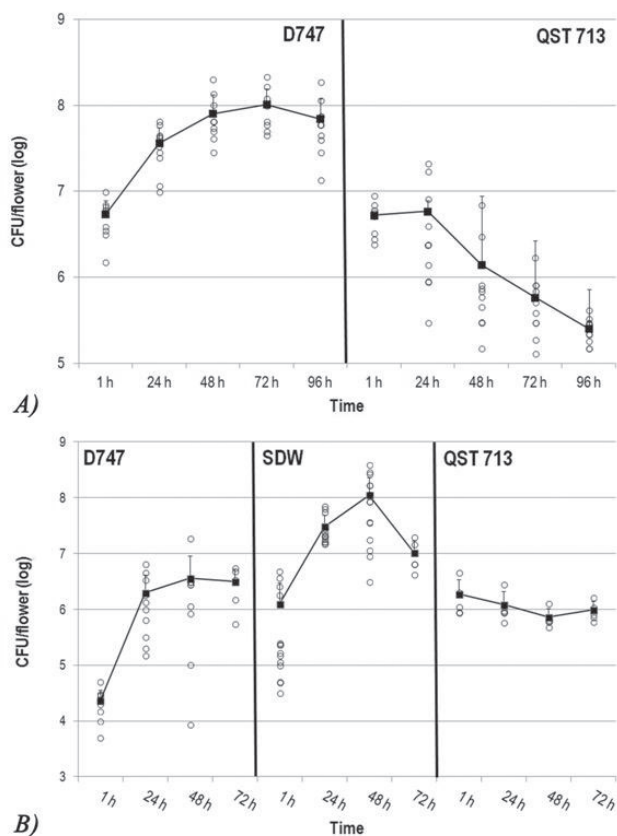


Figure 2. A) Colonization of *Bacillus* strain D747 on flowers of *A. chinensis* ‘Hort16A’ up to 96 h from its application. Empty circles indicate populations on each flower, and black squares and line indicate the mean populations on ten flowers (five flowers per experiment, two replicates). Bars indicate standard deviations ($P \leq 0.05$). B) Colonization of *Pseudomonas syringae* pv. *actinidiae* mutant strain CRA-FRU 3.1rif^r applied to flowers of *A. chinensis* ‘Hort16A’ flowers pre-treated with *Bacillus* spp. strains D747 or QST713, or sterile distilled water (SDW, control). The pathogen population was monitored for 72 h. Empty circles indicate CRA-FRU 3.1rif^r strain populations on each flower, and black squares and line indicate the mean populations present in ten flowers. Bars indicate standard deviations ($P \leq 0.05$).

0.16, while in the control (untreated plot) was *c.* 0.26. In June, the DIs were *c.* 0.17 for untreated and 0.32 from the D747-treated plants. At the last assessment (in September) the mean DI for Amylo-X[®] treated plants (0.26) was less than that in the experimental controls (0.43) (Figure 5).

For the 2-year-old branches, the DIs in both plots were higher than those recorded for 1-year-old branches. In May, the mean DI in Amylo-X[®]-treated plants was *c.* 0.30, significantly lower than that of the control plants (*c.* 0.42); in June, the mean DIs were 0.38 for the treated plot and 0.71 for the untreated plot. In September, the

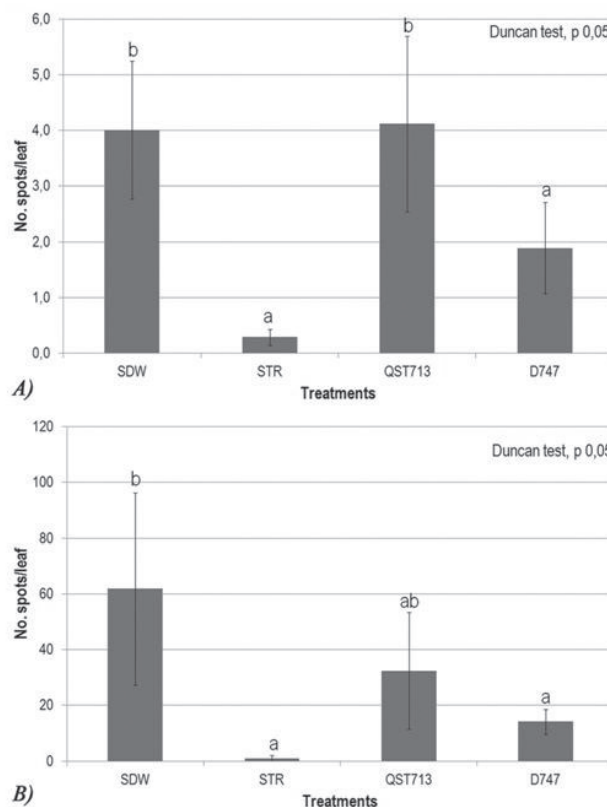


Figure 3. Mean bacterial leafspot severity after treatments with *Bacillus* strains applied to leaves of *A. deliciosa* (A) or *A. chinensis* (B) plants following inoculations with *Pseudomonas syringae* pv. *actinidiae* (strain DISTAL 9312). Treatments applied were: SDW (sterile distilled water, negative control); STR (streptomycin sulphate, positive control); QST713: *B. amyloliquefaciens* strain QST713 (active ingredient in Serenade Max[®]); D747: *B. amyloliquefaciens* strain D747 (in Amylo-X[®]). Bars indicate standard deviations. Histograms accompanied by different letters are different (Duncan’s test, $P \leq 0.05$).

mean DI for treated plants was *c.* 0.40, and less than that in untreated plants (*c.* 0.79) (Figure 5). The proportions of healthy leaves on 1- and 2-year-old branches in May was *c.* 70% in the control plot, less than in the treated plot (*c.* 80%). In June and in September, the proportions of healthy branches in the Amylo-X[®]-treated plot was similar (*c.* 78% in June and 75% in September) to that recorded in May; while in the untreated plot, these proportions were significantly decreased at the June (*c.* 35%) and September (*c.* 28%) assessments (Figure 6).

DISCUSSION

Bacillus bacteria have been described as microbial factories capable of producing many biologically active

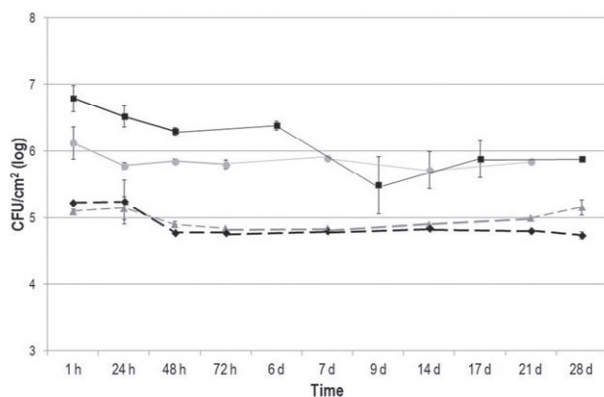


Figure 4. Mean numbers of *Bacillus amyloliquefaciens* strain D747 (active ingredient in Amylo-X[®]) on leaves of field-grown *Actinidia deliciosa* cv. Hayward plants, in Emilia Romagna (continuous line) or Lazio regions (dotted line) during the 2017 (light grey circles and triangles) or 2018 growing seasons (black squares and diamonds). Mean antagonist populations on leaf surfaces (cfu cm²) were monitored for 3 to 4 weeks. Bars indicate standard deviations ($P \leq 0.05$) for each time point.

compounds, which are potential inhibitors of phytopathogen growth. Examples are kanosamine and zwittermycin A from *B. cereus* (Emmert and Handelsman, 1999). The spore-forming capacity of *Bacillus* spp. makes these bacteria good candidates for development of efficient bio-pesticide products. *Bacillus* spp. are frequently used in biocontrol of plant pathogens, and includes a heterogeneous group of Gram-positive, aerobic or facultative anaerobic bacteria (Dworkin, 2006). These bacteria have been utilized for control of several plant diseases, including fire blight of pomaceous plants (caused by *Erwinia amylovora*) (Laux *et al.*, 2003; Broggini *et al.*, 2005; Bazzi *et al.*, 2006;), crown gall of grapevine (*Agrobacterium vitis*) (Biondi *et al.*, 2009b) and bacterial speck of tomato (caused by *P. syringae* pv. *tomato*) (Fousia *et al.*, 2016). *Bacillus* spp. act through a variety of mechanisms, including competition, induction of systemic host resistance, and production of antibacterial compounds, the last of these being commonly recognized as the most important (Zuber *et al.* 1993; Thomashow and Weller, 1996; Koumoutsi *et al.*, 2004; Reva *et al.*, 2004; Lahlali *et al.*, 2013; Chowdhury *et al.*, 2015).

In the present study, results obtained *in vitro* confirmed the capacity of both *Bacillus* strains in each of the biocontrol formulations tested to produce antibiotic compounds. The cell-free diffusion procedure was carried out with a minimal medium that contained low concentrations of nutrients and salts, as would be the case in host phyllospheres (Vanneste *et al.*, 1992). This activity highlighted the antibacterial abilities of both

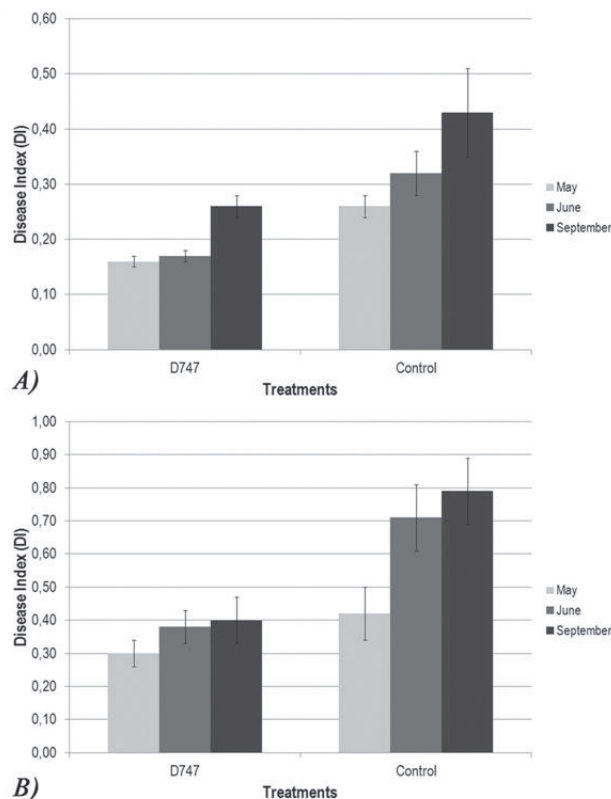


Figure 5. Mean bacterial leafspot indices (DI) caused by natural *Pseudomonas syringae* pv. *actinidiae* infections on kiwifruit plants after treatments with *Bacillus* strain D747 (active ingredient in Amylo-X[®]) or treated trees (control). The DIs were determined from phytopathometric assessments performed in May, June or September 2018, of leaves of 1-year-old (A) or 2-year-old (B) branches. Bars indicated standard deviations ($P \leq 0.05$).

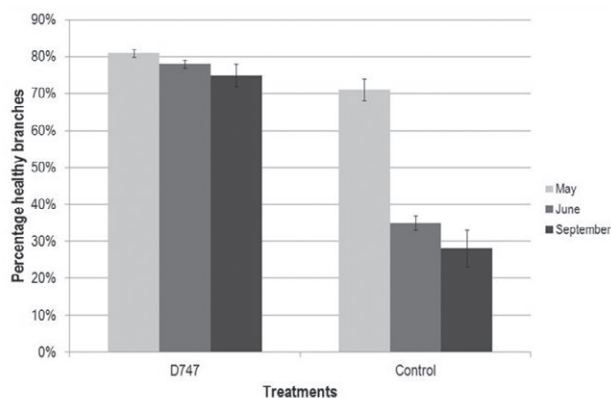


Figure 6. Mean percentage of healthy (disease free) 1-year and 2-year-old kiwifruit branches in May, June or September, 2018, in plots treated with *Bacillus* strain D747 (active ingredient of Amylo-X[®]) or controls (untreated plots) in a kiwifruit orchard in Latium region. Bars indicate standard deviations ($P \leq 0.05$).

antagonists under the unfavourable conditions. The effectiveness, isolation and identification of the antibacterial compounds produced by both antagonist strains have been assessed in previous studies. In particular, the strain QST713 was found to produce three families of non-ribosomal lipopeptides (LPs), the iturins, fengycins and surfactins (Mora *et al.*, 2011; Cawoy *et al.*, 2014). Strain D747 can produce surfactin, iturin and the serine proteinase subtilisin (Caulier *et al.*, 2019; EFSA, 2014). The *in vitro* activity of strains D747 and QST713 was also evaluated against *Xylella fastidiosa* (Zicca *et al.*, 2020), and these strains showed similar effectiveness against three Psa strains, one of biovar 1 and two of biovar 3. The QST713 strain resulted more antibacterial than strain D747.

The *in vitro* experiments assessing the activity of streptomycin sulphate against the two *Bacillus* strains QST713 and D747, carried out in solid and liquid media, showed the sensitivity of both strains to streptomycin sulphate. This antibiotic is commonly used against bacterial plant diseases. In the liquid medium experiment, the concentration of streptomycin sulphate was similar to that used in the field against bacterial diseases (Sundin *et al.*, 2009; Vanneste *et al.*, 2011a). From 0 h, the populations of both *Bacillus* strains were reduced by the antibiotic. After 24 h, the populations of QST713 and D747 were not completely eliminated, but were reduced by 3 to 4 orders of magnitude, thus confirming the need of significant reductions of antibiotic-based treatments applied in orchards, when these compounds are used in combination with biopesticides based on bacterial antagonists.

Flower colonization by strain D747 was higher than that of strain QST713, but strain QST713 survived at constant levels from application to 96 h. Strain D747 showed the highest population level after 72 h, which was more than one order of magnitude higher than that reported immediately after application. The BCA ability to colonize flowers indicated competition for nutrients and physical occupation of infection sites, as has been observed in previous studies. Psa can penetrate kiwifruit plants through stigmata and nectarii (Donati *et al.*, 2018), and the pathogen could be transmitted by contaminated pollen through natural and artificial pollination (Stefani *et al.*, 2011; Balestra *et al.*, 2018). Natural Psa populations can also predominate on *A. chinensis* compared with *A. deliciosa* flowers, indicating that the flowers of *A. deliciosa* may be less susceptible to penetration by the pathogen (Purahong *et al.*, 2018). Treatment of *A. chinensis* flowers with bacterial antagonists may protect against Psa infections, which rapidly become systemic, leading to the death of host plants (Renzi *et al.* 2012). In the present study, the high populations of both

antagonists affected populations of the inoculated Psa mutant strain, which were reduced by more than one order of magnitude compared to the controls, from 48 to 72 h after Psa inoculation.

The ability to colonize flowers made the strain D747 a good candidate for orchard trials to monitor its survival under field conditions. This strain survived on leaves of *A. deliciosa* for almost 1 month at high population levels (*c.* 10^{4-5} cfu cm⁻²), during 2 years in Emilia Romagna and Latium, located, respectively, in Northern and Central Italy. In Emilia Romagna, strain D747 was more abundant in both years than in Latium from the first assessment (1 h post inoculation). This may have been due to the type and/or time of treatment. The capacity of D747 to survive on kiwifruit leaves for long periods also indicates a reliable efficacy of this biocontrol agent.

Purahong *et al.* (2018) correlated the epiphytic bacterial populations present on leaves of kiwifruit plants to the ability of Psa to shape diversity of epiphytic bacterial populations, thus making the plants more susceptible to bacterial canker. Several bacterial genera were identified, particularly, *Bacillus* spp. were not significant compared to other genera. *Pseudomonas* species on leaves, including the pathogens *P. syringae* pv. *syringae* and *P. viridiflava*, were not predominant compared to the other genera, while on *A. deliciosa* these *Pseudomonas* species were predominant, ranging from 30 to 90%. In combination with the lower genetic susceptibility of kiwifruit plants with green fleshed fruit (EPPO, 2016; Perez *et al.*, 2019), treatments of leaves with D747 may protect from Psa penetration, and may reduce the subsequent secondary inoculum sources.

Under controlled conditions, the *A. deliciosa* plants were less susceptible to Psa than those of *A. chinensis*, which confirms previous results of intermediate susceptibility of *A. deliciosa* genotypes compared to several accessions of *A. chinensis* (Cotrut *et al.*, 2013; EPPO, 2016; Perez *et al.*, 2019). Results from the present study showed that Serenade Max[®] was ineffective against bacterial leaf spots in *A. deliciosa*, while Amylo-X[®] reduced the disease severity and provided relative protection of more than 52%. These results were partially confirmed by those on *A. chinensis* against the same pathogen strain; on plants producing yellow-fleshed fruit, Amylo-X[®] gave 77% relative protection, and Serenade Max[®] reduced the disease severity (relative protection *c.* 47%). The streptomycin sulphate treatment provided 93% relative protection on the green fruit variety and 98% relative protection on the yellow fruit variety.

The results on *A. deliciosa* plants, obtained under controlled conditions, partially confirmed those

obtained in similar environmental conditions by Collina *et al.* (2016). They showed that Serenade Max[®] applied 48 h before the pathogen inoculation reduced the disease severity and provided more than 60% relative protection. Amylo-X[®] was more efficient and provided approx. 80% relative protection. In the same study, the ability of both antagonists to reduce the disease severity was similar when they were applied 24 h before Psa inoculation, and both provided c. 40% relative protection.

In open field conditions (in Latium region) and with natural pathogen inoculation pressure, repeated applications of Amylo-X[®] reduced the bacterial canker severity and an increased the number of healthy branches during the entire host vegetative season, in comparison to the control plants. Up to September, where the disease severity was higher in untreated plants, Amylo-X[®] provided 40-50% relative protection on all leaves. On the leaves of 2-years-old branches, the disease severity was reduced by more than 50% compared to control plants. The orchard results confirmed those obtained under controlled conditions. The strain D747-based product consistently reduced bacterial canker severity and achieved protective action against new and re-infections by Psa. This was confirmed by the higher proportions of healthy leaves on all branches (1-year and 2-year old branches) in plants treated with Amylo-X[®] compared to control plants, in all the assessments. On control plants, the disease incidence was higher at each assessment. On plants treated with the antagonist, although the disease increased at each assessment, the incidence was always lower. Daranas *et al.* (2018) have also demonstrated the effectiveness of Amylo-X[®] against bacterial canker of kiwifruit, in semi-field and field conditions. The ability of Serenade Max[®] to reduce kiwifruit bacterial canker was not optimal as against different bacterial pathogens, including those causing bacterial spot of stone fruits, angular leaf spot of strawberry and fire blight of pomaceous plants, although the product reduced the disease incidence and severity (Biondi *et al.*, 2006; Daranas *et al.*, 2018). The reduction of secondary inoculum sources, provided by the first treatments assessed during the optimal environmental conditions for the pathogen (spring, early summer), and the persistence of the antagonist strain D747 on the leaves surfaces throughout the growth season, emphasised the ability of this *Bacillus* strain to survive efficiently in the phyllospheres, and its capacity to persist under the microclimatic conditions of kiwifruit orchards. The Psa infections were detectable until September, but on Amylo-X[®]-treated plants the disease severity was reduced, confirming the ability of strain D747 to survive in different environmental conditions, including the high temperatures during summer.

Bacillus species can form heat-, aridity-, and radiation-tolerant endospores allowing survival under non-optimal conditions (Dworkin, 2006).

In addition, when evaluated on flowers, those treated with Serenade Max[®] and Amylo-X[®], in the climatic chamber and in the field, did not show phytotoxicity.

Purahong *et al.* (2018) showed that *Bacillus* species are not predominant on leaves, with respect of the other bacterial genera. Further research is required to evaluate the influence of *Bacillus* based products on the phyllosphere microbiomes during and after the crop growing season. Risks to biodiversity on kiwifruit organs should be prevented, both by reducing the use of agrochemicals, and by avoiding the persistence of bacterial antagonists (EFSA, 2014; Montesinos *et al.*, 2009).

CONCLUSIONS

This study has demonstrated that the bio-product Amylo-X[®] could be an effective tool for biological control of kiwifruit bacterial canker, because of efficacy against Psa and survival of the D747 *Bacillus* strain, the principal component of Amylo-X[®], on kiwifruit flowers and leaves. The study has also demonstrated that this biocontrol agent is not compatible with antibiotic-based treatments against Psa.

ACKNOWLEDGEMENTS

The authors acknowledge the Italian Ministry for Education, University and Research (MIUR) for financial support for this research (Law 232/216, Department of Excellence).

LITERATURE CITED

- Abelleira A., López M., Peñalver J., Aguin O., Mansilla J., ...García M., 2011. First report of bacterial canker of kiwifruit caused by *Pseudomonas syringae* pv. *actinidiae* in Spain. *Plant Disease* 95(12): 1583–1583.
- Balestra G.M., 2007. Biocontrol of bacterial pathogens of kiwifruit plants. *Acta Horticulturae* 753: 635–638.
- Balestra G., Bovo M., 2003. Efficacy of copper compounds in the control of bacterial diseases on kiwifruit plants. *Acta Horticulturae* 610: 399–402.
- Balestra G.M., Taratufolo M.C., Vinatzer B.A., Mazzaglia A., 2013. A multiplex PCR assay for detection of *Pseudomonas syringae* pv. *actinidiae* and differentiation of populations with different geographic origin. *Plant Disease* 97: 472–478.

- Balestra G.M., Buriani G., Cellini A., Donati I., Mazzaglia A., Spinelli F., 2018. First report of *Pseudomonas syringae* pv. *actinidiae* on kiwifruit pollen from Argentina. *Plant Disease* 102(1): 237. <https://doi.org/10.1094/PDIS-04-17-0510-PDN>.
- Bazzi C., Biondi E., Berardi R., Brunelli A., 2006. Efficacy of bioagents and chemicals against pear shoot blight. *Acta Horticulturae* 704: 283–287.
- Biondi E., Bazzi C., Vanneste J.L., 2006. Reduction of fire blight incidence on apple flowers and colonization of pear shoots in experimental orchards using *Pseudomonas* spp. IPV-BO G19 and IPV-BO 3371. *Acta Horticulturae* 704: 323–327.
- Biondi E., Dallai D., Brunelli A., Bazzi C., Stefani E., 2009a. Use of a bacterial antagonist for the biological control of bacterial leaf/fruit spot of stone fruits. *IOBC Bulletin* 43: 277–281.
- Biondi E., Bini F., Anaclerio F., Bazzi C., 2009b. Effect of bioagents and resistance inducers on grapevine crown gall. *Phytopathologia Mediterranea* 48: 379–384.
- Biondi E., Galeone A., Kuzmanovic N., Ardizzi S., Lucchese C., Bertaccini A., 2013. *Pseudomonas syringae* pv. *actinidiae* detection in kiwifruit plant tissue and bleeding sap. *Annals of Applied Biology* 162(1): 60–70.
- Biondi E., Zamorano A., Vega E., Ardizzi S., Sitta D., ... Fiore N., 2018. Draft whole genome sequence analyses on *Pseudomonas syringae* pv. *actinidiae* hypersensitive response negative strains detected from kiwifruit bleeding sap samples. *Phytopathology* 108: 1–9.
- Borriss R., 2011. Use of plant-associated *Bacillus* strains as biofertilizers and biocontrol agents, in agriculture. In: *Bacteria in Agrobiolgy: Plant Growth Responses*, (D.K. Maheshwari, Heidelberg ed.), Springer, New York, USA, 41–76 pp.
- Broggini G.A.L., Duffy B., Holliger E., Schärer J.H., Gessler C., Patocch A., 2005. Detection of the fire blight biocontrol agent *Bacillus subtilis* BD170 (Bio-pro[®]) in a Swiss apple orchard. *European Journal of Plant Pathology* 111(2): 93–100.
- Butler M.I., Stockwell P.A., Black M.A., Day R.C., Lamont I.L., Poulter R.T.M., 2013. *Pseudomonas syringae* pv. *actinidiae* from recent outbreaks of kiwifruit bacterial canker belong to different clones that originated in china. *PlosOne* doi.org/10.1371/journal.pone.0057464.
- Cameron A., Sarojini V., 2013. *Pseudomonas syringae* pv. *actinidiae*: chemical control, resistance mechanisms and possible alternatives. *Plant Pathology* 63(1): 1–11.
- Caulier S., Nannan C., Gillis A., Licciardi F., Bragard C., Mahillon J., 2019. Overview of the antimicrobial compounds produced by members of the *Bacillus subtilis* group. *Frontiers in Microbiology* 10: 302.
- Cawoy H., Debois D., Franzil L., De Pauw E., Thonart P., Ongena M., 2014. Lipopeptides as main ingredients for inhibition of fungal phytopathogens by *Bacillus subtilis/amyloliquefaciens*. *Microbial Biotechnology* 8(2): 281–295.
- Cellini L., Fiorentini L., Buriani,G., Yu J., Donati I., ... Spinelli, F., 2014. Elicitors of salicylic acid pathway reduce bacterial canker of kiwifruit. *Annals of Applied Biology* 165(3): 441–13.
- Chen X.H., Koumaoutsi A., Scholz R., Schneider K., Vater J., ...Borriss R., 2009. Genome analysis of *Bacillus amyloliquefaciens* FZB42 reveals its potential biocontrol of plant pathogens. *Journal of Biotechnology* 140: 27–37
- Chowdhury S.P., Hartmann A., Gao X., Borriss, R., 2015. Biocontrol mechanism by root-associated *Bacillus amyloliquefaciens* FZB42 – A review. *Frontiers in Microbiology* 6: 780.
- Collina M., Donati I., Bertacchini E., Brunelli A., Spinelli F., 2016. Greenhouse assays on the control of the bacterial canker of kiwifruit (*Pseudomonas syringae* pv. *actinidiae*). *Journal of Berry Research* 6: 407–415.
- Cortesi R., Quattrucci A., Esposito E., Mazzaglia A., Balestra G.M., 2017. Natural antimicrobials in spray-dried microparticles based on cellulose derivatives as potential eco-compatible agrochemicals. *Journal of Plant Diseases and Protection* 124, 3, 269–278.
- Cotrut R., Renzi M., Taratufolo M.C., Mazzaglia A., Balestra G.M., Stanica F., 2013. *Actinidia arguta* ploidy level variation in relation to *Pseudomonas syringae* pv. *actinidiae* susceptibility. *Lucrări Științifice* 56 (1), 29–38.
- Crosse, J. E., 1959. Bacterial canker of stone-fruits: IV. Investigation of a method for measuring the inoculum potential of cherry trees. *Annals of Applied Biology* 47: 306–317.
- Cunty A., Poliakoff F., Rivoal C., Cesbron S., Fischer M., ...Vanneste J.L., 2015. Characterization of *Pseudomonas syringae* pv. *actinidiae* (Psa) isolated from France and assignment of Psa biovar 4 to a de novo pathovar: *Pseudomonas syringae* pv. *actinidifoliorum* pv. nov. *Plant Pathology* 64: 582–596.
- Daranas N., Roselló G., Cabrefiga J., Donati I., Francés J., ...Bonaterra A., 2018. Biological control of bacterial plant diseases with *Lactobacillus plantarum* strains selected for their broad-spectrum activity. *Annals of Applied Biology* 174: 92–105.
- De Jong H., Reglinski T., Elmer P.A.G., Wurms K., Vanneste J.L., .. Alavi M., 2019. Integrated use of *Aureobasidium pullulans* strain CG163 and acibenzolar-s-methyl for management of bacterial canker in kiwifruit. *Plants* 8: 287.

- Dong H., Delaney T.P., Bauer D.W., Beer S.V., 1999. Harpin induces disease resistance in *Arabidopsis* through the systemic acquired resistance pathway mediated by salicylic acid and the NIM1 gene. *The Plant Journal* 20: 207–15.
- Donati I., Cellini A., Buriani G., Mauri S., Kay C., ... Spinelli F., 2018. Pathways of flower infection and pollen-mediated dispersion of *Pseudomonas syringae* pv. *actinidiae*, the causal agent of kiwifruit bacterial canker. *Horticulture Research* 5: 56.
- Dworkin M., 2006. Prokaryotic life cycles. In: *Prokaryotes* (M. Dworkin, S. Falkow, E. Rosenberg, K. -H. Schleifer, E. Stackebrandt ed.), Springer, New York, USA, 2:140–166.
- EFSA, European Food Safety Authority (2014). Conclusion on the peer review of the pesticide risk assessment of the active substance *Bacillus amyloliquefaciens* subsp. *plantarum* strain D747. *EFSA Journal* 12(4): 3624.
- Emmert E.A.B., Handelsman J., 1999. Biocontrol of plant disease: a (Gram-) positive perspective. *FEMS Microbiological Letters* 171: 1–9.
- EPPO, European and Mediterranean Plant Protection Organization, 2016. PM 7/120 (1) *Pseudomonas syringae* pv. *actinidiae*. *Bulletin OEPP/EPPO Bulletin* 44 (3): 360–375.
- Fortunati E., Rescignano R., Botticella E., La Fiandra D., Marsilio M., ... Balestra G.M., 2016. Effect of poly (DL-Lactide-co-Glycolide) nanoparticles or cellulose nanocrystals based formulations on *Pseudomonas syringae* pv. *tomato* (Pst) and tomato plant development. *Journal of Plant Diseases and Protection* 123: 301–310.
- Fortunati E., Verma D., Luzi F., Mazzaglia A., Torre L., Balestra G.M., 2017. Novel nanoscaled materials from lignocellulosic sources: potential applications in the agricultural sector. In: *Handbook of Ecomaterials* (L. Myriam, T. Martínez, O.V. Kharissova, B.I. Khari-sov Springer International Publishing ed.), Cham, Switzerland, 1-24.
- Fortunati E., Balestra G.M., 2018. Overview of novel and sustainable antimicrobial nanomaterials for agri-food applications. *Nanomedicine and Nanotechnology Journal* 1: 1-15.
- Fousia S., Paplomatas E.J., Tjamos S.E., 2016. *Bacillus subtilis* QST713 confers protection to tomato plants against *Pseudomonas syringae* pv. *tomato* and induces plant defence-related genes. *Journal of Phytopathology* 164: 264–270.
- Frampton R.A., Taylor C., Holguín Moreno A.V., Visnovsky S.B., Petty N. K., ... Fineran P.C., 2014. Identification of bacteriophages for biocontrol of the kiwifruit canker phytopathogen *Pseudomonas syringae* pv. *actinidiae*. *Applied and Environmental Microbiology* 80 (7): 2216–2228.
- Fujikawa T., Sawada H., 2019. Genome analysis of *Pseudomonas syringae* pv. *actinidiae* biovar 6, which produces the phytotoxins, phaseolotoxin and coronatine. *Scientific Reports* 9: 3836.
- Gallelli A., Talocci S., Pilotti M., Loreti S., 2013. Real-time and qualitative PCR for detecting *Pseudomonas syringae* pv. *actinidiae* isolates causing recent outbreaks of kiwifruit bacterial canker. *Plant Pathology* 63: 264–276.
- Goto M., Hikota T., Nakajima M., Takikawa Y., Tsuyumu S., 2004. Occurrence and properties of copper resistance in plant pathogenic bacteria. *Annals of the Phytopathological Society of Japan* 60: 147.
- Hoyte S., Elmer P., Parry F., Phipps J., Spiers M., ... McBrydie H., 2018. Development of a new biocontrol product (AUREO® Gold) for control of *Pseudomonas syringae* pv. *actinidiae* in kiwifruit. *IOBC-WPRS Bulletin* 133: 164–166.
- King E.O., Raney M.K., Ward D.E., 1954 Two simple media for the demonstration of pyocyanin and fluorescein. *Journal of Laboratory and Clinical Medicine* 44: 301–307.
- Koh Y., Park S., Lee D., 1996. Characteristics of bacterial canker of kiwifruit occurring in Korea and its control by trunk injection. *Korean Journal of Plant Pathology* 12: 324–330.
- Koumoutsis A., Chen X.H., Henne A., Liesegang H., Hitzeroth G., ... Borriss R., 2004. Structural and functional characterization of gene clusters directing non-ribosomal synthesis of bioactive cyclic lipopeptides in *Bacillus amyloliquefaciens* strain FZB 42. *Journal of Bacteriology* 186: 1084–1096.
- Lahlali R., Peng G., Gossen B.D., McGregor L., Yu F.Q., Boyetchko S.M., 2013. Evidence that the biofungicide serenade (*Bacillus subtilis*) suppresses clubroot on canola via antibiosis and induced host resistance. *Phytopathology* 103:245–254.
- Laux P., Wesche J., Zeller W., 2003. Field experiments on biological control of fire blight by bacterial antagonists. *Journal of Plant Diseases and Protection* 110(4): 401–407.
- Lee J.H., Kim J.H., Kim G.H., Jung J.S., ... Koh Y.J., 2005. Comparative analysis of Korean and Japanese strains of *Pseudomonas syringae* pv. *actinidiae* causing bacterial canker of kiwifruit. *Plant Pathology Journal* 21(2): 119–126.
- Marcelletti S., Ferrante P., Petriccione M., Firrao G., Scortichini M., 2011. *Pseudomonas syringae* pv. *actinidiae* draft genomes comparison reveal strain-specific fea-

- tures involved in adaptation and virulence to *Actinidia* species. *Plos One* 6(11): e27297.
- Mazzaglia A., Studholme D.J., Taratufolo M.C., Cai R., Almeida N.F., ...Balestra G.M., 2012. *Pseudomonas syringae* pv. *actinidiae* (PSA) isolates from recent bacterial canker of kiwifruit outbreaks belong to the same genetic lineage. *Plos One* 7(5): e36518.
- Mazzaglia A., Fortunati E., Kenny J.M., Torre L., Balestra G.M., 2017. Nanomaterials in plant protection. In: *Nanotechnology in Agriculture and Food Science* (M.A.V. Axelos and M. van De Voorde ed.), Wiley-VCH GmbH & Co. 7:408: 115–133.
- McSpadden Gardener B.B., Fravel D.R., 2002. Biological control of plant pathogens: Research, commercialization and application in the USA. *Plant Health Progress* 3(1).
- McSpadden Gardener B.B., Driks A., 2004. Overview of the nature and applications of biocontrol microbes: *Bacillus* spp. *Phytopathology* 94: 1244.
- Michelotti V., Lamontanara A., Buriani G., Orrù L., Cellini A., Spinelli F., 2018. Comparative transcriptome analysis of the interaction between *Actinidia chinensis* var. *chinensis* and *Pseudomonas syringae* pv. *actinidiae* in absence and presence of acibenzolar-S-methyl. *BMC Genomics* 19(1): 585.
- Montesinos E., Pujol M., Badosa E., 2009. Quantitative strain specific molecular methods for monitoring and ecological fitness studies of biological control agents. *IOBC Bulletin* 43: 53–57.
- Mora I., Cabrefiga J., Montesinos E., 2011. Antimicrobial peptide genes in *Bacillus* strains from plant environments. *International Microbiology* 14:213–223.
- Nakajima M., Goto M., Hibi T., 2002. Similarity between copper resistance genes from *Pseudomonas syringae* pv. *actinidiae* and *P. syringae* pv. *tomato*. *Journal of General Plant Pathology* 68: 68–74.
- Perez S., Biondi E., Giuliani D., Bertaccini A., Comuzzo G., Testolin R., 2019. Preliminary results on susceptibility to bacterial canker of *Actinidia* spp. accessions. *Acta Horticulturae* 1243: 115–120.
- Purahong W., Orrù L., Donati I., Perpetuini G., Cellini A., ...Spinelli F., 2018. Plant microbiome and its link to plant health: host species, organs and *Pseudomonas syringae* pv. *actinidiae* infection shaping bacterial phyllosphere communities of kiwifruit plants. *Frontiers in Plant Science* 9: 1563.
- Quattrucci A., Ovidi E., Tiezzi A., Vinciguerra V., Balestra G.M., 2013. Biological control of tomato bacterial speck using *Punica granatum* fruit peel extract. *Crop Protection* 46: 18–22.
- Rees-George J., Vanneste J., Cornish D., Pushparajah I., Yu J., ...Everett K., 2010. Detection of *Pseudomonas syringae* pv. *actinidiae* using polymerase chain reaction (PCR) primers based on the 16S-23S rDNA inter transcribed spacer region and comparison with PCR primers based on other gene regions. *Plant Pathology* 59: 453–464.
- Renzi M., Mazzaglia A., Balestra G.M., 2012. Widespread distribution of kiwifruit bacterial canker by the European genotype of *Pseudomonas syringae* pv. *actinidiae* in the main production areas of Portugal. *Phytopathologia Mediterranea* 51: 402–409.
- Reva O.N., Dixelius C., Meijer J., Priest F.G., 2004. Taxonomic characterization and plant colonizing abilities of some bacteria related to *Bacillus amyloliquefaciens* and *Bacillus subtilis*. *FEMS Microbiology Ecology* 48(2): 249–259.
- Ridé M., Ridé S., Novoa D., 1983. Connaissances actuelles sur la necrose bacterienne de la vigne [*Xanthomonas ampelina*; evolution, symptomes, cycle biologique, lutte, fongicides]. *Bulletin Technologique du Pyrenees Orientales* 106: 10–45.
- Rossetti A., Mazzaglia A., Muganu M., Paolocci M., Sguizzato M. ...Balestra G.M., 2017. Microencapsulated formulations of gallic and ellagic acids for biological control of bacterial diseases of kiwifruit plants. *Journal of Plant Diseases and Protection* 124(6): 563–575.
- Stefani E., Giovanardi D., 2011. Dissemination of *Pseudomonas syringae* pv. *actinidiae* through pollen and its epiphytic life on leaves and fruits. *Phytopathologia Mediterranea* 50: 489–496.
- Stewart A., Hill R., Stark C., 2011. Desktop evaluation on commercially available microbial-based products for control or suppression of *Pseudomonas syringae* pv. *actinidiae*. *Bio-Protection Research Centre – Report No 1*: 1–26.
- Sundin G.W., Werner N.A., Yoder K.S., Aldwinckle H.S., 2009. Field evaluation of biological control of fire blight in the eastern United States. *Plant Disease* 93: 386–394.
- Thomashow L.S., Weller D.M., 1996. Current concepts in the use of introduced bacteria for biological disease control: mechanisms and antifungal metabolites. In: *Plant-Microbe Interactions* (G. Stacey and N. T. Keen, ed.), Springer Nature, Switzerland, 1: 187–235.
- Vanneste J.L., 2017. The scientific, economic, and social impacts of the New Zealand outbreak of bacterial canker of kiwifruit (*Pseudomonas syringae* pv. *actinidiae*). *Annual Review of Phytopathology* 55(1): 377–399.
- Vanneste J.L., Yu J., Beer S.V., 1992. Role of antibiotic production by *Erwinia herbicola* Eh252 in biological control of *Erwinia amylovora*. *Journal of Bacteriology* 174(9): 2785–2796.

- Vanneste J.L., Kay C., Onorato R., Yu J., Cornish D., ...
pv. *actinidiae*, the causal agent of bacterial canker on
kiwifruit. *Acta Horticulturae* 913: 443–455.
- Vanneste J.L., Giovanardi D., Yu J, Cornish D.A., Kay C.,
...Stefani E., 2011b. Detection of *Pseudomonas syringae*
pv. *actinidiae* in kiwifruit pollen samples. *New
Zealand Plant Protection* 64: 246.
- Vanneste J.L., Yu J, Cornish D., Tanne, D., Windner R.,
...Dowlut S., 2013. Identification, virulence, and dis-
tribution of two biovars of *Pseudomonas syringae* pv.
actinidiae in New Zealand. *Plant Disease* 97: 708–
719.
- Versalovic J., Schneider G.M., de Bruijn F.J., Lupski J.R.,
1994. Genomic fingerprint of bacteria using repeti-
tive sequence-based polymerase chain reaction.
Methods in Molecular and Cellular Biology 1: 25–40.
- Zicca S., De Bellis P., Masiello M., Saponari M., Sal-
darelli P.,...Sisto A., 2020. Antagonistic activity of
olive endophytic bacteria and of *Bacillus* spp. strains
against *Xylella fastidiosa*. *Microbiological Research*
236:126467.
- Zuber P., Nakano M.M, Marahiel M.A., (1993). Peptide
antibiotics. In: *Bacillus subtilis* and other Gram-pos-
itive bacteria (A.L. Sonenshein, J.A. Hoch, R. Losick,
ed.), ASM Press, Washington, USA, 897–916.



Citation: A. Yirgu, A. Gezahgne, T. Alemu, M. Havenga, L. Mostert (2021) First report of *Didymosphaeria rubi-ulmifolii* associated with canker and dieback of apple trees in southern Ethiopia. *Phytopathologia Mediterranea* 60(2): 229-236. doi: 10.36253/phyto-12400

Accepted: March 17, 2021

Published: September 13, 2021

Copyright: © 2021 A. Yirgu, A. Gezahgne, T. Alemu, M. Havenga, L. Mostert. This is an open access, peer-reviewed article published by Firenze University Press (<http://www.fupress.com/pm>) and distributed under the terms of the Creative Commons Attribution License, which permits unrestricted use, distribution, and reproduction in any medium, provided the original author and source are credited.

Data Availability Statement: All relevant data are within the paper and its Supporting Information files.

Competing Interests: The Author(s) declare(s) no conflict of interest.

Editor: Vladimiro Guarnaccia, DiSAFA - University of Torino, Italy.

Research Papers

First report of *Didymosphaeria rubi-ulmifolii* associated with canker and dieback of apple trees in southern Ethiopia

ABRAHAM YIRGU^{1,*}, ALEMU GEZAHGNE¹, TESFAYE ALEMU², MINETTE HAVENGA³, LIZEL MOSTERT³

¹ Central Ethiopia Environment and Forest Research Center, P.O.Box 33042, Addis Ababa, Ethiopia

² College of Natural and Computational Sciences, Addis Ababa University P.O.Box 1176, Ethiopia

³ Department of Plant Pathology, Stellenbosch University, Private Bag X1, Matieland, 7602, South Africa

*Corresponding author. E-mail address: abrahamyirguw@gmail.com

Summary. Cultivation of apple trees in the highlands of Ethiopia began in 1955. In 2014, blistering of the bark due to cankers on the main stems mostly below the grafting points, followed by dieback and eventually death of apple trees, was observed in apple orchards in the Hadiya Zone in Ethiopia. This study aimed to identify the causal agent of canker and dieback symptoms on the apple trees. Symptomatic trunks from 20 trees (ten per cultivar) were sampled. Isolations were performed from ten trunks (five per cultivar). Fungus colonies with similar cultural features were obtained from all the samples, and the morphology of a representative isolate was characterized. Phylogenetic analyses of the concatenated internal transcribed spacers 1 and 2 and 5.8S rRNA gene, large subunit and actin gene regions confirmed the identity of two isolates as *Didymosphaeria rubi-ulmifolii*. Pathogenicity was confirmed for one isolate by inoculations of healthy branches of 'Anna' and 'Dorsett Golden' apple trees resulting in lesion formation, and subsequent re-isolation of the inoculated fungus. This study is the first report of *D. rubi-ulmifolii* associated with dieback of apple trees. This pathogen caused death of more than 26% of apple trees in one commercial orchard, and could cause severe losses for smallholder apple growers in Ethiopia. Future studies are required to assess the magnitude, distribution and management options of this economically important canker disease in Ethiopia.

Keywords. *Malus pumila*, *Paraconiothyrium brasiliense*, stem canker.

INTRODUCTION

Malus pumila Mill. (Rosaceae; syn. *M. domestica* Borkh.) is native to southwest Asia (Hedberg *et al.*, 1989), and apple is the fourth most important horticultural fruit crop in the world and is by far atypical temperate fruit tree that can reach 8–12 m high (Hedberg *et al.*, 1989; Tromp, 2005; Bekele-

Tesemma, 2007; FAO, 2010). Although originating and common in temperate regions, apple trees are grown at 2,300 m above sea level in many tropical and subtropical regions, and have become an increasingly important source of income in Ethiopia (Erez, 2000; Bekele Tesemma, 2007). Commercial apple cultivars are grafted on seed grown rootstocks.

Around 1955, missionaries established apple orchards (medium and high-chilling cultivars) in the Chencha highlands of the Southern Nations and Nationalities People (SNNP) Regional state of Ethiopia (Fetena *et al.*, 2014). This region has minimum temperatures of 11 to 13°C and maxima of 18 to 23°C, 900 to 1200 mm annual rainfall, and altitudes of 2300 to 3250 m (Hailemichael, 2006). In recent decades, government and non-government organizations have engaged in propagation of low-chilling grafted apple trees and rootstocks from abroad to improve the livelihood and income of the rural communities in this region. Approximately 138,000 plants (105,000 grafted apples and 33,000 rootstocks) were imported between 1998 to 2007 (Sisay, 2007).

As apple production has expanded, the impacts of biotic agents have increased. Assessments in Chencha and Bonke districts showed that apple scab, powdery mildew, green aphids, scale insects and green plant bugs were the most serious apple diseases and pests (Fetena and Lemma, 2014; Fetena *et al.*, 2014). In addition to significant losses in the production from 'Bond's Red Royal Gala', 'Crispin' and 'Jona Gold', 'Royal Gala' was replaced by 'Crispin' in Chencha district, due to susceptibility of 'Royal Gala' to apple scab (Fetana and Lemma, 2014). White root rot, caused by *Rosellinia necatrix* Berl. ex Prill., also caused death of mother apple trees and grafted plants. The MM106 rootstock, which was once considered as a superior rootstock for Chencha district, was found to be susceptible to crown rot on poorly drained soils (Fetena *et al.*, 2014).

In early 2014, extensive damage due to cankers and dieback was observed on apple trees at Gibagri Farm, located in SNNP Regional State in Ethiopia. The study described here was carried out to identify the causal agent of this disease.

MATERIALS AND METHODS

Sample collection, isolation and characterization of pathogenic fungus

The Foke orchard of Gibagri Farm PLC, is situated at Olewa Peasant Association in Gibe District, Hadiya Zone in SNNPR in Ethiopia, about 260 km from the capital city Addis Ababa. The district has a wet *Woina*

Dega climate, with annual rainfall of 1100 mm, with Nitosol reddish loamy and deeply structured soil (pH 5 to 6), and altitude of 2,000 m. Gibagri Farm PLC grows the apple 'Anna', 'Princesa' and 'Dorsett Golden' imported from Spain in 2009 and 2012, on 14 ha of land. Field survey was conducted in Foke Orchard in December 2015. Symptomatic trunk samples from 20 apple trees, ten each from 'Anna' and 'Dorsett Golden' grafted on rootstocks M7, MM111 and MM106, were systematically sampled and collected, as described by Cloete *et al.* (2011). These samples were separately packed in paper bags, labeled and brought to the Forest Protection Laboratory of the Central Ethiopia Environment and Forest Research Center (CEE-FRC), Addis Ababa. In the laboratory, samples were kept at 4°C in a refrigerator before further analysis.

Three to four segments of wood fragments were collected from the margins between necrotic and healthy tissues of five symptomatic apple trunks per cultivar. The fragments were excised into approx. 2×2 cm pieces. These were then surface sterilized in 70% ethanol followed by 5% sodium hypochlorite, each for 2 min., and then rinsed in sterilized distilled water. The tissue pieces were then air-dried, each aseptically halved using a sterile knife, and then placed in 90 mm diam. Petri dishes containing malt extract agar (MEA, Oxoid Ltd) amended with 100 mg of streptomycin sulphate. In addition, cross-sections cut from stems showing disease symptoms on both sides were placed in 19.5 mm diam. Petri dishes with moistened double-layered filter paper to induce pycnidium formation. The filter papers were regularly monitored and moistened with distilled water. All dishes were placed on a laboratory bench and incubated in 12 h light and 12 h dark, at 20 to 25°C room temperature. Emerging mycelia and pycnidia were transferred to potato dextrose agar (PDA; Oxoid Ltd.) amended with streptomycin sulphate.

The growth characteristics of the isolated fungus were determined based on mycelium growth rate and colony colour on PDA after 7 d incubation at 25°C in darkness. Pycnidium formation in a moist chamber was also examined under a dissecting microscope. Sporulation of the isolated fungus was induced by transferring mycelia from the margin of 7-d-old pure cultures onto 20 g L⁻¹ water agar supplemented with sterilized pine needles (Su *et al.*, 2012). Based on morphological similarities, a fungus isolate obtained from 'Anna' was designated as AY-1 and an isolate from 'Dorsett Golden' was designated as AY-2. Dimensions (length and width) and shape of 50 conidia from the AY-1 isolate were measured and described at 400× magnification using an Olympus BX 63 camera-mounted microscope. Conidiomata

were sectioned (10 µm thick) with a freeze microtome and measured at 400× and 1000× magnification using a Nikon Eclipse E600 compound microscope with a Nikon DMX1200C digital camera attachment. Ten conidiomata and 30 conidiogenous cells were measured. Cultures of both isolates were deposited at the Ethiopian Biodiversity Institute and Forest Protection laboratory of CEE-FRC.

Molecular characterization and phylogenetic analysis

DNA was extracted from 4-d-old cultures of isolates AY-1) and AY-2), and the regions were amplified of the internal transcribed spacers 1 and 2 and 5.8S rRNA (ITS), 28S rRNA the large subunit (LSU) and the partial actin (ACT) genes. The primers used for these regions were V9G/LS266 for ITS, LROR/LR6 for LSU and ACT512F/ACT783R for ACT. The PCR conditions and sequencing were as described by Samson *et al.* (2010), and were carried out at the Westerdijk Fungal Biodiversity Institute (CBS), AD Utrecht, the Netherlands. Consensus sequences were made from the forward and reverse sequences, and were lodged in GenBank (MK167444 to MK167448). For phylogenetic analysis, sequences generated by Ariyawansa *et al.* (2014) were added as reference sequences. *Kalmusia longisporum* CBS 582.83 was included as the out-group. Newly generated sequences of the three gene regions were aligned separately using the E-INS-i algorithm in the MAFFT plugin of Geneious R9 software (Katoch and Standley, 2013), visually inspected for obvious alignment errors, and concatenated in Geneious. Maximum likelihood analysis was performed in PhyML-mpi (Guindon *et al.*, 2010) under the best-fit model (HKY+I+G). Branch support was calculated from 100 bootstrap replicates for the concatenated dataset.

Pathogenicity test

The AY-1 isolate was used in a pathogenicity test conducted on apple trees at Foke apple orchard, in November 2017. Four apple trees each of 'Anna' and 'Dorsett Golden' from different rows of the farm were randomly selected for the inoculation trial. On each tree, two healthy and oppositely situated branches with mean diameter of 11 mm (range 10 to 14 mm) were selected. One branch was inoculated with a mycelium plug of the fungus and the other branch was treated with a sterile PDA plug (as the negative control). In total eight branches were inoculated with the fungus and eight were treated with sterile PDA plugs. The methods of Luque *et al.*

(2006) and Sami *et al.* (2014) were adopted with modifications. The bark of each of the selected branches was cleaned with 70% ethanol before inoculation. Holes (4 mm diam.) were made in the branches using a cork borer. Mycelium plugs (4 mm diam.) cut from colony margins in 10-d-old PDA cultures were placed on the wounds with mycelium facing the host cambium. A 4 mm diam. sterile PDA plug was similarly placed on one of the alternative branches of each tree as the control treatment. Inoculated wounds were wrapped with Parafilm® (American National Can) to prevent contamination and desiccation of the inoculated areas. After 8 weeks, all inoculated branches were destructively sampled and brought to CEE-FRC Forest Protection laboratory. The lengths of developed lesion's development in the cambium of inoculated branches were measured after removing the bark of each branch surrounding the inoculation point. Re-isolations from symptomatic cambium tissues beyond the areas of inoculation were performed onto PDA. ANOVA analysis of the lesion length data was done using XLStat. Differences in mean lesion lengths formed on the two cultivars were assessed with Fishers least significant differences (LSD) at $P \leq 0.05$.

RESULTS

Disease symptoms and severity in the field

Based on the documents available in Gibagri Farm PLC, 31,500 grafted apple trees were imported from Spain between May 2009 and July 2012. Of these, 384 trees were rejected due to their poor rooting and dry wood. As well, 8,186 apple trees were eradicated from the nursery and orchard sites at the farm up to November 2017, due to development of canker symptoms. The trees showed blistering of the bark of the main stems mostly below the grafting points, and eventually produced exudates, lanceolate leaf development, abscission of blossom and fruits, and dieback that progressively led to the death of the trees (Figure 1a). Cross-sectional cuts of stems of symptomatic trees showed either circular or triangular discolorations in the wood tissues (Figure 1b and 1c).

Morphological characteristics of fungi isolated fungi on PDA

Morphology of the fungi isolated from symptomatic samples of the two host cultivars was the same. Colonies on PDA were whitish with short woolly texture (Figure 2a). Black conidiomata formed on the incubated wood

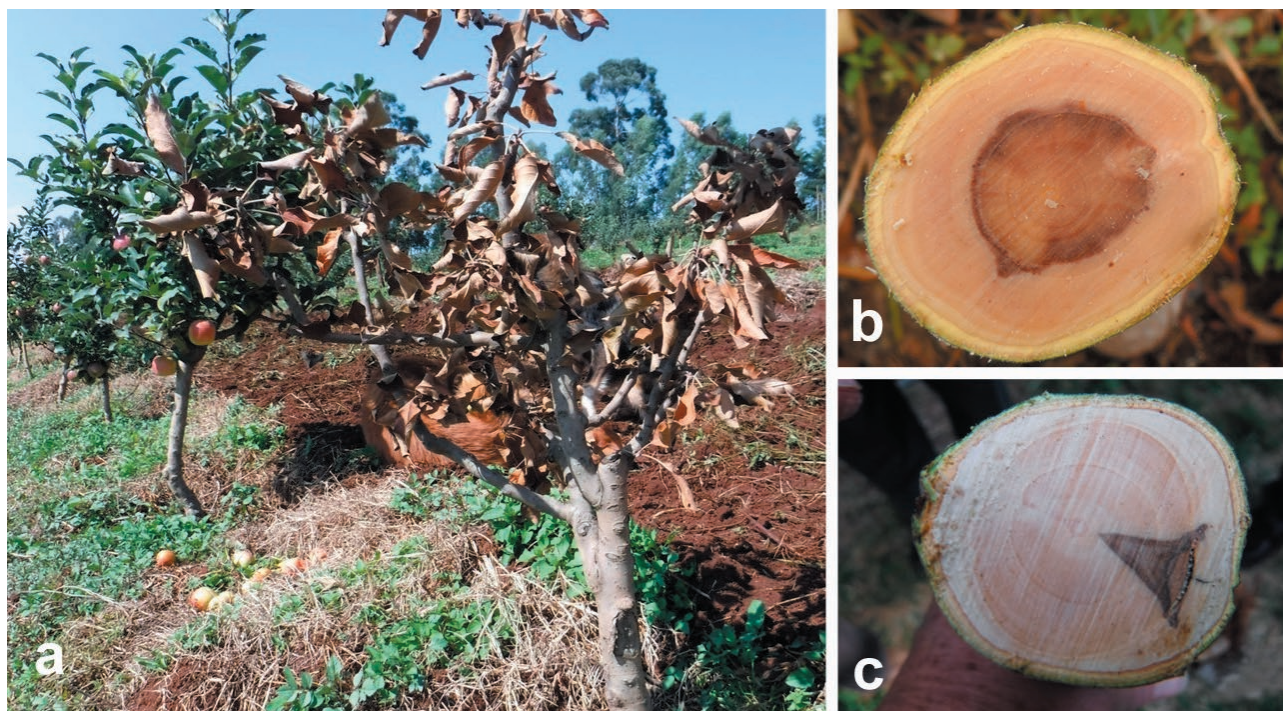


Figure 1. Apple tree at Foke Farm showing dieback symptoms (a) and main stem cross section symptoms (b and c).

samples, and fungus structures are illustrated in Figure 2. Conidiomata on PDA were superficial or immersed in the agar, were dark brown to black, and were $(-316)414-659(-673)$ μm wide and $(-303)494-584(-776)$ μm tall. They were mostly single (sometimes multiple) and clumped together (Figure 2b), with short necked ostioles. And were $75-180$ μm long and $87-256$ μm wide at the base. The conidiomata walls had textured outer layers $21-42$ μm thick with thin, dark brown cells, and were lined with inner layers of hyaline globose cells $16-32$ μm thick (Figure 2c to e). The surfaces of conidiomata walls were covered with dark brown hyphae. Conidiogenous cells were discrete or assembled into protruding masses, and were indeterminate and phialidic, formed from the inner cells all over the conidiomata walls, and were hyaline to pale yellow, and broadly ampulliform to globose (Figure 2f), with distinct periclinal thickening (Figure 2g). Phialide collarettes mostly absent, occasionally with visible annulations, and measured $(-3)4-6(-8)$ $\mu\text{m} \times (-1.5)2-2.5(-3)$ μm (Figure 2h). Conidia were ellipsoidal to short-cylindrical, rounded at both ends, 1-celled, olivaceous, and $3-4(-4.8)$ $\mu\text{m} \times (-1)1.5-2(-2.8)$ μm (Figure 2i). The morphological characteristics were similar to those described for *Paraconiothyrium brasiliense* Verkley (Verkley *et al.*, 2004; Paul and Lee, 2014). This species was synonymised with *Didymosphaeria rubi-ulmifolii* Ariyawansa, Erio Camporesi & K.D. Hydeby

Ariyawansa *et al.* (2014b), based on phylogenetic analyses. The sexual stage as described by Ariyawansa *et al.* (2014a) was not observed in the present study.

Molecular characterization and phylogenetic analysis of fungus isolate

Phylogenetic analyses of the concatenated ITS, LSU and ACT gene regions confirmed the identity of isolates AY-1 and AY-2 as *Didymosphaeria rubi-ulmifolii* (Figure 3). Both isolates grouped together with *D. rubi-ulmifolii sensu stricto*, with a 99% bootstrap support (CBS 100299, the type strain of *P. brasiliense*). The *D. rubi-ulmifolii sensu lato* subclade did not have significant support, only an internal cluster of three *D. rubi-ulmifolii sensu lato* isolates were associated with the present study's two isolates (bootstrap support of 68%).

Pathogenicity test

Prominent brown lesions caused by the fungus after inoculation were observed on the branches of 'Anna' and 'Dorsett Golden' apple trees (Figure 4). For 'Anna', the lesions lengths were from 23 to 86 mm (mean = 54 mm; $n = 4$). For 'Dorsett Golden', the lesion lengths were from 26 to 46 mm (mean = 32 mm; $n = 4$). Mean lesion

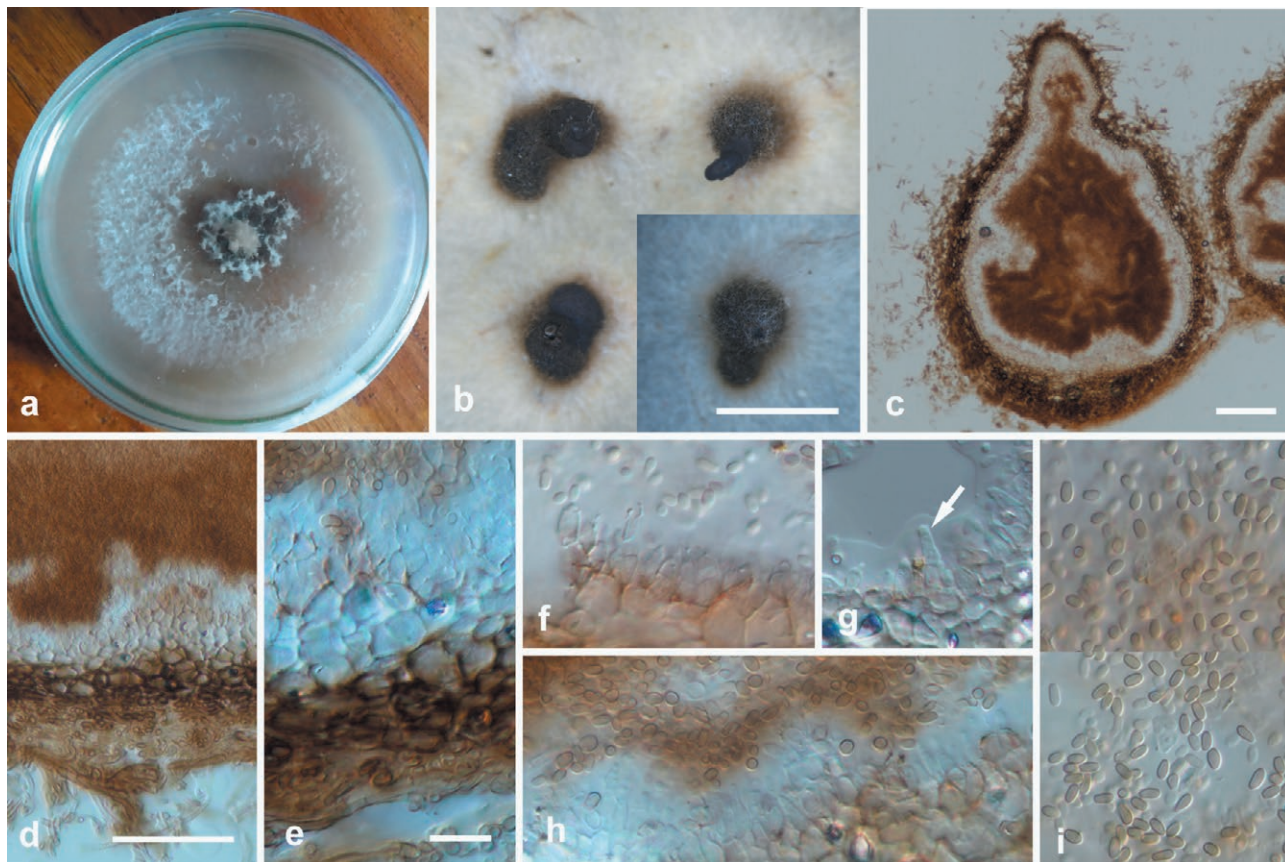


Figure 2. Cultural and morphological structures of *Didymosphaeria rubi-ulmifolii* (isolate AY-1). After 7 d growth on PDA (a), conidiomata with oozing conidia (b), cross section through a conidioma illustrating the neck (c), cross sections through conidioma wall (d and e), conidiogenous cells (f to h), arrow indicating periclinal thickening and conidia (i). Scale bars: in b = 1000 μ m; c = 100 μ m; d = 50 μ m; e to i = 10 μ m.

lengths for the two cultivars were not significantly different ($P = 0.175$). Two of the control branches (one branch each from the two cultivars) had slightly pale brown discolorations at the inoculation sites, which did not exceed 4 mm in length, and no *D. rubi-ulmifolii* was isolated from these lesions. Re-isolation of the same fungus (colony characteristics described above) from each of the pathogen inoculated branches confirmed the pathogenicity of *D. rubi-ulmifolii* on apple trees.

DISCUSSION

This study has confirmed that the trunks of *M. pumila* trees at Foke farm were infected by *D. rubi-ulmifolii* (syn. *Paraconiothyrium brasiliense*). This pathogen caused gradual decline and dieback of apple trees and decreased growth and production of fruit in the affected orchards. The dieback caused by this pathogen was so severe that the orchard owner decided to remove all of the apple trees and plant a different crop.

Previous studies showed that *D. rubi-ulmifolii* has been isolated from a number of plant species, including: fruits of *Coffea arabica* in Brazil; *Ginkgo biloba*, *Pinus tabulaeformis* and leaves of *Pinus glauca* in Canada; *Alliaria petiolata* in the USA; marine fish in China; wetland surface water in Japan; discoloured wood of a living *Platanus acerifolia* tree in Italy; South African peach, nectarine, and plum trees; and Chinese Maple leaves in Korea (reviewed in Paul and Lee, 2014). *Didymosphaeria rubi-ulmifolii* was reported to cause disease on one-year-old commercial apple trees and was also found causing latent infections in certified nursery trees in South Africa (Havenga *et al.*, 2019). The present paper is, therefore, the second report of canker disease on apple trees caused by *D. rubi-ulmifolii*, and the first report in Ethiopia. The potential pathogenicity of *D. rubi-ulmifolii* on detached apple shoots was shown by Cloete *et al.* (2011), who inoculated the fungus isolated from pears onto apple shoots, and showed it to be pathogenic causing significant lesions.

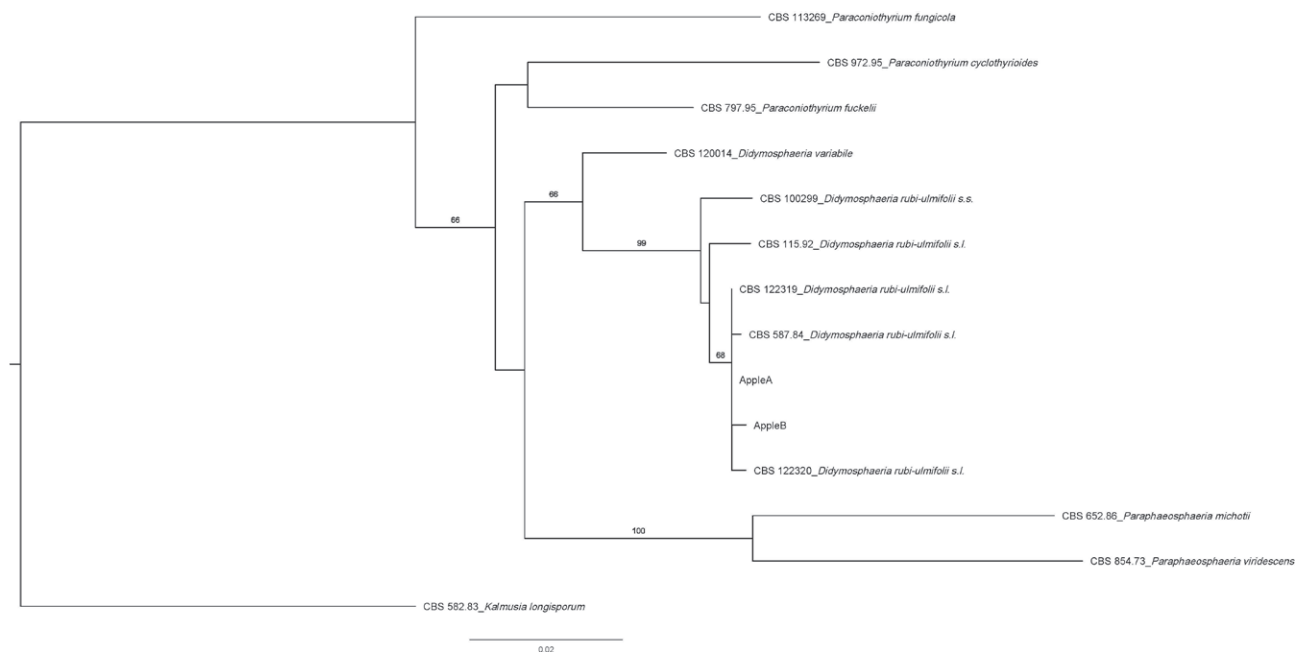


Figure 3. Maximum likelihood phylogeny of the selected genera within *Didymosphaeriaceae*, as estimated from concatenated alignments of the internal transcribed spacers 1 and 2 and 5.8S rRNA gene (ITS), the 28S rRNA large subunit gene (LSU) and the partial actin (ACT) gene regions. Maximum likelihood bootstrap percentages are indicated at the nodes. Support values less than 50% bootstrap were omitted. *Kalmusia longisporum* CBS 582.83 was included as the outgroup.

The main reasons behind the serious damage from *D. rubi-ulmifolii* on apple trees may be a combination of cultivar susceptibility and suitable environmental conditions (high air humidity and low soil pH) for the pathogen. Low soil pH causes stress to apple trees. Due to the slow development of symptoms, the cause of the disease was not initially attributed to fungal canker. *Didymosphaeria rubi-ulmifolii* was isolated from one farm and the incidence of the fungus across other apple-growing districts of Ethiopia has not been established.

In conclusion, in addition to the updating of quarantine measures required for the importation of trees harbouring latent quarantine pathogen infections, future studies are required to determine the magnitude, distribution and consequences of this pathogen on the cultivation and production of apple trees in Ethiopia. This information will assist the livelihoods of the rural communities in different apple production of this country.

ACKNOWLEDGEMENTS

The authors thank Gibagri Farm PLC, for assisting and covering expenses during fieldwork for this study. The CEE-FRC allowed use of laboratory consumables, and the Ethiopian Institute of Biodiversity (EIB) sent specimens to The Netherlands. The Westerdijk Fungal Biodiversity Insti-

tute, AD Utrecht, the Netherlands provided fungus molecular characterization and identification. Prof. Peter Braun and colleagues at the University of Geisenheim, Germany assisted in this study. Ms. Mag. pharm. Hermine Lotz-Winter and her team at the Faculty of Biological Sciences Department of Mycology, Biologicum, Goethe-University, Germany and Dr. Ulrike Damm, Head of Section Mycology, Senckenberg Museum of Natural History, Görlitz, Germany gave assistance with preparation of this paper. Tiruwork Tesfa and Almaz Asefa assisted during laboratory work at CEE-FRC. Dr. Adane Ayele facilitated microscopy at Armauer Hansen Research Institute (AHRI), Addis Ababa, Ethiopia. The assistance of the Editor of the Journal and two anonymous reviewers to improve the manuscript is also gratefully acknowledged.

LITERATURE CITED

- Ariyawansa H.A., Camporesi E., Thambugala K.M., Mapook A., Kang J., ... Hyde K.D., 2014a. Confusion surrounding *Didymosphaeria*—phylogenetic and morphological evidence suggest *Didymosphaeriaceae* is not a distinct family. *Phytotaxa* 176: 102–119. doi: 10.11646/phytotaxa.176.1.12.
- Ariyawansa H.A., Tanaka K., Thambugala K.M., Phookamsak R., Tian Q., Hyde K.D., 2014b. A



Figure 4. Brown lesion caused by *Didymosphaeria rubi-ulmifolii* (isolate AY-1) on a branch of apple 'Anna', and non-inoculated (control) branch, 8 weeks post inoculation.

molecular phylogenetic reappraisal of the Didymosphaeriaceae (=Montagnulaceae). *Fungal Diversity* 68: 69–104. doi: 10.1007/s13225-014-0305-6.

Bekele-Tesemma A., 2007. *Useful trees and Shrubs for Ethiopia: Identification, Propagation and Management for 17 Agroclimatic zones*. World Agroforestry Centre, East Africa Region, Nairobi, Kenya, 552 pp.

Cloete M., Fourie P.H., Damm U., Crous P.W., Mostert L., 2011. Fungi associated with dieback symptoms of apple and pear trees, a possible inoculum source of grapevine trunk disease pathogens. *Phytopathologia Mediterranea* 50: S176–S190. doi: 10.14601/Phytopathol_Mediterr-9004.

Erez A., 2000. Bud dormancy; phenomenon, problems and solutions in the tropics and subtropics. In *Tem-*

perate Fruit Crops in Warm Climates (A. Erez, ed.), Kluwer Academic Publishers, The Netherlands, 17–48.

FAO, 2010. FAOSTAT: statistics database. Food and Agriculture Organization of the United Nations (FAO). Available at: <http://www.apps.fao.org/>.

Fetena S., Lemma B., 2014. Assessment on major apple diseases and insect pests in Chencha and Bonke Woredas of Gamo Gofa Zone, Southern Ethiopia. *Scholarly Journal of Agricultural Science* 4: 394–402.

Fetena S., Shara S., Anjulo A., Gulie G., Woldesenbet F., Yilma B., 2014. Survey on apple production and variety identification in Chencha District of Gamo Gofa Zone, Southern Ethiopia. *Journal of Agricultural Food Technology* 4: 7–15.

Guindon S., Dufayard J.F., Lefort V., Anisimova M., Hordijk W., Gascuel O., 2010. New algorithms and methods to estimate maximum-likelihood phylogenies: Assessing the performance of PhyML 3.0. *Systematic Biology* 59: 307–321. doi: 10.1093/sysbio/syq010.

Havenga M., Gatsi G.G., Halleen F., Spies C.F.J., van der Merwe R., Mostert L., 2019. Canker and wood rot pathogens present in young apple trees and propagation material in the Western Cape of South Africa. *Plant Disease* 103: 3129–3141. doi: 10.1094/PDIS-04-19-0867-RE.

Hailemichael B.G., 2006. Impact of male out-migration on rural women's livelihood: the case of Chencha woreda, South Ethiopia. MSc Thesis, Addis Ababa University, Addis Ababa, Ethiopia, 120 pp.

Hedberg O., 1989. Pittosporaceae to Araliaceae. In: *Flora of Ethiopia and Eritrea*. (I. Hedberg, S. Edwards, ed.), The National Herbarium, Addis Ababa, Ethiopia, and Department of Systematic Botany, Uppsala, Sweden, 732.

Katoh K., Standley D.M., 2013. MAFFT multiple sequence alignment software version 7: Improvements in performance and usability. *Molecular Biology and Evolution* 30, 772–780. doi: 10.1093/molbev/mst010.

Luque J., Sierra D., Torres E., Garcia F., 2006. *Cryptovalsa ampelina* on grapevines in N.E. Spain: identification and pathogenicity. *Phytopathologia Mediterranea* 45: S101–S109. doi: 10.14601/Phytopathol_Mediterr-1838.

Paul N.C., Lee H.B., 2014. First Record of Endophytic *Paraconiothyrium brasiliense* isolated from Chinese Maple Leaves in Korea. *Korean Journal of Mycology* 42: 349–352. doi: 10.4489/KJM.2014.42.4.349.

Sami S., Mohammadi H., Heydarnejad J., 2014. *Phaeoacremonium* species associated with necrotic wood

- of pome fruit trees in Iran. *Journal of Plant Pathology* 96: 487–495. doi: 10.4454/JPP.V96I3.006.
- Samson R.A., Houbraken J., Thrane U., Frisvad J.C., Andersen B., 2010. *CBS Laboratory manual series 2, Food and Indoor Fungi*. CBS-KNAW Fungal Biodiversity Centre Utrecht, The Netherlands, 390 pp.
- Sisay A., 2007. Ethiopia-GTZ Promotes apples in the highlands of Ethiopia. Available at: www.nazret.com/news (Accessed November 10, 2017).
- Su Y.Y., Qi Y.L., Cai L., 2012. Induction of sporulation in plant pathogenic fungi. *Mycology* 3(3), 195–200.
- Tromp J., 2005. Fruit ripening and quality. In: *Fundamentals of Temperate Zone Tree Fruit Production* (J. Tromp, A.D. Webster, S.J. Wertheimeds, ed.), Backhuys Publishers, Leiden, The Netherlands, 295–310.
- Verkley G.J.M., da Silva M., Wicklow D.T., Crous P.W., 2004. *Paraconiothyrium*, a new genus to accommodate the mycoparasite *Coniothyrium minitans*, anamorphs of *Paraphaeosphaeria*, and four new species. *Studies in Mycology* 50: 323–335.



Research Papers

Characterization of *Lasiodiplodia* species associated with grapevines in Mexico

Citation: E.A. Rangel-Montoya, M. Paolinelli, P.E. Rolshausen, C. Valenzuela-Solano, R. Hernandez-Martinez (2021) Characterization of *Lasiodiplodia* species associated with grapevines in Mexico. *Phytopathologia Mediterranea* 60(2): 237-251. doi: 10.36253/phyto-12576

Accepted: April 11, 2021

Published: September 13, 2021

Copyright: ©2021 E.A. Rangel-Montoya, M. Paolinelli, P.E. Rolshausen, C. Valenzuela-Solano, R. Hernandez-Martinez. This is an open access, peer-reviewed article published by Firenze University Press (<http://www.fupress.com/pm>) and distributed under the terms of the Creative Commons Attribution License, which permits unrestricted use, distribution, and reproduction in any medium, provided the original author and source are credited.

Data Availability Statement: All relevant data are within the paper and its Supporting Information files.

Competing Interests: The Author(s) declare(s) no conflict of interest.

Editor: José R. Úrbez Torres, Agriculture and Agri-Food Canada, Summerland, British Columbia, Canada.

EDELWEISS A. RANGEL-MONTOYA¹, MARCOS PAOLINELLI^{2,3}, PHILIPPE E. ROLSHAUSEN⁴, CESAR VALENZUELA-SOLANO⁵, RUFINA HERNANDEZ-MARTINEZ^{1,*}

¹ Departamento de Microbiología, Centro de Investigación Científica y de Educación Superior de Ensenada (CICESE), Ensenada, Baja California, 22860, Mexico

² Consejo Nacional de Investigaciones Científicas y Técnicas (CONICET)

³ Instituto Nacional de Tecnología Agropecuaria. Estación Experimental Agropecuaria Mendoza INTA, Luján de Cuyo, Mendoza, 5534, Argentina

⁴ Department of Botany and Plant Sciences. University of California, Riverside, California, 92521, USA

⁵ Instituto Nacional de Investigaciones Forestales, Agrícolas y Pecuarias (INIFAP). Campo Experimental Costa de Ensenada, Ensenada, Baja California, 22880, Mexico

*Corresponding author. E-mail: ruhernan@cicese.mx

Summary. Botryosphaeria dieback is one of the most prevalent grapevine trunk diseases (GTDs), and is caused by fungi in the *Botryosphaeriaceae*. Fungi invade grapevine vascular systems mainly through pruning wounds, and cause cankers and necrotic lesions, which lead to grapevine decline and death. *Lasiodiplodia theobromae* has been reported as a highly virulent pathogen of grapevine, and was previously reported in Mexican vineyards. The taxonomy of *Lasiodiplodia* was recently revised, adding new species, and some were reduced to synonymy. This study aimed to characterize *Lasiodiplodia* producing grapevine dieback symptoms in Sonora and Baja California, Mexico. Using the phylogenetic markers *tef1-α* and ITS regions, *Lasiodiplodia brasiliensis*, *L. crassispora*, *L. exigua*, and *L. gilanensis* were identified. *Lasiodiplodia exigua* was the most prevalent species. *Lasiodiplodia brasiliensis* and *L. gilanensis* were very virulent to 'Cabernet Sauvignon' plants, while *L. exigua* and *L. gilanensis* were less virulent, and *L. crassispora* did not produce lesions at 2 months post-inoculation. The optimum temperature of the *Lasiodiplodia* spp. was 28°C, but all four species grew up to 37°C, and the isolates of *L. exigua* grew slowly at 40°C. This is the first report of the four of *Lasiodiplodia* species in vineyards of Mexico.

Keywords. Grapevine Trunk Diseases (GTDs), Botryosphaeria dieback, *Botryosphaeriaceae*.

INTRODUCTION

In Baja California and Sonora, Mexico, grapes are one of the most economically important fruit crops (García-Robles *et al.*, 2007; González-Andrade, 2015). Baja California produces close to 90% of Mexico's wines, while Sonora produces approx. 95% of Mexican table grapes (SIAP, 2019).

Botryosphaeria dieback is a degenerative wood disease caused by *Botryosphaeriaceae* fungi, this disease has cosmopolitan distribution and predominates in warm climate regions (Úrbez-Torres, 2011; Gramaje *et al.*, 2018). Fungi in this family are known as opportunistic or latent plant pathogens, as they can remain endophytic for long periods in host tissues without causing symptoms (Slippers *et al.*, 2007).

More than 30 species in the *Botryosphaeriaceae* have been associated with Botryosphaeria grapevine dieback, and these are in *Botryosphaeria*, *Diplodia*, *Dothiorella*, *Lasiodiplodia*, *Neoscytalidium*, *Neofusicoccum*, *Sphaeropsis*, and *Spenceriartinsia* (Úrbez-Torres, 2011; Rolshausen *et al.*, 2013; Stempien *et al.*, 2017; Gramaje *et al.*, 2018). The main symptoms caused by these fungi are vascular discoloration and perennial cankers in host plant vascular bundles, by occlusion of xylem and phloem, which leads to the death of branches and eventually of entire plants. This disease is distinguished from Eutypa dieback because it is not known to cause particular foliar symptoms (Úrbez-Torres, 2011; Bertsch *et al.*, 2013; Billones-Baaijens and Savocchia, 2019). Species in the *Botryosphaeriaceae* were commonly found in grapevines 7 to 10 years old and older, mainly in plants where large pruning wounds had been made in vines (Gubler *et al.*, 2005). However, incidence of symptoms caused by this group of fungi has greatly increased in recent years, especially in young vineyards (Gramaje and Armengol, 2011; Gispert *et al.*, 2020).

Among the *Botryosphaeriaceae*, the *Lasiodiplodia* has been reported as highly virulent on grapevines (Úrbez-Torres and Gubler, 2009), and has also been identified on more than 500 host species (Punithalingam, 1976). Some of the main morphological characteristics of *Lasiodiplodia* include hyaline and smooth conidiogenous cells, with cylindrical to conical shapes, which produce conidia with subovoid to ellipsoid-ovoid shapes and which are hyaline without septa, or dark-brown with single septae (Phillips *et al.*, 2013). *Lasiodiplodia* are globally distributed, mainly in the tropics and subtropics, and are probably spread when plants are transported between regions due to the lack of restrictions on the movement of propagation material (Cruywagen *et al.*, 2017; Mehl *et al.*, 2017). *Lasiodiplodia theobromae* is the type species of the genus (Alves *et al.*, 2008), and this species is comprised of many cryptic species because of their morphological similarity (Alves *et al.*, 2008; Mehl *et al.*, 2017). As a result, the taxonomy of *Lasiodiplodia* has undergone revisions, and new species have been introduced (Dissanayake *et al.*, 2016; Tibpromma *et al.*, 2018). Several *Lasiodiplodia* species have been reduced to synonymy, particularly those with morphology similar

to *Lasiodiplodia mahajangana*, *L. plurivora* and *L. theobromae*. There are currently 34 accepted *Lasiodiplodia* species (Zhang *et al.*, 2021).

The only *Lasiodiplodia* species causing perennial cankers and dieback that has been reported in Mexican vineyards is *L. theobromae* (Úrbez-Torres *et al.*, 2008). However, given the recent taxonomical revision of *Lasiodiplodia*, we hypothesize that the species diversity within that group is broader than initially reported. Hence, the present study aimed to clarify and update the taxonomy of *Lasiodiplodia* present in vineyards from Baja California and Sonora, Mexico, and to evaluate the pathogenicity of these fungi to grapevine.

MATERIALS AND METHODS

Fungal isolation and morphological characterization of Lasiodiplodia spp.

This study encompassed ten vineyards in the main grape-growing areas of the States of Baja California and Sonora, from which 35 samples from grapevines exhibiting Botryosphaeria dieback symptoms were taken from trunks and branches (Figure 1). Small pieces of symptomatic plant tissue were obtained from each diseased plant, and these were immersed in 95% ethanol, quickly flamed, and then placed onto potato dextrose agar (PDA; Difco) supplemented with 25 mg mL⁻¹ chloramphenicol in Petri plates. The plates were incubated at 30°C until fungal growth was observed. Smoke-gray fungal colonies with abundant aerial mycelium were sub-cultured onto PDA plates to obtain pure cultures, and were then preserved at 4°C in 20% glycerol.

Pure cultures were grown on PDA and incubated at 30°C for 7 d to determine morphological characteristics of fungal isolates, including their pigmentation and formation of aerial mycelium. Pycnidium production was induced using liquid Minimal Medium 9 (MM9) (10 g·L⁻¹ glucose, 1.0 g·L⁻¹ NH₄Cl, 0.5 g·L⁻¹ NaCl, 2.5 g·L⁻¹ K₂HPO₄, 2.5 g·L⁻¹ KH₂PO₄) in flasks supplemented with sterile pine needles (5% w/v). The flasks were incubated at room temperature under an ultraviolet electromagnetic radiation lamp, using a 12 h light and 12 h darkness regime for 15 d. Formed pycnidia were suspended in 0.5% Tween 20 to obtain conidia, which were observed under a light microscope (Nikon Eclipse E200). Images of the conidia were captured with an Infinity 1 Lumenera camera, and analyzed using Infinity Analyze v 6.5.4 and ImageJ software. To compare conidium size across species, one-way ANOVA followed by a *post hoc* Fisher LSD analysis ($\alpha < 0.05$) were carried on these data using STATISTICA 8.0.



Figure 1. Locations of study sites and symptoms of *Botryosphaeria* dieback in *Vitis vinifera* associated with *Lasiodiplodia* spp. A) Field study sites in Baja California and Sonora regions. B-D) Grapevine plants showing vascular necroses, wedge-shape cankers and wood necroses. E) Pycnidia observed under a stereoscopic microscope found in some grapevine samples.

DNA extraction and PCR amplification from Lasiodiplodia spp. isolates

Total genomic DNA of each fungus isolate was extracted from mycelia recovered from cultures (3 d in

PDB at 30°C), using the CTAB protocol (Wagner *et al.*, 1987). To characterize *Lasiodiplodia* spp., the ITS region and elongation factor *tef-1a* as phylogenetic markers were used, as recommend in TrunkDiseaseID.org (<http://www.grapeipm.org/d.live/>) (Lawrence *et al.*, 2017). The oligo-

nucleotide primers EF1-728F (5'-CATCGAGAAGTTC-GAGAAGG-3') and EF1-986R (5'-TACTTGAAGGAACCTTACC-3') were used to amplify part of the translation elongation factor-1 α (*tef-1 α*) gene (Carbone and Kohn, 1999); and ITS1 (5'-TCCGTAGGTGAACCTGCGG-3') and ITS4 (5'-TCCTCCGCTTATTGATATGC-3') were used to amplify the ITS region of the nuclear ribosomal DNA, including the 5.8S gene (White *et al.*, 1990). Each PCR reaction contained 2.5 μ L of 10 \times PCR buffer (100 mM Tris-HCl, pH 8.3 at 25°C; 500 mM KCl; 15 mM MgCl₂; 0.01% gelatin), 0.5 μ L of 20 mM dNTPs, 0.625 μ L of 10 μ M of each primer, 0.125 μ L of Taq DNA polymerase (GoTaq[®] DNA polymerase, 5 units $\cdot\mu$ L⁻¹; Promega), and 1 μ L of 30 ng $\cdot\mu$ L⁻¹ template DNA, adjusted with purified water to a final volume of 25 μ L. Amplification reactions were carried out in a Bio-Rad T-100 thermal cycler set to the following conditions: for *tef-1 α* , an initial cycle of 95°C for 3 min, followed by 35 cycles of 95°C for 30 s, 55°C for 30 s, and 72°C for 1 min; for ITS region, an initial cycle of 94°C for 2 min, followed by 35 cycles of 94°C for 1 min, 58°C for 1 min, and 72°C for 90 s. Both programmes had a final cycle of 72°C for 10 min. Once observed in electrophoresis gels, PCR reactions were purified using the GeneJet PCR purification kit (Thermo Scientific), and purified products were sequenced by Eton Bioscience Inc.

Phylogenetic analyses

The sequences were analyzed using BioEdit v.7.0.5.3 (Hall, 1999) and a BLASTn analysis was carried out. Sequences with the greatest similarity were downloaded from the GenBank (Table 1) and aligned with ClustalW (pairwise alignment parameters: gap opening 10, gap extension 0.1, and multiple alignment parameters: gap opening 10, gap extension 0.2. Transition weight was set to 0.5, and delay divergent sequences to 25 %) (Thompson *et al.*, 1994). The alignment was adjusted manually where necessary. Alignment of ITS and *tef-1 α* were imported in BioEdit v.7.0.5.3 to obtain the concatenated matrix. Maximum Likelihood (ML) and Maximum Parsimony (MP) analyses were performed using MEGA-X (Kumar *et al.*, 2018), based on the concatenated sequence alignment. The best model of nucleotide substitution was selected according to the Akaike Information Criterion (AIC). The T3+G+I model was used for the ML analysis (Tamura, 1992). Parameters for Maximum Likelihood were set to Bootstrap method using 1000 replicates. Initial tree(s) for the heuristic search were obtained automatically by applying the Maximum Parsimony method. Gaps were treated as missing data. The tree was visualized in MX: Tree Explorer. New sequences were deposited in the GenBank (<https://www.ncbi.nlm.nih.gov/genbank/>) (Table 1).

Determination of optimum growth temperature of selected *Lasiodiplodia* isolates

The optimum growth temperature of identified *Lasiodiplodia* species was determined. Selected isolates of identified species were grown on PDA plates by inoculating each plate with a 3-mm diam. plug of a 2-d-old colony at the edge of the plate. Three replicates of each isolate for each temperature were included, and plates were then incubated at 20, 23, 25, 28, 30, 37, or 40°C. This temperature range was chosen based on previous reports (Úrbez-Torres *et al.*, 2006; Paolinelli-Alfonso *et al.*, 2016), and considering the prevalent summer temperatures of the zone from which the isolates were obtained. The colony radius was measured every 24 h for 3 d. The optimum growth temperature was determined as the temperature that produced the maximum mycelial growth rate (mm d⁻¹), which was calculated using the formula:

$$GR = \frac{R_f - R_i}{T_f - T_i}$$

where: GR = Growth rate, R_f = Final colony diam. (mm), R_i = Initial colony diam. (mm), T_f = Final time (d) when colony measured, and T_i = Initial time (day 1).

Production of aerial mycelium in *Lasiodiplodia* spp.

To evaluate aerial mycelium production as a phenotypic characteristic to differentiate among species, 2 d-old cultures of selected isolates were each used to inoculate a 3 mm diam. plug of each culture into a glass tube containing 5 mL of PDA medium. Tubes were incubated at 28°C for 5 d and the elevations of mycelia were measured.

Pathogenicity tests of selected *Lasiodiplodia* isolates

Based on the analyses of the morphological and genetic results, the isolates MXL28BC, MXCS01BC, MX50BC, MXV5BC, MXVSM1b, MXVSM6, MXVS-M16a, MXVSM18, and MXVS21b were selected for pathogenicity tests. Grapevine plants of 'Cabernet Sauvignon' were used to evaluate the pathogenicity of these *Lasiodiplodia* isolates. Inoculation of each test plant was carried out through a mechanical wound in woody tissue made with a drill bit (2 mm diam.), and a mycelium plug of a selected isolate was placed inside the hole. An isolate of *L. gilanensis* UCD256Ma (formerly *L. theobromae*) (Úrbez-Torres *et al.*, 2006; Obrador-Sánchez and Hernandez-Martinez, 2020) was used for comparisons.

Table 1. List of GenBank and culture accession numbers of *Lasiodiplodia* spp. used in this study for phylogenetic analyses.

Species	Isolate	Host	Origin	GeneBank accession number	
				ITS	<i>tef-1α</i>
<i>Lasiodiplodia brasiliensis</i>	CMM2184	<i>Carica papaya</i>	Brazil	KC484801	KC481531
<i>L. brasiliensis</i>	CMM2185	<i>Carica papaya</i>	Brazil	KC484800	KC481530
<i>L. brasiliensis</i>	CMM2186	<i>Carica papaya</i>	Brazil	KC484812	KC481542
<i>L. brasiliensis</i>	CMM2188	<i>Carica papaya</i>	Brazil	KC484807	KC481537
<i>L. brasiliensis</i>	CMM2212	<i>Carica papaya</i>	Brazil	KC484806	KC481536
<i>L. brasiliensis</i>	UCD1012BC ^a	<i>Vitis vinifera</i>	USA	EU012372	EU012392
<i>L. brasiliensis</i>	UCD916SN ^a	<i>Vitis vinifera</i>	USA	EU012366	EU012386
<i>L. brasiliensis</i>	UCD923SN ^a	<i>Vitis vinifera</i>	USA	EU012371	EU012391
<i>L. brasiliensis</i>	MXBCL28	<i>Vitis vinifera</i>	Mexico	MT663281	MT711988
<i>L. brasiliensis</i>	MXVSCC1	<i>Vitis vinifera</i>	Mexico	MT663282	MT711989
<i>L. brasiliensis</i>	MXVS15a	<i>Vitis vinifera</i>	Mexico	MT663283	MT711990
<i>L. brasiliensis</i>	MXVS16a	<i>Vitis vinifera</i>	Mexico	MT663284	MT711991
<i>L. brasiliensis</i>	MXVS18	<i>Vitis vinifera</i>	Mexico	MT663285	MT711992
<i>L. brasiliensis</i>	MXVS19a	<i>Vitis vinifera</i>	Mexico	MT663302	MT712009
<i>L. citricola</i>	IRAN1522C	<i>Citrus</i> sp.	Iran	GU945354	GU945340
<i>L. citricola</i>	IRAN1521C	<i>Citrus</i> sp.	Iran	GU945353	GU945339
<i>L. crassispora</i>	WAC12533	<i>Santalum album</i>	Australia	DQ103550	DQ103557
<i>L. crassispora</i>	CBS110492	Unknown	Unknown	EF622086	EF622066
<i>L. crassispora</i>	MXBCV5	<i>Vitis vinifera</i>	Mexico	MT663286	MT711993
<i>L. crassispora</i>	MXVS1b	<i>Vitis vinifera</i>	Mexico	MT663287	MT711994
<i>L. euphorbicola</i>	CMM 4616	<i>Vitis vinifera</i>	Brazil	MG954348	MG979518
<i>L. euphorbicola</i>	CMM 4597	<i>Vitis vinifera</i>	Brazil	MG954347	MG979517
<i>L. exigua</i>	BL104	<i>Retama raetam</i>	Tunisia	KJ638317	KJ638336
<i>L. exigua</i>	BL184	<i>Retama raetam</i>	Tunisia	KJ638318	KJ638337
<i>L. exigua</i>	BL185	<i>Retama raetam</i>	Tunisia	KJ638319	KJ638338
<i>L. exigua</i>	BL186	<i>Retama raetam</i>	Tunisia	KJ638320	KJ638339
<i>L. exigua</i>	BL187	<i>Retama raetam</i>	Tunisia	KJ638321	KJ638340
<i>L. exigua</i>	PD161	<i>Pistacia vera</i>	USA	GU251122	GU251254
<i>L. exigua</i>	MXBCV4	<i>Vitis vinifera</i>	Mexico	MT663288	MT711995
<i>L. exigua</i>	MXBCV6	<i>Vitis vinifera</i>	Mexico	MT663289	MT711996
<i>L. exigua</i>	MXBCV7	<i>Vitis vinifera</i>	Mexico	MT663290	MT711997
<i>L. exigua</i>	MXVS2Ta	<i>Vitis vinifera</i>	Mexico	MT663291	MT711998
<i>L. exigua</i>	MXVS5a	<i>Vitis vinifera</i>	Mexico	MT663301	MT712008
<i>L. exigua</i>	MXVS6a	<i>Vitis vinifera</i>	Mexico	MT663292	MT711999
<i>L. exigua</i>	MXVS16b	<i>Vitis vinifera</i>	Mexico	MT663293	MT712000
<i>L. exigua</i>	MXVS20	<i>Vitis vinifera</i>	Mexico	MT663294	MT712001
<i>L. exigua</i>	MXVS21a	<i>Vitis vinifera</i>	Mexico	MT663295	MT712002
<i>L. exigua</i>	MXVS21b	<i>Vitis vinifera</i>	Mexico	MT663296	MT712003
<i>L. exigua</i>	MXVSS2	<i>Vitis vinifera</i>	Mexico	MT663303	MT712010
<i>L. exigua</i>	MXVSSC1	<i>Vitis vinifera</i>	Mexico	MT663297	MT712004
<i>L. exigua</i>	MXVSV1	<i>Vitis vinifera</i>	Mexico	MT663298	MT712005
<i>L. gilanensis</i>	IRAN1523C	Unknown	Iran	GU945351	GU945342
<i>L. gilanensis</i>	IRAN1501C	Unknown	Iran	GU945352	GU945341
<i>L. gilanensis</i>	UCD256Ma ^a	<i>Vitis vinifera</i>	USA	DQ233594	GU294742
<i>L. gilanensis</i>	MXBC50	<i>Vitis vinifera</i>	Mexico	MT663299	MT712006
<i>L. gilanensis</i>	MXBCCS01	<i>Vitis vinifera</i>	Mexico	MT663300	MT712007
<i>L. gonubiensis</i>	CMW 14077	<i>Syzygium cordatum</i>	South Africa	AY639595	DQ103566

(Continued)

Table 1. (Continued).

Species	Isolate	Host	Origin	GeneBank accession number	
				ITS	<i>tcf-1a</i>
<i>L. gonubiensis</i>	CMW 14078	<i>Syzygium cordatum</i>	South Africa	AY639594	DQ103565
<i>L. iraniensis</i>	IRAN1502C	<i>Juglans</i> sp.	Iran	GU945347	GU945335
<i>L. iraniensis</i>	IRAN921C	<i>Mangifera indica</i>	Iran	GU945346	GU945334
<i>L. margaritacea</i>	CBS122519	<i>Adansonia gibbosa</i>	Australia	EU144050	EU144065
<i>L. margaritacea</i>	CBS122065	<i>Adansonia gibbosa</i>	Australia	EU144051	EU144066
<i>L. mediterranea</i>	BL101	<i>Vitis vinifera</i>	Italy	KJ638311	KJ638330
<i>L. mediterranea</i>	BL1	<i>Quercus ilex</i>	Italy	KJ638312	KJ638331
<i>L. missouriana</i>	UCD2193MO	<i>Vitis</i> sp.	USA	HQ288225	HQ288267
<i>L. missouriana</i>	UCD2199MO	<i>Vitis</i> sp.	USA	HQ288226	HQ288268
<i>L. parva</i>	CBS 456.78	Cassava field-soil	Colombia	EF622083	EF622063
<i>L. parva</i>	CBS 494.78	Cassava field-soil	Colombia	EF622084	EF622064
<i>L. pseudotheobromae</i>	CBS116459	<i>Gmelina arborea</i>	Costa Rica	EF622077	EF622057
<i>L. pseudotheobromae</i>	CBS447.62	<i>Citrus aurantium</i>	Suriname	EF622081	EF622060
<i>L. pyriformis</i>	CBS 121770	<i>Acacia mellifera</i>	Nambia	EU101307	EU101352
<i>L. pyriformis</i>	CBS 121771	<i>Acacia mellifera</i>	Nambia	EU101308	EU101353
<i>L. subglobosa</i>	CMM4046	<i>Jatropha curcas</i>	Brazil	KF234560	KF226723
<i>L. subglobosa</i>	CMM3872	<i>Jatropha curcas</i>	Brazil	KF234558	KF226721
<i>L. theobromae</i>	CBS 164.96	Fruit along coral reef	Papua New Guinea	AY640255	AY640258
<i>L. theobromae</i>	CBS111530	Unknown	Unknown	EF622074	EF622054
<i>L. venezuelensis</i>	WAC12539	<i>Acacia mangium</i>	Venezuela	DQ103547	DQ103568
<i>L. venezuelensis</i>	WAC12540	<i>Acacia mangium</i>	Venezuela	DQ103548	DQ103569
<i>Diplodia mutila</i>	CBS 136015	<i>Populus alba</i>	Portugal	KJ361838	KJ361830
<i>Diplodia seriata</i>	CBS 112555	<i>Vitis vinifera</i>	Portugal	AY259094	AY573220

Isolates from this study are highlighted in bold font.

^aIsolates previously identified as *L. theobromae*.

Plugs of sterile PDA were used in control plants, and all drill wounds were covered with Parafilm®. The grapevine plants were left in greenhouse conditions for 2 months. Samples were then taken to measure the length of the necrotic lesion caused by *Lasiodiplodia* isolates, and attempts were made to recover the inoculated fungus onto PDA. The experiments in plants were conducted twice. Statistical analyses were carried out using one-way ANOVA followed by *post hoc* Fisher LSD analyses, with $\alpha < 0.05$ for determination of significant differences in virulence between isolates using STATISTICA 8.0.

RESULTS

Host symptoms, and morphological characteristics of fungal isolates

Botryosphaeria dieback symptoms observed on sampled grapevine plants were mainly dead spurs, cordons, and arms, and shorter shoot internodes. The collected

wood exhibited wedge-shaped cankers and necrotic lesions in the vascular bundles.

From necrotic tissue placed in PDA, rapid fungus growth was observed after 2 d. From these colonies, 23 fungal isolates with a similar phenotype were recovered, seven from Baja California and sixteen from Sonora. According to their morphological characteristics, these isolates were identified as *Lasiodiplodia*. Morphological characteristics included initially white colonies with abundant aerial mycelium, which became smoke-gray and produced pycnidia in PDA as they aged (Figure 2). Pycnidium induction allowed observation of hyaline and pigmented conidia in all the isolates (Figure 3). Inside pycnidia, only hyaline aseptate conidia, with granular contents, were observed, while one-septate pigmented conidia with longitudinal striations were mainly found in cirri (Figure 3). The dimensions (length and width) of 30 conidia per isolate were measured, and minimum, maximum, mean, and standard deviations were calculated (Table 2). Statistically significant differences in conidium dimensions were observed among the four analyzed

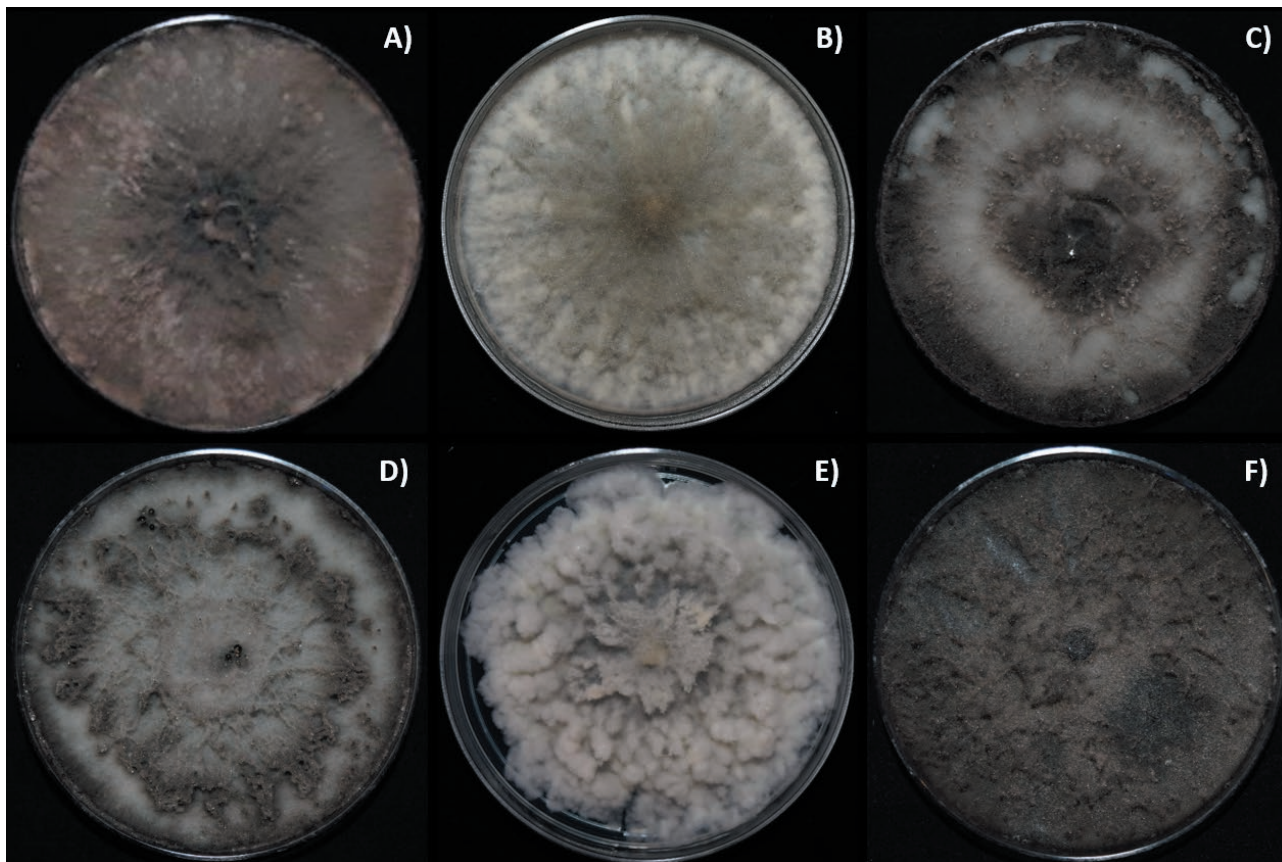


Figure 2. *Lasiodiplodia* spp. isolates grown on PDA at 30°C for 7 d. A) *L. brasiliensis* MXBCL28, B) *L. brasiliensis* MXVS18, C) *L. exigua* MXVS21b, D) *L. exigua* MXVS5a, E) *L. gilanensis* MXBCCS01, F) *L. crassispora* MXVS1b.

Lasiodiplodia species. Isolates characterized as *L. gilanensis*, MX50 (av. = 28.5 × 16.6 mm), and MXCS01 (av. = 30.2 × 15.6 mm), produced larger and wider conidia than *L. brasiliensis*, *L. crassispora*, or *L. exigua*. *Lasiodiplodia brasiliensis* and *L. crassispora* isolates had similar sized conidia (respective mean lengths = 24.0 and 25.6 mm). The *L. exigua* isolates had shorter conidia (av. = 21.2 × 12.2 mm).

Molecular identification of *Lasiodiplodia* isolates

The ITS region and *tef-1α* loci sequences obtained were, respectively, approx. 500 and 263 bp. The combined dataset comprised 832 characters including gaps after alignment (541 corresponded to the ITS gene and 291 corresponded to the *tef1* gene), and 72 taxa. *Diplodia mutila* (CBS 136015) and *Diplodia seriata* (CBS 112555) were used as the outgroup taxa. Maximum parsimony analysis yielded one most parsimonious tree [(length = 151, CI = 0.711864 (0.677885), RI = 0.922197,

RC = 0.714550 (0.656479)] for all sites and parsimony-informative sites. Maximum likelihood analysis using the Tamura 3-parameter model resulted in a tree with the log likelihood value of -2252.61. The rate variation model allowed for some sites to be evolutionarily invariable ([+I], 41.41% sites). Estimated base frequencies were: A = 0.21487, C = 0.28764, G = 0.25966, and T = 0.23783; and a discrete Gamma distribution was used to model evolutionary rate differences among sites [five categories (+G, parameter = 0.5665)].

The phylogenetic analysis of the ITS region and *tef-1α* revealed that the isolates were of four different *Lasiodiplodia* spp. (Figure 4). Most of the isolates were *L. exigua* (syn. *Lasiodiplodia mahajangana*) (isolates MXBCV4, MXBCV7, MXBCV6, MXVSV1, MXVS5a, MXVSSC1, MXVSS2, MXVS2Ta, MXVS6a, MXVS16b, MXVS20, MXVS21a, and MXVS21b). Six isolates were *L. brasiliensis* (isolates MXBCL28, MXVSCC1, MXVS15a, MXVS16a, MXVS18, and MXVS19a); two isolates were *L. gilanensis* (syn. *Lasiodiplodia missouriana*) (isolates MXBCCS01 and MXBC50); and two isolates were

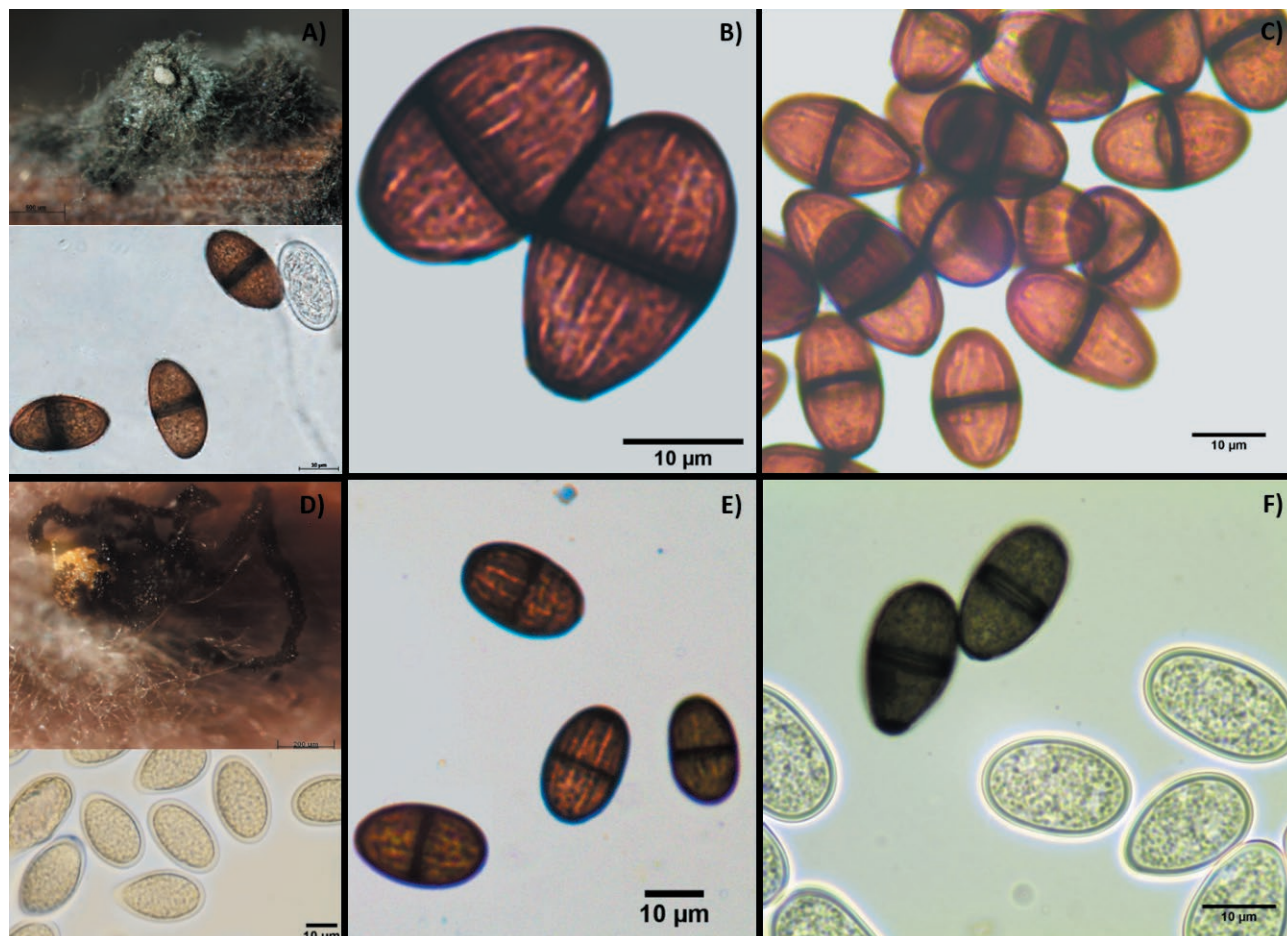


Figure 3. Conidia of *Lasiodiplodia* spp. isolates. A) *L. brasiliensis* MXBCL28, B) *L. brasiliensis* MXVS18, C) *L. exigua* MXVS21b, D) *L. gilanensis* MXBCCS01, E) *L. crassispora* MXVS1b, F) *L. exigua* MXVS5a.

L. crassispora (syn. *Lasiodiplodia pyriformis*) (isolates MXBCV5 and MXVS1b). Previously, only *L. theobromae* had been described in Baja California and Sonora (Úrbez-Torres *et al.*, 2008). Nonetheless, the three *L. theobromae sensu stricto* isolates used as references were clustered separately, and the isolates from the 2008 study of Baja California and Sonora were clustered within the clade of *L. brasiliensis* (Figure 4, Figure S1).

Optimum growth temperature and aerial mycelium production of Lasiodiplodia spp.

The *Lasiodiplodia* isolates selected had optimum growth temperatures of 28°C. Most of the isolates grew at greater than 20 mm d⁻¹ at 30°C (Table 3). *Lasiodiplodia exigua* grew at up to a mean of 24.6 mm d⁻¹ at 37°C, and this was the only species that grew at 40°C. *Lasiodiplodia gilanensis* had the least mycelium growth rate, with a maximum mean growth rate of 19.8 mm d⁻¹ at 28°C.

All the *Lasiodiplodia* isolates produced aerial mycelium, but in *L. gilanensis* this was less (mean = 0.8 ± 0.4 mm) than for the other species. The most abundant and longest aerial mycelium was observed in *L. exigua* isolate MXVS5a (16 ± 4.8 mm), followed by *L. brasiliensis* (9.0 ± 2.56 mm). The species *Lasiodiplodia crassispora* produced less abundant aerial mycelium (5.4 ± 2.3 mm) than the other species, and this species melanized more rapidly than the other species (Figure 5).

Evaluation of the pathogenicity of selected isolates of Lasiodiplodia spp.

Pathogenicity assays on grapevine plants showed that two-months post inoculation *L. brasiliensis* MXBCL28 and MXVS18, and *L. gilanensis* MXCS01 were the most virulent isolates (Figure 5, C, D, and F), in the woody shoots induced necrotic lesions up to 6 cm in

Table 2. Conidium dimensions of the *Lasiodiplodia* spp. isolates from this study.

Isolate	Origin	Conidium size ^a	Mean ± SD ^b
<i>Lasiodiplodia brasiliensis</i> ^b			
MXBCL28	Valle de Guadalupe, B.C.	(21.9-)24-28.4 × (12.8-)13.6-14.7	24.3±1.4 × 13.7±0.7
MXVSCC1	Hermosillo, Sonora	(20.4-)24.6-27.1 × (11.3-)12.5-14.8	23.7±1.7 × 12.8±0.8
MXVS15a	Hermosillo, Sonora	(20.3-)22.3-24.6 × (11.5-)12.5-14.4	22.8±1 × 12.5±0.7
MXVS16a	Hermosillo, Sonora	(22.1-)26.8-27.6 × (10.6-)11.7-13.1	24.7±1.6 × 11.9±0.5
MXVS18	Hermosillo, Sonora	(21.3-)24.8-29.4 × (11.3-)13.5-15.2	24.7±2 × 13.3±0.8
MXVS19a	Hermosillo, Sonora	(20.1-)23.3-26.4 × (11.4)13.4-16.8	23.2±1.7 × 13.3±1.3
<i>Lasiodiplodia crassispora</i> ^c			
MXBCV5	Valle de Guadalupe, B.C.	(23.0-)24.4-29.9 × (13.3-)16.7-20.2	26.1±2.2 × 17.5±1.7
MXVS1b	Hermosillo, Sonora	(23.7-)24.6-27.1 × (13-)14.7-16.7	25.0±0.9 × 14.7±1.1
<i>Lasiodiplodia exigua</i> ^a			
MXBCV4	Valle de Guadalupe, B.C.	(18.6-)21.1-24.8 × (11-)12-13.9	21.5±1.6 × 12.2±0.8
MXBCV6	Valle de Guadalupe, B.C.	(18.4-)19.2-22.5 × (10.5-)11.4-12.7	20.2±1.1 × 11.2±0.7
MXBCV7	Valle de Guadalupe, B.C.	(19.1-)20.1-21.7 × (12.0-)12.9-14.2	20.3±0.7 × 12.9±0.5
MXVS5a	Hermosillo, Sonora	(21.1-)22.5-25.6 × (11.7-)13.2-16	22.7±1.1 × 13.9±1.0
MXVS6a	Hermosillo, Sonora	(21.0-)23.4-24.6 × (11.9-)12.9-13.9	22.8±1.0 × 13±0.5
MXVS2Ta	Hermosillo, Sonora	(19.7-)21.3-22.8 × (11.3-)12.3-12.9	21.3±0.9 × 12.2±0.5
MXVS16b	Hermosillo, Sonora	(19.6-)23-26.9 × (11.1)13-14.9	22.5±2.0 × 12.9±0.9
MXVS20	Hermosillo, Sonora	(20.2-)21.9-23.7 × (11.2-)12.7-13.9	22.2±0.9 × 12.8±0.7
MXVS21a	Hermosillo, Sonora	(18.4-)19.6-23.8 × (10.1-)12.5-13.9	20.6±1.5 × 12.5±0.9
MXVS21b	Hermosillo, Sonora	(19.3-)20.3-23.2 × (10.7-)11.9-13.4	21±1.0 × 12±0.7
MXVSV1	Hermosillo, Sonora	(19.1-)20.8-23.4 × (10.2)12-12.8	20.6±1.0 × 11.6±0.7
MXVSSC1	Hermosillo, Sonora	(18.2-)19.8-24.1 × (10.5-)11.5-13.5	20.8±1.9 × 11.7±0.6
MXVSS2	Hermosillo, Sonora	(18.3-)20-23 × (11.4-)11.9-14.2	20.5±1.2 × 12.5±0.7
<i>Lasiodiplodia gilanensis</i> ^d			
MXBC50	Valle de Guadalupe, B.C.	(25.6-)28-33.8 × (15-)17.1-18.1	28.5±1.7 × 16.6±0.6
MXNCCS01	Valle de Guadalupe, B.C.	(25.4-)28.9-33 × (13.8-)15.4-18.7	30.2±1.8 × 15.6±1.2

^a Minimum size, most repetitive value and maximum size for length and width of 30 conidia selected.

^b SD = standard deviation.

a,b,c,d Means accompanied by the same letters are not significantly different ($\alpha < 0.05$).

length around the inoculation site, and were significantly different from the other inoculated isolates. *L. exigua* MXVS21b caused necrotic lesions in length, similar to *L. gilanensis* UCD256Ma (Figure 5 and 6). *L. crassispora* MXBCV5 and MXVS1b caused lesion below 1 cm in length (Figure 5 and 6) and showed a non-significant difference in comparison to control plants. All isolates were recovered from the inoculate site at three days after incubation at 30°C on PDA plates, which confirmed Koch's postulates. Non-necrotic lesions were observed in the control plants, only the wound effect; instead, green tissue was found, which indicated tissue regeneration of the caused wound.

DISCUSSION

In this study, four *Lasiodiplodia* species causing Botryosphaeria dieback symptoms were identified from Mexican vineyards. *Lasiodiplodia theobromae*, the type species of *Lasiodiplodia*, is one of the most common species associated with Botryosphaeria dieback in grapevine (Úrbez-Torres, 2011; Fontaine *et al.*, 2016), and for several years, it was the only known species within the genus. Later, *L. theobromae* was shown to be a complex of cryptic species (Alves *et al.*, 2008), which led to taxonomic revision of *Lasiodiplodia*. As a result, fungal isolates previously reported as *L. theobromae* have been re-

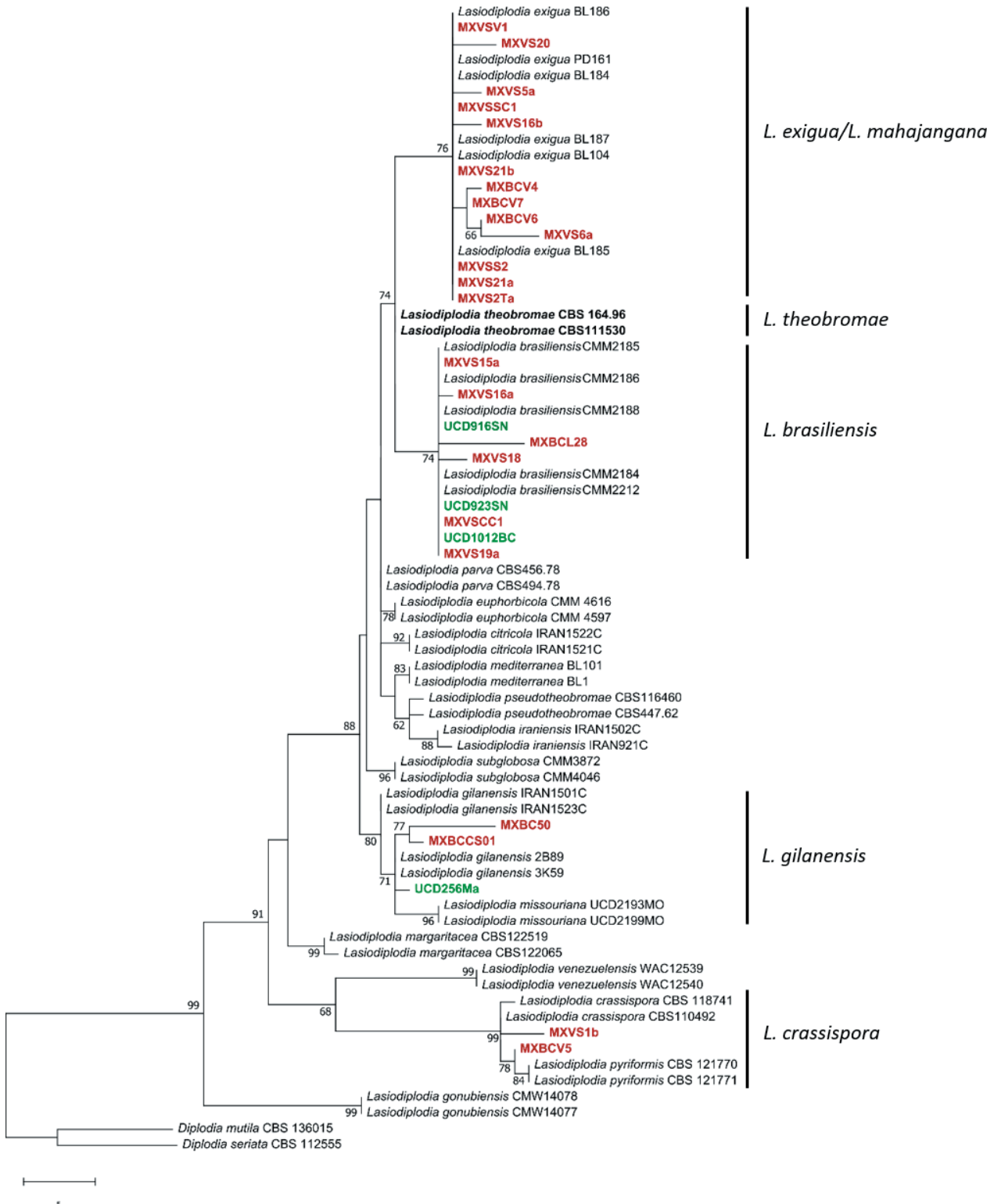
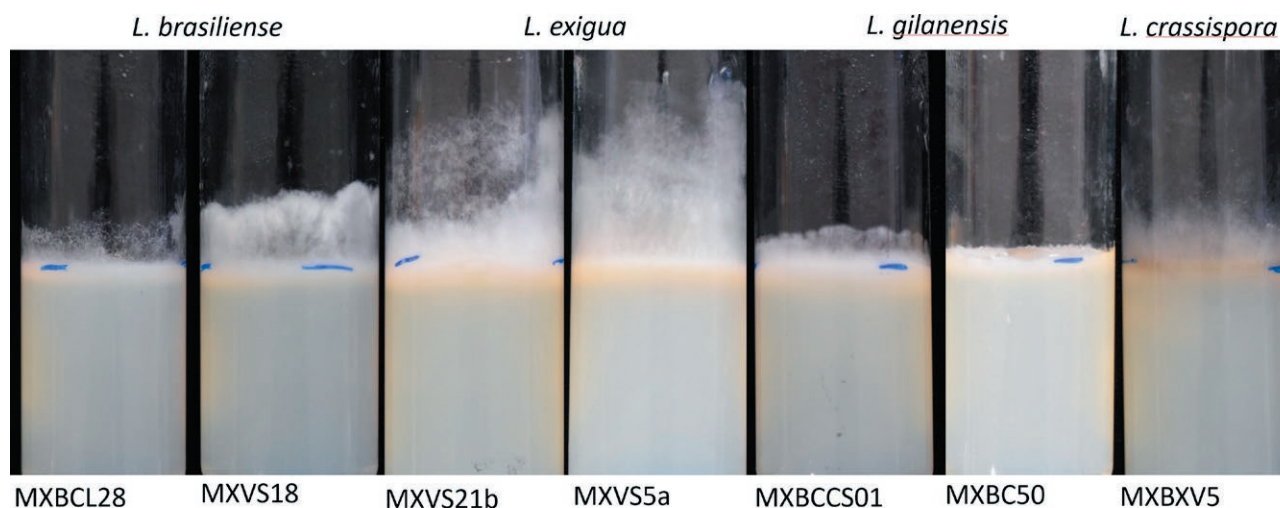


Figure 4. Phylogenetic analysis. Most-parsimonious tree (length = 151) obtained from analysis of ITS and *tef1* concatenated datasets. Bootstrap values from 1000 replicates greater than 50 are indicated at the nodes. The tree is rooted with *Diplodia mutila* (CBS 136015) and *Diplodia seriata* (CBS 112555). The isolates from the present study are indicated in bold red font, isolates previously identified as *L. theobromae* are indicated in bold black font, and the *L. theobromae sensu stricto* isolates are indicated in bold black font.

Table 3. Mean colony diameters at different temperatures for Mexican *Lasiodiplodia* isolates grown in PDA cultures.

Isolate	Temperature						
	20°C	23°C	25°C	28°C	30°C	37°C	40°C
<i>Lasiodiplodia brasiliensis</i>							
MXBCL28	19.1 ± 0.7	21.6 ± 2.4	20 ± 1.3	28.1 ± 0.2	20.6 ± 3.6	6.8 ± 0.57	0
MXVS18	15 ± 0	20 ± 0.8	23.1 ± 1.0	27.3 ± 1.7	22.0 ± 1.0	20.0 ± 1.8	0
<i>Lasiodiplodia crassispora</i>							
MXBCV5	12.6 ± 0.2	17.3 ± 0.2	19.1 ± 1.5	23.1 ± 0.2	20.1 ± 1	3.8 ± 0.7	0
<i>Lasiodiplodia exigua</i>							
MXVS5a	15 ± 1.3	21.3 ± 2	19.8 ± 0.7	28.1 ± 1.5	20.5 ± 2.2	21.6 ± 1	0.5 ± 0
MXVS21b	17.16 ± 0.2	19.6 ± 0.5	20.6 ± 1.5	23 ± 2.1	22.3 ± 0.7	24.6 ± 0.7	0.5 ± 0
<i>Lasiodiplodia gilanensis</i>							
MXBC50	11 ± 2.4	8.1 ± 0.7	5.6 ± 1.6	6.1 ± 1.2	11.3 ± 7.2	5.8 ± 1.6	0
MXBCCS01	16.3 ± 0.35	17.1 ± 2.46	17.5 ± 3.6	19.8 ± 5.0	18.1 ± 1.89	9.5 ± 0.5	0

**Figure 5.** Aerial mycelium growth of different *Lasiodiplodia* spp. isolated from grapevines in Mexico. The isolates were grown in glass tubes containing PDA medium for 5 d at 28°C.

classified as new species (Dissanayake *et al.*, 2016; Cruywagen *et al.*, 2017; Mehl *et al.*, 2017; Tibpromma *et al.*, 2018). Some species were subsequently reduced to synonymy (Zhang *et al.*, 2021). The fungal rDNA internal transcribed spacer region (ITS) is the primary barcode used to identify fungal species, but in *Lasiodiplodia* spp., this region has low interspecific variation. The translation elongation factor 1- α (*tef-1 α*) is more variable than ITS, and has been recommended as a secondary barcode region to estimate species identity for *Botryosphaeriaceae* (Lawrence *et al.*, 2017), and this locus allowed us to segregate *L. brasiliensis* from *L. theobromae*.

Pathogens associated with wood dieback diseases are generally found in vineyards that are at least 10 years

old (Gubler *et al.*, 2005), but we have isolated these fungi in younger vineyards in Mexico. *Lasiodiplodia exigua*, *L. brasiliensis*, and *L. crassispora* were recovered from the two Mexican viticulture areas (Baja California and Sonora), whereas *L. gilanensis* was only found in Baja California. *Lasiodiplodia exigua* was the most prevalent species. Previously, only *L. theobromae* was reported in Mexico in grapevine (Úrbez-Torres *et al.*, 2008), but our phylogenetic analyses indicated that those isolates clustered with *L. brasiliensis*, suggesting that *L. brasiliensis* has been in Mexico for a long time.

Production of reddish-pink pigment by the isolates of *L. brasiliensis* and *L. gilanensis* was observed. This characteristic has been reported in other species

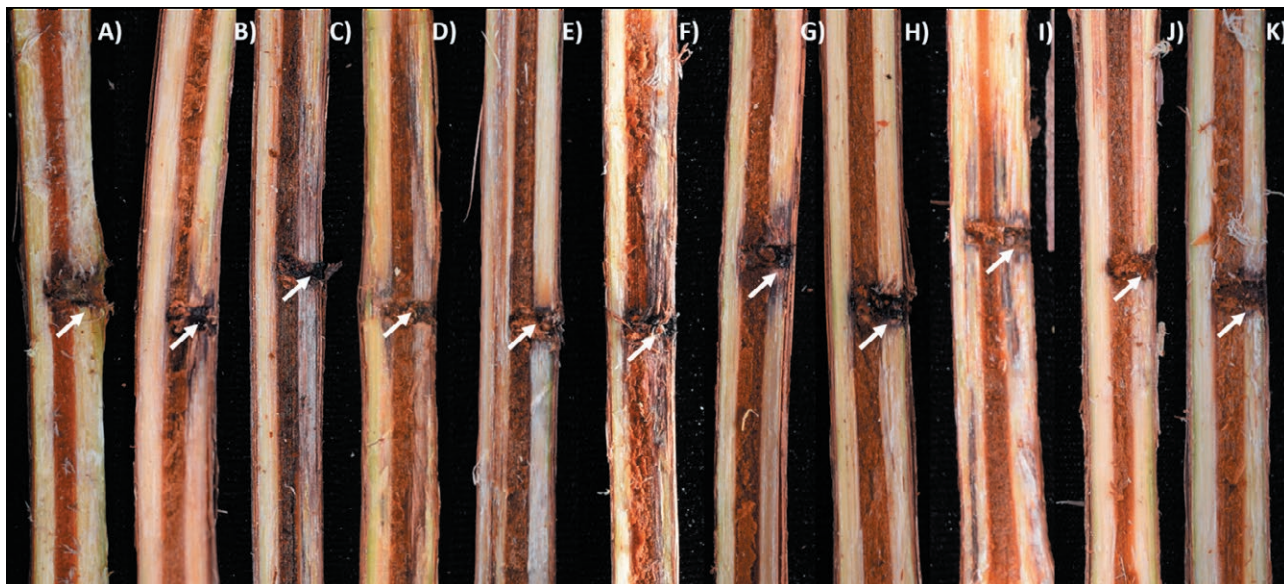


Figure 6. Grapevine woody shoots showing dark-brown lesions at 2-months post inoculation with *Lasiodiplodia* isolates. A) Control plant (PDA), B) *L. gilanensis* UCD256Ma, C) *L. brasiliensis* MXBCL28, D) *L. brasiliensis* MXVS18, E) *L. brasiliensis* MXVS16a F) *L. gilanensis* MXBCCS01, G) *L. gilanensis* MXBC50, H) *L. exigua* MXVS6a, I) *L. exigua* MXVS21b J) *L. crassispora* MXVS1b, and K) *L. crassispora* MXB-CV5. White arrows indicate the point of inoculation.

including *L. pseudotheobromae*, *L. parva*, and *L. theobromae* (Alves *et al.*, 2008; Abdollahzadeh *et al.*, 2010). Although *L. missouriana* has been reduced to synonymy with *L. gilanensis* (Zhang *et al.*, 2021), conidium dimensions of the Mexican isolates of *L. gilanensis* (isolates MX50 and MXSC01) and one from California, USA (isolate UCD256Ma) were larger (av. = 29.6 x 15.6 μm) than those for *L. missouriana* (av. = 18.5 x 9.8 μm) from Missouri, USA (Phillips *et al.*, 2013). On the other hand, *L. theobromae* (av. \pm SD = 26.2 \pm 2.6 x 14.2 \pm 1.2 μm) (Phillips *et al.*, 2013) had conidium dimensions similar to those for *L. brasiliensis* (av. \pm SD = 26.01 \pm 1.36 x 14.64 \pm 1.16 μm) (Netto *et al.*, 2014), making these species difficult to distinguish based solely on morphological traits. In the present study, aerial mycelium height was another morphological characteristic evaluated, and the observed differences suggested that this trait could help with the differentiation of *Lasiodiplodia* species.

The pathogenicity tests showed that the *L. brasiliensis* isolates MXBCL28 and MXVS18, and *L. gilanensis* isolate MXCS01 were the most virulent to grapevine plants ‘Cabernet Sauvignon’. These isolates caused necrotic lesions to the host vascular systems at 2 months post-inoculation. *Lasiodiplodia brasiliensis* was also reported for the first time on grapevine in Brazil, and this was the most virulent species on green shoots, followed by *L. theobromae* (Correia *et al.*, 2016). *Lasidiplo-*

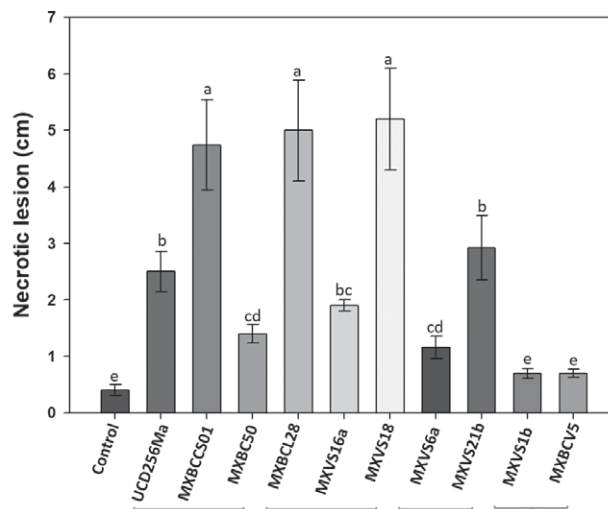


Figure 7. Mean lesion length caused by *Lasiodiplodia* isolates in grapevine plants 2-months post inoculation under greenhouse conditions. Bars indicate the standard deviation of each treatment. Significance letters were grouped based on Fisher's analysis ($P < 0.05$); Bars indicate standard deviations. Means accompanied by the same letters are not significantly different ($\alpha < 0.05$)

dia gilanensis was described for the first time from Iran, from an unknown tree showing branch dieback, cankers, and fruit rot (Abdollahzadeh *et al.*, 2010). Considering isolate UCD256Ma, formerly identified as *L. theo-*

bromae (Úrbez-Torres *et al.*, 2006) belongs to *L. gilanensis*, the present study data supports taxonomic reassignment. *Lasiodiplodia missouriana* has been reduced to synonymy with *L. gilanensis* (Zhang *et al.*, 2021). *Lasiodiplodia missouriana* was isolated from grapevines in 2011, and was one of the most aggressive species to grapevine (Úrbez-Torres *et al.*, 2012), confirming results from the present study.

Lasiodiplodia exigua isolates MXVS6a and MXVS21b were of different virulence than *L. brasiliensis* and *L. gilanensis* isolates. *Lasiodiplodia exigua* was first isolated from broom bush (*Retama raetam*) in Tunisia (Linaldeddu *et al.*, 2015), and was reported to cause brown discolouration and streaks in grapevine wood (Akgül *et al.*, 2019). The *L. crassispora* isolates MXBCV5 and MXVS1b from the present study were the least virulent, which is similar to the results from previous studies (Correia *et al.*, 2016).

Grapevine plants are susceptible to several different wood pathogens during the pruning period, so it is important to consider factors such as climatic conditions and life cycles of GTDs pathogens (Rolshausen *et al.*, 2010; Agustí-Brisach *et al.*, 2015; Gramaje *et al.*, 2018; Waite *et al.*, 2018). Spread of fungus pathogens involved in Botryosphaeria dieback within vineyards is linked with rainfall and associated wind dispersal of inocula (Mehl *et al.*, 2017). *Lasiodiplodia* has been reported to be prevalent in regions with high temperatures and low precipitation (Úrbez-Torres, 2011; Gispert *et al.*, 2020). The isolates examined in the present study had optimum growth temperatures of 28°C, but all grew at 37°C, and the isolates of *L. exigua* grew at 40°C. This could be an adaptation of *L. exigua* to extreme hot weather conditions. This species is the most commonly found in the Baja California and Sonora grape-growing regions. Even when the other isolates did not grow at 40 °C, they recovered their average growth once they were transferred to room temperature, except for *L. gilanensis* isolate MXBC50. These fungi probably entered a dormant state that recovers when temperatures decrease. This could explain why *L. gilanensis* is the most common species in Baja California and Sonora, where prevalent climate conditions are annual precipitation of 280 mm and temperatures greater than 40°C during the summer, conditions which favour growth of *L. gilanensis*. More studies are required of these fungi under extreme growing conditions. However, the present study has contributed to recognizing GTD pathogen species present in Mexico's most economically important viticulture region, representing the first step for epidemiological studies to assist controlling the spread of these pathogens.

ACKNOWLEDGMENTS

Edelweiss A. Rangel-Montoya received a scholarship from CONACYT. Marcos Paolinelli acknowledges the support provided by a CONICET postdoctoral fellowship.

LITERATURE CITED

- Abdollahzadeh J., Javadi A., Mohammadi Goltapeh E., Zare R., Phillips A.J., 2010. Phylogeny and morphology of four new species of *Lasiodiplodia* from Iran. *Persoonia: Molecular Phylogeny and Evolution of Fungi* 25: 1–10.
- Agustí-Brisach C., León M., García-Jiménez J., Armengol J., 2015. Detection of grapevine fungal trunk pathogens on pruning shears and evaluation of their potential for spread of infection. *Plant Disease* 99: 976–981.
- Akgül D.S., Savaş N.G., Özarslandan M., 2019. First report of wood canker caused by *Lasiodiplodia exigua* and *Neoscytalidium novaehollandiae* on grapevine in Turkey. *Plant Disease* 103: 1036.
- Alves A., Crous P.W., Correia A., Phillips A.J.L., Alves A., 2008. Morphological and molecular data reveal cryptic speciation in *Lasiodiplodia theobromae*. *Fungal Diversity* 28: 1–13.
- Bertsch C., Ramírez-Suero M., Magnin-Robert M., Larignon P., Chong J., ... Fontaine F., 2013. Grapevine trunk diseases: complex and still poorly understood. *Plant Pathology* 62: 243–265.
- Billones-Baaijens R., Savocchia S., 2019. A review of Botryosphaeriaceae species associated with grapevine trunk diseases in Australia and New Zealand. *Australasian Plant Pathology* 48: 3–18.
- Carbone I., Kohn L., 1999. A method for designing primer sets for speciation studies in filamentous Ascomycetes. *Mycologia* 91: 553–556.
- Correia K.C., Silva M.A., de Moraes M.A., Jr. Armengol J., Phillips A.J.L., ... Michereff S.J., 2016. Phylogeny, distribution and pathogenicity of *Lasiodiplodia* species associated with dieback of table grape in the main Brazilian exporting region. *Plant Pathology* 65: 92–103.
- Cruywagen E.M., Slippers B., Roux J., Wingfield M.J., 2017. Phylogenetic species recognition and hybridisation in *Lasiodiplodia*: a case study on species from baobabs. *Fungal Biology* 121: 420–436.
- Dissanayake A.J., Phillips A.J.L., Li X.H., Hyde K.D., 2016. Botryosphaeriaceae: current status of genera and species. *Mycosphere* 7: 1001–1073.

- Fontaine F., Pinto C., Vallet J., Clément C., Gomes A.C., Spagnolo A., 2016. The effects of grapevine trunk diseases (GTDs) on vine physiology. *European Journal of Plant Pathology* 144: 707–721.
- García-Robles J.M., Tobón-Quijano J.I., Bringas-Taddei E., Mercado-Ruiz J.N., Luchsinger-Lagos L., Báez-Sañudo R., 2007. Daños y desórdenes fisiológicos en uva de mesa sonoreña después del preenfriado y almacenamiento. *Revista Iberoamericana de Tecnología Postcosecha* 8: 89–100.
- Gispert C., Kaplan J.D., Deyett E., Rolshausen P.E., 2020. Long-Term Benefits of Protecting table grape vineyards against trunk diseases in the California desert. *Agronomy* 10: 1895.
- González-Andrade S., 2015. Cadena de valor económico del vino de Baja California, Mexico. *Estudios fronterizos* 16: 163–193.
- Gramaje D., Armengol J., 2011. Fungal trunk pathogens in the grapevine propagation process: potential inoculum sources, detection, identification, and management strategies. *Plant Disease* 95: 1040–1055.
- Gramaje D., Úrbez-Torres J.R., Sosnowski M.R., 2018. Managing grapevine trunk diseases with respect to etiology and epidemiology: current strategies and future prospects. *Plant Disease* 102: 12–39.
- Gubler W.D., Rolshausen P.E., Trouillasse F.P., Úrbez J.R., Voegel T., 2005. Grapevine trunk diseases in California. *Practical Winery & Vineyard* Jan/Feb: 6–25.
- Hall T.A., 1999. BioEdit: a user-friendly biological sequence alignment editor and analysis program for Windows 95/98/NT. *Nucleic acids symposium series* 41: 95–98.
- Kumar S., Stecher G., Li M., Nnyaz C., and Tamura K., 2018. MEGA X: Molecular Evolutionary Genetics Analysis across computing platforms. *Molecular Biology and Evolution* 35: 1547–1549.
- Lawrence D.P., Travadon R., Nita M., Baumgartner K., 2017. TrunkDiseaseID.org: A molecular database for fast and accurate identification of fungi commonly isolated from grapevine wood. *Crop Protection* 102: 110–117.
- Linaldeddu B.T., Deidda A., Scanu B., Franceschini A., Serra S., ... Phillips A.J.L., 2015. Diversity of Botryosphaeriaceae species associated with grapevine and other woody hosts in Italy, Algeria and Tunisia, with descriptions of *Lasiodiplodia exigua* and *Lasiodiplodia mediterranea* sp. nov. *Fungal Diversity* 71: 201–214.
- Mehl J., Wingfield M.J., Roux J., Slippers B., 2017. Invasive everywhere? Phylogeographic analysis of the globally distributed tree pathogen *Lasiodiplodia theobromae*. *Forests* 8: 1–22.
- Netto M.S., Assunção I.P., Lima G.S., Marques M.W., Lima W.G., ... Câmara M.P., 2014. Species of *Lasiodiplodia* associated with papaya stem-end rot in Brazil. *Fungal Diversity* 67: 127–141.
- Obrador-Sánchez J.A., Hernandez-Martinez R., 2020. Microscope observations of Botryosphaeriaceae spp. in the presence of grapevine wood *Phytopathologia Mediterranea* 59: 119–129.
- Paolinelli-Alfonso M., Villalobos-Escobedo J.M., Rolshausen P., Herrera-Estrella A., Galindo-Sánchez C., ... Hernandez-Martinez R., 2016. Global transcriptional analysis suggests *Lasiodiplodia theobromae* pathogenicity factors involved in modulation of grapevine defensive response. *BMC Genomics* 17, 615.
- Phillips A.J.L., Alves A., Abdollahzadeh J., Slippers B., Wingfield, M.J., ... Crous P.W., 2013. The Botryosphaeriaceae: genera and species known from culture. *Studies in Mycology* 76: 51–167.
- Punithalingam E., 1976. *Botryodiplodia theobromae*. *IMI Descriptions of Fungi and Bacteria* 519: 1–2.
- Rolshausen P.E., Úrbez-Torres J.R., Rooney-Latham S., Eskalen A., Smith R.J., Gubler W.D., 2010. Evaluation of pruning wound susceptibility and protection against fungi associated with grapevine trunk diseases. *American Journal of Enology and Viticulture* 61: 113–119.
- Rolshausen P.E., Akgül D.S., Perez R., Eskalen A., Gispert C., 2013. First report of wood canker caused by *Neoscytalidium dimidiatum* on grapevine in California. *Plant Disease* 97: 1511–1511.
- SIAP Servicio de Información y Estadística Agroalimentaria y Pesquera, 2019. Ministerio de Agricultura de Mexico, Secretaría de Agricultura, Ganadería, Desarrollo Rural, Pesca y Alimentación (SAGARPA).
- Slippers B., Smit W.A., Crous P.W., Coutinho T.A., Wingfield B.D., Wingfield M.J., 2007. Taxonomy, phylogeny and identification of Botryosphaeriaceae associated with pome and stone fruit trees in South Africa and other regions of the world. *Plant Pathology* 56: 128–139.
- Stempien E., Goddard M.L., Wilhelm K., Tarnus C., Bertsch C., Chong, J., 2017. Grapevine Botryosphaeria dieback fungi have specific aggressiveness factor repertory involved in wood decay and stilbene metabolism. *PloS one* 12: e0188766.
- Tamura K., 1992. Estimation of the number of nucleotide substitutions when there are strong transition-transversion and G + C-content biases. *Molecular Biology and Evolution* 9: 678–687.
- Thompson J.D., Higgins D.G., Gibson T.J., 1994. CLUSTAL W: improving the sensitivity of progres-

- sive multiple sequence alignment through sequence weighting, position-specific gap penalties and weight matrix choice. *Nucleic Acids Research* 22: 4673–4680.
- Tibpromma S., Hyde K.D., McKenzie E.H., Bhat D.J., Phillips A.J.L., ... Karunarathna S.C., 2018. Fungal diversity notes 840–928: micro-fungi associated with Pandanaceae. *Fungal Diversity* 93: 13–160.
- Úrbez-Torres J.R., 2011. The status of Botryosphaeriaceae species infecting grapevines. *Phytopathologia Mediterranea* 50: S5–S45.
- Úrbez-Torres J.R., Gubler W.D., 2009. Pathogenicity of Botryosphaeriaceae species Isolated from Grapevine Cankers in California. *Plant Disease* 93: 584–592.
- Úrbez-Torres J.R., Leavitt G.M., Voegel T.M., Gubler W.D., 2006. Identification and Distribution of Botryosphaeria spp. associated with grapevine cankers in California. *Plant Disease* 90: 1490–1503.
- Úrbez-Torres J.R., Leavitt G.M., Guerrero J.C., Guevara J., Gubler W.D., 2008. Identification and pathogenicity of *Lasiodiplodia theobromae* and *Diplodia seriata*, the causal agents of bot canker disease of grapevines in Mexico. *Plant Disease* 92: 519–529.
- Urbez-Torres J.R., Peduto F., Striegler R.K., Urrea-Romero K.E., Rupe J.C., ... Gubler W.D. 2012. Characterization of fungal pathogens associated with grapevine trunk diseases in Arkansas and Missouri. *Fungal Diversity* 52: 169–189.
- Wagner D.B., Furnier G.R., Saghai-Marooof M.A., Williams SM, Dancik B.P., Allard R.W., 1987. Chloroplast DNA polymorphisms in lodgepole and jack pines and their hybrids. *PNAS* 84: 2097–2100.
- Waite H., Armengol J., Billones-Baaijens R., Gramaje D., Hallen F., ... Smart R., 2018. A protocol for the management of grapevine rootstock mother vines to reduce latent infections by grapevine trunk pathogens in cuttings. *Phytopathologia Mediterranea* 57: 384–398.
- White T.J., Bruns T., Lee S.J.W.T., Taylor J., 1990. Amplification and direct sequencing of fungal ribosomal RNA genes for phylogenetics. *PCR protocols: a Guide to Methods and Applications* 18: 315–322.
- Zhang W., Groenewald, J.Z., Lombard, L., Schumacher, R.K., Phillips, A.J.L., and Crous, P.W. 2021. Evaluating species in Botryosphaeriales. *Persoonia-Molecular Phylogeny and Evolution of Fungi* 46: 63–115.



Citation: D. Migliorini, F. Pecori, A. Raio, N. Luchi, D. Rizzo, C. Campani, L. Neri, A. Santini (2021) First report of *Erwinia amylovora* in Tuscany, Italy. *Phytopathologia Mediterranea* 60(2): 253-257. doi: 10.36253/phyto-12817

Accepted: June 10, 2021

Published: September 13, 2021

Copyright: ©2021 D. Migliorini, F. Pecori, A. Raio, N. Luchi, D. Rizzo, C. Campani, L. Neri, A. Santini. This is an open access, peer-reviewed article published by Firenze University Press (<http://www.fupress.com/pm>) and distributed under the terms of the Creative Commons Attribution License, which permits unrestricted use, distribution, and reproduction in any medium, provided the original author and source are credited.

Data Availability Statement: All relevant data are within the paper and its Supporting Information files.

Competing Interests: The Author(s) declare(s) no conflict of interest.

Editor: Nicola Sante Iacobellis, Former Professor, University of Basilicata, Italy.

Short Notes

First report of *Erwinia amylovora* in Tuscany, Italy

DUCCIO MIGLIORINI¹, FRANCESCO PECORI^{1,*}, AIDA RAIIO¹, NICOLA LUCHI¹, DOMENICO RIZZO², CARLO CAMPANI², LORENZO NERI², ALBERTO SANTINI¹

¹ Institute for Sustainable Plant Protection - National Research Council (IPSP-CNR), Via Madonna del Piano 10, I-50019, Sesto Fiorentino, Firenze, Italy.

² Laboratory of Phytopathological Diagnostics and Molecular Biology, Plant Protection Service of Tuscany, 51100 Pistoia, Italy

*Corresponding author. E.-mail: francesco.pecori@ipspp.cnr.it

Summary. 2-years-old plants of *Pyrus communis* showing symptoms of fire blight disease were sampled in an orchard in Tuscany (Italy) during Autumn 2020. Plants were obtained the previous spring from a commercial nursery located in a region where the disease is present since 1994. The collected material was processed in the lab in order to verify the presence of the bacterium *Erwinia amylovora*, the causal agent of fire blight. Pure isolates showing white mucoid colonies and levan producers on Lev-an medium were putatively assimilated to *E. amylovora*. DNA was extracted from the cultures and analysed with three molecular assays, including duplex PCR of the 29-Kb plasmid pEA29 and the *ams* chromosomal region, sequencing of the 16S rDNA and *recA* gene regions, two real-time PCR assays on symptomatic plant tissues. All tests confirmed the presence of *E. amylovora*. Symptomatic and surrounding plants were removed and immediately destroyed according to the regional phytosanitary protocol. This outcome poses a serious threat for fruit orchards in the area.

Keywords. Fire blight, AJ75/AJ76 and AMSbL/AMSbR primers, *recA* gene.

Fire blight symptoms were observed on 2-year-old pear trees (*Pyrus communis* ‘Williams’ and ‘Red Williams’) in October 2020 during an orchard phytopathological survey in south-eastern Tuscany (43.37966 N, 11.81162 E), an important fruit production area.

Plants were obtained in early spring 2020 from a fruit tree nursery located in a “protected area” within the Emilia Romagna region, where the pathogen causing this disease has been present since 1994 (EPPO, 114/1995). Plant material was standard, i.e. without phytosanitary certification proving disease-free status. At the time of the survey, the young pear trees showed a variety of symptoms, including shoot blight, stem canker or complete die-back, dried terminal shoots and shepherd’s crook (Figure 1). During autumn 2020, 21 infected plants were observed (19 *Pyrus communis*, two *Malus domestica*) out of more than 400 plants surveyed.



Figure 1. Symptoms of shoot blight and stem canker on symptomatic *Pyrus communis* 'Williams' and 'Red Williams' plants sampled during the survey.

Table 1. Isolates of *Erwinia* species used in this study. Sequence numbers in bold font were obtained in the present study.

Taxa	Strain	GenBank		Reference
		16S	<i>recA</i>	
<i>Erwinia amylovora</i>	1540	Z96088		Young and Park (2007)
	FB1-DZ		JN812979	Laala <i>et al.</i> (2012)
	ATCC15580	U80195		Arriel <i>et al.</i> , 2014
	IL6		AY217068	Geider <i>et al.</i> , (2006)
	IPSP_EA_001	MW786972	MW916100	This study
<i>E. chrysanthemi</i>	MAFF311151		AB713694	Suharjo <i>et al.</i> , (2014)
<i>E. mallotivora</i>	5705	Z96084	DQ859877	Young and Park (2007)
<i>E. persicina</i>	12532	Z96086	DQ859883	
	XHL2002230201	MT568607		Li <i>et al.</i> , 2021
<i>E. piriflorinigrans</i>	CFBP 5888 strain CECT 7348		GQ421460	López <i>et al.</i> , 2011
	CFBP 5882		GQ421461	
<i>E. psidii</i>	8426	Z96085	DQ859878	Young and Park (2007)
<i>E. pyrifoliae</i>	Ep1/96	AJ009930		Arriel <i>et al.</i> , 2014
	Ep16/96		AY217072	Geider <i>et al.</i> , (2006)
	14143	EF122435	DQ859885	Young and Park (2007)
<i>E. rhapontici</i>	ICMP 1582	Z96087	DQ859882	
	SUPP 355		LC406869	Tsuji <i>et al.</i> , 2020
<i>E. tasmaniensis</i>	Et4/99		AM292088	Geider <i>et al.</i> , (2006)
<i>E. tasmaniensis</i>	Et1/99		AM055718	
<i>E. tracheiphila</i>	5845	Y13250	DQ859879	Young and Park (2007)

Symptomatic shoot samples were collected, transferred to the laboratory on ice, and were processed for bacteria isolation and molecular analyses. Tissue samples were processed according to EPPO standard protocol (2013), as described below. Fragments of symptomatic tissues were surface sterilized in 1% NaClO solution, washed in sterilized distilled water and then ground in an antioxidant maceration buffer. Macerated tissues were enriched in liquid King's B medium (Sigma-Aldrich) and were incubated at 25°C for 48 h. To obtain single colonies, enriched suspensions were streaked onto Levan medium and nutrient glucose agar (NGA; 28 g L⁻¹ nutrient agar, 5 g L⁻¹ glucose: Oxoid), and incubated at 27°C for 48–72 h. Bacterial isolates were selected on the basis of colony morphology, and were purified and evaluated by KOH tests (Buch, 1982) to identify Gram negative bacteria. Isolates showing white mucoid colonies and levan production on Levan medium, were identified as putative *Erwinia amylovora*.

DNA extracted (Wizard® Genomic DNA Purification Kit: Promega) from the bacterial cultures was amplified by duplex PCR, as described by Hannou *et al.* (2013), using primers AJ75/AJ76 (844 bp fragment from the 29-Kb plasmid pEA29) and AMSbL/AMSbR (1.6-Kbp fragment from the *ams* chromosomal region). Both fragments, specific for *E. amylovora*, were successfully amplified.

The 16S rDNA and *recA* genes were amplified and sequenced using primers fD1 and rP1/rP2 (fD1: 5'-AGAGTTTGATCCTGGCTCAG-3'; rP1/rP2: 5'-GGYTACCTTGTTACGACTT-3'; Weisburg *et al.*, 1991), *recA1* and *recA2* (*recA1*: 5'-GGTAAAGGGTC-TATCATGCG-3'; *recA2*: 5'-CCTTCACCATACAT-AATTTGGA-3'; Waleron *et al.*, 2008).

Sequencing of 16S rDNA (GenBank accession no. MW786972; 1392 bp; Table 1) showed 99.61% similarity with *E. amylovora* (GenBank accession no. FN666575, isolate ATCC 49946). Sequencing of *recA* (GenBank accession no. MW916100; 711 bp; Table 1) showed 100% similarity with this reference *E. amylovora* isolate. Similarity with *E. pyrifoliae* (GenBank accession no. FP236842, strain Ep1/96) was of 99.21% for 16S and 96.18% for *recA*. Additional 16S and *recA* gene sequences from different strains of *E. amylovora*, and of different *Erwinia* species used for comparison, were obtained from NCBI (Table 1). Alignments were made using Geneious Prime (version 11.0.9) and phylogenetic analysis was performed with MEGA (version 10.2.2), using the Maximum Likelihood method and Tamura-Nei model. The trees obtained for both genes confirmed the species identification (Figures 2 and 3).

The presence of the pathogen was also confirmed by extraction of DNA with CTAB 2% (Li *et al.*, 2008) and

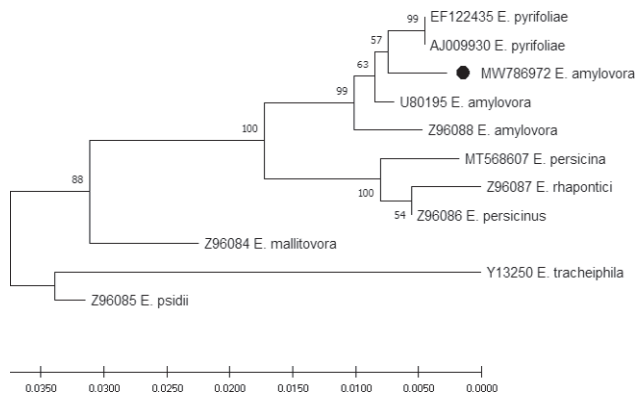


Figure 2. Phylogenetic analysis based on 16S rDNA gene sequences from diverse *Erwinia* spp. strains. The evolutionary history was inferred by using the Maximum Likelihood method and Tamura-Nei model (Tamura and Nei, 1993). The tree with the greatest log likelihood (-2704.47) is shown. The percentage of trees in which the associated taxa clustered together is shown next to the branches. Number of bootstrap replicates = 500. Initial tree(s) for the heuristic search were obtained automatically by applying Neighbor-Join and BioNJ algorithms to a matrix of pairwise distances estimated using the Tamura-Nei model, and then selecting the topology with superior log likelihood value. The tree is drawn to scale, with branch lengths measured in the number of substitutions per site. This analysis involved 11 nucleotide sequences. There were a total of 1285 positions in the final dataset. Evolutionary analyses were conducted in MEGA X (Kumar *et al.*, 2018). The sequence obtain in the present study is marked with a black dot.

two real-time PCR protocols according to Gottsberger (2010) and Pirc *et al.* (2009) carried on the symptomatic plant tissue from which the pathogen had been isolated. All processed samples were identified as *E. amylovora*.

All symptomatic plants were removed and destroyed. In order to check for others possible outbreaks intensive monitoring started in the original orchard and the surrounding areas.

This is the first report of *E. amylovora* in Tuscany. This pathogen may pose a serious threat to apple and pear production in this area. Presence of this pathogen in Tuscany is also a clear example of the spread of a quarantine pathogen by the plants-for-planting pathway. This record supports the need to use certified plant material, especially when nurseries are located in protected areas.

LITERATURE CITED

Arriel D.A.A., Fonseca N.R., Guimarães L.M.S., HERNANDEZ P. S., Mafía R. G., ... Alfenas A.C., 2014. Wilt and die-back of *Eucalyptus* spp. caused by *Erwinia psidii* in Brazil. *Forest Pathology* 44: 255–265.

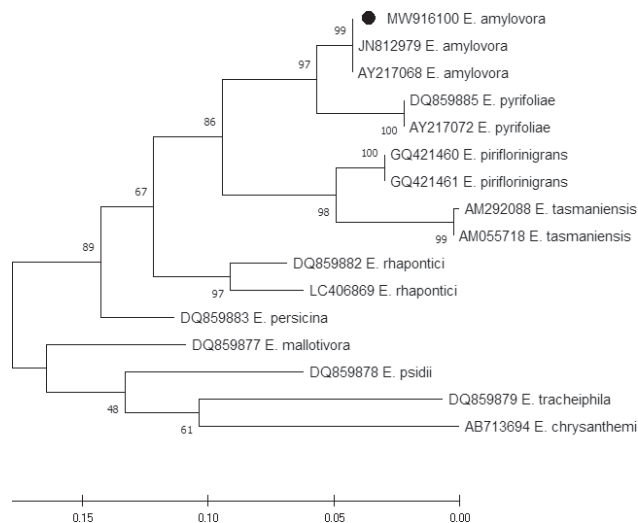


Figure 3. Phylogenetic analysis based on *recA* gene sequences from diverse *Erwinia* spp. strains. The evolutionary history was inferred by using the Maximum Likelihood method and Tamura-Nei model (Tamura and Nei, 1993). The tree with the greatest log likelihood (-1905.63) is shown. The percentage of trees in which the associated taxa clustered together is shown next to the branches. Number of bootstrap replicates = 500. Initial tree(s) for the heuristic search were obtained automatically by applying Neighbor-Join and BioNJ algorithms to a matrix of pairwise distances estimated using the Tamura-Nei model, and then selecting the topology with superior log likelihood value. The tree is drawn to scale, with branch lengths measured in the number of substitutions per site. This analysis involved 16 nucleotide sequences. Codon positions included were 1st+2nd+3rd+Noncoding. There was a total of 399 positions in the final dataset. Evolutionary analyses were conducted in MEGA X (Kumar *et al.*, 2018). The sequence obtain in the present study is marked with a black dot.

Buck J.D., 1982. Nonstaining (KOH) method for determination of Gram reactions of marine bacteria. *Applied Environmental Microbiology* 44: 992–993.

EPPO. 1995. *Erwinia amylovora* present in Emilia-Romagna (IT). *EPPO Reporting Service* 114.

EPPO. 2013. PM 7/20 (2) *Erwinia amylovora*. *Bulletin OEPP/EPPO Bulletin* 43: 21–45.

Geider K., Auling G., Du Z., Jakovljevic V., Jock S., Völksch B., 2006. *Erwinia tasmaniensis* sp. nov., a non-phytopathogenic bacterium from apple and pear trees. *International Journal of Systematic and Evolutionary Microbiology* 56: 2937–2943.

Gottsberger R.A., 2010. Development and evaluation of a real-time PCR assay targeting chromosomal DNA of *Erwinia amylovora*. *Letters in Applied Microbiology* 51: 285–292.

Hannou N., Llop P., Faure D., López M.M., Moumni M., 2013. Characterization of *Erwinia amylovora* strains from Middle Atlas Mountains in Morocco by PCR

- based on tandem repeat sequences. *European Journal of Plant Pathology* 136: 665–674.
- Kumar S, Stecher G, Li M, Knyaz C, Tamura K., 2018. MEGA X: Molecular evolutionary genetics analysis across computing platforms. *Molecular Biology and Evolution* 35: 1547–1549.
- Laala S., Manceau C., Valentini F., Kerkoud M., Kheddami M., 2012. Fireblight survey and first characterization of *Erwinia amylovora* isolates from Algeria. *Journal of Plant Pathology* 693–696.
- Li R., Mock R., Huang Q., Abad J., Hartung J., Kinard G., 2008. A reliable and inexpensive method of nucleic acid extraction for the PCR-based detection of diverse plant pathogens. *Journal of Virological Methods* 154: 48–55.
- Li L., Li H., Shi Y., Chai A.L., Xie X., Li B., 2021. First report of bacterial leaf spot of *Cucurbita pepo* caused by *Erwinia persicina* in China. *Plant Disease* <https://doi.org/10.1094/PDIS-06-20-1241-PDN>.
- López M.M., Rosello M., Llop P., Ferrer S., Christen R., Gardan L., 2011. *Erwinia piriflorinigrans* sp. nov., a novel pathogen that causes necrosis of pear blossoms. *International Journal of Systematic and Evolutionary Microbiology* 61: 561–567.
- Pirc M., Ravnkar M., Tomlinson J., Dreo T., 2009. Improved fireblight diagnostics using quantitative real-time PCR detection of *Erwinia amylovora* chromosomal DNA. *Plant Pathology* 58: 872–881.
- Suharjo R., Sawada H., Takikawa Y., 2014. Phylogenetic study of Japanese *Dickeya* spp. and development of new rapid identification methods using PCR–RFLP. *Journal of General Plant Pathology* 80: 237–254.
- Tamura K., Nei M. 1993. Estimation of the number of nucleotide substitutions in the control region of mitochondrial DNA in humans and chimpanzees. *Molecular Biology and Evolution* 10: 512–526.
- Tsuji M., Kadota I., Takikawa Y., 2020. Genetic and phenotypic characterization of bacterial strains isolated in Japan that resemble *Erwinia rhapontici* and *E. persicina*. *Journal of General Plant Pathology* 86: 24–33.
- Waleron M., Waleron K., Geider K., Lojkowska E., 2008. Application of RFLP analysis of *recA*, *gyrA* and *rpoS* gene fragments for rapid differentiation of *Erwinia amylovora* from *Erwinia* strains isolated in Korea and Japan. *European Journal of Plant Pathology* 121: 161–172.
- Weisburg W.G., Barns S.M., Pelletier, D. A., Lane D.J., 1991. 16S ribosomal DNA amplification for phylogenetic study. *Journal of Bacteriology* 173: 697–703.
- Young J.M., Park D.C., 2007. Relationships of plant pathogenic enterobacteria based on partial *atpD*, *carA*, and *recA* as individual and concatenated nucleotide and peptide sequences. *Systematic and Applied Microbiology* 30: 343–354.



Citation: E. Kopilov, H. Tsekhmister, O. Nadkernychna, A. Kyslynska (2021) Identification of *Plectosphaerella melonis* from cucumber plants in Ukraine. *Phytopathologia Mediterranea* 60(2): 259-263. doi: 10.36253/phyto-12612

Accepted: June 14, 2021

Published: September 13, 2021

Copyright: © 2021 E. Kopilov, H. Tsekhmister, O. Nadkernychna, A. Kyslynska. This is an open access, peer-reviewed article published by Firenze University Press (<http://www.fupress.com/pm>) and distributed under the terms of the Creative Commons Attribution License, which permits unrestricted use, distribution, and reproduction in any medium, provided the original author and source are credited.

Data Availability Statement: All relevant data are within the paper and its Supporting Information files.

Competing Interests: The Author(s) declare(s) no conflict of interest.

Editor: Josep Armengol Forti, Polytechnical University of Valencia, Spain.

Short Notes

Identification of *Plectosphaerella melonis* from cucumber plants in Ukraine

EVGENIY KOPILOV, HANNA TSEKHMISTER*, OLENA NADKERNYCHNA, ANNA KYSLYNSKA

Laboratory of plant microbial interaction, Institute of Agricultural Microbiology and Agro-industrial Manufacture, National Academy of Agrarian Sciences of Ukraine (NAAS), Chernihiv, Ukraine

*Corresponding author. E-mail: anna.tceh@gmail.com

Summary. A fungus was isolated from diseased roots of *Cucumis sativus* grown in greenhouses. The morphological and cultural characteristics of the isolate allowed it to be classified as *Plectosphaerella melonis*. BLASTn analysis revealed 99% homology of the ITS sequence from the isolate with 14 *Acremonium cucurbitacearum* and *P. melonis* isolates, allowing attribution of the isolate to *P. melonis* (syn. *A. cucurbitacearum*). Koch's hypothesis requirements were fulfilled for the isolate. Symptoms on host roots developed after 14 d of growing cucumber plants on infested soil. Plants of the cucumber variety Nizhynskyi 12 were very susceptible at the two leaf growth stage (2 weeks after sowing). Above-ground disease symptoms were absent after 14 d, even with severely diseased roots. This is the first report of *P. melonis* on *C. sativus* in Ukraine.

Keywords. *Acremonium cucurbitacearum*, cucurbits, disease, identification, pathogen, *Plectosphaerella melonis*, soilborne.

INTRODUCTION

Plectosphaerella spp. are known pathogens for a wide range of agricultural crops, including *Cucurbitaceae* (Carlucci *et al.*, 2012; Raimondo and Carlucci, 2018a; 2018b).

In Spain, Alfaro-García *et al.* (1996) reported that the causal agent of this disease, after the mass death of melons at the beginning of fruit ripening, was the fungus *Acremonium cucurbitacearum*. Bruton *et al.* (1996) described the same disease on melon plants in Texas (United States of America). Carlucci *et al.* (2012) determined that *A. cucurbitacearum* was synonymous to *Nodulisporium melonis* and transferred the pathogen to *Plectosphaerella* as *P. melonis* comb. nov.

A *Plectosphaerella* species was consistently isolated from diseased cucumber plants grown in a greenhouse in Ukraine. The aim of the present study was to identify the isolate fungus using morphological cultural and molecular genetic characteristics, and to confirm its pathogenicity to *Cucumis sativus*.

MATERIALS AND METHODS

Plant sampling and fungus isolation

A fungus isolate (coded 502) was collected from affected roots of *C. sativus* (variety Koroliok), at the mass fruiting stage of crop growth. *Cucumis sativus* was grown in greenhouses in Chernihiv district, Chernihiv region (Ukraine). Affected host root segments (3–5 mm) were thoroughly washed for 15 min under running water, surface sterilized with 96% ethyl alcohol for 1 min then washed twice with sterile water, and were then plated into Petri dishes containing 4% barley meal agar (BMA) amended with 250 ppm streptomycin. The plates were incubated at 26°C, and after 4 d the resulting fungus was reisolated onto BMA.

Morphological identification

The cultural and morphological characteristics of the isolated fungus were examined after culture on BMA, Czapek's agar (CZA) or potato dextrose agar (PDA) in the darkness at 26°C. After 10 d in culture, the fungus completely covered the agar surfaces, and colonies were characterised.

Temperature/growth relationship

The temperature optimum for the isolated fungus was studied by culturing the fungus in Petri dishes on BMA at 10, 18, 26 or 35°C. After 10 d, the colony diameters were measured in two mutually perpendicular directions, and colony radial growth rates were determined (Pert, 1978).

Molecular identification

DNA extraction. For DNA isolation, parts of fungus colonies grown on BMA were processed using the AmpliSens DNA-sorb-B kit. The necessary quantity of DNA solution obtainment was carried out in accordance to described methods (Birnboim & Doly, 1979; Chowdhury & Akaike, 2005; Chi *et al.*, 2009; Sika *et al.*, 2015).

PCR analysis. For sequencing, obtained DNA solution polymerase chain reaction was carried out using ITS1 and ITS4 primers (White *et al.*, 1990). The amplification reaction was conducted within Applied Biosystems equipment following prescribed methods (Watts & MacBeath, 2001; Garrido *et al.*, 2009). Analysis of resulting 5.8S rDNA sequences were compared with GenBank

database sequences using by BLAST analyses (<http://www.ncbi.nlm.nih.gov/blast>).

Pathogenicity test

Pathogenicity tests were performed in a pot experiment using *C. sativus* plants (var. Nizhynskyi 12). Pots (2 L capacity) were each filled with 1800 g of soil which had been previously steamed at 70–80°C for 50 min.

Inoculum of the isolated fungus was prepared by growing the fungus on medium containing oat seeds, oat flakes, water, chalk and gypsum in 1 L capacity flasks. This substrate was sterilized twice at 128°C and 1.5 atm pressure for 1 h 30 min, and was then inoculated with pure cultures of the isolate, grown in tubes containing BMA. The flasks were kept at 26°C for 21 d. Then the inoculum was transferred into paper bags, dried to constant weight at 30 °C, and mixed with soil.

Cucumis sativus seeds were sown to a depth of 2 cm. Fungus inoculum was applied to the pots at the equivalent of 5×10^4 CFU g⁻¹ of soil (Bruton *et al.*, 2000a). Experimental controls were cucumber plants grown without added inoculum. Soil in the pots was maintained at 60% of total water holding capacity. The pots were placed randomly in a greenhouse with natural lighting. The experiment was repeated five times. After emergence of the cucumber seedlings, these were thinned to five per pot. After 2 and 4 weeks, the plants were removed, washed from the soil and the root systems were evaluated.

Root segments (3–5 mm each) were thoroughly washed for 15 min under running water, surface sterilized with 96% ethyl alcohol for 1 min, and then washed twice with sterile water. The segments were then placed into Petri dishes containing 4% BMA plus 250 ppm Streptomycin at 26°C, and after 4 d the resulting fungus was reisolated onto BMA.

Statistical analyses

The data obtained were analyzed using Statistica 12. Normality of the data were assessed using Shapiro-Wilks W-test statistics, and homogeneity of variances was assessed using the Brown-Forsythe test. The nonparametric Mann-Whitney *U* test was applied ($P \leq 0.05$) to compare experimental groups, including fungus growth media. One-way Analysis of Variance (ANOVA) and Duncan Multiple Range Tests were used to determine optimum temperature.

RESULTS AND DISCUSSION

Isolate 502 was obtained from affected cucumber plants grown in greenhouses (Figure 1a). Disease symptoms were absent until the onset of the mass plant fruiting phase of cucumber. The symptoms included fading of leaf edges on the lower leaves of affected plants. The root systems had secondary and tertiary roots with necrotic areas (Figure 1b). No reductions in plant growth or delays in development were observed.

The macro-morphological features of isolate 502 differed depending on the culture medium (Figure 2). Colonies were rounded, hyphae were thin, septate and hyaline. The colonies on PDA were white or cream, the colony surfaces were and velvety. On BMA, the colony colours varied from white to rose pink. On CZA the colonies had white aerial mycelium. Colonies had radial wrinkles on the reverse sides, and the colonies were

slow-growing (Table 1), the most rapid growth was on PDA.

Phialides of isolate 502 were unbranched, septate, mostly simple, and measured from $22.4 \times 4.2 \mu\text{m}$ to $42.0 \times 4.2 \mu\text{m}$. The phialides were coloured along their entire lengths. The phialides were located on hyphal filaments and each had a basal septum at the base. Unicellular conidia were assembled into a head at the apex of each phialide. Conidia were oblong, elliptical, smooth-walled and hyaline (granular). Conidia in PDA cultured measured $8.4 \times 2.8 \mu\text{m}$ to $14.0 \times 2.8 \mu\text{m}$, and sporulation was most intense on this medium. On BMA, the conidia were smaller ($5.6 \times 3.1 \mu\text{m}$ to $11.2 \times 2.8 \mu\text{m}$) and sporulation was intense. On CZA, sporulation was not intense and the conidia were $4.2 \times 4.2 \mu\text{m}$ to $8.4 \times 4.2 \mu\text{m}$. Chlamydozoospores were absent. These characteristics were similar to those described for *P. melonis* (Alfaro-Garcia *et al.*, 1996; Carlucci *et al.*, 2012).

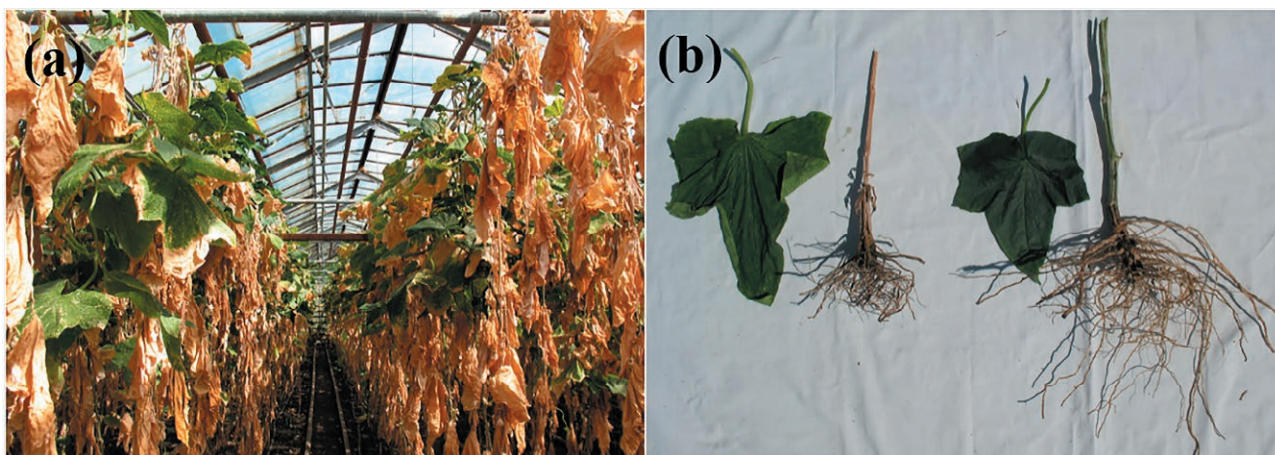


Figure 1. (a) Cucumber plants (variety Koroliok) affected by *Plectosphaerella melonis* (isolate 502) in a greenhouse. (b) Leaf and root of an affected plant (left) and a healthy plant (right).

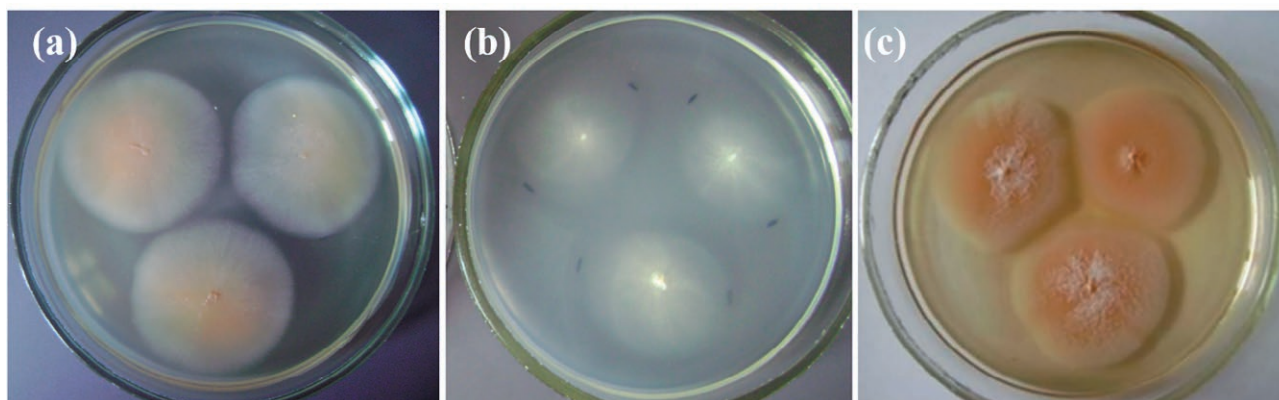


Figure 2. Colonies of *Plectosphaerella melonis* (isolate 502) on (a) PDA, (b) CZA, and (c) BMA.

Table 1. Mean diameters of *Plectosphaerella melonis* (isolate 502) colonies on different nutrient media.

Nutrient medium	Mean colony diameter (mm) after 7 d.	Mean colony diameter (mm) after 10 d.
BMA	20.2 ± 0.2 c	26.8 ± 0.1 c
CZA	17.1 ± 0.1 b	28.5 ± 0.3 b
PDA	21.2 ± 0.3 a	33.0 ± 0.3 a

The values are means ± standard errors for three replicates. Means in each column followed by different letters are significantly different ($P \leq 0.05$; Mann–Whitney test).

Table 2. Mean *Plectosphaerella melonis* (isolate 502) colony diameters and growth rates at different temperatures.

Temperature (°C)	Mean colony diameter (mm, after 10 d)	Mean colony radial growth rate (mm h ⁻¹)
10	5.5 ± 0.3 d	0.023 ± 0.001 d
18	13.2 ± 0.5 b	0.055 ± 0.002 b
26	22.3 ± 0.3 a	0.093 ± 0.001 a
35	8.8 ± 0.3 c	0.037 ± 0.001 c

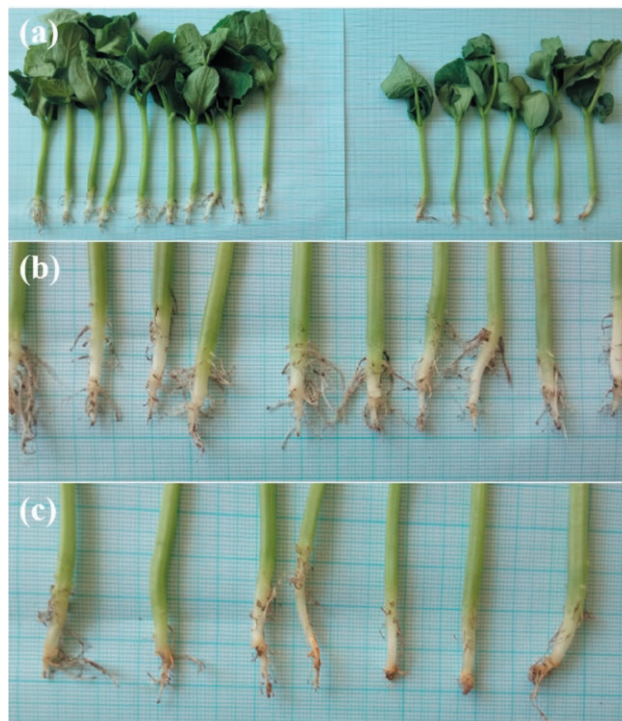
The values are means ± standard errors for three replicates. Means in each column followed by different letters are significantly different ($P \leq 0.05$; Duncan's multiple range test).

The optimum temperature growth for isolate 502 was 26°C (Table 2).

Isolate 502 was deposited at the Depository of the Institute of Microbiology and Virology, NAS of Ukraine, with the number IMB F-100138.

Morphological identification of the isolate was confirmed by the molecular analysis. The sequence of isolate 502 was determined and submitted to GenBank with accession number MK736305.1. The BLASTn analysis showed 99% similarity with 14 strains of *A. cucurbitacearum* and *P. melonis*.

Pathogenicity of *P. melonis* 502 to cucumber plants was confirmed. Symptoms of root system damage were observed after 14 days for cucumber plants grown in soil inoculated with this isolate (Figure 3). The cucumber variety Nizhynskiy 12 was very sensitive to the pathogen at the two true leaf growth stage (after 2 weeks from sowing) (Figure 3c). Above-ground symptoms were absent after 14 d, although severe symptoms were apparent on the root system at this time. Investigating the sensitivity of cucurbit species to Spanish *P. melonis* isolates, Armengol *et al.* (1998) found that cucumber plants ranged from resistant to very susceptible, and that, in field conditions, cucumber plants were less affected by *P. melonis* than melon plants with the same level of susceptibility. In contrast, Bruton *et al.* (2000b), in studies of

**Figure 3.** Healthy cucumber variety Nizhynskiy 12 plants (a - left, and b), and diseased plants (a - right, and c), after 14 d of cultivation.

pathogenicity of American *P. melonis* isolates, concluded that cucumber plants belonged to a high-resistance host group.

The present results are the first to show pathogenicity of *P. melonis* on cucumber plants in Ukraine. This study has confirmed the pathogenicity of this fungus to cucumber, and has shown that young cucumber seedlings were very susceptible to this pathogen.

ACKNOWLEDGEMENTS

The authors express gratitude to Senior Research Fellow, PhD Stanislav Nadkernichnyi for his academic advice in conducting the research described in this paper and his critical analysis of the research results. This research was carried out within the tasks of applied research No. 0116U003070.

LITERATURE CITED

Alfaro-García A., Armengol J., Bruton B.D., Gams W., García-Jiménez J., Martínez-Ferrer G., 1996. The taxonomic position of the causal agent of *Acremonium* collapse. *Mycologia* 88: 804–808.

- Armengol J., Sanz E., Martínez-Ferrer G., Sales R., Bruton B.D., García-Jiménez J., 1998. Host range of *Acremonium cucurbitacearum*, cause of *Acremonium* collapse of muskmelon. *Plant Pathology* 47: 29–35.
- Birnboim H.C., Doly J., 1979. A rapid alkaline extraction procedure for screening recombinant plasmid DNA. *Nucleic Acids Research* 7(6): 1513–1523, DOI: 10.1093/NAR/7.6.1513.
- Bruton B.D., Miller M.E., Garcia-Jimenez J., 1996. Comparison of *Acremonium* sp. from the Lower Rio Grande Valley of Texas with *Acremonium* sp. from Spain. *Phytopathology* 3: 86.
- Bruton B.D., Garcia-Jimenez J., Armengol J., Popham T.W., 2000a. Assessment of virulence of *Acremonium cucurbitacearum* and *Monosporascus cannonballus* on *Cucumis melo*. *Plant Disease* 84: 907–913.
- Bruton B.D., Popham T.W., García-Jiménez J., Armengol J., Miller M.E., 2000b. Disease reaction among selected Cucurbitaceae to an *Acremonium cucurbitacearum* isolate from Texas. *Hortscience* 35 (4): 677–680.
- Carlucci A., Raimondo M.L., Santos J., Phillips A.J.L., 2012. *Plectosphaerella* species associated with root and collar rots of horticultural crops in southern Italy. *Persoonia - Molecular Phylogeny and Evolution of Fungi* 28(1): 34–48.
- Chi M.H., Park S.Y., Lee Y.H. 2009. A quick and safe method for fungal DNA extraction. *Plant Pathology Journal* 25: 108–111.
- Chowdhury E.H., Akaike T. 2005. Rapid isolation of high quality, multimeric plasmid DNA using zwitterionic detergent. *Journal of Biotechnology* 119(4): 343–347, DOI: 10.1016/J.JBIOTECH.2005.05.013.
- Garrido C., Carbú M., Fernández-Acero F. J., Boonham N., Colyer A., Cantoral J. M., Budge G., 2009. Development of protocols for detection of *Colletotrichum acutatum* and monitoring of strawberry anthracnose using real-time PCR. *Plant Pathology* 58: 43–51, DOI: 10.1111/J.1365-3059.2008.01933.X.
- Perth S.J., 1978. *Fundamentals of the Cultivation of Microorganisms and Cells*. World, Moscow, Russia, 330 pp (in Russian).
- Raimondo M.L., Carlucci A., 2018a. Characterization and pathogenicity of *Plectosphaerella* spp. collected from basil and parsley in Italy. *Phytopathologia Mediterranea* 57 (2), 284–295.
- Raimondo M.L., Carlucci A., 2018b. Characterization and pathogenicity assessment of *Plectosphaerella* species associated with stunting disease on tomato and pepper crops in Italy. *Plant Pathology* 67 (3), 626–641.
- Sika K.C., Kefela T., Adoukonou-Sagbadja H., Ahoton L., Saidou A., ... Gachomo E. W. 2015. A simple and efficient genomic DNA extraction protocol for large scale genetic analyses of plant biological systems. *Plant Gene* 1: 43–45.
- Watts D., MacBeath J. R. 2001. Automated fluorescent DNA sequencing on the ABI PRISM 310 Genetic Analyzer. *Methods in Molecular Biology* (Clifton, N.J.) 167: 153–170, DOI: 10.1385/1-59259-113-2:153
- White T.J., Bruns T.D., Lee S.B., Taylor J.W., 1990. Amplification and direct sequencing of fungal ribosomal RNA genes for phylogenetics. In: *PCR Protocols: a Guide to Methods and Applications* (M.A. Innis, D.H. Gelfand, J.J. Sninsky, T.J. White, ed.), Academic Press, New York, USA, 315–321.



Citation: L. Soto-Muñoz, V. Martínez-Blay, M.B. Pérez-Gago, A. Fernández-Catalán, M. Argente-Sanchis, Lluís Palou (2021) Starch-glycerol monostearate edible coatings formulated with sodium benzoate control postharvest citrus diseases caused by *Penicillium digitatum* and *Penicillium italicum*. *Phytopathologia Mediterranea* 60(2): 265-279. doi: 10.36253/phyto-12528

Accepted: March 16, 2021

Published: September 13, 2021

Copyright: ©2021 Author. This is an open access, peer-reviewed article published by Firenze University Press (<http://www.fupress.com/pm>) and distributed under the terms of the Creative Commons Attribution License, which permits unrestricted use, distribution, and reproduction in any medium, provided the original author and source are credited.

Data Availability Statement: All relevant data are within the paper and its Supporting Information files.

Competing Interests: The Author(s) declare(s) no conflict of interest.

Editor: Pervin Kinay Teksür, Ege University, Bornova Izmir, Turkey.

Research Papers

Starch-glycerol monostearate edible coatings formulated with sodium benzoate control postharvest citrus diseases caused by *Penicillium digitatum* and *Penicillium italicum*

LOURDES SOTO-MUÑOZ^{1,2,A}, VICTORIA MARTÍNEZ-BLAY^{1,A}, MARÍA B. PÉREZ-GAGO¹, ASUNCIÓN FERNÁNDEZ-CATALÁN¹, MARICRUZ ARGENTE-SANCHIS¹, LLUÍS PALOU^{1,*}

¹ *Laboratori de Patologia, Centre de Tecnologia Postcollita (CTP), Institut Valencià d'Investigacions Agràries (IVIA), 46113 Montcada, València, Spain*

² *Facultad de Química, Universidad Autónoma de Querétaro. Centro Universitario S/N, Colonia Las Campanas, 76010 Querétaro, Mexico*

^A L. Soto-Muñoz and V. Martínez-Blay contributed equally to this work as first authors.

* Corresponding author. E-mail: palou_llu@gva.es

Summary. The curative antifungal activity of edible composite coatings (ECs) based on pregelatinized potato starch-glycerol monostearate (PPS-GMS) formulated with or without sodium benzoate (SB) to control green mould (caused by *Penicillium digitatum*) and blue mould (*P. italicum*) was assessed on 'Orri' mandarins, 'Valencia' oranges and 'Fino' lemons. These fruit were artificially inoculated with *P. digitatum* or *P. italicum*, treated by immersion in coating emulsions and compared to uncoated control fruit immersed in water and fruit immersed in 2% SB (w/v) aqueous solution. Treated fruit were then stored at either 20°C or commercial low temperature (5°C for mandarins and oranges, 12°C for lemons). Coatings without SB did not exhibit antifungal activity, whereas coatings containing 2% SB reduced incidence and severity of green and blue moulds, in comparison to the controls, on all citrus species and in all storage conditions, without differing from the application of 2% SB alone. For example, incidence reduction on 'Fino' lemons was from 99 to 0% after 7 d at 20°C, and from 99 to 30% after 2 weeks at 12°C. None of the treatments was phytotoxic. These results indicate that applications of SB as antifungal ingredient of PPS-GMS based ECs is a promising non-polluting alternative to control *Penicillium* postharvest decay of citrus, and these ECs are effective substitutes for conventional waxes amended with synthetic fungicides.

Keywords. Green mould, blue mould, alternative disease control, antifungal fruit coatings, GRAS salts.

INTRODUCTION

Fungal pathogens are one of the main factors contributing to citrus spoilage and quality deterioration during postharvest fruit handling, leading to significant economic losses (Zacarias *et al.*, 2020). Green mould (GM;

see Table 1 for definitions of abbreviations used in this paper) and blue mould (BM), caused, respectively, by *Penicillium digitatum* (Pers.: Fr.) Sacc. and *Penicillium italicum* Wehmer, are the most important postharvest citrus diseases, particularly in Mediterranean climate regions. These fungi are strict wound pathogens that infect citrus fruit through rind injuries caused during harvest, transportation, and postharvest handling and commercialization (Palou, 2014; Smilanick *et al.*, 2020).

Treatments with synthetic fungicides applied as aqueous solutions or added to waxes have been traditionally used to reduce postharvest citrus decay to commercially acceptable levels (Erasmus *et al.*, 2013; Njombolwana *et al.*, 2013). However, due to legislative restrictions and consumer trends, the citrus industry demands safer approaches to control postharvest diseases. Alternative control methods include different physical treatments, antimicrobial antagonists used as biocontrol agents, and low-toxicity chemicals classified as food additives or generally recognized as safe (GRAS) compounds. These compounds include organic and inorganic salts, chitosan, essential oils and other plant extracts (MoscOSO-Ramírez *et al.*, 2013; Palou *et al.*, 2016; Palou, 2018; Papoutsis *et al.*, 2019; Sapper *et al.*, 2019).

Among the different disease management alternatives, GRAS salts present important advantages, including high water solubility, availability, and general low cost (Palou, 2018). Thus, their potential to control citrus postharvest decay as aqueous solutions or as ingredients of composite edible coatings (ECs) is an active research field (Palou *et al.*, 2015; Montesinos-Herrero *et al.*, 2016). The effectiveness of GRAS salts, including benzoates, bicarbonates, carbonates, metabisulfites, parabens, silicates, and sorbates, for control of major postharvest citrus diseases has been demonstrated in previous studies (Palou *et al.*, 2002; Smilanick *et al.*, 2008; Valencia-Chamorro *et al.*, 2009a; Askarne *et al.*, 2013; MoscOSO-Ramírez *et al.*, 2013; Youssef *et al.*, 2014; Montesinos-Herrero *et al.*, 2016; Guimarães *et al.*, 2019; Martínez-Blay *et al.*, 2020a; 2020b). We have found that, among these salts, aqueous solutions of sodium benzoate (SB) had substantial curative activity against citrus GM and BM (Montesinos-Herrero *et al.*, 2016). Therefore, we have evaluated ECs containing this salt as an antifungal ingredient.

Since ECs on fruit act as water and gas barriers, the use of ECs formulated with antifungal GRAS ingredients allows coating the fruit directly with a thin layer of edible material to provide antifungal activity, maintain fruit physicochemical quality and extend shelf life (Janjarasskul and Krochta, 2010; Valencia-Chamorro *et al.*, 2011a; Palou *et al.*, 2015; Sapper and Chiralt, 2018). In addition, postharvest use of ECs containing GRAS

compounds may facilitate slow diffusion of active ingredient from coating matrices, compared to application of aqueous solutions (Palou *et al.*, 2015; Palou, 2018). We have previously demonstrated that ECs based on hydroxypropyl methylcellulose (HPMC) containing antifungal GRAS salts reduced brown rot in plums (Karaca *et al.*, 2014; Gunaydin *et al.*, 2017) and *Alternaria* black spot and gray mould in cherry tomatoes (Fagundes *et al.*, 2013; 2015), while the physicochemical and sensory qualities of the fruit were maintained. Furthermore, on citrus fruit, these ECs controlled GM and BM (Valencia-Chamorro *et al.*, 2008; 2009a; 2009b; 2010; 2011b), *Diplodia* stem-end rot (Guimarães *et al.* 2019) and postharvest anthracnose (Martínez-Blay *et al.*, 2020a), while fruit quality was preserved during cold storage. However, the effectiveness and stability of the ECs depended on their composition, and the incorporation of antifungal GRAS salts greatly changed the original coating matrix properties. This indicated the need to optimize the formulations for each target pathogen and fruit species or cultivar (Valencia-Chamorro *et al.*, 2011a; Palou *et al.*, 2015).

In addition to HPMC, starch has been reported as a promising polysaccharide for ECs due to its biodegradability, biocompatibility, availability and low cost, creating odourless, tasteless and transparent films with good fruit preservation properties (Acosta *et al.*, 2015; Sapper and Chiralt, 2018). In addition, some studies have reported the antifungal activity of starch-based ECs amended with GRAS ingredients such as essential oils (Sapper *et al.*, 2019), natamycin-cyclodextrin complex (Yang *et al.*, 2019), biocontrol agents (Marín *et al.*, 2016), lactic acid bacteria (Marín *et al.*, 2019) and potassium sorbate (Mehyar *et al.*, 2011) to control different postharvest diseases in apple, cucumbers, grapes, persimmon or tomatoes. However, no information is available regarding the utilization of GRAS salts as ingredients of starch-based ECs to control major citrus postharvest diseases. Considering the importance of factors such as coating composition (i.e., type of ingredients and relative content) on coating performance, we have developed and optimized ECs formulated with SB as the antifungal ingredient and different ratios of pregelatinized potato starch (PPS), glyceryl monostearate (GMS) and glycerol as hydrophobic and plasticizer components to maintain the physicochemical and sensory quality of 'Orri' mandarins during storage (Soto-Muñoz *et al.*, 2021). From that research, two antifungal ECs were selected as promising treatments to maintain quality, reduce decay and extend postharvest life of mandarins.

The objective of the present study was to assess the efficacy of the optimized antifungal PPS-based ECs containing SB for control of GM and BM on mandarins,

oranges and lemons. Curative activity of the ECs was assessed on fruit artificially inoculated with the postharvest pathogens and stored at either 20°C or commercial low temperatures (5°C for mandarins and oranges, 12°C for lemons).

MATERIALS AND METHODS

Abbreviations used in this paper are presented in Table 1.

Fruit

Experiments were conducted with ‘Orri’ mandarins (*Citrus reticulata* Blanco), ‘Valencia’ oranges (*Citrus sinensis* (L.) Osbeck) and ‘Fino’ lemons (*Citrus limon* (L.) Osbeck). Commercially mature fruit were collected from citrus orchards in the Valencia area (Spain), and were used the same day or stored [5°C, 90% relative humidity (RH)] for up to 1 week before use. No commercial postharvest treatments were applied to the fruit before the experiments. Fruit were selected for uniformity of size and shape, and diseased or mechanically damaged fruit were discarded. Selected fruit were surface disinfected (4-min dips in 0.5% sodium hypochlorite solution), rinsed with tap water, allowed to air dry at room temperature, and then randomized before each experiment.

Fungal inoculations

The fungus strains NAV-7 of *P. digitatum* and MAV-1 of *P. italicum* were obtained from decayed citrus fruit

from local packhouses in the Valencia region. These strains were isolated, identified and maintained in the culture collection of postharvest pathogens of the IVIA CTP, after being selected for their aggressiveness and uniform behaviour on fruit of the most commercially important citrus cultivars. These isolates were deposited in the Spanish Type Culture Collection (CECT, University of Valencia, Valencia, Spain) with the accession numbers CECT 21108 for NAV-7 and CECT 21109 for MAV-1. Prior to the experiments, the two isolates were incubated on potato dextrose agar (PDA) (Scharlab S.L.) in Petri dishes at 25°C for 7–14 d.

For fruit inoculations, conidia from 7- to 14-d-old cultures of *P. digitatum* or *P. italicum* were taken from the PDA surfaces with sterilized inoculation loops and each transferred to a sterile aqueous solution of 0.05% Tween® 80 (Panreac-Química S.A.). Conidium suspensions were then filtered through two layers of cheesecloth. Conidium numbers in suspensions were measured with a hemocytometer, and dilutions with sterile water were made to obtain an inoculum density of 10⁵ conidia mL⁻¹. Each pathogen was wound-inoculated onto different sets of fruit. For each inoculation, the tip of a stainless steel rod (1 mm wide, 2 mm long) was immersed in the conidium suspension and then inserted in the fruit rind. Each fruit was inoculated at one point in the equatorial zone. Inoculated fruit were kept at 20°C and 90% RH for 24 h before application of fruit coatings.

Preparation of edible fruit coatings

The ECs were prepared by combining PPS as biopolymer (Quimidroga, S.A.), GMS as lipidic component (Italmatch Chemicals Spa) and glycerol as plasticizer (Panreac-Química S.A.) suspended in water. SB (Sigma-Aldrich Química S.A.) was added as antifungal GRAS salt in the formulations at 2% (w/v). These ingredients were combined in different proportions to prepare four different ECs designated as F10, F6, F10/SB and F6/SB based on the optimized stable emulsions described by Soto-Muñoz *et al.* (2021), where F10 and F6 were the PPS-GMS-based ECs formulated without GRAS salt and F10/SB and F6/SB were the same ECs formulated with 2% SB. The proportions of each component and the characteristics of these ECs are detailed in Table 2. In all formulations, sunflower lecithin (LEC) and diacetyl tartaric acid esters of mono-diglycerides (DATEM) (Lase-nor S.A.) were also incorporated as emulsifiers at the ratio GMS:emulsifier of 2:1 (dry basis, db).

For each preparation, a PPS solution (5%, w/w) was first stirred at 65°C for 30 min, and then kept under magnetic stirring at 25°C overnight. The required

Table 1. Abbreviations used in this paper.

Abbreviation	Definition
GM	Green mould
BM	Blue mould
ECs	Edible coatings
GRAS	Generally recognized as safe
SB	Sodium benzoate
HPMC	Hydroxypropyl methylcellulose
PPS	Pregelatinized potato starch
GMS	Glyceryl monostearate
RH	Relative humidity
PDA	Potato dextrose agar

Table 2. Composition and characteristics of the edible fruit coatings evaluated in this study.

Composition and characteristics ^a	Edible coating			
	F10	F6	F10/SB	F6/SB
SB concentration (% w.b.)	-	-	2.0	2.0
Solid content (%)	3.9	3.5	5.9	5.5
PPS (% d.b.)	48.3	28.6	32.0	18.2
GMS (% d.b.)	13.2	28.6	8.8	18.2
Glycerol (% d.b.)	25.2	14.3	16.7	9.1
pH	3.3	3.3	5.8	5.4
Viscosity (cP)	55.1	48.6	33.6	11.2

^a SB, sodium benzoate; PPS, pregelatinized potato starch; GMS, glyceryl monostearate (GMS); w.b., wet basis; d.b., dry basis.

amount of SB aqueous solution (10% w/w), the emulsifiers and water were then added to the PPS solution, GMS and glycerol and the resulting emulsion was heated to 90°C. Once the compounds were melted, samples were homogenized using a high-shear probe mixer (Ultra-Turrax IKA® model T25; IKA-Werke) for 1 min at 12,000 rpm followed by 3 min at 22,000 rpm. Emulsions were then cooled under agitation to a temperature below 25°C by placing them in an ice/waterbath under constant agitation for 25 min. The emulsions were kept overnight at 5°C before use.

Assessment of curative activity of fruit coatings

‘Orri’ mandarins and ‘Fino’ lemons were artificially inoculated with each pathogen (as above) and incubated at 20°C for 24 h. Inoculated fruit were then individually treated by immersion (10 s at 20°C) in relevant coating emulsions, drained and allowed to air-dry at room temperature. Curative activity of ECs was assessed since the disease control treatments were applied to already infected fruit. Treatments applied were: control = uncoated (immersion in water at 20°C for 10 s); F10 coating; F6 coating; SB (immersion in 2% (w/v) SB aqueous solution at 20°C for 10 s); F10/SB coating, or F6/SB coating. For each pathogen, each treatment was applied to four replicates of five fruit each. Treated fruit were randomly placed on cavity sockets in plastic trays and incubated at 20°C and 90% RH. Incidence of GM and BM were assessed as the percentage of decayed fruit, and disease severity was determined as individual lesion diameter (mm). All wounds, including asymptomatic wounds (diam. = 0 mm), were considered. Disease inci-

dence and severity were assessed after 4 and 7 d incubation at 20°C. Experiments were repeated once, and average data are presented.

Effectiveness of fruit coatings during cold storage

‘Orri’ mandarins, ‘Valencia’ oranges and ‘Fino’ lemons were inoculated and treated as described above (the six different treatments were applied to each of the three fruit species). For each host and disease (GM or BM), each treatment was applied to four replicates of ten fruit each. Treated fruit were randomly placed on cavity sockets in plastic trays and then cold-stored in recommended commercial conditions. The mandarins and oranges were stored at 5°C, and the lemons were kept at 12°C to avoid chilling injury (Ladaniya, 2008; Zacarias *et al.*, 2020). RH was 90% in all cases. Incidence and severity of GM and BM were assessed as described above. These parameters were evaluated for mandarins after 2, 3, 4 and 5 weeks of cold storage, for oranges after 4, 6 and 10 weeks, and for lemons after 1, 2 and 3 weeks. Every trial was conducted twice, and average data are presented.

Statistical analyses

Data from all experiments were subjected to analysis of variance (ANOVA). Since experiment was not a statistically significant factor, means of repeated experiments are presented. Disease incidence proportions were arcsine square root transformed to improve the homogeneity of variances. Where appropriate, Fisher’s Protected Least Significant Difference (LSD) test, at the 95% level of confidence ($P = 0.05$), was used for means separation. Non-transformed means are presented. All statistical analyses were carried out using Statgraphics Centurion XVII software (Statgraphics Technologies Inc.).

RESULTS

Curative activity of fruit coatings

The ECs formulated without SB (F6 and F10) did not exhibit activity against GM and BM on ‘Orri’ mandarins incubated for 4 and 7 d at 20°C, with similar or greater mean incidence and severity values in all cases than those for uncoated control fruit (Figure 1). In contrast, the ECs formulated with SB (F6/SB and F10/SB) significantly reduced the incidence and

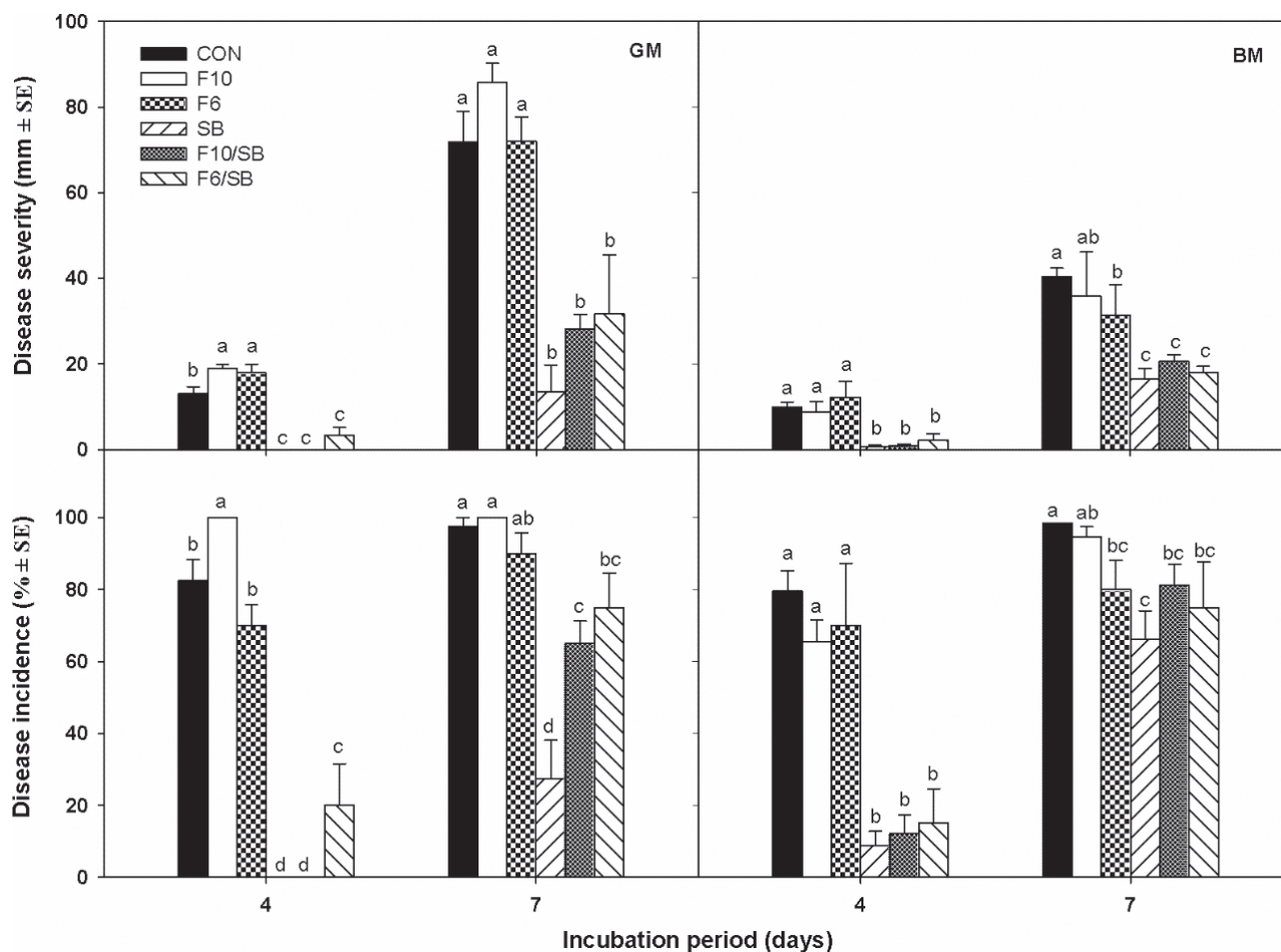


Figure 1. Mean severity and incidence of green mould (GM) or blue mould (BM) on 'Orri' mandarins artificially inoculated, respectively, with *Penicillium digitatum* or *P. italicum*, then coated 24 h later and incubated for 4 and 7 d at 20°C and 90% RH. Treatments applied were: control (CON) = uncoated (immersion in water), F10 coating, F6 coating, 2% sodium benzoate (SB) aqueous solution (w/v), F10/SB coating, or F6/SB coating (see Table 2 for coating composition). For each disease and incubation period, columns accompanied by different letters are significantly different (Fisher's protected LSD test; $P < 0.05$). Vertical lines above columns indicate standard errors. Incidence values were arcsine-transformed before statistical analyses. Non-transformed means are shown.

severity of GM and BM compared to uncoated control fruit after 4 d of incubation. Effectiveness of these antifungal ECs to reduce incidence and severity of GM and BM was similar to that obtained with the SB aqueous treatment. After 7 d, incidence and severity increased significantly in all cases. The antifungal ECs, F6/SB and F10/SB, reduced the severity of GM and BM, with severity reductions of 50–80% with respect to uncoated control fruit, and no significant differences were observed with the SB treatment. However, although both antifungal ECs reduced the incidence of GM, they were less effective than SB in aqueous solution, with reductions of approx. 30% for coated fruit in comparison to 70% for SB-treated fruit. Similar reductions of 20–30% were observed for BM incidence

on coated 'Orri' mandarins after 7 d of storage, but in this case without statistically significant differences from the SB treatment.

On 'Fino' lemons incubated up to 7 d at 20°C, F6 and F10 (without SB) did not reduce the incidence and severity of GM and BM compared to uncoated control fruit, with few exceptions (Figure 2). For example, incidence reductions of approx. 20–30% were obtained with F6 against BM. However, these reductions were always less than those obtained with the antifungal ECs containing SB or the SB aqueous solution, showing that the PPS-based matrices without GRAS salt exhibited no relevant antifungal activity. After 7 d of incubation, the incidence and severity of GM was nil on fruit coated with F10/SB or treated with 2% SB aqueous solution,

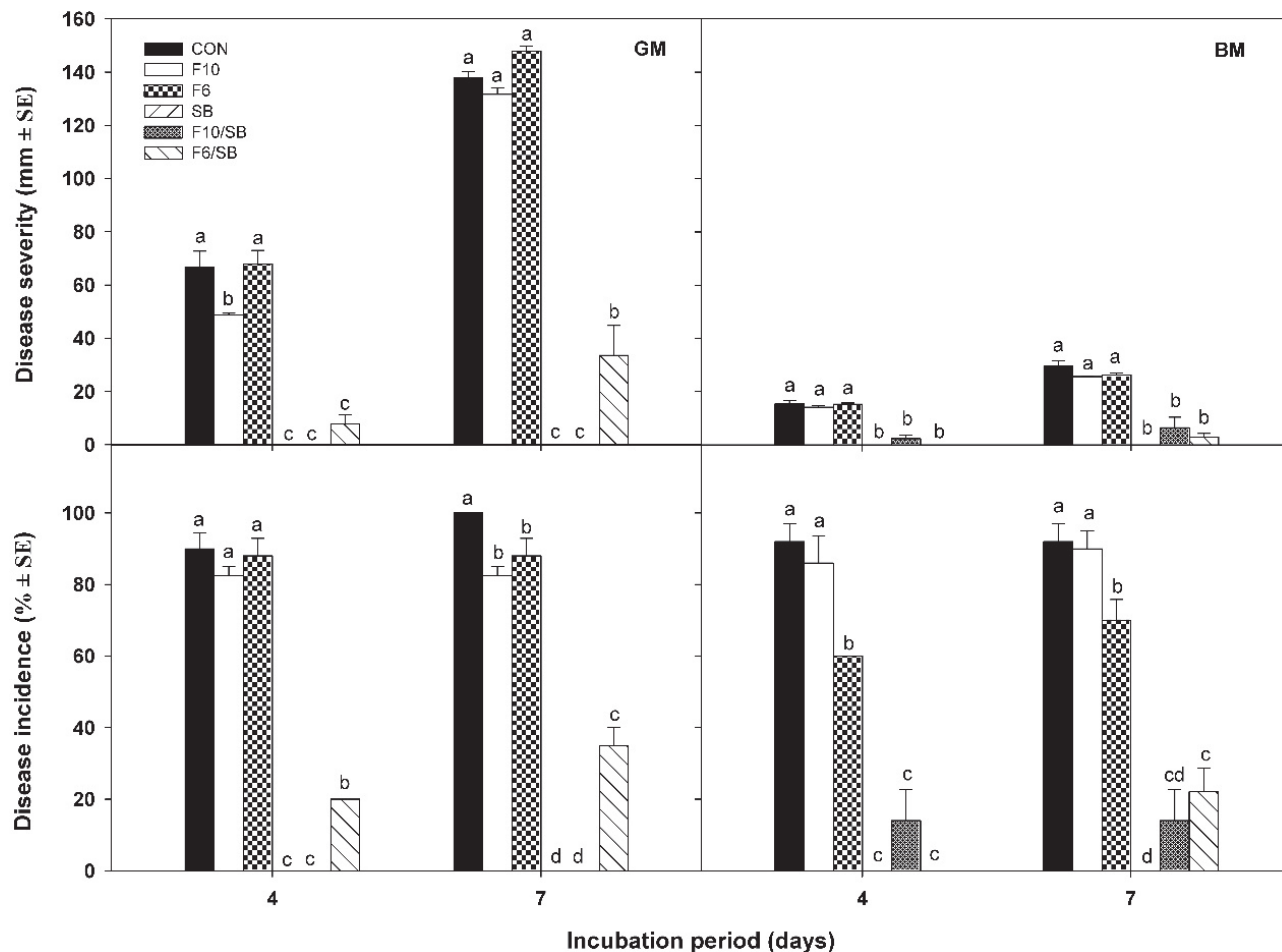


Figure 2. Mean severity and incidence of green mould (GM) or blue mould (BM) on 'Fino' lemons artificially inoculated, respectively, with *Penicillium digitatum* or *P. italicum*, then coated 24 h later and incubated for 4 and 7 d at 20°C and 90% RH. Treatments applied were: control (CON) = uncoated (immersion in water), F10 coating, F6 coating, 2% sodium benzoate (SB) aqueous solution (w/v), F10/SB coating, or F6/SB coating (see Table 2 for coating composition). For each disease and incubation period, columns accompanied by different letters are significantly different (Fisher's protected LSD test; $P < 0.05$). Vertical lines above columns indicate standard errors. Incidence values were arcsine-transformed before statistical analyses. Non-transformed means are shown.

whereas the F6/SB coating reduced incidence of GM by 65% and severity by 75%, compared to control fruit. For BM, the reductions after 4 d of both incidence and severity were 85–100% on coated lemons and lemons immersed in 2% SB solution, without statistically significant differences among these treatments. These reductions were maintained after 7 d of incubation, although the reduction in BM incidence for the lemons coated with F6/SB and F10/SB was less than for the fruit treated with aqueous SB, which completely inhibited GM development. Nevertheless, these antifungal coatings reduced the incidence of BM by approx. 85% compared to control fruit.

In every test, no phytotoxicity was observed on the rind of treated fruit.

Effectiveness of fruit coatings during cold storage

The effectiveness of treatments applied for control of GM and BM on 'Orri' mandarins cold-stored at 5°C for up to 5 weeks is illustrated in Figure 3. The ECs without SB (F6 and F10) did not control either GM or BM. In contrast, the applications of SB, alone as aqueous solution or incorporated into ECs, reduced GM severity, achieving reductions of 80–100% after 2 weeks, 90–100% after 3 weeks, 75–95% after 4 weeks, and 70–90% after 5 weeks, compared to the uncoated control. On the other hand, F10/SB and SB treatments reduced GM incidence, with reductions of 95–100% after 2 weeks, 60–80% after 4 weeks, and 55–65% after 5 weeks, compared to control fruit, without statistically significant differences between

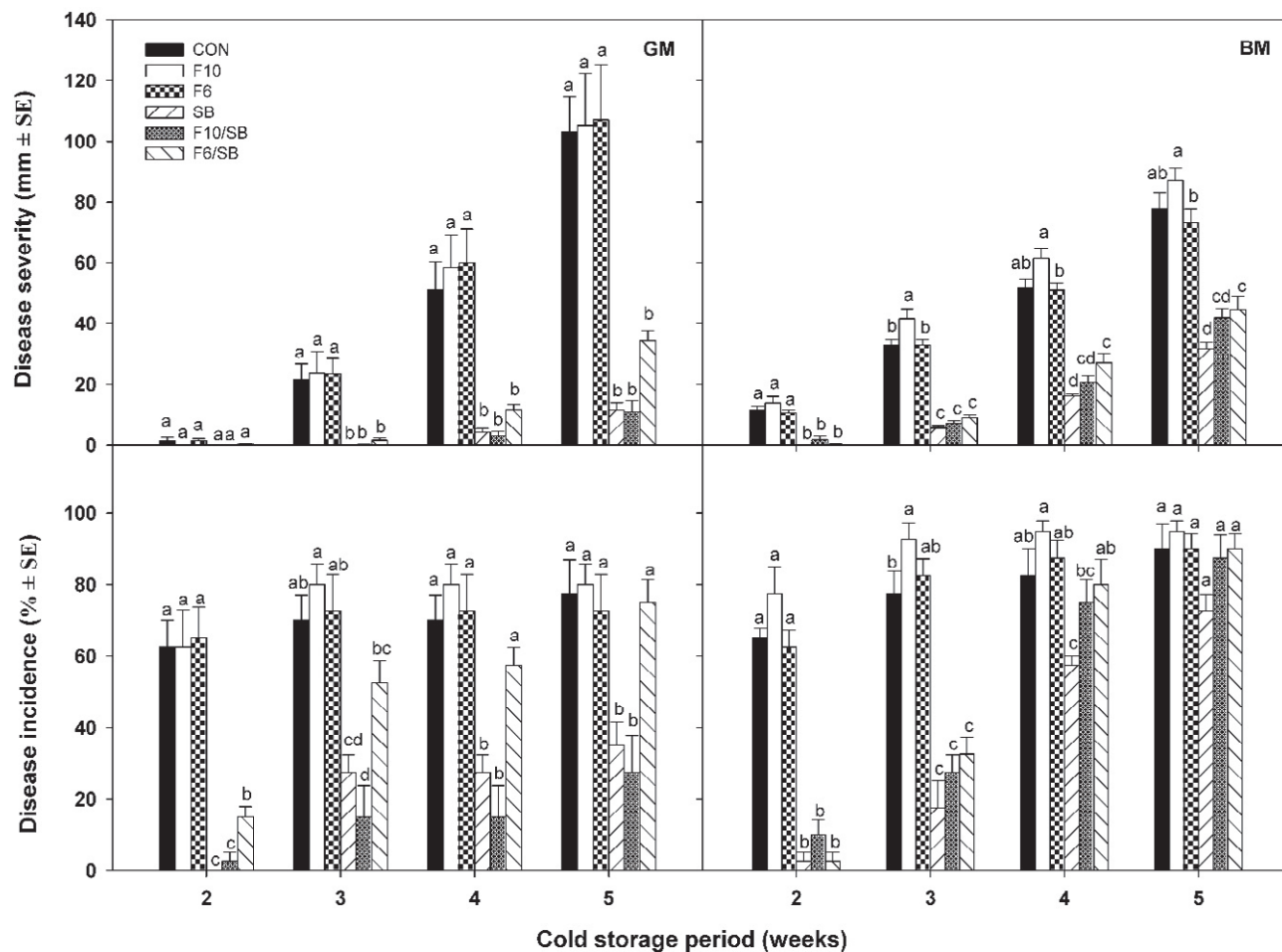


Figure 3. Mean severity and incidence of green mould (GM) or blue mould (BM) on 'Orri' mandarins artificially inoculated, respectively, with *Penicillium digitatum* or *P. italicum*, then coated 24 h later and cold-stored for 2, 3, 4 and 5 weeks at 5°C and 90% RH. Treatments applied were: control (CON) = uncoated (immersion in water), F10 coating, F6 coating, 2% sodium benzoate (SB) aqueous solution (w/v), F10/SB coating, or F6/SB coating (see Table 2 for coating composition). For each disease and incubation period, columns accompanied by different letters are significantly different (Fisher's protected LSD test; $P < 0.05$). Vertical lines above columns indicate standard errors. Incidence values were arcsine-transformed before statistical analyses. Non-transformed means are shown.

these treatments. Effectiveness of F6/SB in reducing GM incidence was less than that of F10/SB or SB, and after 4 weeks of cold storage there were no statistically significant differences between these treatments and the experimental controls. Similar results were observed for BM severity. Only the ECs or the SB aqueous solution reduced BM severity on 'Orri' mandarins during cold storage, and these reductions at the end of the storage period were greater on SB-treated fruit (60% reduction) than on coated fruit (40% reduction). For BM, the ECs reduced disease incidence during the first 3 weeks of cold storage, without statistically significant differences between coated- and SB-treated fruit, whereas, after 4 weeks, only the SB aqueous solution reduced BM incidence (up to 30%), and this effectiveness disappeared after 5 weeks of storage.

Data of severity and incidence of GM and BM on coated and uncoated 'Valencia' oranges stored for up to 10 weeks at 5°C are summarized in Figure 4. Similar to results for mandarins, only the treatments containing SB, alone or incorporated to the PPS-based ECs, reduced GM and BM on 'Valencia' oranges. In general, in all cases, the effectiveness of the fruit coatings was similar to that from the SB aqueous treatment. Thus, for example, after 10 weeks of storage, reductions in severity were 85-90% for GM and 65-75% for BM, and reductions of incidence were 30-50% for GM and 20-40% for BM.

On 'Fino' lemons, incidence of GM and BM on uncoated control samples and fruit coated with F10 and F6 (without SB) were 100% after 1 week of storage at 12°C (Figure 5). The treatments F6/SB, F10/SB and

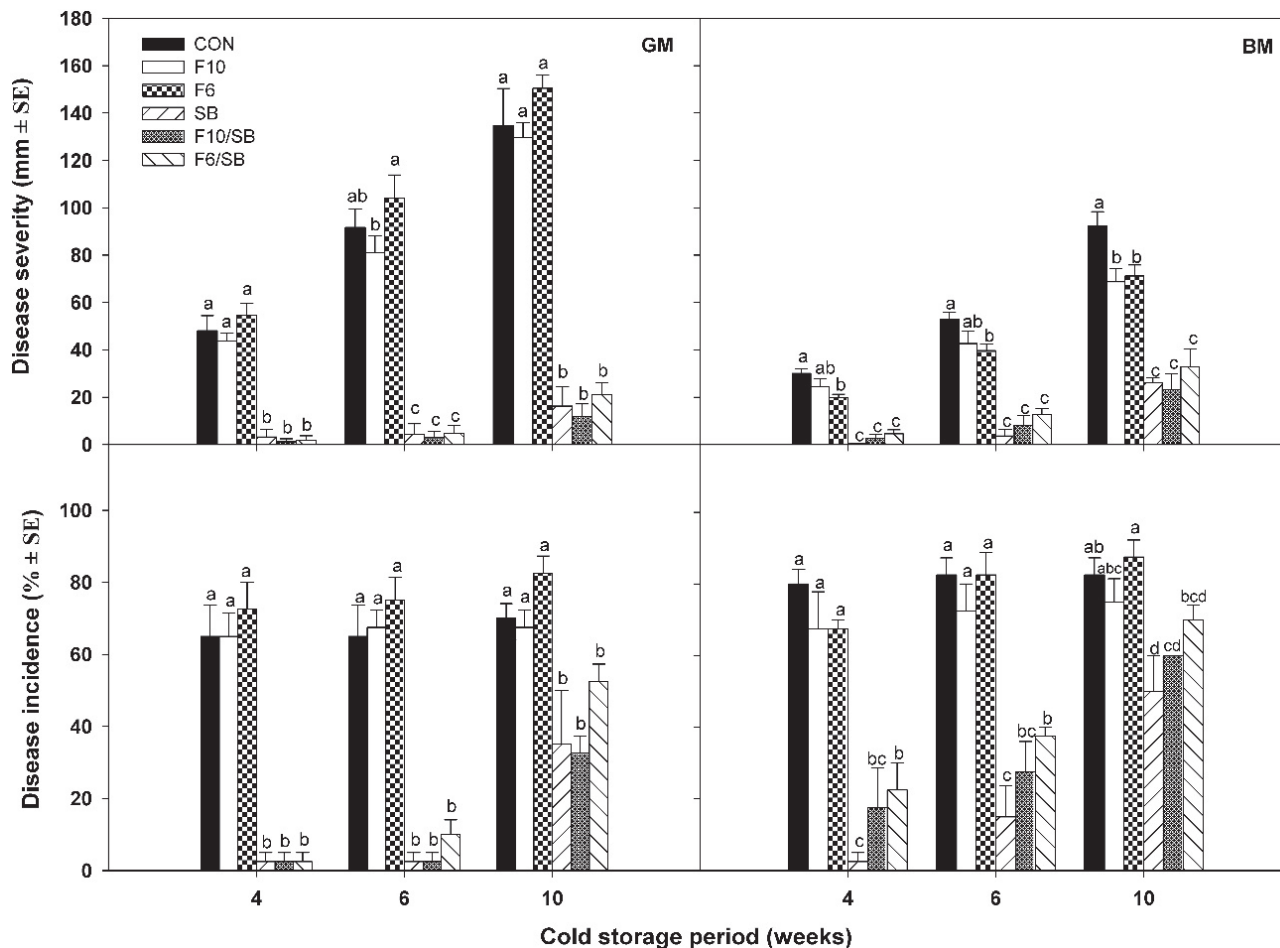


Figure 4. Mean severity and incidence of green mould (GM) or blue mould (BM) on 'Valencia' oranges artificially inoculated, respectively, with *Penicillium digitatum* or *P. italicum*, then coated 24 h later and cold-stored for 4, 6 and 10 weeks at 5°C and 90% RH. Treatments applied were: control (CON) = uncoated (immersion in water), F10 coating, F6 coating, 2% sodium benzoate (SB) aqueous solution (w/v), F10/SB coating, or F6/SB coating (see Table 2 for coating composition). For each disease and incubation period, columns accompanied by different letters are significantly different (Fisher's protected LSD test; $P < 0.05$). Vertical lines above columns indicate standard errors. Incidence values were arcsine-transformed before statistical analyses. Non-transformed means are shown.

SB reduced incidence and severity of GM and BM during the 3-week storage period compared to control fruit and fruit treated with ECs without GRAS salt. Among the treatments, F6/SB was the least effective coating against GM, with reductions of 35% in incidence and 40% in severity after 3 weeks. In contrast, the coating F10/SB and SB aqueous solution reduced GM incidence by 60–65% and severity by 75–80%. Reduction of BM severity ranged from 90–100% after 1 week of storage, and from 50–70% at the end of the 3-week storage period on lemons treated with F6/SB, F10/SB or SB, without statistically significant differences among these treatments. These treatments also reduced BM incidence during storage, and the SB treatment was more effective than F6/SB and F10/SB treatments after 1 and 2 weeks.

However, after 3 weeks, all three treatments were equally effective against BM, reducing incidence of the disease by 30–40% compared to control fruit.

Irrespective of the citrus species and the storage conditions, none of the treatments was visibly phytotoxic.

DISCUSSION

SB is regarded as a GRAS salt by regulations in many countries, and this compound is widely used as a food preservative with broad spectrum activity against yeasts and moulds (Chiple, 2005). Furthermore, the compound is effective for controlling postharvest *Penicillium* decay of citrus fruit (Montesinos-Herrero *et*

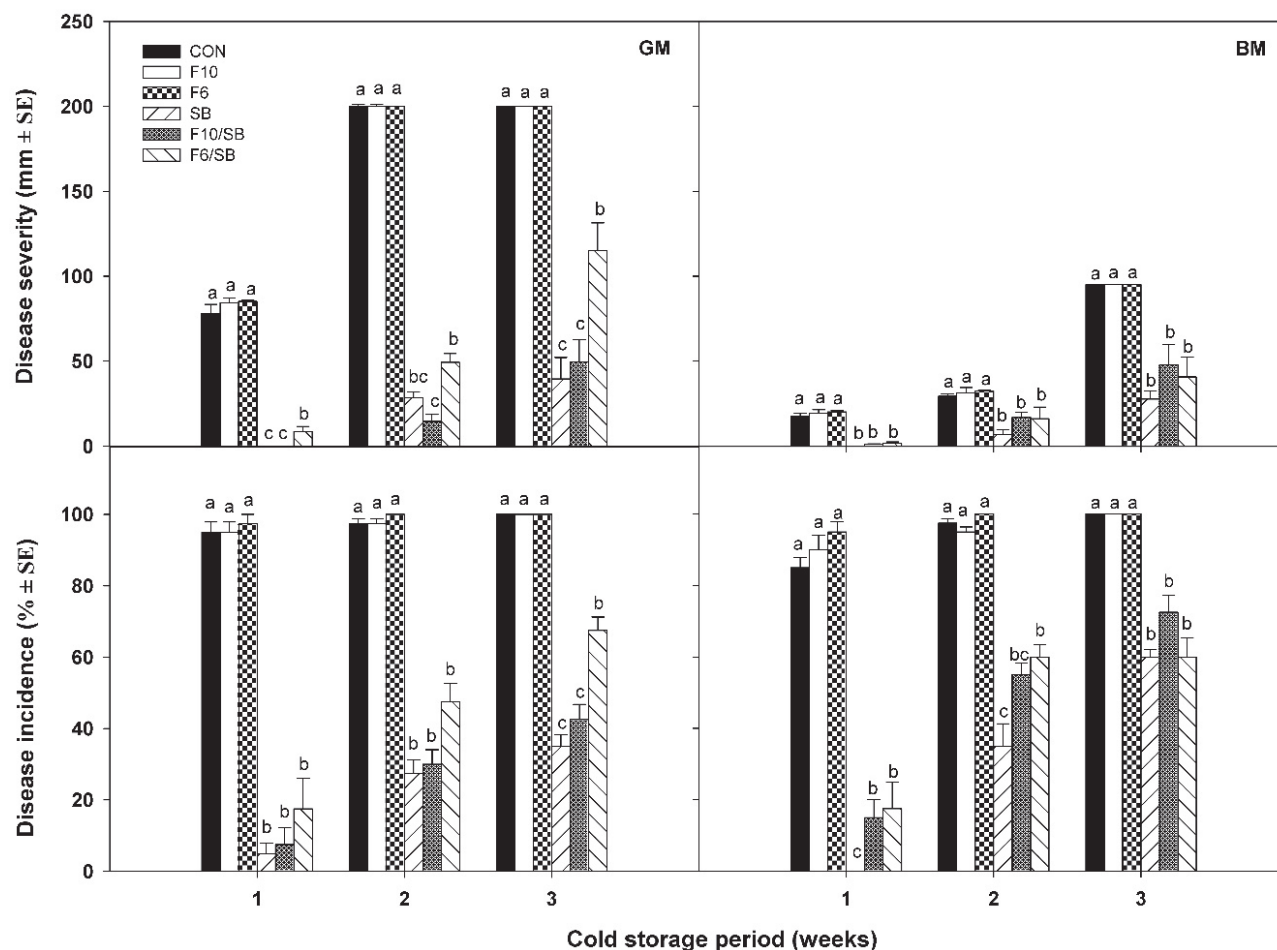


Figure 5. Mean severity and incidence of green mould (GM) or blue mould (BM) on 'Fino' lemons artificially inoculated, respectively, with *Penicillium digitatum* or *P. italicum*, then coated 24 h later and cold-stored for 7, 14 and 21 d at 12°C and 90% RH. Treatments applied were: control (CON) = uncoated (immersion in water), F10 coating, F6 coating, 2% sodium benzoate (SB) aqueous solution (w/v), F10/SB coating, or F6/SB coating (see Table 2 for coating composition). For each disease and incubation period, columns accompanied by different letters are significantly different (Fisher's protected LSD test; $P < 0.05$). Vertical lines above columns indicate standard errors. Incidence values were arcsine-transformed before statistical analyses. Non-transformed means are shown.

al., 2016; Palou, 2018). The present study has evaluated incorporation of SB at a concentration of 2% as an ingredient of novel PPS-GMS-based ECs, after optimization in previous research by response surface methodology of fruit coating ingredients for improving the postharvest quality of 'Orri' mandarins (Soto-Muñoz *et al.*, 2021). The results presented here demonstrate the effectiveness of these antifungal PPS-GMS-based ECs for control of GM and BM on fruits of three citrus species. This is the first report on the effectiveness of these types of ECs for control of major citrus postharvest diseases.

In general, the functionality of ECs based on polysaccharide matrices that do not exert direct inhibitory effects against spoilage microorganisms, in contrast to other ECs such as chitosan or *Aloe vera* gels, can be

improved by incorporation of additional antifungal ingredients such as GRAS salts or food-grade preservatives. In these amended coatings, incorporation of the antifungal ingredients may facilitate slow diffusion of active ingredients from the matrices, regulating temporal and spatial release and facilitating continuous and effective contact with target pathogens, thus enhancing their effectiveness (Mehyar *et al.*, 2011). These incorporations may also reduce possible phytotoxicity risks or adverse sensory properties derived from the direct application of the antifungal ingredient (Vargas *et al.*, 2008; Palou *et al.*, 2015; Palou, 2018; Sapper and Chiralt, 2018).

Overall, we observed that the coatings without SB did not exhibit activity in any of the conditions tested, confirming that the SB salt was responsible for the effec-

tiveness of the emulsions F6 and F10 for control of GM and BM on all three citrus species studied. These results are similar to those from previous studies, which showed that starch-based coatings and films can control pathogenic fungi and bacteria only if the coating matrices are amended with antifungal ingredients. Durango *et al.* (2006) developed antimicrobial ECs based on yam starch combined with chitosan to control microbial growth on minimally processed carrots, and their results showed that only the ECs containing chitosan reduced growth of pathogenic bacteria. Similarly, Ratnawati and Afifah (2019) reported that arrowroot starch-based films alone did not inhibit foodborne pathogenic bacteria, whereas films amended with the GRAS salts SB, potassium sorbate or calcium propionate did inhibit these organisms. SB was the most effective antibacterial salt, and its antimicrobial effect was related to decreased external pH, alteration of the integrity and permeability of bacteria cell membranes, as well as disturbance of nutrient transport (Lucera *et al.*, 2012). A similar mechanism is likely to be associated with the behaviour of the ECs F6/SB and F10/SB applied to control GM and BM in citrus fruit. The pH of the albedo tissue of the citrus fruit rind, the site initially colonized by pathogenic *Penicillium* spp., is between 5 and 6, and is influenced by fruit maturity (Widodo *et al.*, 1996; Smilanick *et al.*, 2005). Since the ionization constant of benzoic acid is 4.1, a substantial portion would be protonated and active within wounds of citrus rind. This reduction in intracellular pH caused by the accumulation of benzoic acid at low external pH inhibits glycolysis at the stage of phosphofructokinase, causing a fall in ATP and consequent inhibition of cell growth (Krebs *et al.*, 1983; Chipley, 2005; Montesinos-Herrero *et al.*, 2016).

In general, both antifungal ECs equally reduced BM incidence and severity in all three citrus fruit and in the studied storage conditions. However, the emulsion F10/SB was more effective than F6/SB for control of GM on 'Fino' lemons after incubation at 20°C and cold storage, and on 'Orri' mandarins during cold storage. On the other hand, overall, no significant differences were found between the antifungal ECs and the application of SB as aqueous solution. When a GRAS salt is incorporated into an EC and the coating is applied to fruit, the contact between the salt and the pathogen may be limited, enhanced or unaltered depending on intrinsic and extrinsic factors. These include the emulsion properties (pH and viscosity), interaction of the salt with the coating matrix and other components (e.g., emulsifiers and plasticizers), release of the salt from the coating, characteristics of the fruit outer structures, and the storage conditions (Chung *et al.*, 2001; Valencia-Chamorro *et al.*,

2011b; Fagundes *et al.*, 2013; Karaca *et al.*, 2014; Valdés *et al.*, 2017; Guimarães *et al.*, 2019; Martínez-Blay *et al.*, 2020a). Although F6/SB and F10/SB are coating matrices containing the same ingredients, their ingredient proportions are different, which confers different physical properties to the resulting coatings. The emulsion F10/SB has greater viscosity than F6/SB, which may lead to the formation of a thicker coating for F10/SB than F6/SB (i.e., greater surface solid content), ensuring greater concentration of the GRAS salt per unit fruit surface area. However, these differences may not completely explain why F10/SB was superior to F6/SB for control GM in some experiments, and further research is required to fully define their roles in disease control, particularly regarding the proportions of components used in the F10/SB and F6/SB matrices. The similar effects of the ECs and the SB in aqueous solution for control of GM and BM suggest that the coating matrix did not limit salt activity, allowing it to act within the infected fruit rind wounds. However, since similar effectiveness of ECs and aqueous SB was also observed on long-term cold-stored fruit, it can also be concluded that the coating matrix played no role in improving the persistence of the aqueous treatment during storage. In contrast, for instance, the study of López *et al.* (2013) showed that corn starch matrices containing potassium sorbate retained this salt for long periods in polymeric matrices, and actively released the salt to product surfaces, where its action was required during product storage. However, if this salt was applied by immersion or spray methods, its surface antimicrobial action decreased rapidly, so highly concentrated solution was necessary to ensure satisfactory antimicrobial activity.

The present results show that both ECs containing SB and aqueous SB controlled both GM and BM more effectively on lemons than oranges and more effectively on oranges than mandarins. Considering that disease on control fruit was similar for all citrus species tested, these results indicate that variations in the efficacy of the treatments were not only caused by differences in fruit species susceptibility. Disease development is affected by complex interactions between the fruit host, the pathogen and the environment. In the case of diseases caused by wound pathogens, efficacy of an antifungal GRAS salt depends on the amount of salt residue present within wound infection sites occupied by fungi, and on interactions between this residue and rind constituents (Palou *et al.*, 2002; Montesinos-Herrero *et al.*, 2016; Palou, 2018). As previously reported, and depending on the citrus species, such interactions may alter the original toxicity of the salt to the pathogen as a consequence of different rind characteristics, composition or pH (Valencia-

Chamorro *et al.*, 2009a; Montesinos-Herrero *et al.*, 2016; Palou *et al.*, 2016). In the present case, the fact that rind pH is lower in lemons than in oranges and mandarins, and that effectiveness of SB is pH-dependent, increasing the effectiveness of the salt as the pH decreases within the rind wounds (Palou *et al.*, 2002; Chipley, 2005), may explain why the effectiveness of the treatments was greater on lemons than on the other citrus species. In addition, release of SB from the polymer matrix to the rind wounds in each type of fruit may vary according to the degree of rind resistance to the diffusion of the salt. Therefore, the same ECs may considerably differ in suitability for management of fungal diseases on different fruit species and cultivars (Park, 1999; Palou *et al.*, 2015). Further research may clarify if histological and/or ultrastructural differences between the rinds of lemons, oranges and mandarins can account for different degrees of SB diffusion.

The ECs F6/SB and F10/SB and the SB treatment reduced GM more than BM, during incubation at 20°C and cold storage at 5°C. Comparing these results with those obtained in previous studies by Valencia-Chamorro *et al.* (2009a; 2009b; 2011), HPMC-beeswax-based ECs containing SB also controlled GM more effectively than BM on 'Clemenules' and 'Ortanique' mandarins and on 'Valencia' oranges incubated for up to 7 d at 20°C or long-term stored at 5°C. However, the present results show greater reductions in disease incidence and severity during incubation at 20°C, which may be due to greater release of SB in the PPS-GMS-based matrix than in the HPMC-beeswax-based matrix. During cold storage, the present results were very similar to those reported for HPMC-based coatings with SB applied to 'Valencia' oranges in equivalent experimental conditions (Valencia-Chamorro *et al.*, 2009a). Moreover, it is well known that at storage at temperatures below 10°C, *P. italicum* is well adapted, and grows more rapidly than *P. digitatum* (Smilanick *et al.*, 2020). In general on cold-stored citrus, therefore, the efficacy of postharvest antifungal treatments such as GRAS salts and antifungal ECs as alternatives to synthetic fungicides is less for control BM than GM. Furthermore, the effectiveness of the PPS-GMS-based ECs formulated with SB and the SB aqueous treatment to control BM and GM decreased during the cold storage period, confirming that the effect of the SB salt, either in aqueous solution or incorporated in the ECs, is probably fungistatic rather than fungicidal, in agreement with previous studies (Valencia-Chamorro *et al.*, 2009a, 2011b; Montesinos-Herrero *et al.*, 2016). In this sense, and considering the importance of the pH, the salt diffusion properties and the fruit host characteristics, further research on the

modes of action of SB and/or ECs containing SB against the pathogens causing citrus GM and BM should focus on the evaluation of actual SB residue levels on fruit, after treatment and during storage. These studies should also consider the role of commercial storage conditions, particularly temperature, on the stability and diffusion of SB on coated and stored fruit, and elucidate the influence of EC emulsion pH on SB persistence and effectiveness. Theoretically, an EC emulsion with low pH would have increased efficacy since a greater portion of the SB would be protonated. Another aspect that deserves further research is the ability of antimicrobial ECs in general and ECs containing SB in particular to kill or inactivate microorganisms of food safety concern, such as *Salmonella* spp., *Listeria* spp. and *Escherichia coli* (Aloui and Khwaldia, 2016). Currently, this is particularly important in citrus packhouses in the United States of America, where sanitation programmes are required to satisfy food safety audits under the Food Safety Modernization Act (FSMA) established by the Food and Drug Administration.

In summary, there is little information available on the addition of antifungal ingredients to starch-based ECs for management of postharvest fruit diseases. Nevertheless, some studies have reported significant antifungal activity when starch-based matrices were amended with antimicrobial ingredients, such as essential oils (Sapper *et al.*, 2019), biocontrol agents (Marín *et al.*, 2016, 2019), natamycin (Yang *et al.*, 2019) and the GRAS salt potassium sorbate (Mehyar *et al.*, 2011). Within this context, the general antifungal activity of starch-based ECs containing antimicrobial compounds outlined in these studies involving a variety of fresh fruit pathosystems is in agreement with the results outlined in the present paper.

The main objective of this work was to assess the antifungal curative activity of PPS-based ECs amended with the GRAS salt SB for control of major postharvest citrus diseases. We have found that PPS-GMS-based ECs reduced GM and BM on 'Orri' mandarins, 'Valencia' oranges and 'Fino' lemons artificially inoculated with *P. digitatum* and *P. italicum*, showing curative activity during fruit incubation in room conditions and postharvest storage at low temperatures. Hence, these new PPS-based ECs containing the GRAS salt SB as antifungal ingredient showed potential as promising treatments to reduce *Penicillium* citrus decay. Although both ECs gave curative antifungal activity, F10/SB was superior to F6/SB for control of GM and BM on three citrus species incubated at room temperature and also for control of GM on citrus stored at low temperatures. Therefore, PPS-GMS-based ECs, and particularly the coating F10/

SB, could be promising means for reducing decay and maintaining fruit quality during long-term cold storage, and thus be effective substitutes for conventional waxes amended with synthetic fungicides.

The information generated in this study provides a basis for further research into the application of antifungal PPS-based ECs on other commercially important citrus cultivars, and their possible combination with other alternative non-polluting methods. This research will assist the establishment of cost-effective multi-strategies to improve the control of *Penicillium* postharvest decay in citrus packhouses while preserving the overall fruit quality.

ACKNOWLEDGMENTS

This research was partially funded by the IVIA (Project No. 51910) and the European Union, through the European Regional Development Fund (ERDF) of the Generalitat Valenciana 2014–2020. Dr Lourdes Soto-Muñoz postdoctoral programme was supported by a scholarship from the Mexican National Council of Science and Technology (CONACYT-160058-México). Dr Victoria Martínez-Blay's research scholarship is supported by the IVIA and the European Social Fund ('Beca IVIA-FSE' 2018 No. 24). Fontestad S.A. (Montcada, Valencia, Spain) is gratefully acknowledged for providing fruit and technical assistance for this research.

LITERATURE CITED

- Acosta S., Jiménez A., Cháfer M., González-Martínez C., Chiralt A., 2015. Physical properties and stability of starch-gelatin based films as affected by the addition of esters of fatty acids. *Food Hydrocolloids* 49: 135–143. <https://doi.org/10.1016/j.foodhyd.2015.03.015>
- Aloui H., Khwaldia K., 2016. Natural antimicrobial edible coatings for microbial safety and food quality enhancement. *Comprehensive Reviews in Food Science and Food Safety* 15: 1080–1103. <https://doi.org/10.1111/1541-4337.12226>
- Askarne L., Boubaker H., Boudyach E.H., Ait Ben Aoumar A., 2013. Use of food additives to control postharvest citrus blue mold disease. *Atlas Journal of Biology* 2: 147–153. <https://doi.org/10.5147/ajb.2013.0128>
- Chipley J.R., 2005. Sodium benzoate and benzoic acid. In: *Antimicrobials in Food* (P.M. Davidson, J.N. Sofos, A.L. Branen, ed.), CRC Press, Boca Raton, FL, USA, 11–48. <https://doi.org/10.1201/9781420028737>
- Chung D., Papadakis S.E., Yam K.L., 2001. Release of propyl paraben from a polymer coating into water and food simulating solvents for antimicrobial packaging applications. *Journal of Food Processing and Preservation* 25: 71–87. <https://doi.org/10.1111/j.1745-4549.2001.tb00444.x>
- Durango A.M., Soares N.F.F., Andrade N.J., 2006. Microbiological evaluation of an edible antimicrobial coating on minimally processed carrots. *Food Control* 17: 336–341. <https://doi.org/10.1016/j.foodcont.2004.10.024>
- Erasmus A., Lennox C.L., Smilanick J.L., Lesar K., Fourie P.H., 2013. Imazalil residue loading and green mould control on citrus fruit as affected by formulation, solution pH and exposure time in aqueous dip treatments. *Postharvest Biology and Technology* 77: 43–49. <https://doi.org/10.1016/j.postharvbio.2012.11.001>
- Fagundes C., Pérez-Gago M.B., Monteiro A.R., Palou L., 2013. Antifungal activity of food additives in vitro and as ingredients of hydroxypropyl methylcellulose-lipid edible coatings against *Botrytis cinerea* and *Alternaria alternata* on cherry tomato fruit. *International Journal of Food Microbiology* 166: 391–398. <https://doi.org/10.1016/j.ijfoodmicro.2013.08.001>
- Fagundes C., Palou L., Monteiro A.R., Pérez-Gago M.B., 2015. Hydroxypropyl methylcellulose-beeswax edible coatings formulated with antifungal food additives to reduce alternaria black spot and maintain postharvest quality of cold-stored cherry tomatoes. *Scientia Horticulturae* 193: 249–257. <https://doi.org/10.1016/j.scienta.2015.07.027>
- Guimarães J.E.R., de la Fuente B., Pérez-Gago M.B., Andradas C., Carbó R.,... Palou L., 2019. Antifungal activity of GRAS salts against *Lasiodiplodia theobromae* in vitro and as ingredients of hydroxypropyl methylcellulose-lipid composite edible coatings to control Diplodia stem-end rot and maintain postharvest quality of citrus fruit. *International Journal of Food Microbiology* 301: 9–18. <https://doi.org/10.1016/j.ijfoodmicro.2019.04.008>
- Gunaydin S., Karaca H., Palou L., De La Fuente B., Pérez-Gago M.B., 2017. Effect of hydroxypropyl methylcellulose-beeswax composite edible coatings formulated with or without antifungal agents on physicochemical properties of plums during cold storage. *Journal of Food Quality* 2017: 8573549. <https://doi.org/10.1155/2017/8573549>
- Janjarasskul T., Krochta J.M., 2010. Edible packaging materials. *Annual Review of Food Science and Technology* 1: 415–448. <https://doi.org/10.1146/annurev.food.080708.100836>
- Karaca H., Pérez-Gago M.B., Taberner V., Palou L., 2014. Evaluating food additives as antifungal agents against

- Monilinia fructicola* in vitro and in hydroxypropyl methylcellulose-lipid composite edible coatings for plums. *International Journal of Food Microbiology* 179: 72–79. <https://doi.org/10.1016/j.ijfoodmicro.2014.03.027>
- Krebs H.A., Wiggins D., Stubbs M., Sols A., Bedoya F., 1983. Studies on the mechanism of the antifungal action of benzoate. *Biochemical Journal* 214: 657–663. <https://doi.org/10.1042/bj2140657>
- Ladaniya M.S., 2008. Physiological disorders and their management. In: *Citrus Fruit: Biology, Technology and Evaluation* (M. Ladaniya, ed.), Academic Press, Cambridge, MA, USA, 451–463. <https://doi.org/10.1016/B978-012374130-1.50019-X>
- López O. V., Giannuzzi L., Zaritzky N.E., García M.A., 2013. Potassium sorbate controlled release from corn starch films. *Materials Science and Engineering C* 33: 1583–1591. <https://doi.org/10.1016/j.msec.2012.12.064>
- Lucera A., Costa C., Conte A., Del Nobile M.A., 2012. Food applications of natural antimicrobial compounds. *Frontiers in Microbiology* 3: 287. <https://doi.org/10.3389/fmicb.2012.00287>
- Marín A., Cháfer M., Atarés L., Chiralt A., Torres R., ... Teixidó N., 2016. Effect of different coating-forming agents on the efficacy of the biocontrol agent *Candida sake* CPA-1 for control of *Botrytis cinerea* on grapes. *Biological Control* 96: 108–119. <https://doi.org/10.1016/j.biocontrol.2016.02.012>
- Marín A., Plotto A., Atarés L., Chiralt A., 2019. Lactic acid bacteria incorporated into edible coatings to control fungal growth and maintain postharvest quality of grapes. Lactic acid bacteria incorporated into edible coatings to control fungal growth and maintain postharvest quality of grapes. *HortScience* 54: 337–343. <https://doi.org/10.21273/HORTSCI13661-18>
- Martínez-Blay V., Pérez-Gago M.B., de la Fuente B., Carbó R., Palou L., 2020a. Edible coatings formulated with antifungal GRAS salts to control citrus anthracnose caused by *Colletotrichum gloeosporioides* and preserve postharvest fruit quality. *Coatings* 10: 730. <https://doi.org/10.3390/coatings10080730>
- Martínez-Blay V., Taberner V., Pérez-Gago M.B., Palou L., 2020b. Control of major citrus postharvest diseases by sulfur-containing food additives. *International Journal of Food Microbiology* 330: 108713. <https://doi.org/10.1016/j.ijfoodmicro.2020.108713>
- Mehyar G.F., Al-Qadiri H.M., Abu-Blan H.A., Swanson B.G., 2011. Antifungal effectiveness of potassium sorbate incorporated in edible coatings against spoilage molds of apples, cucumbers, and tomatoes during refrigerated storage. *Journal of Food Science* 76: M210–M217. <https://doi.org/10.1111/j.1750-3841.2011.02059.x>
- Montesinos-Herrero C., Moscoso-Ramírez P.A., Palou L., 2016. Evaluation of sodium benzoate and other food additives for the control of citrus postharvest green and blue molds. *Postharvest Biology and Technology* 115: 72–80. <https://doi.org/10.1016/j.postharvbio.2015.12.022>
- Moscoso-Ramírez, P.A., Montesinos-Herrero, C., Palou, L., 2013. Characterization of postharvest treatments with sodium methylparaben to control citrus green and blue molds. *Postharvest Biology and Technology* 77: 128–137. <https://doi.org/10.1016/j.postharvbio.2012.10.007>
- Njombolwana N.S., Erasmus A., Fourie P.H., 2013. Evaluation of curative and protective control of *Penicillium digitatum* following imazalil application in wax coating. *Postharvest Biology and Technology* 77: 102–110. <https://doi.org/10.1016/j.postharvbio.2012.11.009>
- Palou, L., 2014. *Penicillium digitatum*, *Penicillium italicum* (Green Mold, Blue Mold), In: *Postharvest Decay. Control Strategies* (S. Bautista-Baños, ed.), Academic Press, Elsevier Inc., London, UK, 45–102.
- Palou, L., 2018. Postharvest treatments with gras salts to control fresh fruit decay. *Horticulturae* 4: 46. <https://doi.org/10.3390/horticulturae4040046>
- Palou L., Usall J., Smilanick J.L., Aguilar M.J., Viñas I., 2002. Evaluation of food additives and low-toxicity compounds as alternative chemicals for the control of *Penicillium digitatum* and *Penicillium italicum* on citrus fruit. *Pest Management Science* 58: 459–466. <https://doi.org/10.1002/ps.477>
- Palou L., Valencia-Chamorro S.A., Pérez-Gago M.B., 2015. Antifungal edible coatings for fresh citrus fruit: A review. *Coatings* 5: 962–986. <https://doi.org/10.3390/coatings5040962>
- Palou L., Ali A., Fallik E., Romanazzi G., 2016. GRAS, plant- and animal-derived compounds as alternatives to conventional fungicides for the control of postharvest diseases of fresh horticultural produce. *Postharvest Biology and Technology* 122: 41–52. <https://doi.org/10.1016/j.postharvbio.2016.04.017>
- Papoutsis K., Mathioudakis M.M., Hasperué J.H., Ziogas V., 2019. Non-chemical treatments for preventing the postharvest fungal rotting of citrus caused by *Penicillium digitatum* (green mold) and *Penicillium italicum* (blue mold). *Trends in Food Science & Technology* 86: 479–491. <https://doi.org/10.1016/j.tifs.2019.02.053>
- Park H.J., 1999. Development of advanced edible coatings for fruits. *Trends in Food Science & Technology* 10: 254–260. [https://doi.org/10.1016/S0924-2244\(00\)00003-0](https://doi.org/10.1016/S0924-2244(00)00003-0)

- Ratnawati L., Afifah N., 2019. Effect of antimicrobials addition on the characteristic of arrowroot starch-based films. *AIP Conference Proceedings*: 2175. <https://doi.org/10.1063/1.5134575>
- Sapper M., Chiralt, A., 2018. Starch-based coatings for preservation of fruits and vegetables. *Coatings* 8: 152. <https://doi.org/10.3390/coatings8050152>
- Sapper M., Palou L., Pérez-Gago M.B., Chiralt A., 2019. Antifungal starch-gellan edible coatings with thyme essential oil for the postharvest preservation of apple and persimmon. *Coatings* 9: 333. <https://doi.org/10.3390/coatings9050333>
- Smilanick J.L., Mansour M.F., Margosan D.A., Mlikota Gabler F., Goodwine, W.R. 2005. Influence of pH and NaHCO₃ on effectiveness of imazalil to inhibit germination of *Penicillium digitatum* and to control postharvest green mold on citrus fruit. *Plant Disease* 89: 640–648. <https://doi.org/10.1094/PD-89-0640>
- Smilanick J.L., Mansour M.F., Gabler F.M., Sorenson D., 2008. Control of citrus postharvest green mold and sour rot by potassium sorbate combined with heat and fungicides. *Postharvest Biology and Technology* 47: 226–238. <https://doi.org/10.1016/j.postharvbio.2007.06.020>
- Smilanick J.L., Erasmus A., Palou L., 2020. Citrus fruits. In: *Postharvest Pathology of Fresh Horticultural Produce* (L. Palou, J.L. Smilanick, ed.), CRC Press, Boca Raton, FL, USA, 3–53. <https://doi.org/10.1201/9781315209180-1>
- Soto-Muñoz, L., Palou, L., Argente-Sanchis, M., Ramos-López, M.A., Pérez-Gago, M.B., 2021. Optimization of antifungal edible pregelatinized potato starch-based coating formulations by response surface methodology to extend postharvest life of ‘Orri’ mandarins. *Scientia Horticulturae* 288: 110394. <https://doi.org/10.1016/j.scienta.2021.110394>
- Valdés A., Ramos M., Beltrán A., Jiménez, A. Garrigós M.C., 2017. State of the art of antimicrobial edible coatings for food packaging applications. *Coatings* 7: 56. <https://doi.org/10.3390/coatings7040056>.
- Valencia-Chamorro S.A., Palou L., Del Río M.A., Pérez-Gago M.B., 2008. Inhibition of *Penicillium digitatum* and *Penicillium italicum* by hydroxypropyl methylcellulose-lipid edible composite films containing food additives with antifungal properties. *Journal of Agricultural and Food Chemistry* 56: 11270–11278. <https://doi.org/10.1021/jf802384m>
- Valencia-Chamorro S.A., Pérez-Gago M.B., Del Río M.A., Palou L., 2009a. Curative and preventive activity of hydroxypropyl methylcellulose-lipid edible composite coatings containing antifungal food additives to control citrus postharvest green and blue molds. *Journal of Agricultural and Food Chemistry* 57: 2770–2777. <https://doi.org/10.1021/jf803534a>
- Valencia-Chamorro S.A., Pérez-Gago M.B., Del Río M.A., Palou L., 2009b. Effect of antifungal hydroxypropyl methylcellulose (HPMC)-lipid edible composite coatings on postharvest decay development and quality attributes of cold-stored ‘Valencia’ oranges. *Postharvest Biology and Technology* 54: 72–79. <https://doi.org/10.1016/j.postharvbio.2009.06.001>
- Valencia-Chamorro S.A., Pérez-Gago M.B., Del Río M.A., Palou L., 2010. Effect of antifungal hydroxypropyl methylcellulose-lipid edible composite coatings on penicillium decay development and postharvest quality of cold-stored ‘Ortanique’ mandarins. *Journal of Food Science* 75: S418–S426. <https://doi.org/10.1111/j.1750-3841.2010.01801.x>
- Valencia-Chamorro S.A., Palou L., Del Río M.A., Pérez-Gago M.B., 2011a. Antimicrobial edible films and coatings for fresh and minimally processed fruits and vegetables: A review. *Critical Reviews in Food Science and Nutrition* 51: 872–900. <https://doi.org/10.1080/10408398.2010.485705>
- Valencia-Chamorro, S.A., Palou, L., Del Río, M.A., Pérez-Gago, M.B., 2011b. Performance of hydroxypropyl methylcellulose (HPMC)-lipid edible coatings with antifungal food additives during cold storage of ‘Clemenules’ mandarins. *LWT-Food Science and Technology* 44: 2342–2348. <https://doi.org/10.1016/j.lwt.2011.02.014>
- Vargas M., Pastor, C., Chiralt A., McClements D.J., González-Martínez C., 2008. Recent advances in edible coatings for fresh and minimally processed fruits. *Critical Reviews in Food Science and Nutrition* 48: 496–511. <https://doi.org/10.1080/10408390701537344>
- Widodo S.E., Shiraishi M., Shiraishi S., 1996. Variations of acidity in the peel of acid citrus. I. Acid contents in the flavedo and albedo of acid citrus. *Journal of The Faculty of Agriculture Kyushu University* 40: 257–262. <https://doi.org/10.5109/24111>
- Yang Y., Huan C., Liang X., Fang S., Wang J., Chen J., 2019. Development of starch-based antifungal coatings by incorporation of natamycin/methyl- β -cyclodextrin inclusion complex for postharvest treatments on cherry tomato against *Botrytis cinerea*. *Molecules* 24: 3962. <https://doi.org/10.3390/molecules24213962>
- Youssef K., Sanzani S.M., Ligorio A., Ippolito A., Terry L.A., 2014. Sodium carbonate and bicarbonate treatments induce resistance to postharvest green mould on citrus fruit. *Postharvest Biology and Technology* 87: 61–69. <https://doi.org/10.1016/j.postharvbio.2013.08.006>

Zacarias L., Cronje P.J., Palou L., 2020. Postharvest technology of citrus fruits. In: *The Genus Citrus* (M. Talón, M. Caruso, F. Gmitter Jr., ed.), Woodhead Publishing, Elsevier Inc., Sawston, Cambridge, UK, 421–446. <https://doi.org/10.1016/b978-0-12-812163-4.00021-8>



Citation: W. Cui, A. Zamorano, N. Quiroga, A. Bertaccini, N. Fiore (2021) Ribosomal protein coding genes *SSU12p* and *LSU36p* as molecular markers for phytoplasma detection and differentiation. *Phytopathologia Mediterranea* 60(2): 281-292. doi: 10.36253/phyto-11993

Accepted: July 7, 2021

Published: September 13, 2021

Copyright: © 2021 W. Cui, A. Zamorano, N. Quiroga, A. Bertaccini, N. Fiore. This is an open access, peer-reviewed article published by Firenze University Press (<http://www.fupress.com/pm>) and distributed under the terms of the Creative Commons Attribution License, which permits unrestricted use, distribution, and reproduction in any medium, provided the original author and source are credited.

Data Availability Statement: All relevant data are within the paper and its Supporting Information files.

Competing Interests: The Author(s) declare(s) no conflict of interest.

Editor: Nihal Buzkan, Kahramanmaraş Sütçü Imam University, Turkey.

Research Papers

Ribosomal protein coding genes *SSU12p* and *LSU36p* as molecular markers for phytoplasma detection and differentiation

WEIER CUI¹, ALAN ZAMORANO¹, NICOLÁS QUIROGA¹, ASSUNTA BERTACCINI², NICOLA FIORE^{1,*}

¹ University of Chile, Faculty of Agronomic Sciences, Department of Plant Health, Santiago, Chile. Av. Santa Rosa 11315, Santiago, Chile

² Alma Mater Studiorum - University of Bologna, Department of Agricultural and Food Sciences, viale G. Fanin 40, 40127, Bologna, Italy

*Corresponding author. E-mail: nfiore@uchile.cl

Shared co-first authorship: Weier Cui and Alan Zamorano

Summary. Detection and classification of phytoplasmas mainly rely on amplification of the 16S rRNA gene followed by RFLP analysis and/or sequencing, because these organisms lack complete phenotypic characterization. Other conserved genomic *loci* have been exploited as additional molecular markers for phytoplasma differentiation. Two *loci*, *SSU12p* and *LSU36p*, selected by whole-genome comparison of 12 phytoplasma strains, were used for primer design, and were successfully tested on DNA samples from plants infected by phytoplasmas belonging to ten 16S ribosomal groups. The phylogenetic trees inferred from *SSU12p* and *LSU36p* *loci* were highly congruent to the trees derived from 16S rRNA and *tuf* genes of the same phytoplasma strains. Virtual RFLP analysis of the amplified *SSU12p* gene showed distinct patterns for most of the phytoplasma ribosomal subgroups tested. These results show that *SSU12p* and *LSU36p* genes are reliable additional markers for phytoplasma detection and differentiation.

Keywords. PCR, 16S rRNA gene, *tuf* gene, RFLP.

INTRODUCTION

Phytoplasmas are obligate intracellular pathogens that reside and multiply in the phloem tissues of plants and in insect hosts. They are associated with severe diseases of economically important plants, including aster yellows, coconut lethal yellowing, apple proliferation, pear decline, peach X disease and ash yellows. Australian grapevine yellows, which is associated with three phytoplasmas, causes up to 54% yield losses (Glenn, 2000). In Brazil, yield losses caused by maize bushy stunt are estimated to be worth \$US 16.5 million (Oliveira *et al.*, 2003). Due to the difficulty to culture phytoplasmas (Contaldo and Bertaccini, 2019) and the lack of a complete phenotypic characterization of these organisms, phytoplasmas classification is based on their 16S rRNA gene sequences, that are conserved and widely used for prokary-

ote identification (Lee *et al.*, 1993; Ludwig and Schleifer, 1994; Seemüller *et al.*, 1994; Schneider *et al.*, 1995; Jenkins *et al.*, 2012). A provisional naming system (IRPCM, 2004) assigned ‘*Candidatus* Phytoplasma’ species to strains whose 16S rRNA gene sequence has less than 97.5% identity to any previously described ‘*Ca.* Phytoplasma’ species. A set of 17 restriction enzymes was selected to generate the restriction fragment length polymorphism (RFLP) profile of the R16F2n/R2 fragment of the 16S rRNA gene. By this approach, 16Sr groups and subgroups have been identified (Lee *et al.*, 1998; Wei *et al.*, 2008). The ‘*Ca.* Phytoplasma’ species and the RFLP-generated ribosomal groups and subgroups are therefore the two approaches used to classify these prokaryotes. However, one 16S ribosomal group may contain one or more ‘*Ca.* Phytoplasma’ species, whereas all the strains within one ribosomal subgroup belong to the same ‘*Ca.* Phytoplasma’ species (Bertaccini and Lee, 2018).

Considering the stringency of the 16S rRNA gene in assigning ‘*Ca.* Phytoplasma’ species, there are limitations in differentiating closely related strains, so other *loci* have been described and utilized as additional molecular markers for phytoplasma strain differentiation. Other markers have been used in phytoplasma phylogenetic studies, including the 16S-23S intergenic spacer, the 23S rRNA gene, the ribosomal protein operon (*rp19-rpl22-rps3*), the elongation factor Tu (*tuf*), protein translocase units (*secA* and *secY*), the chaperonin 60 (*cpn60*), and the subunit β of RNA polymerase (*rpoB*) (Marccone *et al.*, 2000; Martini *et al.*, 2002, 2007; Hodgetts *et al.*, 2008; Lee *et al.*, 2010; Makarova *et al.*, 2012; Valiunas *et al.*, 2013). The methionine aminopeptidase gene (*map*)-*uvrB-degV*, *nusA* and *vmp1* was also used for differentiation of strains within, respectively, the 16SrV, 16SrI and 16SrX-II-A groups and subgroups (Shao *et al.*, 2006; Arnaud *et al.*, 2007; Cimerman *et al.*, 2009). All these markers except *vmp1* have also been used for differentiation of other bacteria (Pérez-López *et al.*, 2016), confirming the suitability of a gene-based strategy also for phytoplasma strain differentiation.

Besides providing classification, the 16S rRNA gene also serves as the most important detection marker for phytoplasmas. Several sets of primers have been designed to amplify different fragments from this gene. The combination of P1/P7 and R16F2n/R2 is the most employed for phytoplasma detection, but other primer sets as well as ribosomal group-specific primers are useful for detection of multiple phytoplasma infections and/or heterogeneous phytoplasma populations (Duduk *et al.*, 2013). Other *loci* are also used as detection markers, including *tuf*, *rpoB*, *cpn60*, *nusA* and *vmp1* (Shao *et al.*, 2006; Cimerman *et al.*, 2009; Makarova *et al.*, 2012;

Valiunas *et al.*, 2013; Dumonceaux *et al.*, 2014). However, the lack of universal primers (*rpoB*, *secY*, *rp*), the narrow detection range (*nusA*, *vmp1*, *map-uvrB-degV*) and the high rate of false positives (*cpn60*) severely reduce their detection efficiency.

In the present study, new molecular markers for phytoplasma detection and differentiation were designed and tested. Using whole genome comparisons, the phytoplasma genome conserved regions *SSU12p* and *LSU36p* were selected for primer design, and tested to verify their usefulness as molecular markers for a range of phytoplasma strains.

MATERIALS AND METHODS

Phytoplasma strains and nucleic acid preparation

Thirty-three phytoplasma strains collected from various host plant species from different geographic regions worldwide were used. The strains were identified on their 16S ribosomal DNA (Cui *et al.*, 2019; EPPO-Q-bank, 2020), and belong to the 16Sr groups: -I, -II, -III, -V, -VI, -VII, -IX, -X, -XII and -XIII. The strain names, acronyms, 16Sr groups/subgroups, and providers are listed in Table 1. The DNAs from strawberry plants infected by the StrPh-CL strains were extracted as described by Cui *et al.* (2019). DNA samples provided by EPPO-Q-bank were extracted as described by Makarova *et al.* (2012).

Primer design

Direct and nested PCR primers were designed by comparing the conserved genomic regions of 12 phytoplasma strains available from the GenBank, including those associated with the diseases aster yellows witches’ broom (AYWB) (CP000061), onion yellows mild strain (OYM) (NC_005303), peanut witches’ broom (PnWB) strain NTU2011 (AMWZ00000000), *Echinacea purpurea* witches’ broom (*E. purpurea* WB) strain NCHU2014 (LKAC00000000), Italian clover phyllody (ItClPh) strain MA1 (AKIM00000000), *Vaccinium* witches’ broom (VacWB) strain VAC (AKIN00000000), milkweed yellows (MWY) strain MW1 (AKIL00000000), poinsettia branch-inducing phytoplasma (PoiBI) strain JR1 (AKIK00000000), ‘*Ca.* P. mali’ strain AT (CU469464), ‘*Ca.* P. australiense’ (AUSGY) (AM422018), strawberry lethal yellows phytoplasma (CPA) strain NZSb11 (CP002548), and phytoplasma Vc33 (LLKK00000000). Whole-genome comparison was performed with the “Sequence-based comparison” tool on the Rapid Annotation using the Subsystem Technology (RAST) server

Table 1. Phytoplasma strains used in this study, and their corresponding *SSU12p* and *LSU36p* amplicons.

16Sr group	Subgroup	Associated disease	Acronym	Provided by	Amplicon size ^a		GenBank Accession Number	
					SSU12p	LSU36p	SSU12p	LSU36p
16SrI	A	Aster yellows witches' broom	AYWB	GenBank	748	465	CP000061	
	B	<i>Catharanthus</i> virescence	CTV	EPPQ-Q-bank	766	468	MT161513	MT161546
	B	Onion yellows mild strain	OY-M	GenBank	766	461	NC_005303	
	B	Primula yellows	PRIVA	EPPQ-Q-bank	766	461	MT161512	MT161545
	B	Maize bushy stunt	MBS	GenBank	766	461	CP015149	
	C	Clover phyllody	KVE	EPPQ-Q-bank	758	462	MT161514	MT161547
16SrII	F	Aster yellows from apricot	A-AY	EPPQ-Q-bank	735	462	MT161515	MT161548
	A	Peanut witches' broom	PnWB	GenBank	703	411	AMWZ000000000	
16SrIII	A	<i>Echinacea purpurea</i> witches' broom	<i>E. purpurea</i> WB	GenBank	703	411	LKAC000000000	
	C	Faba bean phyllody	FBP	EPPQ-Q-bank	703	409	MT161516	MT161549
	D	Tomato big bud	TBB	EPPQ-Q-bank	703	418	MT161517	MT161550
	A	Peach X disease	WX	GenBank	738	417	LHCF000000000	
	A	Peach X disease	CX	EPPQ-Q-bank	739	417	MT161518	MT161551
	A	Peach yellow leaf roll	PYLR	EPPQ-Q-bank	739	417	MT161519	MT161552
	B	Italian clover phyllody	ItClPh	GenBank	740	417	AKIM000000000	
	B	<i>Taraxacum</i> leaf reddening	TA	EPPQ-Q-bank	740	417	MT161520	MT161553
	B	Plum leptonecrosis	LNI	EPPQ-Q-bank	740	417	MT161521	MT161554
	D	Goldenrod yellows	GR	EPPQ-Q-bank	740	417	MT161522	MT161555
	E	Spirea stunt	SPI	EPPQ-Q-bank	739	420	MT161523	MT161556
	F	<i>Vaccinium</i> witches' broom	VacWB	GenBank	740	417	AKIN000000000	
16SrV	F	<i>Solanum</i> big bud	SBB	EPPQ-Q-bank	741	417	MT161524	MT161557
	F	Milkweed yellows	MW1	EPPQ-Q-bank	740	417	MT161525	MT161558
	F	Milkweed yellows	MWY	GenBank	740	417	AKIL000000000	
	H	Poinsettia branch inducing	PoiBI	GenBank	739	417	AKIK000000000	
	H	Poinsettia branch inducing	JR	EPPQ-Q-bank	739	417	MT161526	MT161559
	J	Phytoplasma Vc33	Vc33	GenBank	740	417	LLKK000000000	
	A	Elm yellows	EY	EPPQ-Q-bank	724	419	MT161527	MT161560
	A	Clover proliferation	CPI	EPPQ-Q-bank	722	381	MT161528	MT161561
	A	Ash yellows	ASHY	EPPQ-Q-bank	719	398	MT161529	MT161562
	B	Almond witches' broom	SA213	GenBank	723	489	JPSQ000000000	
16SrX	C	<i>Picris echioides</i> yellows	PEY	EPPQ-Q-bank	737	677	MT161530	MT161563
	C	Naxos periwinkle yellows	NAXOS	EPPQ-Q-bank	737	677	MT161531	MT161564
	A	Apple proliferation	AP	EPPQ-Q-bank	723	443	MT161532	MT161565
	A	Apple proliferation	AT	GenBank	723	443	CU469464	
	B	European stone fruit yellows	ESFY	EPPQ-Q-bank	724	489	MT161533	MT161566

(Continued)

Table 1. (Continued).

16Sr group	Subgroup	Associated disease	Acronym	Provided by	Amplicon size ^a		GenBank Accession Number	
					SSU12p	LSU36p	SSU12p	LSU36p
16SrXII	B	Plum leptonecrosis	LŃp	EPPQ-Q-bank	724	487	MT161534	MT161567
	C	Pear decline	PD	EPPQ-Q-bank	724	442	MT161535	MT161568
	A	Molière disease	MOL	EPPQ-Q-bank	723	406	MT161536	MT161569
	A	Grapevine yellows	SA-1	GenBank	723	406	MPBG000000000	
	A	Grapevine yellows	CHI	EPPQ-Q-bank	723	406	MT161537	MT161570
	B	Australian grapevine yellows	AUSGY	GenBank	745	401	AM422018	
	C	Strawberry lethal yellows	CPA	GenBank	745	401	CP002548	
16SrXIII	F	Strawberry phylloxy	StrPh-CL1	University of Chile	739	406	MT161538	MT161571
			StrPh-CL3		739	406	MT161540	MT161573
			StrPh-CL5		739	406	MT161542	MT161575
			StrPh-CL6		739	406	MT161543	MT161576
			StrPh-CL7		739	406	MT161544	MT161577
			StrPh-CL2	University of Chile	737	406	MT161539	MT161572
	K	Strawberry phylloxy	StrPh-CL4		737	406	MT161541	MT161574

^abp, the length of the primers is not included.

(<http://rast.nmpdr.org/rast.cgi>). The annotated genes were sorted based on similarity, and four genes with the greatest similarities, except for the 16S rRNA, were selected for primer design. These were: the small subunit ribosomal protein S12p (*SSU12p*), and the large subunit ribosomal proteins L2p, L27p and L36p (*LSU2p*, *LSU27p* and *LSU36p*). For each gene, a region containing the gene and 500 bp flanking the region upstream and downstream was used for the alignment. Direct and nested primers were selected within the most conserved regions (Table 2).

Cloning and sequencing

PCRs were carried out using the Invitrogen™ Platinum™ Taq DNA Polymerase system. Each reaction was performed in a 30 µL volume containing 1× reaction buffer, 2.5 mM MgCl₂ and 2 U Taq polymerase, supplied with 0.3 mM dNTP, 0.8 µM of each primer and sterile double distilled water. One µL (20 ng) of nucleic acid was used as template, and 0.2 µL of the amplicon was used as template for the nested assays. A sample devoid of DNA template was enclosed as negative control. PCR was initiated by a 5 min denaturation at 94°C, followed by 35 cycles of 30 s denaturation at 94°C, 45 s annealing at respective temperatures (Table 2) and 1 min extension at 72°C, and a final extension at 72°C for 7 min. A three step annealing strategy was used, with each step of 15 s, for all the primer sets (Table 2).

The PCR products were resolved in 1.2% agarose gels with ethidium bromide. Amplicons, corresponding to approx. 820 bp for the *SSU12p* gene and 420 to 530 bp for the *LSU36p* gene from nested PCR, were recovered and cloned into the vector pGEM⁺-T Easy (Promega). The plasmids were transformed into *E. coli* TOP10 chemically competent cells (Life Technologies), and the clones were sequenced using the T7/SP6 primers in both directions. Each pair of sequences was aligned and assembled using BioEdit. Three individual clones for each amplicon from each sample were analyzed. Each PCR, cloning and sequencing was repeated at least three times.

Phylogenetic analyses

The consensus sequence of each amplicon was submitted to the NCBI GenBank database (Table 1). Sequence information of the 12 phytoplasma strains used for the primer design was obtained from the same database. Sequence information of four other strains, including maize bushy stunt phytoplasma (MBS) strain M3 (CP015149), '*Ca. P. pruni*' strain CX

Table 2. Universal primers designed for amplification of *SSU12p* and *LSU36p* loci.

Target	PCR	Primer	Sequence ^a	T°C ^b		
				1	2	3
SSU12p	Direct	ItSSU12pF	ATGCCTACTRITTCWCAATTAATTA	51.8	48.3	44.0
		ItSSU12pR	ATCTTAAACCTAAAGATTGRCGTC			
	Nested	ItSSu12pFn	AAAACCTAACTCCGCTTT	49.7	45.8	44.1
ItSSu12pR1n		TTATGAAAAGTGGTAAAAAAG				
ItSSu12pR2n		TTATGAAAAGATGGMAAAAAGG				
LSU2p	Direct	ItLSu2pF	CTCATGYAAGTGTATTATCA	55.0	47.0	42.0
		ItLSu2pR	CTAAACGTGYTTTTCKAGG			
	Nested	ItLSu2pFn	YACTAGCAAYGTTTTRCC	56.0	47.0	42.0
ItLSu2pRn		CCTAATTTATGWCCCACCAT				
LSU27p	Direct	ItLSu27pF1	AAAAATATCGTTTAAAAACAAGG	55.0	47.0	42.0
		ItLSu27pF2	AAAAATATCGTTGTAAACAAGG			
		ItLSu27pR	GATATAGTTTGTGCTTCBGTTTC			
	Nested	ItLSu27pFn	GTTCTCTTTGGCGRTAA	56.0	53.0	48.0
		ItLSu27pRn	TTAGAATGAGAATCACGACC			
LSU36p	Direct	ItLSU36pF1	GACTTTTTGCATTGAACC	51.6	47.2	42.2
		ItLSU36pF2	GACTTTTTGTGTTGAACC			
		ItLSU36pR	CGTTGTTTCTAGTTTTTTGHCC			
	Nested	ItLSU36pFn	AAGTGCTCATTTTGAACAYAC	50.0	47.7	43.1
		ItLSU36pRn	TTAYCCTTGTCTTTGATTRT			

^aDegenerate nucleotides: R = A or G, W = A or T, H = A or C or T, Y = C or T.

^bAnnealing temperatures: a three-step annealing was applied: 15 s of T1 followed by 15 s of T2, and then 15 s of T3.

(LHCF00000000), '*Ca. P. phoenicium*' strain SA213 (JPSQ00000000), and '*Ca. P. solani*' (STOL) strain SA-1 (MPBG00000000), was also retrieved from the database for constructing phylogenetic trees. The sequence alignment was performed using ClustalW. *Acholeplasma laidlawii* (CP000896) served as outgroup. The phylogenetic trees were constructed using the Molecular Evolutionary Genetics Analysis program (MEGA7) (Kumar *et al.*, 2016). Diversity indices, represented by the distances within and between groups, were also calculated using MEGA7. Virtual RFLP was performed using Vector NTI.

RESULTS

PCR amplification

In all the PCR reactions, several annealing temperatures were tested to select the best combinations. Since one reaction may include more than two primers and each primer may contain several degenerate nucleotides, a range of melting temperatures was calculated using the online tool (IDT OligoAnalyzer). This range could exceed the suggested melting temperature differ-

ence (5°C) for primer design, and when a single annealing temperature was utilized, not all the primers would anneal as efficiently, and nonspecific amplicons might be produced. Therefore, a three-step annealing strategy was used to optimize the reactions. Three annealing temperatures were selected at the maximum, mean and minimum points in the melting temperature range, each step lasting 15 sec. For each primer set, several adjustments were made before establishing the optimal combination (Table 2).

For all the samples used in this study, the PCR assay using the ItSSU12pF/ItSSU12pR primer pair produced clear bands approximately ranging from 750 bp to 820 bp (Figure 1A, Table 1). Subsequent nested PCR also generated clear bands (data not shown). These PCR amplicons were cloned and sequenced.

The PCR assay using the ItLSU36pF1/2/ItLSU36pR primers generated multiple bands or smears, and, in several cases, the expected products were not visible (Figure 1B). However, the subsequent nested PCR using the ItLSU36pFn/ItLSU36pRn primers always generated a strong and clear amplicon, and, in some cases, longer but significantly weaker bands (Figure 1C, Table 1). The strongest bands from each sample were recovered from the gels, cloned and sequenced.

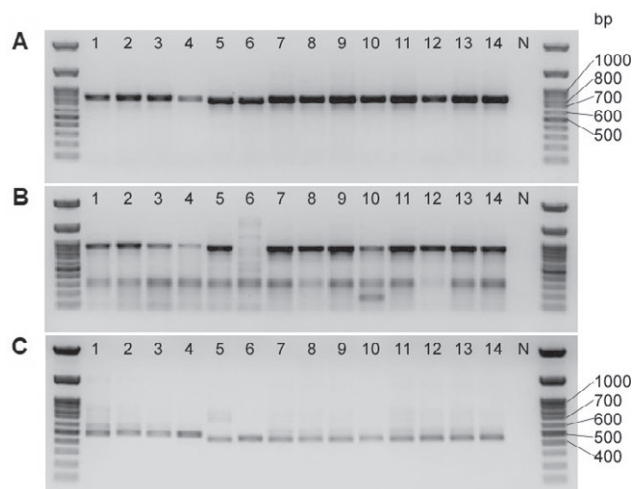


Figure 1. Agarose electrophoresis of the PCR results using the primer sets ItSSU12pF/ItSSU12pR (A), ItLSU36pF1/2/ItLSU36pR (B) and ItLSU36pFn/ItLSU36pRn (C). Lanes: 1. PRIVA, 2. CVT, 3. KVE, 4. A-AY, 5. FBP, 6. TBB, 7. CX, 8. PYLR, 9. TA, 10. LNII, 11. GR, 12. SP1, 13. MW1, 14. JR, N = negative control. Ladder: Maestrogen AccuRuler 100 bp Plus (ThermoFisher).

The direct and nested PCR assays targeting *LSU2p* and *LSU27p* genes failed to produce satisfactory results. In each trial, less than half of the tested samples showed amplification, and the results were not repeatable (data not shown). Optimization of the annealing temperatures failed to achieve consistent results and these primers were therefore discarded.

The specificity of the remaining primers was tested for detection of *Xylella fastidiosa*, *Agrobacterium tumefaciens*, *Pantoea agglomerans*, *Clavibacter michiganensis* subsp. *michiganensis*, *Pseudomonas syringae* pv. *tomato*, *P. syringae* pv. *syringae*, *Ralstonia solanacearum*, *Curtobacterium flaccumfaciens* pv. *flaccumfaciens*, *Xanthomonas arboricola* pv. *juglandis*, ‘*Candidatus Liberibacter solanacearum*’, and ‘*Ca. L. asiaticus*’, with no amplification (data not shown).

Loci structures

The amplicons generated by ItSSU12pF/ItSSU12pR covered the full length of the *SSU12p* gene, the partial sequence of *SSU7p* gene, and the intergenic region between the two genes. In the following text, this amplicon and its corresponding genomic locus are referred to as *SSU12p*. Sequence alignment of all the amplified samples and selected strains retrieved from the GenBank showed that *SSU12p* presented greater variation among ribosomal groups and subgroups compared with 16S rRNA (Supplementary Figure S1). The most relevant var-

iation lay between 396 to 431 nt in strain AYWB (16SrI-A) corresponding to the intergenic region, which was less conserved than the coding genes, where the phytoplasma strains of the same ribosomal group and/or subgroup were featured by specific insertions and deletions.

The amplicon generated by ItLSU36pFn/ItLSU36pRn covered approximately 80% of the *LSU36p* gene, the full length of the gene encoding bacterial protein translation initiation factor 1 (IF-1), approx. 5% of the *map* gene, and the two intergenic regions. This amplicon and its corresponding genomic locus is referred to as *LSU36p* in the following text. Sequence alignment showed that the most conserved region was that encompassing the first 102 nt in the sequence of the strain AYWB, corresponding to the *LSU36p* gene (Supplementary Figure S2). The rest of the amplicon was highly variable among ribosomal groups and/or subgroups, with especially low similarity between the three tested strains in the 16SrIX group and the rest of the strains. However, by comparing this region in AYWB and ‘*Ca. P. phoenicium*’ strain SA213 (16SrIX-B) it was observed that the low similarity was mainly located in the two intergenic regions, which also resulted in differences in length among the tested strains (Supplementary Figures S2 and S3).

Phylogenetic analyses

Phylogenetic trees were constructed with the *SSU12p* and *LSU36p* sequences separately as well as with the concatenated sequences (Figures 2A, 2B and 2C). The three trees showed clear separation of the phytoplasmas classified in the different 16Sr groups, the only exception being the 16SrXII-A subgroup (‘*Ca. P. solani*’), which was more closely related to the 16SrI group than to the other 16SrXII subgroups in the *SSU12p* tree (Figure 2A). A number of subgroups and their corresponding ‘*Ca. Phytoplasma*’ species were also clearly separated, e.g. 16SrI-B (‘*Ca. P. asteris*’), 16SrXII-A (‘*Ca. P. solani*’), 16SrXIII-E, 16SrXIII-K, 16SrX-A (‘*Ca. P. mali*’), 16SrX-B (‘*Ca. P. prunorum*’) and 16SrX-C (‘*Ca. P. pyri*’). The three trees showed significant consistency with those inferred from the 16S rRNA and *tuf* genes (Figure 2D and 2E).

To further evaluate the efficiency of the *SSU12p* and *LSU36p* for phytoplasma strain differentiation, the diversity indices within each 16Sr group and between any two groups were calculated, and paired t-Tests were performed to compare the set of “between group mean distance” indices from each marker (Supplementary Table S1). Both sets of indices from *SSU12p* and *LSU36p* were significantly higher than that of 16S rRNA ($P < 0.01$), suggesting that these two markers could efficiently separate the strains in different ribosomal groups. The indi-

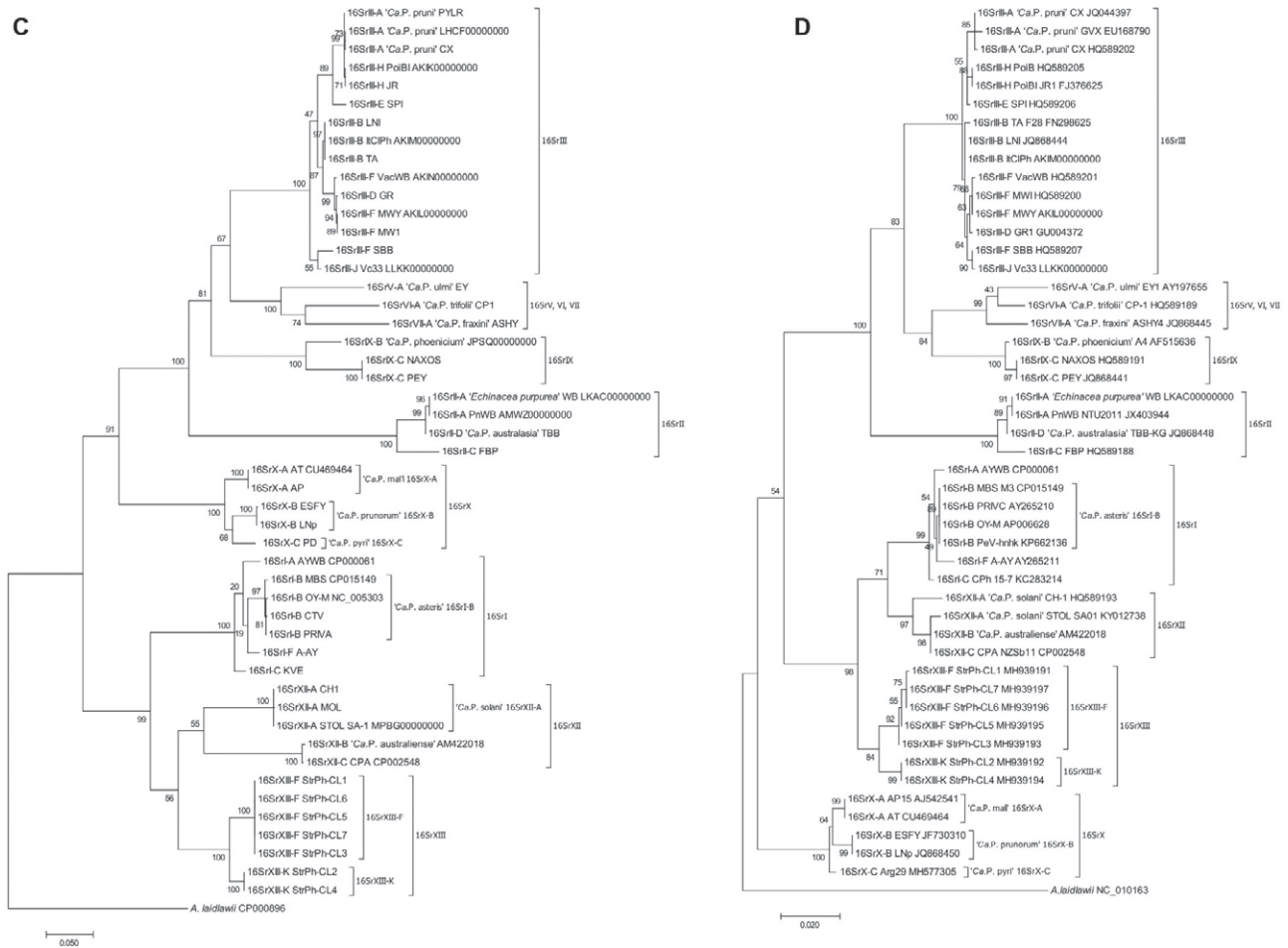


Figure 2. (continued)

strains from the 16SrXIII-F subgroup, and the 576A site of the strains from the 16SrXIII-K subgroup, also resulted in a specific *SspI* restriction site, producing a triple-band pattern for these two subgroups on the virtual RFLP. The 218G site unique to the strains from the 16SrIX-C subgroup resulted in a specific *HpaII* restriction site, generating double bands on the virtual RFLP for this subgroup (Figure 3, Supplementary Figures S1 and S4).

DISCUSSION

Using 33 DNA samples and 16 sequences retrieved from the GenBank belonging to ten 16Sr groups and 27 subgroups, this study has shown that both *SSU12p* and *LSU36p* are suitable *loci* for phytoplasma detection and differentiation. In the RFLP analyses using amplicons generated by *SSU12p*, a set of seven enzymes, including

BfaI, *HinfI*, *HpaII*, *Sau3AI*, *SspI*, *AluI* and *HhaI*, were able to identify all the phytoplasmas in the 16Sr groups, and in all but four subgroups (16SrII-A/-D and 16SrIII-A/-E) examined.

The primers for *SSU12p* and *LSU36p* amplified phytoplasma sequences from all the samples tested, proving that they are amplifying conserved regions in a robust manner. The *SSU12p* primers generated in direct PCR clear, single-band products. According to the literature, *SSU12p* is to date peerless for phytoplasma PCR detection, considering its ability to generate a unique specific band in direct PCR using a single pair of primers from a wide range of phytoplasmas. The high consistency of *SSU12p* for phytoplasma identification with 16S rRNA and *tuf* genes confirms its reliability, suggesting that the application of this pair of primers is appropriate for rapid and efficient phytoplasma detection and identification. The *LSU36p* primers, on the other hand, requires nested amplification, and the resulting products may vary

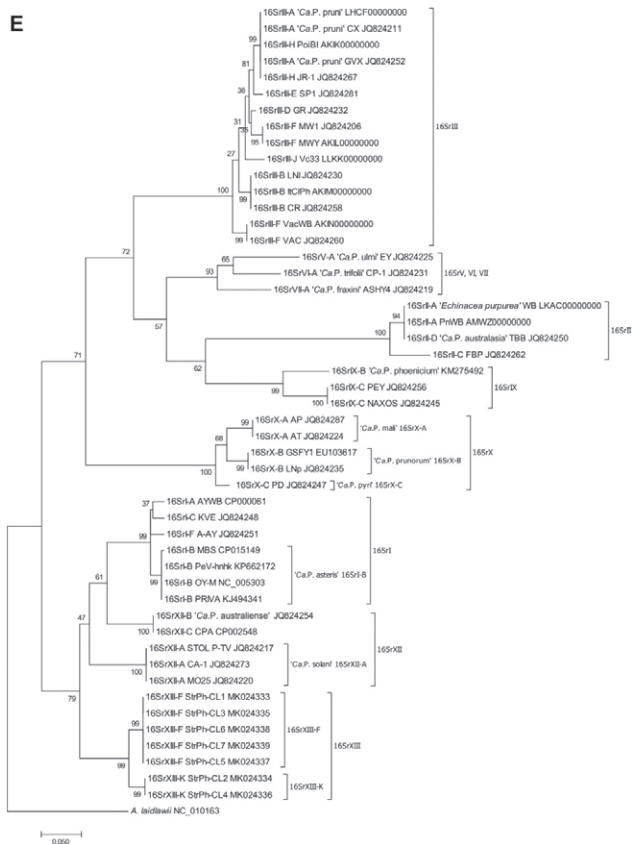


Figure 2. (continued)

significantly in size. However, the relatively high value of between-group mean distance indices suggests that *LSU36p* has potential for resolving closely related strains. Further study focused on other strains belonging to different subgroups from the same ribosomal group is required for confirmation.

Due to different evolutionary processes, phylogenetic trees derived from different genome *loci* may show conflicting structures. One way to interpret the conflicting information is to concatenate the *loci* for phylogenetic analyses. Although concatenation is a controversial method because of potential misspecification of models, it provides longer sequences to overcome sampling errors (Holland *et al.*, 2004). In the present study, the phylogenetic trees inferred from *SSU12p*, *LSU36p* and *SSU12p* plus *LSU36p* showed clear and unambiguous consistency of ramification of phytoplasma subgroups within most of the 16Sr groups, confirming the robustness of the concatenation methods.

The only exception was the 16SrIII group, which showed unclear relationships among several subgroups. For example, in the *SSU12p* tree, the strain SBB from the 16SrIII-F subgroup formed a clade with the Vc33 from

the 16SrIII-J subgroup, while the other two strains from the 16SrIII-F group, MWY and MW1, were grouped with strains from the 16SrIII-B and 16SrIII-D subgroups. This was probably due to the intrinsic structure of the 16SrIII group, since the trees from both *tuf* and 16S rRNA also showed unclear structures within this phytoplasma group. A similar conflict occurred within the 16SrIII group in independent studies analyzing 16S rRNA and *secY* phylogenies (Lee *et al.*, 2010; Fernández *et al.*, 2017). The two copies of the 16S rRNA gene of phytoplasmas in this group very often present interoperon heterogeneity. Data from *secY* and *tuf* genes, both present in the genome in single copy, indicated that the confusing tree structures were not incidental. These results suggest that the subgroup classification within the 16SrIII group may not reflect phylogenetic interrelationship and the RFLP-based classification may be biased, because this classification solely depends on the restriction sites of a selected set of enzymes while the SNPs in sequences other than these sites are neglected.

The reliability of *SSU12p* and *LSU36p* as phytoplasma markers confirms that genome comparison is an approach that could also be used for selecting genes to differentiate these bacteria. A larger number of samples than used in the present study, containing strains from untested groups and subgroups, will help to confirm the wide reliability of this detection system. The development of next-generation sequencing and long-read sequencing has built an expanding genomic database of microbial pathogens. Comparative genomics has been used to study the mechanisms of pathogenicity, molecular epidemiology, molecular diagnostics, multi-locus sequence typing, and transmission prediction (Avarre *et al.*, 2011; Bastardo *et al.*, 2012; Walker *et al.*, 2014; Bayliss *et al.*, 2017; Aly *et al.*, 2019). As more phytoplasma genomes are being sequenced, comparative genomics has also become the trend for analyses in genome reports (Sparks *et al.*, 2018; Wang *et al.*, 2018; Music *et al.*, 2019; Cho *et al.*, 2019). Approaches on the genome level will likely be increasingly applied to phytoplasmas for understanding their adaptations to diverse host species. However, the identification of new markers for detection and differentiation of phytoplasmas strains is still a necessary tool for developing knowledge of epidemiology and management of phytoplasma-associated diseases that aim to avoid their pandemic distribution.

ACKNOWLEDGEMENTS

This study was supported by the National Fund for Scientific and Technological Development (FONDECYT) of Chile, project Nos. 1140883 and 11160719, and Post-doctoral Project 2017, No. 3170120.

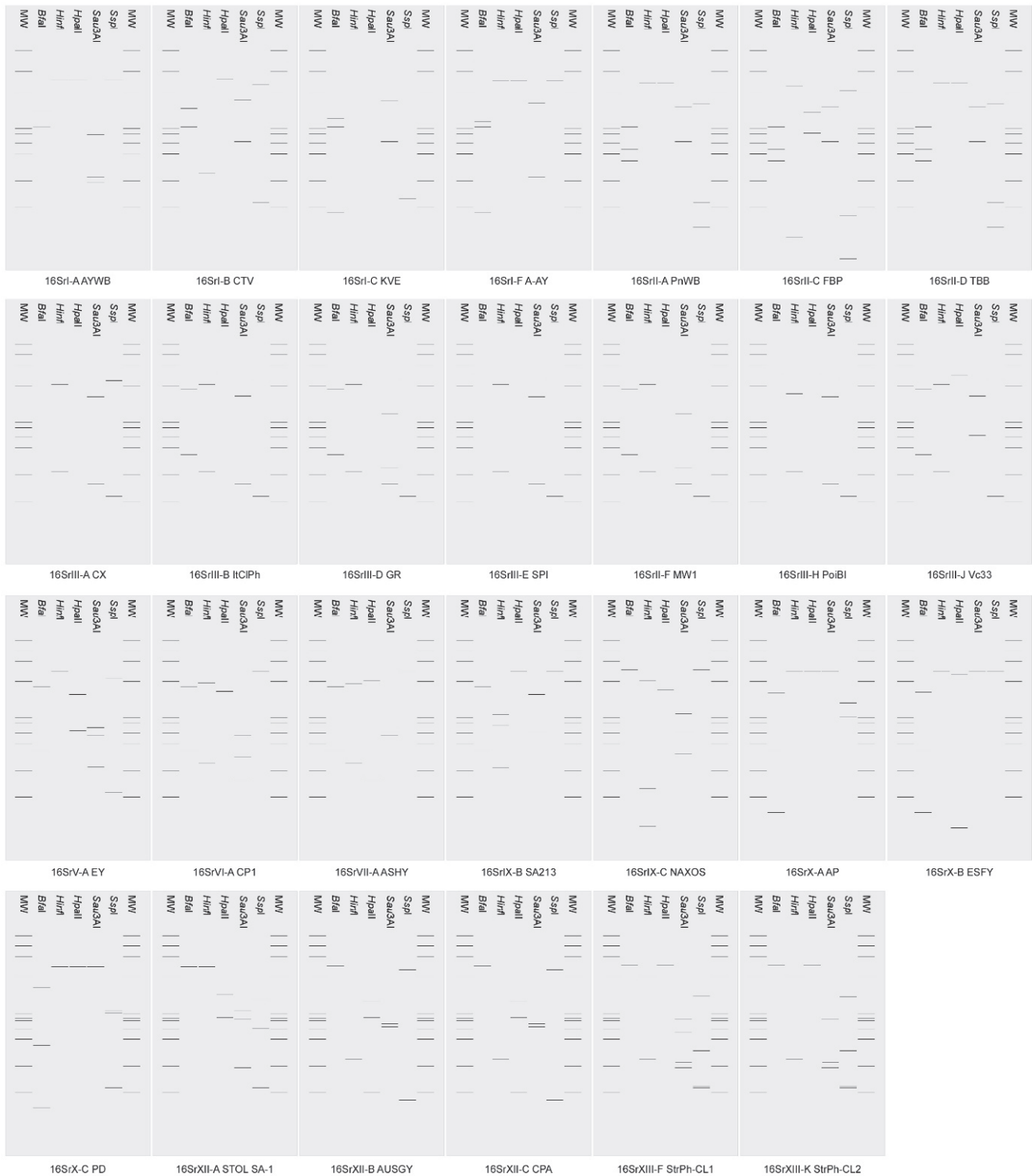


Figure 3. *In silico* RFLP patterns of *SSU12p* sequences from 27 phytoplasma strains, representing all the ribosomal groups and subgroups used. Restriction enzymes: *BfaI*, *HinfI*, *HpaII*, *Sau3AI*, *SspI*. Size marker: phiX174 digested by *BsuRI* and *HaeIII*.

LITERATURE CITED

- Aly M.A., Domig K.J., Kneifel W., Reimhult E., 2019. Whole genome sequencing based comparison of food isolates of *Cronobacter sakazakii*. *Frontiers in Microbiology* 10: 1464.
- Arnaud G., Malembic-Maher S., Salar P., Bonnet P., Maixner M., ... Foissac X., 2007. Multilocus sequence typing confirms the close genetic interrelatedness of three distinct “flavescence dorée” phytoplasma strain clusters and group 16SrV phytoplasmas infecting grapevine and alder in Europe. *Applied and Environmental Microbiology* 73: 4001–4010.
- Avarre J.C., Madeira J.P., Santika A., Zainun Z., Baud M., ... Maskur M., 2011. Investigation of Cyprinid herpesvirus-3 genetic diversity by a multi-locus variable number of tandem repeats analysis. *Journal of Virological Methods* 173: 320–327.
- Bastardo A., Ravelo C., Romalde J.L., 2012. Multilocus sequence typing reveals high genetic diversity and epidemic population structure for the fish pathogen *Yersinia ruckeri*. *Environmental Microbiology* 14: 1888–1897.
- Bayliss S.C., Verner-Jeffreys D.W., Bartie K.L., Aanensen D.M., Sheppard S.K., ... Feil E.J., 2017. The promise of whole genome pathogen sequencing for the molecular epidemiology of emerging aquaculture pathogens. *Frontiers in Microbiology* 8: 1–18.
- Bertaccini A., Lee I.-M., 2018. Phytoplasmas: an update. In: *Phytoplasmas: Plant Pathogenic Bacteria – I: Characterization and Epidemiology of Phytoplasma-Associated Disease* (G.P. Rao, A. Bertaccini, N. Fiore, L.W. Liefting, eds.), Springer Nature, Singapore, 1-29.
- Cho S.-T., Lin C.-P., Kuo C.-H., 2019. Genomic characterization of the periwinkle leaf yellowing (PLY) phytoplasmas in Taiwan. *Frontiers in Microbiology* 10: 2194.
- Cimerman A., Pacifico D., Salar P., Marzachi C., Foissac X., 2009. Striking diversity of *vmp1*, a variable gene encoding a putative membrane protein of the “stolbur” phytoplasma. *Applied and Environmental Microbiology* 75: 2951–2957.
- Contaldo N., Bertaccini A., 2019. Phytoplasma cultivation. In: *Phytoplasmas: Plant Pathogenic Bacteria – III: Genomics, Host Pathogen Interactions and Diagnosis* (A. Bertaccini, K. Oshima, M. Kube, G.P. Rao, ed.s), Springer Nature, Singapore, 89-104.
- Contaldo N., Canel A., Makarova O., Paltrinieri S., Bertaccini A., Nicolaisen M. 2011. Use of a fragment of the *tuf* gene for phytoplasma 16Sr group/subgroup differentiation. *Bulletin of Insectology* 64 (Supplement): S45–S46.
- Cui W., Quiroga N., Curkovic S.T., Zamorano A., Fiore N., 2019. Detection and identification of 16SrXIII-F and a novel 16SrXIII phytoplasma subgroups associated with strawberry phyllody in Chile. *European Journal of Plant Pathology* 155: 1039–1046.
- Duduk B., Paltrinieri S., Lee I.-M., Bertaccini A., 2013. Nested PCR and RFLP analysis based on the 16S rRNA gene. In: *Phytoplasma: Methods and Protocols* (M. Dickinson, J. Hodgetts, ed.), Humana Press, Totowa, New Jersey, United States of America, 159–171.
- Dumonceaux T.J., Green M., Hammond C., Perez E., Olivier C., 2014. Molecular diagnostic tools for detection and differentiation of phytoplasmas based on chaperonin-60 reveal differences in host plant infection patterns. *PLoS One* 9: e116039.
- EPPO-Q-bank, 2020. <https://qbank.eppo.int/>
- Fernández F.D., Meneguzzi N.G., Conci L.R., 2017. Identification of three novel subgroups within the X-disease group phytoplasma associated with strawberry redness disease. *International Journal of Systematic and Evolutionary Microbiology* 67: 753–758.
- Glenn D., 2000. National program for the management of phytoplasmas in Australian grapevines. Final report CRCV 95/2 for Grape and Wine Research and Development Corporation. Loxton, Australia, 174 pp.
- Hodgetts J., Boonham N., Mumford R., Harrison N., Dickinson M., 2008. Phytoplasma phylogenetics based on analysis of *secA* and 23S rRNA gene sequences for improved resolution of candidate species of ‘*Candidatus* Phytoplasma’. *International Journal of Systematic and Evolutionary Microbiology* 58: 1826–1837.
- Holland B.R., Huber K.T., Moulton V., Lockhart P.J., 2004. Using consensus networks to visualize contradictory evidence for species phylogeny. *Molecular Biology and Evolution* 21: 1459-1461.
- IRPCM 2004. ‘*Candidatus* Phytoplasma’, a taxon for the wall-less, non-helical prokaryotes that colonize plant phloem and insects. *International Journal of Systematic and Evolutionary Microbiology* 54: 1243–1255.
- Jenkins C., Ling C.L., Ciesielczuk H.L., Lockwood J., Hopkins S., ... Kibbler C.C., 2012. Detection and identification of bacteria in clinical samples by 16S rRNA gene sequencing: comparison of two different approaches in clinical practice. *Journal of Medical Microbiology* 61: 483–488.
- Kumar S., Stecher G., Tamura K., 2016. MEGA7: Molecular evolutionary genetics analysis version 7.0 for bigger datasets. *Molecular Biology and Evolution* 33: 1870–1874.
- Lee I.-M., Hammond R.W., Davis R.E., Gundersen D.E., 1993. Universal amplification and analysis of patho-

- gen 16S rDNA for classification and identification of mycoplasma-like organisms. *Phytopathology* 83: 834–842.
- Lee I.-M., Gundersen-Rindal D.E., Davis R.E., Bartoszyk I.M., 1998. Revised classification scheme of phytoplasmas based on RFLP analyses of 16S rRNA and ribosomal protein gene sequences. *International Journal of Systematic Bacteriology* 48: 1153–1169.
- Lee I.-M., Bottner-Parker K.D., Zhao Y., Davis R.E., Harrison N.A., 2010. Phylogenetic analysis and delineation of phytoplasmas based on *secY* gene sequences. *International Journal of Systematic and Evolutionary Microbiology* 60: 2887–2897.
- Ludwig W., Schleifer K.H., 1994. Bacterial phylogeny based on 16S and 23S rRNA sequence analysis. *FEMS Microbiology Reviews* 15: 155–173.
- Makarova O., Contaldo N., Paltrinieri S., Kawube G., Bertaccini A., Nicolaisen M., 2012. DNA barcoding for identification of ‘*Candidatus* Phytoplasmas’ using a fragment of the elongation factor *Tu* gene. *PLoS One* 7: e52092.
- Marcone C., Lee I.-M., Davis R.E., Ragozzino A., Seemüller E., 2000. Classification of aster yellows-group phytoplasmas based on combined analyses of rRNA and *tuf* gene sequences. *International Journal of Systematic and Evolutionary Microbiology* 50: 1703–1713.
- Martini M., Botti S., Marcone C., Marzachi C., Casati P., ... Bertaccini A., 2002. Genetic variability among “flavescence dorée” phytoplasmas from different origins in Italy and France. *Molecular and Cellular Probes* 16: 197–208.
- Martini M., Lee I.-M., Bottner K.D., Zhao Y., Botti S., ... Osler R., 2007. Ribosomal protein gene-based phylogeny for finer differentiation and classification of phytoplasmas. *International Journal of Systematic and Evolutionary Microbiology* 57: 2037–2051.
- Music M.S., Samarzija I.S., Hogenhout S.A., Haryono M., Cho S.-T., Kuo C.-H., 2019. The genome of ‘*Candidatus* Phytoplasma solani’ strain SA-1 is highly dynamic and prone to adopting foreign sequences. *Systematic and Applied Microbiology* 42: 117–127.
- Oliveira E. de, Resende R. de O., Pecci M. de la P.G., Laguna I.G., Herrera P., Cruz I., 2003. Occurrence of viruses and stunting diseases and estimative of yield losses by mollicutes in corn in Paraná State, Brazil. *Pesquisa Agropecuária Brasileira* 38: 19–25.
- Pérez-López E., Olivier C.Y., Luna-Rodríguez M., Dumonceaux T.J., 2016. Phytoplasma classification and phylogeny based on *in silico* and *in vitro* RFLP analysis of *cpn60* universal target sequences. *International Journal of Systematic and Evolutionary Microbiology* 66: 5600–5613.
- Schneider B., Seemüller E., Smart C.D., Kirkpatrick B.C., 1995. Phylogenetic classification of plant pathogenic mycoplasma-like organisms or phytoplasmas. In: *Molecular and Diagnostic Procedures in Mycoplasmaology* (S. Razin, J.G. Tully, eds.), Academic Press, San Diego, California, United States of America, 369–380.
- Seemüller E., Schneider B., Maurer R., Ahrens U., Daire X., ... Stackebrandt E., 1994. Phylogenetic classification of phytopathogenic mollicutes by sequence analysis of 16S ribosomal DNA. *International Journal of Systematic Bacteriology* 44: 440–446.
- Shao J., Jomantiene R., Dally E.L., Zhao Y., Lee I.-M., ... Davis R.E., 2006. Phylogeny and characterization of phytoplasmal *nusA* and use of the *nusA* gene in detection of group 16SrI strains. *Journal of Plant Pathology* 88: 193–201.
- Sparks M.E., Bottner-Parker K.D., Gundersen-Rindal D.E., Lee I.-M., 2018. Draft genome sequence of the New Jersey aster yellows strain of ‘*Candidatus* Phytoplasma asteris’. *PLoS One* 13: e0192379.
- Tamura K., Nei M., 1993. Estimation of the number of nucleotide substitutions in the control region of mitochondrial DNA in humans and chimpanzees. *Molecular Biology and Evolution* 10: 512–526.
- Valiunas D., Jomantiene R., Davis R.E., 2013. Evaluation of the DNA-dependent RNA polymerase β -subunit gene (*rpoB*) for phytoplasma classification and phylogeny. *International Journal of Systematic and Evolutionary Microbiology* 63: 3904–3914.
- Walker T.M., Lalor M.K., Broda A., Ortega L.S., Morgan M., ... Conlon C.P., 2014. Assessment of Mycobacterium tuberculosis transmission in Oxfordshire, UK, 2007–12, with whole pathogen genome sequences: an observational study. *The Lancet Respiratory Medicine* 2: 285–292.
- Wang J., Song L., Jiao Q., Yang S., Gao R., ... Zhou G., 2018. Comparative genome analysis of jujube witches’-broom phytoplasma, an obligate pathogen that causes jujube witches’-broom disease. *BMC Genomics* 19: 689.
- Wei W., Lee I.-M., Davis R.E., Suo X., Zhao Y., 2008. Automated RFLP pattern comparison and similarity coefficient calculation for rapid delineation of new and distinct phytoplasma 16Sr subgroup lineages. *International Journal of Systematic and Evolutionary Microbiology* 58: 2368–2377.



Citation: M. Minutolo, M. Cinque, G. Altamura, F. Di Serio, D. Alioto, B. Navarro (2021) Identification, full-length genome sequencing, and field survey of citrus vein enation virus in Italy. *Phytopathologia Mediterranea* 60(2): 293-301. doi: 10.36253/phyto-12180

Accepted: March 5, 2021

Published: September 13, 2021

Copyright: ©2021 Author. This is an open access, peer-reviewed article published by Firenze University Press (<http://www.fupress.com/pm>) and distributed under the terms of the Creative Commons Attribution License, which permits unrestricted use, distribution, and reproduction in any medium, provided the original author and source are credited.

Data Availability Statement: All relevant data are within the paper and its Supporting Information files.

Competing Interests: The Author(s) declare(s) no conflict of interest.

Editor: Anna Maria D'Onghia, CIHEAM/Mediterranean Agronomic Institute of Bari, Italy.

Short Notes

Identification, full-length genome sequencing, and field survey of citrus vein enation virus in Italy

MARIA MINUTOLO¹, MARIA CINQUE¹, GIUSEPPE ALTAMURA², FRANCESCO DI SERIO², DANIELA ALIOTO¹, BEATRIZ NAVARRO^{2,*}

¹ *Dipartimento di Agraria, Università degli Studi di Napoli Federico II, Portici (NA), Italy*

² *Istituto per la Protezione Sostenibile delle Piante, Consiglio Nazionale delle Ricerche, Bari, Italy*

*Corresponding author. E-mail: beatriz.navarro@ips.cnr.it

Summary. Citrus vein enation virus (CVEV) was described in Spain and then it has been reported in several citrus growing areas of Asia, America and Australia. Here, the occurrence of CVEV in Italy has been documented for the first time. The full genome sequence of a CVEV Italian isolate (14Q) was determined by high-throughput sequencing and the presence of the virus was confirmed by RT-PCR and graft-transmission to indicator plants, from which the virus was recovered six-months post-inoculation. Phylogenetic analysis based on the full-length genome of CVEV isolates from different countries showed that they are phylogenetically related to each other based on their geographic origin, rather than on their host and that the Italian isolate is more closely related to the Spanish isolate than to the other ones. A field survey revealed the presence of CVEV in some areas of Campania region (southern Italy), prevalently infecting lemon trees. In the frame of this survey, kumquat was identified for the first time as a host of CVEV. No symptoms were observed in the field so far. The infection of asymptomatic hosts and the transmission by aphid species present in Italy increase the risk that the virus could further spread.

Keywords. Citrus virus, vein enation disease, woody gall disease, CVEV.

INTRODUCTION

Citrus vein enation virus (CVEV), a monopartite, single strand positive sense RNA virus (*Luteoviridae*, *Enamovirus*), has been proposed as the causal agent of citrus vein enation (VE) and woody gall (WG) (Vives *et al.*, 2013). These two graft-transmissible citrus diseases were first described in United States of America in sour orange (VE) and in Australia in rough lemon (WG) (Wallace & Drake, 1953; Fraser, 1959; Moreno, 2000). Although CVEV may remain latent in several commercial citrus cultivars, it has been found associated with small outgrow in the underside tissues of leaves (enations), mainly in correspondence to secondary veins, of some susceptible citrus species, such as Mexican lime [*Citrus aurantifolia* (Christm.) Swingle], sour

orange (*C. aurantium* L.), *C. junos* Siebold ex Tanaka, citron (*C. medica* L.), satsuma (*C. x unshiu*) and various local Chinese citrus varieties (Chen *et al.*, 1992). Woody gall disease, characterized by galls on trunks and/or branches, has been reported in Rangpur lime (*C. x limonia* Osbeck), rough lemon (*C. jambhiri* Lush), and *C. x volkameriana* rootstocks (Fraser, 1959). Based on bioassays, it was shown that both VE and WG diseases were caused by the same transmissible agent (Wallace and Drake, 1960), now identified as CVEV (Vives *et al.*, 2013). This virus is transmitted in a persistent manner by several aphid species, including *Toxoptera citricidus*, *Myzus persicae* and *Aphis gossypii*, (Hermoso de Mendoza *et al.*, 1993; Maharaj and da Graca, 1989) and is considered a quarantine pest in several Mediterranean and American countries (<https://gd.eppo.int/taxon/CVEV00/categorization>). The complete genome of twenty CVEV isolates from six countries (Spain, Japan, China, South Korea, United States of America and Australia) has been sequenced (Vives *et al.*, 2013; Huang *et al.*, 2015; Nakazono-Nagaoka *et al.*, 2017; Wu *et al.*, 2019; Yang *et al.*, 2019). Although VE disease is widespread in Spain, it has not been reported in Italy (Catara and Davino, 1984). Spain is the only European country where the CVEV has been identified and characterized (Vives *et al.*, 2013).

High-throughput sequencing (HTS) is the most effective technology for detection of viruses in plants (Maliogka *et al.*, 2018). This has allowed identification of several novel viruses in citrus hosts (Loconsole *et al.*, 2012a; Loconsole *et al.*, 2012b; Roy *et al.*, 2013; Vives *et al.*, 2013; Harakava *et al.*, 2017; Ramos-González *et al.*, 2017; Chabi-Jesus *et al.*, 2018; Navarro *et al.*, 2018a; Navarro *et al.*, 2018b; Chabi-Jesus *et al.*, 2020; Wu *et al.*, 2020; Xuan *et al.*, 2020). The present study, based on HTS data, reports the first identification of CVEV in Italy. The complete genome sequence and variability of the Italian CVEV isolate is also presented, together with the results of graft-transmission bioassays. In addition, data are reported on the spread of this virus mainly in Campania region (Southern Italy), where lemons are important citrus crops.

MATERIALS AND METHODS

Plant material, RNA preparation and high-throughput sequencing of cDNA libraries

Fresh flushes, collected in 2018 from a non-symp-tomatic sweet orange tree (*Citrus sinensis*, L.) grown in Campania region, were used for generating a cDNA library. Total RNA was extracted with phenol/chloroform (Pallás *et al.*, 1987) followed by elimination of pol-

ysaccharides with the methoxyethanol method (Bellami and Ralph, 1968). After DNase treatment and ribosomal RNA depletion (Navarro *et al.*, 2018a), cDNA libraries were constructed using the Illumina TruSeq Total stranded RNA Sample Preparation Kit, according to the manufacturer's protocol. HTS was performed in a Next-Seq500 analyzer (Illumina) with a configuration of 150 paired ends reads. After removing the reads mapping in the host genome, high quality reads were *de novo* assembled using SPAdes software (Bankevich *et al.*, 2012). The obtained contigs were screened by BlastN and BlastX for homologous viral sequences in the National Center for Technology Information (NCBI). Alignments of HTS reads to the reference genome of CVEV (NC-021564) were performed by Bowtie (Langmead *et al.*, 2009) implemented in the MacVector Assembler platform (15.1.5, MacVector, Inc.).

RT-PCR detection, field survey and bioassays

Total nucleic acids (100 ng) were extracted and reverse transcribed as reported previously (Navarro *et al.*, 2017). Two μ L of the cDNA reaction were used for the PCR amplification in a reaction volume of 25 μ L, using 1.25 units of GoTaq polymerase (Promega) and containing final concentrations of 0.2 μ M of each primer. The two CVEV specific primer pairs VE5f/VE15r and VE16f/VE17r, previously reported by Vives *et al.* (2013) and targeting a CVEV genomic region coding for the polymerase and the coat protein, respectively, were used. The cycling conditions were as follows: initial denaturation at 94°C for 3 min, followed by 32 cycles at 94°C for 30 s, 55°C for 30 s, 72°C for 30 s, and a final extension step at 72°C for 7 min. The reaction products were analysed by electrophoresis on 2% agarose gels buffered in TAE (0.04 M Tris-acetate, 1 mM EDTA, pH 8) and visualized by UV light after ethidium bromide staining. Amplicons were purified, cloned in pGemT-easy (Promega) and sequenced (Macrogen).

A field survey was carried out in spring 2019 in 14 orchards (13 located in provinces of Campania region and one in Latina province of Lazio region). Leaves from fresh flushes from sweet orange [*Citrus sinensis* (L.) Osbeck], clementine (*C. clementina* Hort. ex Tanaka), lemon [*C. x limon* (L.) Burm. f.], mandarin (*C. reticulata* Blanco), kumquat (*C. japonica* Thunb.), tangerine (*C. x tangerina*), grapefruit (*C. x paradisi* Macfad.), sour orange, or citron (*C. medica* L.) trees were analyzed by RT-PCR (as outlined above) using the primer pair VE5f/VE15r. Bioassays were performed by grafting bark tissues from the Italian isolate to three sour orange indicator plants grown at 23-25°C in a greenhouse, which were

then maintained under observation for two consecutive years (Roistacher, 1991).

Phylogenetic analysis

Sequence variability within the CVEV-14Q isolate was investigated by identifying the SNPs using Bowtie (Langmead *et al.*, 2009). Multiple alignments of the full-genome, 5'UTR and 3'UTR nucleotide (nt) sequence, of the amino acid sequence of the putative proteins encoded by the Italian CVEV isolate, and with those available in databases were performed using Clustal Omega (Sievers and Higgins, 2014). A pairwise matrix was generated from each alignment. The multiple alignment of the genomic sequence was used to generate a phylogenetic tree by maximum likelihood method with the best-fit model of kimura-2+G and 1000 bootstraps inferred in the MEGA7 package.

RESULTS AND DISCUSSION

Identification of an Italian isolate of CVEV

To characterize citrus viromes in the Campania region (southern Italy), a cDNA library of total RNAs from a non-symptomatic sweet orange tree (isolate 14Q) was analyzed by HTS. A total of 24,800,000 high quality reads were obtained, and after removing those mapping in the citrus genome (nuclear, chloroplastic and mitochondrial genomes), the remaining 8,510,000 reads were assembled in contigs. BlastN search with the obtained contigs allowed identification of 11 contigs sharing high sequence similarity to CVEV (97 to 99% nt identity). When mapped on the CVEV genome, the contigs covered 84% of the viral genome, indicating a possible infection of the source tree by this virus. The presence of CVEV in the original tree 14Q was confirmed by RT-PCR using two primer pairs (VE5f /VE15r and VE16f/VE17r) specific for this virus and already reported in the literature (Vives *et al.*, 2013). PCR amplicons with the expected size of 426 and 413 nt were obtained using total RNA extracted from leaf samples collected from the 14Q tree during two consecutive springs (in 2018 and 2019). Cloning and Sanger sequencing of the generated PCR fragments confirmed that they had 100% nt identity with the corresponding CVEV sequences obtained by HTS. These data confirmed the CVEV infection by a second and independent detection method. This is the first report of CVEV in Italy.

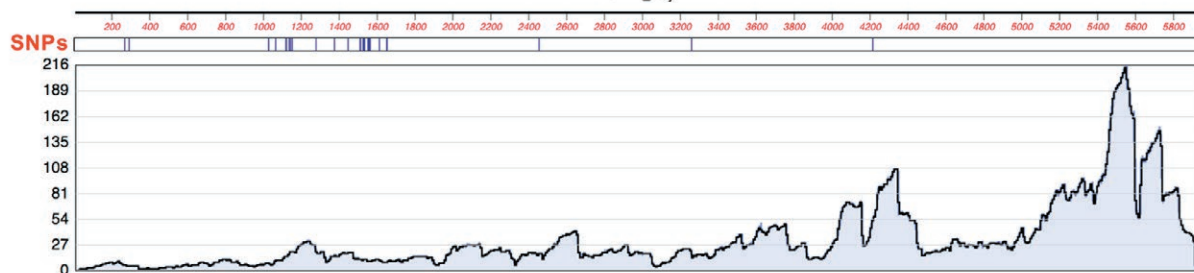
The transmissibility of the CVEV-14Q isolate was tested by graft-inoculating bark tissues from the origi-

nal infected sweet orange tree onto three seedlings of sour orange indicator. RT-PCR assay using VE5f/VE15r oligonucleotides showed that all the inoculated plants were infected by CVEV 6 months post-inoculation. No enations and no wood alterations were observed in the infected plants periodically inspected for symptom expression for more than 2 years after the graft-inoculation. However, additional bioassays with a greater number of tested plants and the other susceptible indicators rough lemon and Mexican lime must be performed to determine the pathogenicity of the CVEV-14Q isolate.

Characterization of the full-length genome of an Italian isolate of CVEV

Alignments of sequenced reads on the reference CVEV genome (VE-1 isolate, NC_021564) using the Bowtie software, allowed assembly of the consensus full-length genomic sequence (mean coverage depth = 33) of the first Italian CVEV isolate. This was named CVEV-14Q (Genbank ID: MW167082) (Figure 1a).

The CVEV-14Q genome is 5983 nt long, with the same organization of the reference isolate VE-1, and consists of five ORFs surrounded by a 5' untranslated region (UTR) and a 3'UTR (Figure 1b). The overlapping ORF0, ORF1 and ORF2 were very likely directly translated from the genomic RNA, while the expression of ORF3 and ORF5 is proposed to occur through the synthesis of a 3' co-terminal subgenomic RNA (Vives *et al.*, 2013). The abundance of this subgenomic RNA in the nucleic acid preparations used for generating the RNA seq library could justify the asymmetric distribution of the sequenced reads on the CVEV genome, with a prevalent coverage in the 3' region including ORF3 and ORF5 (Figure 1a). ORF0 (positions 219-1283) overlaps completely with ORF1, and encodes a putative protein of 39 kDa (P0) that likely is a suppressor of gene silencing (Vives *et al.*, 2013). P0 contains the four conserved amino acids (LPxx(L/I)x10-13P) of a putative F-box-like motif (Huang *et al.*, 2015). ORF1 (positions 208-2016) encodes for a putative peptidase of 100 kDa that contains the conserved serine proteinase domain characteristic of the S39 peptidase superfamily. The ORF2 (positions 2202-4148) is translated via a -1 ribosomal frameshift of ORF1, thus encoding a putative fusion protein of 148 kDa that contains the conserved polymerase and helicase domains (replicase). ORF3 (positions 4301-4876) codes for the putative coat protein (CP) of 21 kDa. ORF5 (positions 4301-5785) is translated by an in-frame readthrough of the amber stop codon of ORF3 allowing the expression of a putative fusion protein (P5) of 55 kDa, which is probably involved in aphid transmission,

a**b**

CVEV genomic RNA

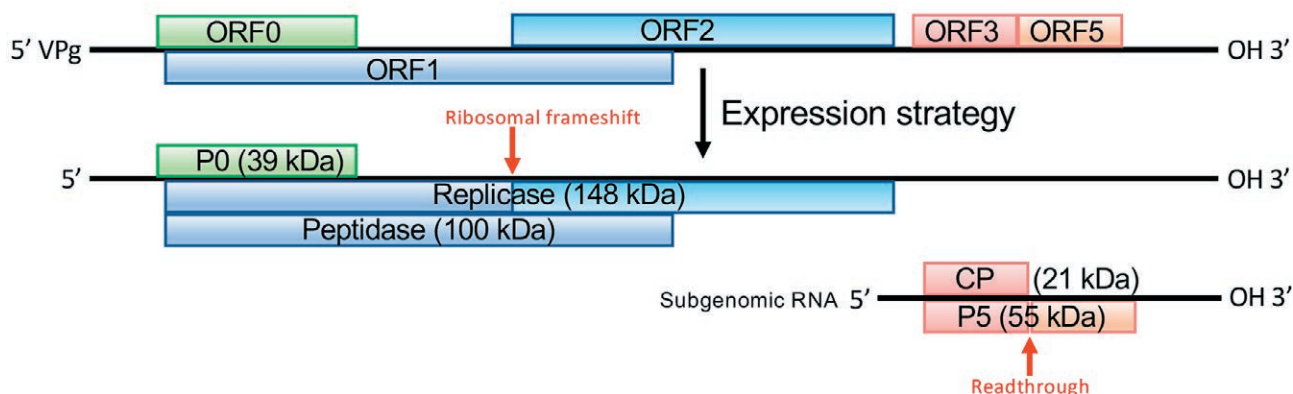


Figure 1. (a) CVEV genome coverage by HTS reads. Alignments were performed using the Bowtie program and the CVEV variant NC_021564 as the reference sequence. Nucleotide (nt) positions are indicated at the top. Single nucleotide polymorphisms (SNPs) are indicated by vertical lines below the respective positions. (b) Genome organization and expression strategy of CVEV. Putative ORFs are indicated by boxes. The predicted proteins expressed from the genomic and subgenomic RNAs are indicated by boxes in the lower part of the panel.

symptom expression and virus accumulation (Vives *et al.*, 2013).

Sequence variability within the CVEV-14Q isolate was investigated by aligning the HTS reads on CVEV-14Q consensus genome using Bowtie. This identified a total of 26 variable nucleotide positions in the CVEV genome of the 14Q virus isolate (Figure 1a; Table 1). Most of them were located between the positions 267 and 1651, which include the ORF0 overlapping with a fragment of ORF1 and a region of ORF1 not overlapping with other ORFs. Since in a sequence with overlapping ORFs one nucleotide change can differently affect the encoded proteins, we further considered the 10 mutations observed in the overlapping ORF0-ORF1 region. Most mutations were synonymous in P0 (six out of ten) and non-synonymous in the peptidase (nine out of ten). These data suggest that the nucleotide variability in this region has a greater effect on the amino acid variability

in the peptidase than in the P0. Two other variable positions were identified in the replicase coding region and in the intergenic region. Although several of the mutations observed in the CVEV-14Q isolate were also identified in other CVEV isolates, most of the mutations are here reported for the first time (Table 1).

Phylogenetic relationships between CVEV-14Q and other reported isolates

Pairwise alignment of the CVEV-14Q full-length genome with genomes of the other 20 isolates that have been characterized from different geographic areas, revealed the greatest similarity (99.08% of nt identity) with the isolate VE-1 from Spain, and the least (97.09%) with the CVEV SM isolate from China (Figure 2). The 5' UTR region of CVEV-14Q, showing the least similarity (92.75% of nt identity) with the Chinese SM iso-

Table 1. Sequence variability in the Italian CVEV isolate 14Q. Nucleotide variability and its effect at amino acid level are reported for polymorphic nucleotide positions.

nt position	Nt in CVEV-14Q ^a (number of reads)	Nt in reads showing variability (number of reads)	Nt in CVEV genomes from other isolates (number of isolates)	ORF	Variability in the codons (encoded amino acid)	Type of mutation	Overlapping ORF	Variability in the codons (encoded amino acid)	Type of mutation
267	A(7)	T(4)	A(0); T(20)	Peptidase	ACA (Thr) to ACT (Thr)	Synonymous	P0	ACT (Thr) to TCT (Ser)	Nonsynonymous
290	C(6)	T(4)	C(14); T(6)	Peptidase	GCT (Ala) to GTT (Val)	Nonsynonymous	P0	AGC (Ser) to AGT (Ser)	Synonymous
1026	T(6)	G(3)	C(16); T(4)	Peptidase	TTT (Phe) to TTG (Leu)	Nonsynonymous	P0	TTC (Ser) to GTC (Val)	Nonsynonymous
1063	A(7)	T(6)	A(20); T(0)	Peptidase	ATC (Ile) to TTC (Phe)	Nonsynonymous	P0	TAT (Tyr) to TTT (Phe)	Nonsynonymous
1118	T(12)	C(8)	T(0); C(20)	Peptidase	ATC (Ile) to ACC (Thr)	Nonsynonymous	P0	CAT (His) to CAC (His)	Synonymous
1121	C(12)	T(8)	C(0); T(20)	Peptidase	TCC (Ser) to TTC (Phe)	Nonsynonymous	P0	CTC (Leu) to CTT (Leu)	Synonymous
1135	A(15)	G(7)	A(20); G(0)	Peptidase	ACG (Thr) to GCG (Ala)	Nonsynonymous	P0	GAC (Asp) to GGC (Gly)	Nonsynonymous
1142	A(18)	G(7)	A(0); G(20)	Peptidase	AAG (Lys) to AGG (Arg)	Nonsynonymous	P0	GAA (Glu) to GAG (Glu)	Synonymous
1151	C(22)	T(7)	C(0); T(20)	Peptidase	GCT (Ala) to GTT (Val)	Nonsynonymous	P0	GGC (Gly) to GGT (Gly)	Synonymous
1277	A(21)	G(3)	A(4); G(16)	Peptidase	AAG (Lys) to AGG (Arg)	Nonsynonymous	P0	GAA (Glu) to GAG (Glu)	Synonymous
1374	A(23)	G(4)	A(3); G(17)	Peptidase	AAA (Lys) to AAG (Lys)	Synonymous			
1446	T(25)	A(7)	A(1); T(19)	Peptidase	ATT (Ile) to ATA (Ile)	Synonymous			
1509	C(10)	T(9)	C(6); T(12); A(2)	Peptidase	TCC (Ser) to TCT (Ser)	Synonymous			
1512	G(10)	A(9)	G(1); A(9)	Peptidase	AAG (Lys) to AAA (Lys)	Synonymous			
1525	G(10)	A(9)	G(20); A(0)	Peptidase	GTT (Val) to AGT (Ser)	Nonsynonymous			
1530	G(11)	A(9)	G(20); A(0)	Peptidase	GTG (Val) to GTA (Val)	Synonymous			
1533	C(11)	T(9)	C(20); T(0)	Peptidase	TAC (Tyr) to (TAT) Tyr	Synonymous			
1551	T(11)	C(5)	T(19); C(1)	Peptidase	GAT (Asp) to GAC (Asp)	Synonymous			
1557	A(11)	T(5)	A(19); G(2)	Peptidase	CTA (Leu) to CTT (Leu)	Synonymous			
1563	G(11)	A(5)	G(20); A(0)	Peptidase	TTG (Leu) to TTA (Leu)	Synonymous			
1611	C(11)	T(6)	C(20); T(0)	Peptidase	CTC (Leu) to CTT (Leu)	Synonymous			
1650	T(11)	C(6)	T(3); C(17)	Peptidase	TCT (Ser) to TCC (Ser)	Synonymous			
1651	T(11)	C(6)	T(0); C(20)	Peptidase	TTC (Phe) to CTC (Leu)	Nonsynonymous			
2454	A(20)	G(7)	A(20); G(0)	Peptidase	CGA (Arg) to CGG (Arg)	Synonymous			
3258	T(13)	C(12)	T(3); C(17)	Replicase	TGC (Cys) to CGC (Arg)	Nonsynonymous			
4214	A(39)	G(12)	A(20); G(0)	Intergenic					

^a Consensus sequence ID: MW16708

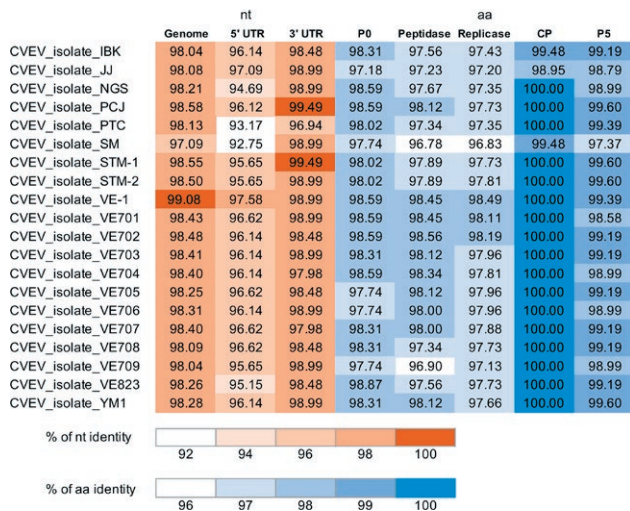


Figure 2. Percentage of nucleotide (nt) and amino acid (aa) sequence identity between the CVEV Italian isolate 14Q and full-length CVEV isolates in databases. Scales of colour identify similar nt and aa identity scores. The accession numbers of the virus isolates are reported in Figure 3.

late, was more divergent than the 3'UTR from the other sequenced isolates. Amino acid sequence comparisons between homologous proteins (Figure 2) identified the putative peptidase protein and the replicase as the proteins of CVEV-14Q that mostly differed from the other isolates, especially from the Chinese isolate SM (96.78% aa identity with the putative peptidase protein and 96.83% aa identity with the replicase). The putative CP is the most conserved protein among the studied isolates, with the exception of the slightly divergent isolates SM from China (99.48% aa identity), IBK from Japan (99.48% aa identity) and JJ from Korea (98.95% aa identity). The other predicted proteins P0 and P5 also showed high sequence similarities with the respective proteins encoded by other isolates.

Although not yet associated with any biological roles, amino acid changes in some CVEV isolates have been previously highlighted (Nakazono-Nagaoka *et al.*, 2017). Four amino acid residues, at positions 83, 104 and 113 of ORF2 and position 41 of ORF5, have been proposed as differential residues among Spanish and Japanese isolates (Nakazono-Nagaoka *et al.*, 2017). Like the Spanish isolates, the CVEV-14Q has a leucine and an arginine at positions 83 and 104 of the protein encoded in ORF2, whereas most of the other known CVEV isolates have a phenylalanine and a glycine at the same positions. The exception is isolate VE823, which also has an arginine at position 104 (Supplementary Figure 1). The amino acid at position 113 of ORF2 is a valine in most isolates, except in the Italian isolate 14Q (a threo-

nine in this position), the Spanish isolate VE-1 (an isoleucine) and the Korean isolate JJ (an alanine). The serine at the position 41 of ORF5 remains specific of the Spanish isolates since in all the other CVEV characterized, including the Italian CVEV-14Q, there is an arginine at that position. Therefore, although closely related to each other, the Italian and Spanish isolates had some diversity.

Relationships between CVEV isolate 14Q and virus isolates from different geographic areas and host species were investigated by generating a maximum likelihood phylogenetic tree using the available full-genomic sequences of the virus (Figure 3). The Italian 14Q and the Spanish VE-1 isolates clustered together. All CVEV isolates from the United States of America were grouped in the same clade, and those from Japan and South Korea clustered in the same phylogenetic subgroup. The CVEV isolate VE709 from Australia was related to the phylogenetic subgroup of American isolates, whereas the isolate from China was unrelated to the other CVEV clades. Therefore, CVEV isolates grouped according to their geographic origins, rather than their host species, indicating a minor role of hosts in the genetic diversity of CVEV isolates.

Field survey

Thirteen citrus growing areas of the Campania region and one on Latium region, at the northwest border of Campania (Suio, Latina Province), were surveyed. In Campania, the most common citrus species are sweet orange and lemon, which are widely grown in commercial citrus orchards as well as in private and public gardens. A total of 229 citrus trees of different species were tested by RT-PCR. The assays showed that 32 tree samples (14.0%) were infected by CVEV, with lemon trees showing the greatest incidence (26.4%) (Table 2). This is the first report of CVEV in Kumquat (<https://gd.eppo.int/taxon/CVEV00>), but only one of two plants analysed, collected from a household garden, tested positive. The tangerine, grapefruit, sour orange, and citron trees from Campania region analyzed in the survey tested negative for CVEV infections. However, in these cases, only very few plants of each host species were tested. None of the infected trees showed the typical symptoms of VE or WG that have been reported to be associated to CVEV in some citrus species. This agrees with previous data reporting symptomless infections of CVEV in lemon, mandarin and orange (Catara and Davino, 1984).

When the geographic distribution of infected samples was considered, the positive samples were only from some areas (mainly in Naples and Salerno province).

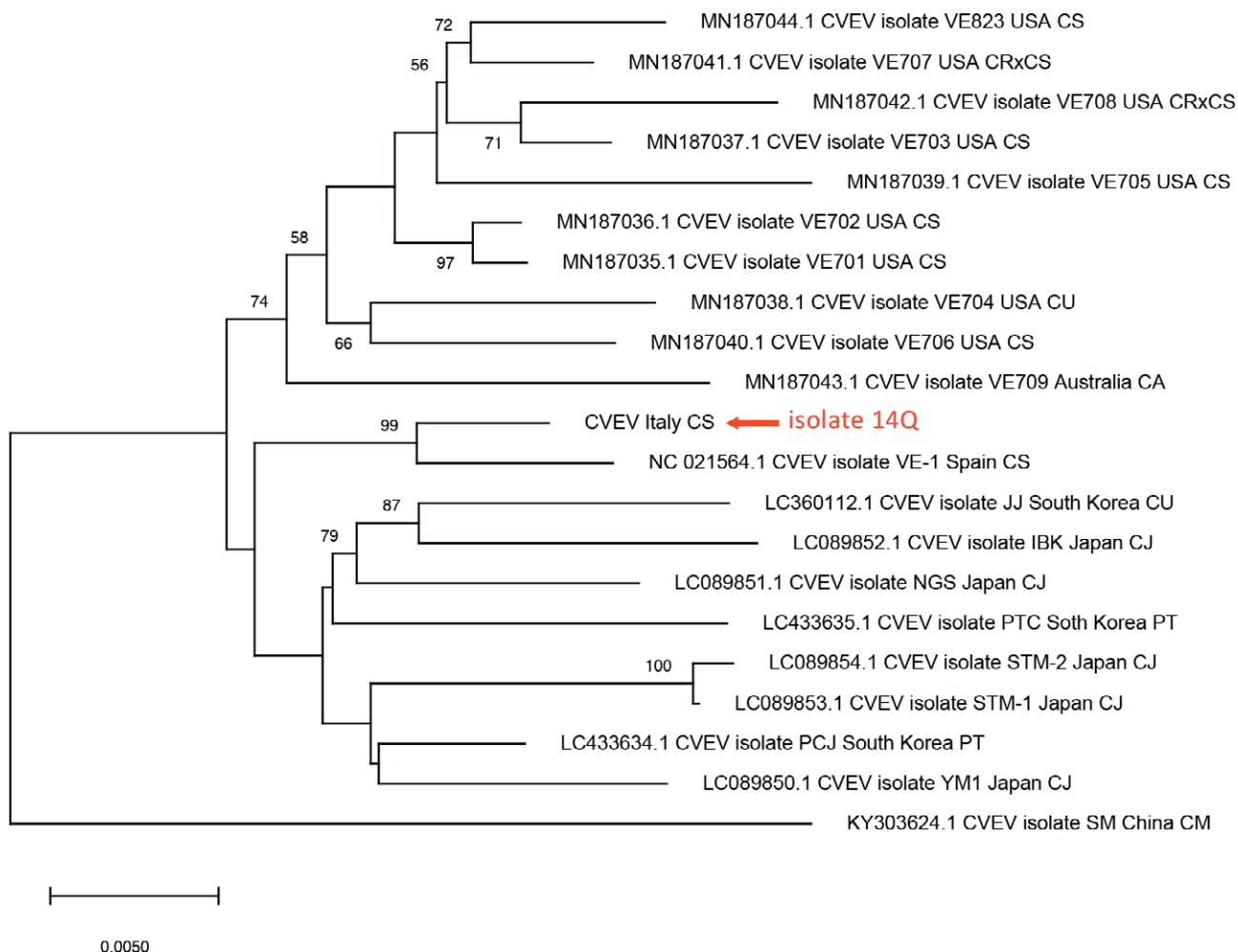


Figure 3. Phylogenetic tree generated using all the full-length CVEEV genome sequences available in databases and the CVEEV-14Q isolate. Clustal omega alignment of the nucleotide sequences was used for inferring the phylogenetic tree using the Maximum likelihood method, and adopting the best-fit model kimura 2+G using MEGA7. Bootstrap probability values (1000 replicates) greater than 50% are shown at the branch nodes. Tree branches are proportional to the genetic distances, with the scale bar indicating substitutions per nucleotide site. The accession number, isolate name, country of origin and citrus host (*Citrus junos*, CJ; *C. maxima*, CM; *C. reticulata*, CR; *C. sinensis*, CS; *C. unshiu*, CU; *Poncirus trifoliata*, PT) are shown at each branch tip.

These data indicate that CVEEV is not widespread in the surveyed area. However, since this virus is transmitted by several aphid species (Hermoso de Mendoza *et al.*, 1993; Maharaj and da Graça, 1989), two of which, *Myzus persicae* and *Aphis gossypii*, are present in the surveyed area, the virus will likely be further disseminated. Asymptomatic infected citrus trees can also be sources of inoculum if used for vegetative propagation. Detection of CVEEV in a symptomless kumquat tree is important. The trees are mainly grown in pots as ornamental plants, so they could favour long distance virus spread. Extension of CVEEV surveys to a greater number of kumquat trees and to other ornamental citrus species would be worthwhile.

Inclusion of CVEEV in the list of quality-affecting organisms in the Italian programs for certification of citrus propagation material is strongly recommended, as the present study has demonstrated that several citrus species can be infected by CVEEV.

ACKNOWLEDGEMENTS

This research was partially supported by the projects 'URCOFI' (funded by Regione Campania, DGR 690/2016, 6th December 2016), and 'INNOCI' (funded by Regione Puglia, DGR n. 903/ 2012, 15th May 2012). The project also received funding from the European

Table 2. Survey of citrus vein enation virus in different orchards of Campania region and one orchard of Latina province. Number of CVEV infected trees /number of total trees analyzed is shown.

Geographic area (Province)	Total citrus trees	Lemon	Sweet orange	Mandarin	Clementine	Kumquat	Tangerin	Grapefruit	Sour orange	Citron
Averno (Naples)	1/6	1/6	-	-	-	-	-	-	-	-
San Antonio Abbate (Naples)	3/19	-	1/8	2/10	0/1	-	-	-	-	-
Agnano (Naples)	0/2	-	-	-	0/2	-	-	-	-	-
Casoria (Naples)	12/23	8/9	2/7	1/4	-	1/2	0/1	-	-	-
Ercolano (Naples)	1/8	1/2	0/1	0/4	0/1	-	-	-	-	-
Napoli (Naples)	3/8	3/3	-	0/1	0/2	-	-	-	0/2	-
Ponticelli (Naples)	2/10	1/3	1/3	0/1	0/3	-	-	-	-	-
Maddaloni (Caserta)	0/16	-	0/7	0/8	0/1	-	-	-	-	-
Sta Maria Capua Vetere (Caserta)	0/10	-	0/8	0/2	-	-	-	-	-	-
Maiori (Salerno)	1/13	1/13	-	-	-	-	-	-	-	-
Minori (Salerno)	8/26	8/26	-	-	-	-	-	-	-	-
Eboli (Salerno)	0/47	0/15	0/26	-	0/2	-	0/2	0/2	-	-
Pontecagnano (Salerno)	0/11	0/5	0/1	0/1	0/2	-	-	-	0/1	0/1
Suio (Latina)	1/30	0/5	1/15	0/6	0/4	-	-	-	-	-
Total	32/229 (14.0%)	23/87 (26.4%)	5/76 (6.5%)	3/37 (8.1%)	0/18 (0%)	1/2 (50%)	0/3 (0%)	0/2 (0%)	0/3 (0%)	0/1 (0%)

Union's Horizon 2020 research and innovation program under the Marie Skłodowska-Curie grant agreement No. 734736. This paper reflects only the authors' views, and the Agencies are not responsible for any use that may be made of the information it contains.

LITERATURE CITED

- Bellamy A.R., Ralph R.K., 1968. Recovery and purification of nucleic acids by means of cetyl trimethylammonium bromide. *Methods in Enzymology* XII: 156–160.
- Bankevich A., Nurk S., Antipov D., Gurevich A.A., Dvorkin M., ... Pevzner P.A., 2012. SPAdes: a new genome assembly algorithm and its applications to single-cell sequencing. *Journal of Computational Biology* 19: 455–477. <https://doi.org/10.1089/cmb.2012.0021>.
- Catara A., Davino M., 1984. Citrus diseases not found in Italy, caused by viruses and virus-like pathogens. *Informatore Fitopatologico* 34: 9–21.
- Chabi-Jesus C., Ramos-González P.L., Tassi A.D., Guerra-Peraza O., Kitajima E.W., ... Freitas-Astúa J., 2018. Identification and Characterization of Citrus Chlorotic Spot Virus, a New Dichorhavirus Associated with Citrus Leprosis-Like Symptoms. *Plant Disease* 102: 1588–1598. <https://doi.org/10.1094/PDIS-09-17-1425-RE>.
- Chabi-Jesus C., Najjar A., Fontenele R.S., Kumari S.G., Ramos-González P.L., ... Varsani A., 2020. Viruses representing two new genomovirus species identified in citrus from Tunisia. *Archives in Virology* 165: 1225–1229. <https://asu.pure.elsevier.com/en/publications/viruses-representing-two-new-genomovirus-species-identified-in-ci>.
- Chen G.Q., Yan S.X., Roistacher C.N., 1992. First report of citrus vein enation disease in China. *Plant Disease* 76: 1077. https://www.apsnet.org/publications/plantdisease/backissues/Documents/1992Abstracts/PD_76_1077C.htm
- Fraser L. R., 1959. Woody gall, a suspected virus disease of rough lemon and other citrus varieties. *Proceedings of the Linnean Society of New South Wales* 84: 332–336.
- Harakava R., Salaroli R.B., Freitas-Astúa J., 2017. Citrus leprosis virus N: A New Dichorhavirus Causing Citrus Leprosis Disease. *Phytopathology* 107: 963–976. <https://doi.org/10.1094/PHYTO-02-17-0042-R>
- Hermoso de Mendoza A., Pina J.A., Ballester-Olmos J.F., Navarro L., 1993. Persistent transmission of Citrus vein enation virus by *Aphis gossypii* and *Myzus persicae*. In: *Proc. 12th Conf. Intern. Organization Citrus Virol.* (P. Moreno, J. V. da Graça, and L. W. Timmer, ed.), IOCV, Riverside, CA, USA: 361–362.
- Huang A., Song Z., Cao M., Chen H., Li Z., Zhou C., 2015. The complete genome sequence of Citrus vein enation virus from China. *Journal of Integrative Agriculture* 14: 598–601. [https://doi.org/10.1016/S2095-3119\(14\)60903-5](https://doi.org/10.1016/S2095-3119(14)60903-5)

- Langmead B., Trapnell C., Pop M., Salzberg S.L., 2009. Ultrafast and memory-efficient alignment of short DNA sequences to the human genome. *Genome Biology* 10: R25. <https://genomebiology.biomedcentral.com/articles/10.1186/gb-2009-10-3-r25>
- Loconsole G., Onelge N., Potere O., Giampetruzzi A., Bozan O., ... Saponari M., 2012a. Identification and characterization of citrus yellow vein clearing virus, a putative new member of the genus *Mandarivirus*. *Phytopathology* 102: 1168–175. <https://apsjournals.apsnet.org/doi/pdf/10.1094/PHYTO-06-12-0140-R>
- Loconsole G., Saldarelli P., Doddapaneni H., Savino V., Martelli G.P., Saponari M., 2012b. Identification of a single-stranded DNA virus associated with citrus chlorotic dwarf disease, a new member in the family *Geminiviridae*. *Virology* 432: 162–172. <https://doi.org/10.1016/j.virol.2012.06.005>
- Maliogka V.I., Minafra A., Saldarelli P., Ruiz-García A.B., Glasa M., ... Olmos A., 2018. Recent Advances on Detection and Characterization of Fruit Tree Viruses Using High-Throughput Sequencing Technologies. *Viruses* 10: 436. <https://doi.org/10.3390/v10080436>
- Maharaj S.B., da Graça J.V., 1989. Transmission of citrus vein enation virus by *Toxoptera citricidus*. *Phytophylactica* 21: 81–82.
- Moreno P., 2000. Protuberancias nerviales-Agallas de la madera (Vein enation-Woody gall). In: *Enfermedades de los cítricos. Monografía de la Sociedad Española de Fitopatología no. 2* (N. Duran-Vila and P. Moreno, ed.), Ediciones Mundi-Prensa, Madrid, Spain: 74–75.
- Nakazono-Nagaoka E., Fujikawa T., Iwanami T., 2017. Nucleotide sequences of Japanese isolates of citrus vein enation virus. *Archives in Virology* 62: 879–883. doi: 10.1007/s00705-016-3139-6. <https://link.springer.com/article/10.1007/s00705-016-3139-6>
- Navarro B., Loconsole G., Giampetruzzi A., Aboughanem-Sabanadzovic N., Ragozzino A., ... Di Serio F., 2017. Identification and characterization of privet leaf blotch-associated virus, a novel ideovirus. *Molecular Plant Pathology* 18: 925–936. <https://doi.org/10.1111/mpp.12450>
- Navarro B., Minutolo M., De Stradis A., Palmisano F., Alioto D., Di Serio F., 2018a. The first phlebo-like virus infecting plants: a case study on the adaptation of negative-stranded RNA viruses to new hosts. *Molecular Plant Pathology* 19: 1075–1089. <https://doi.org/10.1111/mpp.12587>
- Navarro B., Zicca S., Minutolo M., Saponari M., Alioto D., Di Serio F., 2018b. A Negative-Stranded RNA Virus Infecting Citrus Trees: The Second Member of a New Genus Within the Order *Bunyavirales*. *Frontiers in Microbiology* 9: 2340. <https://doi.org/10.3389/fmicb.2018.02340>
- Pallás V., Navarro A., Flores R., 1987. Isolation of a viroid-like RNA from hop different from hop stunt viroid. *Journal of General Virology* 68: 2095–2102.
- Ramos-González P.L., Chabi-Jesus C., Guerra-Peraza O., Tassi A.D., Kitajima EW, ... Freitas-Astúa J., 2017. Citrus leprosis virus N: A New Dichorhavirus Causing Citrus Leprosis Disease. *Phytopathology* 107: 963–976. <https://doi.org/10.1094/PHYTO-02-17-0042-R>
- Roistacher, C.N. 1991. Graft transmissible diseases of citrus. In: *Handbook for Detection and Diagnosis*, F.A.O., Rome.
- Roy A., Choudhary N., Guillermo L.M., Shao J., Govindarajulu A., ... Brlansky R.H., 2013. A novel virus of the genus *Cilevirus* causing symptoms similar to citrus leprosis. *Phytopathology* 103: 488–500. <https://apsjournals.apsnet.org/doi/pdf/10.1094/PHYTO-07-12-0177-R>
- Sievers F., Higgins D.G., 2014. Clustal Omega, accurate alignment of very large numbers of sequences. *Methods in Molecular Biology* 1079: 105–116. https://link.springer.com/protocol/10.1007/978-1-62703-646-7_6
- Vives M.C., Velázquez K., Pina J.A., Moreno P., Guerri J., Navarro L., 2013. Identification of a new enamovirus associated with citrus vein enation disease by deep sequencing of small RNAs. *Phytopathology* 103: 1077–1086. <https://doi.org/10.1094/PHYTO-03-13-0068-R>
- Wallace J.M., Drake R., 1953. A virus-induced vein enation in citrus. *Citrus Leaves* 33: 22–24.
- Wallace J.M., Drake R.J., 1960. Woody galls on citrus associated with vein-enation virus infection. *Plant Disease Reporter* 44: 580–584.
- Wu J., Liu Q., Qiu Y., Zhang S., Li Z., ... Cao M., 2019. First Report of Citrus Vein Enation Virus from Citrus Cultivar Huangguogan in Sichuan Province, China. *Plant Disease* 103. <https://apsjournals.apsnet.org/doi/10.1094/PDIS-03-19-0461-PDN>
- Wu J., Zhang S., Atta S., Yang C., Zhou Y., ... Cao M., 2020. Discovery and Survey of a New *Mandarivirus* Associated with Leaf Yellow Mottle Disease of Citrus in Pakistan. *Plant Disease* 104: 1593–1600. <https://doi.org/10.1094/PDIS-08-19-1744-RE>
- Xuan Z., Li S., Zhang S., Ran W., Zhou Y., ... Cao M., 2020. Complete genome sequence of citrus yellow spot virus, a newly discovered member of the family *Betaflexiviridae*. *Archives in Virology* 165: 2709–2713. <https://link.springer.com/article/10.1007/s00705-020-04794-1>
- Yang H.J., Oh J., Lee H.K., Lee D. S., Kim S.Y., ... Lee S.H., 2019. First Report of Citrus Vein Enation Virus in Satsuma Mandarin (*Citrus unshiu*) in Korea. *Plant Disease* 103: 2703. <https://doi.org/10.1094/PDIS-03-19-0468-PDN>



Citation: Q. Ye, W. Zhang, J. Jia, X. Li, Y. Zhou, C. Han, X. Wu, J. Yan (2021) Fungal pathogens associated with black foot of grapevine in China. *Phytopathologia Mediterranea* 60(2): 303-319. doi: 10.36253/phyto-12353

Accepted: April 11, 2021

Published: September 13, 2021

Copyright: © 2021 Q. Ye, W. Zhang, J. Jia, X. Li, Y. Zhou, C. Han, X. Wu, J. Yan. This is an open access, peer-reviewed article published by Firenze University Press (<http://www.fupress.com/pm>) and distributed under the terms of the Creative Commons Attribution License, which permits unrestricted use, distribution, and reproduction in any medium, provided the original author and source are credited.

Data Availability Statement: All relevant data are within the paper and its Supporting Information files.

Competing Interests: The Author(s) declare(s) no conflict of interest.

Editor: Josep Armengol Forti, Polytechnical University of Valencia, Spain.

Research Papers

Fungal pathogens associated with black foot of grapevine in China

QINGTONG YE^{1,2}, WEI ZHANG¹, JINGYI JIA¹, XINGHONG LI¹, YUEYAN ZHOU^{1,2}, CHANGPING HAN^{1,2}, XUEHONG WU², JIYE YAN^{1,*}

¹ Beijing Key Laboratory of Environment Friendly Management on Fruit Diseases and Pests in North China, Institute of Plant and Environment Protection, Beijing Academy of Agriculture and Forestry Sciences, Beijing 100097, China

² Department of Plant Pathology, China Agricultural University, Beijing 100193, China

*Corresponding author. E-mail: jiyeyan@vip.163.com

Summary. Grapevine trunk diseases (GTDs) are the most destructive diseases in grape-growing regions worldwide. Black foot is one of the important GTDs affecting young vineyards and nurseries. This disease has not been reported in China. During 2017 and 2019, field surveys were carried out in the Guangxi, Hebei, Ningxia, Shanxi, and Xinjiang provinces of China. Incidence of plants with black foot symptoms was 0.1% to 1% in the surveyed vineyards. Plant samples with poorly developed shoots and canes, chlorotic leaves, and necrotic trunks or roots were collected from the five provinces. In total, 50 fungal isolates were obtained from symptomatic tissues. Based on morphological and multi-gene phylogenetic analyses, five species were identified as *Cylindrocladiella lageniformis*, *Dactylonectria torresensis*, *D. macrodidyma*, *D. alcacerensis* and *Neonectria* sp.1. Pathogenicity was assessed using young, healthy detached green shoots of grapevine 'Summer Black' and potted 3-month-old 'Summer Black' cuttings. Inoculated detached shoots developed necroses after 7 d, and inoculated cuttings after 80 d. Fungi were re-isolated from necrotic lesions. Among the five species, *D. macrodidyma* was the most aggressive. This is the first report of *C. lageniformis*, *D. torresensis*, *D. macrodidyma*, *D. alcacerensis*, and *Neonectria* sp. 1 associated with black foot in China. This study has enhanced knowledge of the fungi associated with black foot in China, and will assist development of control measures for this disease.

Keywords. Nectriaceae, morphological characteristics, phylogenetic analyses, *Vitis vinifera*.

INTRODUCTION

Grapevine (*Vitis vinifera* L.) is an economically important fruit crop, with global cultivation area of 7,449,000 hectares in 2018, and China is ranked the second in the world grapevine cultivation area (2019 OIV). More than 70 diseases have been reported in grapevines, most of which are caused by fungi or oomycetes (Wilcox *et al.*, 2006), and among these, at least 27 diseases have been reported in China. Esca complex, Botryosphaeria dieback, black foot (BF), Eutypa dieback, and Phomopsis dieback are major fungal

grapevine trunk diseases (GTDs) worldwide. These diseases have been reported in almost all the main grape-growing countries (Gramaje *et al.*, 2018). GTDs are complexes that affect grape yields, wine quality and lifespan of plants in many grape-growing regions. The global financial losses attributed to GTDs are estimated to be more than \$US 1.5 billion per year (Hofstetter *et al.*, 2012).

Black foot (BF) is one of the most significant GTDs, especially in nurseries and young plantations (Halleen *et al.*, 2006). This disease has occurred in many viticulture regions during the last decade, including Australia, Brazil, California, Canada, (British Columbia, Quebec), France, Iran, Italy, New Zealand, Portugal, South Africa (Western Cape), Spain, Switzerland, Turkey, United States of America, and Uruguay (Agustí-Brisach and Armengol, 2013; Lombard *et al.*, 2014; Carlucci *et al.*, 2017; Aigoun-Mouhous *et al.*, 2019; Lawrence *et al.*, 2019; Berlanas *et al.*, 2020). In France, 50% of losses caused by BF fungal pathogens were recorded in young vineyards of 2 to 8 years old (Larignon *et al.*, 1999). In the Czech Republic, about 30% of plants showed root necroses, reduced root biomass and wood necroses in the basal ends of grapevine rootstocks, which are typical symptoms of BF that appear after one year of cultivation in 2015 (Pecenka *et al.*, 2018). The most common symptoms of BF on grapevine plants include delayed or absent budding, stunted growth, shortened internodes with small trunks, chlorotic leaves with necrotic margins, brown to black necroses on rootstock bases and sunken necrotic root lesions, in nurseries and young plantations (Rego *et al.*, 2000; Halleen *et al.*, 2006; Alaniz *et al.*, 2007; Abreo *et al.*, 2010; Agustí-Brisach and Armengol, 2013).

Ilyonectria destructans (= *Cylindrocarpon destructans*) was first reported in France (Grasso and Magnano Di San Lio, 1975), and to date, 33 fungal species have been reported to be associated with BF. The most common fungal genera associated with BF are *Campylocarpon*, *Cylindrocladiella*, *Dactylonectria*, *Ilyonectria*, *Neonectria*, *Pleiocarpon* and *Theلونectria*. Fungal species that have been associated with BF include: *Campylocarpon fasciculare*, *Ca. pseudofasciculare*, “*Cylindrocarpon*” sp. 2, *Cylindrocarpon didymium*, *Cylindrocladiella parva*, *C. lageniformis*, *C. viticola*, and *C. peruviana*, *Dactylonectria alcacerensis*, *D. estremocensis*, *D. macrodidyma*, *D. novozelandica*, *D. pauciseptata*, *D. pinicola*, *D. torresensis*, *D. riojana*, *D. vitis*, *D. hordeicola*, *Ilyonectria destructans*, *I. europaea*, *I. liriiodendri*, *I. lusitanica*, *I. pseudodestructans*, *I. robusta*, *I. vivaria*, *Neonectria obtusispora*, *N. quercicola*, *Neonectria* sp. 1, fungi in the *N. mammoidea* group, *Pleiocarpon algeriense*.

Theلونectria blackeriella, *T. olida*, and *T. aurea*. (Agustí-Brisach and Armengol, 2013; Lombard *et al.*, 2014; Carlucci *et al.*, 2017; Aigoun-Mouhous *et al.*, 2019; Lawrence *et al.*, 2019; Berlanas *et al.*, 2020). Among these species, *I. liriiodendri* and *D. macrodidyma* are the most widely distributed ones (Agustí-Brisach and Armengol, 2013). These fungi are frequently isolated from BF symptoms in nursery and older grapevine plants (Petit *et al.*, 2011; Carlucci *et al.*, 2017), and from asymptomatic inner tissues from plants (Berlanas *et al.*, 2020). Some BF fungi have also been detected from the soils of grapevine nurseries and vineyards, in Spain and South Africa. (Agustí-Brisach *et al.*, 2013, 2014; Langenhoven *et al.*, 2018).

Eutypa dieback was first reported in China in 2007, *Botryosphaeria dieback* in 2010, *Diaporthe dieback* in 2015 and *Esca* in 2020 (Li *et al.*, 2007; Li *et al.*, 2010; Dissanayake *et al.*, 2015; Ye *et al.*, 2020), while BF has not been reported in China previously.

MATERIALS AND METHODS

Vineyard surveys

Surveys were carried out in ten vineyards, located in Ningxia, Hebei, Shanxi, Guangxi and Xinjiang provinces of China, during 2017 and 2019 (Figure 1a). These provinces belong to the top ten grape cultivated grapevine areas in China, and Xinjiang province ranked the first, followed by Hebei province. The training systems used in the surveyed vineyards was mini “J”. The vineyards were of similar age, from 5 to 6 years old. Typical symptoms associated with diseased vines were shortened shoot internodes, chlorotic leaves, and trunk and root necroses (Figure 1, b–h). Initial disease symptoms included root necroses (especially small roots). As the disease progressed, the above-ground plant parts developed shoot shortened internodes and chlorotic leaves in severe cases. Some grapevines were grafted (rootstock Fercal), and some others were self-rooted (Personal communication, some of the grape growers).

Sample collection, fungus isolation and morphology of the pathogens

Samples were collected from *V. rotundifolia* Michx., and *V. vinifera* cvs Marselan, Cabernet Franc or Cabernet Sauvignon. Typical symptoms were recorded by taking appropriate photographs. The samples were kept at 4°C for further study, and the presence of spores or structures on the surfaces of trunks or roots were detected using a microscope. Isolations were made from

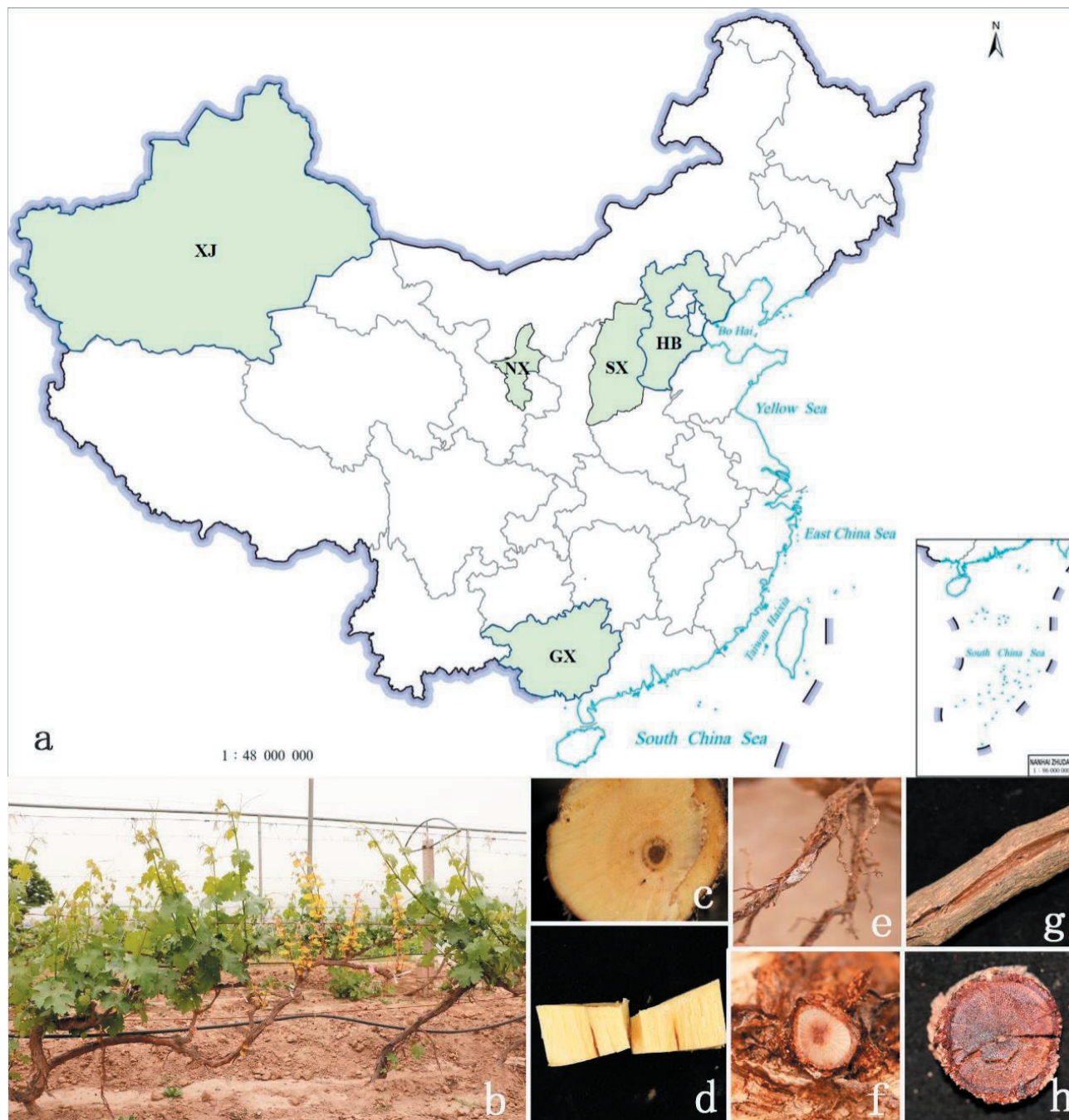


Figure 1. Sample collection sites and disease symptoms. Field surveys were carried out in five provinces of China. GX: Guangxi; HB: Hebei; NX: Ningxia; SX: Shanxi; XJ: Xinjiang (a). Diseased plant (Chardonnay, 5-year-old) showing shortened internodes of shoots (b). Necrotic grapevine roots and trunks (c-h).

symptomatic trunks and roots. Necrotic root and trunk samples were debarked and cut into small pieces (4–5 mm²). These small pieces were then surface-sterilized in 75% ethanol for 30 s, rinsed three times with sterilized water, dried, and cultured on potato dextrose agar (PDA; 20% potatoes, 2% dextrose, 1.5 to 2% agar) in Petri

plates. The plates were incubated at 25°C. Fungi growing from tissue pieces were transferred onto new PDA plates after 7 d, and pure cultures were obtained by isolating single spores. Pure cultures were grown on PDA and malt extract agar (MEA) and incubated at 25°C in the dark for 7 d. Conidia and colonies on the MEA plates

were observed and photographed using the Axio Imager Z2 photographic microscope (Carl Zeiss Microscopy).

DNA amplification and phylogenetic analyses

Single-spore purification were done for all the isolates before DNA extractions. Total genomic DNA was extracted from 50–100 mg of mycelium after 14 d of incubation on PDA (Guo *et al.*, 2000). For initial genus identification, the internal transcribed spacer and intervening 5.8S gene regions (ITS) were amplified and sequenced for all the isolates, and the resulting sequences were searched using BLASTN within GenBank/NCBI (<https://blast.ncbi.nlm.nih.gov/Blast.cgi>), as described by Manawasinghe *et al.* (2019). All the isolates in the present study belonged to *Cylindrocladiella*, *Neonectria* or *Dactyloctenidia*.

For species confirmation, phylogenetic analyses were conducted using multigene phylogenies. For *Cylindrocladiella*, histone H3 (*his3*), β -tubulin (*tub2*), and partial translation elongation factor 1-alpha (*tef1*) were sequenced (Marin-Felix *et al.*, 2019). ITS, *tub2*, *his3*, and *tef1* gene regions were sequenced for *Dactyloctenidia* and *Neonectria* species (Berlanas *et al.*, 2020). The primer pairs and amplification protocols used in the present study are summarized in Table 1. Each PCR mixture comprised 1.0 μ L of genomic DNA, 0.6 μ L of TaKaRa ExTaq DNA polymerase, 5.0 μ L of 10 \times ExTaq DNA polymerase buffer, 4.0 μ L of dNTPs, and 1.0 μ L of each primer, and was adjusted with sterilized double-distilled water to a final volume of 50.0 μ L. The PCR reactions were carried out in a thermal cycler (Bio-Rad, model C1000). Amplification products were visualized on 1% agarose electrophoresis gels under UV light using a Gel Doc™ XR+ Molecular Imager (Bio-Rad). All positive bands obtained by PCR amplification were sequenced by Tsingke Company, Beijing, China,

and the sequence data obtained were deposited in GenBank (Table 2).

Reference sequences of related taxa were obtained from GenBank (Marin-Felix *et al.*, 2019; Berlanas *et al.*, 2020). The sequence data generated in the present study were included, and individual gene regions were aligned using the MAFFT v. 7 webserver (Kuraku *et al.*, 2013; Katoh *et al.*, 2019) (<https://mafft.cbrc.jp/alignment/server/>). The alignments were checked and edited manually, where necessary using BioEdit v7.0.9 (Hall, 1999). Phylogenetic trees were generated using Maximum Likelihood (ML) in RAxML (Silvestro and Michalak, 2016) and Maximum Parsimony (MP) in PAUP (v4.0) (Swofford, 2002). The ML and MP trees were constructed using the methods described by Manawasinghe *et al.* (2019). For MP, heuristic searches were conducted with 1000 bootstrap replicates by random addition. All characters were unordered and equally weighted. Gaps were treated as missing data, and the steepest descent option not in effect, whereas the MulTrees option was used. The Tree Length (TL), Consistency Index (CI), Retention Index (RI), Relative Consistency Index (RC), and Homoplasy Index (HI) were calculated in PAUP. All the resulting trees were saved and checked using Kishino-Hasegawa tests (Kishino and Hasegawa, 1989). The ML analyses of single genes and combined multiple genes were accomplished using the RAxML-HPC2 on XSEDE (8.2.8) in the CIPRES Science Gateway (<https://www.phylo.org/portal2/createTask!create.action>). Phylogenetic trees were visualized using FigTree v1.4.4 (Rambaut, 2018) and were annotated in Microsoft PowerPoint 2016.

Pathogenicity tests

Pathogenicity tests of potential BF pathogens were conducted on detached green shoots or potted 3-month-

Table 1. The primer pairs and their amplified protocols used in present study.

Gene region	Primers	Sequence 5'-3'	Protocols for PCR	References
ITS	ITS1	TCCGTAGGTGAACCTGCGG	94°C: 3 min, (94°C: 30 s, 52°C: 30 s, 72°C: 1 min) \times 34 cycles 72°C: 7 min	White <i>et al.</i> (1990)
	ITS4	TCCTCCGCTTATTGATATGC		
HIS	CYLH3F	AGGTCC ACTGGTGGCAAG	94°C: 3 min, (94°C: 30 s, 58°C: 30 s, 72°C: 1 min) \times 34 cycles 72°C: 7 min	Crous <i>et al.</i> (2004)
	CYLH3R	AGCTGGATGTCCTTGGACTG		
β -tubulin	T1	AACATGCGTGAGATTGTAAGT	94°C: 3 min, (94°C: 30 s, 58°C (62°C): 30 s, 72°C: 1 min) \times 34 cycles 72°C: 7 min	O'Donnell and Cigelnik (1997) Glass and Donaldson (1995)
	Bt2b	ACCCTCAGTGTAGTGACCCTTGCC		
EF1- α	EF1-728F	CATCGAGAAGTTCGAGAAGG	94°C: 3 min, (94°C: 30 s, 54°C: 30 s, 72°C: 1 min) \times 34 cycles 72°C: 7 min	Carbone and Kohn (1999) Udayanga <i>et al.</i> (2012a ; b)
	EF1-986R	TACTTGAAGGAACCCTTACC		

Table 2. Reference sequence data obtained from GenBank and isolate sequence data from the present study which were used for phylogenetic tests.

Species	Isolates	GenBank accession No.			
		ITS	tub2	his3	tef1
<i>Neonectria coccinea</i>	CBS 119158	JF268759	KC660727	N/A	DQ789749.1
<i>N. confusa</i>	CBS 127484	KM515889	KM515886	N/A	N/A
<i>N. confusa</i>	CBS 127485	FJ560437	FJ860054	N/A	JF268736.1
<i>N. ditissima</i>	CBS 226.31	JF735309	DQ789869	JF735594	JF735783
<i>N. ditissima</i>	CBS 835.97	JF735310	DQ789880	JF735595	JF735784
<i>N. faginata</i>	CBS 217.67	HQ840385	JF268730	N/A	JF268746.1
<i>N. faginata</i>	CBS 119160	HQ840384	DQ789883	N/A	N/A
<i>N. fuckeliana</i>	CBS 119200	HQ840387	JF268731	N/A	JF268747.1
<i>N. fuckeliana</i>	CBS 239.29	HQ840386	DQ789871	N/A	JF268748.1
<i>N. hederiae</i>	CBS 714.97	N/A	DQ789878	N/A	KC660461
<i>N. hederiae</i>	IMI 058770	N/A	DQ789895	N/A	DQ789752
<i>N. lugdunensis</i>	CBS 125475	KM231762	KM232019	KM231482.1	KM231887.1
<i>N. lugdunensis</i>	CBS 125485	KM231762	KM232019	KM231482	KM231887
<i>N. major</i>	CBS 240.29	JF735308	DQ789872	JF735593	JF735782
<i>N. neomacrospora</i>	CBS 198.62	AJ009255	HM352865	KM231481	HM364351
<i>N. neomacrospora</i>	CBS 324.61	JF735312	DQ789875	JF735599	JF735788
<i>N. neomacrospora</i>	CBS 503.67	AY677261	JF735436	JF735600	JF735789
<i>N. obtusispora</i>	CBS 183.36	AM419061	AM419085	JF735607	JF735796
<i>N. obtusispora</i>	CPC 13544	AY295306	JF735443	JF735608	JF735797
<i>N. punicea</i>	CBS 242.29	KC660522	DQ789873	N/A	DQ789730
<i>N. punicea</i>	CBS 119724	KC660496	DQ789824	N/A	DQ789681
<i>N. quercicola</i>	CBS 143704	KY676880	KY676874	KY676862	KY676868
<i>N. quercicola</i>	CPC 13530	AY295302	JF735441	JF735605	JF735794
<i>N. ramulariae</i>	MAFF411012	JX034565.1	JX034567.1	N/A	N/A
<i>N. ramulariae</i>	CBS 151.29	AY677291	JF735438	JF735602	DQ789720
<i>N. ramulariae</i>	CBS 182.36	HM054157	JF735439	JF735603	JF735792
<i>Neonectria</i> sp. 1	CPC 13545	N/A	JF735437	JF735601	JF735790
<i>Neonectria</i> sp. 1	JZB3210004	MN988722	MN958534	MN958545	MN956387
<i>N. tsugae</i>	CBS 788.69	KM231763	KM232020	N/A	DQ789720
<i>Dactylonectria alcacerensis</i>	CBS 129087	JF735333	N/A	JF735630	JF735819
<i>D. alcacerensis</i>	Cy134	JF735332	N/A	JF735629	JF735818
<i>D. alcacerensis</i>	JZB3310007	MN988716	MN958528	MN958539	MN956381
<i>D. amazonica</i>	MUCL 55430	MF683706	MF683643	MF683686	MF683664
<i>D. anthuriicola</i>	CBS 564.95	JF735302	JF735430	JF735579	JF735768.1
<i>D. ecuadoriensis</i>	MUCL 55424	MF683704	MF683641	MF683684	MF683662
<i>D. ecuadoriensis</i>	MUCL55425	MF683705	MF683642	MF683684	MF683663
<i>D. estremocencis</i>	CPC 13539	JF735330	JF735458	JF735627	JF735816
<i>D. estremocencis</i>	CBS 129085	JF735320	JF735448	JF735617	JF735806
<i>D. hispanica</i>	CBS 142827	KY676882	KY676876	KY676864	KY676870
<i>D. hispanica</i>	Cy228	JF735301	JF735429	JF735578	JF735767
<i>D. hordeicola</i>	CBS 162.89	AM419060	AM419084	JF735610	JF735799
<i>D. macrodidyma</i>	CBS 112601	MH862898	AY677229	JF735644	JF735833
<i>D. macrodidyma</i>	CBS 112615	AY677290	AY677233	JF735647	JF268750
<i>D. macrodidyma</i>	Cy258	JF735348	JF735477	JF735656	JF735845
<i>D. macrodidyma</i>	CBS 112604	AY677284	AY677229	JF735644	JF735833
<i>D. macrodidyma</i>	JZB3310008	MN988717	MN958529	MN958540	MN956382
<i>D. macrodidyma</i>	JZB3310009	MN988718	MN958530	MN958541	MN956383

(Continued)

Table 2. (Continued).

Species	Isolates	GenBank accession No.			
		ITS	tub2	his3	tef1
<i>D. macrodidyma</i>	JZB33100010	MN988719	MN958531	MN958542	MN956384
<i>D. novozelandica</i>	CBS 112608	AY677288	AY677235	JF735632	JF735821
<i>D. palmicola</i>	MUCL55426	MF683708.1	MF683645.1	MF683687.1	MF683666.1
<i>D. pauciseptata</i>	CBS 120171	EF607089	EF607066	JF735587	JF735776
<i>D. pinicola</i>	CBS 159.43	JF735318	JF735446	JF735613	JF735802
<i>D. pinicola</i>	CBS 173.37	JF735319	JF735447	JF735614	JF735803
<i>D. polyphaga</i>	MUCL55209	MF683689	MF683626	MF683668	MF683647
<i>D. torresensis</i>	CBS 119.41	JF735349	JF735478	JF735657	JF735846
<i>D. torresensis</i>	Cyl1102	KP823905	KP823885	KP823894	KP823874
<i>D. torresensis</i>	Cyl1106	KP823907	KP823887	KP823895	KP823876
<i>D. torresensis</i>	Cyl1110	KP823908	KP823888	KP823896	KP823877
<i>D. torresensis</i>	Cyl1124	KP823912	KP823891	KP823900	KP823881
<i>D. torresensis</i>	CBS 129086	JF735362	JF735492	JF735681	JF735870.1
<i>D. torresensis</i>	JZB33100011	MN988720	MN958532	MN958543	MN956385
<i>D. torresensis</i>	JZB33100012	MN988721	MN958533	MN958544	MN956386
<i>D. vitis</i>	CBS 129082	JF735303	JF735431	JF735580	JF735769.1
<i>D. valentina</i>	CBS 142826	KY676881	KY676875	KY676863	KY676869
<i>Cylindrocladiella addiensis</i>	CBS 143794	MH111383	MH111388	N/A	MH111393
<i>C. addiensis</i>	CBS 143793	MH111385	MH111390	N/A	MH111395
<i>C. addiensis</i>	CBS 143795	MH111384	MH111389	N/A	MH111394
<i>C. arbusta</i>	CMW47295/ CBS 143546	MH017015	MH016958	MH016996	MH016977
<i>C. arbusta</i>	CMW 47296; CBS 143547	MH017016	MH016959	MH016997	MH016978
<i>C. australiensis</i>	CBS 129567	JN100624	JN098747	JN098932	JN099060
<i>C. brevistipitata</i>	CBS 142786	N/A	MF444926	N/A	MF444940
<i>C. camelliae</i>	IMI 346845	AF220952	AY793471	AY793509	JN099087
<i>C. clavata</i>	CBS 129564	JN099095	JN098752	JN098858	JN098974
<i>C. cymbiformis</i>	CBS 129553	JN099103	JN098753	JN098866	JN098988
<i>C. elegans</i>	CBS 338.92	AY793444	AY793474	AY793512	JN099039
<i>C. ellipsoidea</i>	CBS 129573	JN099094	JN098757	JN098857	JN098973
<i>C. hahajimaensis</i>	MAFF238172	JN687561	N/A	N/A	JX024570.1
<i>C. hawaiiensis</i>	CBS 129569	JN100621	JN098761	JN098929	JN099057
<i>C. horticola</i>	CBS 142784	MF444911	MF444924	N/A	MF444938
<i>C. humicola</i>	CBS 142779	MF444906	MF444919	N/A	MF444933
<i>C. infestans</i>	CBS 111795	AF220955	AF320190	AY793513	JN099037
<i>C. kurandica</i>	CBS 129577	JN100646	JN098765	JN098953	JN099083
<i>C. lageniformis</i>	CBS 111060	JN100611	JN098770	JN098918	JN099046
<i>C. lageniformis</i>	CBS 111061	JN100606	JN098771	JN098913	JN099040
<i>C. lageniformis</i>	CBS 112898	AY793445	AY725652	AY725699	JN098990
<i>C. lageniformis</i>	CBS 340.92	MH862360	AY793481	AY793520	JN099003
<i>C. lageniformis</i>	JZB3320001	MN988714	MN958526	MN958537	MN958535
<i>C. lageniformis</i>	JZB3320002	MN988715	MN958527	MN958538	MN958536
<i>C. lanceolata</i>	CBS 129566	JN099099	JN098789	JN098862	JN098978
<i>C. lateralis</i>	CBS 142788	MF444914	MF444928	N/A	MF444942
<i>C. longiphialidica</i>	CBS 129557	JN100585	JN098790	JN098851	JN098966
<i>C. longistipitata</i>	CBS 116075	AF220958	AY793506	AY793546	JN098993
<i>C. malesiana</i>	CBS 143549	MH017017	MH016960	MH016998	MH016979
<i>C. microcylindrica</i>	CBS 111794	AY793452	AY793483	AY793523	JN099041
<i>C. natalensis</i>	CBS 114943	JN100588	JN098794	JN098895	JN099016

(Continued)

Table 2. (Continued).

Species	Isolates	GenBank accession No.			
		ITS	tub2	his3	tefl
<i>C. nederlandica</i>	CBS 152.91	JN100603	JN098800	JN098910	JN099033
<i>C. novazelandica</i>	CBS 486.77	AF220963	AY793485	AY793525	JN099050
<i>C. nauliensis</i>	CBS 143792	MH111387	MH111392	N/A	MH111397
<i>C. nauliensis</i>	CBS 143791	MH111386	MH111391	N/A	MH111396
<i>C. obpyriformis</i>	CMW47194/ CBS 143552	MH017022	MH016965	MH017003	MH016984
<i>C. parvispora</i>	CMW 47197/ CBS 143554	MH017025	MH016968	MH017006	MH016987
<i>C. parva</i>	CBS 114524	AF220964	AY793486	AY793526	JN099009
<i>C. peruviana</i>	IMUR 1843	AF220966	AY793500	AY793540	JN098968
<i>C. pseudocamelliae</i>	CBS 129555	JN100577	JN098814	JN098843	JN098958
<i>C. pseudohawaiiensis</i>	CBS 210.94	JN099128	JN098819	JN098890	JN099012
<i>C. pseudoinfestans</i>	CBS 114531	AF220957	AY793508	AY793548	JN099004
<i>C. pseudoparva</i>	CBS129560	JN100620	JN098824	JN098927	JN099056
<i>C. queenslandica</i>	CBS 129574	JN099098	JN098826	JN098861	JN098977
<i>C. reginae</i>	CBS 142782	MF444909	MF444922	N/A	MF444936
<i>C. solicola</i>	CMW47198/ CBS 143551	MH017021	MH016964	MH017002	MH016983
<i>C. stellenboschensis</i>	CBS 110668	JN100615	JN098829	JN098922	JN099051
<i>C. terrestris</i>	CBS 142789	MF444915	MF444929	N/A	MF444943
<i>C. thailandica</i>	CBS 129571	JN100582	JN098834	JN098848	JN098963
<i>C. variabilis</i>	CBS 129561	JN100643	JN098719	JN098950	JN099080
<i>C. viticola</i>	CBS 112897	AY793468	AY793504	AY793544	JN099064
<i>C. vitis</i>	CBS 142517	KY979751	KY979918	N/A	KY979891
<i>Campylocarpon fasciculare</i>	CBS 112613	AY677301.1	AY677221.1	JF735502.1	JF735691.1
<i>C. pseudofasciculare</i>	CBS 112679	AY677306.1	KJ022328.1	JF735503.1	JF735692.1
<i>Gliocladiopsis sagariensis</i>	CBS 199.55	NR147628	JQ666141	JQ666031	JQ666107

^a CBS: Westerdijk Fungal Biodiversity Institute, Utrecht, The Netherlands; CPC: Culture collection of Pedro Crous, housed at CBS. MUCL: Mycothèque de l'Université catholique de Louvain; JZB: Beijing Academy of Agriculture and Forestry Sciences Culture Collection, China; IMI: International Mycological Institute, CABI-Bioscience, Egham, Basingstoke, UK; IMUR: Institute of Mycology, University of Recife, Recife, Brazil; MAFF: Genetic Resources Centre, National Agriculture and Food Research Organization (NARO), NARO GenBank, Ibaraki, Japan; Cy: *Cylindrocarpon* collection housed at Laboratório de Patologia Vegetal "Veríssimo de Almeida" - ISA, Lisbon, Portugal;

^b Ex-type were in bold.

N/A: The sequence is not available or not applicable to the present study.

old healthy plants of grapevine cv. 'Summer Black'. Five isolates (JZB3320001, JZB3310007, JZB3310008, JZB33100011 and JZB3210004) were selected randomly for pathogenicity tests. Mycelium discs (4 mm diam.) were obtained from the edges of PDA colonies which were grown for 10 d at 25°C.

Detached shoots were surface-disinfected in 75% ethanol and then dried, and each shoot was then wounded (4 mm) using a sterilized scalpel. The mycelium discs were placed onto the wound sites and covered with parafilm (Bemis). Non-colonized sterile PDA plugs were used as negative controls. The shoots were then inserted into moist soil and kept at 25°C. Each experiment included ten shoots for each fungus isolate, with a total of three parallel experiments conducted.

The lengths of the lesions were measured after 7 d, and meanwhile photos were taken.

Pathogenicity tests of BF fungal agents were further conducted on the 3-month old grapevine cuttings which were inoculated in a manner similar to the detached green shoots. The experiment was performed in six cuttings for each tested isolate and the negative controls. The plants were kept in a greenhouse maintained at 25°C, and the trial was conducted twice. Shoots were collected, and lesion lengths were measured upward and downward from the points of inoculation after 80 d.

Fungi were re-isolated from necroses on the test plants in all pathogenicity tests, and fungus identifications were based on cultural and morphological characters. The lesion dimension data were statistically ana-

lyzed with IBM SPSS Statistics 21.0 (IBM Corp.) using a one-way analysis of variance (at $P = 0.05$) to determine differences in shoot lesion dimensions resulting from different fungus isolate inoculations.

RESULTS

Fungus isolation and initial species identifications

Incidence of BF-like symptoms in the investigated vineyards was 0.1% to 1%.

Colony morphology of all the isolates distinguished after 14 d of growth on PDA. In total, 50 isolates were obtained from the symptomatic grapevine tissues. For genus confirmation of the isolates, the ITS regions were amplified for all the isolates. The products of the ITS regions were approx. 0.5 kb. All sequences obtained were compared to those deposited in GenBank, and the isolates possessed 95%–99% similarity with sequences from the genera *Cylindrocladiella*, *Dactylonectria* or *Neonec- tria*. One or two isolates were selected from each of these three genera for pathogenicity tests.

The ML MP trees had similar topologies, so only the ML tree is presented in this study, with ML and MP bootstrap support values.

Identification of *Cylindrocladiella* species The optimization likelihood value of the final ML tree was -9044.171598. The matrix had 563 distinct alignment patterns, with 12.52% of undetermined characters or gaps. The parameters for the GAMMA+P-Invar model were as follows: estimated base frequencies A = 0.217646, C = 0.325293, G = 0.206497, T = 0.250564; substitution rates include TL = 1.662695, AC = 1.021632, AG = 3.427269, AT = 1.399071, CG = 0.562601, CT = 4.088874, GT = 1.000000; proportion of invariable sites (I) = 0.346767, and gamma distribution shape parameter (α) = 0.401996. In the MP tree, the heuristic search produced 1000 trees (length = 1415, CI = 0.529, RI = 0.840, RC = 0.445 and HI = 0.471), and the dataset consisted of 1527 total characters. Of these characters, 1000 were constant, 158 variable characters were parsimony-uninformative and 369 were parsimony-informative. In the ML tree (Figure 2), generated using the combined data, two isolates (JZB3320001 and JZB3320002) clustered with *C. lageniformis* (CBS 340.92) with bootstrap value 100 and 99 obtained from the ML and MP tree, respectively. Based on morphological characteristics and phylogenetic results, isolates JZB3320001 and JZB3320002 were identified as *Cylindrocladiella lageniformis* Crous, M.J. Wingf. & Alfenas.

Identification of the species of *Dactylonectria* and *Neonec- tria* species The ML optimization likelihood value was

-12848.031218. The matrix had 916 distinct alignment patterns, with 16.70% of undetermined characters or gaps. Parameters for the GAMMA+P-Invar model were: estimated base frequencies A = 0.216108, C = 0.328348, G = 0.225791, T = 0.229753; substitution rates include TL = 1.593283, AC = 1.370476, AG = 3.210224, AT = 1.626079, CG = 0.702088, CT = 5.644898, GT = 1.000000; proportion of invariable sites (I) = 0.388010, and gamma distribution shape parameter (α) = 0.971160. In the MP tree, the heuristic search produced 1000 trees (length = 1981, CI = 0.610, RI = 0.911, RC = 0.556 and HI = 0.390), and the dataset consisted of 2041 total characters. Of these, 1225 were constant, 88 variable characters were parsimony-uninformative and 728 were parsimony-informative. In the ML tree (Figure 3), generated using the combined data, three isolates (JZB3310008, JZB3310009 and JZB33100010) collected from Ningxia province clustered with *D. macrodidyma* (CBS 112615) and one isolate (JZB3210004) clustered with *Neonec- tria* sp. 1(CPC 13545); In addition, the isolate (JZB3310007) clustered with *D. alcacerensis* (CBS 129087) and two isolates (JZB33100011 and JZB33100012) clustered with *D. torresensis*(CBS 119.41).

Morphological characteristics

Morphological observations for the five identified species are outlined below.

***Cylindrocladiella lageniformis* Crous, M.J. Wingf. & Alfenas**

Pathogenic on trunks and rootstocks of *Vitis vinifera*. **Asexual morph:** Conidiophores were hyaline and penicillate. Conidia were hyaline, cylindrical, one septate or aseptate, with dimensions of 5.3–9.5 × 1.5–2.8 μm , mean \pm SD = 7.8 \pm 1.1 × 2.1 \pm 0.3 μm . The terminal vesicles were lageniform to ovoid. (Figure 4 c-d). **Sexual morph:** undetermined.

Culture characteristics: Colonies on PDA reached 74.9 \pm 0.8 mm diam. after 6 d incubation at 25°C in the dark, and were yellow to tan, with flourish aerial mycelium (Figure 4 a-b).

Material examined: CHINA, Guangxi province, on trunk and rootstock of *Vitis vinifera*, 8 April 2018, Xing- hong Li, living cultures, JZB3320001, JZB3320002.

***Dactylonectria macrodidyma* (Halleen, Schroers & Crous) L. Lombard & Crous**

Pathogenic on trunks and roots of *Vitis vinifera*. **Asexual morph:** the isolates rarely formed chlamydospores and microconidia, producing abundant macroconidia on MEA. Macroconidia hyaline, cylindrical, straight to slightly curved, one to four septate, with dimensions

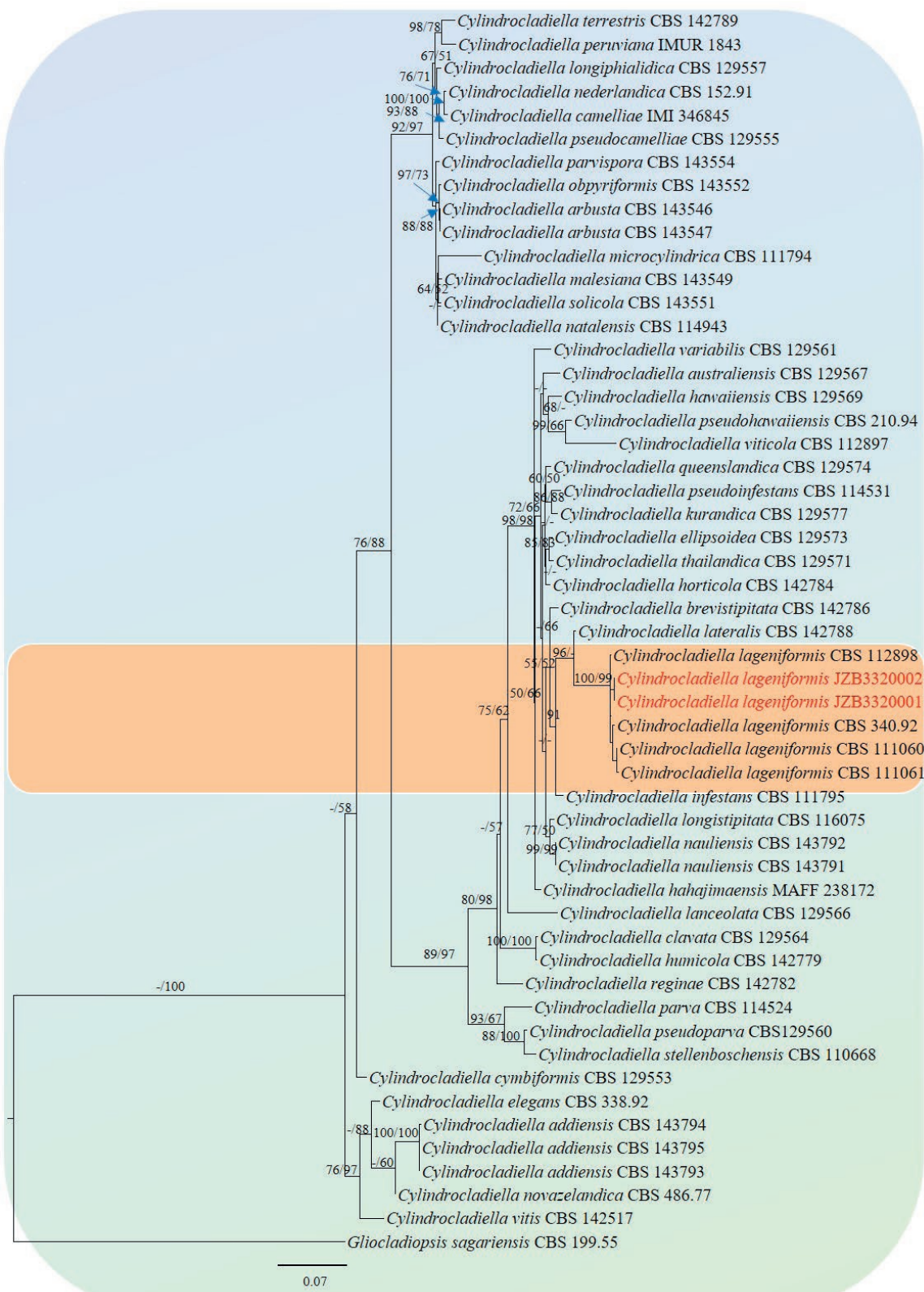


Figure 2. Maximum likelihood tree obtained from the phylogenetic analysis based on *tef1*, *his3* and *tub2* sequence alignments. The scale bar represents 0.07 changes. The tree is rooted in *Gliocladiopsis sagariensis* (CBS 199.55).

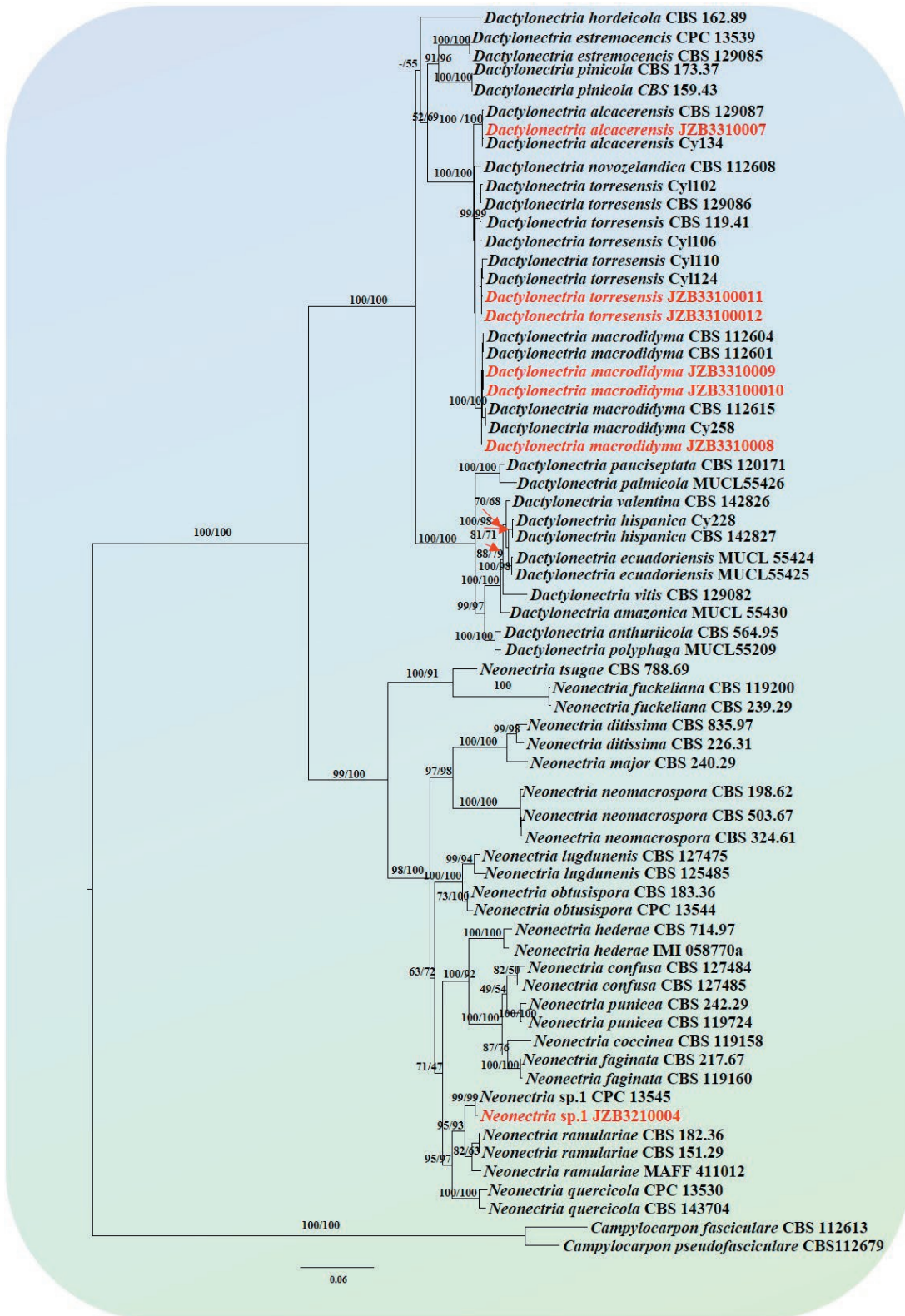


Figure 3. Maximum likelihood tree obtained from the phylogenetic analysis based on combined ITS, *tub2*, *his3*, and *tef1* sequence alignments. The scale bar represents 0.05 changes. The ex-type strains are in bold font. The outgroups of the tree are *Campylocarpon fasciculare* (CBS 112613) and *C. pseudofasciculare* (CBS 112679).

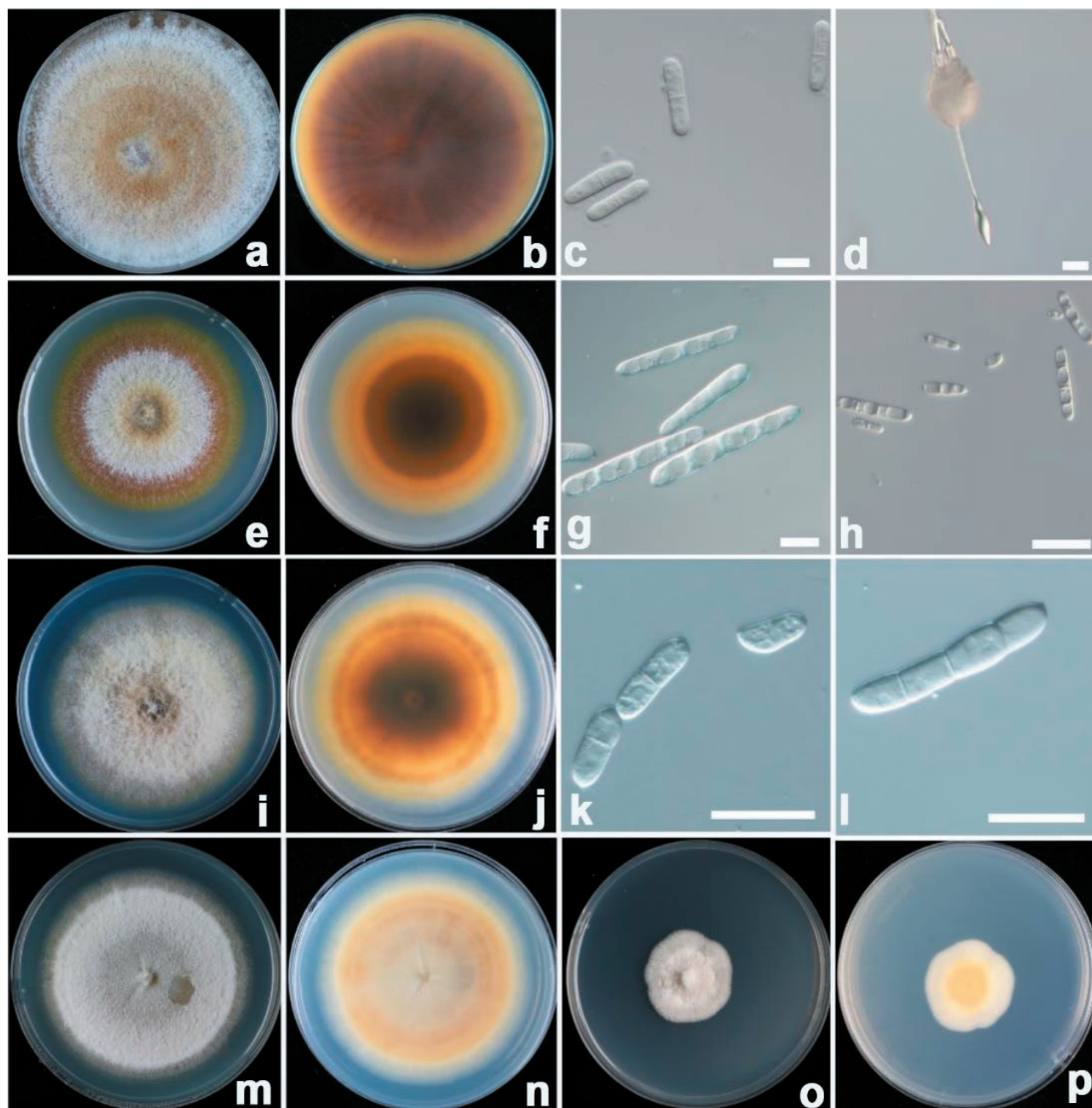


Figure 4. Photographs of isolated fungi and their morphological characterization. Colonies (top and bottom views of cultures) of *Cylindrocladiella lageniformis* (a and b), *Dactinonectria macrodidyma* (e and f), *D. torresensis* (i and j), *D. alcaceresis* (m and n), or *Neonectria* sp.1 (o and p). Conidia and terminal vesicles of *C. lageniformis* (c and d). Conidia of *D. macrodidyma* (g and h), and *D. torresensis* (k and l). All the fungi were grown on PDA for 14 d. Bars = 10 μ m (c and d) or 20 μ m (g, h, k and l).

of 14.4–44.2 \times 4.0–8.2 μ m, mean \pm SD = 31.1 \pm 7.8 \times 6.2 \pm 0.9 μ m (Figure 4, g and h). Microconidia ellipsoid to ovoid, hyaline, straight, aseptate to one septate. **Sexual morph:** undetermined.

Culture characteristics: Colonies on PDA reached 57.3 \pm 5.4 mm diameter after 9 d at 25°C in the dark, and were yellowish, with abundant aerial mycelium (Figure 4e).

Colony reverse sides were burnt umber to raw sienna or brownish yellow on PDA (Figure 4f).

Material examined: CHINA, Ningxia province, on trunk and rootstock of *Vitis vinifera*, 8 April 2018, Qingtong Ye and Xinghong Li, living cultures, JZB3310008, JZB3310009, JZB3310010.

Dactylonectria torresensis (A. Cabral, Rego & Crous) L.

Lombard & Crous

Pathogenic on trunks and rootstocks of *Vitis vinifera*.

Asexual morph: The isolates rarely formed chlamydo-spores and microconidia, producing some macroconidia on MEA. Macroconidia straight or minutely curved, cylindrical, one to four septate. Microconidia zero to one septate, ellipsoid to ovoid. **Sexual morph:** undetermined.

Culture characteristics: Colonies on PDA reached 55.5 ± 3.6 mm diam. after 9 d at 25°C in the dark, and were pale buff to chestnut (Figure 4, i and j). Colony reverse sides were buff to umber to chestnut on PDA.

Material examined: CHINA, Shanxi and Hebei province, on trunk and rootstock of *Vitis vinifera*, 8 April 2018, Qingtong Ye and Xinghong Li, living cultures, JZB3310011, JZB3310012.

Dactylonectria alcacerensis (A. Cabral, H. Oliveira & Crous) L. Lombard & Crous

Pathogenic on roots of *Vitis vinifera*. **Asexual morph:**

isolates did not produce macroconidia, microconidia, or chlamydo-spores on MEA. **Sexual morph:** undetermined. **Culture characteristics:** Colonies on PDA reached 49.3 ± 2.2 mm diam. eafter 9 d at 25°C in the dark, and were felty to slightly cottony (Figure 4 m-n).

Material examined: CHINA, Shanxi province, on trunk and rootstock of *Vitis vinifera*, 8 May 2018, Qingtong Ye and Xinghong Li, living culture, JZB3310007.

Neonectria sp. 1

Pathogenic on the bark of trunk of *Vitis vinifera*. **Asexual morph:** In the present study, the isolates did not produce macroconidia, microconidia, or chlamydo-spores on PDA. **Sexual morph:** undetermined.

Culture characteristics: Colonies on PDA reached 61.1 ± 1.1 mm diameter after 15 d of incubation at 20°C in dark (Figure 4 o-p).

Material examined: CHINA, Xinjiang province, on trunk and rootstock of *Vitis vinifera*, 16 April 2018, Qingtong Ye and Xinghong Li, living culture,

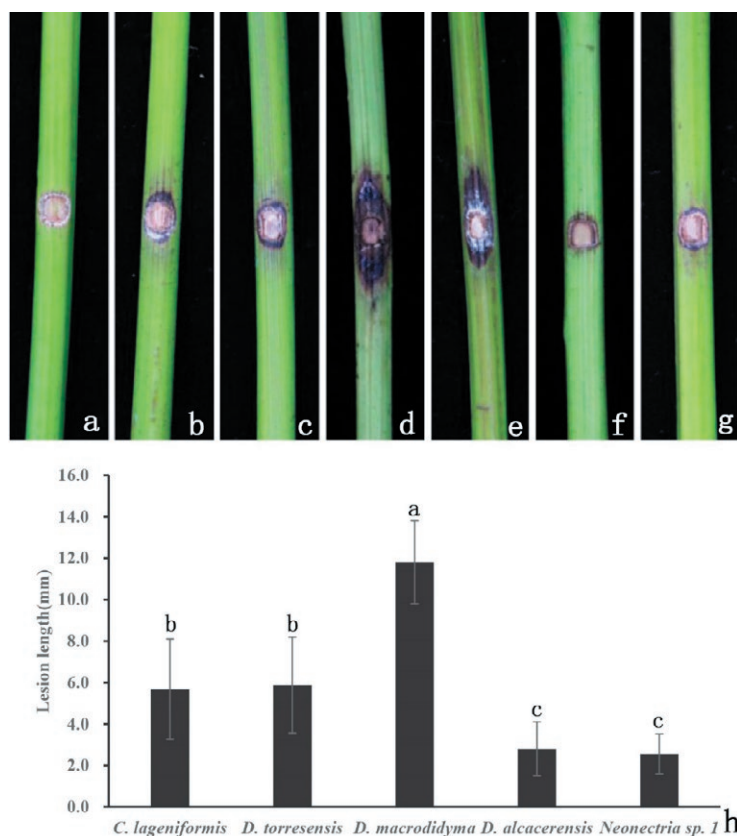


Figure 5. Pathogenicity tests results (after 7 d) of BF fungal agents inoculated onto detached green shoots of grapevine 'Summer Black'. Control (a), *Cylindrocladiella lageniformis*(b), *Dactinonectria torresensis* (c), *D. macrodidyma* (d and e), *D. alcacerensis*(f), or *Neonectria* sp. 1(g). Histogram (h) of mean lesion lengths on wood shoots after inoculations with the different fungi. Means accompanied by different letters are significantly different ($P = 0.05$).

JZB3210004.

Pathogenicity tests

In the pathogenicity tests conducted with detached green shoots, the non-inoculated shoots did not develop any symptoms (Figure 5a). In contrast, shoots inoculated with mycelium discs resulted in necroses. The lesions were brown to black, and the mean lesion lengths differed among the different inoculated fungi ($P < 0.05$) (Figure 5, b to h). *Dactylonectria macrodidyma* was the most aggressive pathogen (mean lesion length = 1.18 cm) among the five species (Figure 5). The re-isolation rates of isolates *C. lageniformis*, *D. torresensis*, *D. macrodidyma*, *D. alcacerensis*, and *Neonectria* sp. 1. were between 70% with 100% from the lesions.

Pathogenicity tests on 3-month-old grapevine cuttings showed different results for the different inoculated pathogens, as well. The non-inoculated controls showed no symptoms on the shoots (Figure 6a). *Dacty-*

lonectria macrodidyma caused brown to black necrotic lesions on the shoots (mean lesion length = 1.95 cm) (Figure 6, d and e). Less necrosis was observed in the cuttings inoculated in *C. lageniformis*, *D. torresensis*, *Neonectria* sp. 1., or *D. alcacerensis* (Figure 6, b to c', f to g'). The re-isolation rates of the different inoculated fungi from the respective lesions were between 70% with 100%.

This is the first report of *C. lageniformis*, *D. torresensis*, *D. macrodidyma*, *D. alcacerensis* and *Neonectria* sp. 1 associated with BF of grapevines in China.

DISCUSSION

Grapevines can be affected by several diseases throughout each year, especially during fruit production. In the present study, 50 isolates obtained from diseased grapevine samples in five provinces of China were identified as *C. lageniformis*, *D. torresensis*, *D. macrodidyma*, *D. alcacerensis*, or *Neonectria* sp. 1. To date, *D. torresen-*

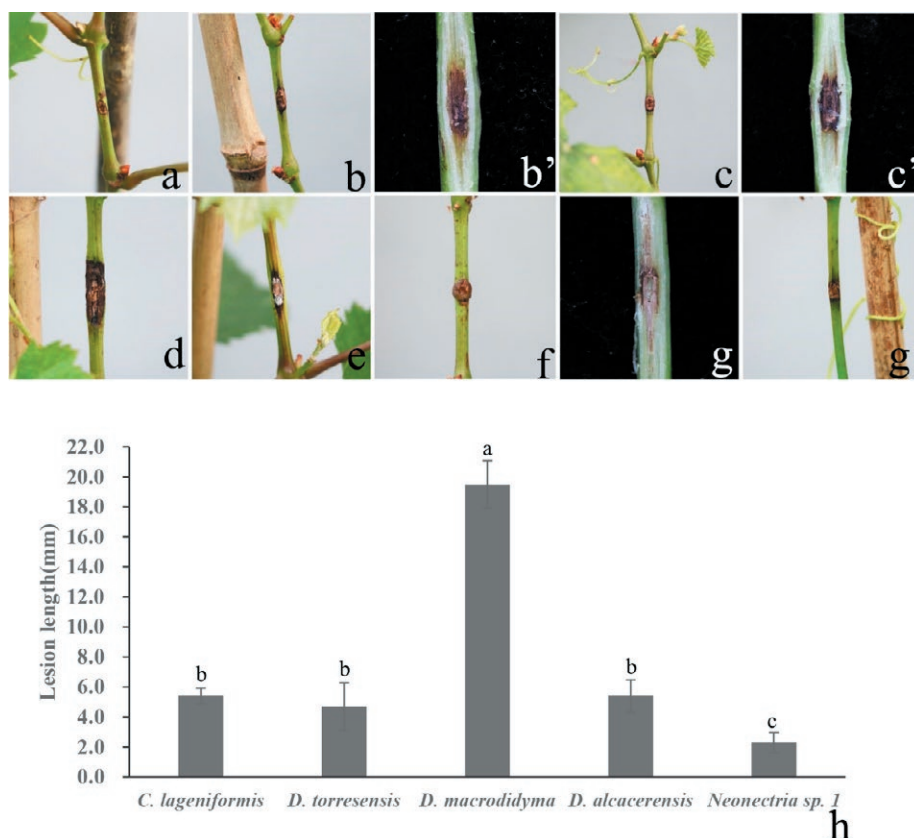


Figure 6. Pathogenicity tests results (after 80 d) of BF fungal agents inoculated onto 3-month-old 'Summer Black' grapevine plants in greenhouse. Control (a), *Cylindrocladiella lageniformis* (b and b'), *Dactylonectria torresensis* (c and c'), *D. macrodidyma* (d and e), *D. alcacerensis* (f and g), *Neonectria* sp. 1 (g'). Histogram (h) of mean lesion lengths caused by inoculations with the different fungi. Means accompanied by different letters are significantly different ($P = 0.05$).

sis has been reported as grapevine pathogen in Australia, Canada, Czech Republic France, Italy, New Zealand, Portugal, South Africa, Spain and USA (Agusti-Brisach *et al.*, 2013; Carlucci *et al.*, 2017; Pecenka *et al.*, 2018; Pintos *et al.*, 2019), and *Cylindrocladiella lageniformis* has been reported mainly from California and South Africa (Van Coller *et al.*, 2005; Koike *et al.*, 2016).

The BF pathogens are soil-borne organisms that affect roots and the basal ends of rootstock vines, and most of the fungi reported in the present study were also reported in California and Spain (Koike *et al.*, 2016; Berlanas *et al.*, 2020). However, whole grapevines in the north grape-growing regions of China are routinely buried under the soil in winter, to allow survival during low temperature winter conditions. It has been proposed that the soil-borne pathogens could infect plants through wounds (to roots, rootstocks, trunks, canes and shoots). Pathogenicity tests of BF pathogens were carried out with canes or roots in previous studies (Koike *et al.*, 2016; Berlanas *et al.*, 2020). Nevertheless, pathogenicity tests of *Cylindrocladiella lageniformis* have also been conducted with green shoots (Van Coller *et al.*, 2005; Koike *et al.*, 2016). Therefore, in the present study, it was important to determine whether the soil-borne fungi could infect host canes or shoots. The fungi were inoculated by wounding between two nodes of each cutting. Among the tested fungi, *D. macrodidyma* produced the longest lesions in the pathogenicity tests. However, Berlanas *et al.* (2020) reported that virulence of *D. alcacerensis* was greater than that of *D. macrodidyma* and *Neonectria* sp. 1., while *D. macrodidyma* was found to be more virulent than *D. alcacerensis* in the present study. Differences in virulence of *D. alcacerensis* or the other species could be attributed to: (1) strain origins (Probst *et al.*, 2019), (2) host genotype susceptibility to black foot fungus infections (Berlanas *et al.*, 2020), (3) methods of inoculation (Alaniz *et al.*, 2009b; Probst *et al.*, 2019; Berlanas *et al.*, 2020), or (4) inoculum dose.

The distribution of BF fungal pathogens in the present study may have been influenced by climate. The climate system of China is diverse due to the varied topography and vast area, including climates of Tibetan plateau, temperate continental, subtropical monsoon, and tropical monsoon (Yan *et al.*, 2013). The characteristics of BF pathogens are likely to vary due to the diverse temperature of China. Based on the present study (data not shown), colony diameter on PDA after 6 d of *C. lageniformis* from the south of China reached up to 60.4 ± 3.3 mm at 30°C while the other fungi (*D. torresensis*, *D. macrodidyma*, *D. alcacerensis* and *Neonectria* sp. 1.) from the north of China hardly grew at 30°C. Most of these fungi could grow below 5°C in PDA, except for *C. lageniformis*.

Although the incidence of diseased plants with BF symptoms was about 1% in the surveyed vineyards in China, which is much less than in France (losses of 50%: Larignon *et al.*, 1999), BF pathogens can infect grapevine roots and trunks in young nurseries and plantations, and the pathogenic fungi can be transmitted to new vineyards by cuttings (De la Fuente *et al.*, 2016). The fungi *C. lageniformis*, *D. torresensis*, *D. macrodidyma*, *D. alcacerensis*, and *Neonectria* sp. 1. are all soilborne, and can infect hosts through the soil (Halleen *et al.*, 2003). In the north of China, grapevines need to be buried under the soil for survival during cold weather, resulting in small wounds that are likely to be susceptible to infection by soilborne fungi, so more attention should be paid to BF in China in future.

Grapevine BF is prevalent in nurseries and new plantations (De la Fuente *et al.*, 2016), and the current strategies for controlling this disease include good hygiene or sanitation, which are the most important means of obtaining healthy vines (Gramaje and Armengol 2011), including treatments with hot water, (Gramaje *et al.*, 2010; Halleen and Fourie 2016), fungicides (Halleen *et al.*, 2007; Rego *et al.*, 2009; Alaniz *et al.*, 2011) and biological control agents (Berbegal *et al.*, 2020; Martínez-Diz *et al.*, 2021; van Jaarsveld *et al.*, 2020, 2021). Chemical treatments during propagation processes in nurseries for control of BF pathogens have been evaluated, including treating cutting prior to cold storage, cutting prior to callusing, rooting pre- and post-grafting, and pre-planting fungicide treatments of rooted cuttings, to eliminate or reduce potential fungal agents before planting (Halleen *et al.*, 2007; Rego *et al.*, 2009, Alaniz *et al.*, 2011, Gramaje *et al.*, 2018). Based on previous research, benomyl was effective for elimination or reducing *Cylindrocarpon destructans* infections (Rego *et al.* 2006). Reductions of *D. torresensis* and *D. macrodidyma* incidence and disease severity on the bases of 2-year-old plants have been reported from applications of *Streptomyces* sp. E1+R4 before preplanting (Martínez-Diz *et al.*, 2021).

Some practices, such as hot water treatments, are useful for sanitizing commercially produced plants. Generally, this practice entails treating the plants at 50°C for 30 min. However, this is stressful for the plants (Waite *et al.*, 2013). Despite treated with these practices, diseases in symptomless plants can still be transmitted to non-infested areas (De la Fuente *et al.*, 2016). The detection of BF fungi in soils or vines is essential for controlling the disease in nurseries and new plantations. Alaniz *et al.* (2009a) reported a multiplex PCR system for specific and early detection of *Ilyonectria liriodendri* (= *Cylindrocarpon liriodendra*), *Dactylonectria macro-*

didyma (= *Cylindrocarpon macrodidymum*), and *Dactylonectria pauciseptata* (= *Cylindrocarpon pauciseptatum*) from pure fungus cultures or diseased plants. Martínez-Diz *et al.* (2020) attempted to detect *I. lirioidendri* in bulk soils, rhizosphere soils, and grapevine endorhizospheres using Droplet Digital PCR (ddPCR) and real-time PCR (qPCR) techniques. They showed that ddPCR was more sensitive than qPCR to lower target concentrations. Nevertheless, the ddPCR technique has not been used for detection of *C. lageniformis*, *D. torresensis*, *D. macrodidyma*, *D. alcaerensis* or *Neonectria* sp.1, and this technology could be useful for detection of BF in China. Further study should also be conducted to develop specific protocols for effective BF management.

ACKNOWLEDGEMENTS

The project was funded by 2018YFD0201301, CARS-29 and JKZX201905. The authors thank the Institute of Forestry and Pomology, Beijing Academy of Agriculture and Forestry Sciences for providing 1-year-old 'Summer black' dormant shoots, and grapevine farmers for their co-operation.

LITERATURE CITED

- Abreo E., Martínez S., Betucci L., Lupo S., 2010. Morphological and molecular characterization of *Campylocarpon* and *Cylindrocarpon* spp. associated with black foot disease of grapevines in Uruguay. *Australasian Plant Pathology* 39: 446–452.
- Agustí-Brisach C., Armengol J., 2013. Black-foot disease of grapevine: an update on taxonomy, epidemiology and management strategies. *Phytopathologia Mediterranea* 52: 245–261.
- Agustí-Brisach C., Gramaje D., García-Jiménez J., Armengol J., 2013. Detection of black-foot and Petri disease pathogens in natural soils of grapevine nurseries and vineyards using bait plants. *Plant and Soil* 364: 5–13.
- Agustí-Brisach C., Mostert L., Armengol J., 2014. Detection and quantification of *Ilyonectria* spp. associated with black-foot disease of grapevine in nursery soils using multiplex nested PCR and quantitative PCR. *Plant Pathology* 63: 316–322.
- Aigoun-Mouhous W., Elena G., Cabral A., León M., Sabaou N., ... Berraf-Tebbal A., 2019. Characterization and pathogenicity of *Cylindrocarpon*-like asexual morphs associated with black foot disease in Algerian grapevine nurseries, with the description of *Pleio-*
carpon algeriense sp. nov. *European Journal of Plant Pathology* 154: 887–901.
- Alaniz S., Leon M., García-Jiménez J., Abad P., Armengol, J., 2007. Characterization of *Cylindrocarpon* species associated with black-foot disease of grapevine in Spain. *Plant Disease* 91: 1187–1193.
- Alaniz S., Armengol J., García-Jiménez J., Abad-Campos P., León M., 2009a. A multiplex pcr system for the specific detection of *Cylindrocarpon lirioidendri*, *C. macrodidymum*, and *C. pauciseptatum* from grapevine. *Plant Disease* 93: 821–825.
- Alaniz S., Armengol J., León M., Garcia-Gimenez J., Abad-Campos P., 2009b. Analysis of genetic and virulence diversity of *Cylindrocarpon lirioidendri* and *C. macrodidymum* associated with black foot disease of grapevine. *Mythological Research* 113:16–23.
- Alaniz S., Abad-Campos P., García-Jiménez J., Armengol J., 2011. Evaluation of fungicides to control *Cylindrocarpon lirioidendri* and *Cylindrocarpon macrodidymum* in vitro, and their effect during the rooting phase in the grapevine propagation process. *Crop Protection* 30: 489–494.
- Berbegal M., Ramón-Albalat A., León M., Armengol J., 2020. Evaluation of long-term protection from nursery to vineyard provided by trichoderma atroviride sc1 against fungal grapevine trunk pathogens. *Pest Management Science* 76: 967–977.
- Berlanas C., Ojeda S., López-Manzanares B., Andrés-Sodupe M., Bujanda R., ... Gramaje D., 2020. Occurrence and diversity of black-foot disease fungi in symptomless grapevine nursery stock in Spain. *Plant Disease* 104: 94–104.
- Carbone I., Kohn L. M., 1999. A method for designing primer sets for speciation studies in filamentous ascomycetes. *Mycologia* 91: 553–556.
- Carlucci A., Lops F., Mostert L., Halleen F., Raimondo M. L., 2017. Occurrence fungi causing black foot on young grapevines and nursery rootstock plants in Italy. *Phytopathologia Mediterranea* 56: 10–39.
- Crous P. W., Groenewald J. Z., Risede J. M., Simoneau P., Hywel-Jones N. L., 2004. Calonectria species and their *Cylindrocladium* anamorphs: species with sphaeropedunculate vesicles. *Study in Mycology* 50: 415–430.
- Dissanayake A. J., Mei L., Wei Z., Zhen C., Udayanga D., ... Hyde K. D., 2015. Morphological and molecular characterisation of *Diaporthe* species associated with grapevine trunk disease in China. *Fungal Biology* 119: 283–294.
- De la Fuente M., Fontaine F., Gramaje D., Armengol J., ... Corio-Costet M.F., 2016. *Grapevine Trunk Diseases A Review*. OIV Publications, 1st Edn. Paris. <https://>

- www.oiv.int/public/medias/4650/trunk-diseases-oiv-2016.pdf
- Glass N. L., Donaldson G., 1995. Development of primer sets designed for use with PCR to amplify conserved genes from Filamentous ascomycetes. *Applied and Environmental Microbiology* 61: 1323–1330.
- Gramaje D., Alaniz S., Abad-Campos P., Garcia-Jimenez J., Armengol J., 2010. Effect of hot-water treatments in vitro on conidial germination and mycelial growth of grapevine trunk pathogens. *Annals of Applied Biology* 156: 231–241.
- Gramaje D., Armengol J., 2011. Fungal trunk pathogens in the grapevine propagation process: potential inoculum sources, detection, identification, and management strategies. *Plant Disease* 95: 1040–1055.
- Gramaje D., Úrbez-Torres J. R., Sosnowski M. R., 2018. Managing grapevine trunk diseases with respect to etiology and epidemiology: current strategies and future prospects. *Plant Disease* 102: 12–39.
- Grasso S., Magnano Di San Lio G., 1975. Infezioni di *Cylindrocarpon obtusisporum* su piante di vite in Sicilia. *Vitis* 14: 38–39.
- Guo L. D., Hyde K. D., Liew E. C. Y., 2000. Identification of endophytic fungi from *Livistona chinensis* based on morphology and rDNA sequences. *New Phytologist* 147: 617–630.
- Hall T. A. 1999. BioEdit: a user-friendly biological sequence alignment editor and analysis program for Windows 95/98/NT. *Nucleic Acids Symposium Series* 41: 95–98.
- Halleen F., Crous P. W., Petrini O., 2003. Fungi associated with healthy grapevine cuttings in nurseries, with special reference to pathogens involved in the decline of young vines. *Australasian Plant Pathology* 32: 47–52.
- Halleen F., Schroers H. J., Groenewald J. Z., Rego C., Oliveira H., Crous P. W., 2006. *Neonectria liriodendri* sp. nov. The main causal agent of black foot disease of grapevines. *Studies in Mycology* 55: 227–234.
- Halleen F., Fourie P.H., Crous P. W., 2007. Control of black foot disease in grapevine nurseries. *Plant Pathology* 56: 37–645
- Halleen F., Fourie P.H., 2016. An Integrated Strategy for the Proactive Management of Grapevine Trunk Disease Pathogen Infections in Grapevine Nurseries. *South African Journal for Enology and Viticulture* 37: 104–114.
- Hofstetter V., Buyck B., Croll D., Viret O., Couloux A., Gindro K., 2012. What if esca disease of grapevine were not a fungal disease? *Fungal Diversity* 54: 51–67.
- Katoh K., Rozewicki J., Yamada K. D., 2019. MAFFT online service: multiple sequence alignment, interactive sequence choice and visualization. *Briefings in Bioinformatics* 20: 1160–1166.
- Kishino H., Hasegawa M., 1989. Evaluation of the maximum likelihood estimate of the evolutionary tree topologies from DNA sequence data, and the branching order in Hominoidea. *Journal of Molecular Evolution* 29: 170–179.
- Koike S.T., Bettiga L.J., Nguyen T.T., and Gubler W.D., 2016. First report of *Cylindrocladiella lageniformis* and *C. peruviana* as grapevine pathogens in California. *Plant Disease* 100: 1783–1784.
- Kuraku S., Zmasek C. M., Nishimura O., Katoh K. 2013. aLeaves facilitates on-demand exploration of metazoan gene family trees on MAFFT sequence alignment server with enhanced interactivity. *Nucleic Acids Research* 41: W22–W28.
- Langenhoven S. D., Halleen F., Spies C. F. J., Stempien E., Mostert L., 2018. Detection and quantification of black foot and crown and root rot pathogens in grapevine nursery soils in the Western Cape of South Africa. *Phytopathologia Mediterranea* 57: 519–537.
- Larignon P., 1999. Black foot disease in France. In: (Morton L, ed.) *Proceedings of the Seminar and Workshop on Black Goo Symptoms and Occurrence of Grape Declines*. Fort Valley, VA, USA: International Ampelography Society 89–90.
- Lawrence D. P., Nouri M. T., Trouillas F. P., 2019. Taxonomy and multi-locus phylogeny of *Cylindrocarpon*-like species associated with diseases roots of grapevine and other fruit and nut crops in California. *Fungal Systematics and Evolution* 4: 59–75.
- Li H., Li R. Y., Wang H. 2007. New Disease for Wine-making Grape-Eutypa Dieback[J]. *Liquor-Making Science & Technology* 155: 48–50.(in Chinese)
- Li X. H., Yan J. Y., Kong F. F., Qiao G. H., Zhang Z. W., Wang Z. 2010. *Botryosphaeria dothidea* causing canker of grapevine newly reported in China. *Plant Pathology* 59: 1170–1170.
- Lombard L., Van Der Merwe N. A., Groenewald J. Z., Crous P. W., 2014. Lineages in *Nectriaceae*: re-evaluating the generic status of *Ilyonectria* and allied genera. *Phytopathologia Mediterranea* 53: 515–532.
- Manawasinghe I. S., Dissanayake A. J., Xing H.L., Mei L., Wanasinghe D. N., ... Ji Y.Y., 2019. High genetic diversity and species complexity of *Diaporthe* associated with grapevine dieback in China. *Frontiers in Microbiology* 10: 1936.
- Marin-Felix Y., Hernández-Restrepo M., Wingfield M. J., Akulov A., Carnegie A. J., ... Crous P.W., 2019. Genera of phytopathogenic fungi: GOPHY 2. *Studies in Mycology* 92: 47–133.

- Martínez-Diz M. P., Andrés-Sodupe M., Berbegal M., Bujanda R., Gramaje D., 2020. Droplet digital PCR technology for detection of *Ilyonectria liriodendri* from grapevine environmental samples. *Plant Disease* 104: 1144–1150.
- Martínez-Diz M.P., Díaz-Losada E., Andrés-Sodupe M., Bujanda R., Maldonado-González M.M., ... Gramaje D., 2021. Field evaluation of biocontrol agents against black-foot and Petri diseases of grapevine. *Pest Management Science* 77: 697–708.
- O'Donnell K., Cigelnik E., 1997. Two divergent intragenomic rDNA ITS2 types within a monophyletic lineage of the fungus *Fusarium* are nonorthologous. *Molecular Phylogenetics and Evolution* 7: 103–116.
- Pecenka J., Eichmeier A., Penazova E., Baranek M., Leon M., Armengol J. 2018. First report of *Dactylonectria torresensis* causing black-foot disease on grapevines in the Czech Republic. *Plant Disease* 102: 2038–2039.
- Petit E., Barriault E., Baumgartner K., Wilcox W. F., Rolshausen P. E., 2011. *Cylindrocarpon* species associated with black-foot of grapevine in northeastern United States and Southeastern Canada. *American Journal of Enology and Viticulture* 62: 177–183.
- Pintos C., Redondo V., Costas D., Aguin O., Mansilla P., 2019. Fungi associated with grapevine trunk diseases in nursery-produced *Vitis vinifera* plants. *Phytopathologia Mediterranea* 57: 407–424.
- Probst C. M., Ridgway H. J., Jaspers M. V., Jones E. E., 2019. Pathogenicity of *Ilyonectria liriodendri* and *Dactylonectria macrodidyma* propagules in grapevines. *European Journal of Plant Pathology* 154: 405–421.
- Rambaut A., FigTree v1.4.4: Tree figure drawing tool. 2018. <https://github.com/rambaut/figtree/releases>
- Rego C., Oliveira H., Carvalho A., Phillips A., 2000. Involvement of *Phaeoacremonium* spp. and *Cylindrocarpon destructans* with grapevine decline in Portugal. *Phytopathologia Mediterranea* 39: 76–79.
- Rego C., Farropas L., Nascimento T., Cabral A., Oliveira H. 2006. Black foot of grapevine, sensitivity of *Cylindrocarpon destructans* to fungicides. *Phytopathologia Mediterranea* 45: 93–100.
- Rego C., Nascimento T., Cabral A., Silva M. J., Oliveira H., 2009. Control of grapevine wood fungi in commercial nurseries. *Phytopathologia Mediterranea* 48: 128–135.
- Silvestro D., Michalak I., 2016. RaxmlGUI: a graphical front-end for RAXML. Retrieved at 29 December 2016, from <http://sourceforge.net/projects/raxmlgui/>.
- Swofford D. L., 2002. PAUP* 4.0: phylogenetic analysis using parsimony (and other methods). Sinauer Associates, Sunderland, Massachusetts, USA.
- Udayanga, D., Liu, X. Z., Crous, P. W., McKenzie, E. H. C., Chukeatirote, E., and Hyde, K. D., 2012a. A multi-locus phylogenetic evaluation of *Diaporthe* (*Phomopsis*). *Fungal Diversity* 56: 157–171.
- Udayanga D., Liu X. X., Crous P. W., McKenzie E. H. C., Chukeatirote E., Hyde K. D., 2012b. Multilocus phylogeny of *Diaporthe* reveals three new cryptic species from Thailand. *Cryptogamie Mycologie* 33: 295–309.
- Van Coller G.J., Denman S., Groenewald J.Z., Lamprecht S.C., and Crous P.W., 2005. Characterisation and pathogenicity of *Cylindrocladiella* spp. associated with root and cutting rot symptoms of grapevines in nurseries. *Australasian Plant Pathology* 34: 489–498.
- van Jaarsveld W. J., Halleen F., Mostert L., 2020. In vitro screening of *Trichoderma* isolates for biocontrol of black foot disease pathogens. *Phytopathologia Mediterranea* 59: 465–471.
- van Jaarsveld, W. J. , Halleen F. , Bester M. C., Pierron R. J., Stempien E., Mostert L., 2021. Investigation of *Trichoderma* species colonization of nursery grapevines for improved management of black foot disease. *Pest Management Science* 77: 397–405.
- Waite H., May P., Bossinger G., 2013. Variations in phytosanitary and other management practices in Australian grapevine nurseries. *Phytopathologia Mediterranea* 52: 369–379.
- White T. J., Bruns T., Lee S., Taylor J., 1990. Amplification and direct sequencing of fungal ribosomal RNA genes for phylogenetics. In: PCR Protocols: A Guide to Methods and Applications. M.A. Innis, D.H. Gelfand, J.J. Sninsky and T.J. White, eds. Academic Press Inc., New York, NY, USA, 315–322.
- Wilcox W. F., Gubler W. D., Uyemoto J. K., 2006. *Compendium of Grape Diseases, Disorders, and Pests*, Second Edition. American Phytopathological Society, St. Paul, Minnesota, USA, 232 pp.
- Yan J. Y., Yue X., Wei Z., Yong W., ... Xing H.L., 2013. Species of *Botryosphaeriaceae* involved in grapevine dieback in China. *Fungal Diversity* 61: 221–236.
- Ye Q.T., Manawasinghe I.S., Wei Z., Mugnai L., Hyde K.D., Xing H.L., Ji Y.Y., 2020. First Report of *Phaeoacremonium minimum* associated with grapevine trunk diseases in China. *Plant Disease* 104: 1259–1259.



Citation: G.L. Bruno, M.P. Ippolito, F. Mannerucci, L. Bragazzi, F. Tommasi (2021) Physiological responses of 'Italia' grapevines infected with Esca pathogens. *Phytopathologia Mediterranea* 60(2): 321-336. doi: 10.36253/phyto-12171

Accepted: March 1, 2021

Published: September 13, 2021

Copyright: © 2021 G.L. Bruno, M.P. Ippolito, F. Mannerucci, L. Bragazzi, F. Tommasi. This is an open access, peer-reviewed article published by Firenze University Press (<http://www.fupress.com/pm>) and distributed under the terms of the Creative Commons Attribution License, which permits unrestricted use, distribution, and reproduction in any medium, provided the original author and source are credited.

Data Availability Statement: All relevant data are within the paper.

Competing Interests: The Author(s) declare(s) no conflict of interest.

Editor: Hanns-Heinz Kassemeyer, Staatliches Weinbauinstitut Freiburg, Germany.

Research Papers

Physiological responses of 'Italia' grapevines infected with Esca pathogens[‡]

GIOVANNI LUIGI BRUNO^{1,*}, MARIA PAOLA IPPOLITO², FRANCESCO MANNERUCCI¹, LUCA BRAGAZZI¹, FRANCA TOMMASI²

¹ Department of Soil, Plant and Food Sciences (Di.S.S.P.A.) - Plant pathology Unit, University of Bari Aldo Moro, Via G. Amendola, 165/A; 70126 - Bari, Italy

² Department of Biology, University of Bari Aldo Moro, Via Orabona, 4; 70125 - Bari, Italy

*Corresponding author. E-mail: giovanniluigi.bruno@uniba.it

‡ Dedicated to the memory of Antonio Graniti (1926-2019), Emeritus Professor of Plant Pathology at the University of Bari, Italy.

Summary. Physiological features were examined of a 20-year-old *Vitis vinifera* 'Italia' table grape vineyard cropped in Apulia, Italy. Healthy vines with no foliar symptoms and any indications of wood or berry alterations, vines with natural wood infections by *Phaeoacremonium minimum* (syn. *P. aleophilum*) and *Phaeoaniella chlamydospora* showing brown wood streaking symptoms, and vines naturally infected with *P. minimum*, *P. chlamydospora* and *Fomitiporia mediterranea* with brown wood streaking and white rot symptoms, were surveyed. Bleeding xylem sap, collected at bud-break from healthy vines showed the greatest total ascorbic acid level, while vines with brown wood streaking and white rot had the greatest viscosity coefficient, glutathione concentration, and plant growth regulator activities. Compared to healthy vines, leaves of wood affected vines, sampled during the unfolded leaf, fruit setting, cluster closing and bunch ripening vine growth stages, had reduced fresh and dry weights, total chlorophyll concentrations, and increased leaf surface area. Low ascorbic acid and reduced glutathione concentrations, weak redox state, and moderate levels of dehydroascorbic acid and oxidized glutathione were also detected in these vines. Analyses also detected reduced activities of dehydroascorbate reductase, ascorbate free radical reductase and glutathione reductase in diseased vines. The cell membrane damage, associated with lipid peroxidation, was coupled with high hydrogen peroxide concentrations. These changes could contribute to the cell death of leaves and foliar symptom development. The ascorbate-glutathione cycle supports grapevine susceptibility to Esca complex-associated fungi.

Keywords. Antioxidant systems, ascorbic acid, glutathione, membrane lipid peroxidation, redox state, hydrogen peroxide.

INTRODUCTION

The disease commonly called "Esca" is one of the longest recognized and most destructive diseases of grapevines (*Vitis vinifera*), and is associated with wood discolouration and decay, and sudden wilting of whole vines

or individual vine arms within a few days (apoplexy or apoplectic symptoms), as well as leaf tiger stripe leaf symptoms (Ravaz, 1898; de Rolland, 1873; Marsais, 1923). Esca is now considered to be a complex of different diseases overlapping in the same vine or developing at different stages of a vine life. Esca-complex comprises brown wood streaking of grapevine cuttings, Petri disease, grapevine leaf stripe disease (GLSD, previously “young esca”), and white rot (which is at the origin of the name Esca). GLSD affects young and old vines, which show wood streaking and discolouration. The association between GLSD and white rot was described as a condition called “Esca proper”. Within the Esca complex, white rot, and Esca proper can also show apoplectic symptoms (Surico, 2009; Mondello *et al.*, 2018). Brown wood streaking, Petri disease and GLSD are also grouped under the name phaeotracheomycosis complex (Bertsch *et al.*, 2012).

Members of the basidiomycetous genus *Fomitiporia* (*F. mediterranea* mainly in Europe and the Mediterranean area) are associated with wood decay of white rot (Fischer, 2002; 2006; Ciccarone *et al.*, 2004). *Phaeoacremonium minimum* (syn. *P. aleophilum*) and *Phaeomoniliella chlamydospora* are the most important etiological agents of brown wood streaking, Petri disease and GLSD (Mugnai *et al.*, 1999; Surico, 2009; Baranek *et al.*, 2018). Other species of *Phaeoacremonium* and *Cadophora* are present in the wood of grapevines affected by Esca complex diseases (Moreno-Sanz *et al.*, 2013; Elena *et al.*, 2018; Jayawardena *et al.*, 2018).

No pathogens have been isolated from leaves or berries of infected plants. Leaf tiger stripe and berry symptoms are considered linked to cultivar susceptibility, vine age, the microorganisms involved, pedoclimatic conditions and other physiological factors (Graniti *et al.*, 2000; Surico *et al.*, 2006; Bertsch *et al.*, 2012; Guérin-Dubrana *et al.*, 2013; Claverie *et al.*, 2020). The substances originating in the discoloured woody tissues of affected trunks and branches contribute to development of the typical symptoms on leaves (Andolfi *et al.*, 2011; Bertsch *et al.*, 2012; Lecomte *et al.*, 2012). These materials could be reaction products of the diseased wood, phytotoxic metabolites excreted by Esca-associated fungi, or a combination of these (Mugnai *et al.*, 1999; Bruno *et al.*, 2007). *P. minimum* and *P. chlamydospora* produce two naphthalenone pentaketides, scytalone and isosclerone, and exopolysaccharides including the α -glucan pullulan (Evidente *et al.*, 2000; Tabacchi *et al.*, 2000; Bruno and Sparapano 2006a; 2006b; 2007). Macro- and micro-nutrients also play roles in Esca complex symptom progression (Calzarano *et al.*, 2009, 2014; Calzarano and Di Marco, 2018).

Stomata closure and changes in the photosynthetic apparatuses affect the pre-symptomatic leaves of Esca diseased grapevines (Petit *et al.*, 2006; Magnin-Robert *et al.*, 2011). Low density cytoplasm, plastids with small starch grains, underdeveloped grana, and elongated thylakoids occur in grapevine leaves before tiger stripes develop (Lima *et al.*, 2010; Fontaine *et al.*, 2016). Glutathione pools, PR-proteins, and phenolic compounds are also affected (Magnin-Robert *et al.*, 2011; Valtaud *et al.*, 2011; Lambert *et al.*, 2013; Calzarano *et al.*, 2016; 2017a; 2017b; Fontaine *et al.*, 2016). Xylem dysfunction also influences water transport and leaf water potential (Bruno *et al.*, 2007; Fontaine *et al.*, 2016), and NMR metabolomics data suggest increased phenylpropanoid compound production and decreased glucose and fructose contents occur in leaves of Esca complex diseased vines (Lima *et al.*, 2010).

The aim of the present study was to gain insight into variations of physiological features of bleeding xylem sap and leaves of ‘Italia’ grapevine plants that were either healthy or naturally infected with *P. minimum* and *P. chlamydospora* showing brown wood streaking, or infected with *P. minimum*, *P. chlamydospora* and *F. mediterranea* showing brown wood streaking and white rot. Special emphasis was placed on the differences in hydrogen peroxide, lipid peroxidation, and antioxidant defence responses associated with the ascorbate-glutathione cycle. The changes in the physiology of diseased plants were assessed as possible factors in development of foliar symptoms.

MATERIALS AND METHODS

Vineyard

A 20-year-old *V. vinifera* ‘Italia’ table grape vineyard (1600 vines) cropped in the countryside of Bari (Apulia, southern Italy) was used for sample collection. The vines, grafted onto 140-Ru rootstock, were trained by the Tendone system, and grown under irrigation in an alkaline clay soil. Since 2006, each vine had been under observation for symptom development of diseases within the Esca complex, i.e., foliar symptoms, or sudden wilting of GLSD or esca proper.

Wood core sampling and vine characterization

To assess the presence of symptoms and fungi in the grapevine trunks, two wood cores per vine were taken with a 95% ethanol pre-sterilised Pressler increment borer at 30 and 110 cm above the ground level. All the 1600

vines were surveyed. To prevent further wood contamination, wood core sampling holes were disinfected with copper oxychloride solution (20% in water) and filled with 2.5% copper oxychloride in linseed oil. Each core was cut to fragments 1.5–2 cm in length. Slices were surface-sterilized for 1 min in 70% ethanol, soaked for 1–2 min in a sodium hypochlorite solution (3% active chlorine), and rinsed three times in sterile distilled water. The slices were then aseptically cut into pieces that were seeded onto 90 mm diam. Petri dishes (five per plate) containing agar media. Malt extract (2%) agar (MEA), MEA amended with 0.25% chloramphenicol (MEAC) and MEA amended with 0.25% benomyl (MEAB) were used as the isolation media. MEAC and MEAB were used as semi-selective media for detection, respectively, of phaeotracheomycotic and basidiomycete fungi. Inoculated plates were incubated at $25\pm 1^\circ\text{C}$ in the dark. The isolation frequency (IF) of each fungus taxon was calculated as $\text{IF} = 100 \times (N_i/N_t)$, where N_i was the number of wood-fragments from which the fungus was isolated and N_t the total number of seeded wood tissue pieces.

At completion of characterizations of the vine wood, associated with leaves and berries symptoms surveyed during 12 years, 15 vines were selected, including five with brown wood streaking, five with brown wood streaking and white rot, and five healthy (symptomless) that did not show any foliar symptoms, and any indications of wood or berry alterations.

Bleeding xylem sap sampling and characterization

To evaluate bleeding sap quantity, viscosity, and ascorbate, glutathione and hormone concentrations, bleeding xylem sap was collected from five vines with brown wood streaking, five with brown wood streaking and white rot, and five healthy vines. Bleeding xylem sap was collected at the bud-break vine growth stage (Baggiolini, 1979; Wilcox *et al.*, 2015). From each selected plant, four vine shoots were cut and the end of each spur was surface-treated with sodium hypochlorite solution (3% active chlorine), then with 95% ethanol, and then rinsed twice with sterile distilled water. The sap exuded during the first 15 min was discarded. A sterile plastic bottle covered with aluminium foil was secured at the end of each bleeding spur to collect the liquid over the following 4 d. All sap samples were filtered through 0.45 mm membranes (Millipore).

The dynamic viscosity (η_x) of each sap sample was calculated as $\eta_x = [(\rho_s \times t_x) / (\rho_w \times t_w)] \times \eta_w$, where ρ_s = sap density, ρ_w = water density, η_w = water dynamic viscosity (0.8937×10^{-3} Poiseuille), t_s = flow time of sap in sec, and t_w = water flow time (sec). Measurements of t_s and

t_w were carried at $25\pm 0.1^\circ\text{C}$ using an Ostwald glass capillary viscometer (Cannon-Fenske Instruments).

For each sap sample, 2 mL were lyophilized, and the resulting powder was treated with 5% metaphosphoric acid (6 mL). After centrifugation (20,000g, 15 min, 4°C), the supernatant was used for total ascorbate and total glutathione determinations following the method of Zhang and Kirkham (1996).

The physiological effects of growth regulator substances in the xylem sap were evaluated using the filter paper disk method (Zhao *et al.*, 1992), with excised cucumber (*Cucumis sativus*) cotyledon root formation (auxin) and cucumber cotyledon expansion (kinetin) bioassays. Indole-3-acetic acid and 6-furfurylaminopurine were dissolved in 95% ethanol and tested in the range of $0.3\text{--}50.0 \mu\text{g mL}^{-1}$, and 95% ethanol was used as a control.

Leaf sampling and characterization

To evaluate leaf fresh and dry weights, and areas, as well as total chlorophyll, hydrogen peroxide, lipid peroxidation, ascorbic acid, dehydroascorbic acid, reduced and oxidized glutathione concentrations and the activity of enzymes involved in ascorbate regeneration, leaves were collected from the selected 15 vines. Leaves (ten per vine) were randomly picked from each vine during the unfolded leaf, fruit setting, cluster closing, and bunch ripening vine growth stages (Baggiolini, 1979; Wilcox *et al.*, 2015). At the cluster closing and bunch ripening vine growth stages of the diseased vines, symptomless and symptomatic leaves were sampled. The leaf petioles were removed, and the leaves were photographed.

Each leaf was weighed with a Sartorius BP 210S analytical balance (Data Weighing Systems, Inc.) to assess leaf fresh weight.

Leaf area was estimated using ImageJ open-source image-processing software (National Institutes of Health).

Leaf dry weight was measured by drying 100 mg of leaves for 20 min at 105°C using an infrared LP 16-M desiccator (Mettler-Toledo SpA). Leaf moisture was calculated as a percentage (%) of fresh weight.

Total chlorophyll concentration was verified by Harborne's method (1973) using leaf lamina samples (2 g each) and 80% acetone (16 mL) as extraction solvent in an ice bath. Absorbance at 645 and 663 nm were measured using a Beckman DU 640 spectrophotometer (Beckman Coulter Inc.).

Hydrogen peroxide content was determined as reported by Lee and Lee (2000), using 1 g of leaf lamina ground with 4 mL of sodium phosphate buffer (0.1 M; pH 6.5).

Lipid peroxidation was assessed as malondialdehyde (MDA) quantity in 200 mg of leaf lamina samples (Heath and Packer, 1968).

Ascorbic acid, dehydroascorbic acid, and reduced and oxidized glutathione were quantified in 2 g of ground leaf lamina samples, at 4°C, in 5% metaphosphoric acid (6 mL). After centrifugation (20,000g, 15 min, 4°C), the supernatant was used as proposed by Zhang and Kirkham (1996). The ascorbate redox state (A-RS) was calculated as $A-RS = [AsA / (AsA + DHA)]$, where AsA represents ascorbic acid and DHA represents dehydroascorbic acid. The glutathione redox state (G-RS) was calculated as $G-RS = [GSH / (GSH + GSSG)]$, where GSH represents reduced glutathione, and GSSG represents oxidized glutathione.

The activity of enzymes involved in ascorbate regeneration was detected on 2 g of leaf lamina homogenized in 6 mL of extraction buffer (50 mM Tris-HCl, pH 7.8; 0.3 mM mannitol; 10 mM MgCl₂; 1 mM EDTA; 0.05% cysteine) at 4°C. After centrifugation (25,000g, 15 min, 4°C), the supernatant was dialyzed against 50 mM Tris-HCl (pH 7.8) and used to determine activities of ascorbate peroxidase (EC 1.11.1.11), dehydroascorbate reductase (EC 1.8.5.1), glutathione reductase (EC 1.6.4.2), and ascorbate free radical reductase (= monodehydroascorbate reductase, EC 1.6.5.4), according to Paciolla *et al.* (2008).

Statistical analyses

Data were subjected to general linear analysis of variance models using the SAS/STAT version 9.0 (SAS Institute Inc.). Normal distributions were assessed using the Shapiro-Wilk tests, and homoscedasticity was assessed using Bartlett's tests. Means were compared using Fisher's LSD test at $P \leq 0.05$. Data of morphological and physiological features of the grapevine leaves were analysed for vine typology (brown wood streaking, brown wood streaking and white rot, or healthy), vine growth stages (unfolded leaf, fruit setting, cluster closing, or bunch ripening), symptoms on leaves (presence or absence), and their interactions.

RESULTS

Wood core and symptom examination

The wood core examinations showed that 562 vines had brown wood streaking, 176 had brown wood streaking and rotted wood in the trunks, and 862 vines were healthy. *P. chlamydospora* and *P. minimum* were always associated with brown wood streaking, while *F. medi-*

Table 1. Isolation frequency (%) of fungus species obtained from 'Italia' vines that were healthy (H), affected with brown wood streaking (BWS) or with brown wood streaking and white rot (BWSWR).

Fungus	Vines ^a		
	H	BWS	BWSWR
<i>Phaeoconiella chlamydospora</i>	0	45±4	38±3
<i>Phaeoacremonium minimum</i>	0	25±2	30±4
<i>Fomitiporia mediterranea</i>	0	0	87±6
Other fungi ^b	3±1	6±1	4±1
No isolations	97±2	10±2	9±2

^a For each group of vines, data are means for 900 woody chips ± standard deviation.

^b *Penicillium* spp., *Alternaria* spp., *Paecilomyces* spp., *Trichoderma* spp., *Chaetomium* spp., *Cladosporium* spp., *Paraconiothyrium* spp. and sterile fungi.

terranea was isolated only from rotted wood (Table 1). Other micromycetes, including species of *Penicillium*, *Alternaria*, *Paecilomyces*, *Trichoderma*, *Chaetomium*, *Cladosporium*, and *Paraconiothyrium*, and sterile fungi, were also isolated from diseased vines. Species of *Penicillium* and *Alternaria* were the only fungi isolated from cores from the healthy vines.

During the survey, symptoms were recorded on leaves and berries of diseased vines (Figure 1). The typical tiger stripe symptoms were first observed in July on vines with brown wood streaking and with brown wood streaking and rotted wood in the trunks. On plants also infected with *F. mediterranea*, trunk cracking was recorded. No apoplexy was viewed on selected vines throughout the survey.

Bleeding xylem sap characterization

Healthy vines discharged the lowest quantities of xylem sap. Both typologies of diseased vines discharged four- and five-fold more sap than the healthy vines, and the sap from these vines had the greatest dynamic viscosity coefficients, total ascorbic acid and glutathione concentrations, and auxin-like and kinetin activities (Table 2).

Leaf characterization

A selection of leaves sampled from the 15 selected vines is illustrated in Figure 1G. Morphological and physiological features were strongly affected by the vine growth stages, vine typology, symptom development, and their interactions (Table 3).

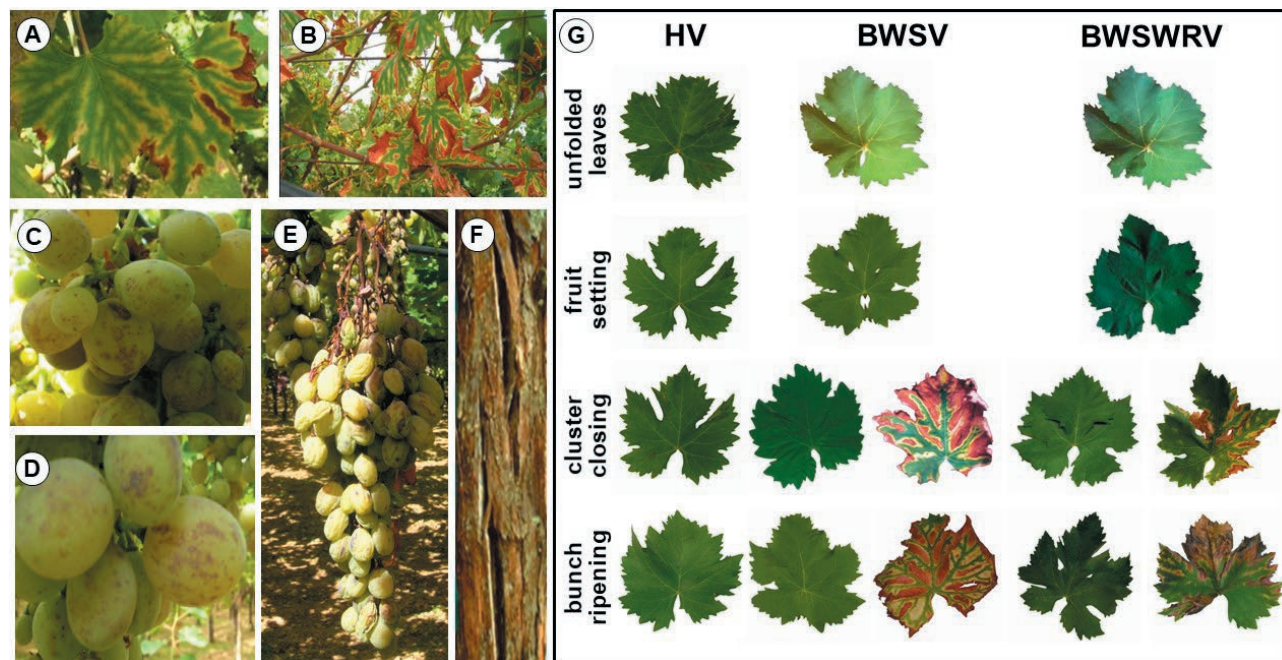


Figure 1. Symptoms developed in the 20-year-old *Vitis vinifera* 'Italia' vineyard. Chlorotic areas (A) and 'tiger stripes' (B) on leaves; spots on the skin (C-D) and wilt (E) of berries and cracking of the trunk (F) of the diseased vine. A selection of leaves (G) collected during the vine growth stages of unfolded leaves, fruit set, cluster closing and bunch ripening, from healthy vines (HV), vines with brown wood streaking (BWSV) or vines with brown wood streaking and white rot (BWSWRV).

Table 2. Flux, viscosity coefficient (h_x), concentrations of total ascorbate (T-ASC), glutathione (T-GLU), and growth regulator activity (GRA) of bleeding xylem sap collected from 'Italia' vines^a that were healthy (H), or had brown wood streaking (BWS) or brown wood-streaking and white rot (BWSWR).

Vines	Flux ^b (mL vine ⁻¹)	h_x ^d (Poiseuille)	T-ASC ^c ($\mu\text{g mL}^{-1}$)	T-GLU ^c ($\mu\text{g mL}^{-1}$)	GRA ($\mu\text{g mL}^{-1}$)	
					Auxin ^e	Kinetin ^e
H	144 ± 9.82 C	0.85 ± 0.04 C	308.6 ± 26.4 A	18.1 ± 3.1 C	10.25 ± 1.7 C	0.91 ± 0.27 B
BWS	677 ± 11.79 A	1.13 ± 0.04 B	211.2 ± 26.6 C	46.4 ± 8.6 B	20.10 ± 3.5 B	22.25 ± 2.45 A
BWSWR	574 ± 9.165 B	1.73 ± 0.07 A	269.1 ± 26.9 B	178.2 ± 38.1 A	30.05 ± 3.9 A	22.45 ± 2.04 A

^a For each column, values accompanied by the same letters are not significantly different ($P < 0.05$), Fisher's LSD test.

^b Each value is the means of five vines ± standard deviation.

^c Data are means of 15 replicates ± standard deviations.

^d Values are means of 50 replicates ± standard deviations.

^e Data are means of 20 replicates ± standard deviations.

Only symptomatic leaves collected from vines with brown wood streaking and white rot at cluster closing stages showed a small decrease (29.6%) in fresh weight compared with symptomless leaves collected from the same vines. At bunch ripening, leaves from healthy vines and symptomless leaves from vines with brown wood streaking and white rot reached maximum fresh weight. Symptomless leaves of vines with brown wood streaking had reduced mean leaf fresh weight compared with healthy vines. Symptomatic leaves from vines with

both disease typologies had leaves with fresh weights that were further 35–40% less.

The greatest leaf dry weight (Figure 2B) was recorded at the bunch ripening phase from symptomatic leaves of vines with brown wood streaking and white rot.

No statistically significant differences were found in leaf moisture content for the different vine disease categories. Leaf moisture contents were in the range 90 to 95% of leaf fresh weight.

Surface areas of leaves sampled at unfolded leaf and

Table 3. Results of general linear analyses of variance considering effects of sampling time (ST), vine typology (VT), symptoms (SY) and their interactions on leaf fresh (Lfw) and dry (Ldw) weights, moisture content (WC), surface area (LSA), and contents of chlorophyll (Chlo), hydrogen peroxide (H_2O_2), malondialdehyde (MDA), ascorbic acid (AsA), dehydroascorbic acid (DHA), reduced (GSH) and oxidized (GSSG) glutathione, and activities of ascorbate peroxidase (APX), dehydroascorbate reductase (DHA-R), glutathione reductase (G-R), or ascorbate free radical reductase (AFR-R).

Sources of variation	df	F values ^a														
		Lfw	Ldw	WC ^b	LSA	Chlo	H_2O_2	MDA	AsA	DHA	GSH	GSSG	APX	DHA-R	AFR-R	G-R
ST	3	19.80**	177.11**	75.27	476.46**	208.09**	47.83**	196.30*	22.67**	67.45*	173.96**	15.11**	0.16	22.45**	27.85**	28.19**
VT	2	27.74**	41.28**	35.80**	47.98**	118.98**	279.69**	250.53**	2193.37**	68.80**	2211.61**	141.76**	5.23*	89.61**	83.32**	168.52**
ST×VT	6	12.67**	17.70**	22.58**	14.71*	23.60**	41.24**	66.28**	18.45**	127.74**	149.93**	59.85**	5.77*	3.40	26.45**	49.21**
SY	1	84.39**	176.76**	22.65	73.09**	94.52**	22.84**	293.71**	187.21	265.55**	6.51**	12.21**	0.12	59.59**	39.94**	2.36
ST×SY	1	5.27**	6.90**	12.15	2.91	14.67**	1.81*	62.38**	6.81*	189.80**	0.37	0.26	1.51	6.62	1.65	0.32
VT×SY	1	27.56**	42.73**	11.24	239.69**	0.78	12.68**	2.56	9.08**	12.32**	0.31	6.13**	0.12	52.59**	38.39**	3.10*
ST×VT×SY	1	2.69	0.89	1.27	235.58**	0.78	1.19	1.65	9.08**	26.24**	1.62	1.19	0.02	5.98	5.54	1.02

^a * and ** indicate, respectively, $P = 0.05$ and 0.01 .

^b ln (Y) transformation used to stabilize variances.

fruit set stages did not show any statistically significant differences, while the leaves of healthy vines were significantly smaller than those of diseased plants during the other two vine growth stages (Figure 2C). At cluster closing stage, the surface areas of symptomless leaves from diseased vines were 2-fold greater than for leave from the healthy vines. At bunch ripening, symptomatic and symptomless leaves of diseased vines had leaf surface areas that were three times greater than leaves from the healthy vines.

During the four sampling times, total chlorophyll concentration in healthy vines was in the range of 160-165 mg g⁻¹ leaf fresh weight (Figure 3A). At the cluster closing and bunch ripening stages, diseased plants had less total chlorophyll. At cluster closing, in comparison with healthy vines, symptomless leaves from vines with brown wood streaking had 20% less total chlorophyll. This loss in symptomatic leaves was greater than 40%. Symptomless leaves from vines with brown wood streaking and white rot had 31% less total chlorophyll compared with healthy vines, and symptomatic leaves had a further 36% less total chlorophyll.

During the assessed four vine growth stages, healthy vines showed the least H_2O_2 concentrations (Figure 3B). Symptomless leaves collected from vines with brown wood streaking had increased H_2O_2 content compared with the healthy vines. Symptomatic leaves collected during cluster closing and bunch ripening had 20% more H_2O_2 than healthy vines. Leaves from vines with brown wood streaking and white rot, had more H_2O_2 than healthy vines at all four growth stages. Symptomatic leaves collected during cluster closing or bunch ripening had 3% more H_2O_2 than symptomless ones.

MDA concentrations were different between healthy vines and the two categories of disease at the four vine growth stages (Figure 3C). Healthy vines reached minimum MDA contents in the unfolded leaf stage, and the greatest MDA concentration was occurred during bunch ripening. A similar trend was recorded in symptomless leaves from vines with brown wood streaking, but the final MDA concentrations were greater than in healthy vines. Symptomless leaves from vines with brown wood streaking and white rot, compared to healthy vines, had greater MDA content at all the sampling times. At the cluster closing and bunch ripening stages, symptomatic leaves from the same vines showed, respectively, further 43% and 11% increases in MDA contents.

During the four sampling times, ascorbic acid concentrations in healthy vines were always greater than in leaves from diseased vines (Figure 4A). At each assessed growth stage, ascorbic acid contents were reduced by up to 78% in leaves collected from vines with brown wood

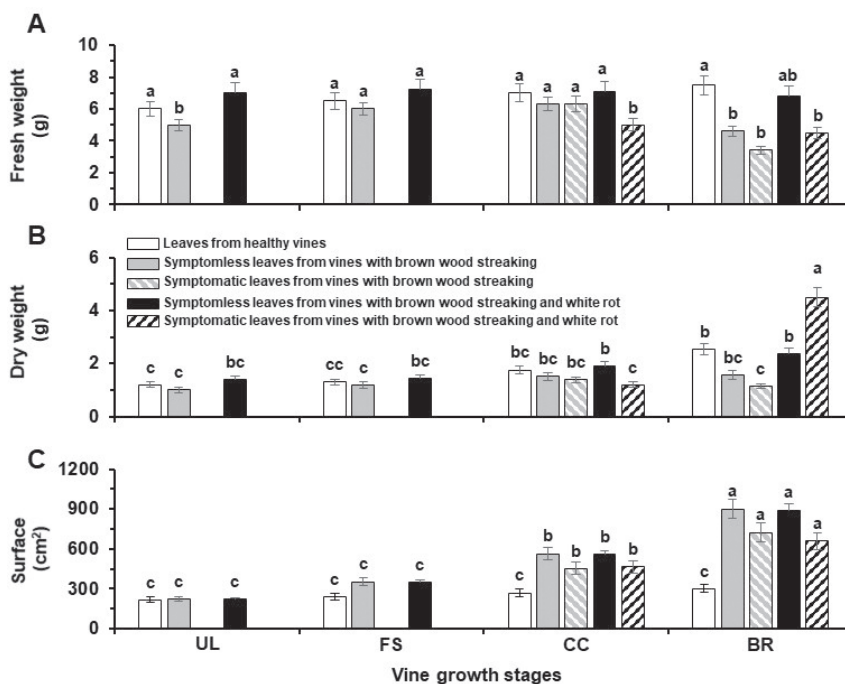


Figure 2. Fresh (A) and dry (B) weights, and surface areas (C) of ‘Italia’ leaves collected during the unfolded leaf (UL), fruit set (FS), cluster closing (CC) and bunch ripening (BR) vine growth stages from infected or healthy vines. Data are the means of 50 replicates \pm standard deviations. For each parameter, values accompanied by the same letters are not significantly different ($P \leq 0.05$) according to Fisher’s LSD test.

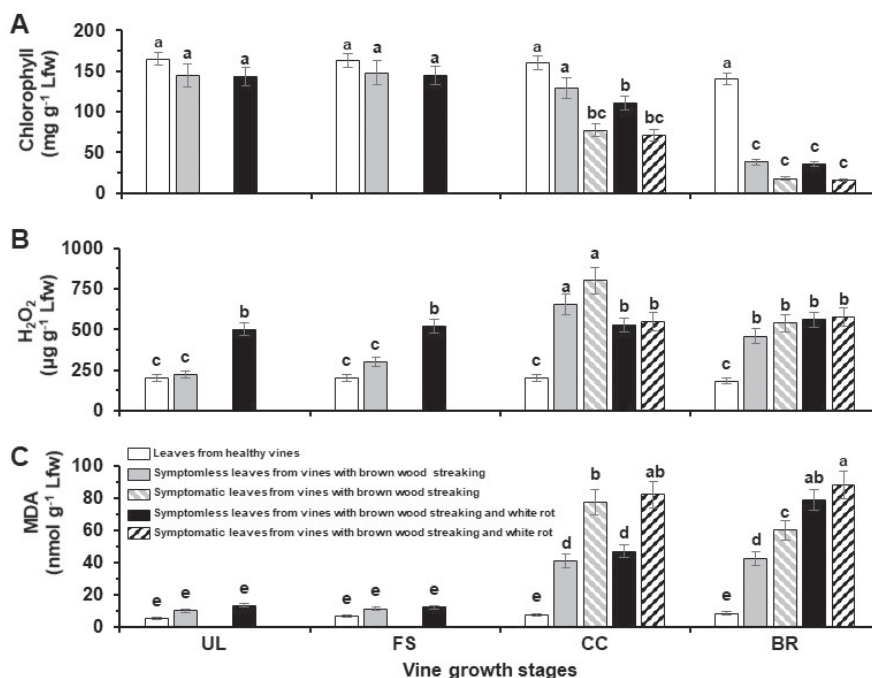


Figure 3. Total chlorophyll (A), hydrogen peroxide (H_2O_2 ; B) and malondialdehyde (MDA; C) concentrations of ‘Italia’ leaves collected during the unfolded leaf (UL), fruit set (FS), cluster closing (CC) and bunch ripening (BR) vine growth stages, from infected or healthy vines. Data are the means of 50 replicates \pm standard deviations. For each parameter, values accompanied by the same letters are not significantly different ($P \leq 0.05$) according to Fisher’s LSD test.

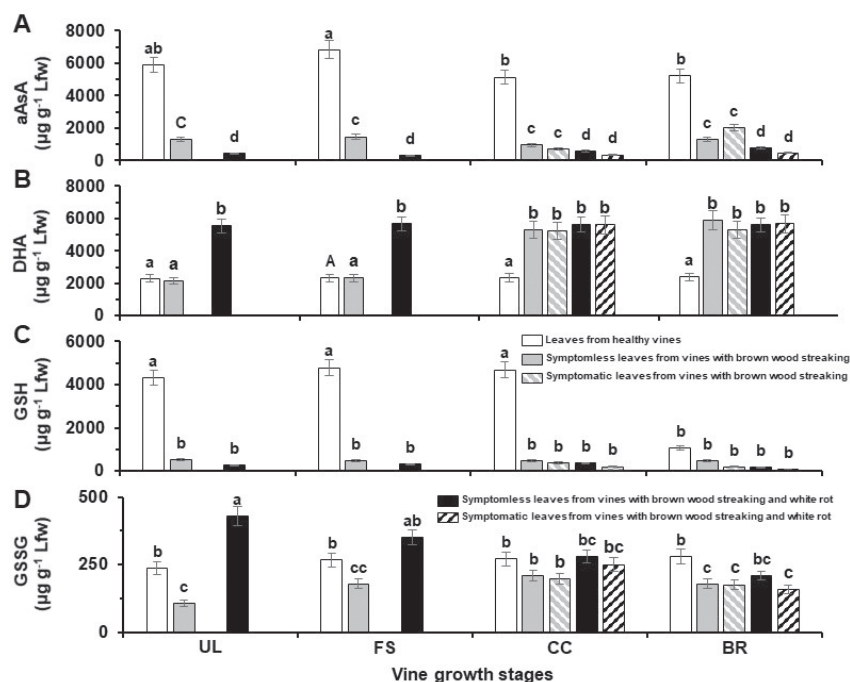


Figure 4. Ascorbic acid (aAsA; A), dehydroascorbic acid (DHA; B), reduced (GSH; C) and oxidized (GSSG; D) glutathione concentrations of 'Italia' leaves collected during the unfolded leaf (UL), fruit set (FS), cluster closing (CC) and bunch ripening (BR) vine growth stages, from infected or healthy vines. Data are the means of 50 replicates \pm standard deviations. For each parameter, values accompanied by the same letters are not significantly different ($P \leq 0.05$) according to Fisher's LSD test.

streaking, and 91% in leaves from vines with brown wood streaking and white rot.

Leaves from healthy vines showed similar levels of dehydroascorbic acid during the four assessed growth stages (Figure 4B). In the unfolded leaf and fruit set stages, leaves collected from vines with brown wood streaking and white rot showed the greatest dehydroascorbic acid concentrations.

The reduced glutathione contents of leaves collected from healthy vines were greater than in leaves collected from diseased plants (Figure 4C).

The oxidized glutathione amounts (Figure 4D) in symptomless leaves collected from vines with brown wood streaking, during the four considered growth stages, were approx. 38% less than in leaves from the healthy vines.

The lowest redox states (Table 4) were recorded in all symptomatic leaves tested.

No significant differences were detected between healthy and diseased vines in ascorbate peroxidase activity (Figure 5A) during the four growth stages.

Dehydroascorbate reductase activity (Figure 5B) in leaves from healthy vines and symptomless diseased vines reached minima in the unfolded leaf growth stage and were greatest at the bunch ripening stage.

Ascorbate free radical reductase activity (Figure 5C) in leaves from healthy vines was the least at the unfolded leaf stage, increased during the next two growth stages, and reached a maximum at the bunch ripening stage. Compared to healthy vines, at the cluster closing and bunch ripening stages, leaves from diseased vines had reduced ascorbate free radical reductase activities.

Glutathione reductase activity (Figure 5D) in leaves from healthy vines was least during the unfolded leaf stage and reached a maximum at bunch ripening. Compared to healthy vines, leaves from diseased vines had reduced glutathione reductase activity. No significant changes in glutathione reductase activity were detected in symptomless compared to symptomatic leaves from diseased vines.

DISCUSSION

In this study, in a 20-year-old 'Italia' vineyard surveyed since 2006 for symptoms of diseases within the Esca complex, we selected vines with brown wood streaking, vines with brown wood streaking and white rot, and healthy vines. The fungus isolation procedure confirmed the presence of *P. minimum* and *P. chlamydo-*

Table 4. Ascorbate and glutathione redox states in symptomless or symptomatic grapevine leaves collected from 'Italia' grapevines during the vine growth stages of unfolded leaves (UL), fruit set (FS), cluster closing (CC) or bunch ripening (BR), from healthy vines (HV), or vines with brown wood streaking (BWSV) or brown wood streaking and white rot (BWSWRV).

Leaves from	Vine growth stages			
	UL	FS	CC	BR
<i>Ascorbate redox state</i> ^a				
HV	0.72 ± 0.05	0.75 ± 0.05	0.69 ± 0.05	0.69 ± 0.05
BWSV symptomless	0.36 ± 0.02	0.38 ± 0.02	0.15 ± 0.01	0.18 ± 0.02
symptomatic	n.p. ^b	n.p.	0.12 ± 0.01	0.28 ± 0.01
BWSWRV symptomless	0.07 ± 0.05	0.13 ± 0.01	0.11 ± 0.01	0.11 ± 0.01
symptomatic	n.p.	n.p.	0.10 ± 0.01	0.10 ± 0.01
<i>Glutathione redox state</i> ^a				
HV	0.95 ± 0.05	0.95 ± 0.05	0.95 ± 0.05	0.79 ± 0.06
BWSV symptomless	0.83 ± 0.04	0.73 ± 0.04	0.69 ± 0.04	0.73 ± 0.04
symptomatic	n.p.	n.p.	0.66 ± 0.04	0.52 ± 0.02
BWSWRV symptomless	0.38 ± 0.01	0.55 ± 0.04	0.56 ± 0.04	0.45 ± 0.02
symptomatic	n.p.	n.p.	0.45 ± 0.02	0.37 ± 0.01

^a Data are means of 15 replicates ± standard deviations.

^b n.p. leaf typology not present.

spora in grapevine wood with brown wood streaking, and *F. mediterranea* was always associated with white rotted tissues. No *Botryosphaeriaceae* fungi or other grapevine trunk disease pathogens were isolated from diseased vines. No symptoms on foliage, wood, or berries were observed on healthy vines. Vines with brown wood streaking and vines with brown wood streaking and white rot showed 'tiger-stripe' symptoms on leaves, and spots, shrivelling and wilt of berries. These observations agreed with those previously described for vines affected by Esca complex pathogens (Bruno and Sparapano, 2007; Mondello *et al.*, 2018).

The present study recorded differences in the contents of bleeding xylem sap and leaves between healthy and diseased vines. Bleeding of xylem sap is a process that characterizes grapevines and many other perennial plants as an effect of positive root pressure that transports water upward. Bleeding occurs in the spring-time because increasing soil temperatures stimulated root pressure. Water fills the xylem vessels, dissolves, and pushes out air bubbles formed during the winter and restores xylem activity (Sperry *et al.*, 1987). Cavitation reduces sap flux density and sap surface tension and induces xylem dysfunction (Hammond-Kosack and Jones, 2015). To bypass obstructions or cavitation, and restore vertical water conductivity, plants respond by producing new xylem conduits or refill cavitated vessels (Nardini *et al.*, 2008).

Xylem-colonising pathogens, including *P. minimum* and *P. chlamydospora*, cause xylem dysfunction asso-

ciated with imbalances between water absorption and transpiration. Permanent xylem blockage results from fungus presence and plant defence responses. Xylem-associated pathogens produce conidia, hyphae, high molecular weight substances and large molecules from cell wall breakdown. Host plants affected by tracheomycoses develop tyloses or gummoses as barriers that limit fungus invasion (Tyree and Zimmermann, 2002). Pathogen metabolites could develop thin films on host vessel inner wall surfaces, minimize sap frictional pressure and change xylem hydraulics, or increase transpiration flux (Yoder, 1980; Bruno *et al.*, 2007). *F. mediterranea*, *P. minimum* and *P. chlamydospora* produce phytotoxic metabolites (Evidente *et al.*, 2000; Tabacchi *et al.*, 2000; Bruno and Sparapano, 2006a; Luini *et al.*, 2010; Andolfi *et al.*, 2011) and enzymes (Chiarappa, 1959; Mugnai *et al.*, 1999; Marchi *et al.*, 2001; Bruno and Sparapano, 2006c). Polyphenol-rich zones, tyloses and gels in xylem (Yadeta and Thomma, 2013), cell wall chemical modifications with suberin deposition (Pouzoulet *et al.*, 2013), and the accumulation of pathogenesis-related-proteins contribute to impeding the spread of xylem-inhabiting pathogens in host wood. Oxidative burst, peroxidases, superoxide dismutase, glutathione S-transferase, phenolic compounds, stilbenes and phytoalexins are also activated by these pathogens (del Rio *et al.*, 2004; Calzarano *et al.*, 2016; 2017a; 2017b).

Presence of *F. mediterranea* and its wood-degrading action could alter xylem conductivity, and thus, the quantity of bleeding sap. As in previous studies (Bruno

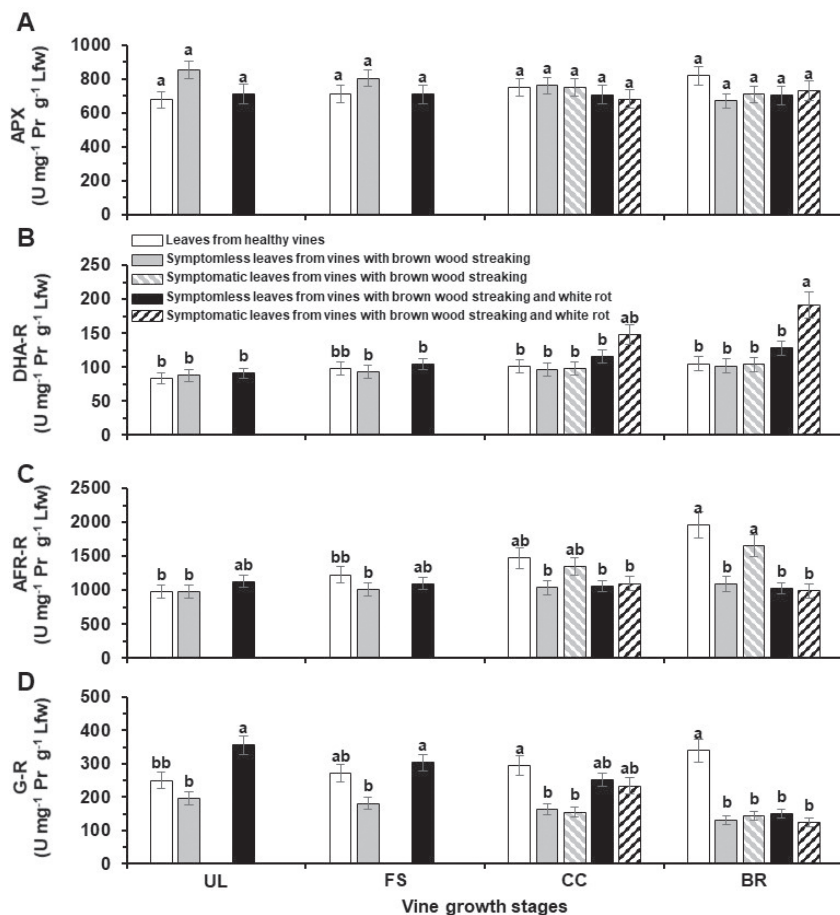


Figure 5. Activities of the redox enzymes: A) ascorbate peroxidase (APX), B) dehydroascorbate reductase (DHA-R), C) ascorbate free radical reductase (AFR-R), D) glutathione reductase (G-R), D) ascorbate free radical reductase (AFR-R) in cv. Italia grapevine leaves, collected during unfolded leaf (UL), fruit set (FS), cluster closing (CC) and bunch ripening (BR) vine growth stages, from infected or healthy grapevines. Data are means of 50 replicates \pm standard deviations. For each parameter, values accompanied by the same letters are not significantly different ($P \leq 0.05$) according to Fisher's LSD test.

and Sparapano, 2006b; Bruno *et al.*, 2007), diseased vines here analysed bled more abundantly than healthy vines.

Viscosity is the capacity of a fluid layer to run with an adjacent layer. In the present study, the dynamic viscosity coefficient increased from healthy vines to the vines with brown wood streaking or with white rot and brown wood streaking. These results suggest that substances produced by fungal pathogens, and molecules resulting from cell component degradation by pathogen lytic enzymes, added to vine response molecules (such as phenols, tannins, flavonoids), could affect dynamic viscosity coefficients, and, thus, the xylem sap flow.

The presence of several plant hormones in host xylem sap has been assessed in herbaceous and woody plants, including grapevine (Niim and Torikata, 1978). In the present study the greatest auxin- and kinetin-like

activities were detected in diseased vines. Auxin activity increased when the vines showed white rot symptoms associated with *F. mediterranea*.

This study also demonstrated that grapevine leaf surface area, leaf fresh and dry weights, and chlorophyll contents varied according to the host growth stages, but were significantly affected by the behaviour of the pathogens inside the woody tissues and, consequently, by altered physiological functions. Symptomatic leaves always had the least fresh and dry weights, and total chlorophyll concentrations. Diseased plants had physiological dysfunctions related to photosynthesis (i.e., reduced photosynthetic pigments) similar to those reported for Esca affected 'Cabernet Sauvignon' and 'Merlot' grapevines (Christen *et al.*, 2007). Decreased gas exchange and chlorophyll fluorescence, and repression of photosynthesis-related genes have been detected

for presymptomatic leaves of Esca-affected vines (Magnin-Robert *et al.*, 2011). Chlorophyll decline leads to decreased photosynthesis efficiency, organic carbon production, host growth, and general plant health. Symptomatic leaves showed further reductions in fresh and dry weights associated with lamina necrosis and wilt. The main aetiological agents of the Esca complex produced phytotoxic metabolites involved, *in vitro* and *in planta*, with symptom development on leaves (Evidente *et al.*, 2000; Bruno and Sparapano, 2006a, 2006b; Luini *et al.*, 2010; Andolfi *et al.*, 2011). Chlorophyll decline could also explain the decrease in leaf weight because of low photosynthesis efficiency. Activation of plant defence mechanisms possibly modified host sugar metabolism, moving towards production of new molecules (Jeandet *et al.*, 2002) and reducing carbohydrates used for plant growth and reproduction.

The experiments carried out in the present study have shown increases in leaf surface area in diseased plants. These results are similar to those where growth regulator activities have been measured for bleeding xylem sap from diseased vines. Hormone-like substances with auxin activity, produced by *P. minimum*, *P. chlamydospora* and especially by *F. mediterranea*, could contribute to host cell hyperplasia, hypertrophy, and leaf lamina expansion.

The most prominent features of plant responses to pathogens and, in general, against stresses, is the 'oxidative burst', i.e. the rapid increase in the cellular concentration of Reactive Oxygen Species (ROS) and mainly H_2O_2 (De Gara *et al.*, 2003; Torres *et al.*, 2009). In the present study, leaves collected from healthy vines had the lowest H_2O_2 concentrations during all the considered growth stages. In leaves of diseased plants, H_2O_2 increased about 3-fold in symptomless leaves compared to healthy ones, regardless of growth stage, and reached greatest amounts in symptomatic plants. This evidence suggests strong correlation between the metabolic activity of pathogens and H_2O_2 production and accumulation in host leaves. H_2O_2 in leaves of diseased plants may act as an antimicrobial to counteract pathogens, or as a strengthener of cell wall polymers, a promoter of phytoalexin synthesis, or in triggering of programmed cell death. However, infected vines failed their defence upgrades and eventually suffered the effects of oxidative stress. H_2O_2 increased oxidative stress and damaged integrity and functionality of cell membranes (Pérez *et al.*, 2002), by lipid peroxidation of unsaturated fatty acids. The lipid peroxidation levels clearly showed changes in cell membranes. Levels of MDA, a product of lipid peroxidation, were correlated to membrane damage (Heath and Packer, 1968; Soares *et al.*, 2019).

Plants produce ROS-scavenging mechanisms under biotic and abiotic stresses. Enzymes, including superoxide dismutase, catalase, peroxidase, ascorbate peroxidase, and glutathione reductase (Zhang and Kirkham, 1996; Lee and Lee, 2000), and non-enzymatic antioxidants such as tocopherols, ascorbic acid, and glutathione (Noctor and Foyer, 1998), functioned as ROS detoxifiers. Ascorbic acid is considered a key molecule for H_2O_2 elimination. Ascorbic acid reacts with H_2O_2 directly or by ascorbate peroxidase, a Class I heme-peroxidase that uses ascorbic acid as an electron donor and is the main peroxidase involved in H_2O_2 detoxification (Asada, 1999). Monodehydroascorbate reductase, dehydroascorbate reductase and reduced glutathione regenerate ascorbic acid. Glutathione controls the redox state in plant cells under abiotic and biotic stresses, and this compound is involved in ascorbic acid regeneration through the Ascorbate-Glutathione cycle (Noctor and Foyer, 1998; Asada, 1999; Mittler, 2002; Hung *et al.*, 2005). If the Ascorbate-Glutathione cycle operated well, ascorbic acid content and ascorbate peroxidase activity increased in host leaves of infected vines as expected (De Gara *et al.*, 2003; Hung *et al.*, 2005). However, leaves of diseased vines, during all the four growth assessed, showed ascorbic acid, and reduced glutathione concentrations that were less than in healthy vines. This trend was also confirmed for total ascorbate presence in bleeding xylem sap. In contrast, presence of pathogens in the grapevine trunks stimulated total glutathione contents.

L-Ascorbic acid (2,3-didehydro L-threo-hexano-1,4-lactone, the well-known functional form of vitamin C) is a multifunction molecule (Gallie, 2013). Ascorbic acid also plays indirect roles in plant responses against pathogens, changes in gene expression and resistance against biotic and abiotic stresses (Khan *et al.*, 2011).

The results from the present study allow development of the hypothesis that *P. minimum* and *P. chlamydospora*, or these fungi in association with *F. mediterranea*, can affect host antioxidant defences based on both glutathione and ascorbic acid. This change could be correlated with an unbalanced host oxidative state, damage to membrane integrity and appearance leaf necrosis symptoms.

Leaves of diseased vines showed significant decreases in redox state, and shift of ascorbic acid and glutathione towards oxidized forms. Ascorbate and glutathione redox states provide reliable estimation of cellular oxidative stress (Munné-Bosch and Alegre, 2003). In the present study, diseased vines were more stressed than healthy vines. To explain this change in physiological status, we suggest that the cause was the metabolic complex produced by *F. mediterranea*, *P. minimum* and

P. chlamydospora (Bruno and Sparapano, 2006a, 2006b; Bruno *et al.*, 2007). The accumulation of resveratrol, benzoic acid derivatives and flavonols as host defence compounds (Amalfitano *et al.*, 2000; Jeandet *et al.*, 2002; Bruno and Sparapano, 2006b; Calzarano *et al.*, 2016, 2017a, 2017b) were also suggested as causes. Phenols or flavonoids contribute to ascorbic acid oxidation in the scavenging of H₂O₂ in grape leaves (Yamasaki *et al.*, 1997), i.e., phenoxy or flavonoxy radicals accept electrons from ascorbic acid and produce the monodehydroascorbate radical (Pérez *et al.*, 2002).

To prevent oxidative stress, following the glutathione-ascorbate metabolic pathway, ascorbate peroxidase reduced H₂O₂ to water converting ascorbic acid to monodehydroascorbate that spontaneously disproportionate into ascorbic and dehydroascorbic acids. Using reduced glutathione, dehydroascorbate reductase reduced dehydroascorbic acid to ascorbate and produced oxidized glutathione. Finally, glutathione reductase reduced oxidized glutathione using NADPH as an electron donor (Asada, 1999). Under our conditions, the activities of enzymes regenerating ascorbic acid, also active in diseased as well as healthy vines, did not show any marked differences. This implied that ascorbate peroxidase, dehydroascorbate reductase, ascorbate free radical reductase, and glutathione reductase made a non-significant contribution to increasing ascorbic acid regeneration in diseased vines. Therefore, our data on ascorbate peroxidase, the key-enzymes of Ascorbate-Glutathione cycle, were in contrast with the low concentrations in cv Sultanina protoplasts (Papadakis *et al.*, 2001) and the absence in 'Sultana' leaves (Pérez *et al.*, 2002). This difference could be due to grape varieties, stress considered, plant materials and assay procedure applied.

In conclusion, the results of the present study suggest that *F. mediterranea*, *P. minimum* and *P. chlamydospora* interfere with several morphological, physiological, and biochemical functions in 'Italia' grapevines. Alterations affected bleeding xylem sap and leaves. Flux, dynamic viscosity, and growth regulator activity distinguished between bleeding xylem sap of vines infected with *P. minimum* and *P. chlamydospora* and those infected with *P. minimum*, *P. chlamydospora* and *F. mediterranea*. Leaf surface area, fresh, and dry weights, chlorophyll, hydrogen peroxide contents, lipid peroxidation, and redox states were altered in leaves of all assessed diseased vines. The presence of *F. mediterranea* in wood tissues of infected vines further debilitated the host physiological status. These alterations were detected in symptomatic leaves and, at low intensity, in symptomless leaves of diseased vines. These deleterious effects

marked a presymptomatic stage, for irreversible changes inducing symptoms appearance. In diseased vines, low concentrations of ascorbic acid, reduced glutathione, and moderate levels of dehydroascorbic acid and oxidized glutathione were also associated with increased amounts of H₂O₂ and MDA, and considerable oxidative stress. Under these conditions, scavenging enzymes were not able to sufficiently restore the balance between ROS and the antioxidants managing host stress conditions. The stresses caused by oxidative unbalance increased lipid peroxidation of unsaturated fatty acids of host membranes, damaged membrane integrity, and contributed to cell death and development of leaf symptoms. The present study has indicated that Ascorbate-Glutathione cycle is likely to be involved in grapevine susceptibility to fungi associated with the Esca complex.

ACKNOWLEDGEMENTS

Mr L. Scarola (University of Bari Aldo Moro - Di.S.S.P.A.) gave technical support in this study. Ms Tonia Gemma and Ms Sylvia J. Stastny provided helpful discussions and skilful proof reading of the manuscript of this paper.

LITERATURE CITED

- Amalfitano C., Evidente A., Surico G., Tegli S., Bertelli E., Mugnai L., 2000. Phenols and stilbene polyphenols in the wood of esca-diseased grapevine. *Phytopathologia Mediterranea* 39: 178–183. <https://oajournals.fupress.net/index.php/pm/article/view/4799/4797>.
- Andolfi A., Mugnai L., Luque J., Surico G., Cimmino A., Evidente A., 2011. Phytotoxins produced by fungi associated with grapevine trunk diseases. *Toxins* 3: 1569–1605. <https://doi.org/10.3390/toxins3121569>.
- Asada K., 1999. The water-water cycle in chloroplasts: scavenging of active oxygens and dissipation of excess photons. *Annual Review of Plant Physiology and Plant Molecular Biology* 50: 601–639. <https://doi.org/10.1146/annurev.arplant.50.1.601>.
- Baggiolini M., 1979. Stades repères de la vigne. In: *La Défense des Plantes Cultivées* (R. Bovey, ed.), Payot, Lausanne, CH, 456–461.
- Baránek M., Armengol J., Holleínová V., Pečenka J., Calzarano F., ... Eichmeier A., 2018. Incidence of symptoms and fungal pathogens associated with grapevine trunk diseases in Czech vineyards: first example from a north-eastern European grape-growing region. *Phytopathologia Mediterranea* 57:

- 449–458. https://doi.org/10.14601/Phytopathol_Mediterr-22460.
- Bertsch C., Ramírez-Suero M., Magnin-Robert M., Larignon P., Chong J., ... Fontaine F., 2012. Grapevine trunk diseases: complex and still poorly understood. *Plant Pathology* 62: 243–265. <https://doi.org/10.1111/j.1365-3059.2012.02674.x>
- Bruno G., Sparapano L., 2006a. Effects of three esca-associated fungi on *Vitis vinifera* L.: I. Characterization of secondary metabolites in culture media and host responses to the pathogens in calli. *Physiological and Molecular Plant Pathology* 69: 209–223. <https://doi.org/10.1016/j.pmpp.2007.04.008>.
- Bruno G., Sparapano L., 2006b. Effects of three esca-associated fungi on *Vitis vinifera* L.: II. Characterization of biomolecules in xylem sap and leaves of healthy and diseased vines. *Physiological and Molecular Plant Pathology* 69: 195–208. <https://doi.org/10.1016/j.pmpp.2007.04.007>.
- Bruno G., Sparapano L., 2006c. Effects of three esca-associated fungi on *Vitis vinifera* L.: III. Enzymes produced by the pathogens and their role in fungus-to-plant or in fungus-to-fungus interactions. *Physiological and Molecular Plant Pathology* 69: 182–194. <https://doi.org/10.1016/j.pmpp.2007.04.006>.
- Bruno G., Sparapano L., 2007. Effects of three esca-associated fungi on *Vitis vinifera* L.: V. Changes in the chemical and biological profile of xylem sap from diseased cv. Sangiovese vines. *Physiological and Molecular Plant Pathology* 71: 210–229. <https://doi.org/10.1016/j.pmpp.2008.02.005>.
- Bruno G., Sparapano L., Graniti A., 2007. Effects of three esca-associated fungi on *Vitis vinifera* L.: IV. Diffusion through the xylem of metabolites produced by two tracheiphilous fungi in the woody tissue of grapevine leads to esca-like symptoms on leaves and berries. *Physiological and Molecular Plant Pathology* 71: 106–124. <https://doi.org/10.1016/j.pmpp.2007.12.004>.
- Calzarano F., Amalfitano C., Seghetti L., Cozzolino V., 2009. Nutritional status of vines affected with esca proper. *Phytopathologia Mediterranea* 48: 20–31. https://doi.org/10.14601/Phytopathol_Mediterr-2872
- Calzarano F., Di Marco S., D'agostino V., Schiff S., Mugnai L., 2014. Grapevine leaf stripe disease symptoms (esca complex) are reduced by a nutrients and seaweed mixture. *Phytopathologia Mediterranea* 53: 543–558. https://doi.org/10.14601/Phytopathol_Mediterr-15253.
- Calzarano F., D'Agostino V., Pepe A., Osti F., Della Pelle F., ... Di Marco S., 2016. Patterns of phytoalexins in the grapevine leaf stripe disease (esca complex)/grapevine pathosystem. *Phytopathologia Mediterranea* 55: 410–426. https://doi.org/10.14601/Phytopathol_Mediterr-18681.
- Calzarano F., Osti F., D'Agostino V., Pepe A., Di Marco S., 2017a. Mixture of calcium, magnesium and seaweed affects leaf phytoalexin contents and grape ripening on vines with grapevine leaf stripe disease. *Phytopathologia Mediterranea* 56: 445–457. https://doi.org/10.14601/Phytopathol_Mediterr-22023.
- Calzarano F., Osti F., D'Agostino V., Pepe A., Della Pelle F., ... Di Marco S., 2017b. Levels of phytoalexins in vine leaves with different degrees of grapevine leaf stripe disease symptoms (Esca complex of diseases). *Phytopathologia Mediterranea* 56: 494–501. https://doi.org/10.14601/Phytopathol_Mediterr-22055.
- Calzarano F., Di Marco S., 2018. Further evidence that calcium, magnesium and seaweed mixtures reduce grapevine leaf stripe symptoms and increase grape yield. *Phytopathologia Mediterranea* 57: 459–471. https://doi.org/10.14601/Phytopathol_Mediterr-23636
- Chiarappa L., 1959. Extracellular oxidative enzymes of wood-inhabiting fungi associated with the heart rot of living grapevines. *Phytopathology* 49: 578–582.
- Christen D., Schönmann S., Jermini M., Strasser R.J., Défago, G., 2007. Characterization and early detection of grapevine (*Vitis vinifera*) stress responses to esca disease by in situ chlorophyll fluorescence and comparison with drought stress. *Environmental and Experimental Botany* 60: 504–514. [Doi:10.1016/j.envexpbot.2007.02.003](https://doi.org/10.1016/j.envexpbot.2007.02.003).
- Ciccarone C., Graniti A., Schiaffino A., Marras F., 2004. Molecular analysis of *Fomitiporia mediterranea* isolates from esca-affected grapevines in southern Italy. *Phytopathologia Mediterranea* 43: 268–272. <https://oajournals.fupress.net/index.php/pm/article/view/5056>
- Claverie M., Notaro M., Fontaine F., Wery J., 2020. Current knowledge on Grapevine Trunk Diseases with complex etiology: a systemic approach. *Phytopathologia Mediterranea* 59: 29–53. [Doi: 10.14601/Phyto-11150](https://doi.org/10.14601/Phyto-11150)
- De Gara L., de Pinto M., Tommasi F., 2003. The antioxidant systems via-à-via reactive oxygen species during plant-pathogen interaction. *Plant Physiology and Biochemistry* 41: 863–870. [https://doi.org/10.1016/S0981-9428\(03\)00135-9](https://doi.org/10.1016/S0981-9428(03)00135-9).
- de Rolland G., 1873. Considérations physiologiques sur l'apoplexie de la vigne. *Bulletin de la Société d'Agriculture de France* 5: 539–545.
- del Rio J.A., Gómez P., Báidez A., Fuster M.D., Ortuño A., Frías V., 2004. Phenolic compounds have a role in the defence mechanism protecting grapevine against

- the fungi involved in Petri disease. *Phytopathologia Mediterranea* 43: 87–94. DOI: 10.14601/Phytopathol_Mediterr-1736.
- Elena G., Bruez E., Rey P., Luque J., 2018. Microbiota of grapevine woody tissues with or without esca-foliar symptoms in northeast Spain. *Phytopathologia Mediterranea* 57: 425–438. Doi: https://doi.org/10.14601/Phytopathol_Mediterr-23337.
- Evidente A., Sparapano L., Andolfi A., Bruno G., 2000. Two naphthalenone pentaketides isolated from liquid cultures of *Phaeoacremonium aleophilum*, a fungus associated with esca disease syndrome. *Phytopathologia Mediterranea* 39: 162–168. <https://oajournals.fupress.net/index.php/pm/article/view/4807/4805>.
- Fischer M., 2002. A new wood-decaying basidiomycete species associated with esca of grapevine: *Fomitiporia mediterranea* (Hymenochaetales). *Mycological Progress* 1(3): 315–324. <https://doi.org/10.1007/s11557-006-0029-4>.
- Fischer M., 2006. Biodiversity and geographic distribution of basidiomycetes causing esca-associated white rot in grapevine: a worldwide perspective. *Phytopathologia Mediterranea* 45(S): 30–42. <https://oajournals.fupress.net/index.php/pm/article/view/5187>.
- Fontaine F., Pinto C., Vallet J., Clément C., Gomes A.C., Spagnolo A., 2016. The effects of grapevine trunk diseases (GTDs) on vine physiology. *European Journal of Plant Pathology* 144: 707–721. <https://doi.org/10.1007/s10658-015-0770-0>.
- Gallie D.R., 2013. L-Ascorbic acid: a multifunctional molecule supporting plant growth and development. *Scientifica* 795964. <https://doi.org/10.1155/2013/795964>.
- Graniti A., Surico G., Mugnai L., 2000. Esca of grapevine: a disease complex or a complex of diseases? *Phytopathologia Mediterranea* 39: 16–20. <https://oajournals.fupress.net/index.php/pm/article/view/4787/4785>.
- Guérin-Dubrana L., Labenne A., Labrousse J.C., Bastien S., Rey P., Gégout-Petit A., 2013. Statistical analysis of grapevine mortality associated with esca or *Eutypa dieback* foliar expression. *Phytopathologia Mediterranea* 52: 276–288.
- Hammond-Kosack K.E., Jones J.D.G., 2015. Responses to plant pathogens. In: *Biochemistry and Molecular Biology of Plants*, 2nd ed. (Buchanan B.B., Gruissem W., Jones, R.L., ed.), John Wiley & Sons Ltd., New Jersey, USA, 984–1050.
- Harborne J., 1973. Nitrogen compounds. In: *Phytochemical Methods. A guide to modern techniques of plant analysis* (J.B. Harborne, ed.), Chapman & Hall, London, UK, 176–221.
- Heath R.L., Packer L., 1968. Photoperoxidation in isolated chloroplasts. I. Kinetics and stoichiometry of fatty acid peroxidation. *Archives of Biochemistry and Biophysics* 125: 189–198. [https://doi.org/10.1016/0003-9861\(68\)90654-1](https://doi.org/10.1016/0003-9861(68)90654-1).
- Hung S.H., Yu C.W., Lin C.H., 2005. Hydrogen peroxide functions as a stress signal in plants. *Botanical Bulletin of Academia Sinica* 46: 1–10. <https://ejournal.sinica.edu.tw/bbas/content/2005/1/Bot461-01.pdf>.
- Jayawardena R.S., Purahong W., Zhang W., Wubet T., Li X., ... Yan J., 2018. Biodiversity of fungi on *Vitis vinifera* L. revealed by traditional and high-resolution culture-independent approaches. *Fungal Diversity* 90: 1–84. <https://doi.org/10.1007/s13225-018-0398-4>
- Jeandet P., Douillet-Breuil A.C., Bessis R., Debord S., Sbaghi M., Adrian M., 2002. Phytoalexins from the Vitaceae: biosynthesis, phytoalexin gene expression in transgenic plants, antifungal activity, and metabolism. *Journal of Agricultural and Food Chemistry* 50: 2731–2741. <https://doi.org/10.1021/jf011429s>.
- Khan T.A., Mazid M., Mohammad F., 2011. Role of ascorbic acid against pathogenesis in plants. *Journal of Stress Physiology & Biochemistry* 7: 222–234. http://www.jspb.ru/issues/2011/N3/JSPB_2011_3_222-234.pdf.
- Lambert C.K.K.I., Lucas S., Téléf-Micoleau N., Mérillon J.M., Cluzet S., 2013. A faster and stronger defence response: one of the key elements in grapevine explaining its lower susceptibility to esca? *Phytopathology* 103: 1028–1034. <http://dx.doi.org/10.1094/PHTO-11-12-0305-R>.
- Lecomte P., Darrietort G., Liminana J. M., Comont G., Muruamendaraz A., ... Fermaud M., 2012. New insights into esca of grapevine: The development of foliar symptoms and their association with xylem discoloration. *Plant Disease* 96: 924–934. DOI: 10.1094/PDIS-09-11-0776-RE.
- Lee D.H., Lee C.B., 2000. Chilling stress-induced changes of antioxidant enzymes in the leaves of cucumber: in gel enzyme activity assays. *Plant Science* 159: 75–85. [https://doi.org/10.1016/s0168-9452\(00\)00326-5](https://doi.org/10.1016/s0168-9452(00)00326-5).
- Lima M.R.M., Felgueiras M.L., Graca G., Rodrigues J.E.A., Barros A., ... Dias, A.C., 2010. NMR metabolomics of esca disease-affected *Vitis vinifera* cv. Alvarinho leaves, *Journal of Experimental Botany* 61: 4033–4042. <https://doi.org/10.1093/jxb/erq214>.
- Luini E., Fleurat-Lessard P., Rousseau L., Roblin G., Berjeaud J., 2010. Inhibitory effects of polypeptides secreted by the grapevine pathogens *Phaeoacremonium aleophilum* and *Phaeoacremonium aleophilum* on plant cell activities. *Physiological and Molecular Plant Pathology* 74: 403–411. <https://doi.org/10.1016/j.pmpp.2010.06.007>.
- Magnin-Robert M., Letousey P., Spagnolo A., Rabenoldina F., Jacquens L., ... Fontaine F., 2011. Leaf strip of

- esca induces alteration of photosynthesis and defence reactions in presymptomatic leaves. *Functional Plant Biology* 38: 856–866. <http://dx.doi.org/10.1071/FP11083>.
- Marchi G., Roberti S., D'Ovidio R., Mugnai L., Surico G., 2001. Pectic enzymes production by *Phaeomonniella chlamydospora*. *Phytopathologia Mediterranea* 40: S407-S416. <https://oajournals.fupress.net/index.php/pm/article/view/4921/4919>.
- Marsais P., 1923. Maladie de l'esca. *Revue de viticulture* 59: 8-14.
- Mittler R., 2002. Oxidative stress, antioxidants and stress tolerance. *Trends in Plant Science* 7: 405–410. [https://doi.org/10.1016/s1360-1385\(02\)02312-9](https://doi.org/10.1016/s1360-1385(02)02312-9).
- Mondello V., Songy A., Battiston E., Pinto C., Coppin C., ... Fontaine F., 2018. Grapevine Trunk Diseases: a review of fifteen years of trials for their control with chemicals and biocontrol agents. *Plant Disease* 102: 1189–1217. <https://doi.org/10.1094/PDIS-08-17-1181-FE>.
- Moreno-Sanz P., Lucchetta G., Zanzotto A., Loureiro M.D., Suarez B., Angelini E., 2013. Fungi associated to grapevine trunk diseases in young plants in Asturias (Northern Spain). *Horticultural Science (Prague)* 40: 138–144.
- Mugnai L., Graniti A., Surico G., 1999. Esca (black measles) and brown wood-streaking: two old and elusive diseases of grapevines. *Plant Disease* 83: 404–418. <https://doi.org/10.1094/PDIS.1999.83.5.404>.
- Munné-Bosch S., Alegre L., 2003. Drought-induced changes in the redox state of α -tocopherol, ascorbate and diterpene carnosic acid in chloroplast of Labiatae specie differing in carnosic acid contents. *Plant Physiology* 131: 1-10. <https://doi.org/10.1104/pp.102.019265>.
- Nardini A., Ramani M., Gortan E., Salleo S., 2008. Vein recovery from embolism occurs under negative pressure in leaves of sunflower (*Helianthus annuus*). *Physiologia Plantarum* 133: 755–764. <https://doi.org/10.1111/j.1399-3054.2008.01087.x>
- Niim Y., Torikata H., 1978. Changes in endogenous plant hormones in the xylem sap of grapevines during development *Journal of the Japanese Society for Horticultural Science* 47 181–187. https://www.jstage.jst.go.jp/article/jjshs1925/47/2/47_2_181/_pdf.
- Noctor G., Foyer C.H., 1998. Ascorbate and glutathione: keeping active oxygen under control, *Annual Review of Plant Physiology and Plant Molecular Biology* 49: 249–279. <https://doi.org/10.1146/annurev.arplant.49.1.249>.
- Paciolla C., Ippolito M.P., Logrieco A., Dipierro N., Mulè G., Dipierro S., 2008. A different trend of antioxidant defense responses makes tomato plants less susceptible to beauvericin than to T-2 mycotoxin phytotoxicity. *Physiological and Molecular Plant Pathology* 72: 3-9. <https://doi.org/10.1016/j.pmpp.2008.06.003>.
- Papadakis A.K., Siminis C.I., Roubelakis-Angelakis K.A., 2001. Reduced activity of antioxidant machinery is correlated with suppression of totipotency in plant protoplasts. *Plant Physiology* 126: 434–441. <https://doi.org/10.1104/pp.126.1.434>.
- Pérez F.J., Villegas D., Mejia N., 2002. Ascorbic acid and flavonoid-peroxidase reaction as a detoxifying system of H₂O₂ in grapevine leaves. *Phytochemistry* 60: 573–580. [https://doi.org/10.1016/S0031-9422\(02\)00146-2](https://doi.org/10.1016/S0031-9422(02)00146-2).
- Petit A.N., Vaillant N., Boulay M., Clement C., Fontaine F., 2006. Alteration of photosynthesis in grapevines affected by esca. *Phytopathologia Mediterranea* 96: 1060–1066. <https://doi.org/10.1094/phyto-96-1060>.
- Pouzoulet J., Jacques A., Besson X., Dayde J., Mailhac N., 2013. Histopathological study of response of *Vitis vinifera* cv. Cabernet sauvignon to bark and wood injury with and without inoculation by *Phaeomonniella chlamydospora*. *Phytopathologia Mediterranea* 52: 313–323. doi:10.14601/Phytopathol_Mediterr-12581
- Ravaz L., 1898. Sur le folletage. *Revue de Viticulture* 10: 184–186.
- Soares C., Carvalho M.E.A., Azevedo R.A., Fidalgo F., 2019. Plants facing oxidative challenges—A little help from the antioxidant networks. *Environmental and Experimental Botany* 161: 4–25. <https://doi.org/10.1016/j.envexpbot.2018.12.009>.
- Sperry J.S., Holbrook N.M., Zimmermann M.H., Tyree M.T., 1987. Tyree, spring filling of xylem vessels in wild grapevine. *Plant Physiology* 83: 414–417. <https://doi.org/10.1104/pp.83.2.414>.
- Surico G., 2009. Towards a redefinition of the diseases within the esca complex of grapevine. *Phytopathologia Mediterranea* 48: 5–10. <https://oajournals.fupress.net/index.php/pm/article/view/5262/5260>.
- Surico G., Mugnai L., Marchi G., 2006. Older and more recent observations on esca: A critical review. *Phytopathologia Mediterranea* 45: S68–S86. DOI: 10.14601/Phytopathol_Mediterr-1847.
- Tabacchi R., Fkyerat A., Poliart C., Dubin G.M., 2000. Phytotoxins from fungi of esca of grapevine. *Phytopathologia Mediterranea* 39: 156–161. <https://oajournals.fupress.net/index.php/pm/article/view/4800/4798>.
- Torres M.A., Jonathan D.G., Dangl J.L., 2006. Reactive oxygen species signaling in response to pathogen. *Plant Physiology* 141: 373–378. <https://doi.org/10.1104/pp.106.079467>.
- Tyree M.T., Zimmermann M.H., 2002. *Xylem structure and the ascent of sap*. 2nd ed. Springer, Berlin, D, 284 pp.

- Valtaud C., Thibault F., Larignon P., Berstch C., Fleurat-Lessard P., Bourbouloux A., 2011. Systemic damage in leaf metabolism caused by esca infection in grapevines. *Australian Journal of Grape and Wine Research* 17: 101–110. <https://doi.org/10.1111/j.1755-0238.2010.00122.x>.
- Wilcox W.F., Gubler W.D., Uyemoto J.K., 2015. *Compendium of Grape Diseases, Disorders, and Pests*. 2nd ed. APS Press, St. Paul, MN, 5–14.
- Yadeta, K., Thomma, B.P.H.J., 2013. The xylem as battleground for plant hosts and vascular wilt pathogens. *Frontiers in Plant Science* 4: Article 97. <https://doi.org/10.3389/fpls.2013.00097>. doi: 10.3389/fpls.2013.00097. eCollection 2013.
- Yamasaki H., Sakihama Y., Ikehara N., 1997. Flavonoid-peroxidase reactions as a detoxification mechanism of plant cells against H₂O₂. *Plant Physiology* 115: 1405–1412. <https://doi.org/10.1104/pp.115.4.1405>.
- Yoder O.C., 1980. Toxins in pathogenesis. *Annual Review of Phytopathology* 18, 103–129. <https://www.annualreviews.org/doi/pdf/10.1146/annurev.py.18.090180.000535>
- Zhang J., Kirkham M.B., 1996. Antioxidant responses to drought in sunflower and sorghum seedlings. *New Phytologist* 132: 361–373. <https://doi.org/10.1111/j.1469-8137.1996.tb01856.x>.
- Zhao Z.R., Wu Z.L., Huang G.Q., Li G.R., 1992. An improved disk bioassay for determining activities of plant growth regulators. *Journal of Plant Growth Regulation* 11: 209–213. <https://doi.org/10.1007/BF02115479>.



Citation: P. Tsopelas, N. Soulioti, M.J. Wingfield, I. Barnes, S. Marincowitz, E.C. Tjamos, E.J. Paplomatas (2021) *Ceratocystis ficiicola* causing a serious disease of *Ficus carica* in Greece. *Phytopathologia Mediterranea* 60(2): 337-349. doi: 10.36253/phyto-12794

Accepted: June 22, 2021

Published: September 13, 2021

Copyright: ©2021 P. Tsopelas, N. Soulioti, M.J. Wingfield, I. Barnes, S. Marincowitz, E.C. Tjamos, E.J. Paplomatas. This is an open access, peer-reviewed article published by Firenze University Press (<http://www.fupress.com/pm>) and distributed under the terms of the Creative Commons Attribution License, which permits unrestricted use, distribution, and reproduction in any medium, provided the original author and source are credited.

Data Availability Statement: All relevant data are within the paper and its Supporting Information files.

Competing Interests: The Author(s) declare(s) no conflict of interest.

Editor: Jean-Michel Savoie, INRA Villenave d'Ornon, France.

Research Papers

Ceratocystis ficiicola causing a serious disease of *Ficus carica* in Greece

PANAGHIOTIS TSOPELAS^{1,*}, NIKOLETA SOULIOTI¹, MICHAEL J. WINGFIELD², IRENE BARNES², SEONJU MARINCOWITZ², ELEFThERIOS C. TJAMOS³, EPAMINONDAS J. PAPLOMATAS³

¹ Institute of Mediterranean Forest Ecosystems, Terma Alkmanos, 11528 Athens, Greece

² University of Pretoria, Department of Biochemistry, Genetics and Microbiology, Forestry and Agricultural Biotechnology Institute (FABI), Pretoria, South Africa

³ Laboratory of Plant Pathology, Agricultural University of Athens, Athens, Greece

*Corresponding author. E-mail: tsop@fria.gr

Summary. *Ceratocystis ficiicola* causes vascular wilt of fig trees in Japan, invading root systems and the main stems eventually leading to tree death. In surveys from 2018 to 2020 in fig orchards in Greece, this fungus was detected in two separated regions. The fungus was consistently isolated from infected wood and from rhizosphere soil. The isolates were identified based on multi-locus phylogenetic analyses of *rpb2*, *bt1* and *tef1* gene regions and detailed morphological characteristics, including comparisons with an ex-type isolate of *C. ficiicola* from Japan. The pathogenicity of Greek isolates was proven on *Ficus carica* and *F. benjamina* plants. *Ceratocystis ficiicola* is a soil-borne pathogen, and the occurrence of vascular wilt outbreaks suggest that the pathogen spreads within and between orchards with infested soil and wood debris during ploughing. The pathogen is also spreading in Greece with infected propagation material. This is the first detailed report of *C. ficiicola* outside Japan, and there is concern over potential spread of the pathogen to other Mediterranean countries, where approx. 70% of the world fig production occurs.

Keywords. *Ceratocystis ficiicola*, *Ficus carica*, soil-borne pathogen, vascular wilt, Greece.

INTRODUCTION

Fig (*Ficus carica* L.) is one of the oldest domesticated tree crops globally. According to Kislev *et al.* (2006) this tree was cultivated for its fruit during the Early Neolithic period (11,400 to 11,200 years ago), preceding cereal domestication. *Ficus* (*Moraceae*) includes more than 700 species, native to the tropics or sub-tropics. *Ficus carica* is indigenous to the Middle East and Asia Minor, and is mostly cultivated in warm and dry areas of the Mediterranean region (Condit, 1955; Flaishman *et al.*, 2008). *Ficus carica* has been cultivated in Greece since ancient times, as mentioned by Homer (8th century BC) *The Odyssey*, and Theophrastus (4–3rd century BC) described cross-

fertilization of wild and domesticated figs (Condit, 1955). Fig continues to be an important crop, in Greece, where production in 2019 was 19,730 t (FAO, 2019). Thus, any negative impact on these trees due to serious disease is considered important from both a cultural and an economic standpoint.

Since the 1970s, a serious disease caused by a *Ceratocystis* species has been reported in Japanese fig orchards. The causal agent of this disease was initially attributed to *Ceratocystis fimbriata sensu lato* (Kato *et al.*, 1982). Kajitani and Masuya (2011) described the pathogen as a new species, *Ceratocystis ficicola* Kajitani and Masuya, based on discernable morphological characteristics and DNA sequence data. Like many other *Ceratocystis* species, *C. ficicola* is a soil-borne pathogen that infects roots and main stems of susceptible hosts, causing vascular wilt and eventually tree death. The pathogen is dispersed by human activities, mainly with contaminated plant material, and has spread to many fig-growing areas of Japan (Kajitani and Masuya, 2011; Kajii *et al.*, 2013).

In 2018, a *Ceratocystis* species was isolated from two neighbouring fig orchards in the Attica region of Greece. The affected trees showed symptoms of wilt and extensive crown defoliation, and some trees had died. The morphological characteristics of the isolated fungus were similar to those of *C. ficicola* (Tjamos *et al.*, 2018). In 2019 and 2020, the same fungus, based on morphology, was also isolated from diseased fig trees at different localities on Euboea Island, where considerable damage was occurring in fig orchards.

The objective of the present study was to identify *Ceratocystis* species, having similar morphology to *C. ficicola*, found causing disease on *F. carica* in the two regions of Greece. This was achieved based on multi-locus phylogenetic analyses and detailed observation of morphological characteristics of the fungus, including

comparisons with the ex-type isolate of *C. ficicola*. Pathways of dispersal of the pathogen were also considered and the extent of damage to fig orchards in Greece is reported. Pathogenicity tests were also conducted with the fungus on plants of *F. carica* and *Ficus benjamina* L.

MATERIALS AND METHODS

Sampling and fungus isolations

Field surveys for disease symptoms were conducted from April to early September, corresponding to the time of year that fig trees retain full foliage. In the fig orchards of the Markopoulo Mesogaia municipality in East Attica, surveys took place in 2018 and 2019, and in the Istiaia-Aidipsos municipality on the Euboea Island, in 2019 and 2020 (Table 1). These two regions are more than 200 km apart.

Trees with symptoms including crown defoliation and leaf wilt were sampled. The lower parts of the main stems were examined for the presence of necrotic bark, which was then removed to expose diseased cambial tissues and discoloured wood (Figure 1C–E). Samples of stained wood were then cut from the lesions using a surface-disinfected chisel. Some of the young plants were uprooted; the root systems examined for disease symptoms, and these were collected for laboratory examination. Soil samples were also collected from a depth of 15–20 cm near the bases of symptomatic trees from most of the surveyed orchards.

For isolation of fungi, PARPH V8 agar medium was used (containing 5% clarified V8 juice, 5 µg mL⁻¹ pimaricin, 250 µg mL⁻¹ ampicillin, 10 µg mL⁻¹ rifamycin, 50 µg mL⁻¹ PCNB, and 50 µg mL⁻¹ hymexazol). This selective medium is widely used for the isolation of *Phytophthora* species (Ferguson and Jeffers, 1999) but was also effective for the isolation of *Ceratocystis* species.

Table 1. Occurrence of *Ceratocystis ficicola* in fig orchards of Greece.

Locality	Fig cultivar	Dates investigated	Number of orchards	Number of trees sampled
<i>Regional Unit of East Attica</i>				
Municipality of Markopoulo Mesogaia	Vasilika honey-white	May 2018	1	4
	Vasilika black	May 2018	1	2
	Vasilika honey-white	April 2019	1	2
<i>Euboea Island</i>				
Municipality of Istiaia-Aidipsos				
Avgaria village	Smyrna	April, September 2019	2	3
Taxiarchis village	Smyrna	September 2019	1	2
Oreoi village	Smyrna	September 2020	2	4
Kastaniotissa village	Smyrna	September 2020	2	3



Figure 1. Field images of infected fig trees. A, infected mature tree of Vasilika honey-white cultivar with symptoms of leaf wilt and defoliation; B, infected young tree of Smyrna cultivar defoliated at the end of summer, with some of the unripe fruit still on the tree; and C, D and E, cankers at the bases of *Ficus carica* trees, with extensive wood staining under the dead bark.

Direct isolation from wood samples was performed after they had been surface-disinfested with 70% ethanol and air dried in a laminar flow cabinet. Small pieces of stained wood were aseptically removed from the samples with a sterile scalpel and transferred to Petri dishes containing PARPH V8A medium.

A carrot baiting method was also used for a sub-set of samples. Small pieces of stained wood were placed between two slices (each 5 mm thick) of carrot root, as described by Moller and De Vay (1968). The carrot baits were then placed in empty Petri dishes with moistened filter paper and incubated for 7–10 d at 25°C. The carrot discs were subsequently examined for the presence of ascomata under a dissecting microscope, and when these

were present, masses of ascospores were transferred to PARPH V8A medium.

Isolations from soil samples were performed using a modification of the trapping technique described by Grosclaude *et al.* (1988) for *Ceratocystis platani* (Walter) Engelbrecht and Harrington. Soil samples (40–50 g) were placed in 250 mL capacity conical flasks, which were filled with 200 mL of sterile deionized water. Freshly cut twigs from fig trees (approx. 10 cm long and 6–10 mm in diameter) with the bark removed were placed in the flasks. Air was continuously pumped into the flasks through a Pasteur pipette, using an aquarium pump (Aqua-Air AP4, Interpet). The flasks were incubated at room temperature (23–25°C). After 7–10 days, the

twigs were examined under a dissecting microscope for the presence of ascomata and, where present, masses of ascospores were aseptically transferred to PARPH V8A medium. In some cases, this trapping technique was also used with pieces of infected wood in the flasks rather than soil. In all cases, resulting, agar medium colonies having *Ceratocystis* morphology were sub-cultured onto V8A medium.

Growth in culture

Growth rates of fungal cultures were determined on 10% V8A at different temperatures from 10 to 40 °C at 5°C intervals. Two measurements of colony diameters were made perpendicular to each other on each culture plate after 7 and 14 d incubation at 25°C.

Measurements of fungal structures were made from 7 to 10d old pure cultures on V8A and malt extract agar (MEA) with fungal structures mounted in water or 85% lactic acid. A Zeiss Axioskop light microscope and SC30 camera (Olympus) or a Nikon Eclipse Ni microscope and DS-Ri2 camera (Nikon) were used to capture images and to take measurements. Ascomata were examined at 50x or 100x magnification and the conidia and ascospores at 400x or 1000x. For each of the two isolates from Greece (CMW 56935 and CMW 54794), the dimensions of 50 conidia of each type were measured.

Besides the isolates from Greece, the ex-holotype culture of *C. ficicola* from Japan (MAFF 625119 = CMW 38543) was also examined.

DNA extraction, sequencing and phylogenetic analyses

To confirm the identity of the *Ceratocystis* species isolated from infected fig trees, two cultures from infected wood and two from the soil baiting (Table 2) were subjected to DNA sequencing. Mycelium from the cultures grown on 2% MEA for approx. 2 weeks was scraped from the surfaces of the agar culture plates and DNA was extracted using the Fungal DNA MiniPrep kit (Zymo Research).

Three gene regions were PCR-amplified and sequenced. Primers RPB2-5Fb and RPB2-7Rb were used to amplify the second largest subunit of the RNA polymerase II (*rpb2*) (Fourie *et al.*, 2015), primers β t1a and β t1b (Glass and Donaldson, 1995) to amplify the β -tubulin 1 (*bt1*) region, and primers EF1-728F and EF1-986R (Jacobs *et al.*, 2004) for the Translation Elongation Factor 1- α (*tef1*) gene region.

PCR reactions and conditions, including optimal MgCl₂ concentrations and annealing temperature for the three gene regions, were carried out as described by Fourie *et al.* (2015), with an Expand-PCR programme of 96°C for 10 min, (94°C for 30 s, primer specific anneal-

Table 2. Details of the *Ceratocystis ficicola* isolates from Japan and Greece analysed in the present study.

Species ¹	Isolate No. ²	Substrate	Country	Locality	Year collected	GenBank accession numbers		
						bt1	tef1	rpb2
<i>C. ficicola</i> ^T	MycoBank 518749; CMW 38543; BPI 843724, MAFF 625119	<i>Ficus carica</i>	Japan	Fukuoka Prefecture	1990	KY685077	KY316544	KY685082
<i>C. ficicola</i>	CMW 38544; NCF0801	<i>Ficus carica</i>	Japan	Fukuoka Prefecture	1991	KY685078	KY685079	KY685083
<i>C. ficicola</i>	CMW 54793; FCE-1	<i>Ficus carica</i> cultivar Smyrna	Greece	Istiaia-Aidipsos, Avgaria village	2019	Same as KY685077	Same as KY316544	Same as KY685082
<i>C. ficicola</i>	CMW 54794; FCE-2	Soil under infected <i>Ficus carica</i> cultivar Smyrna	Greece	Istiaia-Aidipsos, Avgaria village	2019	Same as KY685077	Same as KY316544	Same as KY685082
<i>C. ficicola</i>	CMW 54795; FCE-4	Soil under infected <i>Ficus carica</i> cultivar Smyrna	Greece	Istiaia-Aidipsos, Avgaria village	2019	Same as KY685077	Same as KY316544	Same as KY685082
<i>C. ficicola</i>	CMW 54796; FCM-1	<i>Ficus carica</i> cultivar Vassilika honey white	Greece	Municipality of Markopoulo Mesogaia	2018	Same as KY685077	Same as KY316544	Same as KY685082

¹ T = Ex-type material of *Ceratocystis ficicola*;

² CMW = Culture collection of the Forestry and Agricultural Biotechnology Institute (FABI), University of Pretoria, South Africa; BPI = US National Fungus Collections, Beltsville, Maryland, USA; MAFF = Ministry of Agriculture, Forestry and Fisheries Culture Collection, Tsukuba, Ibaraki, Japan; FCE, FCM= Institute of Mediterranean Forest Ecosystems culture collection numbers

ing temperature for 45 s, 72°C for 1 min) for 10 cycles, (94°C for 30 s, primer specific annealing temperature for 45 s, 72°C for 1 min + 5 s/cycle increase) for 30 cycles, and 72°C for 10 min. All amplicons were purified using 6% Sephadex G-50 columns (Sigma-Aldrich), were sequenced in both directions using the ABI PRISM™ Big DYE Terminator Cycle Sequencing Ready Reaction Kit (Applied BioSystems), and the products were run on an ABI 3100 Genetic Analyzer (Applied BioSystems, Thermo Fisher).

The forward and reverse sequence reads were assembled into contigs in CLC Bio Main workbench v.6 (CLC Bio, www.clcbio.com), and the consensus sequences generated were used in BLAST analyses against the NCBI GenBank database (NCBI; <http://www.ncbi.nlm.nih.gov>) to determine the closest similarity matches with authenticated *Ceratocystis* species.

Sequences were added to the combined *rbp2*, *bt1* and *tef1* *Ceratocystis* database obtained from Barnes *et al.* (2018) (TreeBASE No. S22005), with a focus on retaining all the *Ceratocystis* species in the Asian-Australian Clade (AAC) in the phylogenetic analyses. *Ceratocystis albifundus* was used as the outgroup taxon. Sequences were re-aligned using the online version of MAFFT v. 7 (<http://mafft.cbrc.jp/alignment/server/>). Maximum parsimony (MP) analyses performed in PAUP v. 4.0 (Swofford 2002) and Maximum likelihood (ML) analysis in RAxML (Stamatakis 2014) were carried out on the combined dataset with the same parameters used by Barnes *et al.* (2018).

Inoculation tests

Two isolates of *C. ficicola* collected from different localities were used for inoculation trials. One of these (CMW 56935) from the Attica region was used in the first test (2018) and the other (CMW 54794) from Euboea Island was used in the second test (2019). The isolates used in the inoculation tests were grown for 2 weeks at 25°C in Petri dishes containing V8A. For inoculations, a 3 mm diam. cork-borer was used to remove the bark from stems or branches of test trees (see below), and a mycelium plug of similar size was inserted into each wound which was then wrapped with Parafilm®. Control plants were inoculated in the same way with sterile V8 agar plugs.

The two inoculation tests were carried out at the Institute of Mediterranean Forest Ecosystems in Athens, Greece. In the first test, 11 branches (diam. 1–4 cm) of a wild *F. carica* tree were inoculated in June 2018 with isolate CMW 56935. In the second test conducted in September 2019, a total of 13 *F. carica* saplings (1–2 years-

old) of different size and grown in 7.5 L capacity pots, were inoculated with isolate CMW 54794. Stem diameters of these plants at the inoculation points was from 5 to 20 mm. Non-inoculated control plants were not used in the first test, while in the second test six plants were inoculated with sterile V8 agar plugs.

In September 2019, inoculations were also performed on branches of two *Ficus benjamina* trees, in the same area with isolate CMW 54794. A total of 16 branches on the two trees were inoculated. A third *F. benjamina* tree was used as a control, by inoculating seven branches with sterile V8 agar plugs.

After inoculation, the plants were monitored regularly for expression of disease symptoms. In the first inoculation test (2018), the inoculated branches were harvested after 5 weeks. In the second test (2019), most of the plants were harvested 6 weeks after inoculation, although some of the plants displaying symptoms of wilt were harvested at an earlier time to allow for lesions to be measured. All inoculated stems and branches were sliced open vertically above and below the inoculation points, and the lengths of internal xylem staining were measured. Re-isolations from these lesions were made at different distances from the inoculation points, by aseptically transferring pieces of stained wood onto the selective V8A medium.

Statistical analyses were performed to compare the means of internal lesion lengths for the inoculations on *F. carica* and *F. benjamina* branches or stems of the *F. carica* sapling plants. In these comparisons, only the saplings of *F. carica* that were harvested after 6 weeks were included. A Shapiro-Wilk test was used to test normality of the data, and a Levene's test was used to assess equality of variances. A Kruskal-Wallis H test was then applied to compare the means of lesion lengths between *F. carica* and *F. benjamina* plants, followed by Dunn-Bonferroni *post hoc* method.

RESULTS

Disease symptoms and distribution

In the Markopoulo Mesogaias municipality in East Attica, wilt of fig trees was detected at one location with orchards of mature fig trees (20–30 years-old) of the 'Vasilika honey-white' and 'Vasilika black' cultivars, distributed over approx. 10 ha (Table 1). In the Istiaia-Aidipsos municipality, in the northern part of Euboea Island, the disease was found in fig orchards at four locations (villages) more than 10 km apart, on young as well as mature trees. All the wilt-affected trees on Euboea Island were of the 'Smyrna' cultivar (Table 1).

Wilted mature trees were usually located in one part of each orchard, and the disease appeared to have spread to neighbouring fig trees. In some cases, more than one disease centre was observed. Infected mature trees of all three cultivars showed thinning and yellowing of the foliage, either on some of the branches or over the entire crowns (Figure 1A). In some trees, most of the leaves had dropped by the end of summer, while some of the unripe fruits were retained on the trees indicating rapid death (Figure 1B). In many of the affected mature trees, complete defoliation was observed by the end of the summer, although full foliage had been present on these trees early in the spring. The affected trees eventually died, and in many cases, where dead trees had been replaced with new young plants; these were also dying within 1 to 2 years after replacement.

On mature trees, extensive bark cankers were observed at the bases of the trunks. Necrotic dark brown sapwood was obvious after removal of the bark in the lower part of the trunks (Figure 1C–E), and these lesions extended upwards. Necrotic roots were also observed on affected trees. In some symptomatic young (2–3 years-old) trees, wood staining was not always present at the trunk bases, although in these cases necrotic roots were observed. Wood staining was not found on the branches of wilted trees with chlorotic leaves, or on defoliated trees. Infestations by wood boring insects were not observed on any of the wilted fig trees examined.

In a newly planted 6 ha orchard on Euboea Island, 3 years after planting, approx. 40–50% of the trees were dead or dying with evident disease symptoms. This land had not previously been used for fig tree cultivation.

Fungus isolations

A *Ceratocystis* species was consistently isolated directly from stained fig tree wood on the selective PARPH V8A medium. The fungus was also isolated on plain V8A, but in most of these cases it was overgrown by saprotrophic fungi. On selective medium, colonies were suppressed and scarcely formed ascomata, but they resumed normal growth when transferred to plain V8A medium and ascomata developed after 7–10 d.

The *Ceratocystis* species was also isolated using the carrot baiting technique, but in many cases the carrots were contaminated with bacteria and isolations were inconsistent using this technique. The trapping technique with fig twigs as baits was effective for isolating the *Ceratocystis* species from soil and from wood samples. For twig baiting, the fungus had colonized the twigs and formed ascomata (Figure 2A) after 7–10 d, at the water level. The fungus was easily isolated from

ascospore masses transferred to selective medium. In a few cases, it was not possible to isolate the fungus from wood samples taken from symptomatic trees, especially where these trees had died, but the fungus was readily isolated from soil samples collected near the bases of these trees using the twig baiting technique.

Fungus morphology

Colonies in V8A, after 7–10 d in culture, were circular with slightly undulate margins and were dark olivaceous green. The optimum growth temperature was 25°C, with a radial growth of 20–23 mm week⁻¹. The fungus grew well at 30°C but no growth was observed at 35 or 40°C. When the cultures were transferred to 25°C after 2 weeks incubation at 35°C, the colonies resumed normal growth, but incubation for 2 weeks at 40°C killed the fungus and no growth was observed on the plates after transferring these to 25°C.

Black ascomata (Figure 2A, B) were observed after 7–10 d incubation on V8A, and were partially embedded in the agar. These measured 400–600 µm diam. and had globose bases and long necks (1150–2200 µm long). They had ostiolar hyphae at the tips of the necks (Figure 2C) which were 180–300 µm long. Ascospores exuding from the tips of the ascomata necks formed sticky masses of creamy colour (Figure 2A). Ascospores were one-celled, ellipsoidal in top view, measured 5–7 × 4–5 µm, with the characteristic “bowler-hat” shape typical of *Ceratocystis* spp. (Figure 2D). The fungus produced abundant cylindrical endoconidia (12–40 × 4–7 µm) with rounded apices, and these varied slightly as bulged to straight, from less to more round apices (Figure 2F, G). The conidia were extruded in chains from tubular conidiogenous cells (Figure 2H). Aleurioconidia (Figure 2E) were formed singly or in short chains on short conidiophores, and these were ovoid to subglobose (9–13 × 7–12 µm), pigmented and thick-walled. Doliform endoconidia were not observed.

Morphological characteristics of the Greek isolates were identical to those of the Japanese isolate (exholotype MAFF 625119 = CMW 38543), except that the dimensions of the endoconidia were different. The Japanese isolate had cylindrical endoconidia with dimensions of 5–9.5 × 4.5–8 µm, whereas those made in the present study were 12–40 × 4–7 µm.

Sequencing and phylogenetic analyses

Amplicons of the *rpb2*, *bt1* and *tef1* gene regions produced fragments of approx. 1123, 592 and 754 bp,



Figure 2. Microscopic features of *Ceratocystis ficicola*. A, ascomata on a twig bait; B, ascoma; C, ostiolar hyphae; D, ascospores; E, an aleurioconidium; F and G, cylindrical endoconidia; H, phialides. Scale bars: A = 1.5 mm; B = 500 μ m; C = 100 μ m; D to H = 10 μ m.

respectively. For each of the three gene regions, the sequences for all four isolates were 100% identical to each other. Blast searches against the NCBI GenBank database resulted in 100% identity matches to *C. ficicola* ex-type isolate from Japan [Mycobank MB518749, CMW 38543 for *rpb2* (KY685082), *bt1* (KY685077) and *tef1* (KY316544) gene regions (Table 2)].

The combined dataset (*rpb2*, *bt1* and *tef1*) of the sequences used for the phylogenetic analyses consisted of 2127 aligned characters. MP analyses resulted in eight most parsimonious trees with TL = 299, CI = 0.863, RI = 0.945 and RC = 0.815, with 238 parsimony-informative characters and six uninformative characters. For the ML analyses, using GTR-GAMMA as the best fit model,

the log-likelihood of the most likely tree obtained was -5139.12. MP and ML analyses placed the isolates from Greece, collected from infected *F. carica*, and those obtained from the soil, in the same clade as those of *C. ficicola* from Japan with 100% bootstrap support (Figure 3). These isolates form part of the Asian Australian Clade (ACC) of *Ceratocystis*, as defined by Li *et al.* (2017).

Inoculation tests

All the plants of *F. carica* and *F. benjamina* inoculated with *C. ficicola* developed symptoms of infections (Figure 4), while no symptoms were observed on any

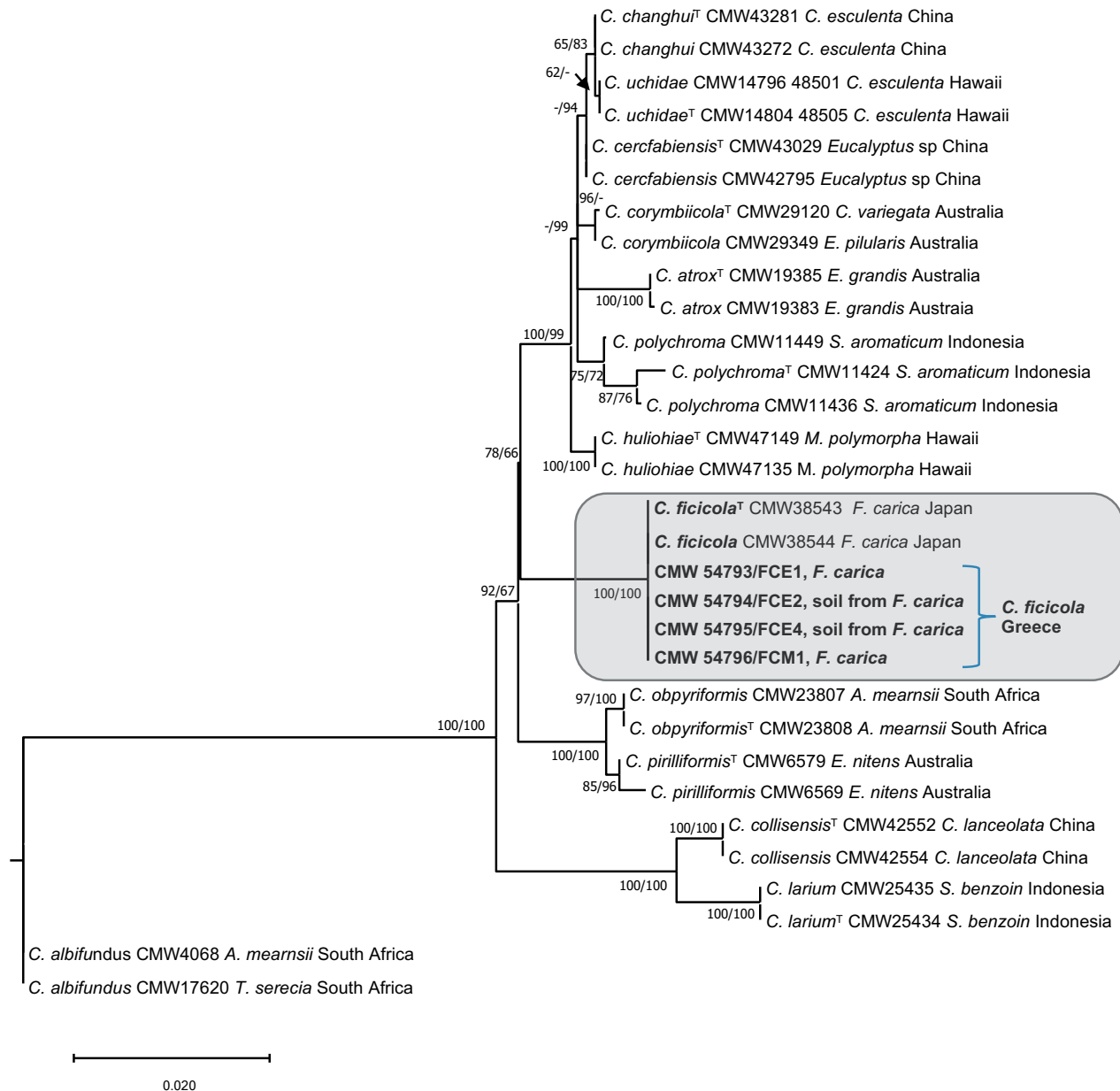


Figure 3. Phylogenetic placement of the isolates from Greece with *Ceratocystis ficicola* from Japan in the Asian-Australian *Ceratocystis* Clade. The ML phylogeny, constructed from the combined regions of the *rpb2*, *bt1* and *tef1* gene sequences, is presented with MP and ML bootstrap values >60 % indicated on the branch nodes. T indicates ex-type representatives of each species. *Ceratocystis albifundus* was used as the outgroup.

of the control plants. Lesions on the inoculated plants included necrotic bark around the inoculation point (Figure 4B), which, in some cases, was evident as early as 2 weeks after inoculation. Exposure of the cambium in stems showed brown-coloured streaked discolouration of the woody tissues, extending longitudinally in the xylem beyond the necrotic bark (Figure 4D, E).

Branch inoculations on *Ficus carica*

The internal lesions associated with the stained wood on the *F. carica* branches inoculated in 2018, and measured after 5 weeks, extended up to 12 cm from the inoculation points. The lesion lengths were 10–23 cm (mean = 14.2 cm).



Figure 4. Inoculations with *Ceratocystis ficicola*. A, *Ficus carica* symptoms of leaf wilt 6 weeks after inoculation; B, canker formed on a branch twig of *F. carica* 5 weeks after inoculation; C, canker formed on a branch twig of *F. benjamina* 6 weeks after inoculation; D and E, main stem of a *F. carica* sapling with xylem discoloration extending longitudinally beyond the necrotic bark 6 weeks after inoculation. Arrows in E show the edges of the lesion.

Inoculations on *Ficus carica* saplings

Three of the *F. carica* saplings inoculated in 2019 that had small diameters (57 mm), showed stem girdling and symptoms of wilt 2 weeks after inoculation. For these three plants, the lesions were 6–12 cm long. For the other ten saplings, the internal lesion lengths were up to 21 cm long at 6 weeks after inoculation. The total lengths of the stained wood associated with these inoculations was from 2.6–37.8 cm (mean = 12.9 cm) (Figure 5).

Branch inoculations on *Ficus benjamina*

Inoculated-branches developed necrotic lesions around the inoculation sites (Figure 4C). On this host, wood staining was very limited, extending only 0.8–1.5 cm from the inoculation points with total length 1.4–3 cm (mean = 2.17 cm). Symptoms of wilt were not evident on branches 6 weeks after inoculation.

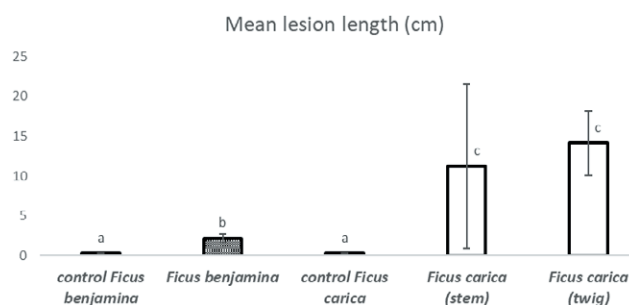


Figure 5. Mean internal lesion lengths (cm), after inoculation of *Ficus carica* sapling stems and branch twigs, or *F. benjamina* branch twigs, with *Ceratocystis ficicola*. Columns accompanied by standard deviations of means, and those accompanied by the same letters are not significantly different ($P \leq 0.05$)

There were no statistically significant differences in the mean internal lesion lengths between *F. carica* saplings (stems) and branches (twigs) in the two experiments, according to Kruskal-Wallis H test and Dunn-

Bonferroni post hoc method ($P \leq 0.05$) (Figure 5). In contrast, the mean lesion lengths on the *F. benjamina* branches differed significantly from both of the *F. carica* inoculations. There were also significant differences between lesion lengths for the control plants and those inoculated with the *C. ficicola* on both hosts (Figure 5). For *F. carica*, wood discolouration was limited to approx. 3 mm around the inoculation sites.

The inoculated fungus was consistently re-isolated from stained wood from *F. carica* and *F. benjamina* plants, and at different distances (up to 17 cm) from the inoculation points. The re-isolated fungus had the typical morphology of the inoculated fungus. The fungus could not be isolated from plants inoculated as experimental controls.

DISCUSSION

This study has provided clear evidence for the presence of *C. ficicola* in fig orchards in two separate regions (Attica and Euboea Island) of Greece. These two areas separated by large distance. This is the first detailed report of the presence of this fungus outside of Japan, in this case also supported by morphological and DNA sequence comparisons. This study also included inoculation trials that confirmed the pathogenicity of Greek isolates of *C. ficicola*.

A similar disease to that caused by *C. ficicola* in Japan and Greece has been reported in Brazil on cultivated fig trees. In that case the pathogen was reported as *Ceratocystis fimbriata* Ellis and Halsted *sensu lato* (Pasura and Harrington, 2004). Kajitani and Masuya (2011) showed that *C. ficicola* is different to the *Ceratocystis* species from fig trees in Brazil, based on morphological differences and ITS sequences. The distinct nature of the fungus killing fig trees in Brazil and Japan was also confirmed by Harrington *et al.* (2011). Results of the present study based on morphological comparisons and DNA sequence data for three gene regions also confirmed that *C. ficicola* from Greece is in the Asian-Australian clade of *Ceratocystis* (Li *et al.*, 2017). In contrast, isolates from fig trees in Brazil form part of the Latin American Clade (Harrington *et al.*, 2011).

Observations in the present study agree with those of Kajitani and Masuya (2011), confirming that *C. ficicola* has morphology that is distinct from other species of *Ceratocystis*. This is relevant as many species of *Ceratocystis*, as defined by De Beer *et al.* (2014), cannot easily be distinguished based on morphology. The most characteristic structures in *C. ficicola* that distinguish it from other *Ceratocystis* species are the large ascomata with

very long necks ($>2000 \mu\text{m}$). Ascospores are very similar in shape and size to those of *Ceratocystis fimbriata sensu stricto* (Marincowitz *et al.*, 2020). Doliform endoconidia were not observed in the present study, and these were also absent from observations of Kajitani and Masuya (2011). However, there was a difference in the size of the cylindrical endoconidia in the present study isolates compared with those described by Kajitani and Masuya (2011). This was confirmed in comparisons of the Greek isolates and the Japanese ex-holotype isolate (CMW 38543) made in the present study.

In Japan, the disease of fig caused by *C. ficicola* is commonly referred to as “*Ceratocystis* canker”, but Kajii *et al.* (2013) stated that the disease is more typical of vascular wilt. The pathogen invades the roots and the main stems of host plants, causing xylem dysfunction and wilt symptoms on infected fig trees. In cross sections of main stems, dark brown radial discolouration of the sapwood tissues was evident at the bases of affected trees, extending upwards and downwards to the roots (Kajii *et al.*, 2013). Consistent with the view of Kajii *et al.* (2013) that infection by *C. ficicola* should be defined as a wilt disease, Morita *et al.* (2016) and Sumida *et al.* (2016) in inoculation studies on mature fig trees, as well as young seedlings, reported that xylem discolourations were correlated with xylem dysfunction. The water supply to leaves decreased when infection progressed causing leaf wilting and extensive xylem dysfunction leading to plant death.

Ceratocystis ficicola also kills host cambium and the bark tissues causing cankers, which were present at the bases of the main stems on most symptomatic trees in Greece. In our surveys, wood discolouration was not evident in the branches of trees displaying wilt of the leaves, and similar observations were made in Japan by Kajii *et al.* (2013). However, the inoculated branch twigs in our experiments developed cankers and extensive wood discoloration. Overall, these symptoms are similar to those of many other tree diseases caused by *Ceratocystis* species, and the disease is best described as canker-wilt (Tsopelas *et al.*, 2017; Nasution *et al.*, 2019).

In the present study, inoculation experiments, showed that *F. benjamina* and not only *F. carica* plants can become infected with *C. ficicola*. However, this species was less susceptible to the pathogen than *F. carica*. In Japan, *Ficus erecta* Thunb., which is an indigenous species, has been proven resistant to *C. ficicola* and has been used in breeding programmes to develop resistant fig tree rootstocks (Yakushiji *et al.*, 2019).

In several studies carried out in Japan, it has been shown that *C. ficicola* is a soil-borne pathogen. It has also been suggested that the fungus persists in the soil as thick-walled aleurioconidia, and newly planted trees in contami-

nated soil are soon infected by the pathogen (Kajii *et al.*, 2013; Yakushiji *et al.*, 2019). Our field observations, in both regions of Greece considered, also suggest soil-borne disease problems, where trees were planted to replace those that had died also became infected. We consistently isolated *C. ficicola* from soils associated with dying trees.

Detection of *C. ficicola* in the soil at an early stage will be important for pathogen detection and application of canker-wilt control strategies. In the present study, using twig baiting, the fungus was readily isolated from soil, even in cases where the pathogen could not be directly isolated from wood samples from nearby symptomatic trees. This baiting method was originally described by Grosclaude *et al.* (1988) for detection and isolation of *Ceratocystis platani*, which causes the canker stain of plane trees (*Platanus*). The method was also successfully used to isolate *C. platani* from adult *Platypus cylindrus* Fab. beetles, a vector of *C. platani* (Soulioti *et al.*, 2015). The present study is the first to use baiting technique to isolate *C. ficicola* from soil and wood samples.

According to Kajitani and Masuya (2011), the dispersal biology of *C. ficicola* is not fully understood. One of the suggested pathways of disease spread in Japan was with infected propagation material (Kajii *et al.*, 2013). This was also evident in one of the orchards examined on Euboea Island. The pathogen was widespread in a new plantation over an area of 6 ha, 3 years after the fig trees had been planted. Since there was no previous use of this land for fig cultivation, the most probable means of pathogen dissemination over such a short period would be with infected nursery stock.

Every effort should be made to avoid further spread of *C. ficicola* with planting material and via contaminated soil. This is a probable pathway for introduction and spread of the pathogen into other areas and countries. The pathogen can survive in soil associated with plants for planting, when symptoms are not evident. While nursery stock should be carefully examined for the presence of *C. ficicola*, disease symptoms may not be always evident, especially during winter when new plants are being established. This problem is exacerbated with fig trees having no foliage during this period, and infected plants may escape the attention during inspections.

Ceratocystis ficicola may also spread with tractors used for ploughing that move infested soil and wood debris within or between orchards. Deep ploughing also causes root wounding, allowing pathogen infection sites. The use of infested ploughing machinery is likely to be a major pathway for pathogen dissemination in the fig orchards of Euboea Island. A major pathway of disease spread for *C. platani* in many areas of Europe has been from terracing machinery that transmit the pathogen

over short and long distances (Tsopeles *et al.*, 2017). Some *Ceratocystis* species can also survive for long periods as aleurioconidia in infected wood. This spore form was also observed by Kajii *et al.*, (2013) in the vessel elements of fig trees infected with *C. ficicola*. Contaminated pruning and cutting tools may therefore be involved in the spread of the pathogen to healthy trees. Precautionary measures, including disinfection of pruning tools and the machinery used in fig orchards have been recommended to avoid further spread of *C. ficicola* in Greece.

Ambrosia beetles (*Euwallacea interjectus* Blandford) have been suggested as possible vectors of *C. ficicola* in Japan. These insects also contribute to expansion of the fungus in sapwood of infected trees (Kajii *et al.*, 2013). The frass produced by the insects may also disseminate the pathogen, as with other *Ceratocystis* species (Harrington, 2013; Tsopeles *et al.*, 2017). Frass can be dispersed by wind, rain splash or running water over short distances, and can contaminate soil or initiate new infections in pruning wounds (Harrington, 2013). In Greece, infestation by wood boring insects in *C. ficicola*-infected fig trees has not been observed. However, future surveys should include careful inspection for the presence of such insects. The ambrosia beetle *Platypus cylindrus* has been reported in Greece to attack *Platanus orientalis* trees already infected by *C. platani*, and this insect may be involved in the spread of that pathogen (Soulioti *et al.*, 2015).

The origin of *C. ficicola* is unknown. Kajitani and Masuya (2011) have suggested two possibilities; one that the fungus is invasive in Japan, or alternatively, that it is native to that country and has, over time, come into contact with the highly susceptible *F. carica*. All evidence emerging from the present study indicates that *C. ficicola* is an alien invasive pathogen in Greece. This because *F. carica* has been cultivated in Greece since ancient times, but canker-wilt has only been detected in recent years and at a small scale. An important question remains as to how the pathogen was introduced into this country, either from Japan or from another source in the Mediterranean region where it is yet to be detected.

Ceratocystis ficicola causes a very important disease of fig trees in Japan, resulting in severe outbreaks of canker-wilt (Kajitani and Masuya, 2011; Yakushiji *et al.*, 2019). The presence of the pathogen in Greece is particularly relevant. Fig is a very important crop in Mediterranean countries, because it is adapted to the dry climatic conditions of the region. About 70% of total world fig production occurs in Mediterranean countries (Flaishman *et al.*, 2008). Consequently, the disease could result in severe losses if the pathogen were to be disseminated to other countries, such as Turkey, Egypt or Morocco where fig production is also important.

ACKNOWLEDGEMENTS

The authors thank Vassilios Bournakas, agronomist in Euboea Island, for valuable help during the field surveys of this region, and Kira Lynn for technical assistance. Dr Hayato Masuya, (Forestry and Forest Products Research Institute, Japan) supplied the ex-type culture of *C. ficicola* from Japan. We acknowledge the Department of Science and Technology/National Research Foundation Center of Excellence in Plant Health Biotechnology, South Africa for financial support.

LITERATURE CITED

- Barnes I., Fourie A., Wingfield M.J., Harrington T.C., McNew D.L., ... Keith L.M., 2018. New *Ceratocystis* species associated with rapid death of *Metrosideros polymorpha* in Hawaii. *Persoonia* 40: 154–181. <https://doi.org/10.3767/persoonia.2018.40.07>
- Condit I.J., 1955. Fig varieties: A monograph. *Hilgardia*, 23: 323–538.
- De Beer Z.W., Duong T.A., Barnes I., Wingfield B.D., Wingfield M.J., 2014. Redefining *Ceratocystis* and allied genera. *Studies in Mycology* 79: 187–219. <https://doi.org/10.1016/j.simyco.2014.10.001>
- FAO, 2019. The FAO statistical database-agriculture. Available at: <http://www.fao.org/faostat/en/#data/QC>. Accessed March 4, 2021.
- Ferguson A.J., Jeffers S.N., 1999. Detecting multiple species of *Phytophthora* in container mixes from ornamental crop nurseries. *Plant Disease* 83: 1129–1136.
- Fourie A., Wingfield M.J., Wingfield B.D., Barnes I., 2015. Molecular markers delimit cryptic species in *Ceratocystis sensu stricto*. *Mycological Progress* 14: 1020. <https://doi.org/10.1007/s11557-014-1020-0>
- Flaishman M., Rodov V., Stover E., 2008. The Fig: Botany, Horticulture, and Breeding. *Horticultural Reviews* 34: 113–197. <https://doi.org/10.1002/9780470380147.ch2>
- Glass N.L., Donaldson G.C., 1995. Development of primer sets designed for use with the PCR to amplify conserved genes from filamentous Ascomycetes. *Applied and Environmental Microbiology* 61: 1323–1330. <https://doi.org/10.1128/AEM.61.4.1323-1330.1995>
- Grosclaude C., Olivier R., Pizzuto J.C., Romiti C., Madec S., 1988. Détection par piégeage du *Ceratocystis fimbriata* f. *platani*. Application à l'étude de la persistance du parasite dans du bois infecté. *European Journal of Forest Pathology* 18: 385–390.
- Harrington T.C., 2013. *Ceratocystis* diseases. In: Gonthier P, Nicolotti G Eds. *Infectious Forest Diseases*. UK: CABI Publishing, 230–255.
- Harrington T.C., Thorpe D.J., Alfenas A.C., 2011. Genetic variation and variation in aggressiveness to native and exotic hosts among Brazilian populations of *Ceratocystis fimbriata*. *Phytopathology* 101: 555–566. <https://doi.org/10.1094/PHYTO-08-10-0228>
- Jacobs K., Bergdahl D.R., Wingfield M.J., Halik S., Seifert K.A., ..., Wingfield B.D., 2004. *Leptographium wingfieldii* introduced into North America and found associated with exotic *Tomicus piniperda* and native bark beetles. *Mycological Research* 108: 411–418. <https://doi.org/10.1017/s0953756204009748>
- Kajii C., Morita T., Jikumaru S., Kajimura H., Yamaoka Y., Kuroda K., 2013. Xylem dysfunction in *Ficus carica* infected with wilt fungus *Ceratocystis ficicola* and the role of the vector beetle *Euwallacea interjectus*. *International Association of Wood Anatomists Journal* 34: 301–312. <https://doi.org/10.1163/22941932-00000025>
- Kajitani Y., Masuya H., 2011. *Ceratocystis ficicola* sp. nov., a causal fungus of fig canker in Japan. *Mycoscience* 52: 349–353. <https://doi.org/10.1007/s10267-011-0116-5>
- Kato K., Hirota K., Miyagawa T., 1982. A new disease, *Ceratocystis* canker of fig caused by *Ceratocystis fimbriata* Ellis et Halsted. *Plant Protection* 36: 55–59 (in Japanese).
- Kislev M.E., Hartmann A., Bar-Yosef O., 2006. Early domesticated fig in the Jordan Valley. *Science* 312: 1372–1374. <https://doi.org/10.1126/science.1125910>
- Li Q., Harrington T.C., McNew D., Li J., 2017. *Ceratocystis uchidaei*, a new species on Araceae in Hawai'i and Fiji. *Mycoscience* 58: 398–412. <https://doi.org/10.1016/j.myc.2017.06.001>
- Marincowitz S., Barnes I., De Beer Z.W., Wingfield M.J., 2020. Epitypification of *Ceratocystis fimbriata*. *Fungal Systematics and Evolution* 6(1): 289–298. <https://doi.org/10.3114/fuse.2020.06.14>
- Moller W.J., De Vay J.E., 1968. Carrot as a species-selective isolation medium for *Ceratocystis fimbriata*. *Phytopathology* 58: 123–124.
- Morita T., Jikumaru S., Kuroda K., 2016. Disease development in *Ficus carica* plants after inoculation with *Ceratocystis ficicola*. (1) Relationship between xylem dysfunction and wilt symptoms. *Japanese Journal of Phytopathology* 82: 301–309. (In Japanese with English summary). <https://doi.org/10.3186/jjphytopath.82.301>
- Nasution, A., Glen, M. Beadle, C., Mohammed C., 2019. *Ceratocystis* wilt and canker – a disease that compromises the growing of commercial *Acacia*-based plantations in the tropics. *Australian Forestry* 82: 80–93. <https://doi.org/10.1080/00049158.2019.1595347>

- Pasura A., Harrington T.C., 2004. Two undescribed species in the *Ceratocystis fimbriata* complex on *Ficus* and *Colocasia* from Asia and Polynesia. *Phytopathology* 94 (supl.): S160-S161 (Abstr.).
- Soulioti N., Tsopelas P., Woodward S., 2015. *Platypus cylindrus*, a vector of *Ceratocystis platani* in *Platanus orientalis* stands in Greece. *Forest Pathology* 45: 367–372. <https://doi.org/10.1111/efp.12176>.
- Sumida S. Kajit C., Morita T., Kuroda K., 2016. Disease development in *Ficus carica* seedlings after inoculation with *Ceratocystis ficicola*. (2) Microscopic analysis of the host-pathogen interaction and internal symptoms. *Japanese Journal of Phytopathology* 82: 310–317. (In Japanese with English summary). <https://doi.org/10.3186/jjphytopath.82.310>
- Stamatakis A., 2014. RAXML Version 8: A tool for phylogenetic analysis and post-analysis of large phylogenies. *Bioinformatics* 30: 1312–1313. <https://doi.org/10.1093/bioinformatics/btu033>.
- Swofford D.L., 2002. PAUP*. Phylogenetic Analysis Using Parsimony (*and other methods). 4 edn. Sinauer Associates, Sunderland. <https://doi.org/10.1111/j.0014-3820.2002.tb00191.x>
- Tjamos E.C., Tsopelas P., Soulioti N., Palavouzis S., Antoniou P., Paplomatas E.J., 2018. A serious infection of fig trees by *Ceratocystis* sp. in Greece: First report of the pathogen in Europe. *Abstracts of the 19th Greek Phytopathological Congress, Hellenic Phytopathological Society*, Athens, Greece, October 30-November 1, 2018, p. 31 (in Greek).
- Tsopelas P., Santini A., Wingfield M.J., De Beer W., 2017. Canker stain: A lethal disease destroying iconic plane trees. *Plant Disease* 101: 645–658. <https://doi.org/10.1094/PDIS-09-16-1235-FE>
- Yakushiji H., Morita T., Jikumaru S., 2019. *Ceratocystis* canker resistance in BC1 populations of interspecific hybridization of fig (*Ficus carica*) and *F. erecta*. *Scientia Horticulturae* 252: 71–76. <https://doi.org/10.1016/j.scienta.2019.03.039>



Citation: Author (2021) Title. *Phytopathologia Mediterranea* 60(2): 351-379. doi: 10.36253/phyto-13021

Accepted: August 12, 2021

Published: September 13, 2021

Copyright: ©2021 Author. This is an open access, peer-reviewed article published by Firenze University Press (<http://www.fupress.com/pm>) and distributed under the terms of the Creative Commons Attribution License, which permits unrestricted use, distribution, and reproduction in any medium, provided the original author and source are credited.

Data Availability Statement: All relevant data are within the paper and its Supporting Information files.

Competing Interests: The Author(s) declare(s) no conflict of interest.

Editor: Alan Phillips, University of Lisbon, Portugal.

Review

***Fomitiporia mediterranea* M. Fisch., the historical Esca agent: a comprehensive review on the main grapevine wood rot agent in Europe**

SAMUELE MORETTI^{1,*}, ANDREA PACETTI^{1,2}, ROMAIN PIERRON¹, HANNS-HEINZ KASSEMAYER³, MICHAEL FISCHER⁴, JEAN-PIERRE PÉROS⁵, GABRIEL PEREZ-GONZALEZ⁶, EVIE BIELER⁷, MARION SCHILLING⁸, STEFANO DI MARCO⁹, ERIC GELHAYE⁸, LAURA MUGNAI², CHRISTOPHE BERTSCH¹, SIBYLLE FARINE^{1,*}

¹ Laboratoire Vigne Biotechnologies et Environnement UPR-3991, Université de Haute Alsace, 33 rue de Herrlisheim, 68000 Colmar, France

² Department of Agricultural, Food, Environmental and Forestry Science and Technology (DAGRI), Plant pathology and Entomology section, University of Florence, P.le delle Cascine, 28, 50144 Firenze, Italy

³ State Institute for Viticulture, Plant Pathology & Diagnostics, Merzhauser Str. 119, 79100 Freiburg, Germany

⁴ JKI-Julius Kühn-Institute, Federal Research Centre for Cultivated Plants, Plant Protection in Fruit Crops and Viticulture, D-76833 Siebeldingen, Germany

⁵ UMR AGAP Institut, Université de Montpellier, CIRAD, INRAE, Institut Agro, F-34398 Montpellier, France

⁶ Department of Microbiology, University of Massachusetts, Amherst, MA 01003, USA

⁷ University of Basel, Swiss Nanoscience Institute - Nano Imaging Lab, Basel, University of Basel, Klingelbergstrasse 50 CH-4056 Basel, Switzerland

⁸ Université de Lorraine, INRAE, IAM, F-54000 Nancy, France

⁹ Istituto per la Bioeconomia, Consiglio Nazionale delle Ricerche, Via Gobetti 101, 40129 Bologna, Italy

*Corresponding authors: samuele.moretti@uha.fr; sibylle.farine@uha.fr

Summary. *Fomitiporia mediterranea* M. Fisch. (*Fmed*) is a basidiomycete first described in 2002, and was considered up to then as part of *Fomitiporia punctata* (P. Karst) Murrill. This fungus can degrade lignocellulosic biomass, causing white rot and leaving bleached fibrous host residues. In Europe *Fmed* is considered the main grapevine wood rot (Esca) agent within the Esca disease complex, which includes some of the most economically important Grapevine Trunk Diseases (GTDs). This review summarises and evaluates published research on *Fmed*, on white rot elimination by curettage or management by treatments with specific products applied to diseased grapevines, and on the relationship between wood symptoms and Grapevine Leaf Stripe Disease (GLSD) in the Esca disease complex. Information is also reviewed on the fungus biology, mechanisms of pathogenicity, and their possible relationships with external foliar symptoms of the Esca disease complex. Information on *Fmed* control strategies is also reviewed.

Keywords. *Fmed*, Basidiomycete, white rot, wood symptoms, foliar symptoms.

INTRODUCTION

Grapevine Trunk Diseases (GTDs), mainly comprising *Botryosphaeria dieback*, *Eutypiosis* and the Esca disease complex, are widespread in vineyards (Mugnai *et al.*, 1999; Bertsch *et al.*, 2013; Bruez *et al.*, 2013; Mondello *et al.*, 2018a). These diseases significantly affect grapevine productivity causing yield losses and quality degradation affecting wine alcohol content and flavour components (Mugnai *et al.*, 1999; Lorrain *et al.*, 2012; Calzarano *et al.*, 2001, 2017).

For several decades the only effective pesticides used to control GTDs were sodium arsenite, to reduce the leaf stripe foliar symptoms in the Esca complex of diseases (Ravaz, 1919; Bonnet, 1926; Rui and Battel, 1963; Svampa and Tosatti, 1977; Del Rivero and García-Marí, 1984), and the fungicides benomyl and carbendazim, to reduce infections by the agents of *Eutypiosis* and *Botryosphaeria dieback*, respectively (Magarey and Carter 1986; Ramsdell, 1995). All these pesticides were banned in European countries in the early 2000s because of their potential environmental and/or user toxicities, more than 10 years after GTDs and especially Esca disease complex were becoming acute problems in Europe and in other grapevine growing countries. GTDs have been described as “the biotic stress of the century” for grapevines (Songy *et al.*, 2019a), and all wine-growing countries are likely to be affected by these diseases. In France, the National Grapevine Trunk Disease Survey assessed incidence and evolution of GTDs during a 10 year survey period. Up to 13% of productive vines were affected by GTDs in French vineyards (Grosman, 2008; Grosman and Doublet, 2012; Bruez *et al.*, 2013). In Italy, incidence of GTDs was between 8 to 19% (Romanazzi *et al.*, 2009), and was of average annual incidence of 12% in vineyards younger than 10 years (Abbatecola *et al.*, 2000), or up to 63% in 30 year old vineyards (Surico *et al.*, 2000).

In several countries within and outside Europe, there has been an upward trend of GTDs since the end of the 20th century (Mugnai *et al.*, 1999; Wicks and Davies, 1999; Rubio and Garzón, 2011; Úrbez-Torres *et al.*, 2014; Fontaine *et al.*, 2016a; Guérin-Dubrana *et al.*, 2019; Kraus *et al.*, 2019). GTDs have also caused severe economic losses. These have been estimated as up to \$US 260 million in California (Siebert, 2001) for GTDs, and \$US 2000 to 3000 per hectare for “Esca disease” (Vasquez 2007, in Rubio and Garzón, 2011), and approx. one billion euros in wine production due to GTDs in France (reported in 2014 by IFV, the French Wine Institute). Annual financial costs of dead vine replacements in all wine production countries were estimated to be 1.132 billion euros (Hofstetter *et al.*, 2012). These losses

have been the major reason that professional winegrowers, research agencies, financial consortia and the scientific community have concentrated on GTDs research in recent decades.

The complexity of symptoms and fungi involved in these diseases is great, and this is particularly true for “Esca disease” (in this paper, when the literature data refer to this generic term – as well as when we will arbitrarily refer to this generic term to avoid nomenclature confusion when critically discussing the literature – we will place quotation marks around the term “Esca disease”). Historically, Esca, a word of indo-european origin meaning “food”, tinder for fire, used to indicate “amadou” i.e. white rot (Viala, 1922, on the chapter written by Gard in “Bulletin de la Société de Pathologie Végétale”, 1922; Montanari, 2010), had been used for a grapevine wood rot disease. Later, the term was associated with foliar symptoms, described as chronic or acute forms (Viala, 1926; Larignon and Dubos, 1997; Letousey *et al.*, 2010; Lecomte *et al.*, 2012), and was shown to involve several different symptoms associated with different pathogens. It was then proposed as a disease complex involving multiple pathogens including basidiomycetes and/or ascomycetes (Mugnai *et al.*, 1999; Surico, 2009; Bertsch *et al.*, 2013). These caused separate diseases including: *i*) white rot (Esca) that develops mostly in old vines; *ii*) vascular diseases, widely present in propagation material and young vines (brown wood streaking of grape cuttings and Petri disease); and *iii*) Grapevine Leaf Stripe Disease (GLSD), which has an unusual epidemiology and symptomatology that can be associated with some or all of the wood pathogens, i.e. only vascular and canker agents, or, very often, also wood decay in all possible combinations. The condition where white rot (Esca) and GLSD occur together can be indicated as “Esca proper”, in recognition of the original disease description.

The frequency of GLSD foliar symptoms has increased considerably over the last two decades. A preliminary study (Fussler *et al.*, 2008) indicated mean incidence increase of 3.25% for “Esca disease” (leaf stripe and apoplexy symptoms) in France between 2003 and 2005. “Esca disease” and *Eutypiosis* were responsible together for 10% of vine replacements in Alsace (Kuntzmann *et al.*, 2010). Also in France, Bruez *et al.* (2013) showed that incidence increase varied according to region. In Austria, Reizenzein *et al.* (2000) estimated a 2.7% annual increase of plants showing “Esca disease” foliar symptoms. In Italy, Surico *et al.* (2006) indicated an increase from 30 to 51% between 2000 and 2006, and Romanazzi *et al.* (2009) showed how disease incidences reached 60 to 80% in many old vineyards of south-

ern Italy. A comprehensive survey for 22 European and Mediterranean vine-growing countries (COST Action; Guérin-Dubrana *et al.*, 2019) described GLSD trends in most surveyed countries as “increasing” and/or “worrying”, particularly in France, Italy, Spain and Turkey. In Germany, in 12 intensively pruned vineyards of red and white grape varieties and resistant and traditional cultivars, incidence of GLSD increased from 1.9% in 2015 to 3.6% in 2018, and was greatest in 2017 at 4.5% of vines affected (Kraus *et al.*, 2019).

Some observations on Esca complex of diseases are now well accepted, despite the complexity, terminology evolution, and difficulties in understanding the interactions of variables that affect symptom expression. These include:

i) The interactions with environmental, pedo-climatic and agronomic factors/practices that can affect symptom expression and disease severity (Marchi *et al.*, 2006; Calzarano *et al.*, 2018a; Lecomte *et al.*, 2018; Fischer and Peighami-Ashnaei, 2019; Songy *et al.*, 2019a).

ii) No completely resistant grape cultivar has been reported, but cultivar and clone contributions to symptom expression and severity have been observed and reviewed (Marchi, 2001; Quaglia *et al.*, 2009; Murolo and Romanazzi, 2014; Kraus *et al.*, 2019; Moret *et al.*, 2019; Songy *et al.*, 2019a; Moret *et al.*, 2021).

iii) The nutritional (especially macronutrient) status of vines can affect foliar symptom expression (Calzarano *et al.*, 2009, 2021).

iv) Although the presence of an exceptionally wide mycoflora in Esca- and GLSD-affected vines has been confirmed by meta-barcoding (Del Frari *et al.*, 2019a; Niem *et al.*, 2020), the pathogens most frequently associated with the wood infections are the two Ascomycota *Phaeoconiella chlamydospora* (W. Gams, Crous, M.J. Wingf. & L. Mugnai) (Crous and Gams, 2000) (*Pch*) and *Phaeoacremonium minimum* (Tul. & C. Tul.) Gramaje, L. Mostert & Crous (Gramaje *et al.*, 2015) (*Pmin*) (syn. *Phaeoacremonium aleophilum*), while the most frequently isolated basidiomycete in Europe has been *Fomitiporia mediterranea* M. Fisch. (Fischer, 2002) (*Fmed*). The two Ascomycota species have mostly been associated with the “phaeotracheomycotic complex” (brown wood streaking, Petri disease and GLSD; Bertsch *et al.*, 2013), while *Fmed* or the other basidiomycetes causing wood decay (Fischer and González-García, 2015) have only been associated with white rot, Esca and “Esca proper”. Nevertheless, decay elimination (curettage) reduced foliar symptoms, and correlations between white rot extent, elimination and foliar symptom expression have been reported (Maher *et al.*, 2012; Thibault, 2015; Cholet *et al.*, 2019, 2021; Pacetti *et al.*, 2021).

Fomitiporia mediterranea (as *Fomitiporia punctata*) was shown to be a primary pathogen by artificial inoculations, either in vineyards or in greenhouse experiments (Sparapano *et al.*, 2000a; 2001a). The need for specific successions of fungi in wood colonization to detoxify wood cellular microenvironments from excesses of polyphenols produced by plant reactions has been suggested but was never fully proved (Larignon and Dubos, 1997; Mugnai *et al.*, 1997; Amalfitano *et al.*, 2000). Microbial combinations between *Fmed*, *Pch* and some bacterial taxa (i.e. *Sphingomonas* spp. and *Mycobacterium* spp.) may have a role in the onset of “Esca disease” in young vines (Bruez *et al.*, 2020). Synergism between *Fmed* and bacteria such as *Paenibacillus* spp. for grapevine wood component degradation has also been confirmed (Haidar *et al.*, 2021).

Despite the year-to-year fluctuations in incidence, foliar symptom surveys represent simple and non-invasive ways to indirectly assess grapevine wood infection by Esca complex pathogens, and for determining epidemiology, crop losses and health status of vineyards (Guérin-Dubrana *et al.*, 2013). Claverie *et al.* (2020) summarised knowledge on foliar symptom outbreak in the “toxins hypothesis” and “hydraulic dysfunction hypothesis”. The first describes how phytotoxic compounds produced by “Esca disease”-associated fungi could diffuse through host transpiration stream sap flow to leaves, inducing the typical tiger-striped leaf patterns (Abou-Mansour *et al.*, 2004; Bruno and Sparapano, 2006b; Andolfi *et al.*, 2011). The second hypothesis explains how impairment of sap flow to leaves, mainly caused by vessel occlusions/pathogen compartmentalization, could lead to cavitation contributing to foliar symptom expression (Pouzoulet *et al.*, 2014, 2017, 2019). Recent findings, however, suggest how these two hypotheses can be complementary and not exclusive, due to observed association between foliar symptoms, disruption of vessel integrity and presence of some “Esca disease”-associated pathogens presence in host trunks, which could elicit a distance-response (Bortolami *et al.*, 2019). Stem vessel occlusion has been related to exacerbation of foliar symptom expression in the following growth season (Bortolami *et al.*, 2021).

Because the two Ascomycota *Pch* and *Pmin* have frequently been associated with foliar symptoms of “Esca disease”-symptomatic plants, considerable research has been carried out on *Pch* and *Pmin* biology and pathogenicity, and a more comprehensive and integrated view on these species was presented by authors such as Valtaud *et al.* (2009), Mostert *et al.* (2006) and Gramaje *et al.* (2015). The same cannot be affirmed for *Fmed*. Despite progress made since taxonomic description of this fungus (Fischer, 2002), knowledge on the pathogen, its wood

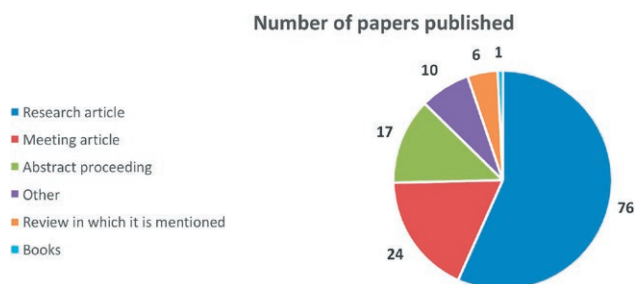


Figure 1. Number of published papers dealing with *Fomitiporia mediterranea* from 2002 (*Fmed* identification date) to 2021, as indexed in the Web of Science™ database (Thomson Reuters).

degradation process and relationship with the other Esca complex diseases, is fragmented. There are few reviews which consider *Fmed* as part of “Esca disease” or GTDs in general, and to our knowledge no comprehensive review on *Fmed* alone has been undertaken (Figure 1).

For this reason, along with contrasting reports of correlations between amounts of white rot necrotic tissues (thus *Fmed* presence) and the leaf stripe symptoms (Maher *et al.*, 2012; Bruez *et al.*, 2014; Bruez *et al.*, 2020; Cholet *et al.*, 2021; Pacetti *et al.*, 2021), and reports of little or no correlation between these factors (Edwards *et al.*, 2001; Calzarano and Di Marco 2007; Romanazzi *et al.*, 2009; Mugnai *et al.*, 2010), a review of *Fmed* is necessary, in order to collect knowledge of the fungus itself, and to stimulate scientific debate and novel ideas in the context of GTDs.

BASIDIOMYCETES ASSOCIATED WITH ESCA

Knowledge on basidiomycetes associated with “Esca disease” has increased, and Fischer (2006), Fischer and González-García (2015), and Cloete *et al.* (2015a, 2016) provided a comprehensive compendium on the topic. Ravaz (1909) was a pioneer in grapevine basidiomycete identification, with the putative identification of *Phellinus igniarius* (L.) Quél. (at the time *Fomes igniarius* (L.) Fr. and formerly *Polyporus igniarius* (L.) Fr. based on fruit bodies found on diseased grapevines in southern France). Vinet (1909) and Viala (1926) also reported the presence of *Stereum hirsutum* (Willd.) Pers. in French vineyards. These two basidiomycetes were long considered as causal agents of Esca wood decay but pathogenicity was only proven for *P. igniarius* (most likely a *Fomitiporia* sp.) by Chiarappa (1997).

Studies on “Esca disease” and its etiology multiplied in the late 1990s, especially when Larignon and Dubos (1997) isolated *Phellinus punctatus* (P. Karst.) Pilát from Esca wood decay in French vineyards. After studies of

the infrageneric structure of *Phellinus* s.l. by Fiasson and Niemelä (1984), Fischer (1996) and Wagner and Fischer (2001, 2002), *P. punctatus* was grouped within *Fomitiporia*, as *F. punctata* (P. Karst) Murrill (= *P. punctatus*). Multiple surveys of Italian vineyards by Cortesi *et al.* (2000) concluded that the main cause of decay in Esca-affected vines was *F. punctata*, later recognized as the new species *F. mediterranea* (Fischer 2002), which is now considered the main white rot agent in “Esca disease” in Europe and Mediterranean regions.

Stereum hirsutum was isolated by Larignon and Dubos (1997) from central decayed grapevine wood inhabited by putative *P. igniarius*, but its role in GLSD is still debated, although it is clearly a white rot basidiomycete agent. Some authors have suggested that this fungus has little or no role in the Esca complex of disease because it is found only rarely in vineyards (Mugnai *et al.*, 1999; Cortesi *et al.*, 2000; Reizenzein *et al.*, 2000; Vicent *et al.*, 2001). In any case, *S. hirsutum* may act as a weak facultative parasite, occasionally penetrating the heartwood of host plants and producing very limited infections and decay of the inner host tissues (Fischer and González-García, 2015).

Many other basidiomycetes have been isolated from decaying grapevine wood. White *et al.* (2011) characterised ten possibly novel taxa belonging to *Hymenochaetales* associated with “Esca disease”, *i.e.* white rot on GLSD symptomatic vines. For Europe, an annotated checklist of GTD-related basidiomycete taxa has been published (Fischer and González-García, 2015). With the advent of metagenomic approaches, reports of basidiomycetes are increasing (Del Frari *et al.*, 2019a; Bruez *et al.*, 2020). A recent study by Brown *et al.* (2020) aimed to clarify the relevance of basidiomycete colonisation within the Esca complex of diseases. They isolated many taxa (including new species, such as *Inonotus vitis* A.A. Brown, D.P. Lawr. & K. Baumgartner, *Tropicoporus texanus* A.A. Brown, D.P. Lawr. & K. Baumgartner, and *Fomitiporia ignea* A.A. Brown, D.P. Lawr. & K. Baumgartner) from white rot and black/brown discoloured wood collected from grapevine plants expressing GLSD foliar or shoot symptoms in Californian and Texan vineyards.

More *Fomitiporia* spp. have been associated with “Esca-diseased” grapevines in other regions, including *Fomitiporia australiensis* M. Fisch., Jacq. Edwards, Cunningt. and Pascoe in Australia (Fischer *et al.*, 2005), *Fomitiporia polymorpha* M. Fisch. in California (Fischer and Binder, 2004), *Fomitiporia capensis* M. Fisch., M. Cloete, L. Mostert, F. Halleen in South Africa (Cloete *et al.*, 2014), *F. ignea* (Brown *et al.*, 2020) in Texas, and, more recently, *Fomitiporia punicata* Y.C. Dai, B.K. Cui & Decock in China (Ye *et al.*, 2021), originally described

on *Punica granatum* (Dai *et al.*, 2008). As well, *Fomitiporia erecta* A. David, Dequatre & Fiasson, and *F. punctata* were mentioned as occurring on grapevine in Spain (Fischer and González-García, 2015). Of these species, *F. australiensis*, *F. capensis* and *F. ignea* were exclusively documented from grapevine.

Geographic distribution and host range of *Fmed* have probably expanded in recent decades. This is supported by the number of host plants in the different regions. In Central Europe the host range is largely limited to *Vitis vinifera*, given the scarcity of reports of the fungus on other hosts: i.e. on *Laurus nobilis* (Fischer, 2006) and on *Robinia pseudoacacia* (Schmidt *et al.*, 2012). However, *Fmed* occurs on several other hosts in the Mediterranean area (see below). This discrepancy in the reported host range indicates a recent invasion of the fungus into the viticultural regions of Central Europe, possibly associated with climatic changes leading to increased temperatures in this region.

These observations indicate that intrinsic geographic and climate conditions play roles in diffusion of Basidiomycota pathogens and influence spread of *Fomitiporia* spp. in vineyards (Fischer *et al.*, 2005; Fischer, 2006; Cloete *et al.*, 2014). Geographical variations influence distribution of fungi among different locations (Hofman and Arnold, 2008; Dietzel *et al.*, 2019), and climate is a major abiotic factor shaping fungal biogeography (Castillo and Plata, 2016; Větrovský *et al.*, 2019). Spatial analyses of “Esca-disease”-related basidiomycete taxa, and comprehensive screening of possible non-*Vitis* host plants, preferably from proximity of vineyards, could help to identify key pedo-agroclimatic factors affecting their diffusion, and could indicate why some *Fomitiporia* spp. are retrieved from some areas but not others.

In Europe information on grapevine white rot agents began to be revised in 2002: Fischer found that strains formerly acknowledged as *F. punctata* collected from grapevines in Italy and Germany differed from strains from other hosts and other geographic areas (Central Europe). Molecular diagnoses (ITS data), pairing tests of single spore isolates, compared with temperature preferences of cultured mycelia allowed description of the new species *Fomitiporia mediterranea* M. Fischer (Fischer, 2002). This is currently considered the main causal agent of white rot in “Esca diseased” grapevines in Europe and in Mediterranean climate areas, while *F. punctata* is more ubiquitous, although a European centred distribution has been suggested by Decock *et al.* (2007).

Due to indistinguishable morphology between *Fmed* and *F. punctata*, but the highlighted phylogenetic differences, previous isolates and findings attributed to *F. punctata* should be reconsidered as possibly assignable to

Fmed (Fischer, 2002; Ciccarone *et al.*, 2004; Fischer, 2006). Recent findings on *P. punctatus* and *P. pseudopunctatus* A. David Dequatre and Fiasson by Polemis *et al.* (2019) and Markakis *et al.* (2019) have reinforced that possible misidentification led to the underestimation of *F. mediterranea* incidence in the Mediterranean region.

This review focuses only on *Fmed* and its role in Esca-related wood degradation, with careful reconsideration of previous reports where the pathogen may have been incorrectly identified.

IDENTIFICATION, TAXONOMY, HOST RANGE, AND SYMPTOMS INDUCED IN GRAPEVINES

Description of fruit bodies and mycelia

Morphology and anatomy of *Fomitiporia mediterranea* (Hymenochaetaceae, Hymenochaetales, Agaricomycetes, Basidiomycota) were described by Fischer (2002).

Fomitiporia mediterranea fruiting bodies (Figure 2) are resupinate, inseparable, and hard woody, up to 15 mm thick with yellowish-brown narrow margins, containing subglobose to oval basidiospores. The hyphal system is dimitic, with generative and skeletal hyphae. Detailed descriptions of the hyphal system, fruiting bodies and basidiospores of this fungus were provided by Fischer (2002, 2009) and Fischer and González-García (2015).

Figure 3, A, B and C show, respectively, a tube mouth with outgrowth of vegetative hyphae, outgrowing hyphae from naturally infected grapevine wood and the pore surface of a fruiting body of *F. mediterranea*.

After isolation from infected wood and/or fruit bodies, mycelial isolates may develop into a so-called “bleaching type” (Type B: Fischer, 1987) or a “staining type” (Type S: Fischer, 1987) (Figure 4).

Type B mycelium has a cottony to woolly appearance, and aerial hyphae are yellowish to brown. Medium pigmentation is sparse or absent. Type S-mycelium has sparse aerial hyphae, and medium pigmentation is strong. Colony growth after 14 days at 21°C on Malt Extract (ME) agar in complete darkness was more rapid in bleaching-type isolates (colony diameter = 3.0 to 4.5 cm) than staining-type isolates (1.5 to 2.5 cm). The two mycelium types may alternate over ensuing inoculations. Growth was confirmed between 15 and 35°C, with optimum growth at 30°C (Fischer, 2002, 2006; Fischer and Kassemeyer, 2003). Under laboratory conditions, sporulation is absent in *Fmed*. Spore germination tests with spores from actively sporulating fruit bodies were performed for some *Fmed* strains, indicating very low germination rates (less than 1%) with a high variation in germination times (Fischer, 2002).



Figure 2. Fruiting bodies of *Fomitiporia mediterranea* on a grapevine trunk. Photograph taken in July 2018, from 'Sauvignon Blanc', in a vineyard in Ehrenkirchen, Germany.

Spread by basidiospores is considered the main dispersal form for *Fmed* and this has been described to be mainly via rain and wind (Cortesi *et al.*, 2000). In Central European vineyards, fruiting body sporulation is increased after rainy periods and is related to daily temperatures greater than 10°C and relative humidity greater than 80% (Fischer, 2009).

Mating system

Studies of the *Fmed* mating system were also affected by misidentification of the pathogen. Fischer

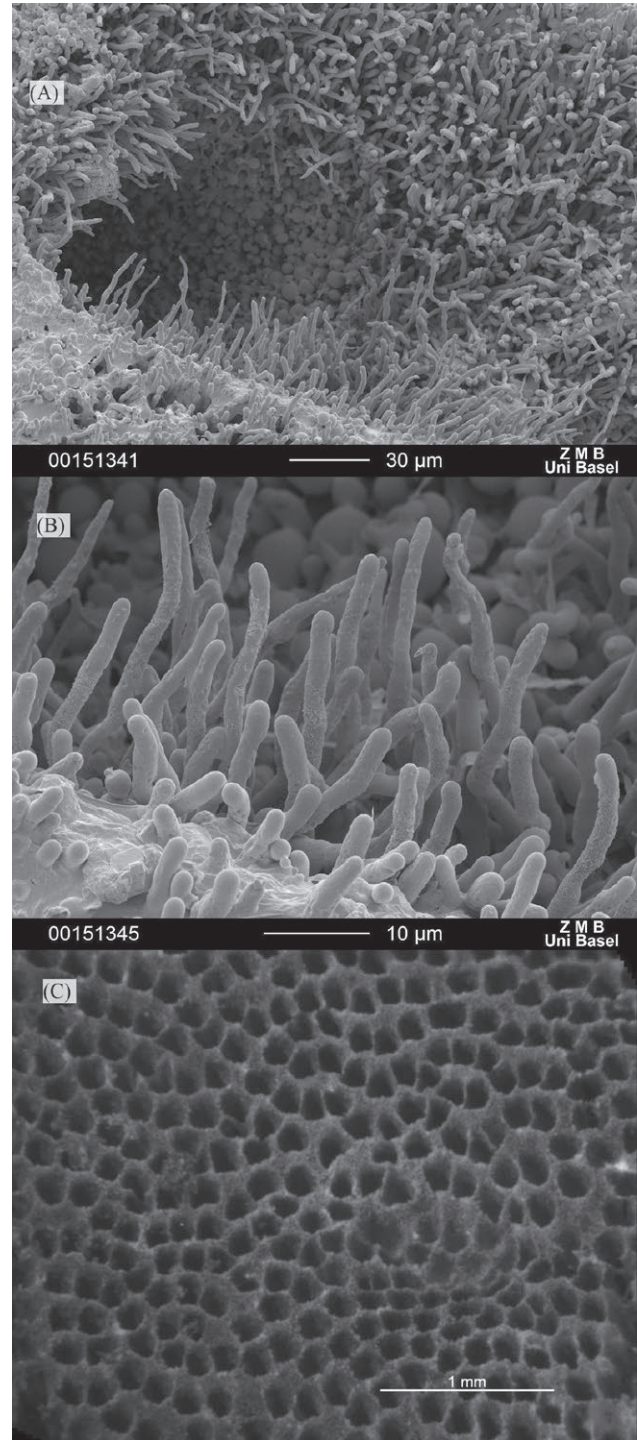


Figure 3. (A), Cryo-Scanning-Electron-Microscopy (Cryo-SEM) micrograph ($\times 500$ magnification) of an *Fmed* tube mouth showing outgrowth of vegetative hyphae. (B), Cryo-SEM micrograph ($\times 2,000$) of hyphae in a cross section of a grapevine trunk naturally affected by white rot. (C), Stereo micrograph of the surface of an *Fmed* fruiting body ($\times 50$). The pores are 5-8/mm. The diseased grapevine specimen was collected in a vineyard in Pfaffenweiler, south-west Germany.

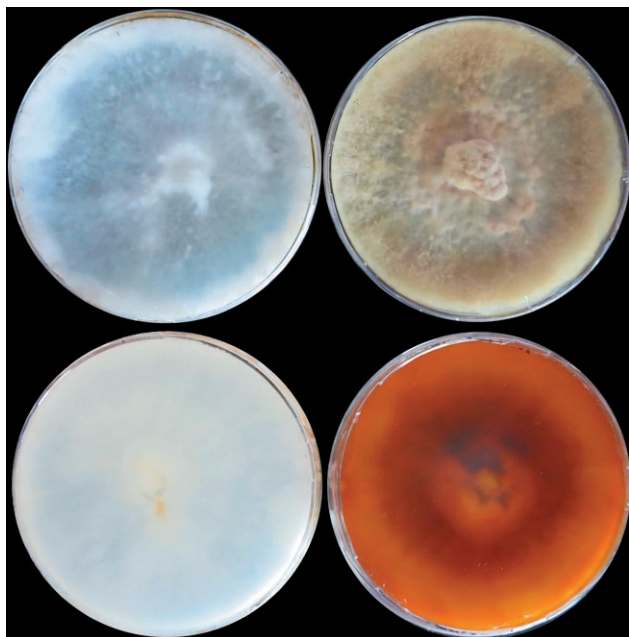


Figure 4. Mycelium cultures of *Fomitiporia mediterranea* on malt extract agar (ME) after 28 days of incubation. “Type B” (left, surface and reverse side) and “Type S” (right, surface and reverse side).

(1996) described *F. punctata* strains (later distinguished from *Fmed*) as homothallic, with no mating types evident in pairings of spores originating from one fruiting body. The time lag between separation of *Fmed* from *F. punctata* by Fischer (2002) and the research of Jamaux-Despreaux and Péros (2003) initially provided conflicting reports of the homothallic mating system described for the fungus. Jamaux-Despreaux and Péros (2003) observed outcrossing populations in France and Italy. This was indicated by high genetic variation within and between vineyards, and random assortment of genetic markers. They therefore suggested possible existence of non-outcrossing populations in other areas. Following correct assignment of species, it was shown that *Fmed* was a heterothallic bipolar species (Fischer, 2002), while *F. punctata* was confirmed as homothallic.

A variety of pairing tests were conducted by Fischer (2002), who demonstrated a range of compatible and incompatible reactions (see Fischer, 2002 for details). Growth of secondary mycelia was stronger in compatible inter-strain than in intra-strain pairings. Mycelia formed from inter-strain pairings could prevail under natural conditions, resulting in high outcrossing rates.

It is now accepted that basidiomycete mating is regulated by different genes, grouped in two types of homeodomain transcription factors (*HD genes*), in pheromone genes and their related receptors and response genes (*PR genes*). These genes can reside in linked or un-linked

chromosome loci (James *et al.*, 2006; Kües *et al.*, 2013, 2015). James *et al.* (2013) highlighted at least four *HD* (two pairs of *HD1* and two pairs of *HD2*), and several apparently functional *PR genes* in the *Fmed* genome, such as 2 *STE3*, several *MAP* kinases and 3 *Prf1*. These authors also suggested that the genes were not linked in a unique mating locus (James *et al.*, 2013; Kües *et al.*, 2015).

Further pairing tests, perhaps with other strains, could better clarify the dispersal system of the fungus, and identify other possible intersterility groups. This would be further clarified if genetic variability data retrieved from German vineyards were considered. Fischer (2012) found 14 different *Fmed* genotypes out of 15 fruit bodies, all derived from one vineyard. Lentes and Fischer (personal communication) identified 56 genotypes out of 64 isolated mycelia, derived from different vines in two vineyards in the Moselle region of Germany.

Available *Fmed* genome could provide new information for expression analysis of mating-associated genes, especially in response to changing environmental conditions which are increasingly affecting European vineyards. Increasing this knowledge could provide a better understanding on pathogen spread and genetic recombination, since *Fomitiporia* spp. are well adapted to different conditions and climates, as reflected by their biogeographical variability.

Field identification

Compared to white rot presence, fruiting bodies of *Fmed* are very rarely found in vineyards, mostly on the uppermost parts of trunks, near pruning wounds, which are the main sites of infection (Cortesi *et al.*, 2000; Fischer *et al.*, 2005; Fischer, 2006; Fischer and González-García, 2015). In vineyards in Central Europe, *Fmed* fruiting bodies were only present on 1 to 3% of “Escadiseased” grapevines that were older than 15 years (Fischer, 2009), and the pathogen was detected as vegetative mycelium in infected hosts. In Germany, a 100:1 ratio is mentioned by Fischer (2006) indicating a low co-occurrence of vegetative mycelium with white rot and fruiting bodies. This was also reported in Tuscan vineyards by Cortesi *et al.* (2000). Because compatibility groups were identified (Fischer, 2002), the occasional occurrence of fruiting bodies in vineyards may be partly explained by the possibly rare contact between sexually compatible basidiospores (Jamaux-Despreaux and Péros, 2003). Dead grapevine trunks are the most favourable substrates for development of fruiting bodies, and the dead trunks are usually removed from vineyards. Another hypothesis to explain the low ratio between white rot and fruiting bodies in non-Central European countries is that the disease

Table 1. Host range and geographic distribution of *Fomitiporia mediterranea* M. Fischer 2002. For each host (and each country), the table includes first reports which used classical isolations, and some of the significant subsequent reports/studies which used molecular classification and metagenomic approaches. References accompanied by “†” refer to studies which used former classifications (as *Phellinus punctatus* or *F. punctata*) which should be carefully reconsidered as representing *F. mediterranea*.

Host	Country	References	
<i>Vitis vinifera</i>	Algeria	Berraf and Péros, 2005	
	Austria	Fischer <i>et al.</i> , 2006	
	Czech Republic	Baranek <i>et al.</i> , 2018	
	France	†Larignon and Dubos, 1997; †Jamaux-Despreaux and Péros, 2003; Péros <i>et al.</i> , 2008; Laveau <i>et al.</i> , 2009; Kuntzmann <i>et al.</i> , 2010; Ouadi <i>et al.</i> , 2019; Bruez <i>et al.</i> , 2020	
	Germany	Fischer, 2002; Fischer and Kassemeyer, 2003; Fischer, 2006; Fischer, 2012; Fischer and González-García, 2015; Fischer, 2019	
	Greece	†Rumbos and Rumbou, 2001	
	Hungary	Rábai <i>et al.</i> , 2008	
	Iran	†Karimi <i>et al.</i> , 2001; Farashiyani <i>et al.</i> , 2012; Mohammadi <i>et al.</i> , 2013; Rajaiyan <i>et al.</i> 2013; Amarloo <i>et al.</i> , 2020; Mirabolfathy <i>et al.</i> , 2021	
	Italy	†Mugnai <i>et al.</i> , 1999; †Cortesi <i>et al.</i> , 2000; Ciccarone <i>et al.</i> , 2004; Romanazzi <i>et al.</i> , 2009; Quaglia <i>et al.</i> , 2009; Del Frari <i>et al.</i> , 2019a; Girometta <i>et al.</i> , 2020; Pacetti <i>et al.</i> , 2021	
	Lebanon	Choueiri <i>et al.</i> , 2014	
	Portugal	Sofia <i>et al.</i> , 2006	
	Slovenia	Rusjan <i>et al.</i> , 2017	
	Spain	†Armengol <i>et al.</i> , 2001; Martin and Cobos, 2007; Sánchez-Torres <i>et al.</i> , 2008; Luque <i>et al.</i> , 2009; Garcia Benavides <i>et al.</i> , 2013; Elena <i>et al.</i> , 2018	
	Switzerland	Fischer, 2006	
	Turkey	Akgül <i>et al.</i> , 2015	
	<i>Acer negundo</i>	Italy	Fischer, 2002
	<i>Actinidia</i> spp.	Greece	†Elena and Paplomatas, 2002
Italy		Fischer, 2002; Di Marco <i>et al.</i> , 2004a; Di Marco and Osti, 2008; Girometta <i>et al.</i> , 2020	
<i>Albizia julibrissin</i>	Greece	Markakis <i>et al.</i> , 2017	
<i>Cistus</i> sp.	Italy	Girometta <i>et al.</i> , 2020	
<i>Citrus</i> spp.	Greece	Elena <i>et al.</i> , 2006	
	Italy	Rocchetti <i>et al.</i> , 2014	
<i>Corylus avellana</i>	Italy	Pilotti <i>et al.</i> , 2010; Girometta <i>et al.</i> , 2020	
<i>Elaeagnus angustifolia</i>	Iran	Ahmadyusefi and Mohammadi, 2019	
<i>Fagus sylvatica</i>	Italy	Girometta <i>et al.</i> , 2020	
<i>Fortunella japonica</i>	Greece	Markakis <i>et al.</i> , 2017	
<i>Hedera helix</i>	Italy	Girometta <i>et al.</i> , 2020	
<i>Lagerstroemia indica</i>	Italy	Fischer, 2002	
<i>Laurus nobilis</i>	Slovenia	Fischer, 2006	
<i>Ligustrum vulgare</i>	Italy	Fischer, 2006	
<i>Olea europaea</i>	Greece	†Paplomatas <i>et al.</i> , 2006; Markakis <i>et al.</i> , 2017; Markakis <i>et al.</i> , 2019	
	Italy	Fischer, 2002 ; Carlucci <i>et al.</i> , 2013	
<i>Platanus x acerifolia</i>	Italy	Pilotti <i>et al.</i> , 2005	
<i>Prunus dulcis</i>	Spain	Olmo <i>et al.</i> , 2017	
<i>Punica granatum</i>	Greece	Markakis <i>et al.</i> , 2017	
<i>Pyrus communis</i>	Greece	Markakis <i>et al.</i> , 2017	
<i>Quercus ilex</i>	Italy	Fischer, 2006	
<i>Quercus robur</i>	Italy	Girometta <i>et al.</i> , 2020	
<i>Quercus rubra</i>	Italy	Girometta <i>et al.</i> , 2020	
<i>Robinia pseudoacacia</i>	Italy	Fischer, 2006; Girometta <i>et al.</i> , 2020	
	Germany	Schmidt <i>et al.</i> , 2012	
<i>Salix alba</i>	Italy	Girometta <i>et al.</i> , 2020	
<i>Ulmus</i> spp.	Iran	Mirsoleymani and Mostowfizadeh Ghalamfarsa, 2019	

and fungus structures could occur in several alternative hosts within or near vineyards (see Table 1). These sources of inoculum could be important. The discrepancies between occurrence of vegetative mycelia and fruit bodies are often large in lignicolous fungi. While the existence of *F. mediterranea* fruiting bodies may be underestimated (Fischer 2006), precise evaluation of exogenous inoculum sources remains a challenging issue.

Field identification of *Fomitiporia* spp. on grapevines is often complex. Because fruiting bodies are very rare and have very similar morphologies, molecular diagnoses after isolations from infected wood tissues or fruiting bodies are likely to be the most reliable tools for identification of mycelia not clearly assignable to particular species (Ciccarone *et al.*, 2004).

Overview of molecular diagnosis, taxonomy and phylogeny

Amplifications and sequencing of ITS regions with or without Large Sub-Unit (LSU) translation elongation factor subunit 1- α (*tef1*) and the second largest subunit of RNA polymerase II (*RPB2*) sequence analysis, have permitted new advances in classification of grapevine basidiomycetes using specific primers. Reports are increasing, differentiating new *Fomitiporia* species (Cloete *et al.*, 2016; Chen and Cui, 2017; Brown *et al.*, 2020; Chen *et al.*, 2021; Ye *et al.*, 2021).

Fischer (2002) reported a specific method for identification, based on the nuclear encoded ribosomal DNA region ITS1-5.8S-ITS2 using the primer pair prITS5 and prITS4 (White *et al.*, 1990). Compared to other *Fomitiporia* spp., *Fmed* strains showed unique small insertions in both ITS regions: between nucleotides 201 and 206 (AATAAT) in ITS1 and between nucleotides 748 and 745 (CCTTTGA) in ITS2 (Fischer, 2002; 2006; Fischer and Binder, 2004). Since 2006, specific primers based on these insertions have been available for differentiation of *Fmed* from other species such as *F. punctata* and *F. australiensis* (Fischer, 2006). The primer sequences and characteristics are as follows: pr*Fmed1*, 5' GCA GTA GTA ATA ATA ACA ATC 3' (GC = 28.6%, TM = 50.1°C); and pr*Fmed2*, 5' GGT CAA AGG AGT CAA ATG GT 3' (GC = 45%, TM = 55.3°C). A 550 bp product is only obtained for *Fmed*. Parameters for successful amplification were described by Fischer (2006).

With basidiospores being the main dissemination agent of *Fmed*, considerable genetic variation in *F. punctata* (probably *Fmed*) has been described by Random Amplified Polymorphic DNA (RAPD) markers. This variation has been shown among isolates derived from individual vineyards (Pollastro *et al.*, 2000; Jamaux-Despreaux and Péros, 2003). Pollastro *et al.* (2001) successfully developed

sequence-characterised amplified region (SCAR) primers suitable as a molecular diagnostic tool for *Fmed*.

The primer pair ITS1 and ITS4 (White *et al.*, 1990) have also been successfully used for identification of *Fmed* isolates within an Italian mycological collection based on fresh mycelial isolates (Girometta *et al.*, 2020).

Other *Fomitiporia* species recorded from grapevine include: *F. polymorpha*, *F. capensis*, *F. australiensis*, *F. ignea*, *F. erecta*, *F. punctata*, and *F. punicata*. For *F. polymorpha*, *F. australiensis*, *F. erecta* and *F. punctata*, characterization of the ITS1-5.8S-ITS2 region was sufficient either to describe them as separate species, or to establish phylogenetic relationships with other *Fomitiporia* spp. (Fischer and Binder, 2004; Fischer *et al.*, 2005; Fischer and González-García, 2015). Implication of other conserved genetic regions has distinguished these other species above mentioned, using the LSU unit ribosomal RNA-encoding regions *tef1* and *RPB2* together with ITS data to describe them (Cloete *et al.*, 2014; Brown *et al.*, 2020; Ye *et al.*, 2021). Nevertheless, species-specific primers are available only for *Fmed* (Fischer, 2006), although unique forward primers paired with ITS4 primers have been designed to successfully detect *F. capensis* (Bester *et al.*, 2015).

Host range and geographical distribution

Fomitiporia mediterranea is considered to be a highly adaptable species, based on the diversity of host plants, and occurrence in different regions and climates.

Isolates from grapevine were retrieved from a range of climate conditions, according to the most updated version of the original Köppen-Geiger climate classification map (Geiger, 1961; Beck *et al.*, 2018): from “Mediterranean and temperate humid-subtropical climates” (for most of non-Central European isolates of the pathogen), to “arid and semi-arid climate” (for Algerian, Iranian and some of the non-Central European isolates), to “cool temperate climate” (for most of the Central-European isolates)” (see Figure 5 for the detailed geographical distribution of *Fmed*). Throughout its geographical range, *Fmed* shows close affinity with *V. vinifera*. However, this may be due to the economic significance of grapevine in these regions, resulting in detailed field observations for vineyards compared with other woody hosts. The fungus is also found on other host plants outside non-Central European countries, potentially resulting in increased infection pressure on grapevines (see Table 1 for a detailed list of hosts in different countries). Fischer (2002, 2006) postulated that, at least for non-Central European countries, alternative hosts could be foci for development of *Fmed* fruiting bodies, reinforcing the observed high adaptability of the pathogen to mul-

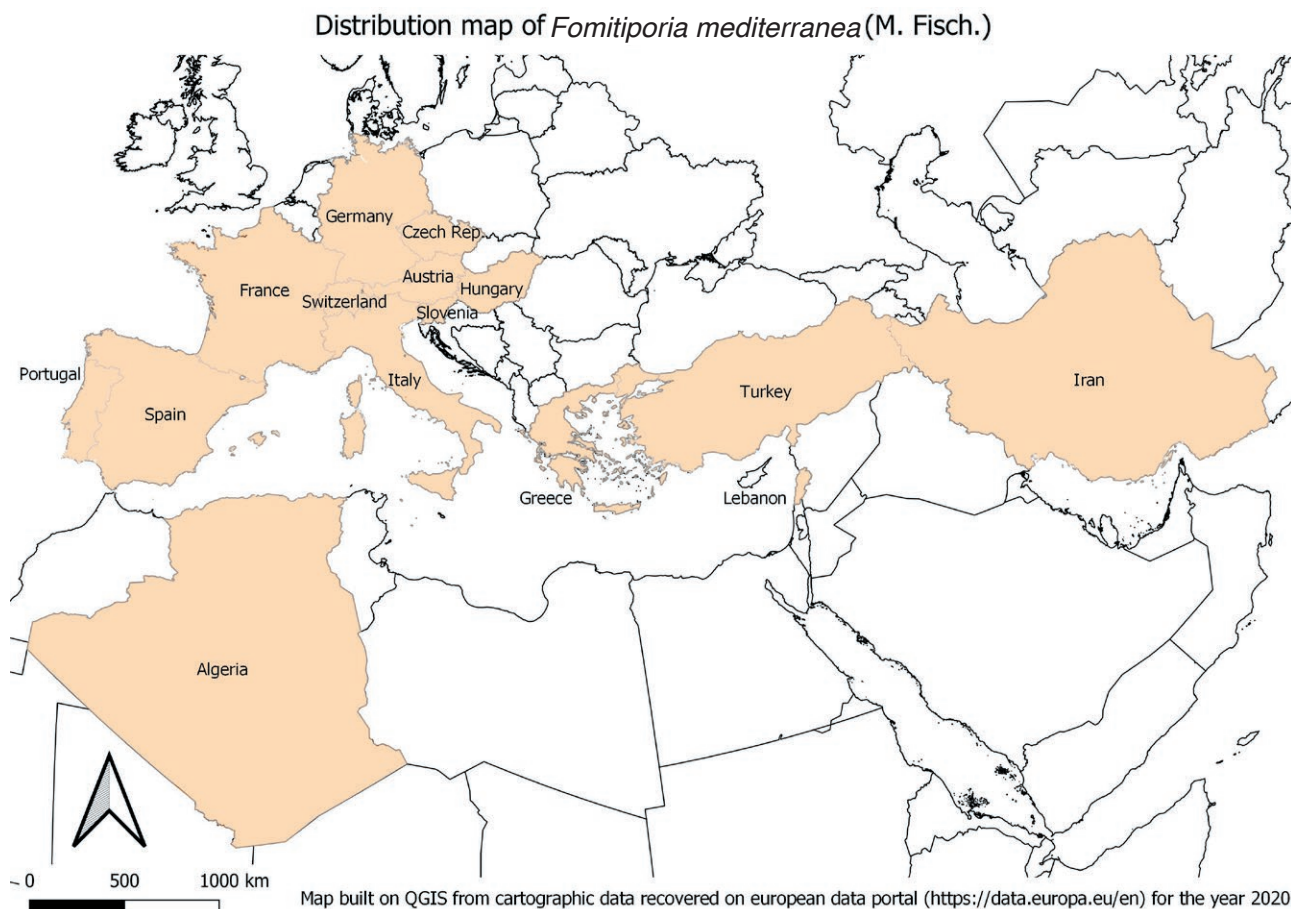


Figure 5. Distribution of *Fomitiporia mediterranea*, based on published reports of isolation of the fungus from grapevine, *Vitis vinifera*. The map was constructed using QGIS software (version 3.10.9-A Coruña).

multiple host species. Although current data show only very few isolations of *Fmed* from Central-European non-*Vitis* hosts, i.e. *Robinia pseudoacacia* in Germany (Schmidt *et al.*, 2012) and *Laurus nobilis* in Slovenia (Fischer, 2006), the potential for the fungus to colonize other hosts is demonstrated. Future studies could focus on: *i*) surveys of fruiting body incidence on alternative hosts in the proximity of vineyards (to better assess inoculum sources); *ii*) performing comparative secretome and metabolome assessment of wood from different hosts to increase knowledge on *Fmed* colonization and growth and fruiting body development; and *iii*) determine pathogenicity to grapevine of isolates from different host plants.

Spread in grapevines and vineyards, wood symptoms and their relationships with foliar symptoms

Fomitiporia mediterranea is mainly retrieved from grapevine white rot necrotic tissue, although its presence

in necrosis borders between white rot and non-necrotic tissues, and adjacent non-necrotic but recently colonised wood has been demonstrated (Fischer, 2002; Péros *et al.*, 2008; Surico, 2009; Bruez *et al.*, 2017; Elena *et al.*, 2018; Bruez *et al.*, 2021; Pacetti *et al.*, 2021). The pathogen needs some time to colonise and decay woody tissues, explaining why it is predominantly found in trunks greater than 10 years old, and only to a lesser extent in young trunks (Sánchez-Torres *et al.*, 2008; Fischer, 2009). White rot has also been mostly reported in old vineyards although it can be sometimes found in young vines and very occasionally in young GLSD symptomatic vines (Edwards *et al.*, 2001; Mugnai *et al.*, 2010).

In the Esca complex of diseases, several diseases have been recognised and have been related to infections by different fungi, and symptom expression can be influenced by many agronomic and environmental factors (cultural practices, host plant age, soil type, weather conditions) (Calzarano *et al.*, 2018a; Gramaje *et*

al., 2018; Lecomte *et al.*, 2018). Distribution of symptomatic vines within a vineyard poorly indicates the dissemination mode of related fungi, including *Fmed*, but diseased vines can be found grouped along vineyard rows. This supports the hypothesis that human-mediated practices are involved in pathogen spread (Mugnai *et al.*, 1999; Guérin-Dubrana *et al.*, 2019). Research on *F. punctata* (likely *Fmed*) isolates obtained from different vines showed they belonged to different somatic incompatibility types (Cortesi *et al.*, 2000), indicating that each vine was colonised by genetically distinct individuals. Similarly, results for *F. punctata* (likely *Fmed*) (Jamaux-Despreaux and Péros, 2003) on the genotypic differences at vineyard level strongly indicated outcrossing reproduction via basidiospores. These results are not consistent with the hypothesis that *Fmed* is spread through wounds by pruning tools. In addition to this genetic evidence, much epidemiological data has shown that “Esca disease” symptoms were spatially random in vineyards (Cortesi *et al.*, 2000; Surico *et al.*, 2000; Sofia *et al.*, 2006; Li *et al.*, 2017), which is consistent with the hypothesis that basidiospores are the likely agents of dispersal for *Fmed* (Cortesi *et al.*, 2000; Fischer, 2002). Although sporulation is rare on grapevine trunks, the inoculum could come from the many other hosts of the pathogen.

Typically, *Fmed* induces white rot in innermost grapevine wood (Figure 6). The decay is most often observed in arms, stem heads and trunks, with colonisation starting from pruning wounds and extending along entire trunks, mostly in the central parts but occasionally also at trunk bases, with desuckering wounds as entrance points (Larignon and Dubos 1997; Mugnai *et al.*, 1999, 2010; Sparapano *et al.*, 2000a, 2001a; Fischer, 2002; Fischer and Kassemeyer, 2003).

Rot diameters vary and decrease from infection origin points to boundaries with healthy wood (Mugnai *et al.*, 2010). Rootstocks are rarely affected because vines die before white rot reaches rootstock tissues, although white rot has been reported in rootstock tissues (Maher *et al.*, 2012; Elena *et al.*, 2018). However, *Fmed*-related white rot is common in rootstock mother plants (Fischer, 2019).

The main symptom induced by *Fmed* on grapevines is spongy yellowish or bleached decay in wood tissues, but the relationship between wood and external foliar symptoms of “Esca diseased” grapevines is debated. To the best of our knowledge, Lafon (in 1921) was the first author to make this association. He assumed that *P. ignarius* (most likely a *Fomitiporia* sp.) present in the decay was the main agent responsible for the apoplectic form of “Esca disease” and leaf dessication (due to sap flow impairment). However, information on *Fmed*,

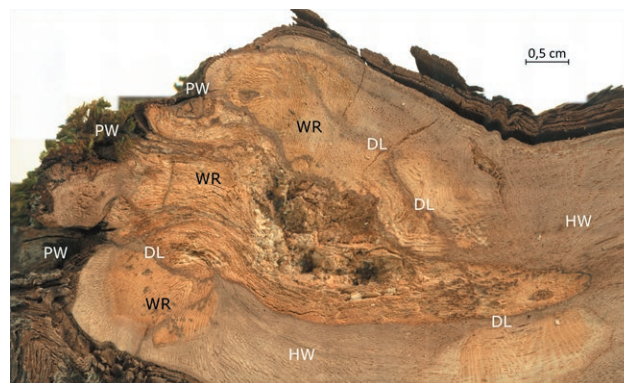


Figure 6. Macroscopic observation by stereo microscopy ($\times 12$ magnification) of a cross section (1 cm thick) of the head of a grapevine stem with a large area of white rot (WR) spreading from pruning wounds (PW) into healthy wood (HW). The necrotic zones are separated from the healthy wood by demarcation lines (DL). Specimen collected in May 2021 from a 28-year-old ‘Sauvignon Blanc’ plant, from a vineyard in Pfaffenweiler, south-west Germany.

grapevine wood symptoms and foliar symptoms needs to be re-examined. Demonstration of *Fmed* to act as a primary grapevine pathogen – after artificial inoculations by mycelial plugs or toothpicks (Sparapano *et al.*, 2000a, 2001a) – confirms the importance of this pathogen within the Esca disease complex. However, research on the actual colonization sequence of “Esca disease”-associated fungi in field-grown grapevines is still required to increase knowledge of relationships between wood decay and foliar symptoms. Under field conditions, basidiospores can be infection agents, and artificial basidiospore inoculations in greenhouses would help to determine the colonization ability of *Fmed* and its role in foliar symptoms. However, basidiospores are difficult to obtain, and rarely germinate under laboratory conditions (Fischer, 2002). Therefore reviewing studies from last two decades will provide insights on the impacts of *Fmed* on “Esca disease” foliar symptoms (GLSD).

Different types of necrosis have been described in “Esca diseased” wood (Larignon and Dubos, 1997). White rot necrosis clearly shows the presence of *Fmed*, which has been the main isolation source of this pathogen in Europe (Larignon and Dubos, 1997; Mugnai *et al.*, 1999; Bruez *et al.*, 2017). Through logistic regression analyses in an old ‘Cabernet Sauvignon’ vineyard, Maher *et al.* (2012) analysed data from presumably 20 to 25 year-old vineyards, and assumed white rot to be the tissue type most strictly associated with the leaf stripe symptoms. A relationship between *Fmed* and “Esca disease” foliar symptoms (GLSD) was shown if white rot presence overcame a 10% necrosis threshold, in vine grafts and/or cordons. Using a similar approach, Calzarano and Di Marco (2007)

showed that, in 32- and 36-year-old vineyards, there was no relationship between severities of wood deterioration and external foliar symptoms. The leaf-symptomatic vines percentage with discoloration (but no white rot) was 46.2% in 32-year-old vineyards and 7.2% in 36-year-old vineyards. Both of these findings have been supported by other authors. Bruez *et al.* (2014) found white rot tissue in cordons from 79% of GLSD-symptomatic 10-year-old vines. Fischer (2012) found 100% of 366 trunks of 28-year-old ‘Traminer’ vines to be affected by white rot, but less than 10% had foliar symptoms. Fischer (2019) also reported a possible correlation between the presence of *Fmed* (but also other GTD related fungi) and leaf symptoms in rootstock mother plants. Ouali *et al.* (2019) observed white rot on 15 to 50% of the total necrotic area of trunks and cordons in 16-year-old ‘Cabernet Sauvignon’ grapevines expressing foliar symptoms. Edwards *et al.* (2010), after fully dissecting trunks of ten GLSD symptomatic vines (aged 4 to 7 years) detected white rot in only one vine. Mugnai *et al.* (2010) dissected nine symptomatic 5- and 6-years-old vines. They found that four of the vines had no white rot and five had traces of decayed wood, mainly following infections from desuckering wounds (Mugnai *et al.*, 2010). These results confirm that white rot, and *Fmed* as the main white rot agent in Europe, becomes increasingly present as vines age, thus becoming increasingly associated with leaf symptoms. The pathogen may play a fundamental role in activating mechanisms leading to the onset of leaf stripe symptoms. However, observations of foliar symptoms not linked to white rot suggest that even if *Fmed* plays a very important role, other factors are also likely to be involved.

In 10-year-old ‘Cabernet Sauvignon’ cordons expressing foliar symptoms, Bruez *et al.* (2020) using meta-barcoding, proposed the link between the onset of GLSD with white rot and a combination of *Fmed*, *Pch* as well as *Sphingomonas* spp. and *Mycobacterium* spp. They suggested that microbiota interactions in white rot necrotic tissues could induce production of phytotoxic secondary metabolites, or increase some shared metabolic pathway, thereby inducing typical GLSD foliar symptoms. *In vitro* production of fungal secondary metabolites by co-culture with bacteria has been documented (Haidar *et al.*, 2016), but occurrence in natural conditions is yet to be assessed.

Cholet *et al.* (2021) and Pacetti *et al.* (2021) have also shown the correlation of white rot with foliar stripe symptoms. Decay elimination (curettage, see below for details) drastically reduced GLSD symptoms during the years following curettage treatment, in 24-year-old ‘Sauvignon Blanc’ and in 14-year-old ‘Cabernet Sauvignon’ plants. Another interesting correlation between white rot

and foliar symptoms came from the curative side: recently, Bruez *et al.* (2021) shown how after sodium arsenite treatment (see below for details), 25-year-old ‘Gewürztraminer’, 27-year-old ‘Chardonnay’ and 40-year-old ‘Merlot’ plants did not shown any foliar symptoms.

In conclusion, the relationship between outbreak of foliar symptoms and white rot in the Esca complex of diseases is widely supported and linked to *Fmed* in Europe, although this is not exclusive as the fungus is absent in young symptomatic vines. Nevertheless, clarifying the mechanisms involved in this relationship will be a big step towards full understanding of the processes leading to the characteristic symptoms and symptom expression timing of GLSD (the symptom fluctuations is not found in other diseases of perennial hosts). Several hypotheses have been proposed for etiology of leaf stripe symptoms, but to understand the role of *Fmed* in development of the disease, an important and essential first step is to detect the signals reaching the leaves and causing the outbreak of these symptoms. In the case of *Fmed* we suggest the following etiology: *i*) joint action of extracellular enzymes and toxins (from *Fmed* or the entire white rot microflora); *ii*) vascular system destruction caused by lignocellulolytic enzymes; *iii*) the formation of low molecular weight diffusible compounds from *Fmed* or from wood degradation-host infection reactions; and *iv*) a combination of these situations and the wood cellular microenvironment.

GENOMIC INFORMATION

Many fungal *Agaricomycetes* genomes have been sequenced by the Joint Genome Institute (JGI) (<http://jgi.doe.gov/fungi>) (Grigoriev IV *et al.*, 2011). According to these data, 93% of the *Agaricomycotina* sequenced genomes are from *Agaricomycetes*. This could be related to the roles of these fungi in trees decay and to their potential applications in biotechnology (Lundel *et al.*, 2014; Hyde *et al.*, 2019). In a comparative genomic study, Floudas *et al.* (2012) sequenced the *Fmed* genome. The final draft assembly was obtained by *in silico* combination of Roche (454), Sanger Fosmids, and Illumina data. Information on genome annotation statistics and composition are available at the MycoCosm portal (<https://mycocosm.jgi.doe.gov>) (Grigoriev IV *et al.*, 2014) and in Floudas *et al.* (2012).

Fmed genome size is approx. 63.35 Mbp which accounts for 11,333 predicted complete gene models with start and stop codons. The genome shows a conspicuous repetitive sequence component, mostly represented by microsatellites and Transposable Elements (TEs). It is

generally accepted that repetitive sequences play roles in *Basidiomycota* genome rearrangements and gene mutations, interrupting genome linearity between strains, and producing strain polymorphisms (Castanera *et al.*, 2017). This could at least partially explain the level of polymorphism detected between strains of *Fmed* (Polastro *et al.*, 2001). Specifically, 4157 microsatellites were detected, most of them (52.27%) being dinucleotides, followed by tri-, mono-, penta-, hexa- and tetra-nucleotide microsatellites. TE analysis revealed a high proportion of TEs coverage (41.42%), representing the greatest for the sequenced genomes in the study. The biggest portion of TEs was LTR-Gypsy elements (21.33%), followed by LTR-Copia, TIR, DNA-transposons and Helitrons. A consistent number of non-classified TEs were reported (Floudas *et al.*, 2012).

Besides constitutive analysis of the genome, Floudas *et al.* (2012) conducted a comparative study with 30 fungal genomes (presenting different ecological strategies), to establish the origin of ligninolytic activity. Through molecular clock analysis of genes encoding Class II Peroxidases (PODs: responsible for lignin degradation), it was possible to date the appearance of ligninolytic activity and the *Agaricomycetes* ancestor (a white rot agent, most likely). The activity probably appeared approx. 290 Ma ago (between the end of Carboniferous and Permian period, Paleozoic era). Subsequently, by Class II PODs-encoding gene expansion through the lineage, five orders of basidiomycetes differentiated, including the *Hymenochaetales* (most likely approx. 237 Ma, during the Triassic period, Mesozoic era). *Fmed* was estimated to have up to 17 Class II PODs-encoding genes in its genome, and these genes can possibly be found clustered with cellobiose dehydrogenase (CDH) encoding genes and other unclassified genes.

Other gene copy numbers expanded in the lineage during *Fmed* genome evolution, such as genes encoding for glycoside hydrolases (GH) families, Fe (III)-reducing glycopeptides (GLP), dye-decolourizing peroxidases (DyP) and laccases (Lac) (Floudas *et al.*, 2012). A detailed report on carbohydrate active enzymes (Cazymes) and class II PODs is presented below.

PATHOGENICITY

In vivo white rot basidiomycete pathogenicity studies on grapevine have been rarely documented (Chiappappa, 1997; Larignon and Dubos, 1997; Sparapano *et al.*, 2000a, 2000b, 2001a; Gatica *et al.*, 2004; Laveau *et al.*, 2009; Luque *et al.*, 2009; Diaz *et al.*, 2013; Akgül *et al.*, 2015; Cloete *et al.*, 2015b; Amarloo *et al.*, 2020; Brown

et al., 2020), but contrasting results to fulfil Koch's postulates were obtained, and the role of basidiomycetes as causes of grapevine foliar symptoms (GLSD) is not clear. Experiments have been conducted either on young or old grapevine plants, but very few of these studies used *Fmed* as inoculum (Larignon and Dubos, 1997; Sparapano *et al.*, 2000a, 2000b, 2001a; Laveau *et al.*, 2009; Luque *et al.*, 2009; Akgül *et al.*, 2015; Amarloo *et al.*, 2020).

The first pathogenicity study on *F. punctatus* (probably *Fmed*) was conducted in France by Larignon and Dubos (1997) to determine the pathogen's role in wood decay. After fungus inoculation of healthy 'Cabernet Sauvignon' wooden blocks or rooted canes, they observed formation of typical white rot only in wooden blocks. As expected the fungus only colonised old wood.

Sparapano *et al.* (2000a), inoculating old vines and assessing wound-induced wood discolouration and white rot symptoms, found that inoculation with *F. punctata* (probably *Fmed*) produced the symptoms with different timing dependant on the cultivar, host plant age and portion inoculated. Specifically white rot formation took: *i*) approx. 6 months after inoculation for symptoms to occur in trunks, branches and spurs of 6-year-old 'Italia', and 9-year-old 'Matilde' plants; *ii*) 2 years after inoculation of 13-year-old 'Sangiovese' vines spurs and branches; or *iii*) 2 years after inoculation in 2-year-old rootstock Kober 5BB grafted with 'Italia'. No symptoms on leaves were induced. While *F. punctata* re-isolation was successful, no other wood degrading fungi were re-isolated. Sparapano *et al.* (2000a) concluded that *F. punctata* (probably *Fmed*) could act as a primary pathogen, and was able to colonize the grapevine woody tissues without other previous fungal infections when inoculated through wounds.

To gain details on the role of each fungus in "Esca disease", Sparapano *et al.* (2000b, 2001a) studied fungus-to-fungus and fungus-to-plant interactions, both *in vitro* and *in planta* co-inoculations. Sparapano *et al.* (2000b) showed *in vitro* competitive interaction of *F. punctata* (probably *Fmed*) with *P. chlamydospora* and antagonism between *P. aleophilum* (= *P. minimum*) and *F. punctata*. They also observed that each fungus could act as a primary pathogen by *in planta* inoculations. Moreover, the effect of *F. punctata* (probably *Fmed*) on the woody tissue of 'Italia' and 'Matilde' grapevines was limited by *P. aleophilum* (= *P. minimum*) but not by *P. chlamydospora*. Only *F. punctata* (probably *Fmed*) alone was able to induce white rot. This fungus was re-isolated, but no foliar symptoms were observed in the co-inoculation experiments. Besides confirming the fungus-to-fungus competitive and antagonistic interactions with *Pch* and *P. aleophilum* (= *P. minimum*), Sparapano *et al.* (2001a)

found that *F. punctata* causes wood discolouration followed by limited and localised white rot lesions within 3 years after single-inoculations or all possible co-inoculations, in 5-year-old 'Italia' and 9-year-old 'Matilde' vines, when they were inoculated in the spurs, spreading slightly more rapidly when trunks of plants were inoculated. Fungus re-isolation was always successful, and few foliar symptoms (even though not fully corresponding to the typical tiger stripe pattern) were observed after 2 to 3 years from inoculation in all the inoculation combinations. Non-inoculated plants (experimental controls) did not develop foliar symptoms.

The most recent study of *Fmed* pathogenicity was conducted by Amerloo *et al.* (2020). They inoculated *Fmed* mycelium on 2-year-old rooted grapevine 'Kolahdari' cutting under controlled greenhouse conditions, obtaining wood discolourations (but not white rot) 10 months after inoculation, confirming that white rot formed only on old wood. The proportion of *Fmed* re-isolation was approx. 60%, and no foliar symptoms were recorded. These results were in agreement with findings in rooted cuttings of 'Cabernet Sauvignon' (Laveau *et al.*, 2009), 1-year-old 'Macabeo' and 'Tempranillo' plants grafted onto Richter 110 rootstock (Luque *et al.*, 2009), and 1-year-old rooted plants of 'Sultana Seedless' (Akgül *et al.*, 2015).

Data from pathogenicity tests of *Fmed* and grapevine are still too scarce for postulation of general concepts, especially considering that multiple factors could play a role in wood symptoms appearance (i.e. grapevine cultivar, age, trunk portion). However, the experimental evidence on ability of the pathogen to primarily colonize grapevine wood, and on relationships between white rot presence/amount and external foliar symptoms, require further investigation, especially considering contrasting results obtained from artificial inoculations versus the ones obtained from curative experiments (see above).

Host specificity should also be considered. *Fmed* isolates from different hosts have been used for pathogenicity tests on citrus trees (Elena *et al.*, 2006). According to the extent of wood discolouration in citrus trees after inoculation with *Fmed* isolates from *Citrus*, *Vitis*, or *Actinidia*, a degree of host specificity for *Citrus* spp. was suggested. Other cross-pathogenicity tests conducted by Markakis *et al.* (2017) shown a certain degree of host-specificity in *Fmed*: grapevine-isolates inoculated in wood of pomegranate tree and kumquat tree shown shorter wood discoloration (and no fungal re-isolation) than in pathogenicity test with isolates from the same trees.

Study of host specificity for different *Fmed* isolates could elucidate dissemination modes for *Fmed*.

As indicated above, most wood and/or foliar vine symptoms could be caused by enzymes, toxins and/or other metabolites secreted by the pathogens individually or in combinations spreading through vines from the colonised wood, together with products of host defence reactions (Sparapano *et al.*, 1998; Graniti *et al.*, 1999; Mugnai *et al.*, 1999; Amalfitano *et al.*, 2000, 2011; Sparapano *et al.*, 2000a, 2000b; Bruno and Sparapano, 2006b; Claverie *et al.*, 2020). Recently, wood degradation in grapevine diseases was critically reviewed in comparison with other tree species by Schilling *et al.* (2021), reinforcing our observation that studying enzymatic and non-enzymatic fungal degradation, together with host defence related compounds, could be the key to understanding fungal adaptation to grapevine, and provide insights into wood and foliar symptoms.

Enzymes

White rot in wood is the result of lignin, cellulose, and hemicellulose degradation (either simultaneously or preferentially) by extracellular enzyme activity (Blanchette, 1991). These enzymes include: *i*) carbohydrate-active enzymes (CAZymes), such as endoglucanases (EC 3.2.14), cellobiohydrolases (EC 3.2.1.91, classified in the Glycoside Hydrolase family, GH), β -glucosidases (EC 3.2.1.21) and cellobiose dehydrogenase, CDH (EC 1.1.99.18); *ii*) laccases (EC 1.10.3.2; p-diphenol:di-oxygen oxidoreductases); and *iii*) Class II peroxidases (PODs), such as manganese peroxidases (MnP; EC 1.11.1.13), lignin peroxidases (LiP; EC 1.11.1.14) and the versatile peroxidases (VPs, EC 1.11.1.16) (Daniel, 2014). Auxiliary activities (AA) redox enzymes are also considered to be present in white rot agents: eight families of ligninolytic enzymes and two of lytic polysaccharide mono-oxygenases (LPMOs) are associated with CAZymes and Class II PODs, since they may contribute jointly to degradation of polysaccharides (Levasseur *et al.*, 2013; Daniel, 2014). Carbohydrate-Binding Modules (CBMs) are non-catalytic modules which were also found to be associated with CAZymes, contributing to polysaccharide degradation activity (Boraston *et al.*, 2004). All these enzymes are currently collected for each fungus in the Carbohydrate Active Enzymes database (CAZy database, <https://www.cazy.org>), including its update for AA (<http://www.cazy.org/Auxiliary-Activities.html>) (Levasseur *et al.*, 2013; Lombard *et al.*, 2014).

Enzymes included in the pool of fungal secreted proteins, the secretome, can be involved in *Fmed* pathogenicity. *Fomitiporia mediterranea* and *F. punctata* (probably *Fmed*) secrete ligninolytic enzymes (such as laccases and peroxidases), and cellulolytic enzymes (such as endo-

1,4- β -glucanases and β -glucosidases), for which *in vitro* activities in *Fmed* cultures have been assessed (Mugnai *et al.*, 1999; Bruno and Sparapano 2006a). Laccases are known for their oxidase activity on a large set of phenolic compounds, and on non-phenolic compounds in the presence of mediators (Pérez *et al.*, 2002). However, the role of laccases in plant-pathogen interactions is still discussed. Their importance in pathogenicity has been suggested for some fungal species, such as the chestnut blight pathogen *Cryphonectria parasitica* (Murrill) M.E. Barr, through tannin detoxification and involvement in several other metabolic pathways, such as fungal morphogenesis and pathogenesis (Singh Arora and Kumar Sharma, 2010). For *Fmed*, Abou-Mansour *et al.* (2009) purified a typical fungal 60kDa laccase from some isolates. This enzyme oxidizes many natural polyphenolic compounds. Complete lignin degradation was not achieved alone, however, but only with the contributions from ligninolytic class II PODs. Three manganese peroxidase genes supplementing laccase activity were characterized in the *Fmed* genome, as *Fmmnp1*, *Fmmnp2* and *Fmmnp3* (Morgenstern *et al.*, 2010). Cloete *et al.* (2015b) highlighted the LiP activity of *Fmed in vitro*. It therefore appears that *Fmed* produces a complete white rot-type enzymatic pool, capable of oxidizing and mineralizing lignin and polysaccharides. In addition, comparative genomic studies supported laboratory data and highlighted a rich enzymatic pool for *Fmed*. Floudas *et al.* (2012) and Riley *et al.* (2014) showed that *CDH* gene copies, several *GH* gene families, *LPMOs* and *CBM* family 1 (*CBM1*) genes were detected for the CAZymes pool. Other AAs were identified for lignin degradation pathways, including multicopper oxidases (MCO), copper radical oxidases (CRO), benzoquinone reductase, iron permease (FTR), and ferroxidase (Fet3) (Floudas *et al.*, 2012). The genes encoding for the latter five proteins have been described as genes involved in the non-enzymatic wood degradation caused by some brown rot pathogens (Sista Kameshwar and Qin, 2020). This could support the hypothesis that a similar non-enzymatic iron-dependent system (as described by Goodell *et al.*, 1997, for brown rot, and by Osti and Di Marco, 2010, for the *Pch* and *Pmin* soft rots) could also be part of the *Fmed* white rot process (Moretti *et al.*, 2019). Low Molecular Weight Compounds (LMWC) Fe^{3+} reductants could also be involved in generating OH radicals through a mediated Fenton reaction ($\text{Fe}^{2+} + \text{H}_2\text{O}_2 \rightarrow \text{Fe}^{3+} + \cdot\text{OH} + \cdot\text{OH}$), as suggested in the Chelator Mediated Fenton (CMF) model proposed by Goodell *et al.* (1997). Three studies support this hypothesis, including: *i*) the *Fmed* draft genome revealed a homologous *SidA* gene responsible for inducing siderophore biosynthesis in *Ustilago maydis* (DC.) Corda (Mei

et al., 1993; Floudas *et al.*, 2012; Canessa and Larrondo, 2013); *ii*) *F. punctata* (probably *Fmed*) produces LMW metabolites *in vitro*, some of which have iron-chelating ability (Sparapano *et al.*, 2000b; Di Marco *et al.*, 2001); and *iii*) the *Fmed* genome includes genes codifying for reducing-polyketide synthase (R-PKS) which upregulate in some brown rot fungi, and these have been related to LMWC production likely involved in the redox chemistry of non-enzymatic degradation models (Goodell *et al.*, 1997; Riley *et al.*, 2014; Goodell, 2020). These observations are in line with Riley *et al.* (2014), who observed that the lignocellulolytic gene pathway does not capture the prevailing paradigm of white rot/brown rot wood decay fungi over several *Basidiomycota* genomes. A more nuanced and less dichotomic categorization of rot types could be implemented.

The *Fmed* genome also includes several gene copies codifying for terpene synthase (TS), cytochrome P450 monooxygenase (CytP450) and glutathione transferases (GSTs) (Floudas *et al.*, 2012). Together with R-PKS, TS could confer competition advantages against other microorganisms through secondary metabolite production (Riley *et al.*, 2014). CytP450 could also be involved in secondary metabolite production, and was originally described with GSTs as part of fungal xenomes, often associated with intracellular detoxification processes against lignin and other secondary metabolites synthesized by plants in reaction to fungus attack (Morel *et al.*, 2013). This could confer the “primary” pathogen character reported by Sparapano *et al.* (2000a, 2001a).

Degradative enzymes (such as laccases, peroxidases and tannases) produced by *Fmed* could also degrade antimicrobial substances synthesized by host plants (tannic acid and resveratrol), playing putative roles in host-pathogen interactions. Moreover, detoxification enzymes such as phenol-oxidases and peroxidases were also detected in the contact zones of dual cultures with *Fmed* and *Pch* or *Fmed* and *Pmin*, suggesting detoxification activity by these enzymes against antimicrobial substances secreted by antagonistic fungi (Bruno and Sparapano, 2006a).

In conclusion, studying the complexity of the enzymatic pool, the secretome and xenome, together with possible presence of a non-enzymatic iron-dependent pathway, could provide further insight into *Fmed*-grapevine interactions and “Esca disease” symptomatology.

Phytotoxic compounds, organic acids, and other molecules

Toxin production and translocation to foliage via sap flow has been often proposed as the possible cause of “Esca disease” foliar symptoms (Claverie *et al.*, 2020),

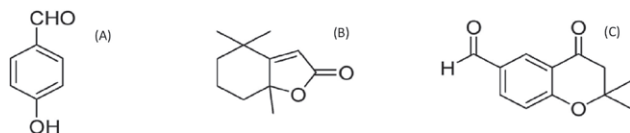


Figure 7. Phytotoxins produced by *Fomitiporia mediterranea*, based on relevant reports. (A), 4-Hydroxybenzaldehyde; (B), dihydroactinolide; (C), 6-Formyl-2,2-dimethyl-4-chromanone. Chemical formulae retrieved by PubChem (<https://pubchem.ncbi.nlm.nih.gov/>).

and its role in GTDs has recently been reviewed (Masi *et al.*, 2018). It has been postulated that an oxidative burst triggered by the toxins in leaves could be more likely involved in foliar symptoms appearance than toxins themselves (Calzarano and Di Marco, 2018b). Toxicity thresholds and possible interference with other foliar susceptibility factors are still unclarified (Claverie *et al.*, 2020). Production of low molecular weight metabolites with potential phytotoxicity was recorded (without identification) by Sparapano *et al.* (2000c), but phytotoxins were identified by Tabacchi *et al.* (2000) in *F. punctata* cultures (probably *Fmed*). They detected 4-hydroxybenzaldehyde, dihydroactinolide and 6-Formyl-2,2-dimethyl-4-chromanone (Figure 7), a phytotoxin related to eutypine produced by *Eutypa lata* (Deswarte *et al.*, 1996a, 1996b; Andolfi *et al.*, 2011). It was suggested that hydroxyl-benzaldehyde and its derivatives (carrying the aldehyde function) play important roles in the toxicity of fungi implicated in “Esca disease”. Phytotoxicity was reported only for 4-Hydroxy-benzaldehyde on living protoplasts from *V. vinifera* ‘Cabernet Sauvignon’ at 10^{-5} and 10^{-6} M, as well as on callus from *V. vinifera* ‘Gamay’ grown in media supplemented with different concentrations of the metabolite (100, 250, and 500 mM) (Tabacchi *et al.*, 2000). Further research is necessary to fully assess phytotoxicity of fungal metabolites and their roles in the diseases of Esca complex.

There is good correlation between fungus pathogenesis and oxalic acid secretion (Dutton and Evans, 1996). This is especially true for wood decay agents, where organic acids (mainly oxalic acid) may facilitate lignocellulosic biomass degradation, due to pH acidification, unstable and toxic divalent metal chelation, and H_2O_2 production (Kuan and Tien, 1993; Shimada *et al.*, 1994; Tanaka *et al.*, 1994; Urzúa *et al.*, 1998). Oxalic acid metabolism is mainly regulated by two enzymes, i.e. oxalate decarboxylase (ODC, EC 4.1.1.2) and oxalate oxidase (OXO, EC 1.2.3.4), both of which catabolize the organic acid and reduce its level, which in high concentrations could be cytotoxic for pathogenic fungi (Svedružić *et al.*, 2005; Zhuang *et al.*, 2015). For *F. punctata* (probably *Fmed*), despite pH lowering in liquid culture (from 6.8 to

5.3; Sparapano *et al.*, 2000c), Liaud *et al.* (2014) observed no organic acid production by *Fmed* in a comparative liquid culture chromatography screening. However, the presence of oxalate decarboxylase/oxidases gene copies in the *Fmed* genome (Floudas *et al.*, 2012) indicates that epigenetic regulation of their expression could often occur.

Basidiomycete species are well known to produce pigments in response to abiotic and biotic stimuli, and these pigments act as chemical mediators during interactions between multiple organisms. Among them, terpene polyketide and amino acid derivatives are known to be inducible, and to confer competition advantage (Spiteller, 2008, 2015; Halbwachs *et al.*, 2016). In co-culture assays with *Hapalopilus rutilans* (Pers.) Murrill, *Fmed* mycelium increased pigmentation earlier compared to axenic culture, via hyperproduction of hypholomine B (Tauber *et al.*, 2018), suggesting a role in interaction modulation. Interactions of *Fmed* with other microorganisms has been studied by Bruno and Sparapano (2006a) and Sparapano *et al.* (2000b, 2001b). In dual cultures with *Pmin* on modified Czapek medium, *Fmed* colony margins turned brown, became thicker and aerial hyphae formed ridge-like barriers, but the fungus growth stops at the contact zone. In dual cultures with *Pch*, after agonistic early growth, *Fmed* overgrew *Pch* mycelium (Sparapano *et al.*, 2000b). The *Pmin* vs *F. punctata* (probably *Fmed*) antagonistic effect was confirmed in triple cultures with *Pch* in that condition, *Pch* was not overgrown by the *Fmed* mycelium, suggesting a suppressive role of *Pmin* (Sparapano *et al.*, 2000b). Sparapano *et al.* (2001b) also studied the possible biochemical motivation of these agonistic and not-agonistic effects: *Pmin* and *Pch* culture filtrates, depending on their dilution in culture media, inhibited or reduced growth of *F. punctata* in Malt Extract Agar (ME). No inhibition of *Fmed* in ME medium was observed for *Pmin* or *Pch* crude organic extracts (ethyl acetate extraction of culture filtrates), purified scytalone from *Pmin* and *Pch* (at 1 mg mL^{-1}), pullulan from *Pch* (at 0.2 mg mL^{-1}) and oligosaccharides up to 2.5 kDa obtained by digestion of *Pch*-pullulan (2 mg mL^{-1}) (Sparapano *et al.*, 2001b).

Study of the metabolome and transcriptome of the contact zones of different dual cultures to assess molecular cross-talking between *Fmed* and its competitor, would be worthwhile, to complete the partially studied secretome of this pathogen (Bruno and Sparapano, 2006a).

HOST PHYSIOLOGY CHANGES AND DEFENSE RESPONSES FOLLOWING *F. MEDITERRANEA* INFECTIONS

Data is sparse on changes in grapevine physiology and defence mechanisms specifically related to *Fmed*.

Effects of GTDs on grapevine physiology were reviewed by Fontaine *et al.* (2016b), but no specific responses to *Fmed* colonization and infection have been reported. Nevertheless, research on re-established plant vigour and quality grape production after 3 years from curettage treatments (see below) has demonstrated that white rot (where the main European decay agent *Fmed* is overabundant; Fischer and Kassemeyer, 2003; Bruez *et al.*, 2017) probably affects grapevine physiology (Chollet *et al.*, 2021). This follows observations by Ouadi *et al.* (2019) on ‘Cabernet Sauvignon’ plants presenting foliar symptoms of “Esca disease”. They linked the abundance of necrotic wood (mainly white rot) in grapevine trunks and cordons with a 30% reduction in vine sap flow circulation, and thus leaf transpiration.

Few experiments have been performed to clarify plant defence mechanisms against *Fmed*. In callus/fungus dual culture experiments, Bruno and Sparapano (2006c) identified a number of phenolic molecules (benzaldehyde derivatives, benzoic acid derivatives, flavonols, flavonol-3-o glycosides, quercetin 3-rhamnoside, catechins and stilbenes) that were differentially induced in ‘Matilde’ and ‘Italia’ grapevines. Other studies have focused directly on vine sap (Bruno and Sparapano, 2006b, d) or brown-red symptomatic wood (Amalfitano *et al.*, 2000, 2011; Agrelli *et al.*, 2009) of “Esca disease”-symptomatic plants. Several stilbene-phenolic molecules were identified, which are theoretically toxic to *Fmed*, that showed greater sensitivity to phenols than *Pch* or *Pmin* (Amalfitano *et al.*, 2001, 2011). Similar results were obtained by Rusjan *et al.* (2017) in wood of leaf stripe symptomatic vines, but with phenolic alterations reflecting both presence of the pathogen and wood condition in different parts of vines (trunks and rootstocks). Rusjan *et al.* (2017) proposed a relationship between the period of presence of the pathogen in different vine portions and their phenolic profiles. However, biomolecule concentration increases observed by Rusjan *et al.* (2017) may not be related exclusively to *Fmed*. Diseased plants are naturally infected by all the “Esca disease”-related fungi (*Pch*, *Pmin*, *Fmed*), and other possible microbial consortia highlighted by metagenomic approaches. Nevertheless, because a *Fmed*-*Pch*-*Pmin* interaction has been demonstrated, a relationship is likely between those compounds and *Fmed* (Sparapano *et al.*, 2001b; Bruez *et al.*, 2020). For this reason, results from most metabolomic studies in leaves responding to “Esca disease”-associated pathogens should be treated with caution, when attempting to understand exact plant responses to *Fmed* (Goufo *et al.*, 2019; Moret *et al.*, 2021). Further studies are necessary to precisely determine grapevine metabolite production burst specifically in response to *Fmed* colonization.

Damage to host hydraulic systems caused by the white rot necrosis could be the most important driver of physiological effects in grapevines, but specific studies are necessary to verify these hypotheses. To the best of our knowledge there have been no reported studies of wood compartmentalization specifically towards *Fmed*. The metabolic changes induced by *Fmed in planta* could generate biochemical markers for presence of the pathogen and wood degrading activity.

CONTROL STRATEGIES WITH A FOCUS ON *F. MEDITERRANEA*

Effective disease management is a major challenge in crop protection, and particularly for disease complexes such as “Esca disease”. Efficiency of individual control methods for Esca complex of diseases is limited, and is best managed using integrated disease management, from nursery to vineyard. This includes cultural or remedial practices, vineyard sanitation, and use of pesticide chemicals or biological agents to protect grapevine wounds from pathogen infections (Gramaje *et al.*, 2018). Methods to reduce or limit disease incidence, especially against *Fmed* infection, are outlined below.

Disease resistance

Incidence of “Esca disease” symptoms have been reported as cultivar-, rootstock-, and clone-related (Marchi 2001; Fussler *et al.*, 2008; Grosman, 2008; Murolo and Romanazzi, 2014; Guan *et al.*, 2016; Kraus *et al.*, 2019; Moret *et al.*, 2019), but they were all related to reduced presence of leaf symptoms, not to wood decay development. Some hypotheses could explain cultivar differences. Rolshausen *et al.* (2008) reported greater lignin levels in ‘Merlot’ grapevines tolerant to *E. lata* compared to susceptible ‘Cabernet-Sauvignon’ vines. A similar correlation has been suggested for *Fmed* affecting different olive tree varieties (Markakis *et al.*, 2019). Assessment of susceptibility of wild grapevine (*V. vinifera* subsp. *sylvestris*) to *Fmed* could be worthwhile, because this host has been shown to be a promising potential source of resistance to *Botryosphaeria dieback* (Guan *et al.*, 2016). Some data are available on other *Vitis* genotypes used in resistance source trials (Kraus *et al.*, 2019). Fischer (2019) also detected regular presence of *Fmed* vegetative mycelium in rootstock mother blocks of rootstocks SO4, 5BB and 125AA in Germany, all of which were a cross population of *Vitis berlandieri* × *Vitis rupestris*.

Grapevine propagation material

The use of a good quality pathogen-free plant material is essential to limit inoculum propagation. Although *Fmed* has been shown to be present in blocks of rootstock mother vines (Fischer, 2009, 2019), and thus the derived plant material could be infected by “Esca disease”-associated fungi before nursery stages or during the propagation processes, *Fmed* has never been isolated from grafted 1-year old cuttings or propagation material. Furthermore, this pathogen has not been reported in grapevine nurseries (Larignon and Dubos 2000; Halleen *et al.*, 2003; Zanzotto *et al.*, 2007; Larignon *et al.*, 2008a; Aroca *et al.*, 2010; Gramaje and Armengol, 2011; Fischer, personal communication).

Protective and curative disease control methods

Curative control

Removing white rot from diseased grapevines seems to be efficient for reducing leaf stripe symptoms. This old technique, called “curettage” or “trunk surgery”, consists of cutting affected vines and removing white rot with small precision chain saws. It provides good results; foliar symptoms are reduced even several years after curetting (Thibault, 2015). Cholet *et al.* (2021) demonstrated how curettage in “Esca disease”-symptomatic plants reduced foliar symptoms during 3 years after treatment, and re-establish vine vigour and grape production. Pacetti *et al.* (2021) confirmed foliar symptom remission in 14-year-old GLSD symptomatic ‘Cabernet Sauvignon’ vines for the following 2 years after complete trunk surgery, and demonstrated microbiome change induced by the treatment. *Fomitiporia mediterranea* abundance decreased after curettage, in parallel to an alpha-diversity increase in fungal population, suggesting a microbiota shift as a likely explanation for foliar symptom reduction during the post-curettage period.

Plant endotherapy is another promising curative technique against white rot. This includes direct treatment of white rot by drilling a vertical hole in grapevine trunks and injecting specific molecule solutions (typically fungicides), aiming to reduce foliar symptoms. However, due to the complexity of microbial consortia in diseased trunks, and because of the wood peculiar structure in old cultivated vines, specificity of the technique against *Fmed* needs to be refined. This approach is the subject of ongoing research (Gellon *et al.*, 2017; Pacetti *et al.*, 2019).

Sodium arsenite has been used in viticulture for a long time as the only effective and curative treatment

against “Esca disease” (Songy *et al.*, 2019b), and studies on modes of action of this compound are increasing. Larignon *et al.* (2008b) suggested *Fmed* as the most sodium arsenite sensitive “Esca disease”-associated fungus, and when Goddard *et al.* (2017) investigated the fate of arsenite within “Esca-diseased” treated plants, they found it concentrated in white rot necroses. Bruez *et al.* (2017) demonstrated that *Fmed* isolations were reduced from white rot necrotic tissue coming from sodium arsenite treated plants. Bruez *et al.* (2021) showed how in sodium arsenite treated ‘Gewürztraminer’, ‘Chardonnay’ and ‘Merlot’ vines (25 to 40 years old) expressing tiger stripe symptoms, the relative abundance of *Fmed* decreased in white rot necroses and necrosis boundaries, confirming *Fmed* as the most sodium arsenite sensitive among GTDs-associated fungi (Larignon *et al.*, 2008b). Previously foliar symptomatic plants did not express these symptoms after treatment, suggesting that the positive effect of sodium arsenite on GLSD was from specific toxicity to *Fmed* in white rot necrotic tissues and their boundaries, where other parasitic and saprobic fungi (*Inonotus hispidus* Bull. P. Karst., *Lepiota brunneoincarnata* Chodat & C. Martín) took place, increasing their relative abundance (Bruez *et al.*, 2021).

Except for host endotherapy, for which experiments are ongoing, up to now curettage is likely to be the most sustainable physical management method against *Fmed*. More user- and environmentally-friendly chemical curative alternative should be proposed. The long-term efficacy of curative treatments has not been fully assessed. Data on reduction of foliar stripe symptoms provided by these two curative techniques (curettage and sodium arsenite) reinforce the link between GLSD and white rot, suggesting that more studies are required on these disease management approaches.

Preventive control

Protection of grapevine pruning wounds is an essential point to reduce pathogen entry (Eskalen and Gubler, 2001; Eskalen *et al.*, 2007). In some European countries, some pesticide products (based on boscalid or pyraclostrobin) and biocontrol products (based on specific strains of *Trichoderma* spp.) are available for protection against GTDs. However, research with these products for management of *Fmed* diseases has not been reported yet.

Beside the authorized and registered products containing boscalid, pyraclostrobin or *Trichoderma* spp., many products or molecules have been tested *in vitro* for the control of GTD pathogens, and these were reviewed by Gramaje *et al.* (2018) and Mondello *et al.* (2018b). For *Fmed*, however, only few reports are available. Chitosan

in *in vitro* tests gave a low EC₅₀ value (1.53 mg L⁻¹) for *Fmed* (Nascimento *et al.*, 2007). Sensitivity of *Fomitiporia* spp. to chitosan was first reported by Bruno *et al.* (2001). Incorporation of resveratrol in culture media gave a direct antifungal effect against *Fmed* growth (Mazzullo *et al.*, 2000). Copper oxychloride and gluconate formulations slightly reduced *Fmed* mycelium growth *in vitro*, with an EC₅₀ of 11.242 mg Cu L⁻¹ (Di Marco *et al.*, 2011). For biological control, sensitivity of *Fmed* to crude protein extracts (CPE) from *Bacillus amiloliquefaciens* AG1 has been recorded as 2.000 AU mL⁻¹ (Alfonzo *et al.*, 2012). Del Frari *et al.* (2019b) demonstrated with *in vitro* dual culture plates that growth of *Fmed* and other “Esca disease”-associated fungi was inhibited by *Epicoccum* spp., a member of ascomycetes which have been commonly identified in grapevine microbiomes. No clear data have been provided about effects of *Trichoderma* spp. on *Fmed*, in contrast to documented effects of these fungi on the growth of *Pch* and *E. lata* (Di Marco *et al.*, 2004b; John *et al.*, 2005).

CONCLUSIONS AND FUTURE PERSPECTIVES

We have made careful attempts to collect and review all relevant published information on *F. mediterranea*, to stimulate debate within the GTD scientific community. Approximately 20 years after formal classification of this fungus, it is well established that it induces white rot in the grapevine wood, but details of the relationships between *Fmed* and GLSD essentially remain unknown. The causes and biomolecular mechanisms of white rot, and their relationships with external grapevine foliar symptoms, has yet to be deciphered, especially in light of knowledge and observations reviewed here. To fully describe these processes could be a standing point in the context of GTDs, and will allow viticulture to adopt new solutions for management of grapevine trunk diseases.

LITERATURE CITED

- Abbatecola A., Dongiovanni C., Faretra F., Pollastro S., 2000. Observations on the fungi associated with Esca and on spatial distribution of Esca-symptomatic plants in Apulian (Italy) vineyards. *Phytopathologia Mediterranea* 39: 206–210.
- Abou-Mansour E., Couché E., Tabacchi R., 2004. Do fungal naphthalenones have a role in the development of esca symptoms? *Phytopathologia Mediterranea* 43: 75–82.
- Abou-Mansour E., Polier J., Pezet R., Tabacchi R., 2009. Purification and partial characterisation of a 60 KDa
- laccase from *Fomitiporia mediterranea*. *Phytopathologia Mediterranea* 48: 447–453.
- Agrelli D., Amalfitano C., Conte P., Mugnai L., 2009. Chemical and spectroscopic characteristics of the wood of *Vitis vinifera* cv. Sangiovese affected by esca disease. *Journal of Agricultural and Food Chemistry* 57(24): 11469–11475.
- Ahmadyusefi Sarhadi F., Mohammadi H., 2019. *Fomitiporia mediterranea* and *Phaeoacremonium rubrigenum* associated to Russian olive trunk diseases in Iran. 4th Iranian Mycological Congress, Sari Agricultural Sciences and Natural Resources University, Sari, Iran. 26–28 August 2019: 104 (Abstract).
- Akgül D.S., Gungor Savas N., Teker T., Keykubat B., Mayorquin J.S., Eskalen A., 2015. Fungal trunk pathogens of Sultana seedless vineyards in Aegean region of Turkey. *Phytopathologia Mediterranea* 54(2): 380–393.
- Alfonzo A., Lo Piccolo S., Conigliaro G., Ventorino V., Burrano S., Moschetti G., 2012. Antifungal peptides produced by *Bacillus amiloliquefaciens* AG1 active against grapevine fungal pathogens. *Annals of Microbiology* 62: 1593–1599.
- Amalfitano C., Evidente A., Surico G., Tegli S., Bertelli E., Mugnai L., 2000. Phenols and stilbene polyphenols in the wood of esca-diseased grapevines. *Phytopathologia Mediterranea* 39(1): 178–183.
- Amalfitano C., Agrelli D., Arrigo A., Mugnai L., Surico G., Evidente A., 2011. Stilbene polyphenols in the brown red wood of *Vitis vinifera* cv. Sangiovese affected by “esca proper”. *Phytopathologia Mediterranea* 50: S224–S235.
- Amarloo O.A., Mohammadi H., Mahdian S.A., Tajick Ghanbary M.A., 2020. Identification and pathogenicity of fungal species associated with grapevine trunk diseases in Khorasan–Razavi province, Iran. *Mycologia Iranica* 7(1): 83–94.
- Andolfi A., Mugnai L., Luque J., Surico G., Cimmino A., Evidente A., 2011. Phytotoxins produced by fungi associated with grapevine trunk diseases. *Toxins* 3(12): 1569–1605.
- Armengol J., Vicent A., Torné L., García-Figueres F., García-Jiménez J., 2001. Fungi associated with esca and grapevine declines in Spain: a three-year survey. *Phytopathologia Mediterranea* 40(3): 325–329.
- Aroca Á., Gramaje D., Armengol J., García-Jiménez J., Raposo R., 2010. Evaluation of the grapevine nursery propagation process as a source of *Phaeoacremonium* spp. and *Phaeoacremonium chlamydospora* and occurrence of trunk disease pathogens in rootstock mother vines in Spain. *European Journal of Plant Pathology* 126: 165–174.

- Baranek M., Armengol J., Holleinova V., Pecenka J., Calzarano F., ... Eichmeier A., 2018. Incidence of symptoms and fungal pathogens associated with grapevine trunk diseases in Czech vineyards: first example from a north-eastern European grape-growing region. *Phytopathologia Mediterranea* 57(3): 449–458.
- Beck H.E., Zimmermann N.E., McVicar T.R., Vergopolan N., Berg A., Wood E.F., 2018. Present and future Köppen-Geiger climate classification maps at 1-km resolution. *Nature Scientific Data* 5: 180214.
- Berraf A., Péros J.P., 2005. Importance of Eutypa dieback and esca in Algeria and structure of the associated fungal community. (Importance de l'eutypiose et de l'esca en Algérie et structure de la communauté fongique associée.). *Journal International des Sciences de la Vigne et du Vin* 39(3): 121–128.
- Bertsch C., Ramírez-Suero M., Magnin-Robert M., Larignon P., Chong J., ... Fontaine F., 2013. Grapevine trunk diseases: Complex and still poorly understood. *Plant Pathology* 62(2): 243–265.
- Bester M.C., Halleen F., Mostert L. 2015. A PCR detection system for South African basidiomycetous isolates from esca affected grapevine. *Australasian Plant Pathology* 44: 647–651.
- Blanchette R., 1991. Delignification by wood-decay fungi. *Annual Review of Phytopathology* 29: 381–398.
- Bonnet L.O., 1926. A promising remedy for black measles of the vine. In: *College of Agriculture. Agricultural Experiment Station*, University of California, College of Agriculture, Agricultural Experiment Station, Berkeley, CA, USA, Circular 303, 10 p.
- Boraston A.B., Bolam D.N., Gilbert H.J., Davies G.J., 2004. Carbohydrate-binding modules: fine-tuning polysaccharide recognition. *Biochemical Journal* 382 (Pt 3): 769–781.
- Bortolami G., Gambetta G.A., Delzon S., Lamarque L.J., Pouzoulet J., ... Delmas C.E.L., 2019. Exploring the hydraulic failure hypothesis of esca leaf symptom formation. *Plant Physiology* 181: 1163–1174.
- Bortolami G., Farolfi E., Badel E., Burlett R., Cochard H., ... Delmas C.E.L., 2021. Seasonal and long-term consequences of esca grapevine disease on stem xylem integrity. *Journal of Experimental Botany* 72(10): 3914–3928.
- Brown A. A. A., Lawrence D. P. P., Baumgartner K., 2020. Role of basidiomycete fungi in the grapevine trunk disease esca. *Plant Pathology* 69(2): 205–220.
- Bruez E., Lecomte P., Grosman J., Doublet B., Bertsch C., ... Rey P., 2013. Overview of grapevine trunk diseases in France in the 2000s. *Phytopathologia Mediterranea* 52(2): 262–275.
- Bruez E., Vallance J., Gerbore J., Lecomte P., Da Costa J. P., ... Rey P., 2014. Analyses of the temporal dynamics of fungal communities colonizing the healthy wood tissues of esca leaf-symptomatic and asymptomatic vines. *PLoS ONE* 9(5): e95928.
- Bruez E., Larignon P., Bertsch C., Rey P., Fontaine F., 2017. Comparison of the wood-microbiome from Grapevine Trunk Disease-plants, treated or not with sodium arsenite. *Phytopathologia Mediterranea* 56(3): 560–561 (Abstract).
- Bruez E., Vallance J., Gautier A., Laval V., Compant S., ... Rey P., 2020. Major changes in grapevine wood microbiota are associated with the onset of esca, a devastating trunk disease. *Environmental Microbiology* 22(12): 5189–5206.
- Bruez E., Larignon P., Bertsch C., Robert-Siegwald G., Lebrun M.-H., ... Fontaine F., 2021. Impacts of sodium arsenite on wood microbiota of esca-diseased grapevines. *Journal of Fungi* 7: 498.
- Bruno G., Muzzarelli R.A.A., Muzzarelli C., Sparapano L., 2001. Biological activity of chitosan and its derivatives on plant pathogenic or antagonistic fungi and on host plants. In: *Proceedings of the 11th Congress of the Mediterranean Phytopathological Union and 3rd Congress of the Sociedade Portuguesa de Fitopatologia*, 17–20 September 2001, University of Évora, Évora, Portugal, 104–106.
- Bruno G., Sparapano L., 2006a. Effects of three esca-associated fungi on *Vitis vinifera* L.: III. Enzymes produced by the pathogens and their role in fungus-to-plant or in fungus-to-fungus Interactions. *Physiological and Molecular Plant Pathology* 69: 182–194.
- Bruno G., Sparapano L., 2006b. Effects of three esca-associated fungi on *Vitis vinifera* L.: II. Characterization of biomolecules in xylem sap and leaves of healthy and diseased vines. *Physiological and Molecular Plant Pathology* 69: 195–208.
- Bruno G., Sparapano L., 2006c. Effects of three esca-associated fungi on *Vitis vinifera* L.: I. Characterization of secondary metabolites in culture media and host responses to the pathogens in calli. *Physiological and Molecular Plant Pathology* 69: 209–223.
- Bruno G., Sparapano L., 2006d. Effects of three esca-associated fungi on *Vitis vinifera* L.: V. Changes in the chemical and biological profile of xylem sap from diseased cv. sangiovese vines. *Physiological and Molecular Plant Pathology* 71: 210–29.
- Calzarano F., Cichelli A., Odoardi M., 2001. Preliminary evaluation of variations in composition induced by esca on cv. Trebbiano d'Abruzzo grapes and wines. *Phytopathologia Mediterranea* 40: 443–448.

- Calzarano F., Di Marco S., 2007. Wood discoloration and decay in grapevines with esca proper and their relationship with foliar symptoms. *Phytopathologia Mediterranea* 46: 96–101.
- Calzarano F., Amalfitano C., Seghetti L., Cozzolino V., 2009. Nutritional status of vines affected with esca proper. *Phytopathologia Mediterranea* 48: 20–31.
- Calzarano F., Osti F., D'agostino V., Pepe A., Di Marco S., 2017. Mixture of calcium, magnesium and seaweed affects leaf phytoalexin contents and grape ripening on vines with grapevine leaf stripe disease. *Phytopathologia Mediterranea* 56(3): 445–457.
- Calzarano F., Osti F., Baránek M., Di Marco S., 2018a. Rainfall and temperature influence expression of foliar symptoms of grapevine leaf stripe disease (esca complex) in vineyards. *Phytopathologia Mediterranea* 57(3): 488–505.
- Calzarano F., Di Marco S., 2018b. Further evidence that calcium, magnesium and seaweed mixtures reduce grapevine leaf stripe symptoms and increase grape yields. *Phytopathologia Mediterranea* 57: 459–471.
- Calzarano F., Pagnani G., Pisante M., Bellocchi M., Cillo G., ... Di Marco, S., 2021. Factors involved on tiger-stripe foliar symptom expression of esca of grapevine. *Plants* 10(6): 1041.
- Carlucci A., Raimondo M.L., Cibelli F., Phillips A.J.L., Lops F., 2013. *Pleurostomophora richardsiae*, *Neofusicoccum parvum* and *Phaeoacremonium aleophilum* associated with a decline of olives in southern Italy. *Phytopathologia Mediterranea* 52(3): 517–527.
- Canessa P., Larrondo L.F., 2013. Environmental responses and the control of iron homeostasis in fungal systems. *Applied Microbiology and Biotechnology* 97: 939–955.
- Castanera R., Borgognone A., Pisabarro A.G., Ramírez L., 2017. Biology, dynamics, and applications of transposable elements in basidiomycete fungi. *Applied Microbiology and Biotechnology* 101: 1337–1350.
- Castillo J.A., Plata G., 2016. The expansion of brown rot disease throughout Bolivia: possible role of climate change. *Canadian Journal of Microbiology* 62: 442–448.
- Chen H., Cui B.K., 2017. Multi-locus phylogeny and morphology reveal five new species of *Fomitiporia* (Hymenochaetales) from China. *Mycological Progress* 16(7): 687–701.
- Chen J.J., Wu Y.D., Ji X.H., Gates G., Xu X., 2021. A new species of *Fomitiporia* (Hymenochaetales) from Australia. *Phytotaxa* 489(2): 200–208.
- Chiarappa L., 1997. *Phellinus igniarius*: the cause of spongy wood decay of black measles (“esca”) disease of grapevines. *Phytopathologia Mediterranea* 36: 109–111.
- Cholet C., Bruez E., Lecomte P., Rey P., Boury T., ... Geny-Denis L., 2019. Intérêt du curetage dans la lutte contre l'esca. *Phytoma* 728: 24–27.
- Cholet C., Bruez E., Lecomte P., Barsacq A., Martignon T., ... Gény L., (2021). Plant resilience and physiological modifications induced by curettage of Esca-diseased grapevines. *OENO One* 55(1): 153–169.
- Choueiri E., Jreijiri F., Chlela P., Mayet V., Comont G., ... Lecomte P., 2014. Fungal community associated with grapevine wood lesions in Lebanon. *OENO One* 48(4): 293–302.
- Ciccarone C., Graniti A., Schiaffino A., Marras F., 2004. Molecular analysis of *Fomitiporia mediterranea* isolates from esca-affected grapevines in southern Italy. *Phytopathologia Mediterranea* 43: 268–272.
- Claverie M., Notaro M., Fontaine F., Wéry J., 2020. Current knowledge on Grapevine Trunk Diseases with complex etiology: a systemic approach. *Phytopathologia Mediterranea* 59(1): 29–53.
- Cloete M., Fischer M., Mostert L., Halleen F., 2014. A novel *Fomitiporia* species associated with esca on grapevine in South Africa. *Mycological Progress* 13: 303–311.
- Cloete M., Fischer M., Mostert L., Halleen F., 2015a. Hymenochaetales associated with esca-related wood rots on grapevine with a special emphasis on the status of esca in South African vineyards. *Phytopathologia Mediterranea* 54(2): 299–312.
- Cloete M., Mostert L., Fischer M., Halleen F., 2015b. Pathogenicity of South African Hymenochaetales taxa isolated from esca-infected grapevines. *Phytopathologia Mediterranea* 54(2): 368–379.
- Cloete M., Fischer M., Du Plessis I.L., Mostert L., Halleen F., 2016. A new species of *Phellinus* sensu stricto associated with esca on grapevine in South Africa. *Mycological Progress* 15(25): 1–9.
- Cortesi P., Fischer M., Milgroom M.G., 2000. Identification and spread of *Fomitiporia punctata* associated with wood decay of grapevine showing symptoms of esca. *Phytopathology* 90(9): 967–972.
- Crous P.W., Gams W., 2000. *Phaeoconiella chlamydospora* gen. et comb. nov., a causal organism of Petri grapevine decline and esca. *Phytopathologia Mediterranea* 39: 112–118.
- Dai Y.C., Cui B.K., Decock C., 2008 A new species of *Fomitiporia* (Hymenochaetales, Basidiomycota) from China based on morphological and molecular characters. *Mycological Research* 112(3): 375–80.
- Daniel G., 2014. Fungal and Bacterial Biodegradation: White Rots, Brown Rots, Soft Rots, and Bacteria. In: *Deterioration and Protection of Sustainable Biomaterials* (T.P. Schultz, B. Goodell, D.D. Nicholas, ed.), American Chemical Society, Washington DC, 23–58.

- Decock C., Figueroa S.H., Robledo G., Castillo G., 2007. *Fomitiporia punctata* (Basidiomycota, Hymenochaetales) and its presumed taxonomic synonyms in America: taxonomy and phylogeny of some species from tropical/subtropical areas. *Mycologia* 99: 733–752.
- Del Frari G., Gobbi A., Aggerbeck M.R., Oliveira H., Hansen L.H., Ferreira R.B., 2019a. Characterization of the wood mycobiome of *Vitis vinifera* in a vineyard affected by esca. Spatial distribution of fungal communities and their putative relation with leaf symptoms. *Frontiers in Plant Science* 10: 910.
- Del Frari G., Cabral A., Nascimento T., Boavida Ferreira R., Oliveira H., 2019b. *Epicoccum layuense* a potential biological control agent of esca-associated fungi in grapevine. *PLoS ONE* 14(3): e0213273.
- Del Rivero J.M., García-Marí F., 1984. Ensayo de productos contra la yesca de la vid y la piral de la vid en tratamientos de invierno. *Boletín de Sanidad Vegetal, Plagas* 10: 17–30.
- Deswarte C., Eychenne J., Davy de Virville J., Roustan J., Moreau F., Fallot J., 1996a. Protonophoric activity of eutypine, a toxin from *Eutypa lata*, in plant mitochondria. *Archives of Biochemistry and Biophysics* 334: 200–205.
- Deswarte C., Canut H., Klæbe A., Roustain J.P., Fallot J., 1996b. Transport, cytoplasmic accumulation, and mechanism of action of the toxic eutypine in *Vitis vinifera* cells. *Journal of Plant Pathology* 149: 336–342.
- Di Marco S., Osti F., Mazzullo A., Cesari A., 2001. How iron could be involved in esca fungi development. *Phytopathologia mediterranea* 40: 449–452.
- Di Marco S., Calzarano F., Osti F., Mazzullo A., 2004a. Pathogenicity of fungi associated with a decay of kiwifruit. *Australasian Plant Pathology* 33: 337–342.
- Di Marco S., Osti F., Cesari A., 2004b. Experiments on the control of esca by *Trichoderma*. *Phytopathologia Mediterranea* 43(1): 108–115.
- Di Marco S., Osti F., 2008. Foliar symptom expression of wood decay in *Actinidia deliciosa* in relation to environmental factors. *Plant Disease* 92 (8): 1150–1157.
- Di Marco S., Osti F., Mugnai L., 2011. First studies on the potential of a copper formulation for the control of leaf stripe disease within esca complex in grapevine. *Phytopathologia Mediterranea* 50: S300–S309.
- Diaz G.A., Auger J., Besoain X., Bordeu E., Latorre B.A., 2013. Prevalence and pathogenicity of fungi associated with grapevine trunk disease in Chilean vineyards. *Ciencia e Investigación Agraria* 40(2): 327–339.
- Dietzel K., Valle D., Fierer N., U'Ren J.M., Barberan A., 2019. Geographical distribution of fungal plant pathogens in dust across the United States. *Frontiers in Ecology and Evolution* 7: 304.
- Dutton M., Evans C.S., 1996. Oxalate production by fungi: its role in pathogenicity and ecology in the soil environment. *Canadian Journal of Microbiology* 42: 881–895.
- Edwards J., Marchi G., Pascoe I.G., 2001. Young esca in Australia. *Phytopathologia Mediterranea* 40: 303–310.
- Elena K., Paplomatas E.J., 2002. First report of *Fomitiporia punctata* infecting Kiwi fruit. *Plant Disease* 86: 1176.
- Elena K., Fischer M., Dimou D., Dimou D.M., 2006. *Fomitiporia mediterranea* infecting citrus trees in Greece. *Phytopathologia Mediterranea* 45(1): 35–39.
- Elena G., Bruetz E., Rey P., Luque J., 2018. Microbiota of grapevine woody tissues with or without esca-foliar symptoms in northeast Spain. *Phytopathologia Mediterranea* 57: 425–438.
- Eskalen A., Gubler W.D., 2001. Association of spores of *Phaeoconiella chlamydospora*, *Phaeoacremonium inflatipes*, and *Pm. aleophilum* with grapevine cordons in California. *Phytopathologia Mediterranea* 40: 429–431.
- Eskalen A., Feliciano J., Gubler W.D., 2007. Susceptibility of grapevine pruning wounds and symptom development in response to infection by *Phaeoacremonium aleophilum* and *Phaeoconiella chlamydospora*. *Plant Disease* 91(9): 1100–1104.
- Farashiyani A., Mousavi Jorf S., Karimi M., 2012. Study of esca disease of grapevine in bojnourd. *Iranian Journal of plant pathology* 48: 143–153.
- Fiasson J.L., Niemelä T., 1984. The Hymenochaetales: a revision of the European poroid taxa. *Karstenia* 24(1): 14–28.
- Fischer M., 1987. Biosystematische Untersuchungen an den Porlingsgattungen *Phellinus* Quél. und *Inonotus* Karst. *Bibliotheca Mycologica* 107: 1–133.
- Fischer M., 1996. On the species complexes within *Phellinus*: *Fomitiporia* revisited. *Mycological Research* 100: 1459–1467.
- Fischer M., 2002. A new wood-decaying basidiomycete species associated with esca of grapevine: *Fomitiporia mediterranea* (Hymenochaetales). *Mycological Progress* 1(3): 315–324.
- Fischer M., Kassemeyer H.H., 2003. Fungi associated with Esca disease of grapevine in Germany. *Vitis* 42(3): 109–116.
- Fischer M., Binder M., 2004. Species recognition, geographic distribution and host-pathogen relationships: A case study in a group of lignicolous basidiomycetes, *Phellinus* s.l. *Mycologia* 96(4): 799–811.
- Fischer M., Edwards J., Cunnington J.H., Pascoe I.G., 2005. Basidiomycetous pathogens on grapevine: a new species from Australia - *Fomitiporia australiensis*. *Mycotaxon* 91: 85–96.

- Fischer M., 2006. Biodiversity and geographic distribution of basidiomycetes causing esca-associated white rot in grapevine: A worldwide perspective. *Phytopathologia Mediterranea* 45(4): 30–42.
- Fischer M., 2009. Nischengebundene Sippenbildung bei Holz bewohnenden Pilzen – experimentelle Befunde. In: *Bayer. Akademie der Wissenschaften (Hrsg.): Ökologische Rolle von Pilzen. Rundgespräche der Kommission für Ökologie*, 37. Pfeil, München, Germany, 53–62.
- Fischer M., 2012. Ein Basidiomycet als Neubürger: Vorkommen und Ausbreitung von *Fomitiporia mediterranea* (Hymenochaetales) in den badischen Weinbaugebieten, mit Hinweisen zum Vorkommen in Deutschland. *Andrias* 19: 229–236.
- Fischer M., González-García V., 2015. An annotated checklist of European basidiomycetes related to white rot of grapevine (*Vitis vinifera*). *Phytopathologia Mediterranea* 54(2): 281–298.
- Fischer M., Peighami-Ashnaei S., 2019. Grapevine, esca complex, and environment: The disease triangle. *Phytopathologia Mediterranea* 58(1): 17–37.
- Fischer M., 2019. Grapevine trunk diseases in German viticulture. III. Biodiversity and spatial distribution of fungal pathogens in rootstock mother plants and possible relation to leaf symptoms. *Vitis: Journal of Grapevine Research* 58(4): 141–149.
- Floudas D., Binder M., Riley R., Barry K., Blanchette R.A., ... Hibbett D.S., 2012. The Paleozoic origin of enzymatic lignin decomposition reconstructed from 31 fungal genomes. *Science* 336: 1715–1719.
- Fontaine F., Gramaje D., Armengol J., Smart R., Nagy Z.A., ... Corio-Costet, M.F., 2016a. *Grapevine trunk diseases: a review*. 1st ed. OIV Publications, Paris, France, 24p.
- Fontaine F., Pinto C., Vallet J., Clément C., Gomes A.C., Spagnolo A., 2016b. The effects of grapevine trunk diseases (GTDs) on vine physiology. *European Journal of Plant Pathology* 144(4): 707–721.
- Fussler L., Kobes N., Bertrand F., Maumy M., Grosman J., Savary S., 2008. A characterization of grapevine trunk diseases in France from data generated by the National Grapevine Wood Diseases Survey. *Phytopathology* 98(5): 571–579.
- García Benavides P., Martín Zamorano P., Ocete Pérez C.A., Maistrello L., Ocete Rubio R., 2013. Biodiversity of pathogenic wood fungi isolated from *Xylotrechus arvicola* (Olivier) galleries in vine shoots. *Journal International des Sciences de la Vigne et du Vin* 47: 73–81.
- Gard M., 1922. L'Apoplexie de la Vigne et les formes résupinées du *Fomes igniarius* (L.) Fries. *Bulletin de la Société de pathologie végétale de France IX* (1) (séances de Janvier) 22–28.
- Gatica M., Césari C., Escoriza G., 2004. *Phellinus* species inducing hoja de malvón symptoms on leaves and wood decay in mature field-grown grapevines. *Phytopathologia Mediterranea* 43: 59–65.
- Gellon M., Fuchs J., Farine S., Mazet F., Laloue H., ... Bertsch C., 2017. A new mode of treatment to cure GTDs: vegetal endotherapy? *Phytopathologia Mediterranea* 56(3): 572–573 (Abstract).
- Girometta C.E., Bernicchia A., Baiguera R.M., Bracco, F., Buratti S., ... Savino E., 2020. An Italian research culture collection of wood decay fungi. *Diversity* 12(2): 58.
- Goddard M.L., Boos A., Larignon P., Fontaine F., Bertsch C., Tarnus C., 2017. Arsenite experiments in the program CASDAR V1301 - Arsenic speciation in grapevines and impact on fungal population. *Phytopathologia Mediterranea* 56(3): 573–574 (Abstract).
- Goodell B., Jellison J., Liu J., Daniel G., Paszczynski A., ... Xu G., 1997. Low molecular weight chelators and phenolic compounds isolated from wood decay fungi and their role in the fungal biodegradation of wood. *Journal of Biotechnology* 53: 133–162.
- Goodell B., 2020. Fungi Involved in the Biodeterioration and Bioconversion of Lignocellulose Substrates. In: *The Mycota (A Comprehensive Treatise on Fungi as Experimental Systems for Basic and Applied Research) vol 2. Genetics and Biotechnology* (Benz J.P., Schipper K., eds.), Springer, Cham, Switzerland, 369–397.
- Goufo P., Marques A. C., Cortez I., 2019. Exhibition of local but not systemic induced phenolic defenses in *Vitis vinifera* L. affected by brown wood streaking, grapevine leaf stripe, and apoplexy (esca complex). *Plants* 8(10): 412.
- Gramaje D., Armengol J., 2011. Fungal trunk pathogens in the grapevine propagation process: potential inoculum sources, detection, identification, and management strategies. *Plant Disease* 95(9): 1040–1055.
- Gramaje D., Mostert L., Groenewald J.Z., Crous P.W., 2015. *Phaeoacremonium*: From esca disease to phaeohyphomycosis. *Fungal Biology* 119(9): 759–783.
- Gramaje D., Urbez-Torres J.R., Sosnowski M.R., 2018. Managing grapevine trunk diseases with respect to etiology and epidemiology: Current strategies and future prospects. *Plant Disease* 102(1): 12–39.
- Graniti A., Surico G., Mugnai L., 1999. Considerazioni sul mal dell'esca e sulle venature brune del legno della vite. *Informatore Fitopatologico* 49(5): 6–12.
- Grigoriev I.V., Cullen D., Goodwin S.B., Hibbett D., Jeffries, ... Baker S.E., 2011. Fueling the future with fungal genomics. *Mycology* 2(3): 192–209.

- Grigorie I.V., Nikitin R., Haridas S., Kuo A., Ohm R., ... Shabalov I., 2014. MycoCosm portal: gearing up for 1000 fungal genomes. *Nucleic Acids Research* 42(D1): D699–D704.
- Grosman J., 2008. Observatoire national des maladies du bois: bilan de 4 années d'observations. In: *Euroviti - Colloque viticole et œnologique*, Angers, France, 8–17.
- Grosman J., Doublet B., 2012. Maladies du bois de la vigne. Synthèse des dispositifs d'observation au vignoble, de l'observatoire 2003–2008 au réseau d'épidémiologie-surveillance actuel. *Phytoma* 651: 31–35.
- Guan X., Essakhi S., Laloue H., Nick P., Bertsch C., Chong J., 2016. Mining new resources for grape resistance against Botryosphaeriaceae: A focus on *Vitis vinifera* subsp. *sylvestris*. *Plant Pathology* 65(2): 273–284.
- Guérin-Dubrana L., Labenne A., Labrousse J.C., Bastien S., Rey P., Gegout-Petit A., 2013. Statistical analysis of grapevine mortality associated with esca or eutypa dieback foliar expression. *Phytopathologia Mediterranea* 52: 276–288.
- Guérin-Dubrana L., Fontaine F., Mugnai L., 2019. Grapevine trunk disease in European and Mediterranean vineyards: occurrence, distribution and associated disease-affecting cultural factors. *Phytopathologia Mediterranea* 58(1): 49–71.
- Haidar R., Roudet J., Bonnard O., Dufour M.C., Corio-Costet M.F., ... Fermaud M., 2016. Screening and modes of action of antagonistic bacteria to control the fungal pathogen *Phaeoconiella chlamydospora* involved in grapevine trunk diseases. *Microbiological Research* 192: 172–184.
- Haidar R., Yacoub A., Vallance J., Compant S., Antonielli L., ... Rey P., 2021. Bacteria associated with wood tissues of Esca-diseased grapevines: functional diversity and synergy with *Fomitiporia mediterranea* to degrade wood components. *Environmental Microbiology*. doi: 10.1111/1462-2920.15676
- Halbwachs H., Simmel J., Bassler C., 2016. Tales and mysteries of fungal fruiting: How morphological and physiological traits affect a pileate lifestyle. *Fungal Biology Review* 30(2): 36–61.
- Halleen F., Crous P.W., Petrini O., 2003. Fungi associated with healthy grapevine cuttings in nurseries, with special reference to pathogens involved in the decline of young vines. *Australasian Plant Pathology* 32: 47–52.
- Hofman M.T., Arnold A.E., 2008. Geographic locality and host identity shape fungal endophyte communities in cupressaceous trees. *Mycological Research* 112: 331–344.
- Hofstetter V., Buyck B., Croll D., Viret O., Couloux A., Gindro K., 2012. What if esca disease of grapevine were not a fungal disease? *Fungal Diversity* 54: 51–67.
- Hyde K.D., Xu J., Rapior S., Jeewon R., Lumyong S., ... Stadler M., 2019. The amazing potential of fungi: 50 ways we can exploit fungi industrially. *Fungal Diversity* 97: 1–136.
- Jamaux-Despréaux I., Péros J.P., 2003. Genetic structure in populations of the fungus *Fomitiporia punctata* associated with esca syndrome in grapevine. *Vitis* 42(1): 43–51.
- James T.Y., Srivilai P., Kües U., Vilgalys R., 2006. Evolution of the bipolar mating system of the mushroom *Coprinellus disseminatus* from its tetrapolar ancestors involves loss of mating type-specific pheromone receptor function. *Genetics* 172: 1877–1891.
- James T.Y., Sun S., Li W.J., Heitman J., Kuo H.C., ... Olson A., 2013. Polyporales genomes reveal the genetic architecture underlying tetrapolar and bipolar mating systems. *Mycologia* 105: 1374–1390.
- John S., Wicks, T.J., Hunt J.S., Lorimer M.F., Oakey H., Scott E.S., 2005. Protection of grapevine pruning wounds from infection by *Eutypa lata*. *Australasian Plant Pathology* 34: 569–575.
- Karimi M.R., Mahmoodi B., Kazemiyani M., 2001. First report of esca of grapevine in Iran. *Phytopathologia Mediterranea* 40: S481 (Abstract).
- Kuan I.-C., Tien M., 1993. Stimulation of Mn peroxidase activity: a possible role for oxalate in lignin biodegradation. *PNAS - Proceedings of the National Academy of Sciences of the United States of America* 90(4): 1242–1246.
- Kües U., 2013. Mating type genes as master regulators of mushroom development. In: *Proceedings of the 7th International Medicinal Mushroom Conference* (Chinese Academy of Engineering, China Chamber of Commerce of Foodstuffs and Native Products, ed.), Jiangsu Alphay Biological Technology Co., Nantong City, China, 33–59.
- Kües U., 2015. From two to many: Multiple mating types in Basidiomycetes. *Fungal Biology Reviews* 29 (3-4): 126–166.
- Kuntzmann P., Villaume S., Larignon P., Bertsch C., 2010. Esca, BDA and Eutypiosis: Foliar symptoms, trunk lesions and fungi observed in diseased vinestocks in two vineyards in Alsace. *Vitis - Journal of Grapevine Research* 49(2): 71–76.
- Kraus C., Vögele R., Fischer M., 2019. The Esca complex in German vineyards: does the training system influence occurrence of GLSD symptoms? *European Journal of Plant Pathology* 155: 265–279.
- Lafon R., 1921. *Modifications à apporter à la taille de la vigne des Charentes, taille Guyot-Poussart mixte et double: l'apoplexie, traitement préventif (méthode Poussard), traitement curatif*. Imp. Roumégous et Déhan, Montpellier, France, 96 pp.

- Larignon P., Dubos B., 1997. Fungi associated with Esca disease in grapevine. *European Journal of Plant Pathology* 103: 147–157.
- Larignon P., Dubos B., 2000. Preliminary studies on the biology of *Phaeoacremonium*. *Phytopathologia Mediterranea* 39: 184–189.
- Larignon P., Giansetto K., Salancon E., Girardon K., Berud F., ... Coarer M., 2008a. Champignons associés aux maladies du bois: une enquête en pépinières. *Rhône en VO - Revue de Viticulture et d'Oenologie de la Vallée du Rhône* 3: 26–31.
- Larignon P., Darne G., Menard E., Desache F., Dubos B., 2008b. Comment agissait l'arsénite de sodium sur l'esca de la vigne? *Progrès Agricole et Viticole* 125: 642–651.
- Laveau C., Letouze A., Louvet G., Bastien S., Guérin-Dubrana L., 2009. Differential aggressiveness of fungi implicated in esca and associated diseases of grapevine in France. *Phytopathologia Mediterranea*, 48(1): 32–46.
- Lecomte P., Darrieutort G., Liminana J.-M., Comont G., Muruamendiariáz A, ... Fermaud, M. 2012. New insights into esca of grapevine: the development of foliar symptoms and their association with xylem discoloration. *Plant Disease* 96: 924–934.
- Lecomte P., Diarra B., Carbonneau A., Rey P., Chevrier C., 2018. Esca of grapevine and training practices in France: results of a 10-year survey. *Phytopathologia Mediterranea* 57: 472–487.
- Letousey P., Bailleul F., Perrot G., Rabenoelina F., Boulay M., ... Fontaine F., 2010. Early events prior to visual symptoms in the apoplectic form of grapevine esca disease. *Phytopathology* 100: 424–431.
- Levasseur A., Drula E., Lombard V., Coutinho P.M., Henrissat B., 2013. Expansion of the enzymatic repertoire of the CAZy database to integrate auxiliary redox enzymes. *Biotechnology for Biofuels* 6(1): 41.
- Li S., Bonneau F., Chadoeuf J., Picart D., Gégout-Petit A., Guérin-Dubrana L., 2017. Spatial and temporal pattern analyses of esca grapevine disease in vineyards in France. *Phytopathology* 107(1): 59–69.
- Liaud N., Giniés C., Navarro D., Fabre N., Crapart S., Sigoilloit J.C., 2014. Exploring fungal biodiversity: organic acid production by 66 strains of filamentous fungi. *Fungal Biology and Biotechnology* 1(1): 1.
- Lombard V., Golaconda Ramulu H., Drula E., Coutinho P.M., Henrissat B., 2014. The Carbohydrate-active enzymes database (CAZy) in 2013. *Nucleic Acids Research* 42: D490–D495.
- Lorrain B., Ky I., Pasquier G., Jourdes M., Dubrana L.G., Gény L., ... Teissedre P.L., 2012. Effect of Esca disease on the phenolic and sensory attributes of Cabernet Sauvignon grapes, musts and wines. *Australian Journal of Grape and Wine Research* 18: 64–72.
- Lundell T.K., Mäkelä M.R., de Vries R.P., Hildén K.S., 2014. Chapter Eleven - Genomics, lifestyles and future prospects of wood-decay and litter-decomposing Basidiomycota. In: *Advances in Botanical Research*, (Francis M. Martin, ed.), Academic Press, 70, 329–370.
- Luque J., Martos S., Aroca A., Raposo R., Garcia-Figueroes F., 2009. Symptoms and fungi associated with declining mature grapevine plants in northeast Spain. *Journal of Plant Pathology* 91(2): 381–390.
- Magarey P. A., Carter M.V., 1986. New technology facilitates control of *Eutypa dieback* in apricots and grapevines. *Plant Protection Quarterly* 1: 156–159
- Maher N., Piot J., Bastien S., Vallance J., Rey P., Guérin-Dubrana, L., 2012. Wood necrosis in ESCA-affected vines: Types, relationships and possible links with foliar symptom expression. *Journal International Des Sciences de La Vigne et Du Vin* 46(1): 15–27.
- Marchi G., 2001. Susceptibility to esca of various grapevine (*Vitis vinifera*) cultivars grafted on different rootstocks in a vineyard in the province of Siena (Italy). *Phytopathologia Mediterranea* 40(1): 27–36.
- Marchi G., Peduto F., Mugnai L., Di Marco S., Calzarano F., Surico G., 2006. Some observations on the relationship of manifest and hidden esca to rainfall. *Phytopathologia Mediterranea* 45: 117–126.
- Markakis A.M., Kavroulakis N., Ntougias S., Koubouris G.C., Sergentani C.K., Ligoixigakis E.K., 2017. Characterization of fungi associated with wood decay of tree species and grapevine in Greece. *Plant Disease* (101): 1929–1940.
- Markakis E.A., Ligoixigakis E.K., Roussos, P.A., Sergentani C.K., Kavroulakis N., ... Koubouris, G.C., 2019. Differential susceptibility responses of Greek olive cultivars to *Fomitiporia mediterranea*. *European Journal of Plant Pathology* 153: 1055–1066.
- Martin M.T., Cobos R., 2007. Identification of fungi associated with grapevine decline in Castilla y Leon (Spain). *Phytopathologia Mediterranea* 46: 18–25.
- Masi M., Cimmino A., Revegilia P., Mugnai L., Surico G., Evidente A., 2018. Advances on fungal phytotoxins and their role in grapevine trunk diseases. *Journal of Agricultural and Food Chemistry* 66(24): 5948–5958.
- Mazzullo A., Di Marco S., Osti F., Cesari A., 2000. Bioassays on the activity of resveratrol, pterostilbene and phosphorous acid towards fungi associated with esca of grapevine. *Phytopathologia Mediterranea* 39(3): 357–365.
- Mirabolfathy M., Hosseinian L., Peighami Ashnaei S., 2021. Fungal communities of grapevine decline

- in the main grapegrowing regions of Iran. *Indian Phytopathology* 1-7.
- Mirsoleymani Z., Mostowfizadeh Ghalamfarsa R., 2019. *Fomitiporia mediterranea*, a new basidiomycete species for mycobiota of Iran. *Rostaniha* 19: 189–191.
- Mohammadi H., Banihashemi Z., Gramaje D., Armengol J., 2013. Fungal pathogens associated with grapevine trunk diseases in Iran. *Journal of Agriculture, Science and Technology* 15:137–150.
- Mondello V., Larignon P., Armengol J., Kortekamp A., Vaczy K., ... Fontaine F., 2018a. Management of grapevine trunk diseases: knowledge transfer, current strategies and innovative strategies adopted in Europe. *Phytopathologia Mediterranea* 57 (3): 369–383.
- Mondello V., Songy A., Battiston E., Pinto C., Coppin C., ... Fontaine F., 2018b. Grapevine trunk diseases: A review of fifteen years of trials for their control with chemicals and biocontrol agents. *Plant Disease* 102(7): 1189–1217.
- Montanari E., 2010. Per una storia linguistica di Esca. In: *Il mal dell'esca della vite* (G. Surico, L. Mugnai, ed.), ARSIA Regione Toscana, Firenze, Italy, 26-34.
- Morel M., Meux E., Mathieu Y., Thuillier A., Chibani K., ... Gelhaye, E., 2013. Xenomic networks variability and adaptation traits in wood decaying fungi: Fungal xenomic networks. *Microbial Biotechnology* 6: 248–263.
- Moret F., Lemaître-Guillier C., Grosjean C., Clément G., Coelho C., ... Adrian M., 2019. Clone-dependent expression of esca disease revealed by leaf metabolite analysis. *Frontiers in Plant Science* 9: 1960.
- Moret F., Delorme G., Clément G., Grosjean C., Lemaître-Guillier C., ... Fontaine F., 2021. Esca-affected grapevine leaf metabolome is clone- and vintage-dependent. *Physiologia Plantarum* 171: 424–434.
- Moretti S., Pierron R., Pacetti A., Gellon M., Tarnus C., ... Farine S. 2019. Non-Enzymatic *in lignum* degradation mechanism: a way to control Grapevine Trunk Disease? *Phytopathologia Mediterranea* 58(2): 414–415 (Abstract).
- Morgenstern I., Robertson D.L., Hibbett D.S., 2010. Characterization of three mnp genes of *Fomitiporia mediterranea* and report of additional class ii peroxidases in the order Hymenochaetales. *Applied and Environmental Microbiology* 76(19): 6431–6440.
- Mostert L., Halleen F., Fourie P., Crous P.W., 2006. A review of *Phaeoacremonium* species involved in Petri disease and esca of grapevines. *Phytopathologia Mediterranea* 45: S12–S29.
- Mugnai L., Bertelli E., Surico G., Bruno E., 1997. Effetto di alcune sostanze fenoliche sulla crescita di funghi del legno di viti colpite dal “mal dell'esca”. *Petria* 7: 35–46.
- Mugnai L., Graniti A., Surico G., 1999. Esca (black measles) and brown wood-streaking: two old and elusive diseases of grapevines. *Plant Disease* 83(5): 404–418.
- Mugnai L., Guiggiani M., Bazzo F., Marchi G., Surico G., 2010. Il mal dell'esca e la carie bianca del legno: agenti causali, sintomatologia e casi studio di esca giovane. In: *Il mal dell'esca della vite* (G. Surico, L. Mugnai, ed.), ARSIA Regione Toscana, Firenze, Italy, 65–88.
- Murolo S., Romanazzi G., 2014. Effects of grapevine cultivar, rootstock and clone on esca disease. *Australasian Plant Pathology* 43: 215–221.
- Nascimento T., Rego C., Oliveira H., 2007. Potential use of chitosan in the control of grapevine trunk diseases. *Phytopathologia Mediterranea* 46: 218–224.
- Niem J.M., Billones-Baaijens R., Stodart B., Savocchia S., 2020. Diversity profiling of grapevine microbial endosphere and antagonistic potential of endophytic *Pseudomonas* against grapevine trunk diseases. *Frontiers in Microbiology* 11: 477.
- Olmo D., Gramaje D., Armengol J., 2017. Hongos asociados a las enfermedades de la madera del almendro en la Isla de Mallorca. *Revista de Fruticultura* 54: 18–29.
- Osti F., Di Marco S., 2010. Iron-dependent, non-enzymatic processes promoted by *Phaeoconiella chlamydospora* and *Phaeoacremonium aleophilum*, agents of esca in grapevine. *Physiological and Molecular Plant Pathology* 74(5–6): 309–316.
- Ouadi L., Bruez E., Bastien S., Vallance J., Lecomte P., ... Rey P., 2019. Ecophysiological impacts of Esca, a devastating grapevine trunk disease, on *Vitis vinifera* L. *PLoS ONE* 14(9): e0222586.
- Pacetti A., Pierron R., Farine S., Mugnai L., Tarnus C., ... Gellon M., 2019. Vertical vegetal endotherapy: a new mode of treatment to cure grapevine trunk diseases? *Phytopathologia Mediterranea* 58(2): 426 (Abstract).
- Pacetti A., Moretti S., Pinto C., Compant S., Farine S., ... Mugnai L., 2021. Trunk surgery as a tool to reduce foliar symptoms in diseases of the esca complex and its influence on vine wood microbiota. *Journal of Fungi* 7: 521.
- Paplomatas E.J., Elena K., Tsopelas P., Tzima A., Paraskevopoulos A., Papanikolaou A., 2006. Infection of olive trees with the fungus *Fomitiporia punctata* (*Phellinus punctatus*). *Phytopathologia Mediterranea* 45(1): 69 (Abstract).
- Pérez J., Muñoz-Dorado J., de la Rubia T., Martínez J., 2002. Biodegradation and biological treatments of cellulose, hemicellulose and lignin: an overview. *International Microbiology* 5: 53–63.
- Péros J.-P., Berger G., Jamaux-Despréaux I., 2008. Symptoms, wood lesions and fungi associated with Esca in organic vineyards in Languedoc-Roussillon (France). *Journal of Phytopathology* 156: 297–303.

- Pilotti M., Gervasi F., Brunetti A., 2005. Molecular identification of *Fomitiporia mediterranea* and *Eutypa lata*/*Libertella blepharis* in *Platanus acerifolia*. *Journal of Phytopathology* 153: 193–202.
- Pilotti M., Tizzani L., Brunetti A., Gervasi F., Di Lernia G., Lumia V., 2010. Molecular identification of *Fomitiporia mediterranea* on declining and decayed hazelnut. *Journal of Plant Pathology* 92(1): 115–129.
- Polemis E., Dimou D.M., Fryssouli V., Zervakis G.I., 2019. Diversity of saproxylic basidiomycetes in *Quercus ilex* woodlands of central and insular Greece. *Plant Biosystem* 153: 385–397
- Pollastro S., Dongiovanni C., Abbatecola A., Faretra F., 2000. Observations on the fungi associated with esca and on spatial distribution of esca-symptomatic plants in Apulian (Italy) vineyards. *Phytopathologia Mediterranea* 39(1): 206–210.
- Pollastro S., Dongiovanni C., Abbatecola A., De Guido, M.A., De Miccolis Angelini R. M., Faretra F., 2001. Specific SCAR primer for fungi associated with wood decay of grapevine. *Phytopathologia Mediterranea* 40: S362–S368.
- Pouzoulet J., Pivovarov A.L., Santiago L.S., Rolshausen P.E., 2014. Can vessel dimension explain tolerance toward fungal vascular wilt diseases in woody plants? Lessons from Dutch elm disease and esca disease in grapevine. *Frontiers in Plant Science* 5: 253.
- Pouzoulet J., Scudiero E., Schiavon M., Rolshausen P.E., 2017. Xylem vessel diameter affects the compartmentalization of the vascular pathogen *Phaeoemoniella chlamydospora* in grapevine. *Frontiers in Plant Science* 8: 1442.
- Pouzoulet J., Scudiero E., Schiavon M., Santiago L.S., Rolshausen P.E., 2019. Modeling of xylem vessel occlusion in grapevine. *Tree Physiology* 39: 1438–1445.
- Quaglia M., Covarelli L., Zizzerini A., 2009. Epidemiological survey on esca disease in Umbria, central Italy. *Phytopathologia Mediterranea* 48: 84–91.
- Rábai A., Dula T., Mugnai L., 2008. Distribution of esca disease in Hungary and the pathogens causing the syndrome. *Acta Phytopathologica et Entomologica Hungarica* 43(1): 45–54.
- Rajaiyan M., Karimi Shahri M.R., Pirnia M., Dehvari V., Ghezeli Sefloo N., 2013. Detection and identification of some fungal agents causing grapevine decline in Northern Khorasan province vineyards using PCR technique. *Applied Entomology and Phytopathology* 81: 167–177.
- Ramsdell D. C., 1995. Winter air-blast sprayer application of benomyl for reduction of *Eutypa* dieback disease incidence in a concord grape vineyard in Michigan. *Plant Disease* 79: 399–402.
- Ravaz L., 1909. Sur l'apoplexie de la vigne. *Progrès Agricole et Viticole* 30: 547–579.
- Ravaz L., 1919. Encore l'apoplexie de la vigne. *Progrès Agricole et Viticole* 52: 601–603.
- Reisenzein H., Berger N., Nieder G., 2000. Esca in Austria. *Phytopathologia Mediterranea* 39: 26–34.
- Riley R., Salamov A.A., Brown D.W., Nagy L.G., Floudas D., ... Grigoriev I.V., 2014. Extensive sampling of basidiomycete genomes demonstrates inadequacy of the white-rot/brown-rot paradigm for wood decay fungi. *PNAS - Proceedings of the National Academy of Sciences of the United States of America* 111 (27): 9923–9928.
- Rocchetti A., Schena L., Sanzani S.M., Cacciola S.O., Mosca S., ... di San Lio G.M., 2014. Characterization of Basidiomycetes associated with wood rot of citrus in southern Italy. *Phytopathology* 104: 851–858.
- Rolshausen P.E., Greve L.C., Labavitch J.M., Mahoney N.E., Molyneux R.J., Gubler W.D., 2008. Pathogenesis of *Eutypa lata* in grapevine: identification of virulence factors and biochemical characterization of cordon dieback. *Phytopathology* 98: 222–229.
- Romanazzi G., Murolo S., Pizzichini L., Nardi S., 2009. Esca in young and mature vineyards, and molecular diagnosis of the associated fungi. *European Journal of Plant Pathology* 125(2): 277–290.
- Rubio J.J., Garzón E., 2011. Las enfermedades de madera de vid como amenaza del sector vitícola. *Revista Winetech* 2 (Noviembre): 18–21.
- Rui D., Battel C., 1963. Mise au point d'un nouveau moyen de lutte contre l'esca de la vigne. *Notiziario sulle malattie delle piante* 63: 9–18.
- Rumbos A., Rumbou I., 2001. Fungi associated with esca and young grapevine decline in Greece. *Phytopathologia Mediterranea* 40 (3): 330–335.
- Rusjan D., Persic M., Likar M., Biniari K., Mikulic-Petkovsek M., 2017. Phenolic responses to esca-associated fungi in differently decayed grapevine woods from different trunk parts of "Cabernet Sauvignon." *Journal of Agricultural and Food Chemistry* 65(31): 6615–6624.
- Sánchez-Torres P., Hinarejos R., González V., Tuset J.J., 2008. Identification and characterization of fungi associated with esca in vineyards of the Comunidad Valenciana (Spain). *Spanish Journal of Agricultural Research* 6(4): 650–660.
- Schilling M., Farine S., Péros J.P., Bertsch C., Gelhay E., 2021. Wood degradation in grapevine diseases. In: *Advances in Botanical Research*, (Mélanie Morel-Rouhier, Rodnay Sormani, eds.), Academic Press, 99, 175–207.
- Schmidt O., Gaiser O., Dujesiefken D., 2012. Molecular identification of decay fungi in the wood of urban

- trees. *European Journal of Forest Research* 131: 885–891.
- Shimada M., Ma D.-B., Akamatsu Y., Hattori T., 1994. A proposed role of oxalic acid in wood decay systems of wood-rotting basidiomycetes. *FEMS Microbiology Reviews* 13(2-3): 285–295.
- Siebert J.B., 2001. Eutypa: The economic toll on vineyards. *Wines & Vines* (April): 50–56.
- Singh Arora D., Kumar Sharma, R., 2010. Ligninolytic fungal laccases and their biotechnological applications. *Applied Biochemistry and Biotechnology* 160: 1760–1788.
- Sista Kameshwar A.K., Qin W., 2020. Systematic meta-data analysis of brown rot fungi gene expression data reveals the genes involved in Fenton's reaction and wood decay process. *Mycology* 11: 22–37.
- Sofia J., Goncalves M.T., Oliveira H., 2006. Spatial distribution of esca symptomatic plants in Dão vineyards (centre Portugal) and isolation of associated fungi. *Phytopathologia Mediterranea* 45: 87–92.
- Songy A., Fernandez O., Clément C., Larignon P., Fontaine F., 2019a. Grapevine trunk diseases under thermal and water stresses. *Planta* 249(6): 1655–1679.
- Songy A., Vallet J., Gantet M., Boo A., Ronot P., ... Fontaine F., 2019b. Sodium arsenite effect on *Vitis vinifera* L. Physiology. *Journal of Plant Physiology* 238: 72–79.
- Sparapano L., Bruno G., Graniti A., 1998. Esopolisaccaridi fitotossici sono prodotti in coltura da due specie di *Phaeoacremonium* associate al complesso del 'mal dell'esca' della vite. *Petria* 8: 210–212.
- Sparapano L., Bruno G., Ciccarone C., Graniti A., 2000a. Infection of grapevines by some fungi associated with esca. I. *Fomitiporia punctata* as a wood-rot inducer. *Phytopathologia Mediterranea* 39(1): 46–52.
- Sparapano L., Bruno G., Ciccarone C., Graniti A., 2000b. Infection of grapevines by some fungi associated with esca. II. Interaction among *Phaeoacremonium chlamydosporum*, *P. aleophilum* and *Fomitiporia punctata*. *Phytopathologia Mediterranea* 39: 53–58.
- Sparapano L., Bruno G., Graniti A., 2000c. Effects on plants of metabolites produced in culture by *Phaeoacremonium chlamydosporum*, *P. aleophilum* and *Fomitiporia punctata*. *Phytopathologia Mediterranea* 39: 169–177.
- Sparapano L., Bruno G., Graniti A., 2001a. Three year observation of grapevines cross-inoculated with esca-associated fungi. *Phytopathologia Mediterranea* 40: S376–S386.
- Sparapano L., Bruno G., Campanella A., 2001b. Interactions between three fungi associated with esca of grapevine, and their secondary metabolites. *Phytopathologia Mediterranea* 40(3): 417–422.
- Spiteller P., 2008. Chemical defence strategies of higher fungi. *Chemistry* 14(30): 9100–9110.
- Spiteller P., 2015. Chemical ecology of fungi. *Natural Product Reports* 32: 971–993.
- Surico G., Marchi G., Ferrandino F.J., Braccini P., Mugnai L., 2000. Analysis of the spatial spread of esca in some tuscan vineyards (Italy). *Phytopathologia Mediterranea* 39: 211–224.
- Surico G., Mugnai L., Marchi G., 2006. Older and more recent observations on esca: A critical overview. *Phytopathologia Mediterranea* 45(S1): 68–86.
- Surico G., 2009. Towards a redefinition of the diseases within the esca complex of grapevine. *Phytopathologia Mediterranea* 48: 5–10.
- Svampa G., Tosatti E.M., 1977. Prove di lotta contro il "mal dell'esca" della vite. *Informatore Fitopatologico* 12: 21–24
- Svedružić D., Jónsson S., Toyota C.G., Reinhardt L.A., Ricagno S., ... Richards N.G., 2005. The enzymes of oxalate metabolism: unexpected structures and mechanisms. *Archives of Biochemistry and Biophysics* 433(1): 176–92.
- Tabacchi R., Fkyerat A., Poliar, C., Dubin G. M., 2000. Phytotoxins from fungi of esca of grapevine. *Phytopathologia Mediterranea* 39(1): 156–161.
- Tanaka N., Akamatsu Y., Hattori T., Shimada M. 1994. Effect of oxalic acid on the oxidative breakdown of cellulose by the Fenton reaction. *Wood Research: Bulletin of the Wood Research Institute Kyoto University* 81: 8–10.
- Tauber J.P., Matthäus C., Lenz C., Hoffmeister D., Popp J., 2018. Analysis of basidiomycete pigments *in situ* by Raman spectroscopy. *Journal of Biophotonics* 11(6): e201700369.
- Thibault M., 2015. Le curetage. In: *Les maladies du Bois de la Vigne - Réunion du groupe national Maladies du Bois de la Vigne*, 17–18/11/2015, Université de Haute-Alsace, Colmar, France, 55–57.
- Úrbez-Torres J.R., Haag P., Bowen P., O'Gorman D.T., 2014. Grapevine trunk diseases in British Columbia: incidence and characterization of the fungal pathogens associated with esca and petri diseases of grapevine. *Plant Disease* 98: 469–482.
- Urzúa U., Kersten P.J., Vicuña R., 1998. Manganese peroxidase-dependent oxidation of glyoxylic and oxalic acids synthesized by *Ceriporiopsis subvermisporea* produces extracellular hydrogen peroxide. *Applied and Environmental Microbiology Journal* 64(1): 68–73.
- Valtaud C., Larignon P., Roblin G., Fleurat-Lessard P., 2009. Developmental and ultrastructural features of *Phaeoconiella chlamydospora* and *Phaeoacremonium aleophilum* in relation to xylem degradation in esca

- disease of the grapevine. *Journal of Plant Pathology* 91: 37–51.
- Vasquez S.J., Gubler W.D., Leavitt G.M., 2007. Economic loss in California's table grape vineyards due to measles. *Phytopathologia Mediterranea* 46: 118 (Abstract).
- Větrovský T., Kohout P., Kopecký M., Machac A., Man M., ... Baldrian P., 2019. A meta-analysis of global fungal distribution reveals climate-driven patterns. *Nature Communication* 10: 5142.
- Viala P., 1926. Recherches sur les maladies de la vigne. Esca. *Annales des Epiphyties* 12: 5–108.
- Vicent A., García-Figueroles F., García-Jiménez J., Armengol J., Torné L., 2001. Fungi associated with esca and grapevine declines in Spain: a three-year survey. *Phytopathologia Mediterranea* 40: 325–329.
- Vinet E., 1909. L'apoplexie de la vigne en Anjou. *Revue de Viticulture* 32: 676–681.
- Wagner T., Fischer M., 2001. Natural groups and a revised system for the European poroid Hymenochaetales (Basidiomycota) supported by nLSU rDNA sequence data. *Mycological Research* 105: 773–782.
- Wagner T., Fischer M., 2002. Proceedings towards a natural classification of the worldwide taxa *Phellinus* s.l. and *Inonotus* s.l., and phylogenetic relationships of allied genera. *Mycologia* 94 (6): 998–1016.
- White T.J., Bruns T.D., Lee S., Taylor J.W., 1990. Amplification and direct sequencing of fungal ribosomal RNA genes for phylogenetics. In: *PCR protocols* (Innis M.A., Gelfand D.H., Sninsky J.J., White T.J., ed.), Academic Press, San Diego, USA, 315–322.
- White C.L., Halleen F., Fischer M., Mostert L., 2011. Characterisation of the fungi associated with esca diseased grapevines in South Africa. *Phytopathologia Mediterranea* 50: 204–223.
- Wicks T., Davies K., 1999. The effect of *Eutypa* on grapevine yield. *The Australian and New Zealand Grape-grower & Winemaker* 426a:15–16.
- Ye Q., Jia J., Manawasinghe I.S., Li X., Zhang W., ... Yan J., 2021. *Fomitiporia punicata* and *Phaeoacremonium minimum* associated with Esca complex of grapevine in China. *Phytopathology Research* 3: 11.
- Zanzotto A., Autiero F., Bellotto D., Dal Cortivo G., Lucchetta G., Borgo M., 2007. Occurrence of *Phaeoacremonium* spp. and *Phaeomoniella chlamydospora* in grape propagation materials and young grapevines. *European Journal of Plant Pathology* 119: 183–192
- Zhuang L., Guo W., Yoshida M., Feng X., Goodell B., 2015. Investigating oxalate biosynthesis in the wood-decaying fungus *Gloeophyllum trabeum* using ¹³C metabolic flux analysis. *RSC Advances* 5(126): 104043–104047.



Citation: Author (2021) Title. *Phytopathologia Mediterranea* 60(2): 381-385. doi: 10.36253/phyto-12805

Accepted: May 12, 2021

Published: September 13, 2021

Copyright: ©2021 Author. This is an open access, peer-reviewed article published by Firenze University Press (<http://www.fupress.com/pm>) and distributed under the terms of the Creative Commons Attribution License, which permits unrestricted use, distribution, and reproduction in any medium, provided the original author and source are credited.

Data Availability Statement: All relevant data are within the paper and its Supporting Information files.

Competing Interests: The Author(s) declare(s) no conflict of interest.

Editor: Josep Armengol Forti, Polytechnical University of Valencia, Spain.

Research Papers

Adult plant resistance to white rust in *Lunaria annua*

DIANA CERVANTES¹, MARY RIDOUT¹, CLAUDIA NISCHWITZ², GEORGE NEWCOMBE^{1,*}

¹ College of Natural Resources, University of Idaho, Moscow ID, USA

² Department of Biology, Utah State University, Logan, UT 84322, USA

*Corresponding author. E-mail: georgen@uidaho.edu

Summary. Wild plants produce abundant seeds and seedlings, but most die before reaching maturity, and these premature deaths are often caused by pathogens. Major genes for resistance protect some seedlings or juveniles. These selected individuals can become a resistant, mature cohort. Alternatively, plants can exhibit mature, adult plant resistance. These two explanations can be indistinguishable in the field, when epidemics in natural pathosystems occur regularly resulting in annual selection for resistance. This study included multi-year observations of a biennial plant where the distinction could be made. White rust of *Lunaria annua*, a pathosystem native to the Mediterranean Basin, took time in its introduced range in Idaho, USA, to generate epidemics. After years of minimal white rust, an epidemic occurred in 2017 in which first-year, juvenile plants had 20 times the sorus density of second-year, adult plants. Since white rust incidence had been minimal for years prior to 2017, the greater resistance of 2017 adults over 2017 juveniles may have been due to adult-plant resistance. This could also be due to phenology: adult plants have mature leaves, and are flowering and maturing seed, by the time that white rust begins to build up on leaves of juveniles. The juvenile-adult difference was maintained in 2018. In white blister rusts, interpretation of resistance can also be complicated by the frequency of asymptomatic infections that adult plants would pass on to the next generation. However, we found no asymptomatic infection of seeds of *L. annua* in our sampling of the Idaho population.

Key words. Plant defense, biotrophic parasite, *Brassicaceae*, *Albugo*.

INTRODUCTION

Plants in nature vary in life history, and some pathogens only affect early or late stages of the life history of their host plants (Agrios, 1997). For example, damping-off pathogens attack seedlings of many plants, but wood decay fungi only affect later stages of woody plants that may by then be many years of age. Resistance to certain pathogens changes with the age of their host plants. This is frequently called ‘age-related resistance’ (Panter and Jones, 2002), although ‘mature plant resistance’ and ‘adult plant resistance’ are also terms that are sometimes employed. Adult plant resistance has been inten-

sively studied in crop hosts (e.g., wheat, maize, tomato, *Brassica* spp. – Nazareno and Roelfs, 1981; Stewart et al, 1983; Bansal et al, 1999; Lin and Chen, 2007) and also in model plants such as *Arabidopsis* and tobacco (Pantier and Jones, 2002; Develey-Rivière and Galiana, 2007). Biennial plants are likely to be good hosts for study of adult plant resistance in this way. First-year plants are juveniles, and second-year plants are mature, having flowered and set seed for the first and only time.

Lunaria annua (money plant) is a biennial native to the Mediterranean Basin, that is introduced and somewhat weedy in North America (Newcombe et al, 2009). Many of the fungus and oomycete pathogens of *L. annua* have only been reported from western Europe (Farr and Rossman, 2018), where the plant is an archaeophyte. White rusts are economically important pathogens (Saharan and Verma, 1992), and the host range of *Albugo candida* is well known (Choi et al, 2009). The probable first specimen of white rust, or ‘white blister rust’, of money plant, caused by *Albugo candida*, was collected in England in 1960 (BPI 184980). This disease was not reported in North America until 2004, in Washington State (Glawe et al., 2004), and was collected in Oregon in 2000 and deposited in CUP as CUP-065639. Subsequently, the disease was found in the neighboring state of Idaho (Newcombe et al., 2009). The present authors have made annual observations since 2000 of this reconstituted pathosystem (i.e., it is reconstituted in that both host and pathogen are native elsewhere).

Annual observations have been made in the Shattuck Arboretum of the University of Idaho. *Lunaria annua* is a common understory plant in the ‘Old Arboretum’, with thousands of individuals representing each of the two age cohorts. White rust was at very low incidence and severity at the time of its discovery (Newcombe et al., 2009), and observations have been made annually since then.

In 2017 an epidemic of white rust developed on *L. annua*. The disease became obvious by early summer and juvenile plants were much more diseased than adult plants. This epidemic was seen as an opportunity to gain insights, using observational methods, into adult-plant resistance in a biennial, non-crop plant. In particular, this allowed possible distinction between selection in the juvenile phase and expression of adult-plant resistance. Adult-plant resistance to white rust has been noted in *Arabidopsis thaliana* (Holub, 2008), and in many other pathosystems, where different names for this phenomenon have been used (e.g., ontogenic, developmental, or age-related resistance; Develey-Rivière and Galiana, 2007).

MATERIALS AND METHODS

Observations on white rust of Lunaria annua from 2009 to 2016

Incidence and severity of white rust were recorded each year from 2009 to 2016, in early summer each year, on paths through the ‘Old Arboretum’, where a robust population of thousands of *L. annua* plants has been present for several decades. Each year, incidence was determined as the percentage of 500 plants (250 juveniles and 250 adults) with any white rust on any of their leaves. Severity was determined as the number of white rust sori on the worst affected leaf of each affected plant.

Severity of white rust during the epidemic years of 2017 and 2018

Intermixed juvenile and adult plants were scored for white rust severity throughout the ‘Old Arboretum’ during the epidemic in early July of 2017 and 2018. A 1 m² quadrant was used to designate 26 representative quadrants containing totals of 194 adult and 348 juvenile plants. Sori were counted on each plant on the second set of leaves from the bottom (i.e., the third and fourth oldest leaves), that were typically the most severely affected by white rust. Each sorus was counted, occasionally using a dissecting microscope to differentiate between closely clustered sori. These data consisted of counts of individual *A. candida* sori on the undersides of the second sets of leaves of 542 plants in 2017 and 100 in 2018. This measure of incidence was conservative, in that plants with no sori on the second set of leaves sometimes had rust sori on other leaves.

Molecular testing for Albugo candida in seeds of infected plants

Seeds from 25 plants with some leaf white rust infections were collected and tested for the presence of *Albugo candida*. Ten seeds from each of 13 plants were combined for testing (No. = 13). Ten seeds of each of 12 plants were tested individually (No. = 120). DNA was extracted using the Qiagen DNeasy Plant Mini kit following the manufacturer’s protocol. Twenty-five microliter PCR reactions were set up using Accuprime Pfx Supermix and a two-step PCR was carried out using oomycete- and *Albugo*-specific primers and conditions described by Ploch and Thines (2011). The resulting PCR products were visualized in a 1% agarose gel stained with ethidium bromide.

Statistical analyses

The Shapiro-Wilk and the Anderson-Darling tests were used to evaluate normality of the data collected. The data were then analyzed using the nonparametric Kruskal-Wallis test to determine difference in disease severity between the juvenile and adult individuals of *L. annua*.

RESULTS

Observations on white rust of *Lunaria annua* from 2009 to 2016

Annual surveys from 2009 to 2016 inclusive, of the 500 plant samples from the population of thousands of *L. annua* plants in the 'Old Arboretum', revealed low white rust incidence. Each year only one to five plants were found with white rust. Severity was also low with from one to four sori on the worst affected leaves, that were typically the third or fourth oldest on each affected plant. In 2016, the last year preceding the 2017 epidemic, incidence was negligible, with three white-rusted plants with, respectively, two, four and four sori per most affected leaf.

Severity of white rust during the epidemic years of 2017 and 2018

During the epidemic of 2017, 71% of 542 surveyed plants had some white rust on the two surveyed leaves per plant. According to this conservative measure of incidence, 90% of 348 juvenile plants, and 36% of 194 second-year, adult plants were diseased. This was a highly significant difference between the juvenile and adult cohorts ($\chi^2 = 79.276$, $P < 0.0001$). Average numbers of sori, as a measure of disease severity, were more than 20 times greater on juvenile than in adult plants (Figure 1a). This difference was also highly significant ($\chi^2 = 230.927$, $P < 0.0001$). Numbers of sori on adult plants averaged 4.2% of numbers on juvenile plants. Only 1% of adult plants had 30 or more sori compared to the 49.1% of juveniles with this white rust severity (Figure 2a). Therefore, the second-year, adult plants had much less white rust than first-year juveniles during the 2017 epidemic, and this difference was obvious from visual observations.

During the epidemic of 2018, 83% of the 100 surveyed plants had some white rust on the two surveyed leaves per plant. According to this conservative measure of incidence, 96% of 50 juvenile plants, and 70% of

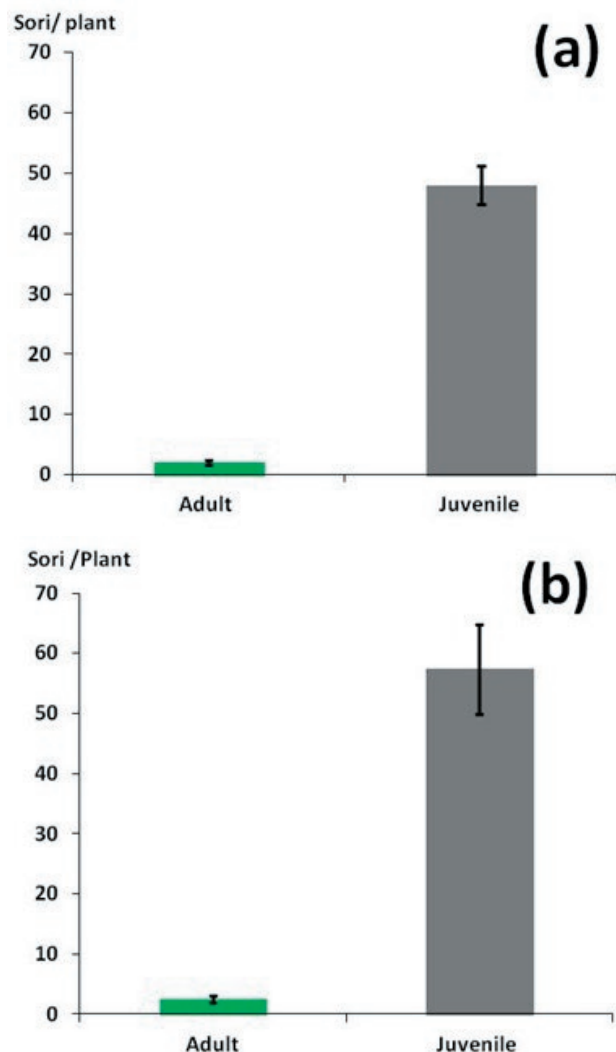


Figure 1. (a) Average numbers of *Albugo candida* sori per plant on *Lunaria annua* plants in 2017. (b) Average numbers of *A. candida* sori per plant on *L. annua* plants in 2018.

50 second-year, adult plants were diseased. This was a highly significant difference between the juvenile and adult cohorts ($\chi^2 = 7.1241$, $P = 0.0076$). Numbers of sori on leaves of juvenile plants were more than 23 times greater than those on leaves of adult plants (Figure 1b). This difference was highly significant ($\chi^2 = 58.205$, $P < 0.0001$). Numbers of sori on adult plants averaged 0.043% of those on juvenile plants. Only 2% of the adult plants had 30 or more sori compared to the 80% of juveniles with this severity (Figure 2b). Therefore, the second-year, adult plants had much less white rust than first-year juveniles, and this difference was visually obvious.

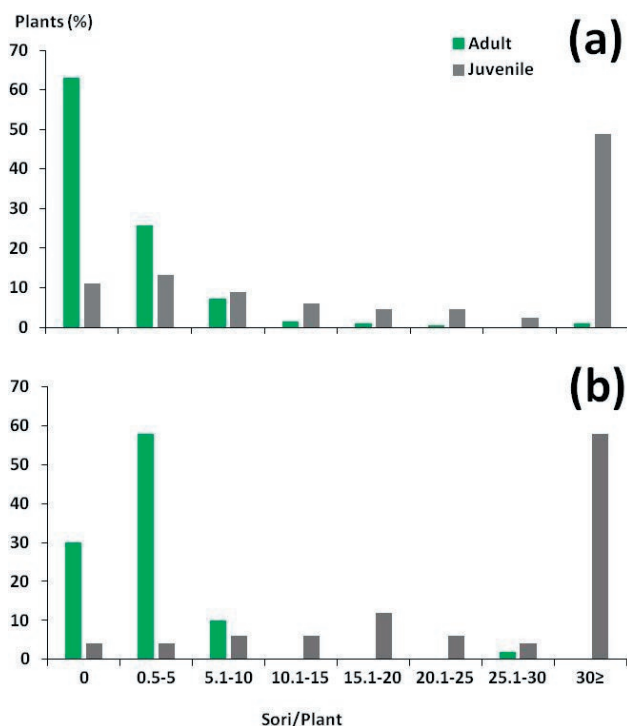


Figure 2. Distributions of average numbers of *Albugo candida* sori on *Lunaria annua* plants, in (a) 2017 and (b) 2018.

Molecular testing for *Albugo candida* in seeds of infected plants

Any PCR products close to the expected size for the *Albugo*-specific primers were sequenced. The sequences were very variable, and were probably randomly attached to the host genome at multiple sites. No *Albugo* was detected in any seeds of leaf-infected *L. annua*. To confirm that no *Albugo* was present, primers ITS 4 and ITS 5 (White *et al.*, 1990) were used on the DNA extracted from seeds. Only part of the ITS region of *L. annua* was amplified. Sequences of *Albugo* or other microorganisms were not detected.

DISCUSSION

This study has detected greater incidence and severity of white rust in juvenile *L. annua* plants than in adult plants. The study considered the possibility that greater resistance of adult plants could be due either to prior selection for resistance or to persistent, systemic infections. However, the observations and data did not support these hypotheses. Instead, they indicated that there were differing phenologies for juvenile and adult plants.

Plants in this study were naturally interspersed. However, without controlled inoculations, inferences about juvenile and adult plant resistance face different challenges. Firstly, there is the problem of prior selection. 2017 was the first year of a severe white rust epidemic, so the detection of stronger adult plant than juvenile resistance in that year was supported. Prior selection was unlikely given the much lower levels of white rust in the preceding years.

A second challenge was the possibility of persistent systemic infections, since simple counts of pustules would then have been an inaccurate measure of infection. Systemic infection has been reported for *Albugo candida* in some species of *Brassicaceae*, including *Lepidium campestre*, *Erysimum menziesii* subsp. *eurekaense*, and *Arabis lyrata* (Jacobson *et al.*, 1998). Systemic infections frequently, but not always, result in sterile, distorted host inflorescences that are commonly described as ‘stag-heads’. In *Brassica napus*, stagheads are associated with greatly reduced seed yields (Harper and Pittman, 1974; Petrie, 1988). Stagheads in *L. annua* were not observed in the UI Arboretum. Assessments for presence of *A. candida* in bulked and individual seeds of 25 plants showed no evidence of systemic infections, and no reports of systemic white rust infections in *L. annua* have been found in the literature. The absence of systemic infection may in part be a function of the host responses, but there are also likely to be differences related to host specificity that were at first thought to be at the ‘strain’ level in *A. candida* (Sansome and Sansome, 1974).

Another possible explanation for the present results could be the difference in phenology of juvenile and adult *L. annua* plants. Adult plants flower in the UI Arboretum before juvenile plants begin to become infected by *A. candida*. By early July, adult plants have finished flowering and their seeds are maturing. Juvenile plants, in contrast, possess only relatively young and susceptible leaves in late June and early July.

Differences in resistance between juvenile and adult of species of *Brassicaceae* have been previously reported. Adult plants usually showed greater resistance to white rust than juvenile seedlings in a study involving growth-chamber inoculations of *Lepidium campestre*, *Erysimum menziesii* subsp. *eurekaense*, and *Arabis lyrata* (Jacobson *et al.*, 1998). This was true even for new leaves of adult plants, in that they were less susceptible than new leaves of young seedlings in the three species examined by Jacobson *et al.* (1998).

The present study has demonstrated adult plant resistance in *L. annua* to white rust, and this allows speculation on the theory of optimal host defense for this pathosystem. This theory proposes that at the level

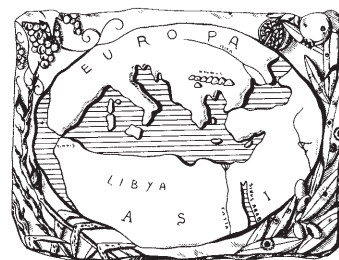
of an individual host plant, defense is weakest when tissues are most expendable, and is strongest when tissues are most valuable. Vegetative tissues are considered to be more expendable, and reproductive tissues more valuable, for overall plant fitness. This distinction has been demonstrated in another species of *Brassicaceae*, *Boechera stricta* (Keith and Mitchell-Olds, 2017), in which defense-related glucosinolates were more concentrated in reproductive than in vegetative tissues. But this idea might be difficult to disentangle from the phenological differences between juveniles and adults.

LITERATURE CITED

- Agrios G.N., 1997. *Plant Pathology, Fourth Edition*. Academic Press. CA.
- Bansal V.K., Thiagarajah M.R., Stringam G.R., Tewari J.P., 1999. Inheritance of partial resistance to race 2 of *Albugo candida* in canola-quality mustard (*Brassica juncea*) and its role in resistance breeding. *Plant Pathology* 48(6): 817–822.
- Choi Y.J., Shin H.D., Thines M., 2009. The host range of *Albugo candida* extends from Brassicaceae through Cleomaceae to Capparaceae. *Mycological Progress* 8(4): 329.
- Develey R.M.P., Galiana E., 2007. Resistance to pathogens and host developmental stage: a multifaceted relationship within the plant kingdom. *New Phytologist* 175(3): 405–416.
- Farr D.F., Rossman A.Y., Fungal Databases: U.S. National Fungus Collections. Available at: <https://nt.ars-grin.gov/fungalDATABASES/>. Accessed October 29, 2018.
- Glawe D.A., Glass J.R., Putnam M.L., 2004. First report of white rust of *Lunaria annua* caused by *Albugo candida* in North America. *Plant health progress*: 1–2.
- Harper F.R., Pittman U.J., 1974. Yield loss by *Brassica campestris* and *B. napus* from systemic infection by *Albugo cruciferarum*. *Phytopathology* 64: 408–410.
- Holub E.B., Springer D., 2008. Natural history of *Arabidopsis thaliana* and oomycete symbioses in the downy mildews-genetics. *Molecular Biology and Control*: 91–109.
- Jacobson D.J., LeFebvre S.M., Ojerio R.S., Berwald N., Heikkinen E., 1998. Persistent, systemic, asymptomatic infections of *Albugo candida*, an oomycete parasite, detected in three wild crucifer species. *Canadian Journal of Botany* 76(5): 739–750.
- Keith R.A., Mitchell O.T., 2017. Testing the optimal defense hypothesis in nature: variation for glucosinolate profiles within plants. *PLoS one* 12(7): 0180971.
- Nazareno N.R.X., Roelfs A.P., 1981. Adult plant resistance of Thatcher wheat to stem rust. *Phytopathology* 71: 181–185.
- Newcombe G., Gaylord R., Yenish J.P., Mastrogiuseppe J., Dugan F.M., 2009. New records for pathogenic fungi on weedy or non-indigenous plants. *North American Fungi* 4: 1–12.
- Panter S.N., Jones D.A., 2002. Age-related resistance to plant pathogens. *Advances in Botanical Research* 38: 252–281.
- Petrie G.A., 1988. Races of *Albugo candida* (white rust and staghead) on cultivated Cruciferae in Saskatchewan. *Canadian Journal of Plant Pathology* 10: 142–150.
- Ploch S., Thines M., 2011. Obligate biotrophic pathogens of the genus *Albugo* are widespread as asymptomatic endophytes in natural populations of Brassicaceae. *Molecular Ecology* 20: 3692–3699.
- Saharan G.S., Verma P.R., 1992. White rusts: a review of economically important species. *International Development Research Centre*.
- Sansome E., Sansome F.W., 1974. Cytology and life-history of *Peronospora parasitica* on *Capsella bursa-pastoris* and of *Albugo candida* on *C. bursa-pastoris* and on *Lunaria annua*. *Transactions of the British Mycological Society* 62(2): 323–IN24.
- Stewart H.E., Taylor K., Wastie R.L., 1983. Resistance to late blight in foliage (*Phytophthora infestans*) of potatoes assessed as true seedlings and as adult plants in the glasshouse. *Potato Research* 26(4): 363–366.
- White T.J., Bruns T., Lee S., Taylor J., 1990. *PCR Protocols: A guide to methods and applications*. Academic Press Inc., San Diego, California, USA.

Mediterranean Phytopathological Union

Founded by Antonio Ciccarone



The Mediterranean Phytopathological Union (MPU) is a non-profit society open to organizations and individuals involved in plant pathology with a specific interest in the aspects related to the Mediterranean area considered as an ecological region. The MPU was created with the aim of stimulating contacts among plant pathologists and facilitating the spread of information, news and scientific material on plant diseases occurring in the area. MPU also intends to facilitate and promote studies and research on diseases of Mediterranean crops and their control.

The MPU is affiliated to the International Society for Plant Pathology.

MPU Governing Board

President

DIMITRIOS TSITSIGIANNIS, Agricultural University of Athens, Greece – E-mail: dimtsi@aua.gr

Immediate Past President

ANTONIO F. LOGRIECO, National Research Council, Bari, Italy – E-mail: antonio.logrieco@ispa.cnr.it

Board members

BLANCA B. LANDA, Institute for Sustainable Agriculture-CSIC, Córdoba, Spain – E-mail: blanca.landa@csic.es

ANNA MARIA D'ONGHIA, CIHEAM/Mediterranean Agronomic Institute of Bari, Valenzano, Bari, Italy – E-mail: donghia@iamb.it

DIMITRIS TSALTAS, Cyprus University of Technology, Lemesos, Cyprus – E-mail: dimitris.tsaltas@cut.ac.cy

Honorary President, Secretary-Treasurer

GIUSEPPE SURICO, DAGRI, University of Florence, Firenze, Italy - E-mail: giuseppe.surico@unifi.it

Affiliated Societies

ARAB SOCIETY FOR PLANT PROTECTION (ASPP), <http://www.asplantprotection.org/>

FRENCH SOCIETY FOR PHYTOPATHOLOGY (FSP), <http://www.sfp-asso.org/>

HELLENIC PHYTOPATHOLOGICAL SOCIETY (HPS), <http://efe.aua.gr/>

ISRAELI PHYTOPATHOLOGICAL SOCIETY (IPS), <http://www.phytopathology.org.il/>

ITALIAN PHYTOPATHOLOGICAL SOCIETY (SIPAV), <http://www.sipav.org/>

PORTUGUESE PHYTOPATHOLOGICAL SOCIETY (PPS), <http://www.spfitopatologia.org/>

SPANISH SOCIETY FOR PLANT PATHOLOGY (SEF), <http://www.sef.es/sef/>

2021 MPU MEMBERSHIP DUES

INSTITUTIONAL MPU MEMBERSHIP: : € 200.00 (college and university departments, libraries and other facilities or organizations). Beside the open-access on-line version of *Phytopathologia Mediterranea*, the print version can be received with a € 50 contribution to mail charges (total € 250,00 to receive the print version). Researchers belonging to an Institution which is a member of the Union are entitled to publish with a reduced page contribution, as the Individual Regular members.

INDIVIDUAL REGULAR MPU MEMBERSHIP*: € 50.00 (free access to the open-access on-line version of *Phytopathologia Mediterranea* and can get the print version with a contribution to mail charges of € 50 (total € 100,00 to receive the print version).

*Students can join the MPU as a Student member on the recommendation of a Regular member. Student MPU members are entitled to a 50% reduction of the membership dues (proof of student status must be provided).

Payment information and online membership renewal and subscription at www.mpunion.com

For subscriptions and other information visit the MPU web site:

www.mpunion.com

or contact us at: Phone +39 39 055 2755861/862 – E-mail: phymed@unifi.it

Phytopathologia Mediterranea

Volume 60, August, 2021

Contents

- Biological and molecular characterization of seven *Diaporthe* species associated with kiwifruit shoot blight and leaf spot in China**
Y. Du, X. Wang, Y. Guo, F. Xiao, Y. Peng, N. Hong, G. Wang 177
- Distribution and identification of luteovirids affecting chickpea in Sudan**
A. Moukabel, S.G. Kumari, A.A. Hamed, M. Sharman, S. Ahmed 199
- Bacillus*-based products for management of kiwifruit bacterial canker**
E. Biondi, L. Gallipoli, A. Mazzaglia, S.P. Fuentealba, N. Kuzmanović, A. Bertaccini, G.M. Balestra 215
- First report of *Didymosphaeria rubi-ulmifolii* associated with canker and dieback of apple trees in southern Ethiopia**
A. Yirgu, A. Gezahgne, T. Alemu, M. Havenga, L. Mostert 229
- Characterization of *Lasiodiplodia* species associated with grapevines in Mexico**
E.A. Rangel-Montoya, M. Paolinelli, P.E. Rolshausen, C. Valenzuela-Solano, R. Hernandez-Martinez 237
- First report of *Erwinia amylovora* in Tuscany, Italy**
D. Migliorini, F. Pecori, A. Raio, N. Luchi, D. Rizzo, C. Campani, L. Neri, A. Santini 253
- Identification of *Plectosphaerella melonis* from cucumber plants in Ukraine**
E. Kopilov, H. Tsekhmister, O. Nadkernychna, A. Kyslynska 259
- Starch-glycerol monostearate edible coatings formulated with sodium benzoate control postharvest citrus diseases caused by *Penicillium digitatum* and *Penicillium italicum***
L. Soto-Muñoz, V. Martínez-Blay, M.B. Pérez-Gago, A. Fernández-Catalán, M. Argente-Sanchis, L. Palou 265
- Ribosomal protein coding genes *SSU12p* and *LSU36p* as molecular markers for phytoplasma detection and differentiation**
W. Cui, A. Zamorano, N. Quiroga, A. Bertaccini, N. Fiore 281
- Identification, full-length genome sequencing, and field survey of citrus vein enation virus in Italy**
M. Minutolo, M. Cinque, G. Altamura, F. Di Serio, D. Alioto, B. Navarro 293
- Fungal pathogens associated with black foot of grapevine in China**
Q. Ye, W. Zhang, J. Jia, X. Li, Y. Zhou, C. Han, X. Wu, J. Yan 303
- Physiological responses of 'Italia' grapevines infected with Esca pathogens[†]**
G.L. Bruno, M.P. Ippolito, F. Mannerucci, L. Bragazzi, F. Tommasi 321
- Ceratocystis ficala* causing a serious disease of *Ficus carica* in Greece**
P. Tsopelas, N. Soulioti, M.J. Wingfield, I. Barnes, S. Marincowitz, E.C. Tjamos, E.J. Paplomatas 337
- Fomitiporia mediterranea* M. Fisch., the historical Esca agent: a comprehensive review on the main grapevine wood rot agent in Europe**
S. Moretti, A. Pacetti, R. Pierron, H.-H. Kassemeyer, M. Fischer, J.-P. Péros, G. Perez-Gonzalez, E. Bieler, M. Schilling, S. Di Marco, E. Gellhaye, L. Mugnai, C. Bertsch, S. Farine 351
- Adult plant resistance to white rust in *Lunaria annua***
D. Cervantes, M. Ridout, C. Nischwitz, G. Newcombe 381

Phytopathologia Mediterranea is an Open Access Journal published by Firenze University Press (available at www.fupress.com/pm/) and distributed under the terms of the Creative Commons Attribution 4.0 International License (CC-BY-4.0) which permits unrestricted use, distribution, and reproduction in any medium, provided you give appropriate credit to the original author(s) and the source, provide a link to the Creative Commons license, and indicate if changes were made.

The Creative Commons Public Domain Dedication (CC0 1.0) waiver applies to the data made available in this issue, unless otherwise stated.

Copyright © 2021 Authors. The authors retain all rights to the original work without any restrictions.

Phytopathologia Mediterranea is covered by AGRIS, BIOSIS, CAB, Chemical Abstracts, CSA, ELFIS, JSTOR, ISI, Web of Science, PHYTOMED, SCOPUS and more